Cranfield University

Benjamin John Phillips

Multidisciplinary Optimisation of a CFRP Wing Cover

School Of Engineering

EngD

Cranfield University

School of Engineering

EngD

2009

Benjamin John Phillips

Multidisciplinary Optimisation of a CFRP Wing Cover

Supervisors: Dr Shijun Guo, Prof John Fielding & Graham Clark

Academic Year 2004 to 2009

This thesis is submitted in partial fulfilment of the requirements for the degree of Engineering Doctorate

Abstract

With the market introduction of both the Airbus A350XWB and the Boeing 787, Carbon Fibre Reinforced Plastics (CFRP) has been applied to primary structure of large commercial aircraft, as a means of enhancing overall performance. Both these aircraft are being developed and produced in a unique way where Airbus and Boeing are acting as System Integrators and using Risk Sharing Partners to develop the majority of the principal components.

To support this new business and technological model it is necessary that the System Integrator has sufficient knowledge and tools to support the development of the components. Of particular interest are items such as the wing covers, as they are both heavy and expensive items, thus offering large opportunities for optimisation, in particular when the benefits of applying CFRP are considered. This creates the forum for this thesis, i.e. to thoroughly understand all factors that influence a CFRP wing cover, from which an optimisation methodology is developed, incorporating design constraints, while seeking the lightest weight solution, with a resultant Life Cycle Cost (LCC). Based on this, different solutions can be compared based on weight and LCC.

In general stringer-stiffened panels are, from a weight perspective, the optimal configuration for wing covers, and thus are solely considered. Serendipitously, due to their prismatic shapes, buckling calculations of stringer-stiffened panels can be solved with reasonable accuracy and ease using the Finite Strip Method (FSM), as opposed to more time consuming methods such as the Finite Element Method. A suitable FSM program is available from ESDU, which when used in combination with a configured Excel spreadsheet can take into consideration constraints established from the extensive literature review. Once the lowest weight solution is obtained under buckling constraints, the solution is then checked for in-plane and if desired out-of-plane strength.

Based on the structurally optimised wing cover, the manufacturing cost is calculated using a Process Based Cost Model (PBCM), which has been developed based on different CFRP materials for the skin and stringer fabrication, as well as suitable manufacturing and integration methods. In order to consider the LCC, i.e. all costs from cradle to grave, the PBCM factors in both the cost of recycling scrap material during manufacture and after retirement. Furthermore, when more than one solution is compared then the Economic Value of Weight Saving, which is based on the range equation, can be factored in to consider the financial benefit of weight saving.

The optimisation methodology and PBCM has been evaluated on diverse wing cover examples, which has considered both uni-directional prepreg, non-crimp fabric and braids materials in combination with autoclave and liquid composite moulding techniques. The results demonstrated a trend which can be considered realistic, although the cost estimation is very much dependent on the assumptions made. In conclusion, the thesis and the optimisation methodology can be used to compare different configurations.

Acknowledgements

I would like to express my appreciation to Airbus Operations GmbH, who had the foresight to allow me to study for this EngD, in order to improve my overall competence and increase my scope of knowledge. I hope that I will be given the opportunity to reimburse this long-term investment taken by Airbus, to help in improving their future position in the market place. I would also like to thank the Engineering and Physical Science Research Council (EPSRC) for the Engineering Doctorate Grant.

There are many people I would like to pay particular thanks to. Firstly, Bodo Zapf from Airbus, who originally supported my wish to study and established the foundations to enable this. Furthermore, he has mentored me through my EngD with his immense knowledge that he has attained through decades of work in the aerospace industry. Further thanks go to Dr Eberhard Greff, who sanctioned me to study whilst at work, and has since supported my studies. Manuela Schradick, who has been my Project Manager since the beginning of my studies, without her support and understanding the possibility to study, while at the same time working, would not have been possible. I am truly indebted to her for this. Further noteworthy thanks go to Dr Eckhard Neise, who also mentored me through my studies, his multi-disciplinary engineering knowledge has been very beneficial. Finally, Dr Shijun Guo, my supervisor at Cranfield, who has provided excellent support when necessary.

Thanks also go to Michael Brüns-Treml, Markus Gibbert and Ivar Wiik, who have spent many hours assisting me in various topics. Further thanks go to the following Airbus colleagues: Ian Beaumont, Günter Döhle, George Kolmaniatis, Ingo Kröber, Xavier Hue, Jonathon Komadina, Sebastian Kaschel, Barnaby Law, and Wolfgang Vöge. From Cranfield University: Anita Beal, Graham Clark, Deborah Hiscock, Andrew Mills, and Kath Tipping. From IHS ESDU: Adam Quilter.

I have also had the pleasure throughout my studies to mentor the following students, who have assisted me in various investigations: Oleg Diehl, Daniel Hofmann, Ata Iyiyazici, Vinayak Patil, Varun Singhania, Feng Wang, and Zhiqiang Zhou.

A special thanks go to my Mother and Father, who have supported me throughout my life, they are truly good examples of how parents should be. The determination that my parents have shown through various endeavours has been an example to me, and has helped me to complete this thesis. Finally, to my Wife, Christina, who has shown great understanding, throughout my thesis, I truly hope now we can start enjoying our lives together to the full!

Acronyms

AAI	Advanced Affordability Initiative
ABC	Activity-Based Costing
AC	Acquisition Cost
ACEE	Aircraft Energy Efficiency
ACCEM	Advanced Composite Cost Estimating Model
ACT	Advanced Composite Technology
ADP	Advanced Pultrusion
AEA	Association of European Airlines
AFP	Automated Fibre Placement
ALCAS	Advanced Low-Cost Aircraft Structures
AST	Advanced Subsonic Technology
ATL	Automated Tape Layer
AVIC	Aviation Industries of China
BAVAMPAC	Buckling And Vibration Analysis of Multi-term Plate Assemblies using CPT
BAVAMPAS	Buckling And Vibration Analysis of Multi-term Plate Assemblies using SDPT
BB	Bearing/Bypass
BMC	Bulk Moulding Compound
BMI	Bismaleimide
BVID	Barely Visible Impact Damage
CAI	Compression After Impact
CF	Cost Factor
CLF	Closed Form
CFRP	Carbon Fibre Reinforced Plastic
CNC	Computer Numerical Control
COM	Cost of Manufacture
CONMIN	Constrained function Minimisation
COSTADE	Composite Optimisation Software for Transport Aircraft Design Evaluation
CPT	Classical Plate Theory
CS	Certification Specification
CTE	Coefficient of Thermal Expansion
CTL	Contour Tape Layer
CWB	Centre Wing Box
DAC	Douglas Aircraft Company
DOC	Direct Operating Costs
DSD	Discrete Source Damage
DP-RTM	Differential Pressure Resin Transfer Moulding
EA	Evolutionary Algorithm
EADS	European Aeronautic and Defence Space Company
EAL	Engineering Analysis Language
EASA	European Aviation Safety Agency
EDM	Electrical Discharge Machining
E-Glass	Electric Glass

EKDF	Environmental Knockdown Factor
EMI	Electro-Magnetic Interference
EOP	Edge of Part
ESD	Electro-Static Dissipation
ESDU	Engineering Sciences Data Unit
EU	European Union
EVWS	Economic Value of Weight Saving
FB	Fuel Burn
FE	Finite Element
FEM	Finite Element Model (Modelling)
FHT	Filled Hole Tension
FML	Fibre Metal Laminate
FTL	Flat Tape Layer
FRP	Fibre Reinforced Part
FSM	Finite Strip Method
FTAC	Fuel Tank Access Cover
FVF	Fibre Volume Fraction
FY	Financial Year
GA	Genetic Algorithm
GFRP	Glass Fibre Reinforced Plastic
HS	High Strength
HSB	Handbuch Struktural Berechnung
HTF	Heat Transfer Fluid
HTP	Horizontal Tail Plane
IM	Intermediate Modulus
IML	Inner Mould Line
IPR	Intellectual Property Rights
IPT	Integrated Product Team
IPPD	Integrated Product and Process Design
ISTR	Innovative Light Structures
JF	Jig Factor
KBE	Knowledge Based Engineering
KDF	Knockdown Factor
KE	Kinetic Energy
KM	Knowledge Management
LCC	Life Cycle Cost
LCM	Liquid Composite Moulding
LF	Length Factor
LHS	Left Hand Side
LL	Limit Load
LSP	Lightning Strike Protection
LWB	Lateral Wing Box
MC	Manufacturing Cost
MCMC	Manufacturing Cost Model for Composites
MDO	Multi Disciplinary Optimisation
MLG	Main Landing Gear
MVI	Modified Vacuum Infusion
NASA	National Aeronautics and Space Administration

NC	Numerically Controlled
NCF	Non-Crimp Fabric
NDT	Non-Destructive Testing
NLR	Nationaal Lucht- en Ruimtevaartlaboratorium
NPD	New Product Development
NRC	Non Recurring Cost
OEM	Original Equipment Manufacturer
OHC	Open Hole Compression
OHT	Open Hole Tension
OLGA	Optimisation of Laminates using Genetic Algorithms
OML	Outer Mould Line
OOP	Out Of Plane
PAN	Polyacrylonitrile
PANDA	Panel Design Analysis
PASCO	Panel Analysis and Sizing Code
PBCM	Process Based Cost Model
PC	Process Cost
PEEK	Polyetheretherketone
PFE	Precision Feed End-effector
PT	Process Time
QCD	Quality, Cost and Delivery
RC	Recurring Cost
R&D	Research and Development
RF	Reserve Factor
RFI	Resin Film Infusion
RHS	Right Hand Side
ROA	Return on Assets
ROI	Return on Investment
RT	Room Temperature
RTM	Resin Transfer Moulding
S-Glass	High Strength Glass
SDPT	Shear Deformation Plate Theory
SFC	Specific Fuel Consumption
SI	System Internationale
SMC	Sheet Moulding Compound
SR	Specific Range
SRO	Stringer Run Out
SQRTM	Same Qualified Resin Transfer Moulding
STAGS	Structural Analysis of General Shells
TAI	Tension After Impact
TANGO	Technology Application to the Near Term Business Goals and Objectives of the Aerospace Industry
TCW	Thermoset Composite Welding
TE	Textile
TQM	Total Quality Management
UD	Uni-Directional
UDL	Uniformly Distributed Load
UL	Ultimate Load

US	United States
USAF	United States Air Force
UV	Ultra Violet
VAP	Vacuum Assisted Process
VARI	Vacuum Assisted Resin Infusion
VARTM	Vacuum Assisted Resin Transfer Moulding
VARTM-PB	Vacuum Assisted Resin Transfer Moulding – Pressure Bleed
VICON	VIPASA with Constraints
VICONOPT	VIPASA with Constraints and Optimisation
VID	Visible Impact Damage
VIPASA	Vibration and Instability of Plate Assemblies including Shear and Anisotropy
VOC	Volatile Organic Compounds
VTP	Vertical Tail Plane
WBS	Work Breakdown Structure
XWB	Extra Wide Body
ZFW	Zero-Fuel Weight

Notation

a	Panel Length
$\bar{a}$	Longitudinal Wavelength
A	Amperes
A	Area
A_b	Bulb Area
b	Panel Width
$\bar{b}$	Speed of Sound
BH	Blade Height
BT	Blade Thickness
c	Specific Fuel Consumption
C	Cost
C	Clamped (Boundary Conditions)
c_o	Material Cost
$\gamma_{xy(F)}$	Shear (Failure) Strain
d	Bolt Diameter
d	Discrete Stringer
D	Drag
d_b	Diameter of Bulb
δ	Geometric Imperfection
ΔW_{FO}	Extra Weight of Fuel
ΔW_A	Extra Structural Weight
e	Eccentricity Factor
E	Young's Modulus
E_{11}	Young's Modulus in Longitudinal Direction
E_{22}	Young's Modulus in Transverse Direction
ε_x	Strain in Longitudinal Direction
ε_{xFC}	Compressive Strain in Longitudinal Direction
ε_{xFT}	Tensile Strain in Longitudinal Direction
ε_y	Strain in Transverse Direction
ε_{yFC}	Compressive Strain in Transverse Direction
ε_{yFT}	Tensile Strain in Transverse Direction
F	Free (Boundary Conditions)
F	Applied Axial Running Load
FC	Flight Cycles
FP	Fuel Price
FVF	Maximum Fibre Volume Fraction
θ	Angle
θ	Seydel's Orthotropic Parameter
g	Gravity
G_c	Critical Strain Energy Release Rate
G_{12}	Shear Modulus
h	Height
h	Hours
h'	Distance from Centre of Gravity to Wing Box Neutral Axis
I	Second Moment of Inertia

I_b	Bulb's Second Moment of Inertia
J	Joules
J	Polar Moment of Inertia
k	1000's of filaments (tow)
k_x	Curvature in Plate
k_y	Curvature in Plate
Kc	Buckling Coefficient
K_{IC}	Critcal Stress Intensity Factor
L	Lift
LFT	Lower Flange Thickness
LFW	Lower Flange Width
λ	Half-Wavelength
m	Mass
M	Moment
m_x	Shear Coupling Coefficient
m_y	Shear Coupling Coefficient
N	Newton
N_x	Axial Running Load
N_{xy}	Shear Running Load
N_y	Transverse Running Load
ν_{12}	Major Poisson's Ratio
ν_{21}	Minor Poisson's Ratio
p	Performance
P	Load
P	Pressure
ρ	Density
r	Lift to Drag Ratio
R	Range
s	Smeared Stringer
SH	Stringer Height
SP	Stringer Pitch
SS	Simply Supported (Boundary Conditions)
σ	Stress
σ_{13}	Interlaminar Longitudinal Shear Stress
σ_{22}	Transverse In-Plane Stress
σ_{23}	Interlaminar Transverse Shear Stress
t	Thickness
t	Time
t_{ply}	Ply Thickness
T_g	Glass Transition Temperature
τ	Shear Stress
u	Axial Load Factor for Beam Column
u	Buckling Displacement in Longitudinal Direction
UFT	Upper Flange Thickness
UFW	Upper Flange Width
υ_e	Elastic Poisson's Ratio
v	Buckling Displacement in Transverse Direction
V	Velocity

w	Buckling Displacement in Vertical Direction
w	Width
W	Weight
WT	Web Thickness
Ψ_{xy}	Twist in Plate
Z_1	Distance from Laminate's Mid-Plane

Table of Contents

Table of Figures

Table of Tables

1 Introduction

1.1 Cost Effectiveness

The aerospace industry has a rich history of innovation and technological leadership. Revolutionary development has often occurred during wars that were both 'Hot' and 'Cold', giving birth to the race for "faster, higher, and farther". However, today, this has given way to "better, cheaper, and faster", where "better" means improved product quality and productivity; "cheaper" relates to reduced product cost; whereas "faster" is the response to market demand[1]. Thus the aircraft's cost effectiveness must be maximised throughout its life-cycle[2], in order to comply to the demands of the customer.

The time to market is of extreme importance to both the customer and the manufacturer. The customer will typically require their new aircraft delivered expediently in order to maximise their benefit from the aircraft's improved efficiency. For the manufacturer, the time to market period, which is also known as the development time, incurs large Non-Recurring Costs (NRC), thus by reducing this time, the overall cost can be reduced, as illustrated in Figure 1-1[3]. The assumption of Figure 1-1 is that the same amount of money is spent; it is just spent in a shorter time. As an example of the criticality of this, by reducing the time to market by 12 months can yield the same benefit in terms of Direct Operating Cost (DOC), as having an advanced composite wing[3].

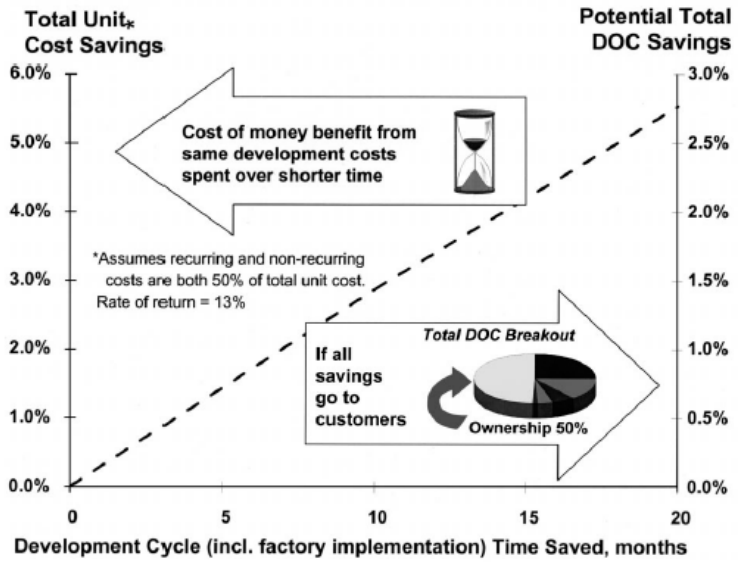

Figure 1-1: Estimated value of reduced cycle time to market

The cost of aircraft ownership is principally governed by the acquisition cost and the running costs. The acquisition cost has been affected by a 400-600% increase in labour rate, between 1970 to 2000, in the Western World[4], which means the cost of a Boeing 737 is 6 times more expensive today than it was 30 years ago[5]. Furthermore, the running costs are heavily influenced by the fuel price, which is often very turbulent, as shown in Figure 1-2[6].

Using more automated, but capital intensive, manufacturing methods, has mitigated the influence of labour rate on the aircraft cost. However, the fluctuation in fuel price can make it hard for the aircraft manufacturer to decide on how best to design the aircraft to maximise value over a life span of more than 30 years. Is it more prudent to design the aircraft to minimise the acquisition cost; or is it best to minimise the structural weight, in order to maximise fuel economy? The answer is principally dependent on the price of fuel, although

increasingly the negative impact that aircraft operation has on the environment, has meant that legislation and regulation is being imposed to reduce the amount of pollution caused by the aircraft.

Figure 1-2: Change in fuel price (based on kerosene from Rotterdam) from 1986 to 2008

The influence that fuel price has on the DOC can be seen in Figure 1-3. Shown on the left hand side (LHS) of Figure 1-3 is the Association of European Airlines (AEA) defined DOC breakdown for a short-range aircraft, carrying 150 passengers over 2800 nautical miles at a fuel price of $0.75/gallon[7]. The right hand side (RHS) of Figure 1-3 reflects the DOC if the fuel price is $2.60/gallon. It can be seen that the acquisition cost represents between 40-54% of the total DOC, dependent on the price of fuel. Based on 1995 aluminium technology, the acquisition cost as a percentage of total DOC for a long-range and short-range aircraft was 33% and 42%, respectively[8]. The relative difference between the two is due to long-range aircraft having higher fuel costs. This is evidenced by the airliner Emirates, who has a pure long-haul fleet[9], where fuel costs account for 34% of operating costs"[10]. Thus, long-range aircraft are influenced more by the fuel price, and hence are more sensitive to variation in fuel price.

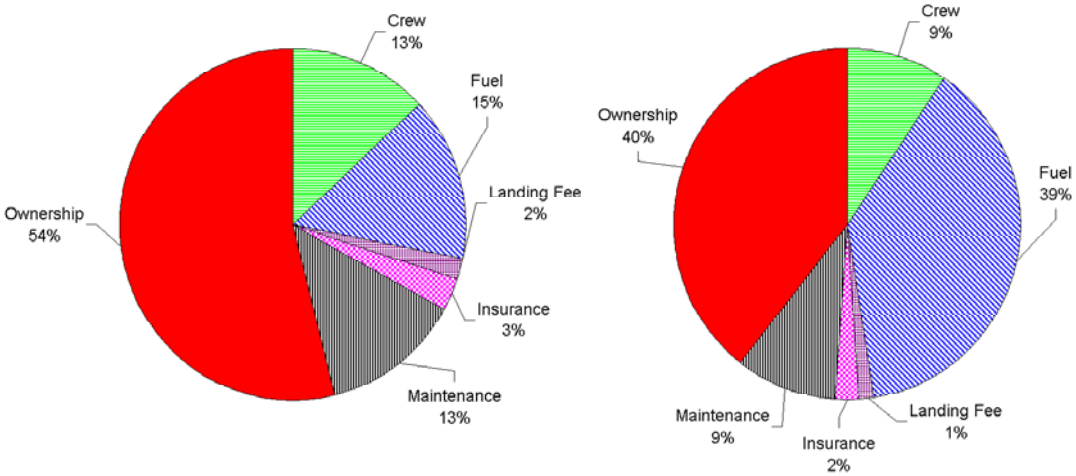

Figure 1-3: DOC of a regional aircraft at $0.75 (LHS) & $2.60 (RHS) per gallon

1.2 Aircraft Demand

In recent years, there has been a steady increase in the demand for commercial aircraft, as shown in Figure 1-4[11]. Demand is particularly high for newly developed aircraft, due to the improved operational efficiency in comparison to their predecessors. As a consequence of this demand, the life cycle of commercial aircraft is being reduced.

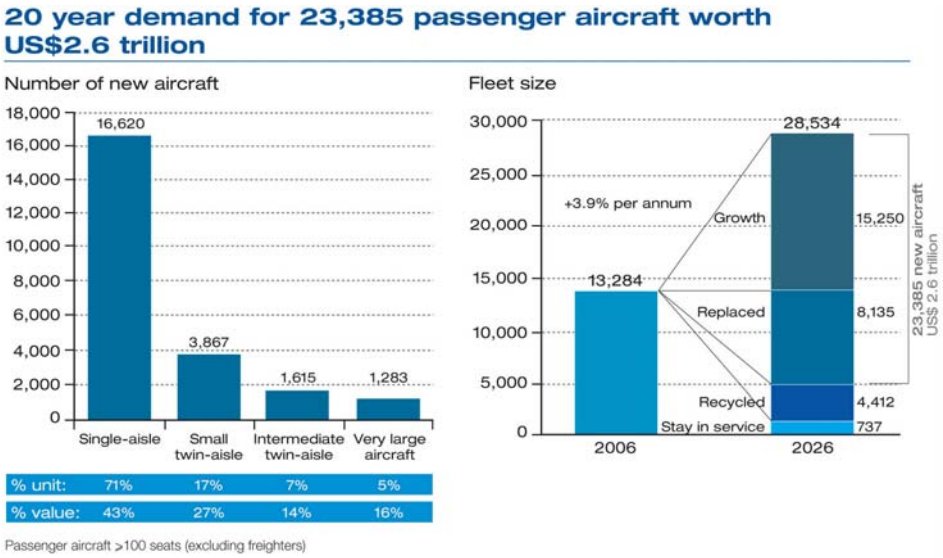

Figure 1-4: Increase in demand for aircraft

For the aircraft manufacturer, it is only worthwhile to develop a new aircraft when there is both significant demand and the available technology that can provide a clear step-change in efficiency over the aircraft that it replaces. This is due to new aircraft programs requiring heavy investment; for example, the Airbus A350 XWB requires an estimated $10 billion purely for the development costs[12], thus the aircraft must have a certain future, in which to accumulate revenue from sales, to pay back the debt and, in the long-term, to make profit to allow investment in future work.

1.3 Market Structure

There have been two forces that have impacted on commercial airlines from the late 1970s, namely deregulation and privatisation. This has increased competition between airlines, causing an overall improvement in financial efficiency, which has led to a reduction in profit margins[13]. Since then, the airline industry has shown rapid development, typified by boom-and-bust cycles, as it is affected by both business cycles and human influences[14], which impinge on the dynamics of supply and demand. A typical cycle in the world airline industry is every 10.5 years[15].

This has culminated in the rise of no frills airlines, in the short-haul market, deflating fares for tickets, to such a degree that air travel has now become a commodity. The financial burden, of increased competition and lower margins, has cascaded down to the aircraft manufacturers, who are then pressured to produce aircraft with increased overall value, with both reduced acquisition and running costs[16], coupled with improved environmental efficiency.

Today, aircraft manufacturers must vie competitively with other manufacturers, for the sale of an aircraft. This means that during the development of the aircraft, the aircraft manufacturer

must control and forecast effectively their costs. Due to increase competition, firms have adopted Total Quality Management (TQM), which introduced a number of new approaches to conducting their business[17]:

- Identification of customer requirements
- Creation of supplier partnerships
- Cross-functional teams to identify and resolve issues
- Utilisation of scientific methods for performance measurement

Amongst the above points, the creation of supplier partnerships has led to the rise of the 'System Integrator' and its' associated supply-chain, where expertise and financial support from specialist suppliers are required. This approach has been evidenced in other industries, but principally the high-volume industries, which exhibit the following attributes[18]:

- Outsourcing of non-core activities
- Focusing on operations
- Reduction in supplier base, due to a switch from multi-source to single-source procurement
- Long-term relationships with suppliers

Such an approach has already been witnessed in engine and landing gear design, making the aircraft manufacturer dependent on suppliers for crucial parts of the corporate well-being[19]. This is now witnessed further with niche composite material suppliers, who can offer particular knowledge for different applications, which is not always possible to replicate within one large organisation.

Finally, the last decade has witnessed the rise of developing countries, which have attained high levels of equity, and want to either move up the supply chain or divest from their traditional industries; for example, the United Arab Emirates with its Dubai Aerospace Enterprise and China with Aviation Industries of China (AVIC). The governments in these developing countries can provide significant incentives to the System Integrator by offering tax relief and direct subsidies and they obtain the benefit in knowing that the System Integrator will have to develop their indigenous suppliers to a significant level to ensure the System Integrator's project is a success.

1.4 Affect of Novel Materials & Processes on Cost

The Specific Range (SR) of an aircraft, or in other terms how efficient it is, can be defined by Equation 1-1:

$$SR = \frac{1}{c} \times \frac{V \times L}{D} \times \frac{1}{W} \qquad \textbf{1-1}$$

Where c = Specific Fuel Consumption (SFC) ($kg \cdot s^{-1} \cdot N^{-1}$), V = Velocity (m/s), L = Lift (N), D = Drag (N), and W = Weight (N). The first term in the equation can be improved through more efficient engines, the second term through improved aerodynamic performance, and the final term through using advanced materials, as well as improved structural analysis. The ability of advanced materials, such as Carbon Fibre Reinforced Plastic (CFRP), to aid in the reduction of DOC is due to the following reasons:

- Light weight materials can reduce fuel consumption
    - This allows the range or payload to be increased
- Cost effective materials applied to suitable parts can reduce the acquisition cost
- Advanced materials with better fatigue and corrosion properties should reduce supportability costs

Since the discovery of continuous carbon fibre in 1964 by the Royal Aircraft Establishment, in Farnborough, UK[20], CFRP has been applied to many parts. The Douglas Aircraft Company (DAC) realised that wings with higher aspect ratio could be designed due to CFRP's inherent stiffness advantage over aluminium, leading to a reduction in drag, while minimising weight[21]. In terms of pure weight, the application of CFRP has achieved savings between 15-20% in comparison to legacy aluminium designs[22]. Furthermore, as the fuselage and the wing together typically account for 75% of the airframe structural weight[21], the new generation of aircraft, such as the Airbus A350 XWB, and the Boeing 787 shown in Figure 1-5[23], have applied CFRP to these parts. This should allow a 787 flying on the same route as a smaller aluminium based 767, to consume $5 million less fuel per year[24]. However, of equal importance, by applying new materials can aid innovation, which is of extreme importance to the aerospace industry.

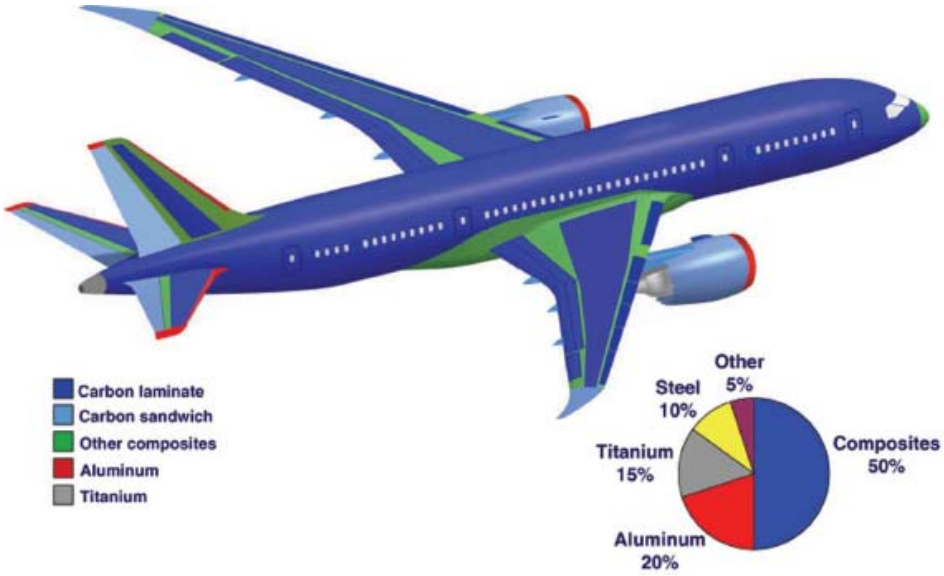

Figure 1-5: Material usage for Boeing 787 (The Boeing Company©)

In order to fairly appraise the benefit of applying CFRP, it is necessary to consider both the structural weight and manufacturing cost, in comparison to a conventional aluminium design. Towards the end of the 1980s, National Aeronautics and Space Administration (NASA) launched the Aircraft Energy Efficiency (ACEE) program, which illustrated that wings and fuselages made from conventional CFRP technology would cost significantly more than the then current aluminium structures[25]. For structures, with a large surface area and high thickness, like wing covers, will be expensive to manufacturer due to the additive nature of the manufacturing process, which is exacerbated by the high price of the raw material and the capital equipment. In order to reduce the manufacturing cost, concepts other than an Automated Tape Layer (ATL) depositing Uni-Directional (UD) prepreg, which is subsequently cured in an autoclave, should be applied. This mindset at tackling the high cost of CFRP parts has resulted in much research. For example, the NASA funded Advanced Composite Technology (ACT) program, which had the target of a 25% weight reduction and 60% part-count reduction in comparison to conventional aluminium[26], considered the

application of integrated "affordable" composite technology, using dry fibre and Liquid Composite Moulding (LCM) techniques.

Similarly, the European funded "Technology Application to the Near Term Business Goals and Objectives of the Aerospace Industry" (TANGO) program, which investigated the application of CFRP to fuselage and wings, had targets of 20% reduction in both weight and cost in comparison to current structures[26]. This has been followed on by the "Advanced Low-Cost Aircraft Structures" (ALCAS) program, the objective of which was to reduce the operating costs of aircraft by 15% through cost effective full application of CFRP to primary structure[27]. Furthermore, the Japanese Innovative Light Structures (ISTR) program produced a wing box, which was 27% lighter and had a 54% reduction in part count[26].

Despite all the research into novel materials and manufacturing solutions, the application of CFRP to wings and fuselage on both the Airbus A350 XWB and Boeing 787 uses the traditional ATL or Automated Fibre Placement (AFP) UD prepreg with autoclave cure. This is perhaps justifiable for the long-range market, as the largest part of the aircraft's DOC is fuel consumption, therefore weight reduction must always be reasonably minimised[28]. Furthermore, due to the popularity of both aircraft, economies of scale can assist in reducing the acquisition cost, due to the capital intensive nature of the industry, with the variable cost primarily being the material, thus a greater production volume should result in lower costs[29]. However, for future short-range aircraft, a principal requirement will be any new technologies that are implemented must then add to the economic value of the aircraft by reducing the overall DOC[22].

1.5 Contemporary Engineering

Up until now DOC has been mentioned, however this only considers the cost due to operation. Of greater importance is to consider the holistic life of the aircraft from "cradle to grave". In order to do this, Life Cycle Cost (LCC) analysis can be used, which considers amongst other additions to DOC the cost of disposal at the end of the aircraft's life.

In order to find the right balance to optimise the LCC, engineering teams are facing the challenge of making important design decisions early on in the design phase as the LCC can be heavily influenced at the preliminary design phase[30], where the use of new technology, such as advanced design concepts, innovative materials, and new manufacturing techniques, can be best applied[31]. The economic and market conditions will influence how much new technology can be risked, i.e. if a large gain in efficiency is required due to more stringent environmental legislation, then riskier technology might be adopted. For these reasons it is necessary to consider the cost effectiveness of new technology, as well as the traditional concerns for production, finance, operations and support[32], in both the product line and the supply chain.

Cost should therefore be one of the design variables in the conceptual and preliminary design phase, and not just weight. Within this forum it is possible to logically discuss trade-offs between cost and weight, and converge to a configuration that offers an efficient compromise. Initial cost estimates should be built upon, using a continuous process to improve the accuracy, which helps in justifying each subsequent phase of the products development[33]. In particular, it can be beneficial to prepare for product manufacture, and to support activities in design trades and make/buy decisions. Furthermore, based on the theory of strategic cost

management, accurate product costs can be of immense benefit to firms that want to make strategic positioning decisions[34].

The ability to predict the cost of a complicated product like an aircraft is not without its difficulties, with many firms struggling to estimate the product's cost early in the design phase[35]. In fact, a well known aircraft design book, used as reference until the 1960s, recommended that "to obtain the optimum combination, the only solution is to design a series of three or four airplanes with different combinations and choose the one with the lowest operating cost"[36].

Even today, it is only once the product has been designed and a prototype has been built that a realistic cost estimate can be attained, and from this point a decision can be taken, based on the product's profitability, if a costly redesign needs to be incurred[5]. However, at this stage it is very hard to justify large design changes, hence, the course of action taken is to try to reduce the manufacturing costs based on the existing design, which typically leads to a reduction in quality[37]. The issues that affect the ability to accurately predict the cost are: financial risk; high unit cost; low production runs; high capital investment; skilled workmanship; unpredictable markets; changing and evermore stringent certification standards, etc[38].

It has been found that companies which have successfully re-engineered their business processes have adopted a "system oriented approach which focuses on the integration of all disciplines", and that their business processes are "re-engineered around a flow of information instead of a flow of tasks"[39]. A systems engineering approach, considers the complete product life cycle, from cradle to grave, and searches for the solution that offers the best value. To do this, the pertinent requirements must be considered, and the value of the product verified through ensuring that the requirements are fulfilled. Concurrent engineering techniques must be grasped and enhanced by conducting succinct analysis throughout the different design phases, in order to accomplish a systems engineering approach. This will involve improved teamwork throughout the organisation, and not just between the design, stress and manufacturing departments. This systems engineering approach, and the tasks involved, are of equal importance as the traditional aspects such as the mechanical design itself. This had led to a holistic approach in aircraft development, which can be encompassed within the term: Multidisciplinary Optimisation (MDO).

1.6 Multidisciplinary Optimisation of a CFRP Wing Cover

The wing box is probably the most structurally difficult part to optimise, due to the various constraints imposed on the design, such as the contradicting aerodynamic and structural performance requirements, having to act as a fuel tank and its affect on structural performance, attachment of many devices, such as the engine, main landing gear (MLG), and high lift systems, as well as due to the physical size in comparison to other components, meaning that weight and cost is very critical. Furthermore, the wing box is composed typically of wing covers, ribs and spars, with the largest and by far the most complicated part to design being the wing covers.

It is known that the ability to perform a good initial design is very critical to the overall performance of the final design, and hence this initial design phase, where information is lacking, needs to be augmented through improved design methodologies. For this reason, optimisation methods are applied during the early design phases to search for the best

configuration. However, traditional optimisation methods used at the preliminary design phase have optimised the external configuration such as wing shape and size, but not internal features like wing covers[40], although the configuration of the internal structure, and the materials used, will have a large consequence on LCC, i.e. the weight and cost.

Therefore, an optimisation methodology is required that can perform a LCC analysis, at the initial design phase, for a CFRP wing cover, which is constituted from a skin and multiple stringers. The optimisation procedure should initially find the lightest weight solution, based on a number of physical, certification and manufacturing constraints, and then the manufacturing cost is calculated for this resultant design. The structural sizing can be based on a number of methods, but the Finite Strip Method (FSM), would seem the most appropriate for stability sizing of prismatic structures such as stringer-stiffened covers, whereas strength can be verified based on simple maximum strain theory, although out-of-plane issues and bearing/bypass should also be considered when applicable. The cost relationship can be defined based on the structural definition, material and process information[41].

However, such an optimisation methodology will be based on accrued knowledge and a number of assumptions. This is necessary to ensure the design is realistic. For this reason, a system view has been taken in writing this thesis, to consider the holistic problem, through a fastidious investigation, of all factors that influence the design of a CFRP wing cover. Although not all this information can be included in an optimisation methodology, it can be used to help understand the decisions being made, as well as to consider the bigger picture of wing cover optimisation. Only be doing this can it be considered MDO of a CFRP Wing Cover.

The structure of this thesis is broken down into the following major sections: Contemporary Engineering Environment; Materials and Processes; Laminate Design; Assembly Techniques; Damage Tolerance and Repair; General Wing Box Design; Optimisation Procedure; Cost; Results; Discussion; Further Work; and Conclusion.

2 Contemporary Engineering Environment

There has been a large change to the way the global aircraft industry performs and perceives their business since the 1960s. This can be basically summarised by two terms: "Systems Engineering" and "Global Supply Chain Management", which cater respectively for both the internal and external nature of the business. The changes in the practices of the industry has occurred due to a number of factors, but mainly due to globalisation, which has increased the efficiency of businesses in the global market economy. The functioning of the industry impinges greatly on the optimisation of the aircraft, and thus will be explained further.

2.1 Introduction to the Global Industry Environment

The following points characterise the market for large commercial aircraft:

- High capital outlay and high asset specificity
- Demanding customers in a technologically changing environment
- Shorter aircraft life cycle, albeit, the cost of development is increasing
- High-risk of each new program, can jeopardise the company's future, due to:
    - Technical risks and the extreme fluctuation in demand for aircraft

For these reason new entrants find it hard to enter the market, as they require heavy capital investment and a steep learning curve, which means that the incumbents typically earn an economic rent. Conversely, the incumbents find it financially difficult to differentiate into other markets[i], which has meant that this industry requires protection by governments. The original goal of supporting the aerospace industry is to promote a high-wage workforce, which promotes overall economic wellbeing throughout the industries it supports. Moreover, due to the high cost and risk of an aircraft development program, it is not ideally suited to being financed through private capital markets. This risk can be mitigated by having a star[ii] in the product-mix, like the Airbus A320 or Boeing 737[42], to ensure that the aircraft manufacturer can withstand a loss-making product on its books for a number of years.

In the 1960s, the Primary Manufacturers themselves would finance the complete program expenses, and as such although outsourcing existed, it was a means of seeking extra capacity, due to the cyclical nature of the industry, where build-to-print contracts were given to the supplier[iii]. Boeing, for example, would even lend the production equipment to the supplier[43]. However, it has been evidenced that when an internal team was working on a build to print contract, if it was to be manufactured by a supplier, there was little attention paid to the issues of efficient manufacture[44].

From the mid-1970s, Boeing created offset packages that transferred production to some countries that would in return, give market access to Boeing[45]. Furthermore, this was beneficial as it reduced the funding required for the project, as the supplier financed the capital equipment required for the manufacture of the parts.

[i] This is different to the Japanese heavy industry players.
[ii] With reference to the Boston Matrix, the A320 is a Star as it has a large percentage of the market and the market is expanding.
[iii] Component was manufactured based on a given specification.

During this time period, Airbus, the new entrant in the market, received government repayable loans, which covered up to 100% of the development cost of a new aircraft. Subsequently, since the mid-1990s, a duopoly of prime contractors for aircraft with a seating capacity over ≈ 120 seats has existed, namely Airbus and Boeing. The traditional Airbus business model could possibly be the ultimate model of risk-sharing, as it not only brings together large international business partners, but also their respective governments[45]. Airbus, also realised that due to the high cost of labour in Western Europe, it would adopt a capital intensive approach to manufacturing[14]. Airbus formed internal clusters with centres of excellence to design certain aircraft parts, such as Airbus UK, for the wing. This provided economies of scale with the consolidation of responsibilities.

In the late 1980s and early 1990s, a worldwide recession created a wave of change in the aerospace community, which brought about rationalisation, through mergers for example, down-sizing, cost reduction drives, inventory reduction, and quality improvement[17,46,47]. This has resulted in Boeing, today having approximately half the suppliers it had a decade ago[48].

In 1992, a European Union – United States (EU-US) Large Aircraft agreement was signed that limited launch aid to 33%. In 2004, the 1992 EU-US Large Aircraft agreement was abandoned by the US – which set the precedent of 0% launch aid. This was a strategy employed by Boeing who instead relied on their new foreign risk-sharing partners to receive state-aid from their own governments. The consequence on Airbus was that they could not, under the agreement, legally receive aid from the EU. Thus, for the A350 XWB, which requires $13.5 billion for Research and Development (R&D), as well as the $2 billion for capital expenditure[49], Airbus is taking a three-tiered approach to financing the program:

- Generating cash flow from savings made by the Power8 program
- Courting the European governments for financial support
- Sourcing risk-sharing partners

Furthermore, within the Power8 program, Airbus intends to centralise the purchasing organisation, using first-tier suppliers to control the lower tiers, and to source from lower-cost areas like Asia, with Airbus stipulating that first-tier suppliers should outsource to Asia[43]. In order to qualify themselves as potential risk-sharing partners, they must finance the development costs, and the RC currency shall be in dollars[43]. Thus, they must have financial and technical prowess, with a competent workforce.

This has resulted in both Airbus and Boeing being termed ‘System Integrators’. It was only at the turn of this century that it would have been deemed incredible that Boeing would allow Japanese companies, to develop, design and manufacture the whole wing of a new Boeing aircraft, i.e. the 787. Boeing has outsourced almost 90% of the parts for the 787, with Boeing only manufacturing part of the VTP[43]. Previously, both Boeing and Airbus outsourced, at most, 50%[50]. Likewise, Airbus had always kept the development of new products in-house, and only sub-contracted out the manufacturer of production parts for the older models[43]; this has also changed with the development of the A350 XWB.

2.2 Introduction to Systems Engineering

Systems engineering can be considered a holistic approach that should ascertain the most optimum product, in terms of customer requirements, cost and quality[7]. The capabilities within the System Engineering approach are[7]:

- Life cycle analysis and modelling
- Requirements and functional analysis
- Multidisciplinary design synthesis
- Risk and uncertainty modelling
- Concurrent planning and control
- Verification and validation

Figure 2-1[2] shows the life cycle for a commercial aircraft wing, which is divided into four phases. Throughout the life cycle, the product can become obsolete due to various occurrences of physical, legal, economic, social, functional, and technological change[2]. The 'birth' phase involves the initial planning, the various design phases, and the manufacturing, which is assumed to take about 12 years. The 'life' phase represents the operation of the aircraft, the duration of which is dependent on the aircraft utilisation, but can be up to 25 years. The 'death' phase represents the dismantling and recycling/disposal of the aircraft, which may take up to 1 year. Finally the 'rebirth' phase represents the selling of the recycled materials.

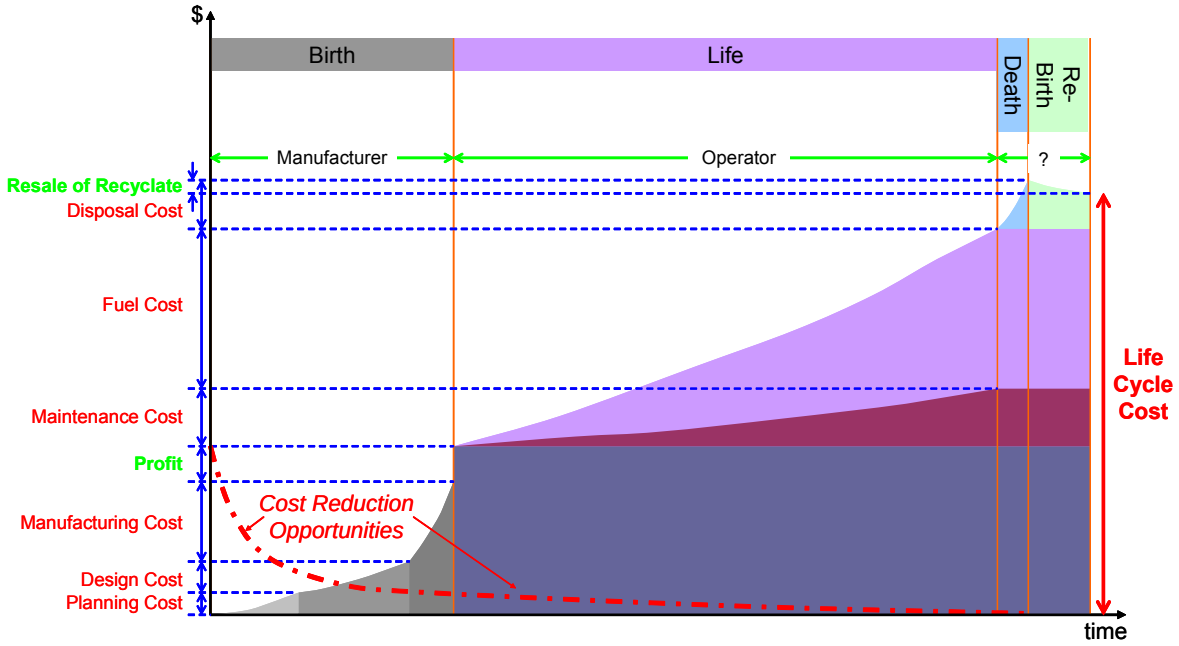

Figure 2-1: Typical life cycle cost for a wing

During the 'birth' phase, the design itself will increase in fidelity, capital equipment and tooling will be invested in, extensive testing will be conducted, certification will be carried out, and then production will commence. Thus, a large amount of resource is invested in the product before any physical sale of an aircraft occurs. This is exacerbated by the extremely high investment cost, which is compounded by the long duration of each phase of the aircraft's life cycle.

Normally, once the program is committed to the detail design phase, there is no stopping. However, the program can be cancelled before the heavy investment in capital equipment and

tooling begins. It is necessary to define the production rate, as this will determine the quantity of equipment and tooling required. Once in production, the rate can be increased, if deemed necessary, by investing in more equipment and tooling; conversely, to reduce production, this would require the scrapping of tools and the underutilisation of capital equipment, which would incur a significant financial penalty.

It is prudent to ensure that the firm can survive the investment in a new program, thus the program must be both financially and technically strong. Uncertainty will be encountered during the different phases of the aircraft program. Technical uncertainties will affect the aircraft's ability to meet the performance requirements; whereas, financial uncertainties relate to the value of an aircraft, whether in terms of demand, manufacturing expense, or future revenue[51]. Should the original performance requirements not be met, there are three scenarios that can happen once the program reaches maturity[51]:

1. The aircraft is sold at the higher weight to be used at less than its maximum (intended) range, or with added fuel volume, if possible, to achieve its intended range. The aircraft will be more expensive to operate, thus the aircraft is sold at a lower price.
2. The aircraft is redesigned to eliminate weight in order to meet the original specification, resulting in higher non-recurring development costs.
3. The aircraft is unable to meet its performance guarantees, either due to outside sources or failed redesign. Additional Non-Recurring Costs (NRCs) may be incurred from attempts to fix the problem, and Recurring Costs (RCs) will be higher despite a lower selling price due to missed performance goals.

As shown in Figure 2-1, between 70-85% of the aircraft's LCC is influenced by design, in terms of the cost to develop, produce, operate and retire the product[52,53]. Contributable to this effect is the allocation of NRC early in the production program[33]. The greatest opportunity to influence the LCC is at the conceptual and preliminary design phases, as at this stage innovative design solutions, advanced materials and manufacturing technological progression can be implemented[54]. Conversely, the decisions taken early on can limit the design freedom and constrain the number of materials and manufacturing processes that can be used. This is why it is important that the influence that the materials and the manufacturing methods have on the overall cost are considered early in the design cycle.

2.2.1 Multidisciplinary Design Process

The traditional design process, as shown in Figure 2-2, starts in earnest with the conceptual phase, which explores various concepts that can fulfil the requirements, in terms of performance. At this stage it is very fluid, with the basic layout changing many times, as learning is accrued. A rating matrix will be developed, based on weight, cost and risk, in order to down select a concept, in which to develop further in the preliminary design phase.

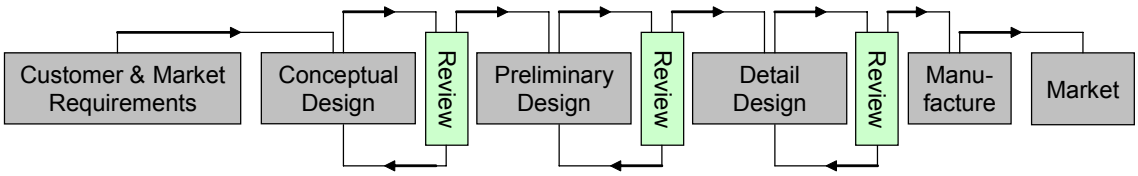

Figure 2-2: Stochastic design phases

During the preliminary design phase, specialists will design parts of the overall system in isolation, such as the wing covers; while system architects and integrators will control

interfaces and overall assembly design. However, as the individual teams only primarily know their own discipline requirements, they will not appreciate that some of the decisions they take might have a negative impact on the other disciplines and their requirements. Therefore, multiple design iterations have to be repeated until all the requirements are achieved, which means that the whole process is not efficient as it has a longer cycle time. This is followed by the detail design phase, which will mature the design in readiness for manufacture, which will effectively determine the weight and cost of the product. In each subsequent design phase, the ability to model and analyse the product increases, as shown in Figure 2-3[55].

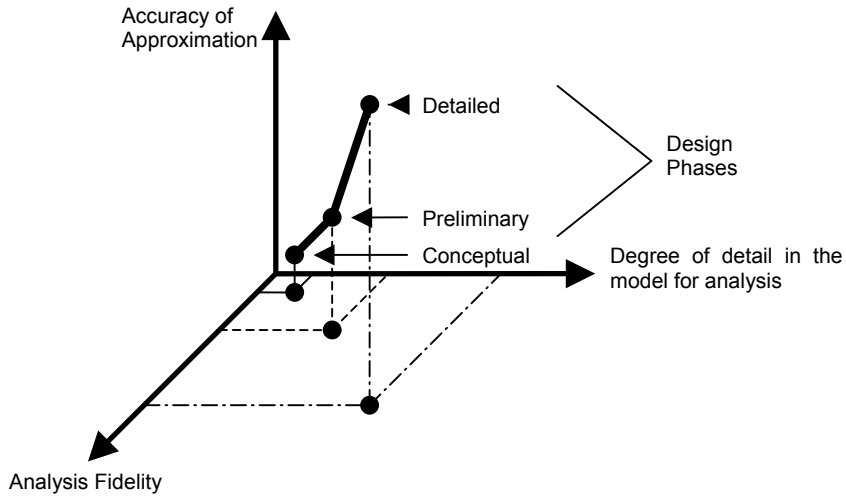

Figure 2-3: The design paradigm

As each design phase has a limited duration, the constrained initial analysis can lead to a mid design-cycle heavy modification in order to make it competitive. Therefore, to improve the efficiency of the overall design time it is necessary for the early phases to go far greater in depth, hence requiring greater resources. However, such a proposal may be warranted from an engineering perspective, but financially, by spending a higher proportion of the available money earlier on in the program is not prudent. This is because later cash flows incur heavier discounting, thus spending more of the available money towards the end of the program will impact less on the overall profitability.

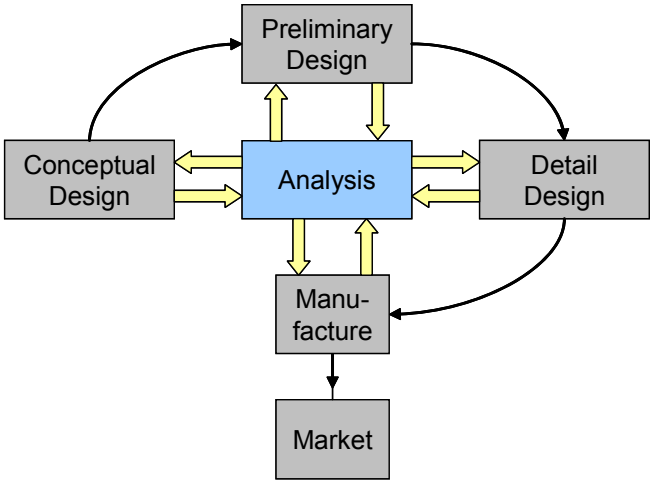

Figure 2-4: Analysis driven design procedure

Alternatively, an analysis driven concurrent design process, as shown in Figure 2-4[56], can be used, which incorporates more knowledge of the configuration, to get it "right the first time",

as opposed to "re-do until right", which is typical of the stochastic engineering process[57]. To better achieve this aim, Integrated Product and Process Design (IPPD) teams have been created so that more informed decisions can be made[58]. Therefore, an analysis driven concurrent engineering process, using IPPDs, improves coordination which leads to a better product, created in a faster time[59].

The increasing influence of taking a systems engineering approach has meant that the key activities conducted by the engineering team has changed, as shown in Figure 2-5[60]. There is greater onus in terms of integration and requirements, whereas the core design itself has a smaller overall emphasis; however, this is counteracted by improved analysis tools.

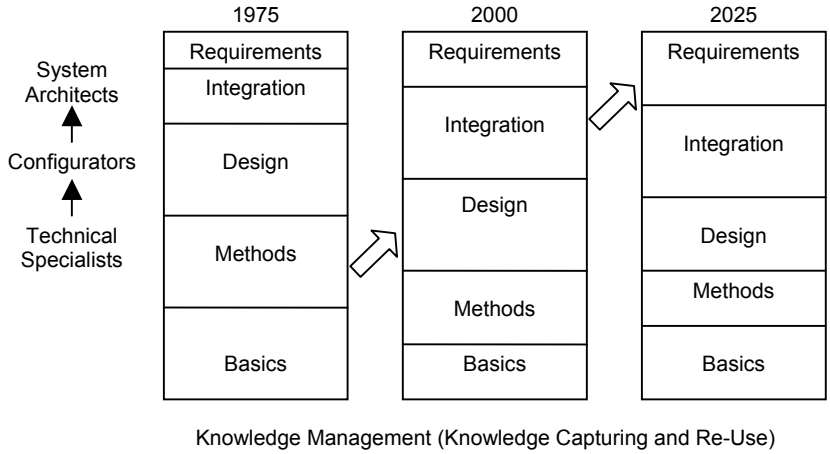

Figure 2-5: Changing emphasis on engineering work

2.2.1.1 Team

The design of a product, such as a wing cover, is both a scientific and social/organisational process[40]. To have a successful product, both of these processes must work in harmony together. It is known that poor coordination and communication, within large organisations, of engineering data hinders the product design, rather than the complexity of the actual engineering problem[61]. For concurrent engineering and MDO to succeed, the traditional organisational breakdown must be amended to reflect the required process flow[54]. This has led to the IPPD team, or more commonly termed Integrated Project Team (IPT)[60], which is an interdisciplinary team, comprising of members from different disciplines, ranging from engineering to finance. It is essential that all departments that influence the product be integrated into one team, as there are important interactions between them. An example of which is between engineering (product) and finance (program)[62]: The performance from a technical perspective will be based on range, capacity and the operating costs of the aircraft. These attributes will affect the demand for the aircraft, which will determine the price, and consequently, the number of aircraft sold. Those same technical attributes also determine the cost of producing the aircraft in terms of NRC (development) and RC (manufacturing). Therefore, cost and revenue, which both fall under financial control, are linked by performance, which is governed by engineering.

Within an IPT, the role of the system architect and integrator will continue in their importance, as shown in Figure 2-6[60], as architects communicate and provide guidance for the design and optimisation process, whereas the integrator interacts between the teams.

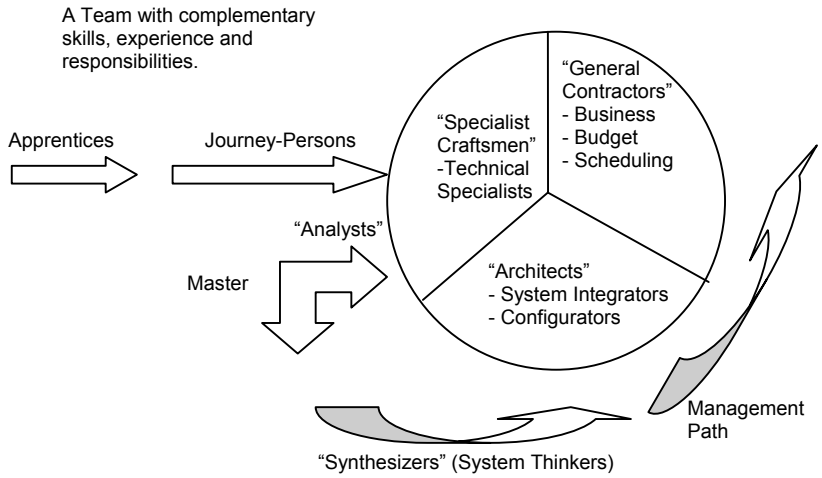

Figure 2-6: Team composition

2.2.2 Value

Today, the customer is more powerful and the market place is more dynamic, which requires the aircraft manufacturers to adapt to a market where they cannot dictate what the market requires, and in what timeframe the aircraft will be delivered. The consequence of this new environment can be summarised as 'value' as shown in Equation 2-1, where the functions with subscripts p, c, and t are performance, cost and time respectively[63].

$$Value = \frac{f_p}{f_c \times f_t} \qquad \textbf{2-1}$$

Value is a measure of worth to a customer, and is a function of the following characteristics[64]:

- The product's usefulness in satisfying customer needs (performance related)
- The relative importance of the need being satisfied (performance related)
- The availability of the product relative to when needed (lead time)
- The cost of ownership to the customer (cost)

As commercial aircraft are high-value products, it is prudent to link the objective function of the costing to the customer requirements. For example, if the customer's requires reduced fuel consumption, then a lighter weight solution needs to be sought. Cost at the conceptual stage can be linked loosely to the requirements, which allows a high-level function objective to control the cost and performance. This can be done with parametric optimisation, which identifies key parameters that drive either cost or performance.

2.3 Introduction to Global Supply Chain Management

2.3.1 Market or Vertical Integration

'Vertical integration is the organisation form not of first but of last resort – to be adopted when all else fails. Try markets, try long-term contracts and other hybrid models, and revert to hierarchy only for compelling reasons'[65]. However, if the invention and the subsequent manufacture of every input can be regulated by the price mechanism in an open market – why

is it that there are many "companies", where several functions are performed under one management structure[13]? This is due to the transaction cost of using the price mechanism[66]. Thus, the transaction cost determines whether to use a market or vertical integrated approach[67]. This will consider factors such as switching costs, the importance of the purchase, the product complexity[68], and production and bargaining costs[69,70], where bargaining costs include:

- Costs arising from contract negotiation
- The costs of making changes after the contract has been agreed upon
- The cost of monitoring performance
- The cost of disputes which arise if neither party want to use the in-built mechanisms

The last three bargaining points will occur after the contract has been signed, with costs occurring when both parties are acting for themselves, but in good faith[65]. Opportunism on the other hand, which typically occurs after the contract has been signed, is when one party acts with self interest and in bad faith, by trying to change the agreed terms of the contract[70]. The inability to distinguish between bargaining and opportunism can also raise the costs of using the market[71]. Equally, there can be bargaining within a vertically integrated structure, such as demands for higher wages.

In a competitive market environment, a profit-maximising firm will have to produce at the lowest marginal cost, which vanquishes inefficient practices. It is most unlikely that internal operations are under such pressure, although this can be simulated through comparisons with internal factories. Furthermore, when a vertically integrated company exceeds a certain size, in terms of departments and the number of employees, due to it performing a number of functions in-house, there are costs associated to organise all the required information pertaining to transactions within the company[19]. By using the market approach, this can reduce the financial risk of performing a number of functions in-house by concentrating on core-competencies, and outsourcing major components to suppliers[72].

A third way is to create an alliance when the market fails and hierarchical governance is not wanted, this is also known as relational governance. In order for this to work in a non-discriminatory manner, non-juridical means are required such as: mutual dependence, trust, parallel expectations, joint action and procedural fairness[73]. Only through repeated exchanges can the cooperative nature of the relationship be established, to understand if the supplier and buyer can trust one another[74]. Relational governance should be ideal for products of high asset specificity, as this mitigates against the safeguarding issues. With the buyer and supplier creating closer vertical ties, they are trying to benefit from vertical integration without the incumbent bureaucratic costs[75].

It has been argued that asset specificity is the key to decide whether the market or a hierarchical approach should be used[76]; however, this has been challenged by the findings of Geyskens[77]. Furthermore, the uncertainty and frequency of transactions also influences the decision[76]. Asset specificity is idiosyncratic in nature and can be defined into various sub-categories, based on human based capital, goodwill through brand awareness, or some physical asset, be it a site or a piece of machinery. With asset specificity and longevity, enforceable contracts can potentially be prone to higher governance costs due to them not being adaptable to the dynamic situation and conflict resolution[78]. Assets that are bespoke to a specific transaction, which can only be conducted between particular parties, are called 'transaction-specific assets'. With such a transaction, opportunistic behaviour can occur and a way to safeguard against this is to bring those parts back in-house, as within a vertically

integrated company greater control is assumed[77]. Transaction-specified assets and uncertainty requires hierarchical governance, otherwise the supplier could exploit the position of the buyer[77].

Uncertainty occurs either when it is not possible to specify beforehand in a contract every contingency for an exchange due to environmental uncertainty, or when the performance, after the exchange has been made, cannot be guaranteed due to behavioural uncertainty. Again, environmental uncertainty can be resolved by making the product in-house, as under a hierarchical jurisdiction it is far easier to adapt the part or conditions, without dramatic change in transaction costs[77]. Environmental uncertainty can be subdivided into two categories, namely, volume uncertainty and technological uncertainty[79].

Volume uncertainty is the inability to predict the amount required over a given time. When there is acute volume uncertainty this impacts both on the supplier and buyer, in terms of too much or too little stock and the inability to amortise recurring costs over a significant production run. Technological uncertainty is where the parties are incapable of establishing the technological requirements needed. This can be, for example, due to changes in standards or step changes in required technology. This is best handled through market governance, as new suppliers can be quickly switched, which avoids being locked into technology that could become superseded[77].

2.3.1.1 Aircraft Market Specific

Neoclassical economic theory states the benefits of exchanging money for goods through normal markets, but purchases of aerospace goods provide multi-dimensional benefits, such as jobs and technology, which might be acquiescent to a single efficiency criterion[80]. Traditionally, aircraft manufacturers have had a high degree of vertical integration, as the parts and systems produced required particular raw materials and specialised capital equipment. This was then feasible, and arguably optimum, as they could produce these parts internally more efficiently in terms of quantity, quality, timeliness and cost, while minimising transaction costs[47]. They would also employ many scientists and engineers who had a wide range of skills encompassing all necessary technologies. This allowed the company to take a long term view and to remain aware of future technologies[81]. However, large vertically integrated firms can be affected by diseconomies of scope, as they must manage several different activities[70].

The trend currently is for the prime contractor to consider their business as selling, marketing, overall system design, and supply chain management. Hence, they are known as ‘System Integrators’, who should provide the following benefits[43]:

- Risk reduction
- Market penetration
- Containment of launch costs
- Court foreign government funding through strategic risk-sharing partners

There are four basic modes of operandi for a System Integrator:

1. Centralised – all product development resources are owned by the System Integrator and can include different project teams working in multiple countries

2. Local Outsourcing – such as using on-site contractors to support product development. This way access can be gained to specialised skills or to meet temporary demand for employees
3. Captive Offshoring – suitable for carrying out product development in a country where it has not previously been. This will require setting up a business, which will require personnel as well as an understanding of local laws and tax regulations. Typically for an engineering centre, around 200 people are required to be justifiable, from an economic perspective. Even if it is economically justifiable, it may take many years to integrate this satellite unit into the company's culture and processes[82]
4. Global Outsourcing – Typically starts with a supplier undertaking basic engineering activities to initiate knowledge transfer and to construct a working relationship, which can then proceed to the supplier taking on a larger role

System integration reduces the unit cost for the System Integrator and spreads financial risk across the supply chain, albeit the total program cost will increase[83]. The management of such projects can be difficult, due to work-share issues, interface agreements etc. The systems supplier should be a "jack of all trades" and preferably, the best in class for one or more of the subsystems[84]. The System Integrator should be knowledgeable in the innovation process[81], whereas the suppliers will be experts in their fields.

The System Integrator must consider the interests of the suppliers involved in the value chain so as to minimise the global costs of the system[85]. Likewise, the suppliers who wish to work with the System Integrator, need to acquiesce to the System Integrator and ensure there is adequate capacity, relevant planned R&D, etc. Due to their reliance on the suppliers, the System Integrator expects higher levels of attention from their suppliers[86]. The suppliers must also maximise their own position and therefore have to grow to seek cost reductions through economies of scale[85]. In order to minimise the cost to the System Integrator, the risk-sharing partners will not be allowed to pass back to the System Integrator the non-recurring development cost, and hence will instead attempt to recoup the cost over several programs, including rivals' aircraft[43].

An essential part of using the market is supply chain management, the very essence of which is to reduce cost, condense development time, manage risk, while trying to maximise value added[18]. Within the supply chain, the transactions between the companies should add value up through the chain, and incur costs – hence payment, down the chain[18]. There are a number of suppliers who fulfil different roles and levels of responsibility in the supply chain, depending on their hierarchically tier level, as shown in Figure 2-7[16].

The first tier constitutes the prime contractors, such as Airbus or Boeing. The second tier includes both the engine manufacturers such as Rolls Royce, and the makers of landing gear, hydraulic systems, nacelles and sections of fuselage. Today's second tier suppliers must be sufficiently large to be able to be partake in a more active role with the development of new products[47]. The third tier will produce products such as electrical subassemblies and fuselage parts; however, even at this level it is still very concentrated with a small number of large companies. The next tier down consists of a multitude of companies who may have divisions that specialise in aerospace products, but will also offer services to other industries[16]. These suppliers might provide parts with "low intellectual property", however, such items typically make up a large part of the product, hence should delays or difficulties occur, then the effect of lower tier suppliers can be considerable[87]. However, lower-tier suppliers have recently taken on greater responsibility, including design, certification work and even supply chain management due to Primary Manufacturers producing only 30% of their parts in house

whereas the other 70% is outsourced[88]. Furthermore, their significance increases as they help determine overall product quality, manufacturing cost and product or process innovations[89].

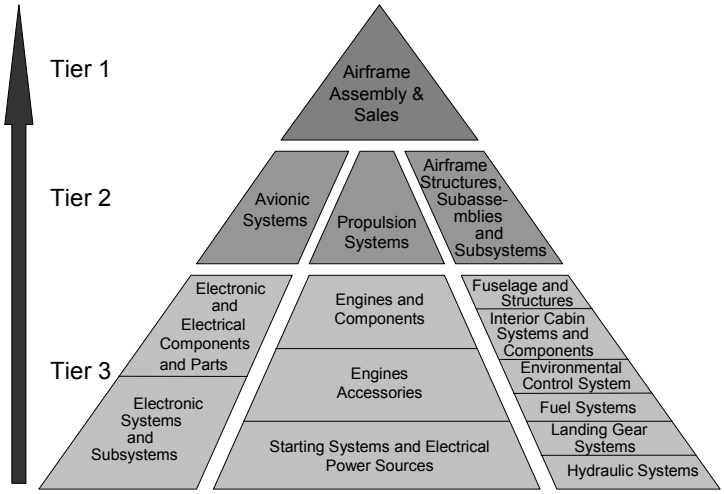

Figure 2-7: The producers' pyramid

The prominence of strategic outsourcing in the last 15 years has coincided with the rise of globalisation. This has been achieved using two approaches: either setting up their own base in a low-cost country; or working with local suppliers, which is termed "global outsourcing". By employing global outsourcing, not only is there the typical loss of organisational proximity, but they are geographically separate. Thus, with global outsourcing, the emphasis is on cost and quality control with limited knowledge transfer[90].

Traditionally, during the product life cycle, as the process technology becomes more mainstream, a larger, global, group of suppliers can produce such a component, which pushes the product into becoming a commodity, meaning that the suppliers compete on price[16]. This makes suppliers in countries where labour costs are lower, and where the market may not be fully penetrated, attractive for mature products[91]. Furthermore, based on the premise that the cost of capital equipment is the same around the world, and full equipment utilisation can be achieved, then by outsourcing in countries where labour costs are lower, this should provide competitive advantage[92]. However, this scenario has changed, due to the greater financial power of formerly low cost areas, such as Asia, plus the increase in development cost of an aircraft, which means risk-sharing partners are sought. Developing countries like China, will see the advancement of many legacy industrialised nations, and recognise that they must diversify away from a reliance on heavy industries such as producing steel, or the production of commodity products, and progress up the value chain.

Furthermore, the traditional aircraft suppliers are a niche group of companies that wish to bid for fixed-price long-term contracts, thus these suppliers are reluctant to bid for risk-sharing work, as their existing cash flow does not allow them to do so[43]. As witnessed on the 787 program, many suppliers who can offer composite expertise are at capacity to fulfil the demands of this program, where as the laggard, in this case Airbus, with the A350 XWB, must develop new suppliers to become risk-sharing partners. These suppliers require huge financial and technical support, and hence need major government funding[43], which is typically available from Asian governments. The Chinese are successful at gaining technology transfers because of their perceived market size, thus entry into their market is the key card that the Chinese play[45]. For this reason, Airbus has set-up an A320 final assembly line in Tianjin, China. The idea behind this is to transfer low-end engineering work, i.e. there have been over 3300 A320 family aircraft assembled[93], and that by producing them inside

China this avoids the 23% import duty on its products, as well as a subsidised production line[43].

2.3.2 Make-Buy Decision

In order to increase overall efficiency, the firm must decide which tasks should be performed internally and which are best performed by suppliers, this is known as the make-buy decision which can heavily influence the ability of the firm to make a profit[94], as through outsourcing, improvements in the financial metrics of the firm can be achieved. For instance, by decreasing the amount of assets within the company can allow an increase in the Return on Assets (ROA) as well as Return on Investment (ROI). Furthermore, by decreasing the amount of employees it is possible to improve on the revenue per employee[95].

Traditionally, the decision whether to make or buy was primarily based on cost. Despite greater emphasis being placed on quality and delivery, evidence exists to suggest it is still cost that is the key determinant of contracts being awarded[96,97]. The issues involved with the make-buy decision can be broken down into three discrete categories[98]:

1. Technology matrix
2. Cost model
3. Analysis of the company's strategic issues

It is prudent for procurement to have early proactive involvement in the make-buy decision, as cost is so crucial in the design development phase. If 80% of total avoidable cost is controllable at the design stage[99], and 80% of total costs for design and contract companies are for bought-out components[18], then the involvement of procurement at the early development stage is of extreme importance if cost reduction is sought. Therefore, procurement can use the supply chain to create cost saving opportunities, while also providing direct feedback to the design process in terms of technology change, fabrication best practice and cost expectancy, to provide knowledge to make the correct make or buy decision. With reference to Figure 2-8[13], there are four categories for potential make-buy situations[13]:

1. The component or process involves a technology that is quickly evolving, and the company is substantially behind the leading firms with respect to its technological competitiveness (top left quadrant)
2. The component or process involves a technology that is quickly evolving, and the company is among the leading firms with respect to its technological competitiveness (top right quadrant)
3. The technology behind the component or process is relatively mature, and the company is substantially behind the leading firms with respect to its technological competitiveness (bottom left quadrant)
4. The technology behind the component or process is relatively mature, and the company is among the leading firms with respect to its technological competitiveness (bottom right quadrant)

Each quadrant is then split according to whether or not the company regards the particular design or manufacturing activity as critical to one of its core competencies.

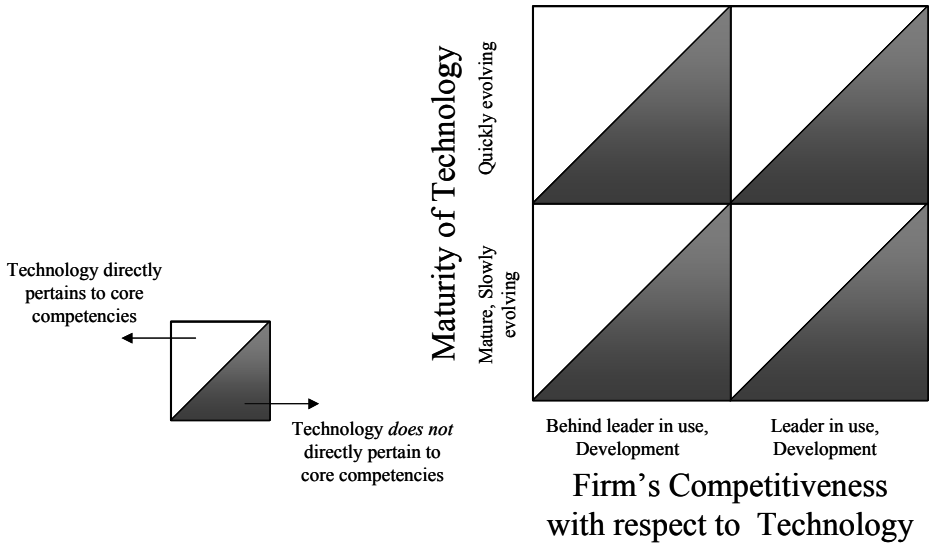

Figure 2-8: Field of potential Make-Buy scenarios

The technological readiness is of importance as there is a higher level of confidence when sourcing something that is a known quantity[13], thus they feel happy to allow such work to be conducted outside of the firm's boundaries. The firm's competitiveness with respect to a particular technology is also of importance[13], although this can be questioned, as with the increased dependency on suppliers, who have greater knowledge of new technology, there may be greater risk by bringing it in-house. The actual technology capability of the supplier should also be understood; if they lack readiness, then it can affect cost, quality and delivery timescale.

The make-buy decision can be based on environmental factors too. For example Boeing outsources titanium parts to a Russian supplier VSMPO-AVISMA in Verkhnaya Salda, where the forgings are made, then rough machined[100]. This means the majority of swarf created for that part, is at the source where it can be most efficiently recycled.

2.3.2.1 Core Competencies

The basic aim to concentrate on core-competencies is to provide both managerial and financial flexibility to take capital away from manufacturing non-core products, and instead to concentrate on innovation, marketing etc[90]. A "Core competency is a skill/asset/technology that underpins the growth of the business and differentiates from its current and future competitors"[iv]. A core competence can be a product, a manufacturing process, a business process etc, and is unlikely to be something that is highly codified, as this should be easily imitable, which is typically the case for all mature technologies. A core competency can be created through tacit relationships, which if taken outside of the organisational boundaries could lose some, if not all, of its value[101], thus it should not be outsourced. A core-competence should have at least one of the following traits[102]:

- Have a large influence on the product attributes that the customer perceives as being the most important

[iv] Definition defined by the UK LAI[640].

- Focused design and manufacturing is required which needs specialised assets, that, at most, only a very few suppliers can do
- Requires technology which should provide a clear technological lead

The core-competencies that should be retained are those that occur frequently and have high asset specificity. For this type of product, Williamson[13] says that "economies of scale can be as fully realised by the buyer as by the outside supplier", however, if the transaction is highly specific but infrequent, then as recommended by Williamson, the item should be outsourced. This is because "the production costs for an internal hierarchy are higher than for a market because the company must acquire capital and maintain a trained staff, even though these resources are only used periodically"[13].

A firm should identify which core-competencies they want to acquire and maintain, and based on this, the outsourcing principles can be devised. Alternatively, they can consider where the maximum learning and information can be extracted through the development and/or manufacture of the part. An example of this philosophy can be found with the Japanese automotive companies who outsource parts like seats and braking assemblies, whereas they produce internally the infrastructural elements such as robots and database software[13]. The logic to this is through developing the manufacturing equipment, the limitations of the design and process are recognised, thus allowing the parts to be manufactured efficiently with the production equipment. Furthermore, if they do develop their own machines, when it comes to buying them in, they have a far better understanding. The closer the firm gets to outsourcing parts nearer to the core competencies, the higher the strategic risk[59].

As it is difficult to foresee when, where and how the next innovation will occur, it is plausible that a supplier may be the first to develop a new idea. The fundamental idea of making or buying is to allow a firm to use the innovativeness of its suppliers to influence its own core competencies, thus giving flexibility to move nimbly in the marketplace. Using the correct supplier relationship, it is possible to learn the new technology from the supplier to benefit its own core competencies, but not switch to production in-house until it has the foundations in place[13]. Therefore, the issue of core competency and supplier relationship can be linked in this respect.

By using supply chain management to work with suppliers, who are specialists themselves in their core-competencies, this should create the best product in terms of price, quality, and innovation[90]. The strategic benefits of using best-in-class suppliers are[18]:

- Enhanced flexibility in the purchase of rapidly developing new technologies
- A reduction is design cycle times
- Higher quality

2.3.2.2 The Pitfalls of Outsourcing

There are a number of strategic risks with outsourcing, which is influenced by both internal and external factors. As shown in Figure 2-9[19], the worst situation for outsourcing a part is when the principal manufacturer is forced to use a supplier for a part as they do not have enough knowledge, and the part itself is integral to the complete product, which is complicated to incorporate. Conversely, a part that requires limited integration into the overall product, and is outsourced due to reasons of capacity, is the most opportune to outsource. In

general, it is important that the 'System Integrator' should only be dependent on component knowledge, not system knowledge.

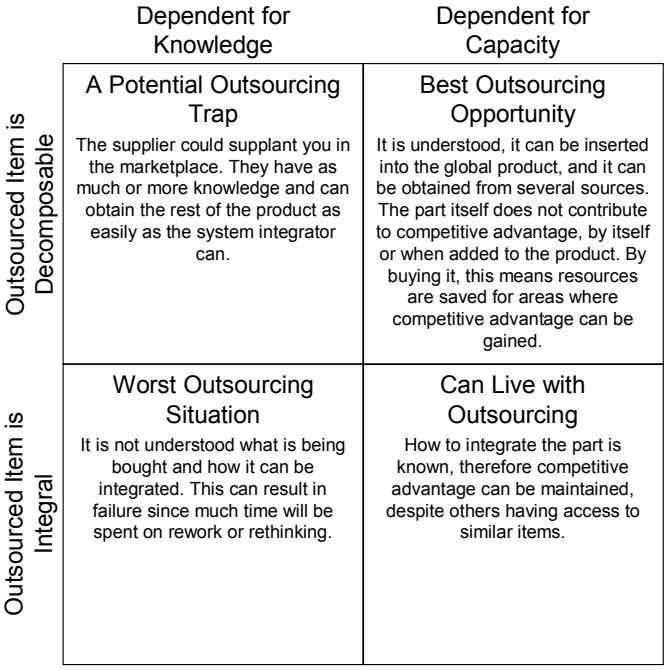

Figure 2-9: The matrix of dependency and outsourcing

When assessing the supplier, research should be conducted into the strategic intent of the supplier, i.e. the ultimate result that the supplier obtains from the relationship. Results could be economies of scale, utilising excess capacity, the acquisition of technology or market data. The riskiest proposition would be when the supplier wants to tap into technological or market knowledge on products that are close to the firm's core competencies. In such a situation, the supplier may well offer incentives such as the lowest price bid to tap into that knowledge[59]. This implies that the most dangerous suppliers may seem initially the most favourable.

The ability to outsource large parts of the total product can be helped if it is designed in a modular fashion. If it is modular then there is fairly simple one-to-one communication between the functional and structural elements of a product; however, if the interfaces are not straightforward the interdependence between the product functions and the product structure is complex[90]. This is why parts, such as the flap bodies themselves, are perfect for outsourcing, as after the preliminary design phase, the interface to the wing and attachment structure is fairly well defined, hence modular. The supplier can control the interaction, of the parts that constitute a flap body. However, a wing cover for example, which typically is a far larger part, has many interfaces, thus outsourcing the design of such a part, would require for more liaison with the customer, which could increase the chances of critical system knowledge leak to the supplier, as well as significant delays due to definition of interfaces.

In a technological dynamic industry, innovations could occur anywhere in the supplier market place[103]. Thus, if a new competence is required outside of the competencies of the existing suppliers, then a cost will need to be incurred to qualify and integrate the new supplier[104]. Furthermore, adverse selection can occur when a supplier is not truthful about their abilities or standards, and the Principal Manufacturer cannot verify them either during the bidding process or after they have won it[105].

The issue of outsourcing, when based on core competency can be problematic, as evidenced by the following anecdote: "First, we started with outsourcing the large series, but we kept the small series and special products in house. However, after a while someone inevitably noticed that making only small series and special products is very expensive[v], so they were outsourced as well. After that, it is only a matter of time before it becomes clear that the people who make the products are much better positioned for developing the product. Thus, product development is outsourced as well. In the end, the only activities that remain in-house are research on one hand and branding on the other hand[90]." Thus the company becomes a "head-and-tail" firm, which might not be best placed to carry out R&D, as no longer are any of the key activities carried out in-house.

However, if 'research' is concerned with future products and 'development' is concerned with existing products, then it is quite possible that if manufacturing is outsourced then development may also be best outsourced[90]. This is because learning cannot only be conducted through an R&D environment; it must also be extracted from series manufacturing. Moreover, as there is limited investment in plant machinery, the firm has little knowledge of advances in manufacturing techniques, therefore new designs will not take this into account[59]. Design engineers, typically, have limited understanding of manufacturing processes, thus having the ability to be able to visit the shop floor and talk to manufacturing engineers is beneficial.

Another issue, when outsourcing manufacturing, is that it is very hard to protect the design data from the manufacturer. This is due to engineers coordinating the activities, which can involve both unrestricted and some restricted information being tranferred[59]. Therefore, as observed by Eindhoven University of Technology and KM consultancy Squarewise, the protection of corporate knowledge should be the shared responsibility of the chief technology officer, a legal officer, human-resources director and/or an innovation manager[106]. However as it is shared responsibility, often the role is secondary in nature, and they have no proper education in the value of corporate knowledge; thus when in a critical meeting with the Chief Financial Officer, with their easy metrics such as ROA or ROI, it is sometimes hard to justify the benefit of not outsourcing.

Outsourcing key components, where the supplier has overall responsibility for both the design and manufacture, can simply overwhelm suppliers. For example, the Boeing 787 program set a precedent for the amount of work that was outsourced. The suppliers faced both cash flow and logistical problems due to the inherent design and manufacturing changes, which were not foreseen during the contractual agreement phase. As the suppliers themselves are, to a certain extent, responsible for paying for design changes and for lateness, despite the fact that the supplier may not be responsible for creating the design change, this may in the future mean that suppliers refuse to enter into such a contract[107]. Furthermore, certain elements of the Boeing 787 supply chain have been vertically integrated back into the Boeing company, such as the fuselage from supplier Global Aeronatica[108], in order to have better control and to minimise the cost of coordinating a large supply chain.

With respect to global outsourcing, the pitfalls can carry greater risk to the Primary Manufacturer. The issues with low cost Asian countries such as China, has already been witnessed with Japan. Western firms outsourced to Japanese firms as a way of reducing costs. The Western firms viewed this as the Japanese firms being dependent on the business from

[v] This is due to allocation of total overhead charges being divided by the remaining products, which will increase their overall cost.

the Western firms, however the Japanese firms saw this as a way to increase manufacturing economies of scale as well to understand the technology and the market of the Western firms[59]. This would then allow them to enter the market and progress higher up the value chain[vi].

This has been evidenced, in terms of the diffusion of technology, between Boeing and the three Japanese "Heavies". For the 777 and 787, the "Heavies" have increasingly played a bigger role in the actual development of the aircraft, as shown in Table 2-1[43]. Based on the experienced gained, through working with Boeing, it is likely that Mitsubishi Heavy Industries Ltd will start to develop a 72-92 seat passenger jet in 2008, with about $1 billion of launch aid from the Japanese government[43]. It is further evidenced that since mid-2006, the "Heavies" have been returning work packages to Airbus, Bombardier, and Embrear, such as Kawasaki Heavy Industries not renewing its contract for the A321 aft fuselage section. The reason for this could be that the 'Heavies' want to have enough capacity, and to ensure that there are no contractual conflicts, when Japan start their own commercial aircraft industry[43].

Airframe	**727**	**777**	**787**
Wing assembly	US	US	Japan
Centre wing	US	Japan	Japan
Front fuselage	US	Japan	Japan/US
Aft fuselage	US	Japan	Italy
Empennage	US	Foreign	Italy/US
Nose assembly	US	US	US

Table 2-1: Boeing's 727/777/787 foreign content

It is known that China's government wants to create an indigenous aerospace industry, thus by outsourcing today to China, this will instigate the creation of an aerospace hub in China, which could result in creating a very strong competitor in the future[95]. However, China's ability to compete with Airbus and Boeing can be contested, as they have only thrived in cost-conscious emerging markets or in cost-sensitive areas of developed markets defined by clear specifications and minimal innovation[109].

A further issue with outsourcing in Asia is that the Original Equipment Manufacturers have progressively become more reliant on traditional Western-based suppliers, in particular since the late 1980s. In this traditional supply chain, knowledge, skills and expertise are passed upstream and downstream, which creates a powerful learning channel. If a new supply chain is sought in Asia, this long-term relationship, which has been honed, will disappear. Furthermore, the System Integrator approach with Asian suppliers will lose ownership of intellectual property to a more global industry that is pursuing an open architecture type perspective[43]. This is because many Asian countries are very much people-driven, where knowledge and intellectual property are considered a public good[106]; whereas in Western society, it is considered private property.

Other general issues with global outsourcing are that by having geographically dispersed suppliers this will increase delivery time, and that parts are shipped in batches as opposed to one-piece flow, which is more desirable due to lean production. Mike Bair (Head of the 787 Program) let it be known after the breakdown in the initial supply-chain of the 787, which led to at least a 6 month slip in schedule, that he saw the business model of the 787 being dispersed across the world and connected only with three 'Dreamlifter' 747s, as wrong, and

[vi] Early value-adding steps in the overall supply chain are typically the most contestable, hence least profitability, whereas later value-adding steps are more specialized, hence less contestability, and higher potential profit.

instead structured like a Toyota plant with all suppliers located within walking distance of the final assembly line[110].

2.3.3 Specifications & Requirements

Traditionally, aircraft were developed based on the manufacturers' perception of the market need. However, today, it is necessary to fully understand the requirements of the customer, which will define the aircraft's performance, cost and time to market. Therefore, a specification defined by requirements is critical to the success of the product[19]. A specification can be considered to be an envelope, which bounds the design extent and will transform the idea of the customer into requirements that can be used by the supplier to carry out design work[111]. Specifications should encompass the following aspects[111]:

- Ensure broad input into the overall specification, including direct customer, distributor, and supplier feedback, and previously verified requirements stemming from analysis of previous development projects
- Create a customer specification, and see it as a lowest level imperative. In parallel, create compliance cards (internal product specifications) setting internal innovative goals in order to create a positive value gap for customers
- Ensure validation plans at each specification level
- Identify priorities through risk and bottleneck analysis
- Ensure feedback at all levels of the specification process, and ensure memorising of all solutions and changes

An aircraft has to be developed as a holistic system, with the components and sub-systems defined by a top down approach to flow down requirements. This approach is typically known as systems engineering[19]. Such a process will consider the product at a series of levels, with the lower levels detailed far more, or alternatively containing subsidiary components, subsystems, or single parts[19]. The requirements start from the customer's needs, and is broken down to delineate the next lower level, and so on.

The system or sub-system should, at each level, be broken down into elements that have clear and concise interfaces with each other and the levels above. If there are complex interactions, then these should be kept within the subsystem's boundary[19]. If this is not adhered to then the System Integrator will have difficulty finding a way to keep the suppliers from interacting too much with each other, as well as to define what they are responsible for delivering[19]. If the subsystem can have its performance requirements derived that are clear and independent of other subsystems, then it can be decomposed, developed separately and can be outsourced. If not, then it may need to be decomposed further.

The decision tree for either make or buy, based on systems engineering is shown in Figure 2-10[19]. The product development process initiates with a customer-driven statement of requirements, which is then broken into sub-requirements. There are different exit points in the product development process where it is possible to outsource the work. If the work is outsourced early on, then the immediate steps in the LHS column will have to be conducted by the supplier. Evidence exists to suggest that the early involvement of suppliers in the design process will improve quality and productivity, while reducing lead-time[81,112,113]. At whichever level outsourcing takes place, there is a high amount of communication needed between the disciplines to help reduce uncertainty[114].

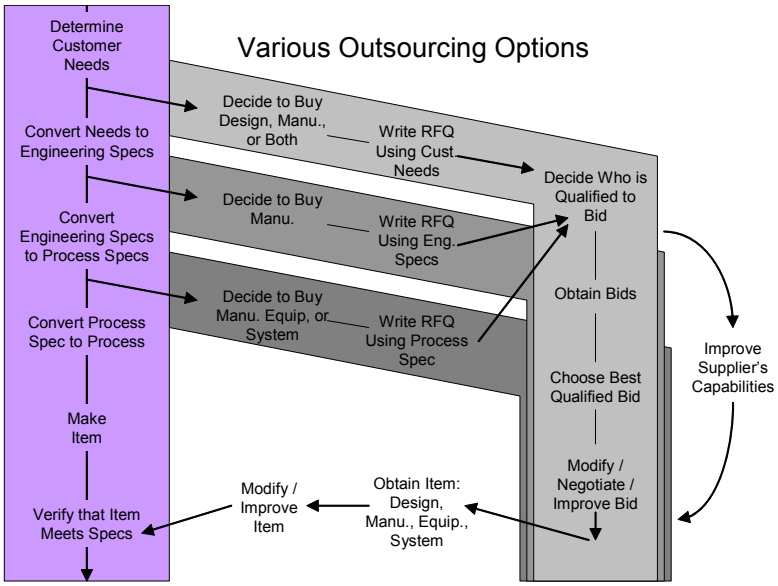

Figure 2-10: Decision trees in outsourcing

Should it be deemed logical to outsource a complicated sub-system that adds value, such as a wing cover, then "architectural knowledge" from the System Integrator is key to its success. Architectural knowledge is the innate ability to codify the customer requirements into a subsystem performance specification. Understanding the links between user requirements, system parameters, and component specification manifests this. It is unique to the company and is developed intuitively by exchanging knowledge between the engineers, marketers, and strategists[102]. Through this architectural knowledge, the buyer can remain in control of both the design and manufacture of the subsystem, despite the fact that it is outsourced. The pitfall of this strategy is that if architectural knowledge is lost then it is very hard to regain.

2.3.3.1 New Product Development

The very purpose of systems engineering is to enhance the process of New Product Development (NPD). NPD is a key strategic activity and source of competitive advantage, as new products often contribute highly to overall sales. With a new distinctive offering, a firm can either sell the new product at a premium price or in high quantities, until a competitor creates something similar[114], as has been witnessed by the Boeing 787.

Inter-firm NPD has become more prevalent due to the increase in R&D being outsourced[115]. A benefit of more than one company working together is that their capabilities can overlap, which aids learning[115]. The success of the partnership is based on the ability to reduce the transaction costs and decision time for new technologies. The expertise in outsourcing of technology can be a key core competence of a System Integrator, which has been evidenced to decrease R&D costs in 12 distinct industries[116].

Typically, the System Integrator should have higher bargaining power to mandate that suppliers invest in advanced technology, which is risky for the suppliers as if the NPD activities become defunct then the System Integrator can fairly easily switch to other suppliers who have newer technologies. However, NPD is enhanced when know-how and technology flows in both directions, creating close collaboration, which means the System Integrator is more cautious with switching to new suppliers[115].

Typically with complex NPD, there will be too many teams with their own intentions, thus informal team processes cannot be relied upon[117]; instead frequent and concentrated communication between the different teams will be required[118]. It is prudent in each of the supplier's teams to have an 'integrator' from the System Integrator who acts as the focal point. The integrator has to facilitate design compatibility between the different sub-systems as well as within the subsystem itself, and acts as an arbitrator.

2.3.4 Supplier Selection

The most important criteria to judge suppliers on are: Quality, Cost and Delivery (QCD)[119]. Traditionally, the Primary Manufacturer would have a large base of suppliers, for the procurement of the same part, which created market competition between the suppliers in order to secure the lowest price, as well as the highest quality. For this strategy to be effective, the term of the contract would be short and the switching cost to change the supplier would be low[105]. However, today the System Integrator wishes to employ a 'strategic sourcing' strategy, which entails initiatives such as: supply base rationalisation; spend consolidation; single sourcing; and long-term agreements[95]. The benefits of supply base rationalisation are that less effort is required to monitor the suppliers as well as the recurring bid processes are reduced. By entering a long-term relationship, the transaction costs are reduced due to[105]:

1. Reduced governance and coordination requirements
2. Increase in purchased volumes which spread transactional costs over more items
3. Eliminates non-value added activities such as inspection

Furthermore, due to agency theory, suppliers who feel secure in the knowledge that they have a long-term relationship will be more willing to invest in equipment, research or whatever the buyer desires. Therefore, a relationship must be established that is based on co-prosperity, which is a reason for the success of the Japanese automotive industry[120]. The Primary Manufacturer should have a vested interest in improving their suppliers' capabilities and not just in improving the products purchased[121].

2.3.4.1 Supplier Relationship

Shown in Figure 2-11[122] are five types of supplier relationship structures, based on the "asset specificity" to the buyer's core competency of the product supplied by the supplier. The most commonly found type of external contractual relationship is the *adversarial leverage*, where the customer has a choice of suppliers, and the suppliers have no strategic advantage in terms of ownership of the part manufactured. Further up the scale of asset specificity are *preferred suppliers* who supply products of medium asset specificity, however with low strategic importance to the customer[123]. The *single source* relationship is for parts that have fairly high sensitivity to the core competency of the firm; however the buyer wants to minimise transaction costs without having to vertically integrate. Where the supplier holds key expertise and without vertically integrating that supplier, this relationship is known as *network sourcing*. Finally *strategic alliances* or commonly known as joint ventures are where both the supplier and the customer have some Intellectual Property Right on the product.

Variables that effect the supplier relationship includes information exchange, outcome uncertainty, goal conflict, relationship length, adverse selection and moral hazard[124]. Moral hazard is where the supplier could shirk their responsibility. With a supplier focussed

commitment strategy, shirking is a threat due to the lack of competitors. If shirking is avoided, it can still mean that suppliers fail to innovate as they do not have the pressure to do so[125]. To safeguard against this, it is possible that clauses can be included in the contract, but in order to mitigate against every eventuality this can increase overall transaction costs.

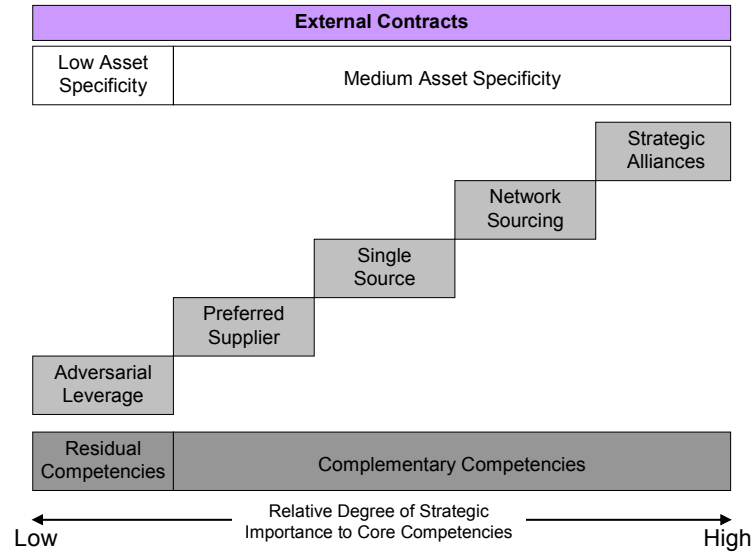

Figure 2-11: Supplier relationship model

However, in general a supplier focussed commitment strategy does reap benefits to a certain level, beyond that point the buyer will then suffer from diminishing returns, which can eventually negate the transactions and scale-related benefits[105]. Having this close relationship with suppliers can lead to the firm's core competency knowledge being exposed[126]. Evidence exists that outsourcing relations are only stable for limited periods of time, and there are often systematic barriers within firms which impede fully cooperative relationships with suppliers[117].

However, in the pursuit of lean practices, and the build up of a close relationship with the customer, the supplier may focus too deeply in-line with the customer that emergence in the marketplace of novel technological opportunities might not be captured[127]. It is therefore necessary if suppliers can be innovative, that the Primary Manufacturer manages the relationship in such a way that this innovation is captured and not stifled. Innovation can involve both the product and the process, where process is often more abundant as this is where the suppliers excel[47].

It has been found that both customised and formal contracts, in combination with high-levels of trust, can improve the performance of complex exchanges between the supplier and the customer[74]. For example, if the contract explicitly stipulates the consequences of performing well or under performing, this should generate trust. As shown in Figure 2-12[128], based on the concept that parties neither fully trust nor fully distrust each other then they are in a state of flux. Shown in quadrant 1 of Figure 2-12, there exists both low trust and distrust, where basically there are no expectations. Such a relationship will develop into quadrant 2, where the relationship is optimistic without encompassing a high level of trust. If the relationship does turn a little sour due to repeated misgivings then the relationship can move into quadrant 3, where the business relationship is present but the quality of information is likely to be poor[129]. In this quadrant, the party with least power will try to regain control via filtered information and knowledge to deal with the imbalance. Finally, quadrant 4 is where parties trust each other but the relationship must be verified, which is the most mature and balanced

of relationships. Therefore, it is trust that determines the level of information and knowledge sharing, and influences the exploitation of the power perceived with the generation of knowledge and its exchange and use.

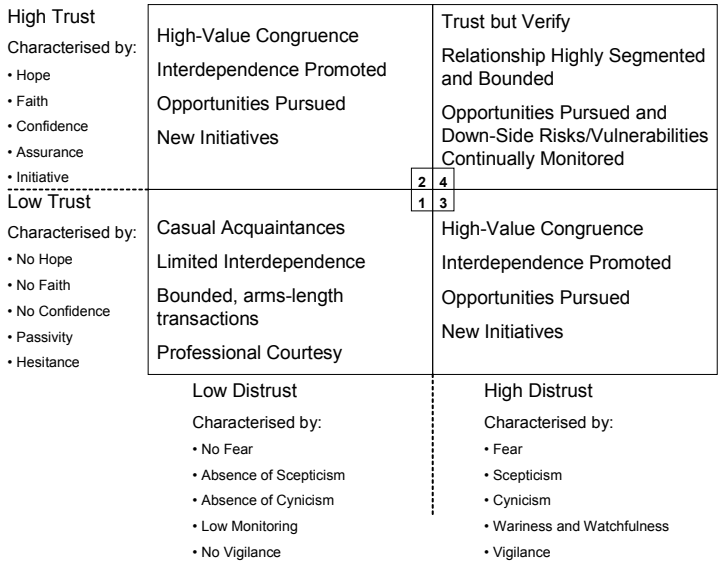

Figure 2-12: Trust and distrust

However, trust is being depleted by Primary Manufacturers through enforcing the following initiatives[95]:

- Year upon year price reductions of 3-5%, for example
- Forced 90-120 day payment terms, with which the powerful customers are manipulating their smaller suppliers to increase their cash flow, instead of trying to balance risk and cost of capital across the supply chain
- Forced inventory levels, where suppliers hold the majority of safety stock, which increases the suppliers' costs and risks

By enforcing cost cutting, this can sour relationships, which is particularly detrimental with suppliers that are in a powerful position. This is further compounded by the fact that since the mid-1990s, many suppliers belong to diversified groups, who have varied revenue sources and therefore do not have to compete on marginal work[95].

2.4 Summary

Based on the systems engineering approach, the simplest and perhaps most efficient method, from an engineering perspective, is to use an IPT approach; the members of which are from the same company, working towards the same goal. However, the overriding strategy of major aerospace Primary Manufacturers today is to outsource work, typically with a global perspective. Therefore, combining systems engineering and global supply chain management, can result in conflicting requirements arising. However, it is necessary that both of these global influences should work in harmony with each other. Finding suitable strategic suppliers, who can competently undertake the responsibility of designing and manufacturing complete CFRP parts, can be difficult when experienced Western suppliers are considered. This issue is exacerbated when suppliers from developing nations are considered.

Between the strategic supplier and the System Integrator there should be interorganisational processes in order to augment communication, as shown in Figure 2-13[81]. This should be augmented through a small core team that liaises between the buyer and the supplier, who should remain in their positions, as this can aid communication in terms of content and frequency and helps to build trust and stability[118]. A quasi-IPT, perhaps with duplication on both sides due to members fulfilling similar roles should be used, with an architect and integrator working at the systems level, controlling the interfaces.

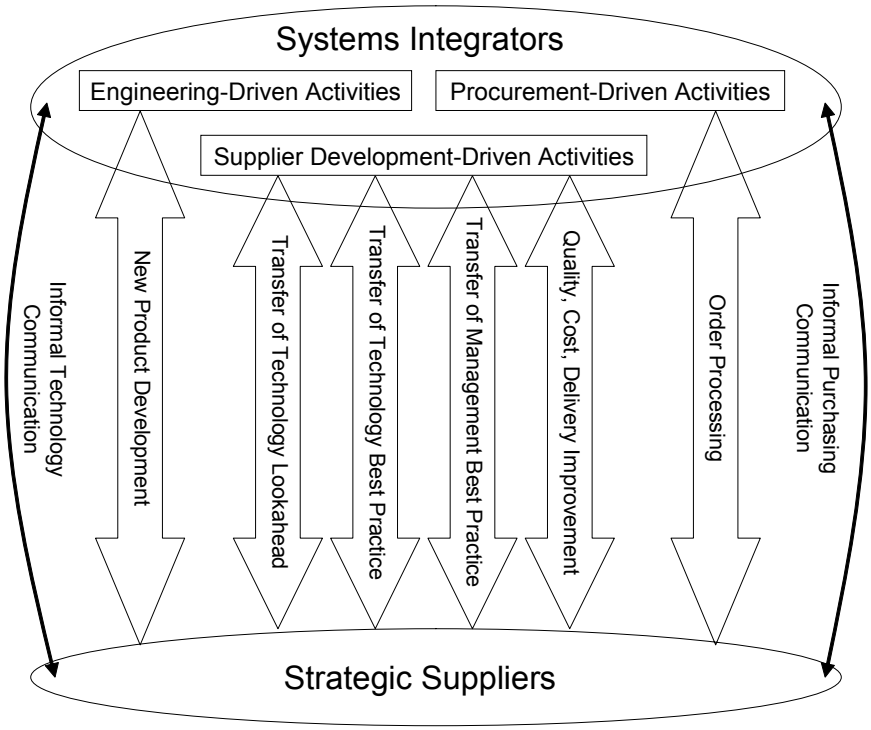

Figure 2-13: Conceptual diagram of interorganisational processes between System Integrators and their suppliers

In particular, at the preliminary design phase, but also in subsequent design phases, information will be both imprecise and subject to change which, if relied upon at an early stage, can lead to a subsequent costly redesign; however, if more concrete information is waited upon then the process will slow down[117]. At this phase, the suppliers are bound by a contract, which is hard to write in order to include every eventuality. Therefore, when such instances occur, such as design changes, then difficulties of the ex-ante (beforehand) cost and technical specification will then create ex-post (after the fact) coordination issues[130,131]. One possible method is that within the tumultuous preliminary design period, the supplier will not be compensated for any changes in design, but thereafter, once the configuration has been frozen, if changes should occur then they receive adequate compensation to amend the design[117].

Furthermore, an issue when relying on suppliers for overall product performance is that without incentives, once the supplier has reached their subsystem objectives, they will not go any further, as that will detract from their profit potential. Or if design changes occur after the contract has been written, which is based on a design with defined interfaces, it can be hard to instigate this change as the supplier could see this as a way of making a claim, and hence profiting from the contract.

It can be argued that the best systems to outsource are those easily decomposed[19], such as a modular unit. Therefore, the outsourcing of a wing cover, or parts of the wing cover, can

become an organisational challenge. Due to the considerable amount of interfaces with a wing cover, such as the spar, ribs and various systems, a thorough but flexible process will be required to manage this. Such a process is hard to deal with inside one organisation, controlling this with globally dispersed suppliers who work in different time zones, would increase the complexity significantly. Decomposing the wing cover further, into the stringers and skin, could also be considered, with a supplier perhaps being responsible for the design and manufacture of the stringers. However, this is even more complicated, as not only will there be an interface issue, similar to between the spars and wing covers, but there will also be load distribution; therefore, the interaction between the skin and stringer team would have to be even more integrated.

Like all parts, they have to be certifiable; therefore methodologies and sizing procedures used by the supplier will have to be harmonised with the System Integrator. Due to this very reason, much tacit knowledge will need to be codified and given to the suppliers, such as manufacturing procedures and mechanical properties, without which the design of the part has no foundations. Therefore, the global strategic supplier can expect to learn a great deal from the incumbent Primary Manufacturer, which strategically is of high importance to them. However, even by codifying a manufacturing process or creating a sizing methodology, this still does not mean that a developing supplier can perform the work. There are many steps in between, which cannot be codified, as this comes from tacit knowledge, both from the experienced engineer as well as through organisational learning. Thus in order to obtain an optimum part it will be necessary to plug these gaps in the experience, which will either mean that the System Integrator has to use their own people to assist the process directly, or instead they will have to liaise with the supplier to train their employees.

Outsourcing can be beneficial if successfully implemented, and with the correct organisation, a systems engineering approach can work in harmony when working with strategic suppliers. The benefits of systems engineering is clear, however with outsourcing, this is only beneficial if the correct strategy and organisation is used. Therefore, the following three broad conclusions based on experience gathered in the Western world, should be considered[59]:

1. A defensive incremental approach to outsourcing decisions, often driven by a general lack of competitiveness in manufacturing, can initiate a spiral of decline that ultimately leaves firms without the skills and competences they need to compete
2. Outsourcing firms often make four questionable assumptions:
   - Strategy primarily involves competitive position in the market place
   - Brand share is defensible without manufacturing share
   - Design and manufacturing are separable
   - Market knowledge is separable from manufacturing
3. Properly understood and managed outsourcing can be an important part of overall strategy

3 Materials & Processes, Tooling and Assembly

3.1 Introduction

Marcus Langley gave a lecture to the Royal Aeronautical Society of England in December 1969 titled "The History of Metal Aircraft Construction". He said "Although, we shall still have metal aircraft for many years to come, quite new materials are beginning to appear and they have as many advantages over metal as metal had over wood. I am referring to such materials as carbon fibres used in matrices of synthetic resins.[132]" However, this prediction of all composite aircraft has still not been realised today.

In today's capitalistic led environment, market forces should drive the development of material science, so that the designer can satisfy the market requirements with advanced materials, in order to reduce the cost of ownership. However, if it was purely market forces pushing the further use of composite materials on civil aircraft, then the current inability to accurately estimate design costs, and the high manufacturing costs, would not be acceptable. Instead, the principal aircraft manufacturers have been previously cosseted in a financially subsidised environment, which has aided the establishment of composite structures in civil aircraft[133]. The increased application of composites to aircraft structure is illustrated in Figure 3-1[134], which has been an evolutionary approach due to the safety consciousness of the civil aerospace industry. Overall, composite materials have received a very high level of funding for a long time, which no other class of material has previously received[135].

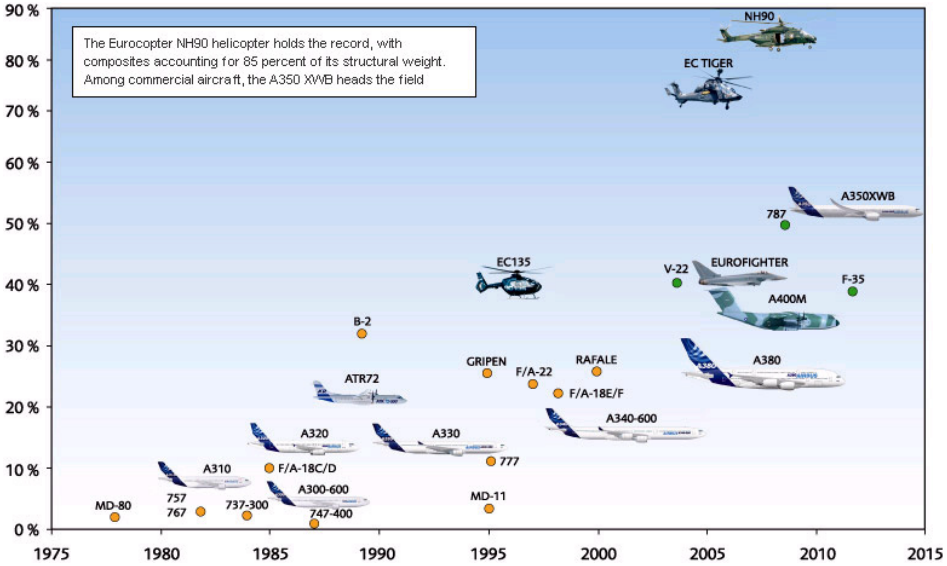

Figure 3-1: Progression of composite parts on EADS aircraft

Demand for aerospace grade CFRP has increased due to the market introduction of the Airbus A380, A400M and the A350 XWB, as well as the Boeing 787, which, based on today's production targets, will require 3000 metric tons of CFRP per annum[136]. Furthermore, demand is also being increased by other engineering sectors, such as the wind turbine and automotive industries[137], as they too require higher performance materials. For example, the wind turbine industry has traditionally used Glass Fibre Reinforced Plastic (GFRP) to manufacture the windmill-blades, but because of the increasing span of the blade to greater than 40m[138], stiffer CFRP is instead required. The quantity of CFRP required by these other industries, has the potential to eclipse the quantity required by the aerospace industry.

The demand for aerospace grade CFRP is directly linked to the demand for new aircraft. During the 1970s and 1980s, CFRP material supply grew 15% annually, and peaked by 1990 at 50% due to the demands of military and civil aerospace programs[29]. However, due to the end of the Cold War, many aircraft programs were cancelled, thus demand fell away, so much so that CFRP material suppliers were selling their product at cost in order to ensure that their facilities still ran[29]. This led to consolidation of the industry, as evidenced by DuPont's closure of its Advanced Materials Systems division[139]. This has created a risk adverse industry exhibiting the classic demand-pull behaviour[29]. Currently material suppliers are increasing supply of aerospace grade CFRP, based upon both Airbus and Boeing being more certain of the future demand, as they have full order books for the next five to ten years[137]. Increased usage, from an economic market perspective, should increase the supply, diminish the economic rent available and hence reduce the cost of composites materials. The upper constraint on producing carbon fibre is the amount of acrylonitrile[vii] available.

3.2 Materials

3.2.1 Material Choice

The specific tensile strength and stiffness of composites compared to that of three ubiquitous metals found in aircraft design is shown in Figure 3-2[140]. It should be noted that the epoxy resin composites have a range of tensile strength and stiffness values, as shown in Figure 3-2, with the lower extremity values representing a quasi-isotropic laminate, while the upper extremity represents a UD laminate.

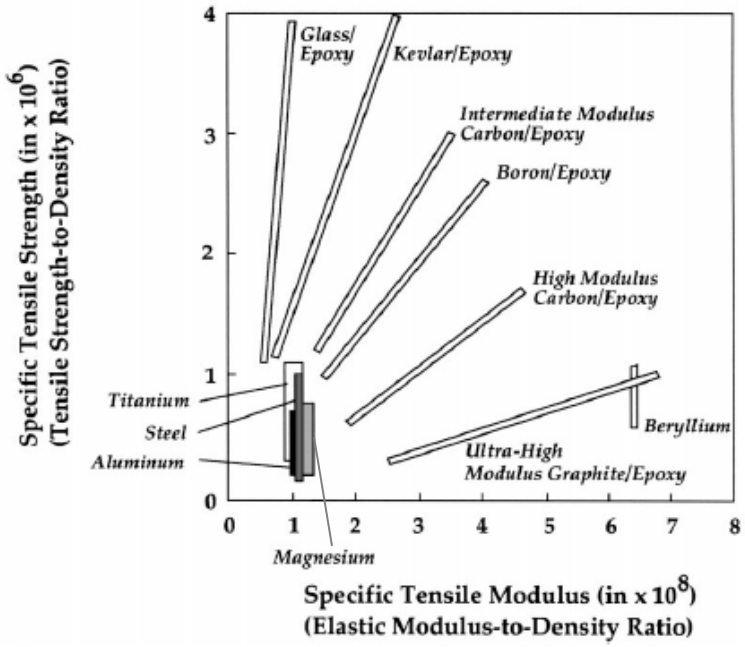

Figure 3-2: Comparison of specific tensile strength and stiffness of composites and metals

A composite has two constituent parts: the fibre and the resin (matrix). It is known that a typical UD CFRP prepreg ply has a modulus of 125GPa, whereas the resin alone has only a

[vii] Acrylonitrile is a monomer that produces synthetic polymers, which can then be used for carbon fibres, synthetic rubber and Nylon.

modulus of 3.5GPa[141]. In general, the factors that determine the performance of a composite material are:

- Fibre properties
- Resin properties
- Fibre Volume Fraction (FVF)
- Fibre orientation

The laminate will have greater stiffness and strength with a higher modulus fibre, a high fibre content, and a greater proportion of fibres along the principal axis.

Shown in Table 3-1[142] are the typical dominant material failure modes of CFRP, and the cause of this failure, albeit this is a very simplistic view. The interface between the fibre and resin is critical, as it is through the resin that the properties of the fibre are imparted into the part. The interface also affects the fracture properties of the laminate, with a weak interface resulting in a laminate exhibiting low compressive strength and stiffness, but conversely high fracture resistance. When a strong interface exists, the laminate exhibits high strength and stiffness, but low fracture resistance. Other properties that are dependent on the interface are creep resistance, fatigue, and environmental degradation[143].

Property/Failure Mode	Dominant Constituent	Stress-Strain Behaviour	Factors Affecting Properties
Stiffness			
Elastic Constants	Fibre	Linear (except shear)	Temperature
Buckling	Fibre	Linear	Fibre Alignment
Crippling	Fibre	Linear	Element Geometry
In-Plane Strength			
Tension	Fibre	Linear	Low Temperatures
Compression	Resin/Interface	Some Non-Linearity	Moisture/Elevated Temperature
Shear	Interface	Nonlinear	Moisture/Elevated Temperature
Pin Bearing	Resin/Interface	Some Non-Linearity	Element Geometry
Bearing/Bypass	Resin/Interface	Some Non-Linearity	NA
Out-of-Plane Strength			
Interlaminar Shear	Resin	Nonlinear	Elevated Temperatures
Interlaminar Tension	Resin	Nonlinear	Moisture Content
Free-Edge Failure	Resin	Nonlinear	Chemical Exposure
Damage Tolerance			
Notched Tension and compression	Interface	Some Non-Linearity	Elevated Temperatures
Compression After Impact	Resin/Interface	Nonlinear	Moisture Content
Fatigue	Resin (only for properties sensitive to fatigue)	NA	Load History

Table 3-1: Composite material failure modes

The FVF is the ratio of fibre volume to resin volume, and is primarily dependent on the manufacturing process, but also on the resin system and the permeability of the fibres. As the mechanical properties of the fibres are superior to the resin, a high FVF is desired; with 60% FVF being typical for high-performance parts such as wing covers, however, there is an upper limit, as the fibres must be fully wetted. The density of resin and fibre are approximately 1.28kg/m³ and 1.8kg/m³ [141] respectively, hence a greater FVF will result in a higher overall density.

Resin dominated properties like compression strength and toughness can be improved through increasing the amount of resin in the laminate, albeit this will reduce the tensile properties and compressive stiffness. With increasing the amount of resin, the flexural stiffness improves with the same number of plies, due to flexural stiffness being dependent on the squared function of the overall thickness[144]. Furthermore, by increasing the resin content, the laminate has higher strain to failure and ultimate compressive strength, however cost and weight must also be considered.

The thickness of the laminate can also affect the part's strength, with an increase in thickness typically resulting in a decrease in FVF, greater fibre waviness, and an increase in void content. Fibre waviness has a detrimental effect on compressive strength[145], whereas voids cause stress concentrations and weak bond interfaces between the resin and the fibre, resulting in strength and stiffness degradation[145].

3.2.1.1 Fibre

The role of the fibre is to provide the mechanical stiffness and strength properties of the composite, with the fibres carrying 70-90% of the load[146]. Shown in Table 3-2[147] are typical values for various common fibre types. It can be seen that carbon has by far the highest stiffness and is nevertheless the lightest. It does have a somewhat limited strain in comparison to glass, and is more expensive, in particular thermoplastic Polyetheretherketone (PEEK).

	Carbon Fibre / 914 Epoxy		Carbon Fibre / PEEK		Glass Fibre / 913 Epoxy		Kevlar / 913 Epoxy	
	Plain	**Notched**	**Plain**	**Notched**	**Plain**	**Notched**	**Plain**	**Notched**
E_{11} (MPa)	126000	126000	129873	129873	41650	41650	73659	73659
E_{22} (MPa)	7400	7400	7318	7318	12333	12333	4111	4111
G_{12} (MPa)	5580	5580	3750	3750	4000	4000	2000	2000
v_{12}	0.28	0.28	0.3	0.3	0.28	0.28	0.344	0.344
ε_{xFT}	0.00944	0.00456	0.01423	0.007004	0.02795	0.0135	0.01766	0.008694
ε_{xFC}	-0.00714	-0.00545	-0.006700	-0.005343	-0.0247	-0.01885	-0.003446	-0.002748
ε_{yFT}	0.00324	0.00249	0.007297	0.007685	0.00346	0.00266	0.003940	0.004150
ε_{yFC}	-0.02095	-0.01745	-0.01616	-0.01499	-0.0096	-0.008	-0.02245	-0.02082
γ_{xyF} shear failure strain	0.01075	0.00689	0.01600	0.01282	0.01599	0.01025	0.02399	0.01923
ρ (g/cm³)	1.63	1.63	1.7	1.7	1.93	1.93	1.38	1.38
c_0 (£/m²)	14	14	38	38	10	10	16	16
G_c (N/mm)	0.5	0.5	2.5	2.5	1	1	1	1

Table 3-2: Material properties for carbon fibre (thermoset/thermoplastic), glass and Kevlar

3.2.1.1.1 Carbon

Carbon is the most widely used fibre in the aerospace industry due to superior strength and stiffness properties, particularly under tensile loads, and the low specific weight. Typically, polyacrylonitrile-based (PAN) fibres are used as they have higher failure strains and are lower in cost, in comparison to pitch-based carbon fibre[148]. PAN-based fibres are manufactured in both small (1-24k) and large (≥ 40k)[137] tows. The fibres, applicable to the aerospace industry, are typically classified by their modulus, as[149]:

- Intermediate Modulus (IM) [≈ 290GPa]
- High Strength (HS) [≈ 230GPa]

Shown in Table 3-3[150], is a comparison, between HS and IM fibres, with the higher value indicating superior performance. As can be seen, based on pure performance the IM fibre is superior, however if normalised to the comparative costs of the two, then HS is advantageous. The difference in cost between the two, apart from marketing reasons, is due to IM fibres having a crystalline microstructure that is more aligned with the fibre axis, which results in smaller diameter fibre having a high modulus and low strength, whereas HS fibres have a less aligned crystalline microstructure with the fibre axis, which results in low modulus and high strength. Furthermore, larger diameter fibres, like HS, have higher buckling resistance[151], as they are not so prone to fibre micro-buckling[143], however the sensitivity at component level to micro-buckling is minimal.

	Stiffness index for minimum mass			Stiffness index for minimum cost		
	Tension	Bending	Torsion	Tension	Bending	Torsion
Performance Index =>	E/ρ	$E^{1/2}/\rho$	$G^{1/2}/\rho$	$E/\rho C$	$E^{1/2}/\rho C$	$G^{1/2}/\rho C$
High Strength Carbon	1.00	1.00	1.00	1.00	1.00	1.00
Intermediate Modulus Carbon	1.28	1.33	1.11	0.58	0.52	0.51

Table 3-3: Relative performance indices for UD prepreg laminates normalised to HS

In general carbon fibres are highly susceptible to damage and have typically limited elongation before breakage (strain) rates of between 0.5-2.4%[152], due to the low interlaminar shear and tensile strengths of carbon fibres. However, through the development of the HS fibre, this has led to high-strain fibres, which have a strain of 2% before fracture. Carbon fibres, when compared to glass fibres, have a low negative coefficient of thermal expansion and are conductive. They are also affected by Ultraviolet (UV) radiation, with the effect being greater for laminates with higher FVF[153].

3.2.1.1.2 Glass

The most common glass fibre is electric glass (E-glass), which is an all-purpose glass. E-glass has high strength to weight ratio, very good dielectric, fatigue and thermal properties as well as environmental resistance. There is also high strength glass (S-glass), which has higher compressive and tensile strengths, as well as having a lower density in comparison to E-glass.

3.2.1.1.3 Aramid

Aramid fibres, commonly referred to as Kevlar®, have high specific mechanical strength, are very tough and damage tolerant, hence they are used for ballistic parts. However, there are a number of disadvantages with these fibres, such as low compressive strength in comparison to carbon, poor adhesion to resins, degradation in UV light, and moisture absorption in humid conditions. In 1994, the US Navy excluded the use of aramid/epoxy due to corrosion issues with aviation fuel and salt water[44].

3.2.1.2 Resin

The resin performs a number of functions[146,149]:

- Transferring the fibre properties into the global laminate
- Matrix isolates the fibres so that each fibre acts individually – this also impedes crack propagation

- Stabilising the fibre in compression by providing lateral support
- Provides out-of-plane properties
- Minimises damage due to impact and chemical attack
- Protects the fibre surfaces from damage during handling and in service
- Provides a good surface finish

Resins can be broadly classified as either thermoset or thermoplastic. Thermosets have a cross-linked polymer structure, whereas thermoplastics do not, which means they are capable of being repeatedly softened and hardened through temperature change. Therefore, from a recycling perspective, thermoplastic composites have a significant advantage over thermosets due to the comparative ease of recycling them[154].

The most commonly used resin system in the aerospace industry is epoxy, which is a thermoset resin. It has a cure temperature of either 120-135ºC or 180 ºC, with the latter being more typical due to its better environmental degradation tolerance[143]. The first generation of epoxy resins applied to carbon fibre in the 1960s and 1970s were brittle, which meant that the laminate had high susceptibility to impact damage. Today's new toughened systems, which have an element of thermoplastic resin added to the principal thermoset resin, are a vast improvement to the original thermoset resin systems, but are still not as damage tolerant as a CFRP using a pure thermoplastic resin system. Thus, even today, the resin system remains the Achilles heel of the laminate. Resins with a high proportion of thermoplastic, will have higher viscosity in comparison to an untoughened resin, which although improves the toughness, can hinder the use of such resins with LCM techniques.

Thermoplastic resins are inherently tougher than epoxy resins, thus the laminate should have a higher strain allowable[155]. Thermoplastics do however suffer from a greater knockdown in their compression performance when notched[149], due to the increased fibre/matrix bond. Pure thermoplastic resins suffer from low thermal stability, lack of chemical resistance, reduced fibre-matrix interfacial bonding and creep[156], and are expensive[154], all of which has hindered their application.

In humid conditions, composite materials will absorb moisture until the laminate is completely saturated, which results in plasticisation of the resin, resulting in deterioration of the laminate's strength and stiffness[157]. In this respect, thermoplastics are advantageous as they retain their properties better under hot/wet conditions, absorbing normally around 0.2% of their weight in moisture, as opposed to 1-3% for thermosets[148].

3.2.2 Fibre Format

Random flaws exist in all materials, however if the material is in a solid form, then the theoretical maximum performance cannot be reached[158]. However, when in the form of a fibre, despite the random flaws still existing in the filaments that constitute the fibre, failure will occur in only a number of the thousands of filaments, thus the material's theoretical strength can be maintained. Despite this, the fibre will incur knockdowns in performance due to the upstream fabrication processes.

Figure 3-3[159] illustrates the value chain for carbon fibre, from its lowest denominator to the end part. When deciding whether a textile or UD format is most suitable, the main considerations will be the mechanical properties and overall cost. Typically, the more

processed the composite materials are, the more expensive they will be, albeit they should be easier to process thereafter[160].

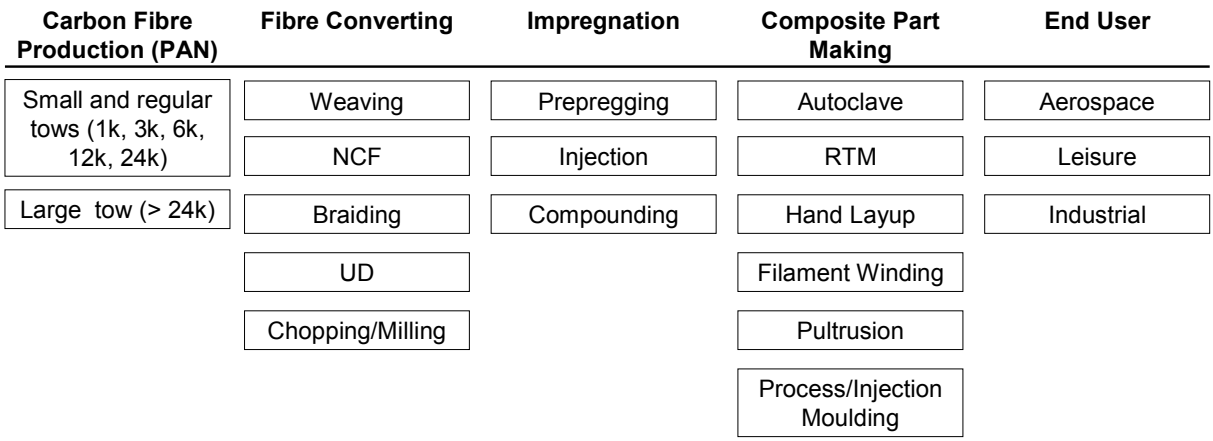

Figure 3-3: Carbon fibre value chain

From a stiffness performance perspective [FVF × orientation factor], Table 3-4[150] shows which reinforcement format offers the best performance[viii]. As would be expected, the UD tow and tape have the best performance.

Reinforcement Format	FVF_{max}	Orientation Factor	Stiffness Performance	Applicable Processes
UD Tow	0.80	1.0	0.8	Filament winding, pultrusion
UD Prepreg	0.65	1.0	0.65	Autoclave, Resin Film Infusion (RFI)
Multi-Axial Prepreg	0.60	0.3(Quasi-Isotropic)	0.18	Autoclave, RFI
2D NCF	0.55	0.3(Quasi-Isotropic)	0.17	RFI and Resin Transfer Moulding (RTM)
Woven 2D Fabric	0.50	0.27(Quasi-Isotropic)	0.14 (Crimp in Fibre)	RTM, wet contact moulding
Orthogonal 3D Fabric	0.40	0.3	0.12	RTM
Random Planar	0.30	0.3	0.09	Wet lay up, Sheet Moulding Compound (SMC)
Random 3D Short-Fibre	0.20	0.12	0.024	Bulk Moulding Compound (BMC) and injection moulded thermoplastics

Table 3-4: Efficiency of different reinforcements

3.2.2.1 Roving

A fibre roving consists of untwisted arrays of filaments, which are fabricated as continuous tows that are woven, for example, into a fabric or UD tape. The tows, which are also known as continuous fibres, are normally available in filament counts of 3k, 6k, 12k or 24k. A 24k tow produces a thicker ply than a 3k tow, resulting in a higher fabrication rate and reduced cost per weight[161,162]. The tows can be flattened to provide the desired ply thickness, although this is more easily achieved with smaller tow sizes.

[viii] Orientation factor is the ability to tailor the reinforcement format to suit the loads.

3.2.2.2 Uni-Directional Prepreg

Pre-impregnated UD, more commonly referred to as UD prepreg, has the resin impregnated into the fibres. The fibre alignment is straight, and the structure is two-dimensional and homogenous, which results in excellent in-plane properties, thus they are best applied to large, highly in-plane loaded shell elements, such as wing covers. Furthermore, the flexibility with the ply orientation angle and higher FVF of 60%[160], enriches its suitability. However, there are a number of disadvantages with UD prepreg, such as:

- Prepreg has limited shelf-life even when stored in a freezer
- Lay-up is a time consuming activity
- Poor out-of-plane properties
- May be difficult to lay up into double-curved shapes – slit tapes can overcome this problem[160]
- Is typically more expensive than its constituent parts – resin, hardener and fibre

In order to minimise interlaminar shear stresses at ply drop offs and free-edges, as well as reduce thermal stress issues, UD prepreg plies are thin, with typical tape thicknesses of 0.125mm (6k tow), 0.184mm or 0.25mm (24 k tow). Consequently, it has high flexibility in tailoring the thickness to suit the loads. The resin content of uncured prepregs vary between 34-42%, and when at the upper limit, the prepreg has 15% more resin content than required to attain the desired FVF[148]. With a higher initial resin content, this can help in the fabrication of the part, as the prepreg will be tackier, giving adhesion between mating plies. However, upon cure, it will be necessary to bleed-off this excess resin, which although ensuring good resin flow during cure, is both wasteful and requires greater control. The latest resin systems are more viscous, thus low-bleed or non-bleed processes can be used, resulting in a more uniform thickness.

Due to the resin already being activated, i.e. the hardener has been added, the prepreg needs to be stored below -18°C, which gives it a shop-life of between 6-12 months. At room temperature, the shop-life is reduced to approximately 28 days, which means careful auditing of out-times is required[163] and it constrains the time to fabricate the part. The tack of the prepreg deteriorates with time due to the resin curing, which not only ensures the plies are harder to lay-up, but also during cure there will be less resin flow, which can result in a thicker laminate, and the resin may not cure properly. The storage and handling of the material incurs an additional cost, due to the temperature constraints, hence the part manufacturer must have sufficient freezer capacity, or alternatively, it could be delivered on demand from the supplier.

The UD laminate has low interlaminar and fracture resistance, due to the lack of through-thickness reinforcement. Typically, the through-thickness properties in comparison to the in-plane properties are just 7% for the tensile modulus and only 3% for tensile strength[164], hence they are not suitable to support high through-the-thickness or interlaminar shear loads.

3.2.2.3 Textile Composites

In general, textiles have poorer in-plane mechanical behaviour in comparison to UD, however, they excel when factors such as high strain-to-failure, out-of-plane properties,

damage tolerance, and drapeability are considered[165,166]. The factors that determine the dry fibre's drape are[167]:

- Fibre architecture
- The locking angle influences the shearing force
- Fibre tensile properties

However, these very factors that improve drape, are detrimental to the in-plane properties[166], although the principal reason for the poorer in-plane properties, relative to UD, is due to the waviness of the tows generating off-axis local stresses[166]. Net-shape or near-net-shape techniques such as braiding, weaving and stitching can reduce cost and potentially enhance the mechanical properties of the resultant part[168]. Table 3-5[169] highlights the advantages and limitations of each process, which highlights that Non-Crimp Fabric (NCF), might lend itself very well to large shell like structures, and that either 2D or 3D braids could be applicable for stringer fabrication. Furthermore, stitching may be beneficial to help integrate the parts of a wing cover and also improve the through-thickness properties of the laminate.

Textile Process	Advantages	Limitations
2-D Woven Fabric	Good in-plane properties Good drapeability Highly automated preform fabrication process Integrally woven shapes possible Suited for large area coverage Extensive database	Limited tailorability for off-axis properties Low out-of-plane properties
3-D Woven Fabric	Moderate in-plane and out-of-plane properties Automated preform fabrication process	Limited tailorability for off-axis properties Poor drapeability Limited woven shapes possible
2-D Braided Preform	Good balance in off-axis properties Automated perform fabrication process Well suited for complex curved shapes Good drapeability	Size limitation due to machine availability Low out-of-plane properties
3-D Braided Preform	Good balance of in-plane and out-of-plane properties Well suited for complex shapes	Slow preform fabrication process Size limitation due to machine availability
NCF	Good tailorability for balanced in-plane properties Highly automated perform fabrication process Multilayer high throughput material suited for large area coverage	Low out-of-plane properties
Stitching	Good in-plane properties Highly automated process provides excellent damage tolerance and out-of-plane strength Excellent assembly aid	Small reduction of in-plane properties Poor accessibility to complex curved shapes

Table 3-5: Summary of advantages and disadvantages of various textile technologies

Textiles can also be differentiated based on their fibre architecture. If a textile, without the matrix, can transmit loads continuously in three dimensions then it is a 3D textile, whereas a 2D textile can only transmit loads in two dimensions. It should be mentioned that a 2D UD prepreg could be converted into a 3D composite, for example, by Z-pinning. Fabrics can be either supplied dry, or as a prepreg[148], albeit the ability to pre-impregnate the fabric becomes more difficult with an increase in thickness, as the resin must be viscous enough to ensure complete wetting. For this reason, a prepreg NCF is uncommon, albeit in non-aerospace applications, semipreg NCF is used to ensure a void free laminate.

In comparison to the standard method of ATL deposited UD prepreg, the 3D preform manufacturing processes, including the process control required to design and cost-effectively manufacture a preform for a specific application, is currently lacking in maturity.

Furthermore, as their performance is harder to quantify, their qualification would require greater analysis, and due to greater variability in their properties, could lead to more conservative allowables.

3.2.2.3.1 2D & 3D Woven

2D woven biaxial fabric consists essentially of two sets of yarns interlaced at right angles, with the longitudinal yarns known as 'warp', while the transverse yarns are known as 'weft'. The weaves can be balanced or can be biased in one direction, by up to 90%. Woven fabric are typically produced in widths between 1.8-2.5m and at a production rate of several meters per minute[164], with ply thicknesses varying from 0.1–5mm[160]. This means that large areas of material are produced at a low associated fabrication cost[166].

A 2D weave can be woven into various orthogonal patterns as illustrated in Figure 3-4[165], which will determine the drapeability, mechanical performance and achievable FVF. Fabrics, in particular twills and satins, have superior drapeability over prepregs[160], as they have lower shear rigidity, although this reduces the fabrics performance[166]. Therefore, the manufacturing engineer would prefer to use a woven fabric for part conformity and higher deposition rate, whereas the structural engineer must determine the knockdown in performance in comparison to a UD laminate.

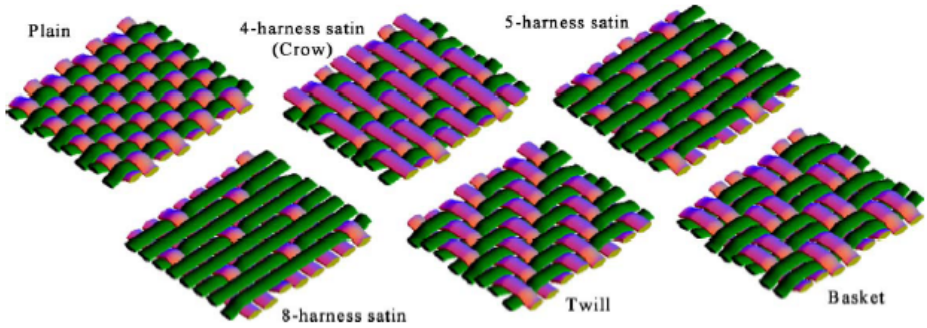

Figure 3-4: 2D weave patterns

Cox and Flanagan[166] investigated the difference between the plain and notched tensile properties of a 5-harness satin, with a UD laminate, for various laminates. Despite the woven laminates having a 10% lower FVF in comparison to the UD laminate, thus being 12-17% thicker, the woven fabrics had up to a 30% knockdown in performance, although with a higher proportion of ±45° plies, this was reduced. For this reason, woven fabrics have had limited application on primary structures. Due to the lack of shear stiffness, triaxial woven fabrics could be sought, however as identified by NASA, the aerospace industry sees CFRP woven fabrics as such a small market that it is not worth further investment[25].

Much effort has been expended in 3D woven fabric techniques to produce integrally woven structures such as I-beams where the fibres in the web and flange sections are interwoven[170], an example of which were woven H-joint connectors used to join honeycomb-sandwich wing panels together on the Beech Starship[148]. Contemporary 3D weaves are fabricated with only 0° and 90° in-plane yarns, thus the fabric exhibits poor torsional and shear mechanical performance[171]. To overcome the lack of ±45° plies in the preform, a great deal of research has been conducted, but in terms of commercial production little has so far been realised. Albany Techniweave Inc. has manufactured a 3D integrally woven skin/stringer preform with ±45° plies in the skin as well as for the ribs[166,170]. Edgson and Temple[172] also have a patent for producing woven I-beams, T-beams and sandwich structures, which contain bias plies in the

web and can be manufactured with curvature. Furthermore, 3D woven preforms suffer from excessive fibre crimping and a maximum achievable FVF of 55%, which results in a minimum knockdown of 20% for the tensile modulus in comparison to a 2D laminate[148], and is worse under compression. However, 3D weaves have good impact performance and are an ideal fabric for the RTM process, with great repeatability due to the preform's resistance to 'fibre-wash'[ix].

3.2.2.3.2 Non-Crimp Fabric

An NCF ply construction is defined, by the standard, as: 'a textile structure constructed out of one or more laid parallel non-crimped non-woven thread plies, which are differently oriented, with different thread densities of single thread plies and in which integration of fibre fleeces, films, foams, or other materials is possible'[173]. In simple terms, it is one to five UD plies compiled to form a stack, which are typically stitched to consolidate it. If stitching is used, then NCF has the potential to outperform normal 2D laminated in terms of damage tolerance, as there is a degree of through-thickness reinforcement. Alternatively, the plies can be tacked together, such as Saertex's latest generation of NCFs, which are held together with a 'hot melt grid' system[174].

NCF potentially creates the utopia for applications where good in-plane properties are required, such as wing skins, due to their straight fibres. Furthermore, due to their reasonable thickness, higher deposition rates than standard UD prepreg can be achieved. A triaxial NCF can create a 44/44/12 (% of 0°/ % of ±45°/ % of 90°) laminate using 12, 6 and 3k tows respectively, thus reducing the cost of the NCF.

Typically NCF conforms well to relatively complex shapes with minimal wrinkling, due to the individual layers ability to shear relative to each other. By specifying and controlling the tension of the stitch thread it is possible to alter the drape properties[175]. Due to the double curvature of the NASA ACT semi-span wing lower cover, the Saertex NCF used developed wrinkles, which was alleviated by cutting the fabric span-wise in the manhole region in a staggered butt-joint fashion[176]. In general, a biaxial NCF has better drapeability in comparison to a triaxial NCF, due to the greater stiffness and limited ability to shear.

There are a number of issues that can affect the performance of NCF relative to UD-prepreg. If stitching is used to join the plies together this can induce crimp into the fabric, for example Miller[177] found that the mean crimp of NCF was 2.32°, whereas for UD prepreg it was only 0.71°. Stitching can also cause the fibres to be pushed together, leading to resin rich areas, which reduce the FVF and can cause cracking, leading to residual stresses and stress concentrations[178,179]. Other limitations of NCF are[175]:

- Thickness and stacking sequence tailoring is reduced
- Large amounts of scrap material may result due to the width of the standard NCF, particularly if the part profile is complex and tapered
- Industrialised process has not yet been developed, and the handling of large textiles must be done with care, due to the delicate NCF architecture
- The requirement to store various NCFs may offset the savings made on freezer costs

[ix] 'Fibre-wash' can be mitigated using a binder.

However, NCF can reduce the part's lead time and there are no tack-life issues with NCF. The principal advantage of NCF is that it has a higher deposition rate in comparison to UD prepreg, such that over a 1m length, 16 times[x] the amount of material can be deposited. Over the part, due to the relative high thickness of the NCF textiles, it is beneficial to minimise the number of butt joints, thus the NCF should be as wide as possible. However, a consequence of this is for a fairly complex contour, such as the wing cover shown in Figure 3-5, there may be a large quantity of off-cut material, if a standard roll width is used. This material may be very hard to utilise again, due to the size and shape of the residual material, and also due to its particular lay-up. This can be reduced, by decreasing the width of the NCF roll, but this will consequently increase the deposition time, and could potentially lead to a weight increase due to the effect of increased butt joints.

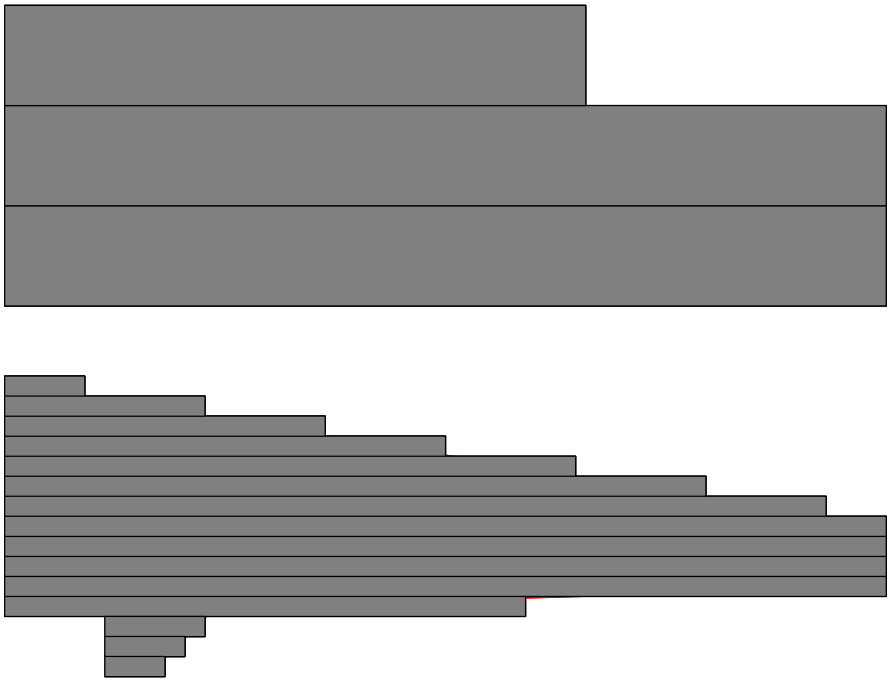

Figure 3-5: Material utilisation of both 1500mm wide NCF and 300mm wide prepreg

Liba machines, as shown in Figure 3-6[25], can produce widths up to 2.5m, however a width of 1.27m is most common, and with production rates of 45m/h[164], meaning LIBA fabrication is typically the lower cost option. There are Liba Max 3 and Liba Max 5 machines, with their capabilities highlighted in Table 3-6[180], with the former laying continuous strands of fibres from a centre point over the top of the machine, whereas the latter has bands of fibres that run across the machine from a creel set at the desired angle, and once the fibre is inserted it will pass through a spreading zone, with the band passed across the width of the machine, cut and transferred down on to the conveyer[180].

NCF was used in the NASA ACT program, which used a 1st generation LIBA machine, for the NCF fabrication. In comparison to the contemporary UD prepregs in the mid-1990s, the NCF had a 25% knockdown in its compressive properties, due to the waviness in the NCF. However, the critical notched properties such as Open Hole Tension (OHT) / Open Hole Compression (OHC) were similar to prepreg, whereas Compression After Impact (CAI) was 50% higher[176]. Today, improved NCFs are available such as Hexcel's NC2, which uses

[x] Prepreg at 300 by 0.25, whereas NCF could be 1500 by 0.8, hence a factor of 16 difference.

lower-cost high tow-count carbon fibres (24k plus)[139]. Furthermore, for LCM techniques, larger tows facilitate higher permeability to allow for rapid resin impregnation[181]. A thermoplastic binder or veil can also be applied to each ply to enhance the toughness of the laminate. An example of which is Hexcel's DX69 thermoset binder with an integrated thermoplastic toughener, which provides, at the laminate level, toughness properties very similar to the M21 prepreg system[182].

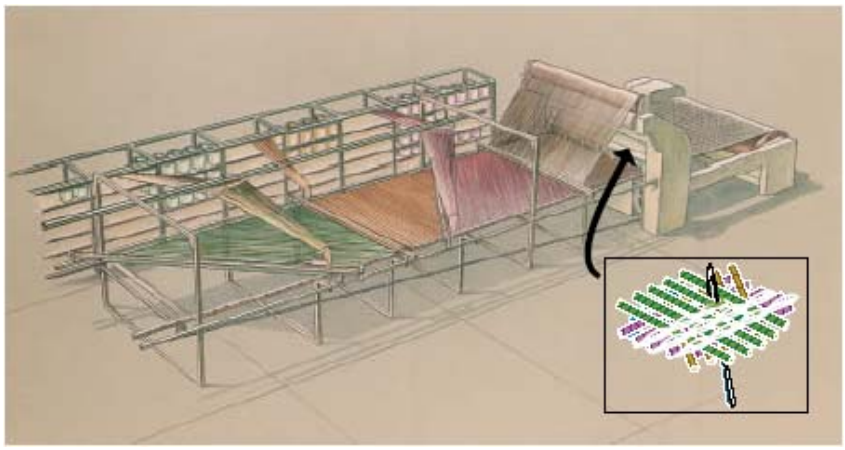

Figure 3-6: Liba Max 3 machine

	Liba Max 3	Liba Max 5	
Carbon Tow	**Min Layer (gsm)**	**Current Min Layer (gsm)**	**Target Min Layer (gsm)**
HS 6K / IM 12K	150	Concentrating on higher tow counts	80-100
HS 12K / IM 24K	200	135	100
HS 24K	300	200	150
HS 50K +	400	200	150

Table 3-6: Liba Max 3 & 5 NCF comparison

3.2.2.3.3 Braiding

The common fibre types can be used with braids, although the tow size should not be greater than 12K, otherwise it will hinder the braiding operation[146]. Braids typically come in a dry format, as when coupled with an LCM process this can lead to cost effective components, although prepreg braids do exist, such as from the firm TCR™ Composites[183]. Braids can be cured using a variety of processes from autoclave to RTM[184]. There are two general categories of braids, namely 2D and 3D. 2D braids can be supplied as sleeves or flat braids, with the difference between the two being[184]:

- Sleeves – two sets of continuous yarns, one clockwise, the other anticlockwise, are produced using the bias weaving process. Each fibre from one set is interwoven with every yarn from the other set in a continuous spiral pattern
- Flat braids – one set of yarns, with each yarn interwoven with every yarn in the set in a zigzag pattern

The *braid angle* is one of the most important parameters of a braid, which is the acute angle measured between the axis of the braid to the axis of the bias yarns, as shown Figure 3-7. The biaxial braid is the most common form, typically using ±45° braid angle, although lesser angles are often used. The triaxial braid, as shown in Figure 3-7, involves a third set of yarns in the axial (0°) direction. The biggest issue is that the third set of yarns effectively locks the diameter, thus inhibiting the braid's ability to expand and contract.

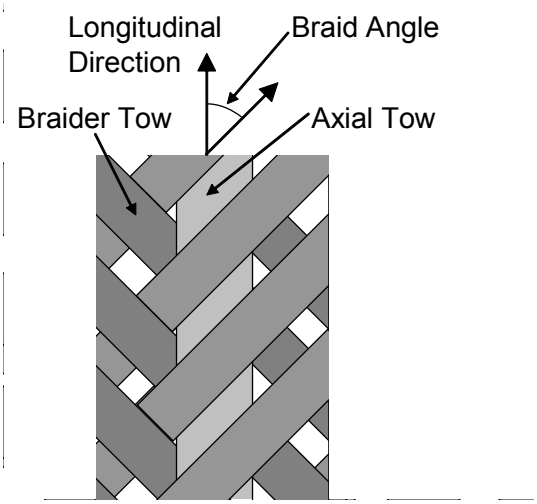

Figure 3-7: Schematic of 2D triaxial fibre architecture

An example of the notation for tri-axial braids is: [0_{15K} / ±60_{6K}] 50% Axial, which means there are 15K axial yarns and 6K bias yarns at 60º, with 50% of the total fibre in the axial yarns. The limitations of braiding technology are[184]:

- Biaxial and triaxial sleeves from 12.7-1200mm in diameter
- Biaxial and triaxial flat tape up to 200mm in width

The mechanical performance of braids is dependent on a number of factors. The braid angle has a large effect, with an increase in angle corresponding to a substantial decrease in Poisson's ratio, tensile strength and stiffness[165], however this has little affect on the fatigue performance. Typical endurance limit[xi] for braided composites is 40-50% of the ultimate tensile strength[165], which makes braids ideal for fatigue critical parts.

As the braid's yarns are mechanically interlocked, the load applied is evenly distributed, resulting in no knockdown in performance due to the inherent crimp[184]. However, during the fabrication of the braid, the fibres are typically unavoidably bent and twisted, due to their manipulation through the series of guides and pulleys on the carrier, which results in a knockdown in the fibre's performance by as much as 20%[185]. Cox and Flanagan[166] investigated the tensile and compressive modulus and strength of 2D triaxial braided in comparison to equivalent UD tape coupons. For a [0_{36K} / ±45_{15K}] 46% axial braid, the braid's principal tensile and compressive modulus was slightly better than the UD equivalent. In terms of tensile strength, the plain and notched strength was 37% and 17% lower than the UD equivalent, although it does demonstrate that braids are less notch sensitive. This is verified by work conducted by Falzon and Herszberg[185], who showed that 2D braids had a 10% decrease in tensile and compressive modulus, and a 20-30% and 40% knockdown in tensile and compressive strength, respectively.

Through the fabrication of a triaxial braid, all fibre angles, such as 0°, ±60°, are incorporated into one layer, whereas a UD laminate would require 3 plies. This means that the braid is less prone to delamination[174]. This is further aided through each lamina having the same properties, meaning the interlaminar stresses are reduced if all layers have the same orientation, meaning that braided laminates should have better interlaminar strength[186]. Impact tests have shown that fracture only occurs local to the point of impact on a braided

[xi] Endurance set at 1x 10^6 Cycles.

laminate, whereas typically a UD prepreg laminate can suffer badly from damage propagation[174].

Triaxial braids were used on the NASA ACT lower wing cover for the stringers, as illustrated in Figure 3-8[176], as the fabrication was more cost-effective than NCF, although the component performance was slightly inferior[187]. The 2D triaxial braid had a (0°±60°) laminate, with AS4 6K bias fibres and IM7 36k axial fibres, with bias being 56% and axial being 44% of the fibres[176]. The braided tubes are folded flat, with a resultant thickness of 1.2mm, with each tube having the same width, hence the 45° bevelled edge. The drapeability of the stringers was also considered to be advantageous in comparison to NCF and UD-prepreg alternatives[166].

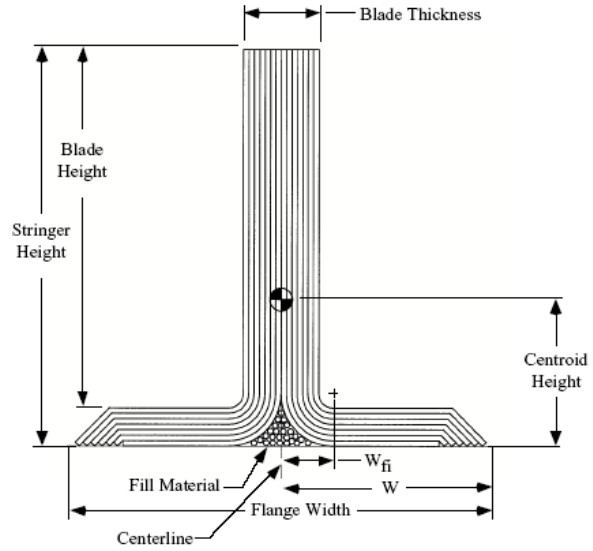

Figure 3-8: Fourteen-tube stringer

3D braiding is where more than one layer of yarn is intertwined in the through-thickness direction, providing enhanced damage tolerance. However, when compared to 2D laminates with similar lay-ups and FVF, 3D braiding has lower in-plane properties, mainly due to the crimping of the fibres. It is possible to have various braid angles, although 90° yarns are not possible with the standard process.

3.3 Processes

With the impetus on maximising structural efficiency it is important that the manufacturing process supports this, by ensuring that the raw material properties are not degraded by the manufacturing process, albeit ease of fabrication and inspection/reliability[188] must also be considered.

To date, the manufacture of high-performance composite parts, in particular large shell structures like wing skins, use ATL deposited UD prepreg with an autoclave cure; which results in a structurally efficient yet expensive product[149]. Much experience has been accrued with this approach, thus making further major gains along the learning curve unlikely. However, as it is now an established process, with the principal composite manufacturers having invested significant capital funds to obtain this capability, this process is likely to remain the baseline process for the foreseeable future. Therefore, any novel technology that can substitute this traditional process must provide a significant advantage for it to be adopted, most notably a large reduction in manufacturing cost. Removal of the high-cost

autoclave is one of the key targets to reduce the cost of CFRP manufacture[189]. However, although many LCM techniques have been developed that have reduced the cycle time in comparison to an autoclave process, they typically have lower mechanical performance and are still expensive[160].

Furthermore, stacking layer upon layer to create the part, independent of it being UD prepreg or NCF, is not compliant with a lean production methodology. If this is the only way of fabricating such a part, then the fabrication of the preform should be pushed down the supply chain. Thus, risk sharing partners and increased outsourcing opportunities should be sought.

3.3.1 Material Deposition

3.3.1.1 CNC Cutters

Computer Numerical Control (CNC) cutting equipment is used to cut ply shapes out of the sheet feedstock, as this is faster and more precise than by hand[160], and can reduce off-cut material by optimising the ply nesting. Furthermore, it also eliminates the need for cutting templates, which will require maintenance, can be lost, and could lead to mistakes being made. For cutting uncured prepreg laminates either a reciprocating knife or ultrasonically driven cutter is used[190]. Typically, such machines, as shown in Figure 3-9[191] can cut several layers of stacked prepregs at one time, up to a thickness of 5mm, with release film between each ply, thus improving the process efficiency[146], with cutting speeds of 66m/min[192]. Such a cutting and collation machine costs $1.5 million[160].

Figure 3-9: Typical flatbed ultrasonic cutter

In preparation for cutting the flat laminate, the cutting bed is first covered with a plastic film and a vacuum is applied. The laminate is laid on top and covered with a layer of release paper. Finally, a layer of plastic film covers the stack and a vacuum is applied to hold the stack flat in readiness for the cutting operation. Such a machine could be used for cutting out the stringer blanks.

3.3.1.2 Automated Tape Layer

The manual lay up of large skin panels is expensive and impractical[193], as it requires a high amount of labour and frequent inspection steps to ensure that the plies have been laid correctly. Due to the constraint of the prepreg's tack-life, hand lay-up for wing skins would be too slow. A method that mitigates against these factors, as well as ensuring consistent results, for UD prepreg, is an ATL, which is an expensive piece of capital equipment, but is the most efficient method today of laying up parts such as wing skins[194]. An ATL is a purpose built,

multi-axis, numerically controlled, machine tool system[195], which has two basic configurations:

- Contour Tape Layer (CTL)
- Flat Tape Layer (FTL)

The CTL and FTL are very similar, however the CTL is more flexible in that it can lay both contoured and flat laminates, thus it is used for wing skins due to the typically complex Outer Mould Line (OML) definition, and the highly architectured skins. The costs for a CTL and FTL are $3m and $3.5m respectively (E-mail from Coyle, E. from MAG Advanced Technologies 09/03/09), however with software and installation costs, a factor of 1.45 should be applied[196], thus the costs for a CTL and FTL are $4.35m and $5.075m respectively.

Typical tape width is 300mm, with 200 to 300m length of tape on a roll, although up to 914m of material is possible[190]. There exists 'broad goods' with widths greater than 1m as well as narrow slit tapes with a width of 150mm[175]. Typically, the tape width is determined by the curvature of the tool, with greater curvature resulting in narrower tapes being used[195]. ATLs are limited in its ability to drop plies off, and on the ply cutting angle. In terms of off-cut material, as shown in Figure 3-10[197], the wider the part, the less off-cut material produced. The scrap rate achieved for an Airbus Industries horizontal stabiliser skin is on average 5%[193], although the buy-to-fly ratio is typically 1:1.3-1.4[198].

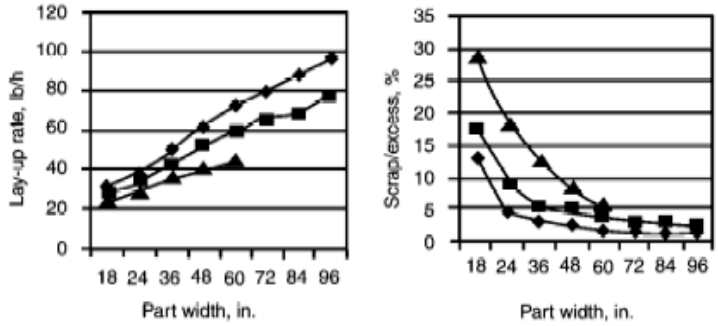

Figure 3-10: Estimated flat lay-up and scrap rates for 300mm ATL deposition

Tape courses can be laid either unidirectionally or bidirectionally, with bidirectional taking less time for courses greater than 1m[197]. There are three different material delivery processes for the ATL:

1. Single-phase
2. Two-phase
3. Dual-phase

The baseline solution is the single-phase process, where a spool of prepreg tape is loaded onto the machine head and feed through rollers and a cutter mechanism. The tape can then be fed and cut to shape with the backing paper continuously taken off and re-spooled on a take-up reel, while the CFRP is deposited. To cut the CFRP, the machine will either stop or slow down[199], and due to the complexity of profiling the edge of the cut, this is one of the reason why the deposition rate is low[181]. For a single-phase ATL the constant deposition rates are 15-20m/min (108-144kg/hr[xii]) for flat or shallow curved shapes[189], although 30kg/hr for 0.25mm

[xii] Based on 0.25 mm tape with 300 mm width.

tapes can be considered average (E-mail from Coyle, E, from MAG Advanced Technologies 09/03/09), which means for wing covers many hours will be required to lay-up the skin. For stringers 30kg/hr[xiii] can be considered typical using an FTL.

The two-phase system involves one machine to prepare the tapes to a particular length, which will mean that it is first un-spooled, the backing tape is taken off, cut to size and then re-spooled on a "cassette"[199]. The cassette can then be loaded onto the ATL. Using this system, the ATL must not stop or slow down for cutting the tape or to remove scrap. Dual-phase combines both single- and two-phase, as the head is configured for both single-phase and two-phase processing on opposite sides of the head, as shown in Figure 3-11[199]. This is the most industrious and flexible ATL process, and was chosen for the wing skins of the Boeing 787[199]. The machine only concentrates on lay-up, time is not wasted on cutting and removing the off-cuts. This should provide a deposition speed of 60m/min[198].

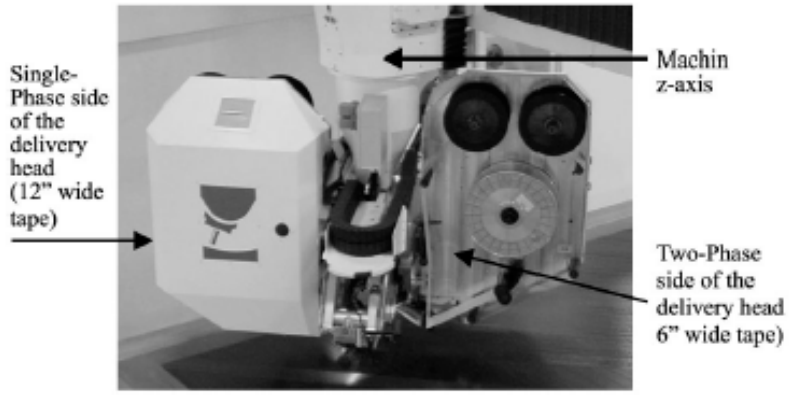

Figure 3-11: Dual-phase ATL head

The compaction afforded by the head is somewhat limited when the uncured laminate is thin. For this reason, the wing skin's first layer, which is the Lightning Strike Protection (LSP) mesh[193], is consolidated through vacuum bagging. Thereafter, the first layer of UD prepreg can be laid.

The latest ATL advancement is to "steer" the tape so that the tape does not follow the geodesic contour, but instead the desired path so that excessive gaps can be eliminated (E-mail from Coyle, E. from MAG Advanced Technologies 09/03/09). Furthermore, MAG Cincinnati has integrated an ultrasonic cutter into the tape head, so that there is no need to transfer and re-align the laminate on the cutting table.

3.3.1.3 Automated Fibre Placement

The choice between using an ATL or AFP is based on steering radius required by the surface. The steering surface is defined as the deviation from the geodesic path that must be given to the tape course so that it follows the surface orientation[194], thus fibre placement is more efficient for a highly profiled part than an ATL[200]. Furthermore, even a large relatively flat surface, such as a wing skin, will have relatively few long continuous tape courses, with AFP outperforming an ATL in its ability to perform short course placement[198].

[xiii] Note that the ply thickness for stringers is assumed to be 0.184mm, not 0.25mm as for wing skins.

Tows have a typical width of 3.2mm, although a minimum tow width of 2.3mm is deemed cost effective for large structures[171]. Gaps can form when depositing the tows if the component width changes or the surface is too undulating, with this problem being exacerbated when a wider tow is used. A wider tow impedes the ability to steer the tow, and hence counteracts the benefits of such a process. The material width can be changed through terminating or adding tows on the outside, which means thickness build-up is possible with one head pass. AFP will reduce the amount of scrap as the material is directly placed where it is needed, as the head can cut or restart any of the individual tows during the course[194].

Ingersoll Machine Tools have developed an AFP machine with a deposition speed of 30m/min[201]. With this increase in speed, the focus is on the amount of off-cut material produced; hence AFP can be more competitive against an ATL. A new machine called TORRESFIBERLAYUP aims to have productivity similar to an ATL but the ability to lay-up over complex surfaces like an AFP[194]. This machine can lay-up at rates of up to 85m/min, or 30-45kg/hr dependent on geometry[194], can be built as a gantry system so can lay up wing skins[194], and has between 4-32 tows (50.8-406.4mm)[194], which has demonstrated productivity higher than an ATL[194].

3.3.1.4 Automated NCF Depositor

The deposition of NCF by hand for a large complex component, like a wing skin, is not feasible. This is due to the large pieces of material requiring a number of people to handle them, the accurate positioning would be difficult, but also the QA issues, such as with manual prepreg deposition, rules out such a process for serial production. However, due to some technical issues, but also that the majority of development has occurred within the UD prepreg ATL/AFP technology domain, there exists no baseline method for the automated deposition of NCF for large structures. The benefits of automating any process is to standardise the process, to reduce variation between parts, as well as to increase the speed, which then offsets the high cost of the capital equipment, resulting in a minimised machine hourly charging rate. It would also be beneficial if the NCF depositing machine, like an ATL, can be universally applied to a number of similar parts.

A significant advantage with depositing NCF, is that it needs only to be laid up in one direction, typically in the 0° direction of the plies, which normally is the longest dimension of the part. This is due to the NCF incorporating angle plies in the textile. Therefore, the idea as proposed by Composite Systems Inc. as shown in Figure 3-12[202] could offer a suitable method for NCF deposition. A gantry, similar to an ATL is used, with a Precision Feed End-effector[xiv] (PFE), which can be used in conjunction with commercial robotic systems. The roll of material is loaded into the PFE at a "tool crib" offline, which is located adjacent to the robot cell[202]. The tool crib can house many different PFE devices, which are configured for different material widths, from 25.4-1524mm[203]. The tool crib can also house "end of arm" devices for the small plies that are not on a roll. This PFE device can manipulate the mould so it can place the material to the contour of the tool without having to program each point along a given path[203]. A deposition feed rate of 30m/min is foreseen[202].

[xiv] An end effector is the device at the end of the robotic arm, i.e. this is the part that interacts with the work environment.

Using the gantry system as shown in Figure 3-13[204], it is possible to have two gantries, or one gantry straddling two tools to improve production rate, i.e. the port and starboard wing skin could be deposited at the same time.

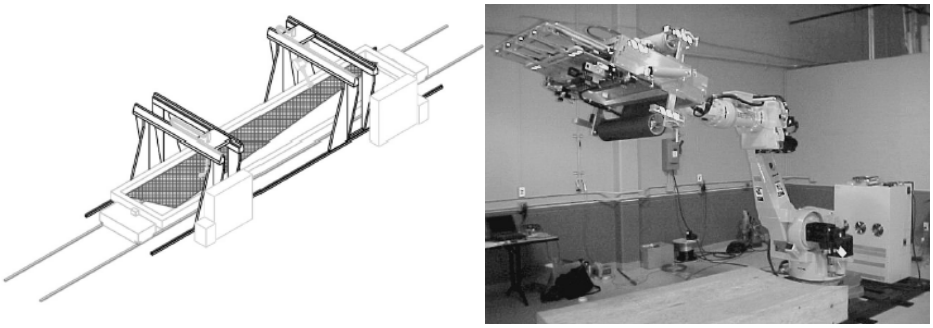

Figure 3-12: Gantry system for wing skin deposition and PFE device

Figure 3-13: Gantry system and robotic arm

As shown in Figure 3-14, a single layer of the overall NCF laminate can be fairly complex, due to the varying thickness of the skin. How such a layer is deposited is dependent on a number of factors, such as financially permissible amount of off-cut material, tolerable number of spanwise butt joints, and deposition time. Figure 3-14, shows 3 different methods in order to achieve the deposition of a single complex layer. The method shown in the top RHS of Figure 3-14 would require the complete layer to be cut to profile, using an ultrasonic cutter, which can then be rolled up onto the roll. Such a method could result in a large amount of off-cut material, but will minimise deposition time, as well as maximise the laminates strength, as there will be minimal butting of layers required. Alternatively, the method shown in the bottom LHS of Figure 3-14, has a roll width equal to the stringer pitch, and the strips of NCF can be deposited spanwise. This too will result in a fairly fast deposition rate, particularly as the strips have a constant width, but there will be many spanwise butt joints, which could be problematic. The third method, shown in the bottom RHS of Figure 3-14, has strip widths that are equal to a number of multiple integer pitches. Thus, for a basic 165mm stringer pitch, roll widths of 330mm, 495mm, 660mm, etc, are possible, with the upper limit set by the constraints of the machine. A decision could be made either to cut the NCF to the desired width as an internal process, or to order the material with the correct widths. This method could result in a number of spanwise, but more crucially chordwise butt joints, which can dramatically reduce the strength of the structure. Therefore, the first method, of pre-cutting the layers to the desired profile, will be considered as baseline.

For areas such as doublers, which will require a number of different size textiles, with no set width, and are likely to be too small to be collected onto a roll, then the method investigated

by Buckingham and Newell[205] can be applied. They considered the automation of depositing prepreg broad goods, with the setup of such a cell shown in Figure 3-15[205]. As this solution is for prepreg broad goods there was a necessity to remove the plastic protective layers, hence the fairly complex system in the area of de-reeling, however for NCF this would not be needed. The cutting area uses an ultrasonic cutter. The material handling robot[206] can then accurately put the ply where it is needed on the mould tool, to create the doubler preform.

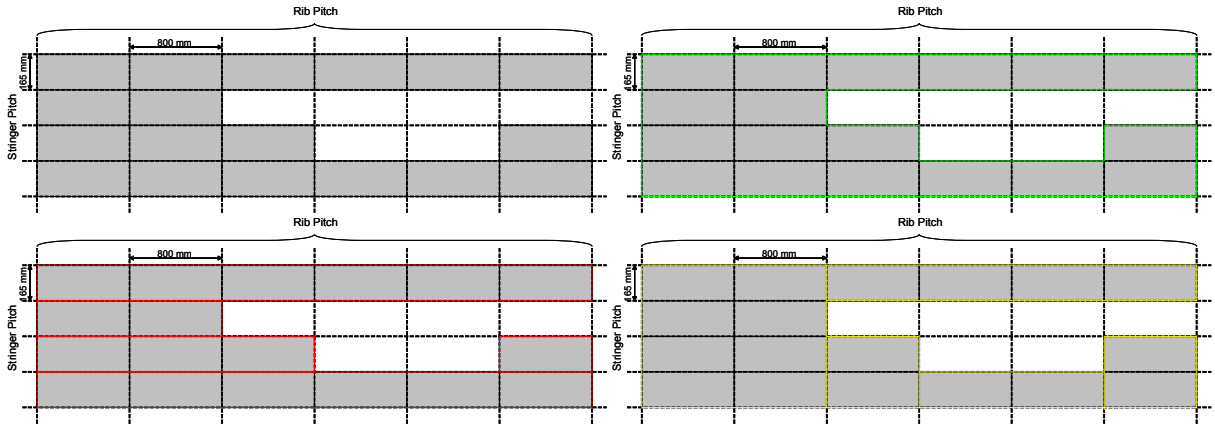

Figure 3-14: Different methods of depositing NCF based on skin architecture

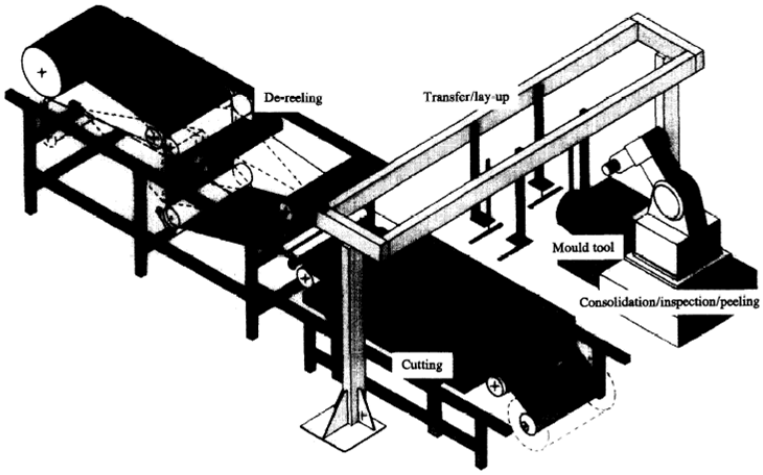

Figure 3-15: Setup for automated lay-up of CFRP broad goods

An issue with NCF is the lack of tackiness, which aids preforming of the overall skin. However, this can be overcome using a compatible epoxy resin binder, which can be applied to the NCF as part of the de-reeling and cutting process. A similar solution has been proven by Mills (2006)[181], using Cytec's Cycom 790[207] epoxy powder binder. Upon deposition, the fabric being laid can be heated to 80°C so that the binder becomes tacky and adheres to the adjacent material, to ensure that the NCF remains in position during skin deposition.

3.3.2 Autoclave Curing

An autoclave produces high quality and reproducible components, through the compacting and curing of the prepreg, with typically less than 1% porosity and a high FVF between 55-60%[143]. With autoclave curing, the thermal curing energy to initiate the polymerisation propagates through the monomers creating an exotherm, which can lead to thermal degradation[208], which is exacerbated with thick composites where heat dissipation is protracted. Therefore, long cure cycles are required, as shown in Figure 3-16[148], due to the

exothermal issues as well as to heat up and subsequently cool down the autoclave, with typical temperature increase/decrease at 1.5°C/min. The maximum pressure reached is 8 bar[143], which is 1 bar atmosphere, plus the 7 bar from the autoclave, although lower pressures are permissible as shown in Figure 3-16.

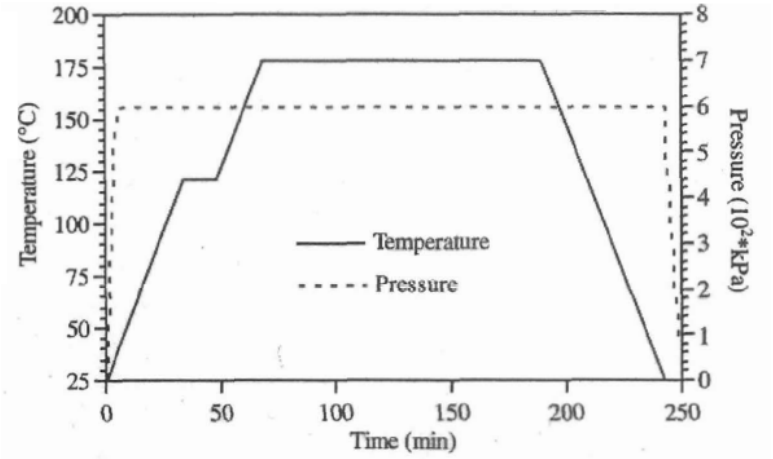

Figure 3-16: Typical autoclave cycle including dwell

In general, the process is expensive and time consuming, where the process time, including preparation can be up to 16 hours, and with an associated estimated cost of $640/kg[160], which includes the material cost and the preceding fabrication steps. An autoclave costs an estimated $2.0 million to purchase, although this is dependent on size, with an associated charging rate of $100/hour[160]. The typical process flow for an autoclaved part is as follows[143]:

- Lay up component on mould
- Enclose in flexible bag tailored to approximate shape and seal to tool
- Put into autoclave
- Flexible bag is evacuated thus removing trapped air and organic vapours from the composite
- Chamber is pressurised to provide extra consolidation during cure

3.3.3 Secondary Processes

3.3.3.1 Tool Preparation

Tools need to be thoroughly cleaned and inspected before lay-up commences, as tool indents can lead to surface defects on the cured laminate, as well as a clean surface is required for the mould release agent. Following this, at least one coat of mould sealer should be applied to seal in any micro-porosity. Prior to lay-up, it is necessary to coat the tool with mould release agent, which ensures the resin does not adhere to the tool during cure. Normally, release agent would be applied as required, however due to the high-value nature of aerospace CFRP components it is considered prudent to apply release agent each time the tool is used (E-mail from Rigby, M. from Marbocote Ltd 03/07/09).

3.3.3.2 Vacuum Bagging

The main purpose of the vacuum-bagging phase is to ensure all entrapped air is removed, so that a high-quality laminate with no voids or dry spots is produced. Shown in Figure 3-17 is a typical schematic for vacuum bagging both a co-cured and co-bonded (wet stringer) stringer-stiffened panel, and an uncured skin laminate.

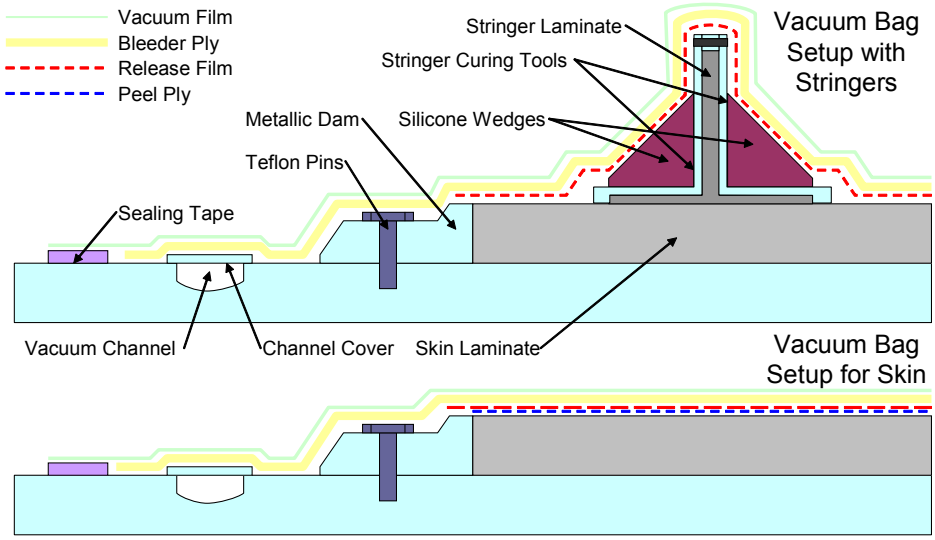

Figure 3-17: Vacuum-bagging schematic

A dam is required to ensure resin cannot escape from the part's edges, which can be assumed to be made from metal for large parts such as wing covers, which are held in place by either double-sided tape or Teflon pins[190]. The metallic dams are butted up against the edge of the laminate to prevent resin forming in the gap.

For all processes except co-curing with U-profile stringers, a peel ply is required on the Inner Mould Line (IML) of the skin. When subsequent bonding is required, such as for co-bonding (soft stringer) or secondary bonding, then the peel ply ensures upon removal that the surface is clean. Furthermore, a peel ply acts as a bridge between the laminate and the bleeder ply, helping to draw out the resin, as it is in direct contact with the uncured laminate and due to its fibrous nature. Therefore, either the complete IML is covered with a peel ply, or between the discrete stringers, for a co-curing or co-bonding (soft skin).

Subsequently, a layer of porous release material is required, which is typically a porous glass cloth coated in Teflon. This ensures that both resin and air can pass through this layer, while ensuring the bleeder material does not adhere to the laminate. For operations such as secondary bonding, release material is still required, but is only used locally, it does not have to be applied over the complete part, but only in the areas of the bond.

The bleeder itself is either a synthetic material, like a polyester mat, or dry fibreglass cloth. The thickness of the bleeder material is dependent on the thickness of the laminate itself, and the amount of resin to be bled off. A typical bleeder ratio of 0.3[190] can be used for a 42±3% resin content prepreg using style-120 glass cloth, hence for a 30mm thick laminate, 9mm thickness of style-120 glass cloth is needed.

The actual vacuum bag, made from nylon-6 or nylon-66, is then applied, which is sealed to the tool with a butyl-rubber or chromate-rubber sealing compound. If caul plates are to be used then they are placed either above the bleeder material or within it. For wing cover tooling, a vacuum channel is incorporated into the tool itself, as shown in Figure 3-17; therefore, the vacuum bag must extend over this line.

To ensure that the corners of the part are not bridged, which includes the breather material, it is necessary to use pleats to prevent bag rupture, which for a stringer-stiffened panel will mean much manual work. Bag rupture can lead to costly rework or the scrapping of the part. Without using cleats, the vacuum bag can wrinkle, which can leave an impression on the part, which is termed a "mark-off". Furthermore, deep channels can be filled with preformed rubber inserts[209]. For this reason, highly trained employees are required to carefully prepare the vacuum bag, which can take days to complete for complex stringer-stiffened parts, as shown in Figure 3-18[209].

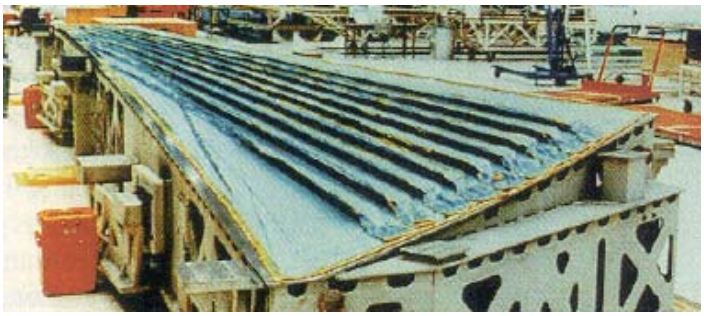

Figure 3-18: Vacuum bagging of the Boeing 777 empennage

It is possible to use reusable high-strength silicone rubber vacuum bags, in order to reduce the chance of a leak or rupture during cure, as the bag is thicker. An example of such a reusable vacuum bag is shown in Figure 3-19[190], which was used on the NASA ACT wing project. Reusable vacuum bags also reduce waste, have better part-to-part consistency, fewer fabrication steps, and can better accommodate complex structures[209], thus they can be more cost-effective. For large parts, these bags are heavy and difficult to handle, they also lack flexibility, for instance if there is a modification to the cover, the bag may not be able to accommodate the change. However, in general, the more complex the cover design, the more beneficial a reusable vacuum bag becomes.

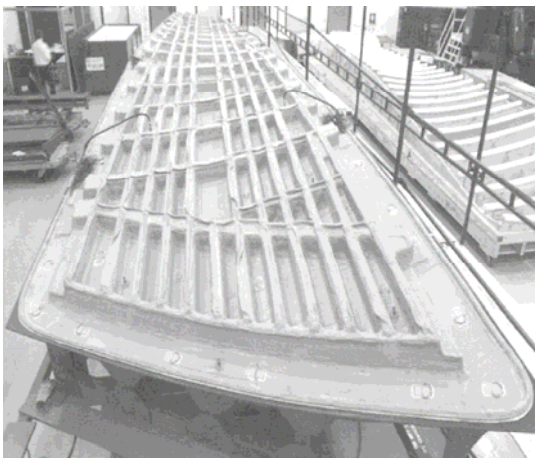

Figure 3-19: Re-usable bag (The Boeing Company)

Reusable bags can be particularly effective for an NCF solution, where debulking will be required, where costs can be cut by up to 50% in comparison to the single-use bags[210]. Such bags can be used for 30-100 cure cycles[211].

3.3.3.3 Debulking

After 3 to 5 plies have been laid up, it is necessary to debulk the plies using a vacuum[190], although for ATL plies, this is not typically required. Debulking is carried out by covering the laminate with a layer of porous release material, then several layers of breather material and finally, a temporary vacuum bag. A vacuum, of 1 bar, is then created to consolidate the laminate[158]. For complex parts, such as stringers, it may be necessary to hot debulk in an oven at a temperature between 66-95°C.

3.3.3.4 Bonding

Both paste and film adhesives can be applied. Paste adhesives may be supplied as either one-part or two-part systems, with the two-part systems needing to be mixed beforehand[190]. When applying film adhesive, it is necessary to ensure bubbles do not form; this can be achieved by using a roller or puncturing the bubbles. For elevated temperature (120-180°C) curing film adhesives, an autoclave is typically used to force the two adherends together. The bonding tool is similar to the curing tool, with the bagging technique also being similar except that no bleeder is required for secondary bonding. As the adhesive is used to join the stringer to the skin, it is advantageous to use a film adhesive, which has been cut-out to the profile of the stringer foot. The adhesive film is then positioned onto the stringer foot, while concurrently applying hot air to tack the film to the stringer foot, in readiness for subsequent process steps. The typical process for a 180°C adhesive system is as follows[190]:

- Pull a 0.68-0.98 bar vacuum and check for leaks
- Apply autoclave pressure between 1.03-3.45 bar. Vent once 1.03 bar has been reached
- Heat to 180°C at a rate of 1 to 3°C/min
- Cure at 180°C for 1 to 2 hours under autoclave pressure
- Cool to 65°C before releasing the autoclave pressure

3.3.3.5 Secondary Tooling Options

There are a number of secondary machining operations involved with CFRP wing box manufacture, such as[212]:

- Trimming/routing
- Drilling
- Milling

When machining, it is necessary to adhere to the given tolerances, for the basic dimensions, as well as an allowance on surface roughness. Machining of a CFRP structure is very critical, as it is one of the final processes, after a lot of added value has been inputted into the part, thus the cost of scrapping the part at this phase is enormous, which is compounded by the potential

impact on production schedule if a problem were to occur. With mechanical machining there are many variables that can affect the process, such as:

- Spindle speed
- Depth of cut
- Feed rate

Each composite part will have different machining characteristics, due to the nature of composites, which can result in varying levels of tool wear. Tool wear is primarily dependent on the following variables: fibre type, fibre orientation, and the resin, with tool wear primarily being attributable to the high mechanical resistance of the fibres[212], with IM causing greater wear than HS, due to the material's higher tensile strength. For a typical skin fabricated from IM fibre[xv] it is possible to route 17m in length before the tool has to be replaced[213], whereas with HS, 34m is assumed. With an increase in machining time, the tool cutting edges become progressively blunt[214], as well as an increase in cutting velocity will lead to an decrease in the tool life. The temperature during machining should not exceed the cure temperature of the resin system, otherwise the material could disintegrate[146]. For today's machine tools, the downtime due to tool failure is between 10-20%[215,216], which is exacerbated due to the limited ability to predict when the tool bit has to be replaced.

Routing can lead to matrix cracking, fibre pullout, inter-laminar voids, delamination, and resin melting[217]. The amount of delamination is also very dependent on the tool wear[212]. This results in costly rework for the damaged edges, which also slows down production. Issues can also be encountered with drilling, due to surface delamination and fibre pullout, with the quality of the drilled hole being dependent on the cutting parameters, tool geometry, and cutting forces (thrust and torque)[218].

Typically, high-speed steel in combination with a hard-wearing coat, such as tungsten carbide, titanium nitride, or diamond, are used to avoid excessive tool wear[146], with carbide being the hardest wearing, but also the most expensive. Cutter costs are far higher (up to 10 times more) for CFRP in comparison to metal[189]. A typical cost for a polycrystalline diamond router bit is $1400, whereas the solution offered by the Diamond Tool Company[219], with their chemical vapour deposition method of attaching the diamond substrate onto the tool costs $300 (E-mail from Bollier, R. from Diamond Tool Company 19/06/09). However, these tools cannot be reground or recoated after use.

The machining of large composite covers is carried out within a machine centre, with each machine having a universal table, which provides the following advantages:

- Can be used for different parts
- Does not need a jig to hold the part in position
    - Reduce tooling cost
    - No jig errors
    - No maintenance or calibration required of the jig itself
- Quick set up time

Such a universal table is available from MTorres, called the Torrestool, and from MAG Cincinnati, called the Universal Tooling System. When used in combination with a

[xv] Assumption is F-35 uses IM fibre – high performance aircraft, therefore high performance fibre is required.

routing/milling/drilling machine as shown in Figure 3-20[220], this can provide a very flexible machining centre. The cost of a basic machine is $1.9m (E-mail from Coyle, E. from MAG Advanced Technologies 19/06/09) to $2.8m (E-mail from Solano, J. from MTorres 20/06/09).

Figure 3-20: MTorres Torresmill and Torrestool

Alternatives to mechanical methods are: water-jet cutting, laser trimming, ultrasonic machining, and Electrical Discharge Machining (EDM). The disadvantage of laser trimming is that it produces heat affected zones, whereas the ultrasonic and EDM methods have low cutting rates[212].

3.3.3.5.1 Water-Jet Cutting

Water-jet cutting is most suitable for trimming cured CFRP laminates, although the CNC machines are expensive, it reduces the number of tools required. Water-jet cutting rates can be used for CFRP thicknesses between 2.5-75.0mm, with a resultant surface finish within the standard set by aerospace manufacturers[217]. Feed rates are dependent on the thickness of CFRP, as shown in Table 3-7[221], with thicker parts requiring a slower feed rate.

Material Thickness (mm)	Feed Rate (mm/min)
≤ 12.7	381
25.4	254
25.4 – 50.8	127-152

Table 3-7: Water jet cutting speeds

However, there are a number of issues with the process. As it is a noisy process it must be isolated within a sound proof room[190], hence the facilities may have to be adapted to suit. Further issues include, the need to filtrate the water, due to both the abrasive material in the water (garnet grit), as well as the CFRP particles; the nozzle has to be checked for wear; if used for drilling holes and slots, then delamination can result[222]; also it is not always suitable for 3D applications[223], as it can damage features behind the one being trimmed Finally, there is a chance that the trimmed CFRP may absorb some of the water, as well as the abrasive solution may remain on the part, which then requires a separate cleaning operation[223]. Large gantry systems, enclosed in a working envelope of 7.5×3×1m, can cost between $1.2-1.8 million[224].

There are hybrid gantry systems that incorporate both a 5-axis water jet cutter and a 5-axis router, with the water jet cutter having a catcher on the 6th axis to catch the exit water, which is then collected in a tank[217]. The router is used to drill and countersink holes, or trim critical areas not accessible with the water jet cutter. Such machines can be up to 46m long and 15m wide.

3.3.3.6 Inspection

Inspection techniques range from visual inspection to automated techniques. Non-Destructive Testing (NDT) using a C-Scan technique can be used to find the following flaws in a laminate:

- Delaminations
- Porosity
- Inclusions
- Debonds

C-Scan is a highly effective way of measuring most flaws, due to its high penetrating power. However, local inhomogeneities, due to the stacked laminate, reduces the reflected energy, which requires skilled operators to decipher the results. The cost for an NDT machine with C-scan, which can scan a wing cover similar to the A350XWB, should cost approximately $2.8m (E-mail from Brown, M. from M-Tech UK (aeromachinery) 19/06/09).

3.3.3.7 Painting

Typically the standard process is to apply an epoxy primer and then a polyurethane topcoat. Before painting, the surface should be cleaned to remove all dirt and oily substances. If a peel ply has been used then it must be removed. The surface should then be prepared for painting by scuff sanding, using 150-180 grit sandpaper or with light sand blasting[190]. The epoxy primer should be applied within 36 hours of surface preparation[190].

3.3.3.7.1 Primer

The most common primer is an epoxy-primer, as the epoxy component acts as a binder, which gives the primer excellent adhesion and chemical resistance[225]. The other component of the two-component system is polyamide, this gives the primer durability. Once the two components are mixed, the curing reaction begins, which after a dwell time of 30 minutes can be sprayed onto the part that requires painting. The dry film thickness is typically between 15-24μm, unless a double coat is applied. The primer is applied and then cured for at least 6 hours at room temperature.

3.3.3.7.2 Top Coat

Polyurethane paint is typically applied as a top-coat as it protects against the operational environment and enhances the optical quality of the surface[225]. The typical dry film thickness is 50.8±7.6μm. For the polyurethane coat, the initial cure takes between 2-8 hours and a full cure within 7-14 days at room temperature[225].

3.4 Cost Effective CFRP Solutions

There are two basic issues hindering the further application of CFRP, namely cost and damage tolerance. The acquisition cost and through-life costs for CFRP products are far

higher than for metallic components[189], with more than half the cost associated with the deposition, cure and assembly, with assembly representing the largest cost[226], which can typically constitute 40% of the total manufacturing cost[189]. To improve the applicability of CFRP, a complete shift in the airframe cost versus weight curve is required. In order to achieve this, the following technologies need to be developed[22]:

- Lower cost materials
- Preforms
- LCM techniques
- Advanced curing technologies
- New sandwich technologies
- Automation of component manufacture

40-50% of the cost of a CFRP piece part is the raw material[154], however this might not be the most likely source of large reductions in cost of CFRP parts. Even if wider spread use of carbon fibre meant a reduction in roving cost, the carbon fibre manufacturers cannot be expected to commission and ramp up production without a strong commitment from the major aircraft manufacturers[227]. Therefore, a reduction in CFRP waste, as a by-product of the process, should be sought. Hence the need for net shaped preforms, fabricated from the lowest cost carbon fibre source, i.e. rovings.

The NASA Advanced Subsonic Technology (AST) project considered the issue of the substantially higher cost of toughened resins, in comparison with standard un-toughened resins but using through-the-thickness stitching, as a cost-effective alternative to counteract the damage tolerance of CFRP[176]. The study was based on a wing stub box, which represented the inboard portion of a high-aspect ratio commercial aircraft wing[228]. The following manufacturing methods were investigated[229]:

- Aluminium riveted solution
- "B" stage hand lay-up autoclave process
- Standard ATL
- Advanced ATL (today's state of the art)
- Automated "B" stage tow placement
- Dry fibre uniwoven fabric/resin infusion process (one-shot)
    - Utilises stitching of skin and stringers
- Dry fibre NCF/resin infusion process (one-shot)
    - Uses 12k tows as opposed to 3k tows for uniwoven fabric
    - Utilises stitching of skin and stringers

A cost exercise, based on a 6.1×2.4m panel, was conducted to see which of the methods could provide the most competitive CFRP solution in comparison to the metallic baseline. The results, based on recurring manufacturing costs are shown in Table 3-8[229]. This illustrates that using large complex preforms with NCF/stitching and untoughened resin system, could match the cost of the aluminium baseline.

The concluding cost estimation from the NASA ACT wing project, showed that a highly integrated cover with stitched stringers, intercostals and spar caps, using RFI, could achieve an overall RC saving of 20%[xvi], as shown in Table 3-9[176], in comparison to the baseline

[xvi] Based on averaged RC over 300 ship sets for both material and labour.

aluminium design. The highly integrated wing covers reduced the number of mechanical fasteners needed[230], by 86% in this project[176], which consequently minimises the labour effort required. Such an approach has been found to be cost effective in the aerospace industry[160].

Fabrication Method	Material ($)	Labour ($)	Total ($)	% of Aluminium
Aluminium	21,056	11,366	32,392	100
Uniwoven "B" Stage Hand Layup & Autoclave Cure	45,453	120,600	166,053	512
Standard ATL / Autoclave Cure 12k Tow	29,692	16,550	46,242	143
Advanced ATL / Autoclave Cure 12k Tow[xvii]	29,692	13,056	42,748	132
"B" Stage Automated Tow Placement / Autoclave Cure 12k Tow	29,692	13,103	42,795	132
Uniwoven Dry Fibre Stitched Preform RIP Impregnation and Cure 3k Tow	40,347	26,375	66,722	205
NCF Dry Fibre Stitched Preform RIP Impregnation and Cure 12k Tow	20,410	10,505	30,915	95

Table 3-8: Costs for different material and manufacturing techniques for wing covers (FY 1995)

	Aluminium Wing Box Cost (M$)	Stitched/RFI Wing Box Cost (M$)	Reduction (%)
Total Structural Wing Box	3.181	2.544	20
Structural Wing Cover	1.516	1.147	24
Wing Substructure	0.461	0.429	7
Wing Assembly	1.204	0.968	20

Table 3-9: Wing box cost analysis (FY 1996)

Lockheed Martin initiated a self-funded project called Advanced Affordability Initiative (AAI), the aim of which was to find a radical new manufacturing process to heavily reduce the manufacturing costs[231]. They investigated the feasibility of fabricating a basic skin from IM7 UD prepreg, due to the superior in-plane properties, whereas the doublers were fabricated from fabric IM7/5HS. The fabric used was preimpregnated with 9% resin, in order to give it enough tack on fabrication, but dry enough to allow an RTM process to be used, which has been specifically developed by Cytec[231].

Finding the best compromise between capital equipment utilisation and material utilisation is also very important. For instance, a highly tailored skin may require less time to lay-up using an ATL, in comparison to an AFP, but the amount of off-cut scrap could be far higher. Matching the number of tooling sets with the capital equipment needs to be considered to maximise the utilisation of the capital equipment. For instance, an autoclave might typically only be used once a day using a single set of tooling, thus if the same tooling is used to lay-up the part, then additional sets of tooling may be required, to ensure that the autoclave can be fully utilised. Alternatively, for RTM parts, a rate of a 1000 parts a year can be achieved from a single set of tools[160].

[xvii] For the "B" Stage Hand Layup, the materials cost should be about 50% higher as the costs were assumed for an un-toughened resin system.

3.4.1 Lower Cost Materials

3.4.1.1 Material Qualification

Typically for each new aircraft program, the aircraft manufacturer wishes to have a higher performance CFRP system. However, the cost of developing new systems is expensive, and the material suppliers must do this without securing a viable financial future. The aircraft manufacturers will take the view that they are already taking a big enough risk in developing and marketing the aircraft, without taking on further risk further down the supply chain. In order to reduce the risk to the material manufacturers, some will only develop part of the new system, such as Cytec often uses fibres developed by their rival Hexcel[232].

It can be argued that a government-controlled institute could create a material database, which could then be used by a multitude of companies who pay a subscription fee, in order to reduce the cost of establishing material allowables. However, with such a proposal there are a number of foreseeable problems. If the institute created its own standards, as might be expected, the material suppliers would have to adhere to those new standards, which could be far more complex and stringent than those previously used to place the material into the marketplace. Under such circumstances, this could stifle the iterative improvement in materials, as seen today. Furthermore, as the major aerospace composite manufacturers have their own manufacturing procedures, this can lead to slight variation throughout the life cycle of the raw material, from its transportation, storage conditions, lay-up environment, technique of bagging, cure cycles, and amount of resin content in the basic system. This variation means that no two manufacturers will be able to use the same allowables[233]. Therefore, it is not considered possible to have universal allowables similar to those available for metal alloys.

3.4.1.2 Hybrid Laminates

Due to the anisotropic nature of the CFRP laminate, varying the fibre type used through the laminate's thickness can enhance both the mechanical properties and the cost effectiveness. This is known as a hybrid laminate, which can entail the following permutations:

- Glass and carbon fibre hybrid:
  - Has potential to eliminate durability/damage tolerance as a design driver[135]
  - Thermal mismatch between carbon and glass can cause distortion in the laminate
- IM and HS carbon fibre hybrid
- Titanium (thin layers with equivalent thickness to carbon layers) and carbon hybrid[234]:
  - Beneficial where bearing strength is critical
  - Will not necessarily lead to a lighter structure but should be thinner

From these choices, a hybrid laminate combining HS/IM fibres and the CFRP/titanium should offer the greatest advantage for wing covers, and hence will be discussed in greater detail.

3.4.1.2.1 Intermediate Modulus/High Strength Hybrid Laminate

In a multidirectional laminate, the plies that are not orientated along the principal stress direction are under-utilised in terms of their load-bearing capability[235]. Therefore, based on

this assumption, lower performance HS fibres are employed in the ±45° and 90° orientations, whereas IM fibres are used in the 0° orientation, which can lead to a better match of stability and strength performance of the laminate.

This concept has already been investigated, as part of the NASA ACT program, using Hexcel's IM7 fibres in the 0° orientation and AS4 fibres in the other orientations[236]. Furthermore, Hitchen and Kemp[235], found that the hybrid laminate had very similar performance to the pure IM with respect to tensile strength, as would be expected as tensile strength is dominated by the fibres in the principal stress direction. The compression strength was better with the HS laminate, however the hybrid laminate's performance was between that of the HS and IM laminates. In terms of the flexural stiffness the hybrid was superior, which can be explained, as the flexural stiffness is generally dependent on the Young's modulus and the shear modulus, with the IM fibres in the hybrid improving the Young's modulus, while perhaps the shear modulus of the HS fibres is slightly better. The CAI strength, after an impact of 7J, for the IM laminate was superior to the hybrid, whereas the HS laminate had the lowest performance.

It is known that the laminate's bending stiffness, and hence the buckling performance, is dependent on the D-matrix, thus ±45° plies on the outside of the stack is very important, and a fibre with higher modulus will improve the overall performance. This is shown in Figure 3-21, for a 5mm laminate using 0.25mm thick plies with a stacking sequence of $[+/-/0_2/90/0/-/0/+/0]_s$, and a panel dimension of 160×700mm. Figure 3-21 illustrates that the normal hybrid, is slightly better than a pure HS laminate, however it has over a 10% knockdown in performance when compared to the pure IM laminate. It can be seen that a significant improvement can be made if the outer ±45° plies use IM fibre, as opposed to the minimal contribution that the innermost ±45° plies from IM make. Therefore, a hybrid laminate, with the outermost ±45° plies using IM fibre, can offer a cost effective alternative to a pure IM laminate.

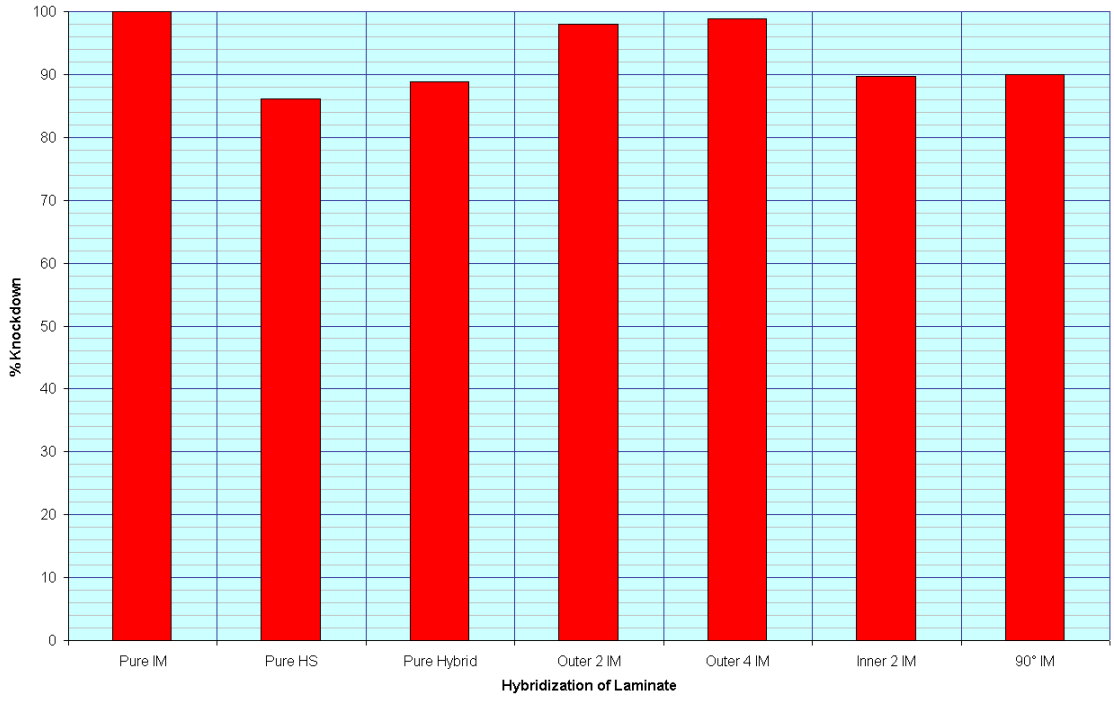

Figure 3-21: Knockdown in axial stability performance for a 5mm laminate with varying degrees of hybridisation

NCF is particularly compliant to a hybrid laminate, as the stacks can be pre-ordered with the required ply architecture. It is, however, not inconceivable that an ATL, such as a two-phase system[199] could be used to deposit a hybrid UD prepregs laminate.

3.4.1.2.2 CFRP/Titanium Hybrid Laminate

A CFRP laminate's bearing and shear capabilities can be improved using high strength metals like titanium[237], to form a Fibre-Metal Laminate (FML). Such titanium foils could be integrated into the laminate locally, where a joint exists, either by adding the plies to the base laminate or substitution, as shown in Figure 3-22. It has been evidenced that by adding titanium to the base CFRP laminate, the bearing strength is improved. The bearing strength for a 70/20/10 laminate and a CFRP/titan 45/0/0 [55] laminate, i.e. 55% of the laminate is titanium, is 571MPa and 1574MPa[238] respectively, whereas for a 50/40/10 laminate and a 70/0/0 [30] laminate, the bearing strengths were 927MPa[237].

The load carrying ability of the hybrid area is dependent not only on the amount of titanium, but also the transition from pure CFRP to the hybrid laminate[237]. A well-designed transition zone will ensure that this is not the weakest part of the joint; hence the joint area should not limit the part's performance.

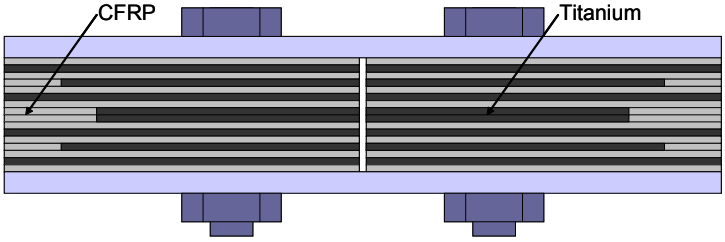

Figure 3-22: CFRP/Titanium joint and transition zone

Due to the inclusion of titanium in the laminate, aspects such as CAI strength and the influence of environmental conditioning should be considered. The difference in stiffness, between the carbon fibre and titanium layers, can cause greater delamination upon impact. However despite this, evidence exists that the residual CAI strength of a titanium/carbon hybrid laminate is higher than for an equivalent homogenous CFRP laminate[237]. Environmental conditioning does not seem to adversely affect the interlaminar shear strength of the laminate[237].

Bearing/bypass strength can be critical for both normal joints, such as for a stringer coupling, but also if bolted repair is considered. Thus, for a CFRP/titanium hybrid to be purposeful when repair is considered, such a hybrid laminate would be required for every part of the structure where the load is above the critical limit, where bearing will size the structure. Thus in this respect, the hybrid laminate is no longer a local consideration, but instead global.

3.4.2 Preforming

Textile preforms allow complex three-dimensional geometries to be created, in a cost and structural effective manner. Near net-shape preforms should have the following advantages:

- Aligned and optimised fibre direction

- High FVF
- Automated fabrication
- Online quality control
- Enhanced damage tolerance

In general, the principal issues that hinder the widespread application of preforms are:

- Dimensional stability of the preform itself
  - Inability to handle long and continuous items, such as the stringers and skin
- Dimensional tolerance of the cured part
- The preform has a complicated microstructure, and the ability to parameterise and model the preform is limited by the fidelity of structural analysis methods

In general the production of preforms can be carried out via two methods:

- Binder preforming
  - Uses a polymer that binds fibre textiles together through heat activation
- Textile preforming
  - Adopted techniques from the clothing industry

3.4.2.1 Binder Preforming

The binder is either a liquid or powder, which is heated to activate the binder's adhesive properties. A liquid binder is less expensive than powder binders[xviii] and is easier to tailor the quantity over a given area, as it can more easily penetrate the fibres, which improves cohesion. However, liquid binders may impede the ability to lay the plies quickly.

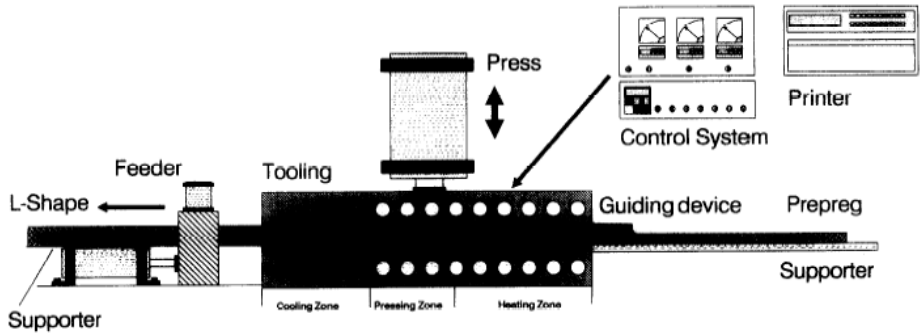

Figure 3-23: Continuous compression moulding technique

Preforming stringers is possible with a continuous compression moulding technique, due to the stringer's long prismatic shape. This technique amalgamates the pultrusion and hot-press techniques and is a continuous operation. Although in the work by Pantelaskis et al.[239], this technique was envisaged for the manufacture of thermoplastic stringers; it can also be used for consolidating preforms. The experimental setup shown in Figure 3-23[239], illustrates the material being placed on a linear steel support with a guiding device. The mould, incorporated into the press machine, is divided into three zones. In the first zone, the material is heated so that the binder can react, whereas in the second zone the material is pressed, and the third

[xviii] Lecture notes from Mills, A. Investigation of the Design, Manufacture, Processing and Performance of Carbon Fibre Preforms for Lower Cost Manufacturing of Aerospace Composite Components.

zone is where cooling is done, typically using water. By the time the material passes through the tooling area, the stringer has been preformed to the desired cross-sectional shape.

There are also 'binder yarns'[240] that are activated via oscillation or radiation, and will adhere to other binder yarns, carbon fibres, mandrels or any other suitable surface. Issues exist with the use of binder yarns, such as ensuring compatibility with the resin system, hence epoxy binders are preferred.

3.4.2.2 Textile Performing

Much can be learnt and adapted from the clothing industry, concerning textile preform fabrication. The industrialised process for the production of clothing involves four distinct steps:

1. Fabric cutting
2. De-stacking/ply separation
3. Handling/transportation of the fabric panels
4. Sewing/making-up

Through ply nesting techniques, dry fabric and prepreg can be cut to reasonable accuracy in an efficient manner to produce net-shaped plies[241]. These plies can then be positioned by hand, using laser positioning, in the mould. Currently, in the aerospace industry, it is economical to cut single layers, as opposed to cutting multiple layers in the clothing industry[242]. However, if it was deemed necessary for economic reasons to cut a stack of plies, then a number of automated processes, which are used in the clothing industry, could be applied to separate the individual layers after cutting, such as:

- Blowing a jet of air
- Electro-adhesion
- Chemical-adhesion
- Piercing pins
- Human finger like arrangement

However, such automated processes are not reliable due to several issues, for example, the air stream displacing the fibres[241]. However, this can be improved through the use of binders, which allows the preform to be more easily handled and impregnated without any serious fibre re-orientation. A number of devices have also been developed to transport a fabric panel to a joining station[242]:

- Vacuum grippers
- Friction plates
- Electro-static grippers

3.4.2.2.1 Textile Preforming Example

A stitched stringer preform can be created as shown in Figure 3-24[229]. The first step, as shown in the LHS of Figure 3-24, is to pre-fabricate two separate textiles using 4 stacks of 9 plies that are stitched together with a 25.4mm stitch density over the complete area. In order to

form the T-profile stringer, the two textiles are brought together and in the region of the blade they are stitched using a 12.7mm stitch density as shown in the RHS of Figure 3-24. The final step is for the feet to be folded out and trimmed to size.

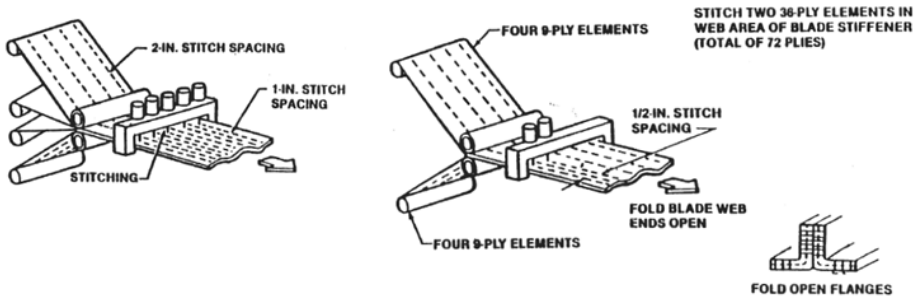

Figure 3-24: Preformed stringer with stitching

This idea can be enhanced at wing cover level, as shown in Figure 3-25[176], with integrated intercostals for attachment of ribs, and integrated spar caps to attach the spar web. The intercostal clips are designed to transfer compressive crushing and tensile fuel pressure loads[169], whereas the spar cap is interleaved into the cover for effective shear transfer from spar to skin.

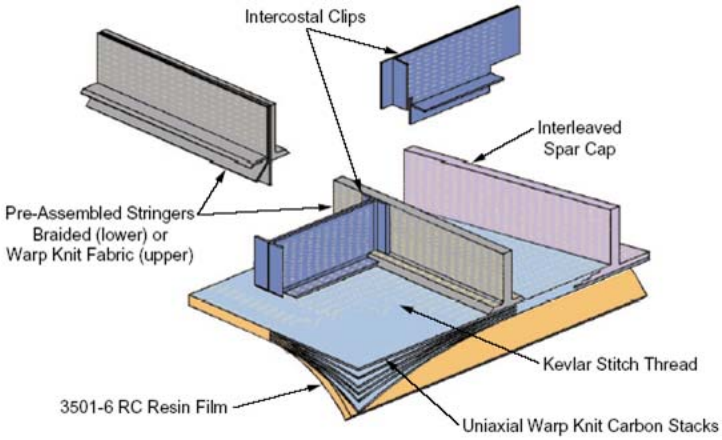

Figure 3-25: Integrated wing covers

3.4.3 Liquid Composite Moulding Techniques

LCM in combination with textile preforms offers the potential for cost-effective composite manufacturing, as it uses the lowest cost constitutive materials, i.e. a dry fibre and a separate resin. All LCM processes have a common attribute, in that a liquid monomer is injected into a cavity filled with a preform, which means a low viscosity resin is required to ensure complete wet-out of the preform[243]. Some of the different LCM techniques applicable to the manufacture of aerospace parts include:

- RTM
- Vacuum Assisted Resin Transfer Moulding (VARTM)
- Differential Pressure Resin Transfer Moulding (DP-RTM)
- Vacuum Assisted Resin Infusion (VARI)
- Vacuum Assisted Process (VAP)
- RFI

A drawback with most LCM processes is the possible degradation in the control of the FVF, which affects the parts dimensional accuracy, although techniques exist to mitigate this. LCM techniques are being used by Airbus to produce wing panels, vertical stabiliser ribs, rear pressure bulkheads and other primary structure[136]. The use of an oven and a vacuum bag over an autoclave reduces the capital cost from $2.0M to $0.5M[160]. Furthermore, as illustrated by Figure 3-26, the oven can be built to the required dimensions, in order to maximise utilisation, whereas an autoclave, due to it acting as a pressure vessel, is cylindrical in shape, hence space utilisation can be fairly poor.

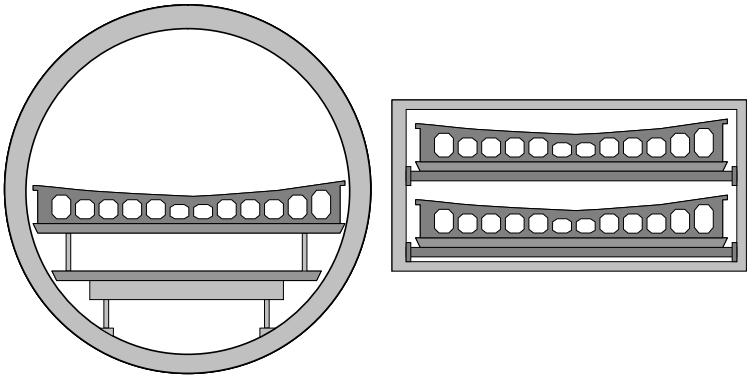

Figure 3-26: Comparison between space and its utilisation for an autoclave and oven

3.4.3.1 Resin Issues

The low-viscosity resin systems used for LCM, such as RTM6, are typically variants of conventional systems, albeit with added diluents to lower the resin's molecular weight[243]. Furthermore, the critical addition of toughening additives used in prepreg resins are omitted, hence the impact and notched performance of traditional LCM parts are fairly poor. The addition of toughness additives to the resin will typically result in higher viscosity and elasticity, principally due to the higher molecular weight of the thermoplastic[244], which reduces the chance to ensure complete wetting of the preform to avoid the pitfalls of voids or porosity[245].

Contemporary toughened LCM systems use two methods to integrate the thermoplastic element into the complete system. The first method is to use a powder binder, however the amount has typically been fairly small, thus its effect is localised[243], resulting in an uneven distribution of the toughening agent through the part. Alternatively, a fleece binder can be used, which is a thin veil of thermoplastic and structural fibres, with an areal weight of less than 20g/m² [243], which upon cure is a way of interleaving the toughening agent to ensure a homogenous structure. This is the principle that Cytec's Priform™ system uses[243], which has very similar properties to Cytec's 977-2 prepreg system[245].

3.4.3.2 Particular Processes

3.4.3.2.1 (Vacuum Assisted) Resin Transfer Moulding

An RTM process should result in reduced manufacturing cost due to lower associated assembly time and cost of the raw material, albeit the preforming of the woven fabrics can be higher than that of prepreg manufacture[181]. As there is no need for vacuum bagging, as well as fewer trimming and finishing operations, this will reduce the overall labour costs and result in

shorter cycle times[182]. High FVF of between 55-60% can be achieved[164]. The basic processing steps of RTM are as follows[146]:

1. A thermoset resin and catalyst are placed in separate tanks of the dispensing apparatus
2. A release agent is applied to the form tool
3. Preform is placed in the mould and the mould is clamped shut
4. The mould is heated
5. The mixed resin is injected through inlet ports at a pre-determined temperature and pressure (for VARTM a vacuum can be created in the mould)
6. Resin is injected until mould is filled. Vacuum is then switched off, and outlet port is closed
7. After curing the part is removed from the mould

Tooling is made from either aluminium or steel[146] and is normally double sided, therefore close dimensional tolerances and improved surface finish can be achieved and reduce Volatile Organic Compounds (VOC) emissions. Tooling costs are high for parts that are over a few meters in dimension[167].

VARTM is based on the same principles as RTM, but using only single sided tooling, as illustrated in Figure 3-27[182], with a vacuum applied to the preform, which improves the resin infiltration due to an increase in differential pressure. A pure vacuum moulding process uses the atmospheric pressure to consolidate the material during cure, which means there is no need for physical pressure from an autoclave or a hydraulic press[143]. The typical resin systems used for vacuum only processing are cured at 60-120°C, and then post-cured at 180°C to fully develop the resin properties.

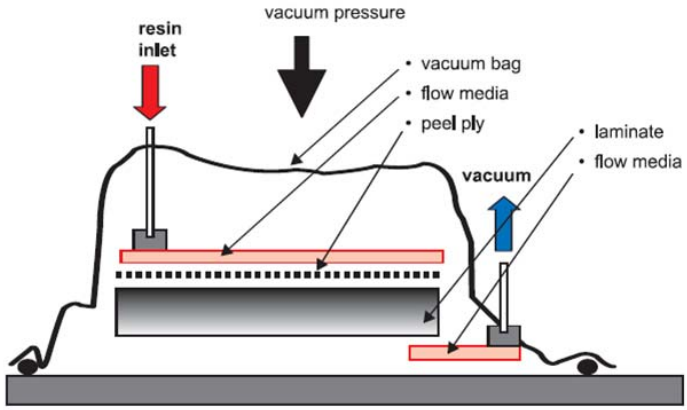

Figure 3-27: Cross-section of VARTM tool

The FVF for VARTM is typically less than 54%[176], however if used on sufficiently thick parts, such as wing skins, significant pressure is needed to infuse the resin, which will ensure a FVF of between 57-60%. To achieve this, several debulking operations are required prior to resin infusion. Alternatively, a VARTM-PB (pressure bleed) process can be used, which should achieve a FVF of over 57%, and due to the use of an autoclave this enhances the dimensional tolerance[176], albeit at a subsequent increase in manufacturing cost.

Similar processes such as the VAP process, which is a patented process owned by European Aeronautic and Defence Space Company (EADS), ensures both low porosity and enhanced FVF, which is a consequence of maximum pressure being maintained throughout the complete infiltration process[174]. Furthermore, Modified Vacuum Infusion (MVI) has been used on an advanced wing technology within Airbus, with NCF material achieving less than 1% porosity and approximately a 60% FVF[246].

3.4.3.2.2 Resin Film Infusion

RFI is based on a resin film media concept, where heat and pressure is applied to allow the infiltration of the resin through the thickness. The RFI process has the resin film laid, which is pre-calculated based on the volume required to achieve the desired FVF, onto the tool surface with the dry fibre preform on top, as shown in Figure 3-28[166].

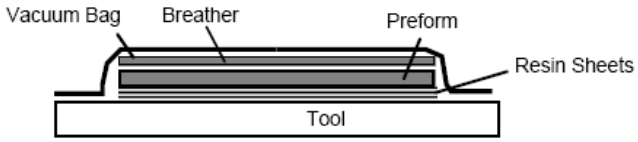

Figure 3-28: RFI process

The advantages of this process are that only one major tool surface is required, and that there is no economical or technical restriction on part size, as the resin flows through the thickness. The cost of the film resin is often twice the cost of a normal liquid resin, and because of the low areal weight, many plies of film are required[164]. The RFI process used on the lower cover panel on the NASA ACT semi-span wing cover panel for a co-infused process achieved a FVF of 59% in the skin and 57% in the stringers[176].

3.4.3.2.3 Hybrid Process

Another strategy as shown in Figure 3-29, is to combine a prepreg skin and a dry preform stringer with a resin film between the two constituent parts; this can provide the following advantages:

- Stringers can be ordered as preforms
- Skin can be laid using ATL
- Better than trying to resin infuse the whole cover, resin has to only infuse the stringer preform
- Still one shot so minimal use of autoclave

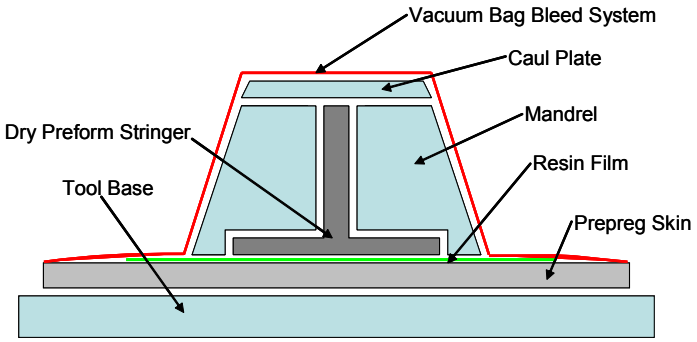

Figure 3-29: Possible tooling philosophy for an RFI stringer preform on a prepreg skin

3.4.4 Advanced Curing Techniques

3.4.4.1 Same Qualified Resin Transfer Moulding

Radius Engineering Inc. has developed an approach called Same Qualified Resin Transfer Moulding (SQRTM), which uses contemporary prepreg woven materials to create net-shaped CFRP parts[247].

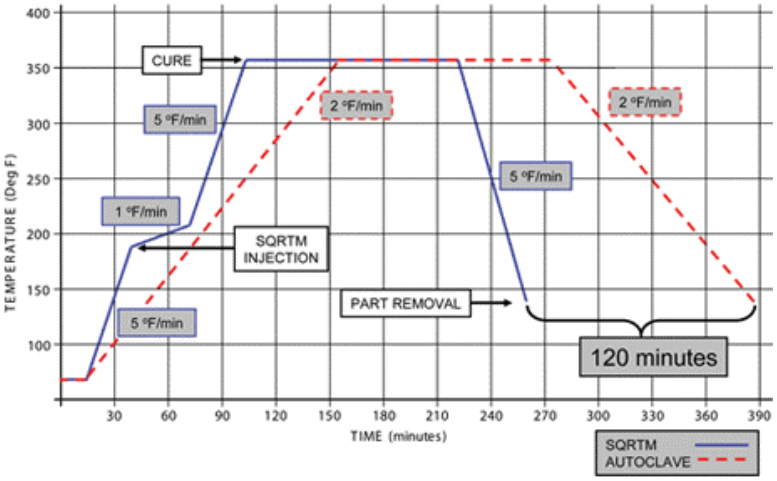

Figure 3-30: Comparison in the process time required between SQRTM and autoclave cure

There are two principal benefits of using this system. Firstly, by using an already qualified prepreg system there are no associated costs of resin qualification, which would be required for a new liquid resin needed for traditional RTM. Secondly, as shown in Figure 3-30[247], by using a hydrostatic-pressure process, i.e. further resin is injected, this can save about 120 minutes in curing time.

3.4.4.2 Quickstep™

The Quickstep™ process is a patented process, which cures prepreg material under a vacuum pressure, with the heating and cooling of the tool through a glycol based Heat Transfer Fluid (HTF) medium[248], using a pressure of 1.1 bar for curing, which is far lower than with an autoclave[249]. This lower pressure is sufficient to consolidate the laminate due to the lower initial resin viscosity with the Quickstep™ process. An autoclave or an oven will impart the heat into the part (and the tooling) via the medium of the gas inside the autoclave, which results in long cure cycles. Fluids though, as used by the Quickstep™ process, have higher thermal conductivity, heat capacity and lower thermal inertia in comparison, thus achieving the same dwell and curing times, but within a shorter time[248]. A reduction in the total curing time of 43% can be achieved with the Quickstep™ process, in comparison to an autoclave, due to the increased temperature rate, from 1.5°C/min for the autoclave to 6-9°C/min for the Quickstep™ process[249].

A cost comparison between a 1.8×5m autoclave and a 1.8×1.8m Quickstep™ curing chamber, including the associated equipment, showed that the Quickstep™ required a 62% reduction in capital expenditure[248], although as the autoclave is larger, the comparison is not totally fair. Similarly, a reduction in RC of 25% and 80%, for labour and energy respectively, are achievable using the Quickstep™ process[248].

In general, the mechanical performance of the laminate is not adversely affected by the Quickstep™ process when compared to an autoclave process[249]. Furthermore, it need not necessarily inhibit part integration, as it can also be applied to co-curing parts together[248]. Furthermore, as lower pressure is used with the Quickstep™ process, caul plates can be applied to define the critical interface surfaces such as for the ribs and spars of the wing-box, thus avoiding the witness marks that occur when caul plates are used with the higher-pressure autoclave cure.

3.4.4.3 Electron Beam (Microwave) Curing

This process directs the heat/energy straight into the part to be cured, rather than by surface heating and thermal diffusion, which reduces the cure time significantly. In terms of the economic benefits of such a process, it has been shown through independent studies that cost savings of 10-50% can be obtained, however this is dependent on the design of the part, production volume, etc[250]. However, such technology is novel and hence carries high risk but with huge potential[135]. It also does not suffer from the residual thermal stresses associated with autoclave cure[251], due to exothermal issues[208].

3.4.5 Sandwich Structure

The development of structural sandwich components is driven by lower component price, enhanced recyclability and improved work environment, and not necessarily the desire to achieve further weight saving[252]. The basic concept of a sandwich structure is to combine two thin and stiff face sheets bonded to a comparatively thick and light core, as shown in the LHS of Figure 3-31[253]. By sandwiching the core between the two face sheets a product with high bending stiffness and low weight is created[252], and typically at a lower cost than a monolithic laminate. The face sheets can be made from fibre-reinforced composites or other materials. The reinforcing fibres used are typically glass, carbon or Kevlar[252], in combination with either thermoset or thermoplastic resins. The sandwich is mainly honeycomb using either Nomex®[xix] or aluminium, and foam cores[254]. Some of the advantages of composite sandwich structures are[255]:

- High strength-to-weight and high bending stiffness-to-weight ratios
    - Hence carry in-plane and out-of-plane loads and maintain stability under compression
- Two load-carrying face sheets reacting the tensile and compression stresses, which maintain their stability across their whole length
- Have fewer parts and manufacturing steps when compared to bonded monolithic parts

Failure characteristics of sandwich structure are very different to that of monolithic CFRP, with limited knowledge of low velocity impact behaviour and its effects on the structural performance[254]. When impact occurs it may be difficult to detect, due to the possibility that the damage might be internal, creating uncertainty, which can result in large knockdowns in strength and stiffness[256]. Furthermore, sandwich processing requires a lower cure pressure of

[xix] A registered trademark of DuPont. Nomex is an aramid fibre-paper which is impregnated with a phenolic resin.

3.5 bar, which can induce fibre waviness and increase the amount of rework required, in comparison to 7 bar, which is typically used for a monolithic laminate[189].

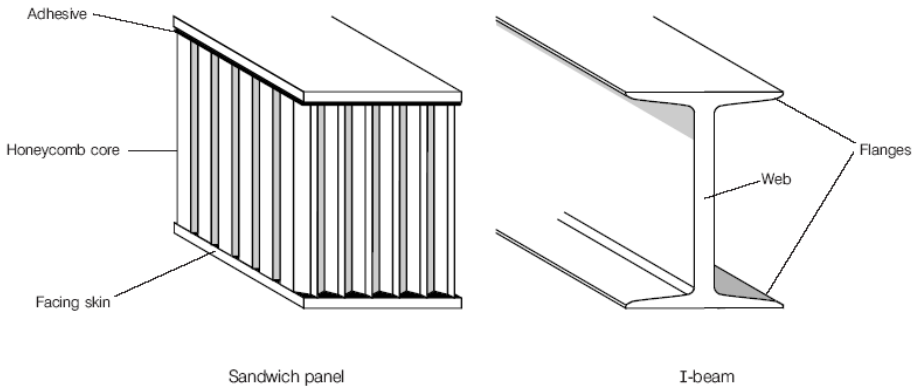

Figure 3-31: Comparison of sandwich panel to I-beam

In the advent of damage during service or assembly, honeycomb sandwich structures can become saturated in fuel or water, which is exacerbated through freeze-thaw cycling resulting in damage propagation. This occurred in secondary structure sandwich panels on the Boeing 737-300, 757 and 767[3]. Due to these issues, sandwich components must be inspected more regularly, which increases the maintenance costs. Other issues associated with honeycomb include face-sheet debonding and costly repair of damaged skins[44,257], leading to the US Navy excluding the use of honeycomb for aircraft in its service, as well as aircraft manufacturers having replaced or phased out many honeycomb structures[44]. Finally, for highly loaded parts a substantial and dense core could be required, which may negate some of the benefits of a sandwich part, i.e. low weight and low cost.

3.5 3D Conversion of 2D Laminates

3.5.1 Stitching

Stitching involves passing a thread through the prepreg or dry fibre, and is considered a low cost option to produce 3D composites. It is more effective with dry fibre as the needle can easily push aside the fibres, which means that the in-plane fibres are damaged less, and the stitching process is faster and can be used on thicker preforms, as prepregs are tackier, which impede the action of the needle[166]. The amount of stitching is normally 1-5% of the total fibre in the preform which is comparable to the through-thickness reinforcement found in 3D woven and braided composites[164].

Investigations have previously been conducted into integrated wing skins and spar joints, using stitching, which demonstrated that the stitched joint was similar if not superior to secondary bonding or co-curing, and mechanical fastening[164]. Stitching can be beneficial in the following respects[258]:

- Enhances resistance to delamination, especially at free-edges and cut-outs
- Improves impact damage tolerance
- Constructs three-dimensional shapes from separate plies
- Can ease handling by joining the fabric plies together
- Stitching can be applied only to areas where it is beneficial

Stitching has a number of parameters that can be varied:

- Stitching thread
  - Material type (carbon, glass or Kevlar), tex/denier, finish, twist
- Stitching pattern
  - Pitch, row spacing, direction, angle
- Stitching process
  - Machine type, thread tension, needle size, needle type

Kevlar or polyester yarns are normally used, as opposed to carbon or glass, as they are more resistant to rough handling, as both carbon and glass suffer from brittleness. However, Kevlar yarns, as well as polyester yarns will, under hot and humid conditions, acts as a pathway to absorb moisture[258], resulting in microcracks forming. Furthermore, they do not bond well to normal polymer resin systems[164]. Kevlar 49, in particular, has some drawbacks as a stitching material[259], thus Kevlar 129 should be used[256].

Tufting is a single sided stitching process, which can be used to attach parts together or provide through-thickness reinforcement, as shown in Figure 3-32[260]. The tufting process involves a needle carrying a thread that penetrates the preform but does not interact with another mechanism at the furthest point of the stroke. Instead, the balance of friction between the withdrawing needle and the thread, and between the thread and the surrounding material into which it has been inserted, encourages the thread to remain in-situ whilst the needle is withdrawn[164].

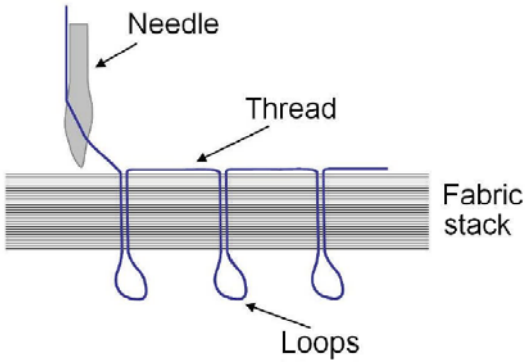

Figure 3-32: Schematic of tufting

From the plethora of published literature on the virtues of stitching, there is much contradictory information concerning the influence on mechanical performance of stitching. As stated by Tong et al.[164] "This implies that tension, compression and flexural failure is not determined by the collective action of many stitches but rather that a single stitch or a small number of stitches and the damage arising from them can determine strength." Furthermore, it seems that high density stitching to provide efficient impact damage tolerance will not reduce further the in-plane properties than if it had low density stitching. The types of defects stitching can cause in the laminate are:

- Fibre breakage
  - The stitching speed can be reduced to negate this effect
- Fibre misalignment which primarily affects the compressive properties
  - The stitching speed can be reduced to negate this effect
- Fibre crimping which primarily affects the compressive properties
  - Has greater effect on a thinner laminate than a thicker one[261]

- Resin-rich regions due to crimping and fibre misalignment
- Micro-cracking
- Compaction, resulting in a higher FVF than considered

As shown in Figure 3-33[166], the effect of stitching leads to a knockdown in plain strength performance, however the allowables that size a structure, i.e. notched and CAI, are all higher with stitching, so much so that a NCF with Hercules 3501 can outperform the 8551-7 toughened epoxy for CAI. Similar results were found by Cox and Flanagan[166].

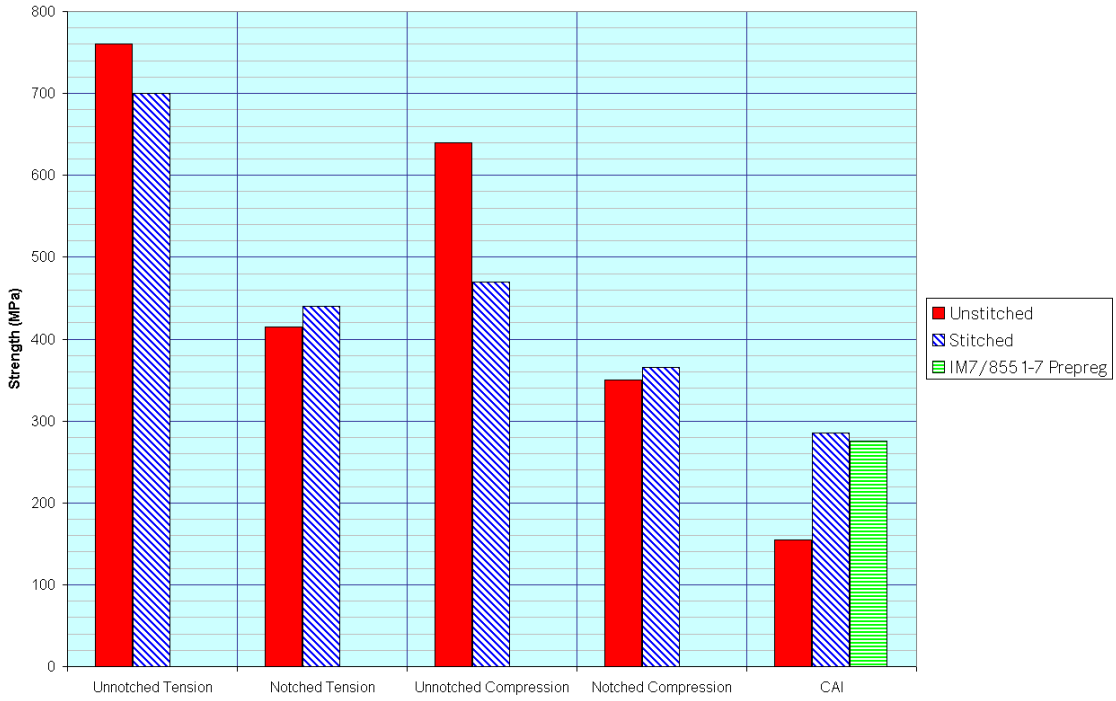

Figure 3-33: Tensile and compressive strength of unstitched and stitched laminates

Stitching provides an extra number of variables, which must be modelled and understood so that confident structural analysis can be performed. Alternatively, much testing must be carried out to create a comprehensive database of mechanical properties. Only with these methods will certification be possible to allow stitching to become a standard process on commercial aircraft.

Examples of the application of stitching includes work conducted by the University of Aachen, Germany, who stitched preforms consisting of multiple layers of NCF with blade stringers attached on one surface[175]. Furthermore, Fuji Heavy Industries Ltd have produced panels representing wing covers with top-hat-profile stringers, which was manufactured using the RTM method and was reinforced by stitched fibre to provide better damage tolerance properties[262].

The most outstanding work carried out to date was during the third phase of the NASA ACT project, with a large multi-head sewing machine that stitched layers of carbon fibre NCF together to form a wing cover. The machine was 28m long, stood 5.2m tall and was built over a pit 6.4m deep, as shown in Figure 3-34. The pit allowed for the movement of the table sections and the supporting equipment. Modified lock stitching type was used on the wing cover preform, thus access to both sides of the preform was required. This meant the table which supported the preform during stitching was divided into 50 sections. This allowed for a single section at a time to be locally removed, so that the stitching could take place, while the

remaining 49 sections remained in place to support the preform. The machine, with its high-speed stitching heads, was capable of 800 stitches/min[135]. The stitching of the complete cover took 14 hours without the need for manual intervention, which included the stitching of the stringers and intercostals to the wing cover.

Figure 3-34: NASA ACT sewing machine and cover manufacture

3.5.2 Z-Pinning

Z-pinning is a simple method of applying through-thickness reinforcement, however in comparison to stitching it cannot be used as a medium to fabricate preforms. However, Z-pinning is advantageous to stitching due to:

- Size and shape is limited for stitching, or less a large purpose-built machine is used
- Z- pinning is better for reinforcing regions with small radii of curvature
- Careful tension control is required with stitching to minimise fibre crimping, Z-pins are independent of each other
- Z-pinning does not break so many fibres, just disorientates them, the hole created is filled by the Z-pin and not a resin rich area, due to the needle diameter being greater than the thread diameter

However, using Z-pins will limit the integration process to co-curing. Other concerns with Z-pins are their longevity and repair. Z-pins can be fabricated from Silicon Carbide/Bismaleimide (BMI), T650/BMI, T300/Epoxy, T300/BMI, P100/Epoxy, S-Glass/Epoxy, titanium, stainless steel, aluminium and Kevlar[263,264], the choice of which is dependent on the application. Pin diameters can range from 0.15-1mm in diameter[263], although typical diameters are either 0.25 or 0.5mm.

Z-pins are inserted using a preform that is initially placed on top of the fully laid up but uncured prepreg laminate or dry fibre, in the area where the laminate needs to be reinforced. A layer of Teflon coated glass fabric[148], whose function is to protect the surface of the laminate from damage and contamination, is inserted between the laminate and the preform[263]. This method of inserting the Z-pins involves a combination of pressure and heat in an autoclave, which compacts the preform and forces the Z-pins into the laminate. Such a process is very good in terms of being able to process many areas, however it is limited to a very low pinning density of <0.5% due to the high pressures required to insert the pins[263].

Aztex Inc. has created another method called Ultrasonically Assisted Z-Fiber™ insertion, which is shown in Figure 3-35[164], and is the common process currently used. With an ultrasonic head the process is far more adaptable with different size and shape heads available. Once the fibre is inserted, the compacted foam from the preform is removed and any excess pin length is further compacted by the ultrasonic 'hammer'[263]. However, it is still an expensive additional manufacturing process[256].

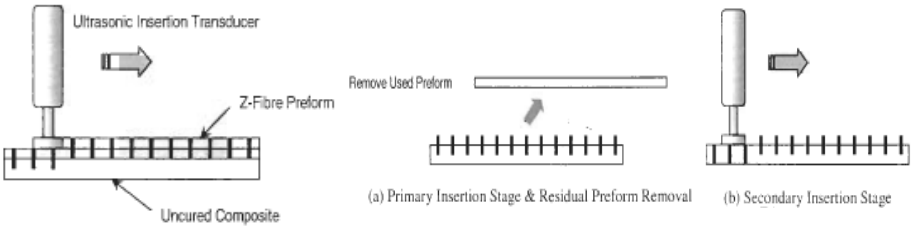

Figure 3-35: Z-Fibre™ insertion process using ultrasonics

3.6 Stringer Manufacturing Methods

3.6.1 Conventional UD Prepreg Stringers

The varying thickness laminate is laid up using a 2D ATL, with the laminate typically having a sufficient area, so that a multiple number of stringer profiles can be cut out of it. A comparison is shown in Figure 3-36, illustrating the nesting of several stringer preforms (RHS), or just a laminate large enough for just a single stringer preform (top LHS). By nesting the preforms, this should result in slightly better material utilisation, in particular when the ±45° plies are considered, but it will also result in a far higher average deposition rate per stringer angle, as the time to lay up will be more efficient with longer strips. However, due to the odd profile of the stringer preforms, it can be easily seen why a material utilisation of 50% might only be possible. It could also be envisaged to nest both stringer angles, for one stringer, on the same laminate, as the thickness distribution will be the same, as shown in the bottom LHS of Figure 3-36, however this could lead to even lower material utilisation.

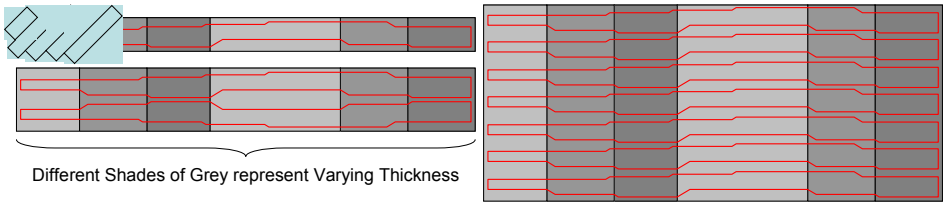

Figure 3-36: Nesting to make a family of parts versus single strip for single stringer

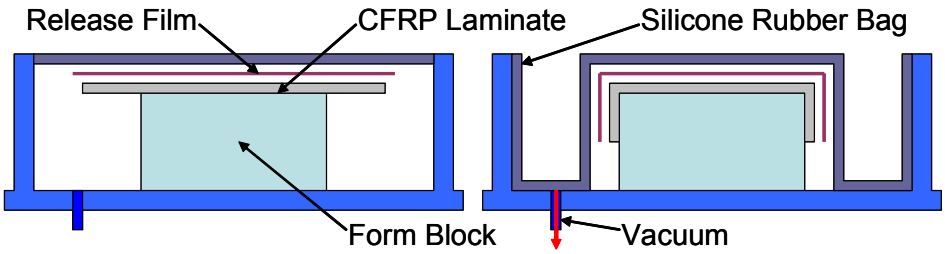

Figure 3-37: Vacuum forming

The traditional stringer manufacturing method involves curing at least two separate parts together, as explained later in section 7.3.6.8, which are preformed to shape and cured together to form the profile of the stringer. The preforming process for the stringer's constitutive angles, as shown in Figure 3-37, involves heating the laminate to 70°C to soften the laminate. Once the laminate is softened, a vacuum is applied, which brings the silicone rubber bladder onto the tool, to form the laminate to the desired shape. If the laminate is too thick, i.e. greater than 5mm, the process of preforming to the desired shape can be done in several steps, in order to prevent wrinkling of plies. If required to maintain equal tension during the forming, a double diaphragm can be used, where the plies are sandwiched between

two thin flexible diaphragms that are pulled together with a vacuum, which is done with heat to aid the forming[190].

The preforming process for the complete stringer is highlighted in Figure 3-38, where diaphragm vacuum forming is used to preform the angles, as explained previously, then a matching pair of preformed angles are brought together, sandwiching if necessary the spine laminate, to obtain the correct blade thickness. Subsequently, a noodle is positioned in the area of the Bermuda triangle then the capping plate laminate is placed on top. The tooling and the stringer preform are enclosed within a vacuum bag, which is typically lined with a bleeder ply, and then a vacuum is applied. This will remove any trapped air between the laminates, and reduce the preform in thickness. Finally, the stringer can be prepared for curing, if required, by attaching the curing plate. Although Figure 3-38 illustrates a discrete T-profile stringer; an I-profile stringer can be similarly formed.

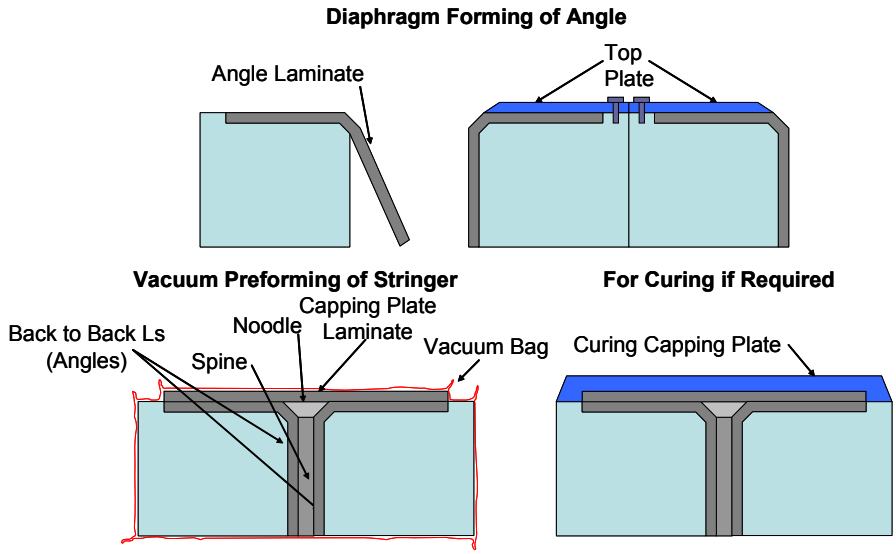

Figure 3-38: Discrete stringer forming process

Not only is the approach both time consuming, but it also can limit the total length of the stringer that can be manufactured, due to difficulties in handling the long slender laminate lengths. If the stringer is to be subsequently co-cured or co-bonded, with the stringer being soft, then principally the profile of the stringer will be determined when it is ultrasonically cut out before forming. However, pre-cured stringers, used for secondary bonding or co-bonding, with the stringer being hard, will incur a machining operation to finish off the profile.

3.6.2 Conventional NCF/Braid Stringers

The manufacture of NCF stringers is similar to UD prepreg stringers, the major difference occurs in collating the laminate. For NCF stringers, the required plies are cut out individually from the NCF textile, which should increase the utilisation of the material. The plies required for the angles, the spine and the capping plate are brought together and debulked/preformed, using a binder in the NCF that is activated under applied heat and pressure. The individual parts are brought together, including the roving for the Bermuda triangle, then again heat and pressure is applied to preform the stringer profile. A braid stringer is very similar, except that the braid sleeve is cut only lengthwise as required.

3.6.3 Pultrusion

Pultrusion techniques for aerospace applications are reaching maturity, with improved part quality[171], offering one of the few continuous automated processes for composite part manufacture, high material utilisation, and has excellent dimensional control and fibre alignment. Mainly dry fibres in the form of rovings[160] are used with the traditional pultrusion process[265], although fabrics and mats can be used to give multidirectional strength properties[146]. Epoxies are not the ideal resin system to use due to processing issues, which is further compounded with lower pulling speeds due to the lower resin reactivity.

A problem with conventional pultrusion techniques is the inability to fabricate parts with varying cross-section, which is a prerequisite for wing covers. New processes such as Pulforming, Selective Interval Pulshaping™[266] and 3D Pultrusion™ have the ability to overcome the limitations of conventional pultrusion technology[171], although this technology lacks maturity today.

3.6.3.1.1 Advanced Pultrusion

Jamco Corp. has developed an Advanced Pultrusion (ADP) method, which uses prepreg to manufacture constant section stringers. The purported advantages are an increase in FVF from 55% for traditional pultrusion processes up to 65%, if desired, with ADP, as well as a decrease in porosity, and an increase in angular tolerance[265].

As shown in Figure 3-39[265], the process starts with prepreg rolls being fed into a preforming device, which shapes the plies to the desired cross-section profile. This preformed shape is then heated and pressed to ensure consolidation of the laminate, before being cured, and thereafter machined. Using one machine, about 2m of stringer can be processed in an hour.

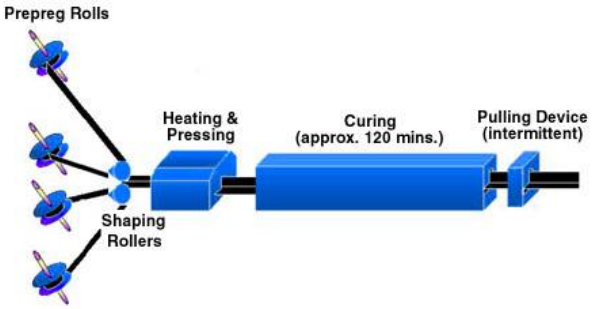

Figure 3-39: ADP process

3.6.4 Roll & Fold Forming

Roll forming uses pre-consolidated UD prepreg laminate, heated to the required temperature for moulding, which is typically carried out using an infrared preheating oven. The steps to form a T-profile stringer, as shown in Figure 3-40, is to start with a flat laminate, pre-develop the profile through a series of rolling stations, then based on the required stringer height, the web and foot are formed, thereafter the profile is consolidated[267]. Further steps will involve curing and being machined to profile. It is possible for the thickness of the laminate to change along its length[268], as well as the blade height and foot width to vary. A constant feed rate of 1.5m/min is possible[268]. Braided tubes or dry fibres with a heat-activated binder can be used

as well[268], with the resin infused after forming. The major advantage of this approach to stringer fabrication is to eliminate matched tooling, vacuum bagging & autoclave tooling.

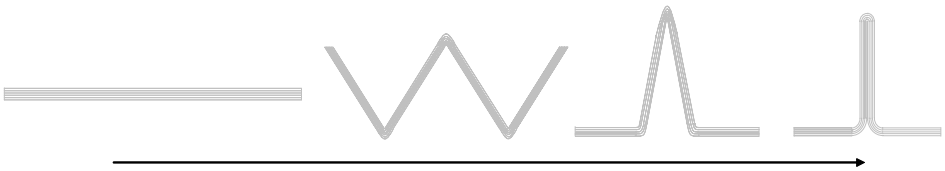

Figure 3-40: Stages of stringer roll forming

A similar method, as shown in Figure 3-41[269], can produce stringers with varying cross-section, with the principal forming steps being:

- The flat laminate is positioned between the lower and upper jigs
- The laminate is pushed down by the rod to fold the laminate
- Rod is extracted and outer jigs are squeezed together

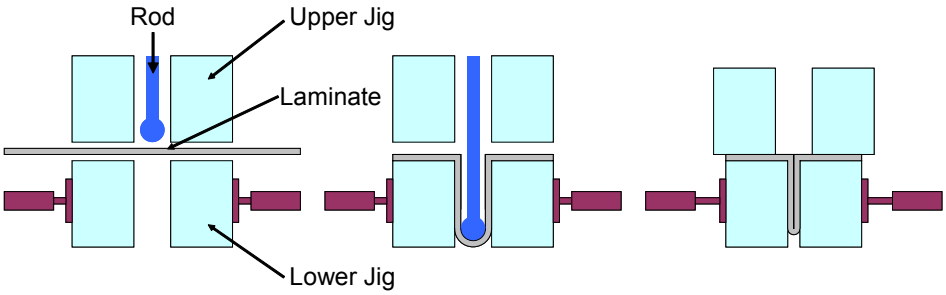

Figure 3-41: Folding stringer manufacturing method

This process could be augmented by replacing the rod with a pre-cured spine, so that the stringer's blade thickness can be easily altered without having to thicken the uncured laminate being formed. Furthermore, the hard spine could have a bulb at its extremity, so that buckling efficient T-profile bulb stringers can be fabricated.

3.6.5 Top-hat Stringer Manufacture

In order to manufacture CFRP top-hat stiffened panels, a mandrel is required to fill the cavity between the skin and the stringer during cure. Semi-solid mandrels such as low Coefficient of Thermal Expansion (CTE) flexible metal mandrel, or a silicon mandrel[270] could be considered. However, when designing metal mandrels, it is necessary to minimise the interference between the stringer and mandrel, otherwise the extraction of the mandrel will be difficult[271].

Alternatively, a sandwich core can be used as a mandrel. However, honeycomb sandwich cannot withstand the autoclave cure pressure, but ROHACELL does[272]. Furthermore, a top-hat-profile stringer filled with ROHACELL will improve the strength and fatigue life of the stringer, with the possibility that the wall thickness can be reduced due to the foam, in comparison to a hollow section. Top-hat-profile stringers filled with ROHACELL have been applied to the A340 and A380 rear pressure bulkhead, with the ROHACELL mandrels being delivered direct to Airbus Stade (Germany)[272]. Normal 180°C cure with 3.5 bar cure pressure can be used, but it can also be used with LCM techniques[272].

3.7 Tooling

3.7.1 Principal Forming Tooling

Invar® tool steel is typically used due to its thermal stability, damage resistance, and longer life, however it is heavy, expensive and requires a long heat soak to bring it up to temperature[189]. To increase the surface finish of the moulded parts, as well as extend the life of the tool, the tool surfaces can be hard chromium plated[160].

The different methods of wing cover integration will require different tooling. The modular aluminium block co-curing procedure, as illustrated in Figure 3-42, is known to produce high-quality parts. Through controlled thermal expansion of the aluminium blocks, due to the internal heat and pressure of the autoclave, both the skin and stringers will be consolidated. However, due to the high setup times and tooling costs this approach has recently lost favour, particularly when design changes would require modification or new tooling.

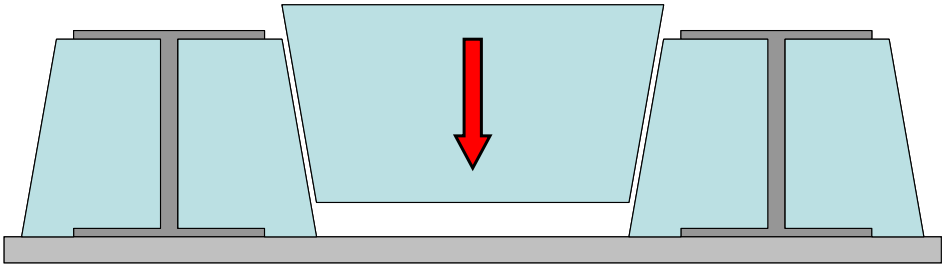

Figure 3-42: Modular one-shot approach

An adaptation to the above co-curing method is shown in Figure 3-43. This is a co-curing or co-bonding (with wet stringers) approach that uses intensifying local tooling on the stringers, to ensure that the form of the stringer is maintained. With such a tooling philosophy, the amount of tooling effort is reduced in comparison to the modular methodology.

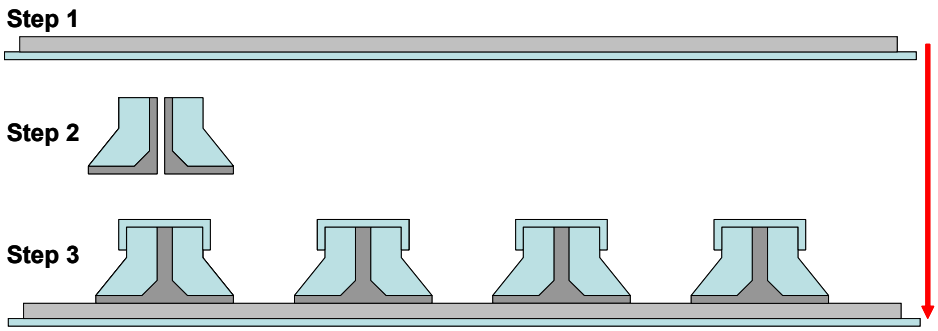

Figure 3-43: Discrete stringer (T- or I-profile) Co-Bond (Skin Pre-Cured) sequence (Co-Cure similar)

The integral U-profile stringer concept can only be accomplished using a co-curing philosophy, with a set of mandrels as shown in Figure 3-44. With such a philosophy, the tooling cost will be high, and design changes will be harder to integrate, however it should result in a high-quality part.

To maximise structural efficiency locally, the stringer webs are typically orientated normal to the skin, as shown in Figure 3-45 (LHS), however due to the chordwise curvature of the cover, this can lead to closed angles between each adjacent pair of stringers. Therefore, if mandrels are used between the adjacent stringers, then it will be necessary to use modular mandrels, similar to the concept shown in Figure 3-42. Alternatively, the stringer webs can be

parallel to the true vertical, which simplifies the tooling, as shown in Figure 3-45 (RHS). This can also be beneficial under global buckling conditions, as the stringer blade is kept straight along the length of the wing cover, which improves the global stability performance.

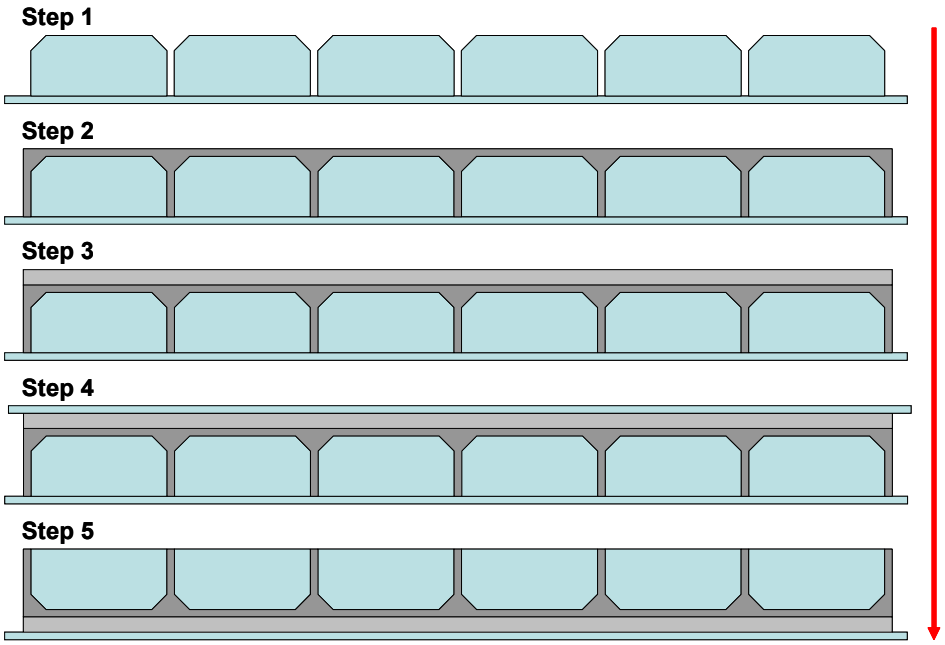

Figure 3-44: U-profile stringer co-cure sequence

With co-bonding (with hard stringer) and secondary bonding, the stringer forming tooling can be considered separate to the tool required for the skin and the subsequent bonding of the stringers to the skin. In terms of co-bonding (with hard stringer), the integration tooling is slightly simpler, as shown in Figure 3-46, as the pre-cured stringers only need to be positioned and held on the skin, with a vacuum bag encompassing both the skin and stringers.

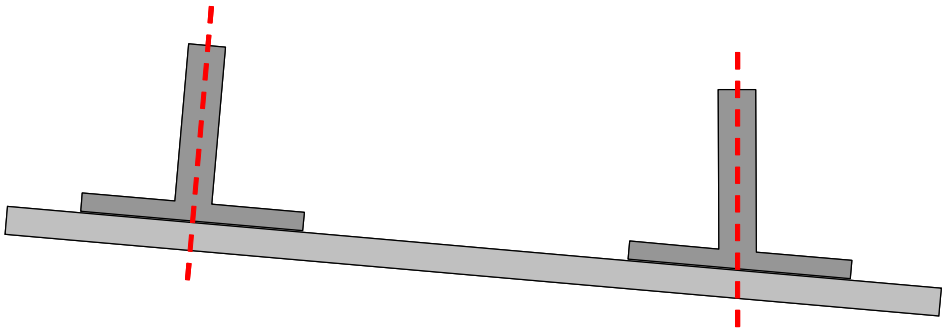

Figure 3-45: Stringer web orientation (LHS normal & RHS parallel to true vertical)

The sequence for secondary bonding is shown in Figure 3-47, where the stringers and skin are formed and cured separately, and then the stringers are positioned and fixed and encompassed in a vacuum bag. It is possible when using a pre-cured T-profile stringer, with either the co-bonding (hard stringer) or secondary bonding process, to form instead an I-profile stringer, which can then be post-machined, primarily along the web, to create two matched stringers, as shown in Figure 3-48, one for the port wing and the other for the starboard wing. This is possible as the stringer parameters, i.e. the thicknesses, height, etc will typically be exactly the same for the same stringer, just on opposite wings. However, the stringer has to be fabricated as shown in the top example of Figure 3-48, for two reasons. The first is due to the orientation of the material principal axes, and the second is that the thickness along the stringer will vary, therefore due to the limitations of the ATL, the tapering in thickness can only be achieved

straight, not in the chevron pattern as shown in the bottom example of Figure 3-48. This does however mean, as the stringer height can vary from approximately 30-100mm in height, that this can lead to a large amount of cured CFRP scrap material. If the stringers were made individually, then it would be possible to reduce the amount of material wasted, by better nesting the parts in the flat laminate. However, serendipitously, by having this area of scrap, this also gives the process greater flexibility, as if the stringer height changes, then this can be easily incorporated, as it is only a matter of updating the NC cutter program, whereas for all the other processes matched tooling is used, thus the tool depth matches the height of the stringer. It is necessary to use matched tooling, as voids can quickly fill with resin during cure, as shown in Figure 3-49, which would then need to be post machined, to clean the edge up, and it could also lead to a reduction in FVF.

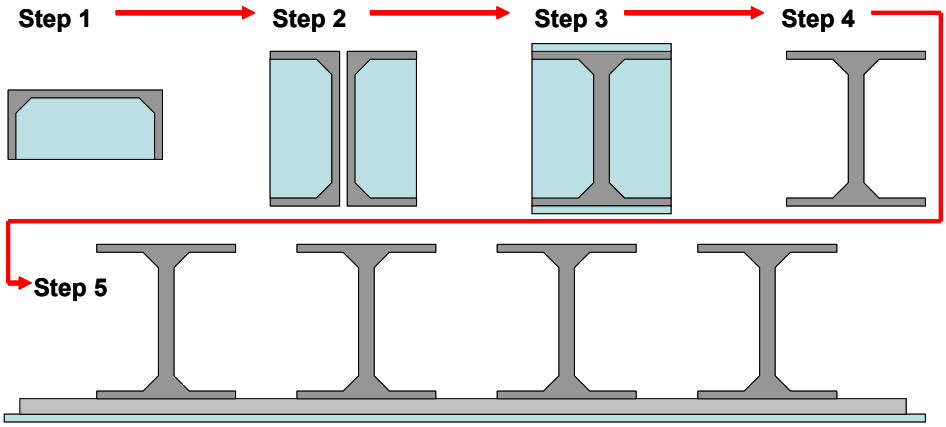

Figure 3-46: Discrete stringer (T- or I-profile) Co-Bonded (Stringer Pre-Cured) sequence

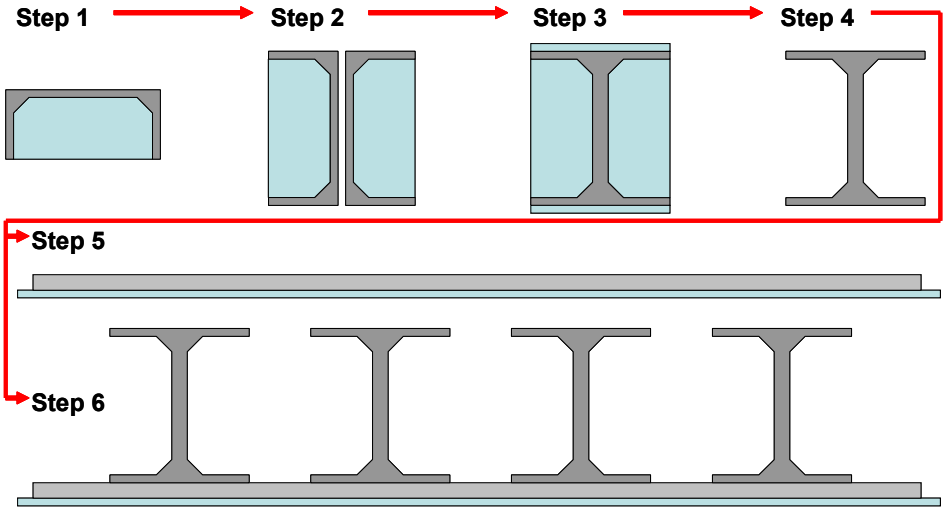

Figure 3-47: Discrete stringer (T- or I-profile) Secondary-Bonded (Stringer Pre-Cured) sequence

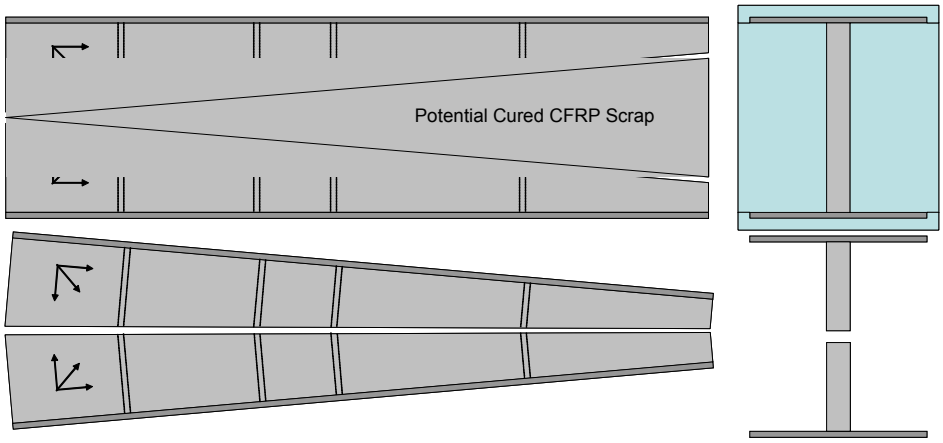

Figure 3-48: Alternative method to manufacture T-profile stringers

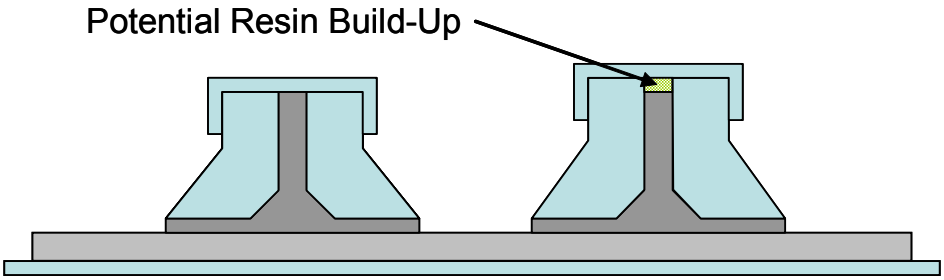

Figure 3-49: Resin build up if tools are not matched

3.7.2 Positioning Tooling

The principal integration of the skin and stringers is shown in Figure 3-50 for co-curing, although fundamentally it can be used for all integration methods. The baseline tooling setup for the integration of both uncured and pre-cured stringers onto the skin is shown in Figure 3-51. For uncured stringers, the tooling for the stringer has to run the complete length, as not only must the tooling assist in the stringer's positioning, it must also form the stringer's profile under curing. For pre-cured stringers, only local tooling is necessary. The basic principle of this tooling configuration is that the master tooling datum's for the stringers are defined by the docking stations, which uses a tongue between the docking station and the stringer tooling, to exactly position the stringer. As highlighted in Figure 3-51, a slot is integrated into the tongue to alleviate thermal expansion issues during the cure cycle.

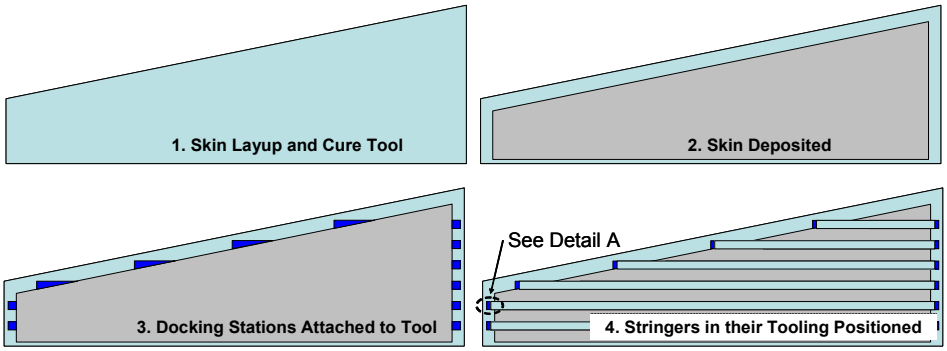

Figure 3-50: Process flow for Co-Cure cover integration

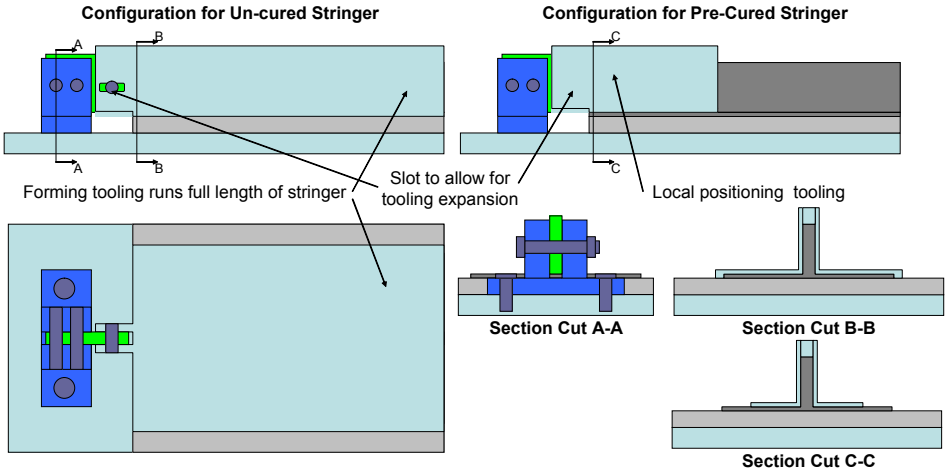

Figure 3-51: Baseline setup for positioning and curing of covers

Shown in Figure 3-52, is an alternative stringer positioning tool that is employed both at the root and the tip, using the stringer feet to position the stringers. Such tooling does not interfere directly with the stringer blade, thus it is applicable for stringers that are cured and uncured, as there is no interface to the stringer form tool for uncured stringers. However, as a number of stringers terminate along the span, and also to provide some inter-span support, it is necessary to have fixtures, such as shown in Figure 3-53. These too can be adapted to accommodate both cured and uncured stringers, and will be positioned approximately every 3m along the cover span.

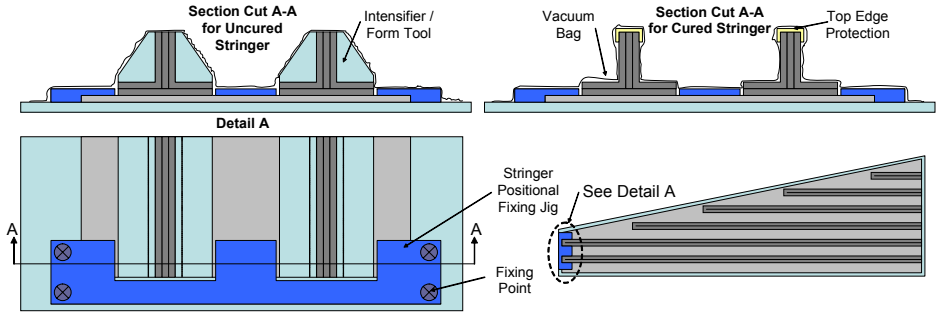

Figure 3-52: Alternative procedure for positioning stringers on skin

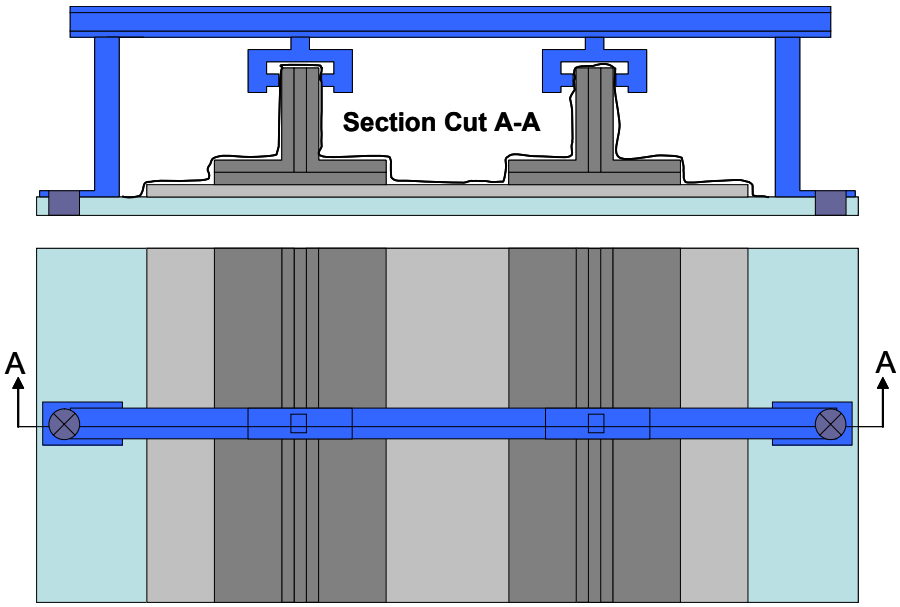

Figure 3-53: Stringer positioning tool at inter-span positions (cured stringer setup shown)

As shown in Figure 3-54 the stringers can be pre-loaded into a trolley, either pre-cured or uncured. If pre-cured the stringer blade is simply clamped in, or if uncured then the tooling is clamped into position instead, with the stringer inside the tooling. The stringers can be lowered onto the docking station individually.

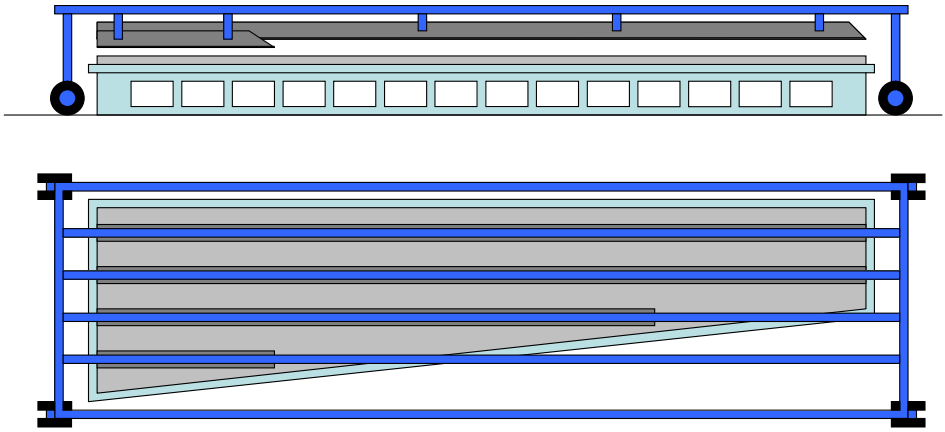

Figure 3-54: Stringer trolley/gantry

3.8 Recycling

Both governmental legislation and customer awareness of environmental issues are today driving recycling. Before 1970, the environmental legislation was either not established or legally binding, which gave the aircraft manufacturer a freehand in designing aircraft without necessarily considering the impact that their choice of materials and processes would have on the environment. This lack of foresight can impact heavily on the cost of disposal today[273], in particular when it is considered that between 2005-2025, there will be at least 200 commercial aircraft retired each year[274]. Not only must the end-of-life disposal be considered but also the scrap material, other associated waste and general pollution produced during the manufacture of the aircraft. This affects not just the materials and processes used but also the design, as it must be ensured that the aircraft can be easily disassembled and that the parts are identifiable so that they can be recycled at the minimum cost, or to maximise the value of the recyclate.

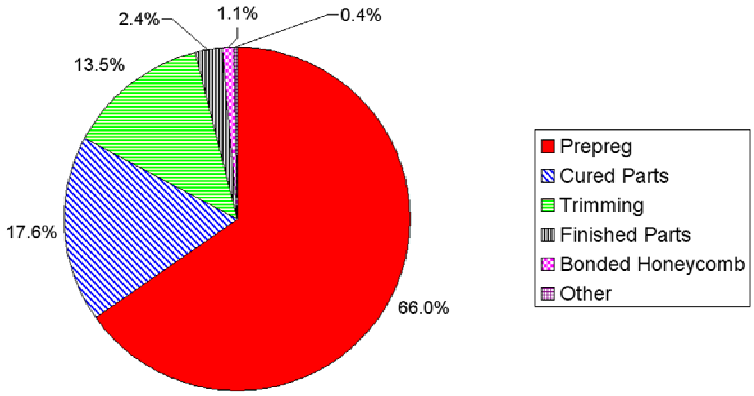

Figure 3-55: Average distribution of composite waste in aerospace industry

The issues of recycling aircraft is exacerbated, with the increasing application of thermoset composites, as there is a lack of recycling methods[189]. As shown in Figure 3-55[146,275], unused prepreg constitutes the majority of the composite waste produced in the aerospace industry, with cured parts and trimmed off-cuts making up nearly the rest. Uncured waste is classified as hazardous waste, thus it must be cured before being transported for disposal[28]. As

highlighted in Table 3-10[28], the knowledge of the waste is dependent on who produces or receives the waste. For instance, the manufacturing waste is simpler to deal with in comparison to end of life scrap because[28]:

- The waste type is well known, e.g. is it HS or IM fibre
- It is not chemically affected due to ageing
- It is not contaminated

Waste producer/receiver	Type of waste	Level of knowledge
Material manufacturer	Manufacturing	High
Product manufacturer	Manufacturing and products	Varying
Product user	End of life	Low
Contractor	All types	Low

Table 3-10: Waste producer and knowledge of the waste

Within the EU there is a hierarchy of routes for dealing with waste[276]:

- Prevent waste through prevention at source during manufacture
- Reuse a product
- Recycle material
- Incinerate waste
    - With material and energy recovery
    - With energy recovery
    - Without energy recovery
- Landfill

The prevention or minimisation of waste during manufacture could be improved by optimising the manufacturing process. Currently, it is estimated that 40% of UD prepreg is wasted as off-cuts[277]. Dry fibre technology is advantageous as the constitutive parts are already separated, unlike in prepreg.

The option of land filling will, due to forthcoming legislation, be no longer available, which along with the increase in the quantity of waste produced, should help to create a large market for disposal/recycling of composite waste. The option of incineration could also be moderated, as the acceptance of incineration is based on the level of energy content that can be gained[278]. For Fibre Reinforced Plastics (FRP) typically only 10% of the energy required to produce the FRP product is recovered due to incineration, as it contains over 60% inorganic material, which results in a high ash content[28,278]. Furthermore, incineration will destroy valuable fibres, which could potentially be reused.

It has been verified that recycling of composites is the best method economically and environmentally[28], however, there is an inherent lack of a market for waste composite materials, such as there is for metals, which is due to the following major barriers[278]:

- Lack of cheap size reduction technology
- Design rules for composite recyclate are not well known
- Lack of sufficient, high tech applications
- Lack of an infrastructure to recover and recognise thermoset components
- Lack of a system to guarantee the FRP recyclate quality for the specific applications

Carbon fibre is a more valuable product than glass, thus the prospects for recycled carbon is perhaps more financially viable than glass[276]. FRP can be recycled using the following techniques:

- Mechanical
- Chemical
- Thermal

The different recycling processes available have their own advantages and disadvantages, and the down-selection of an appropriate process will be dependent on the use of the recovered fibres and resin. The best case should enable the recyclate to achieve[277]:

- Efficient removal of resin from the fibres
- Capture and recycling of the resin side-products
- Preservation of the fibre's mechanical properties

The recycling processes can be broken down into three categories:

- Primary recycling: Reprocesses the waste to obtain the original or comparable product
- Secondary recycling: Transforms the waste into products that do not require the virgin material properties
- Tertiary recycling: Transforms the waste into their chemical building blocks

Thermoplastics can be recycled into the primary or secondary categories, whereas thermoset can be recycled into the secondary or tertiary categories.

Mechanical processing is currently the most common process, and involves cutting, shredding, grinding and milling of the scrap material. The resultant material will vary in size from powder to various fibre lengths. To ensure longevity of the grinding equipment, it is necessary that all metal parts are first removed from the scrap composite part[28]. Therefore, this could push for a fastenerless design. Alternatively, a hammer mill can be used which should require less maintenance as there are no blades that require sharpening[276]. Typically, the strength and stiffness of the ground composite is reduced in comparison to the virgin material[28] due to their decreased length and also due to the reduced interfacial bonding between the recycled fibre and the resin. The by-product can be used as a filler in secondary structures, for SMC, bulk moulding, or reinforced concrete[146], and as an additive in paint to improve the Electro-Magnetic Interference (EMI) shielding.

Acid digestion applies severe chemicals and conditions to dissolve the polymer, and hence from an environmental perspective is impractical[146]. From an economical perspective, the most viable recycling process would be to recover the long fibres for use on another product[277]. This can be achieved by using the thermal methods, such as pyrolysis and hydrogenation. Alternatively hydrolysis can be used, which is a chemical process that breaks the polymer chains into monomers[28].

Pyrolysis is a tertiary process where the polymer is thermally decomposed at elevated temperatures in the absence of oxygen. Such a process breaks the polymer into monomers, fuels, and chemicals, whereas the fibres are separated[146]. The pyrolysis method used by Milled Carbon Ltd is based on pyrolysis in air, which can continuously recycle carbon and glass composites[279]. With the current setup parts 2m wide and 0.25m high can be processed[279]. For this process, the ideal recyclate would be out of date complete rolls of

prepreg. To process virgin NCF, the heat required would be 200°C, however, for a prepreg the temperature would be 400°C. It is known that braided and woven materials are harder to process [meeting with J. Davidson (Milled Carbon Ltd) 27/02/08].

The fluidised bed process, as shown in Figure 3-56[276], was developed by the University of Nottingham, for thermoset glass and carbon composites, which both recycle the materials and recovers energy. This is done through a fluidised bed, with the fibres and fillers sucked into a cyclone and the organic gases captured for energy recovery. Any metallic parts should sink into the fluidised bed.

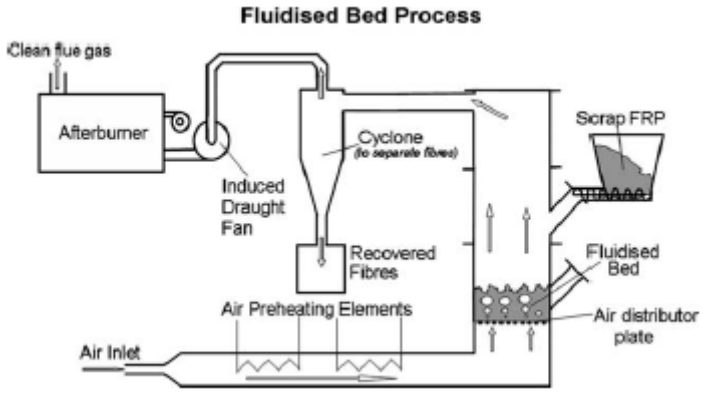

Figure 3-56: Fluidised bed process

If this process can be run economically, then the cost of the recycled material can be 80% of the cost of the virgin material[28]. Furthermore, the stiffness is unchanged and the strength is 80-93% of the virgin material[28,137]. Epoxy resins require processing temperature up to 550°C for rapid volatilisation of the polymer[276].

3.9 Building Block Approach

It has been proven that the most efficient and successful framework to develop an aircraft structure is to use the building-block approach, as shown in Figure 3-57[140], which, when used in combination with a realistic time-schedule, will ensure methodical development of the aircraft[44]. This approach can be applied to both structural and manufacturing development of composite structures[280].

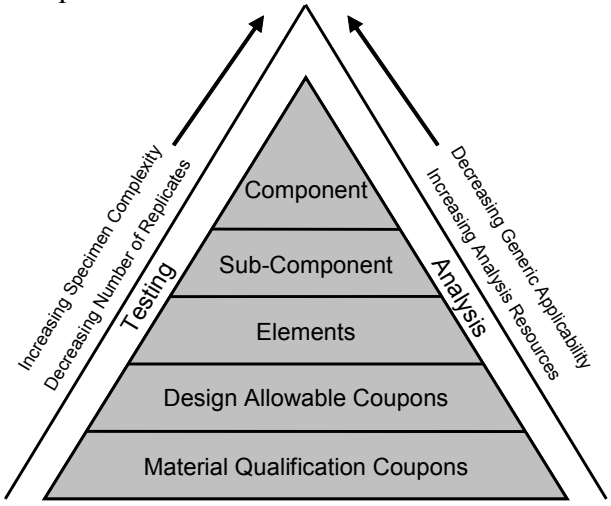

Figure 3-57: Test pyramid

To find the effects of local details and internal load paths on structural behaviour, elements and sub-components are used, such as shown in Figure 3-58[133] from the NASA ACT full-scale wing project. Applying the building block approach to the development of a commercial composite aircraft, but excluding the final full scale test, can cost £10M[281], thus it is both time consuming and expensive. However, if a 2-3 year building block validation program is used, then the risk due to applying composites to a structure should be severely reduced[44]. Such a test program can only legitimately be avoided when high-fidelity design tools are used, or when a conservative design is acceptable. The consequences of not strictly adhering to the building block approach is failure at a late stage in the development, which can be very damaging to the aircraft program.

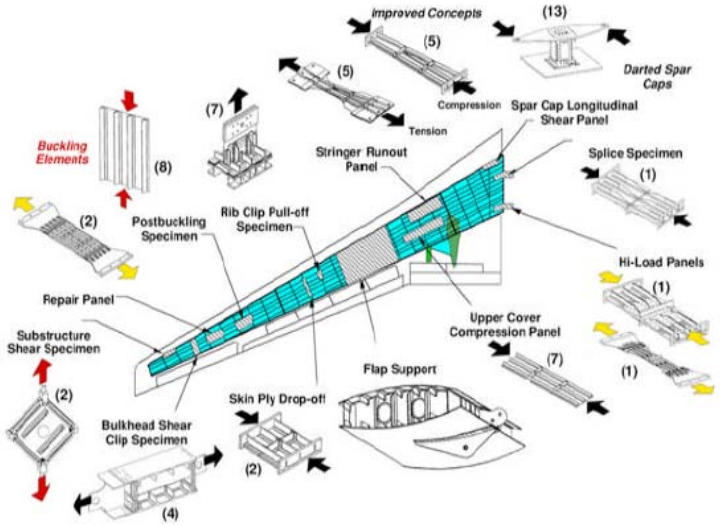

Figure 3-58: Elements and sub-components for the ACT full wing program

When each hierarchical level of detail is reached, the results are then reflected in the design. However, it cannot be guaranteed that each subsequent level will show a good correlation to the proceeding one. For example, design allowables that are derived from coupon tests can be so inaccurate, that when sub-components are made and tested based on these allowables, a costly re-design could be required due to sub-component failing at a lower or higher applied load[282]. This has been evidenced, through the difference between a multi-cell wing test box and a plain 8mm thick laminate, which led to the plain laminate having a failure strain 31% higher than the wing box, due to the difference in support conditions[282].

Complementary to the building-block approach is to focus on design, manufacturing, and maintenance issues at each level and solve any issues found. Product scaling can also be considered in the building block approach. This is where the flow time of the product from raw material to end product can be analysed. This is important to analyse early on, as it is typically done after the first production run, at which time it is too late, and a failure can lead to a major loss in profit. During the development, the credibility of product scaling should ensure confidence in the cost analysis being carried out. Aspects such as material utilisation, defects, and process flow must be understood based on the design characteristics. This information is necessary so that equipment, material, labour, tooling and facilities can be determined to support scheduled production rates.

3.10 Summary

This chapter has outlined a number of materials and processes that could be applicable to the manufacture of a composite wing cover. For high performance parts only CFRP can be considered, GFRP and Kevlar would simply result in a sub-optimal wing cover. The baseline solution for the manufacture of a CFRP wing cover, is to use a UD prepreg solution, with either IM or HS fibre that is deposited using an ATL, with a toughened resin system that requires a 180°C cure in an autoclave, to ensure a FVF close to 60% is attained. Due to the size of wing skins 0.25mm thick plies will be used, whereas 0.184mm plies will be used for stringers, in order to ensure good axial performance. A hybrid laminate should also be considered, as this should provide a good balance between performance and cost.

Contemporary toughened NCFs are a viable alternative to UD prepreg, which could reduce the cost of CFRP wing cover manufacture, as long as the material can be well utilised and that the ability to tailor the thickness is similar to a comparable UD prepreg example. Furthermore, an automated solution such as previously explained, must be used for the deposition of the NCF. An RTM process could be considered for the manufacture of the skins, but due to the colossal size of tooling required for the RTM process, then VARTM, VAP or MVI are more suitable. These processes can also be applied to the manufacture of stringers.

Despite a number of potentially superior methods to manufacture stringers being outlined, the simple method of forming the constituent parts through vacuum forming will be considered the baseline solution, as such methods are used today.

Using a FML can improve the bearing strength, however at the preliminary design phase, such a laminate is hard to consider. This is because the bearing strength is dependent on a number of factors, which cannot be optimised at the preliminary design phase. Similarly, 3D reinforcement, by either stitching or z-pinning, can again be beneficial. In particular, the damage tolerance of the parts as well as their integration, however this can limit the available integration techniques to co-curing. However, the benefit of such is hard to justify at the preliminary design phase.

Finally, braid sleeves can be used for the fabrication of stringers, as this should offer a cost effective solution, although the performance of braids is inferior when compared to UD prepreg or NCF.

4 Laminate Design

4.1 Introduction

The ability to tailor the laminate to suit the load conditions is well known. In terms of in-plane strength and resultant strain, i.e. the extensional stiffness (A-Matrix), it is the percentage of each ply orientation in the laminate, typically limited to 0°, ±45° and 90° orientations[175], that is of importance. The positioning of the individual plies in the stack is not important, although certain design rules will need to be obeyed. Programs like ESDUpac A9636[283] can calculate the required thickness of a certain stacking sequence to suit the loading conditions, which caters for biaxial and shear loaded laminates.

The bending stiffness (D-Matrix) is dependent on the positioning of the plies in the laminate, thus the performance, if buckling is critical, for a given weight can be improved through careful positioning of the individual plies in the laminate, with the outermost plies being the most critical to the bending stiffness. Genetic Algorithms (GA) are ideally suited to search for the optimal stacking sequence[284]. From the closed-form Equations 4-1 to 4-4[285,286], which assume simply-supported conditions, it can be seen that the D-terms wholly determine the laminate's buckling performance, in particular the D_{66} term.

To calculate the axial compressive load capability of a laminate, the closed form Equation 4-1 can be used:

$$N_{x\,critical} = 2\left(\frac{\pi}{b}\right)^2 \times \sqrt{D_{11} \times D_{22}} \times \left(1 + \frac{1}{\theta}\right) \qquad \textbf{4-1}$$

Where θ is Seydel's orthotropic parameter[286], and is given by Equation 4-2. When θ=1, the material is considered isotropic.

$$\theta = \frac{\sqrt{D_{11} \times D_{22}}}{D_{12} + 2D_{66}} \qquad \textbf{4-2}$$

Similarly, to calculate the shear load capability of a laminate when θ>1, Equation 4-3 can be used:

$$N_{xy\,critical} = \frac{4}{b^2} \sqrt[4]{D_{11} \times D_{22}^3} \times \left(8.125 + \frac{5.05}{\theta}\right) \qquad \textbf{4-3}$$

And, when θ<1, Equation 4-4 can be used:

$$N_{xy\,critical} = \frac{4}{b^2} \sqrt{D_{22} \times \left(D_{12} + 2D_{66}\right)} \times \left(11.7 + 0.532 \times \theta + 0.938 \times \theta^2\right) \qquad \textbf{4-4}$$

4.2 Effect of Panel Aspect Ratio

The panel, defined by the boundary set by adjacent stringers and ribs, will have a certain aspect ratio (a = length, b = width), which for a wing panel is typically a/b ≥ 3. When reacting

primarily axial load, such as wing skins, with an aspect ratio >3 then the buckling coefficient is independent of the panel's aspect ratio[287,288]. Shown in Figure 4-1 to Figure 4-4 are graphs representing different load conditions on a 4mm thick constant volume panel, but with varying aspect ratio and ply orientations. ESDUpac A0817[289] was used to obtain the results, and due to the 0° and 90° laminates being specially orthotropic, the results should be very accurate[xx]. Figure 4-1 illustrates the optimum fibre orientation to react axial compressive load. As can be seen for a normal panel aspect ratio of >3, a ±45° laminate is optimum, whereas for an aspect ratio less than 0.8, then 0° plies are ideal, which has been verified with other work[288,290].

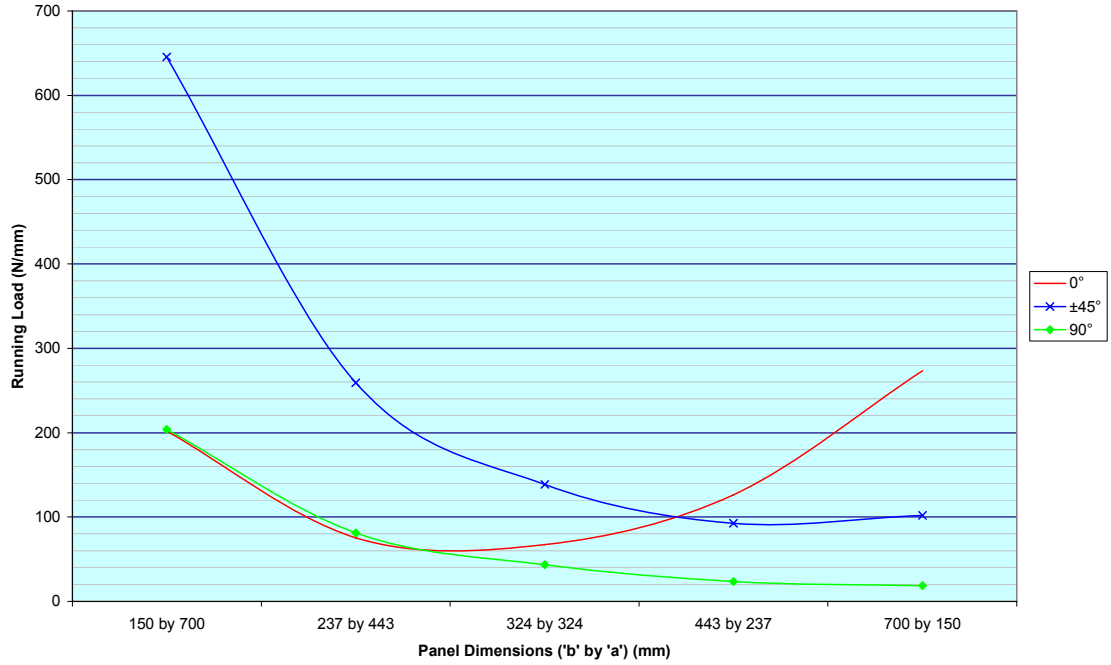

Figure 4-1: Influence of aspect ratio and fibre orientation on axial compressive stability performance

A useful observation from Figure 4-1 is the comparison between the performance for the 0° and the 90° laminate, with an aspect ratio >3. It can be seen they both have the same buckling load, therefore from a buckling perspective, which ply orientation should be applied to the wing skin? To answer this question, the ratio of wavelength is calculated using Equation 4-5[291]:

$$\frac{\overline{a}}{b} = \sqrt[4]{\frac{D_{11}}{D_{22}}} \qquad \textbf{4-5}$$

Where '$\overline{a}$' is the longitudinal wavelength. For the pure 0° laminate, the ratio of wavelength is 2.04, for the 90° laminate it is 0.87, whereas for a ±45° it is 1. Thus for a panel length of 700mm, the 0° laminate has a wavelength of 1428mm, whereas the 90° laminate has a wavelength of 609mm, similarly the laminate $[0/0/90/90]_s$ has a far higher value than a $[90/90/0/0]_s$ laminate. The rib pitch for a wing box will be influenced by ensuring the maximum amplitude of the unsupported plate, thus using a 0° dominated laminate will allow the rib pitch to be maximised[292].

[xx] See Chapter 8 for FSM background information and limitations.

Under pure shear load, as shown in Figure 4-2, for an aspect ratio >1 the ±60° laminate is optimal, albeit a ±45° laminate has only slightly lower performance, and the pure 90° laminate performs far better than the pure 0° laminate. With an aspect ratio <1 then a ±45° laminate is superior. Again, these results are similar to other published results[288].

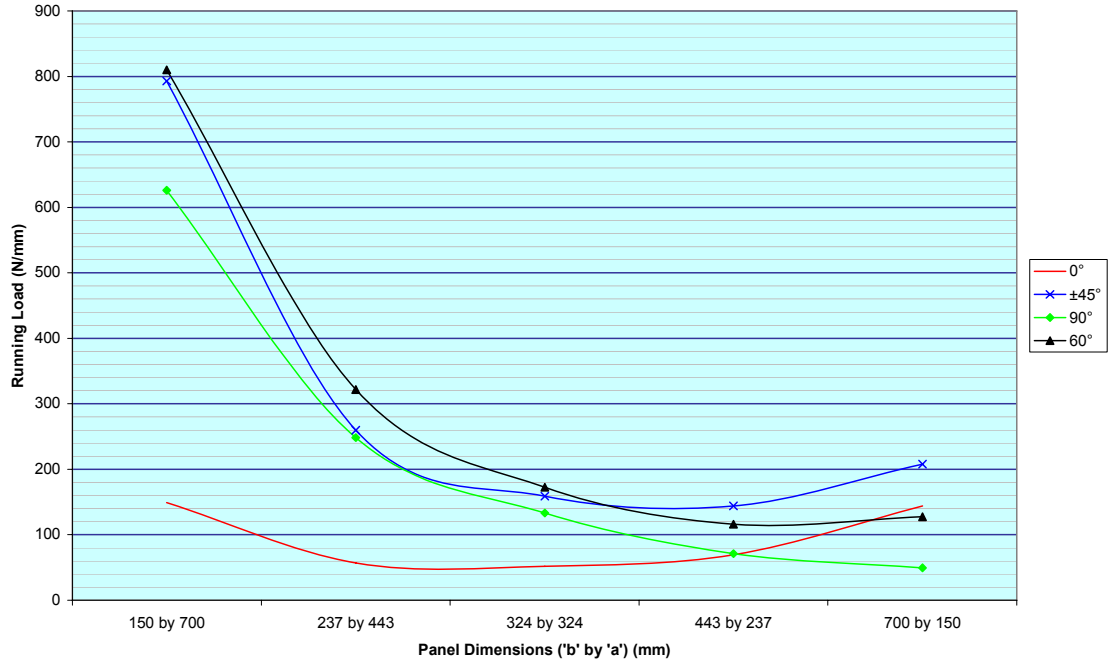

Figure 4-2: Influence of aspect ratio and fibre orientation on shear stability performance

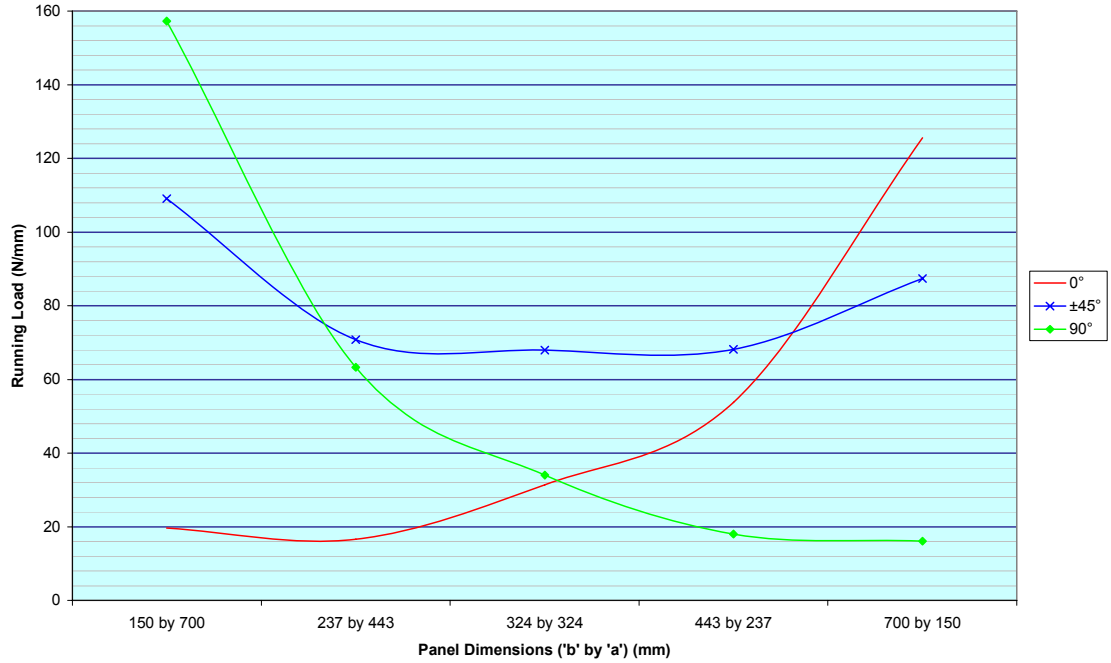

Figure 4-3: Influence of aspect ratio and fibre orientation on biaxial compressive stability performance

It is known that flexural anisotropy, i.e. the D_{16} & D_{26} terms, which is intrinsically related to the stacking sequence, can increase the shear buckling load[293]. As seen in Figure 4-2 the ±60° laminate resists shear well, which is due to the term D_{22} having greater influence on N_{xy} than D_{11}, thus the angle should be greater than 45°, helping to better resist the anticlastic (D_{12}) and torsion (D_{66}) terms. However, as the laminate is typically limited to 0°, ±45° and 90° ply orientations, if the panel must principally react shear load then 90° plies should be used[292].

Shown in Figure 4-3 is a panel reacting an equal distribution of a biaxial compressive running load. For an aspect ratio >2, a pure 90° laminate is optimal, whereas a ±45° laminate is optimal for an aspect ratio between 0.5 and 2, and a 0° laminate is optimal for an aspect ratio < 0.5. Again, these results are similar to other published results[288].

The equal distribution biaxial running load, shown in Figure 4-4, has both a compressive axial load and a tensile transverse load. Under this loading condition, the pure 0° laminate is optimal; however, the most important observation is how this tensile load increases the stiffness of the laminate to resist the axial load. It is known that if the panel is under destabilising stresses, i.e. compression and shear, then the bending stiffness is reduced, whereas tensile stresses increase the bending stiffness[294].

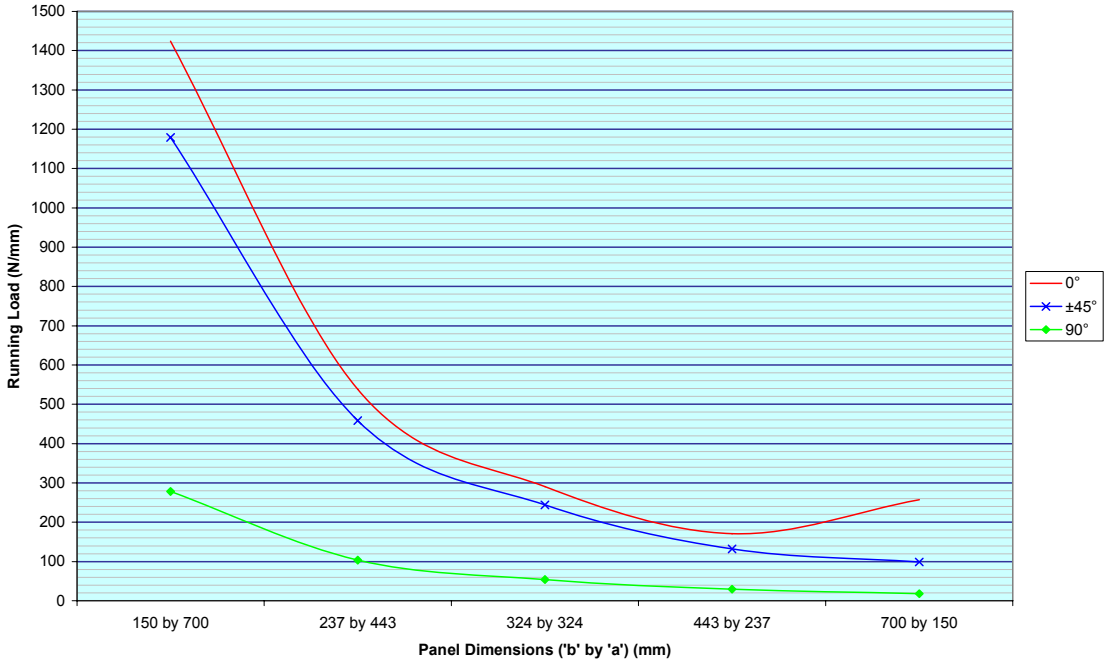

Figure 4-4: Influence of aspect ratio and fibre orientation on biaxial stability performance

4.3 Effect of Laminate Thickness

It is known that the buckling load is proportional to the cube of the thickness. The effect of thickness is considered, in Figure 4-5 to Figure 4-7, on the pure orientation laminates, with panel dimension of 150mm width by 700mm length. As shown in Figure 4-5 for a thickness from 4-13mm a ±45° laminate is optimal, thereafter a pure 0° laminate is superior. In reality, at such a thickness the wing cover is not likely to be stability critical, instead strength will be the design driver. This is despite the bending stiffness being superior for pure 0° laminate, regardless of thickness as shown in Figure 4-6. The influence of thickness on shear performance is shown in Figure 4-7, where a ±45° laminate is superior, and the pure 0° laminate has the lowest performance.

In terms of the effect of thickness on strength, a thinner laminate can attain a higher plain (i.e. undamaged) stress than a thicker laminate, with the resultant plain strength strain for a 2mm laminate at 9700με, whereas a 8mm laminate attains a strain of 7200με[145]. In terms of notched (OHC) strength performance, the effect is similar. This has been evidenced using Hexcel's IM7/8552 prepreg system, with laminate thicknesses of 4mm, 8mm, and 16mm, fabricated

from 0.25mm thick plies and a stacking sequence of $[+/90/-/0]_{ns}$, with values of 288MPa, 284MPa, and 276MPa, respectively[281] [E-mail from C. Soutis, The University of Sheffield, 2008]. This loss in performance of thicker laminates can be attributed to greater void content and fibre waviness.

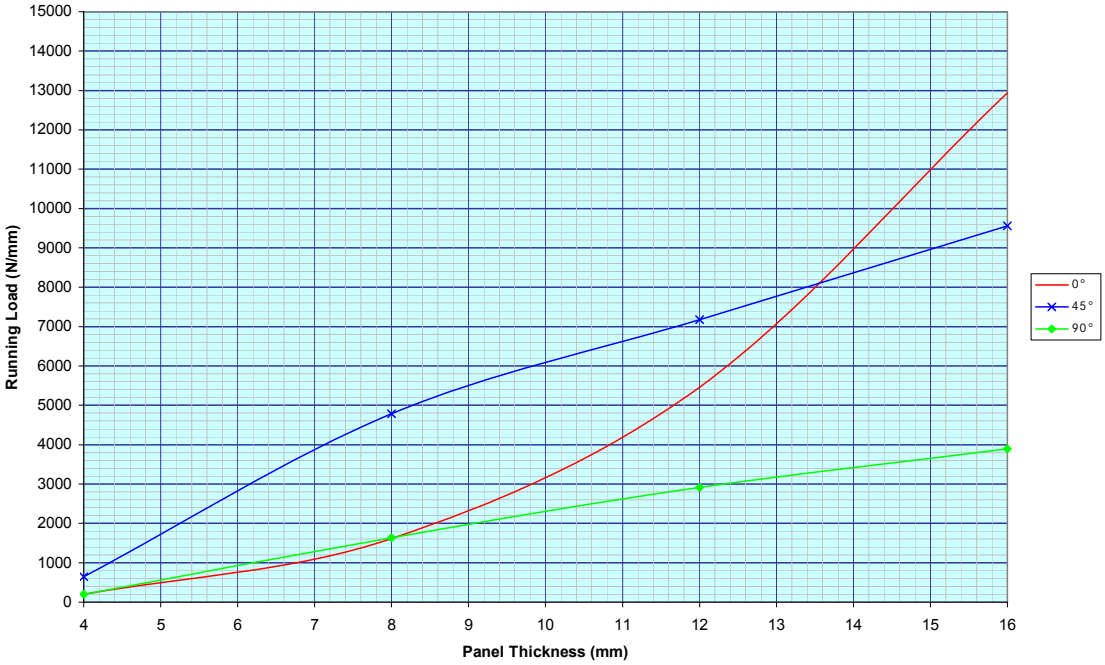

Figure 4-5: Influence of fibre orientation and increasing thickness on axial compressive stability performance (150×700mm)

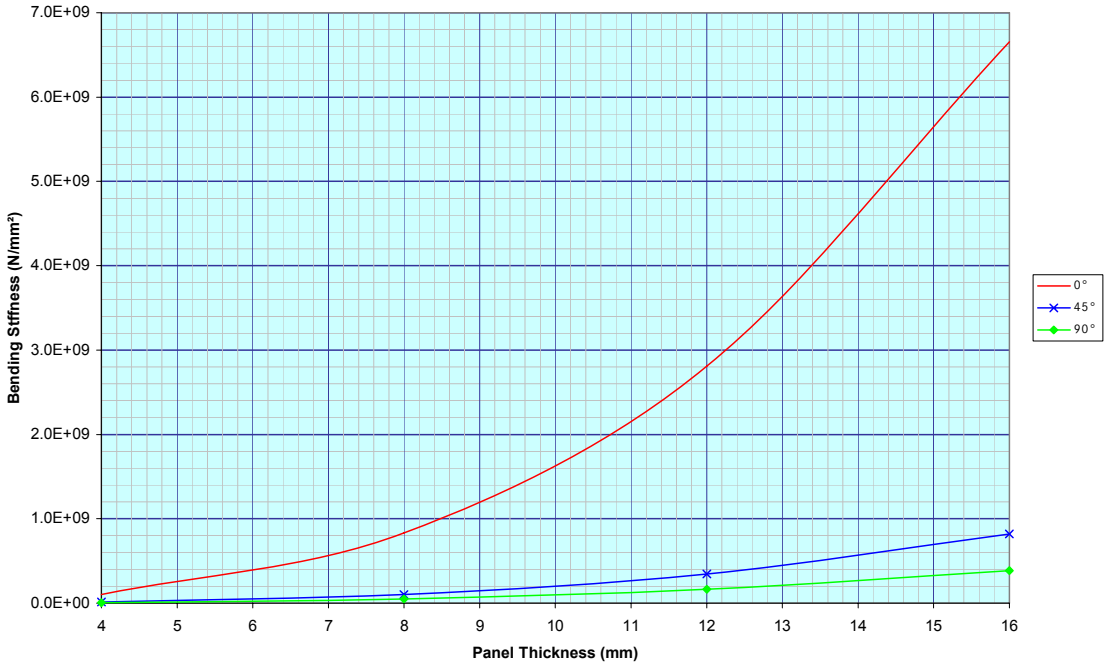

Figure 4-6: Influence of fibre orientation and increasing thickness on bending stiffness (150×700mm)

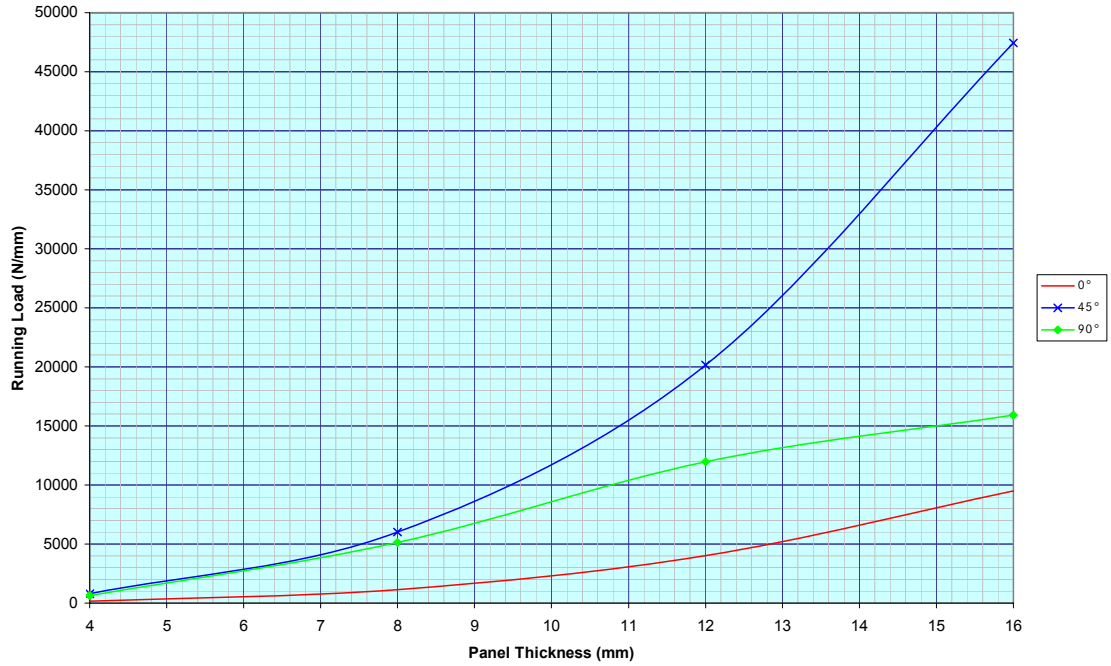

Figure 4-7: Influence of fibre orientation and increasing thickness on shear stability performance (150×700mm)

4.4 Laminate Design Guidelines

A symmetric laminate will have for every ply with orientation +θ° at a distance Z_l from the laminate's mid-plane, another ply with orientation +θ° at a distance $-Z_l$. Symmetric laminates reduces the warping effect during cool down of the laminate after it has been cured, as it minimises the difference in thermal expansion between the plies. Should there be a large difference in thermal expansion between the plies, the cooled laminate could have matrix cracks, which reduces the laminate's impact resistance properties[295]. Furthermore, it minimises the extension-bending (B-Matrix) coupling effects[292], so that pre-buckling deformations are purely in-plane[296,297].

A balanced laminate is required to prevent deformations causing internal stresses, and minimise shear-extension coupling effects[296,297,298]. Therefore, for every ply with a +θ° there is a –θ°. This requirement to have a balanced laminate is not compliant with the ability to reduce interlaminar shear[xxi] through reducing the angle between adjacent plies, if possible, following a spiral stairwell method (+/90/-/0). Thus a contradiction exists, on the one hand to have a balanced laminate that curtails coupling effects, against a laminate that eludes interlaminar shear. Coupling effects pose a greater problem for thinner laminates; hence thin laminates should have the ±45° plies paired, whereas the thicker laminates can use the stairwell method.

Placing a pair of ±45° plies on the outside of the laminate maximises the D_{66} term, which enhances the buckling performance[148], and reduces the flexural strains in the 0° plies[299,300]. If followed by a 90° ply, i.e. +/-/90, this provides lateral support to the 0° fibres helping them to

[xxi] Interlaminar shear is the maximum shear stress existing between layers of laminated material.

achieve failure closer to their fundamental compressive strength[301], as well as increasing transverse bending stiffness for the transverse load paths[302].

By uniformly banding 0° and ±45° plies through the laminate, this creates multiple shear paths for the 0° plies, which minimises interlaminar shear stress concentrations, and provides a high degree of buckling stability[302]. By placing the 0° plies towards the mid-plane this allows the strength requirement to be achieved without negating the buckling performance[292]. However, if there are changes in stiffness over the skin which can encourage delamination[303], then the laminate's overall bending stiffness can be enhanced by placing the laminate's 0° plies as far away from the neutral plane as possible[304], and preferably under the ±45° plies.

Interlaminar shear can be mitigated under tensile loads by placing the 90° plies far from the neutral axis, which also improves the shear buckling performance[292], conversely under compression load they should be placed close to the neutral axis[305]. However, as both the upper and lower wing covers react tensile and compressive loads, it is hard to satisfy this design guideline.

It is recommended that no more than 4 plies of the same orientation should be grouped together, or a maximum thickness of 1.0mm, to reduce crack propagation, transverse shear stress, interlaminar shear stress at the edge and minimise edge splitting[148,298,299,301,306,307,308], which can reduce the laminate's overall strength[145].

4.4.1 Laminate Families

Shown in Figure 4-8[140] is the range of recommended percentages of 0°, ±45°, and 90° plies in a laminate, with a minimum of 10% 0° and 90° plies, as well as a minimum of 20% ±45°. The reason why the laminates should remain in the blue shaded area of Figure 4-8 is due to Poisson's ratio effects. Furthermore, a reasonably quasi-isotropic laminate is applicable to a wing cover, as they are subjected to multiple structural constraints[309], provide a safety net for unexpected loads[307], and has good damage tolerance[292]; although a more orthotropic laminate may be more optimal.

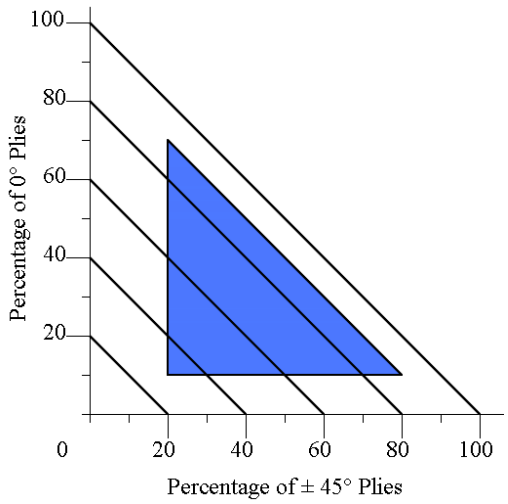

Figure 4-8: Guideline to picking a damage tolerant and durable laminate

For a wing cover, typical laminates can range from 10/80/10, for a soft skin, to 70/20/10, for a stiff stringer, with the average overall angle for the laminate being 45° and 18°[xxii] respectively. Figure 4-9 and Figure 4-10 illustrates the stability performance under axial and shear loads respectively, for different laminates. It can be seen that the best performing laminates are those with the highest percentage of ±45° plies, such as the 10/80/10 laminate.

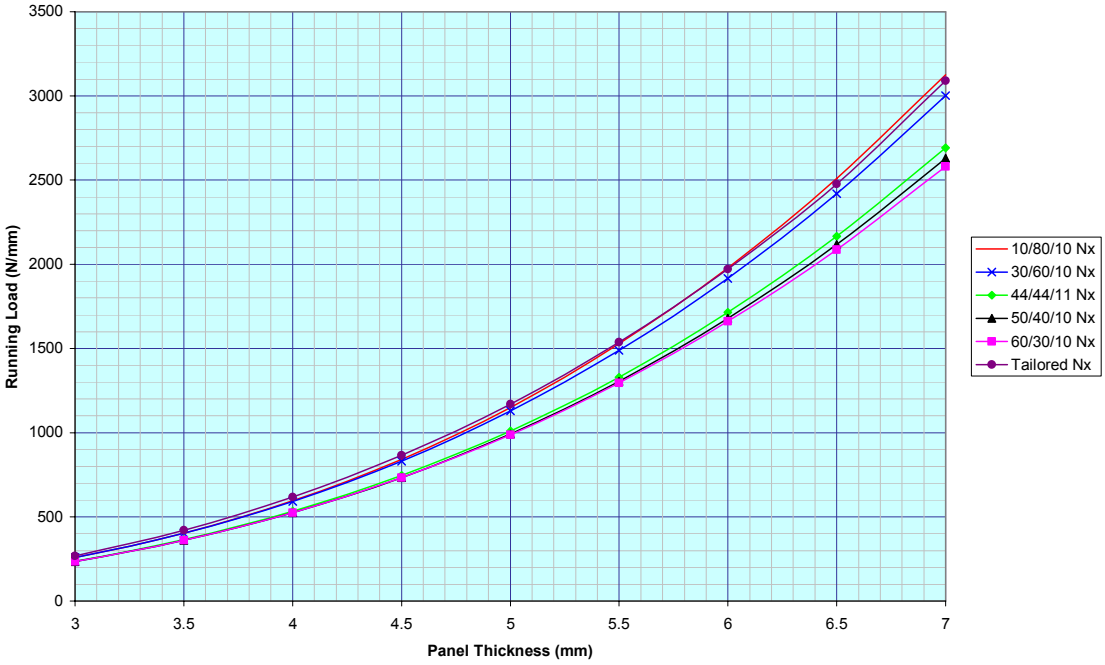

Figure 4-9: Critical axial stability running load for different laminates (150×700mm)

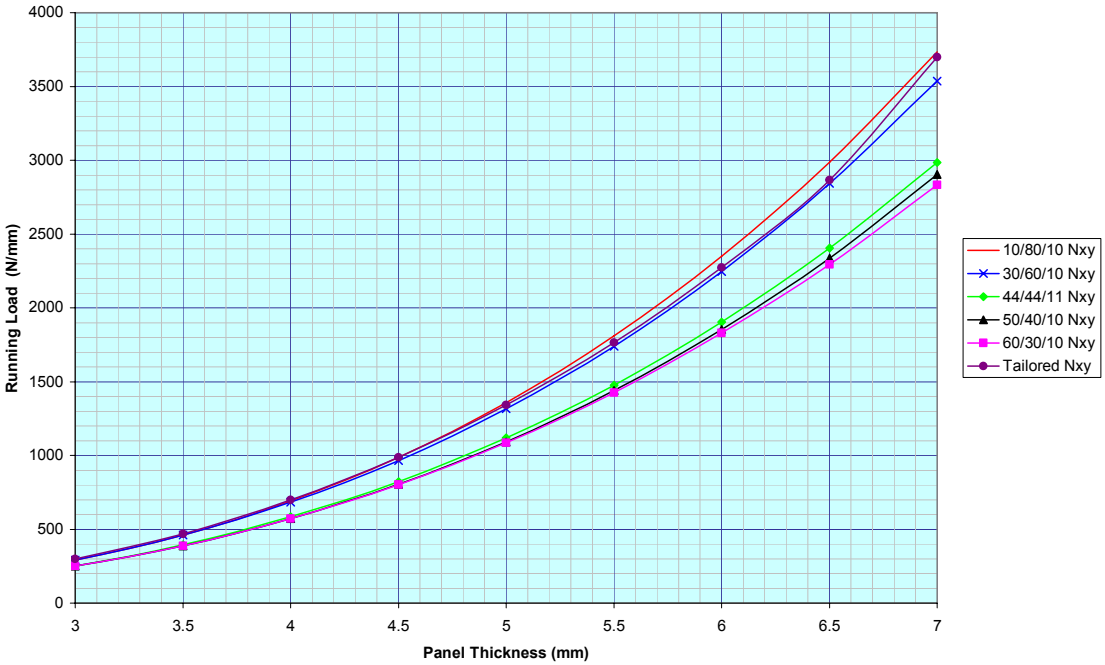

Figure 4-10: Critical shear stability running load for different laminates (150×700mm)

The opposite is true for strength as shown in Figure 4-11 and Figure 4-12, for axial and shear strength respectively, where laminates with a high proportion of 0° are superior. It should be

[xxii] ((20*45)+(10*90))/100 = 18° for a 70/20/10 laminate.

noted that the results shown in both Figure 4-11 and Figure 4-12 are for a laminate under biaxial and shear load, using ESDUpac 84018[310], which is an iterative method based on the modified Puck criterion. For these reason, the curves in Figure 4-11 and Figure 4-12 have slight undulation, however despite this the trend of the curves is clear. Shown in Figure 4-9 to Figure 4-12 is a laminate named "tailored", which does not have a fixed percentage of different ply orientations, instead the laminate when stability driven, i.e. when it is thin, has a higher percentage of ±45° plies, whereas when it is strength driven it has a higher percentage of 0° plies. In reality, both strength and stability performance of the laminate should be matched as far as possible, after all there is no point having a good stability performance, while strength is poor, and vice versa. Figure 4-13 illustrates the crossover point at which the laminate is strength driven instead of stability, for a 44/44/11 and 10/80/10 laminate. For the 44/44/11 laminate, this crossover point is at a thickness of 6.25mm, whereas for the 10/80/10 laminate it is at 4.25mm, this is due to a 10/80/10 laminate being very soft, thus strength is nearly always critical.

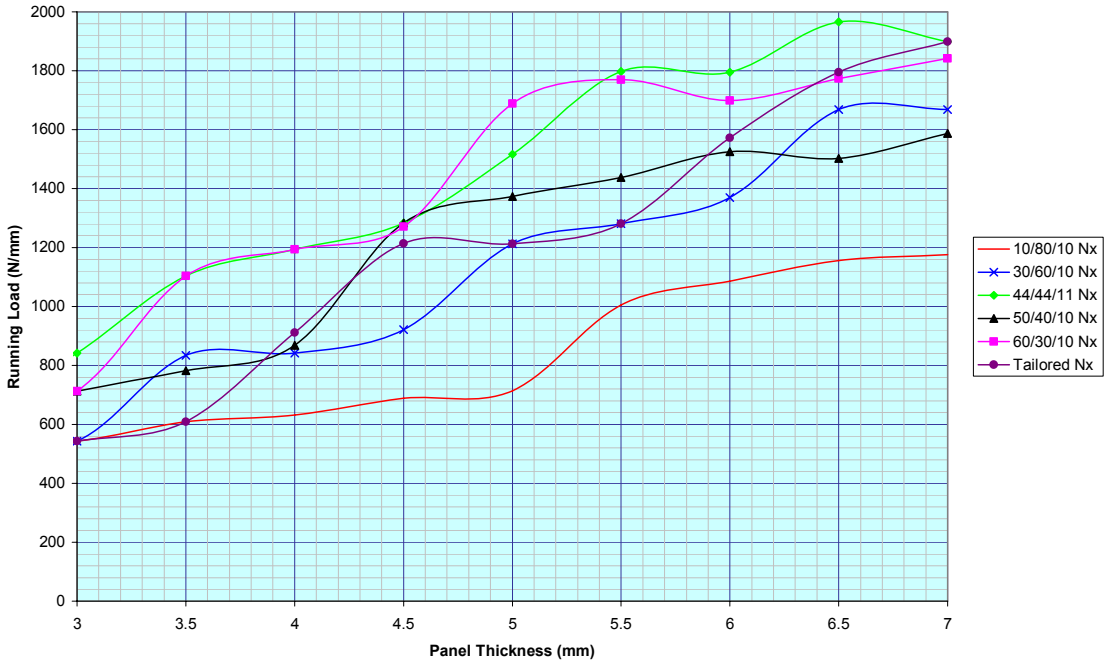

Figure 4-11: Critical axial strength running load for different laminates (150×700mm)

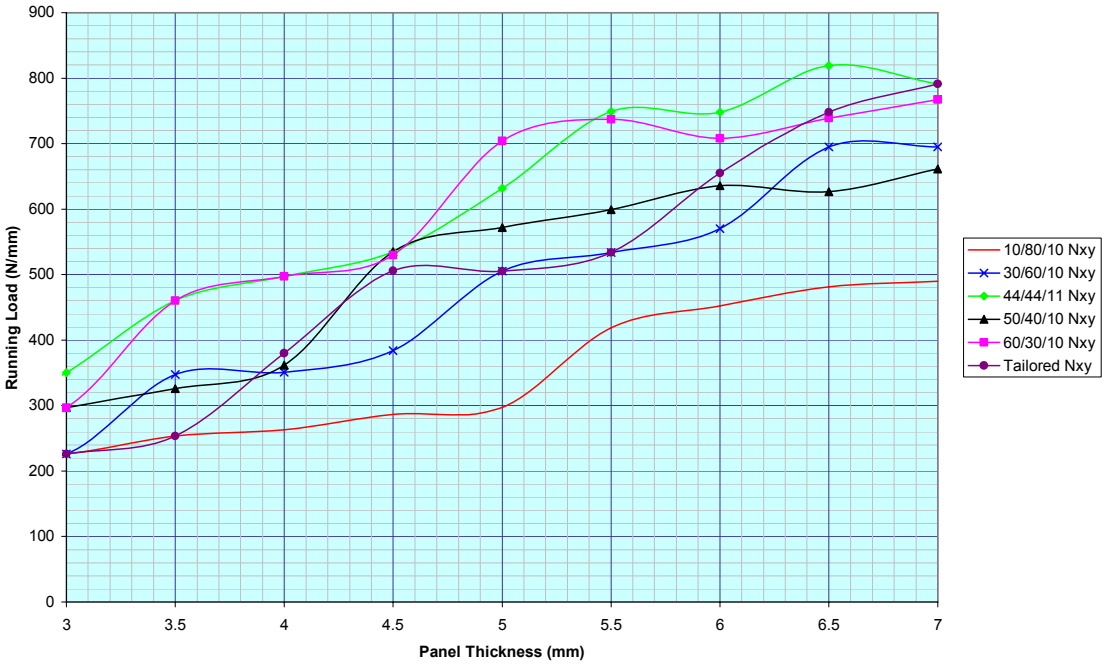

Figure 4-12: Critical shear strength running load for different laminates (150×700mm)

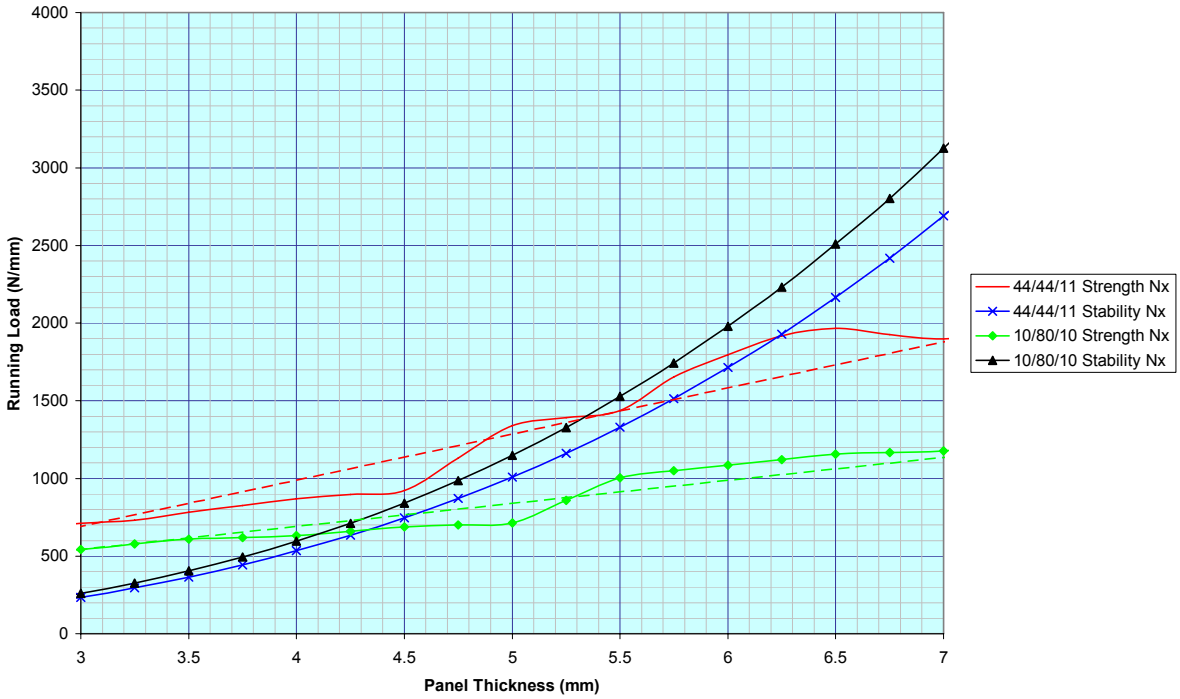

Figure 4-13: Crossover point for compressive axial strength or stability criticality for 44/44/11 and 10/80/10 laminates (150×700mm)

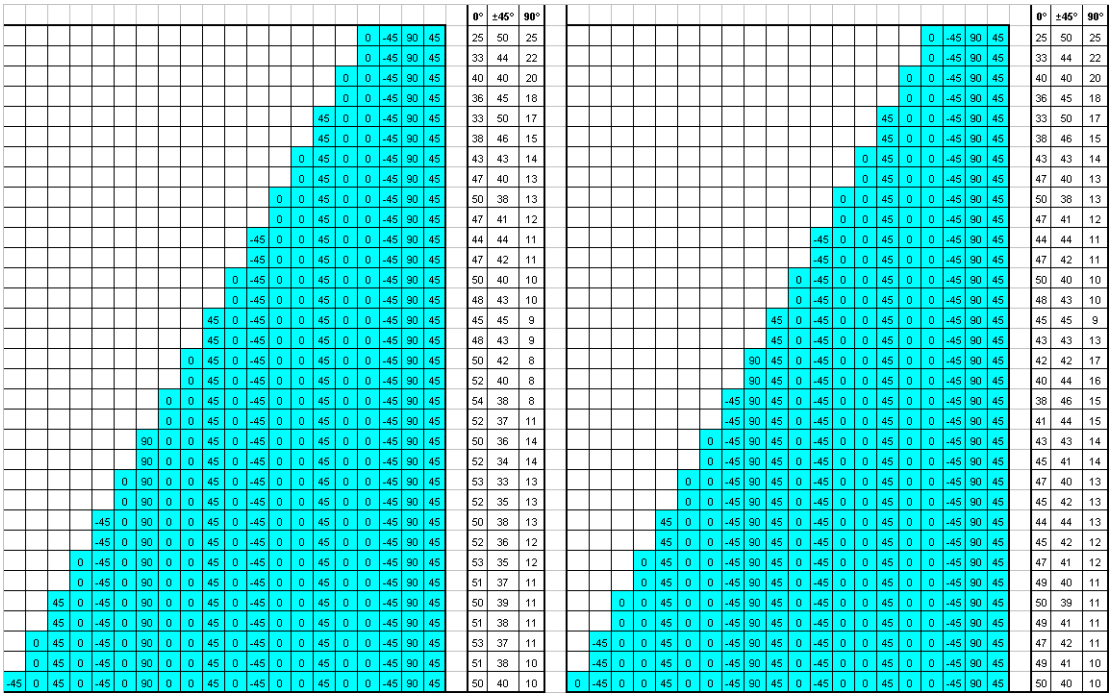

Figure 4-14: Ply table for 50/40/10 laminate (LHS Tailored; RHS Grouped)

Designers have had considerable success by staying with similar families of laminates for most applications[44], and uniformly distributing the different ply orientations through the laminate. However, uniformly distributing the plies through the laminate can be quite difficult the more orthotropic the laminate becomes. For a quasi-isotropic laminate, the repeatable band of plies to always achieve exactly 25/50/25 is [+/-/0/90], for example. Thus with a ply thickness of 0.25mm, then each band has a thickness of 1mm, and the resulting symmetric laminate is only 2mm with a lay-up of $[+/-/0/90]_s$. For a more orthotropic laminate, such as a 50/40/10 laminate, it is harder to obtain the desired laminate, as this can only be achieved with a symmetric and balanced laminate, such as the following stacking sequence, resulting in a laminate thickness of 5mm:

- $[+/90/-/0/0/+/0/0/-/0]_s$

Throughout the build-up of the laminate it is possible to minimise the difference between the actual laminate percentages and the target of 50/40/10 by selectively choosing which ply orientation to use, as shown in the LHS of Figure 4-14, while following the laminate design rules. However, if there should be consistent grouping of plies, as shown in the RHS of Figure 4-14, then the laminate will diverge more from the 50/40/10 target. This divergence from a perfect 50/40/10 laminate is shown in Figure 4-15, where it can be clearly seen that the grouped laminate has a far greater divergence than the tailored. On average, for the 0°, ±45° and 90° plies, the tailored diverges by 0.86%, -0.36% and -0.5% respectively, whereas the grouped diverges by 2.14%, -0.95%, and 1.19%.

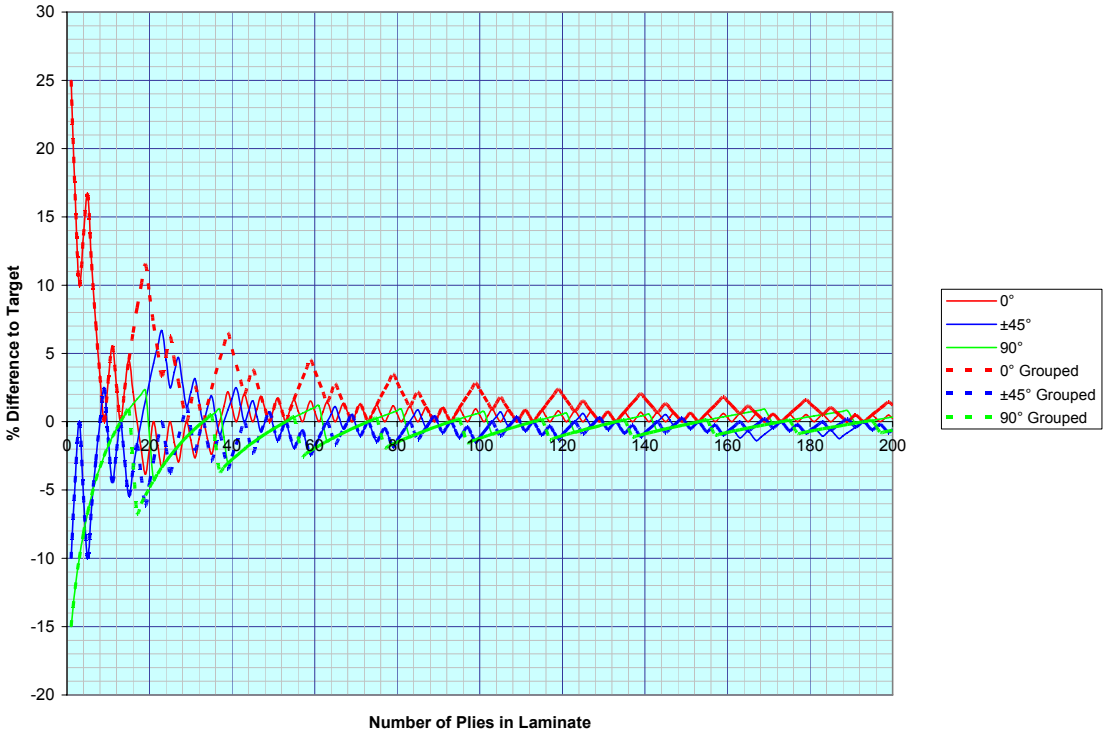

Figure 4-15: Difference between desired 50/40/10 laminate and reality due to ply integers and stacking guidelines

4.4.2 Damage Tolerance Influence

The outermost plies should not be aligned with the principal stress direction, thus ±45° plies should be used[306]. This increases the delamination initiation energy in comparison to when 0° plies are placed on the outside[188,311,312,313], as the laminate can absorb more energy elastically, and hence has increased residual strength[311]. The damage tolerance of the laminate is further improved if mainly ±45° plies for carrying in-plane shear are used, as opposed to a principally 0° ply dominated laminate, as shown in Figure 4-16[157].

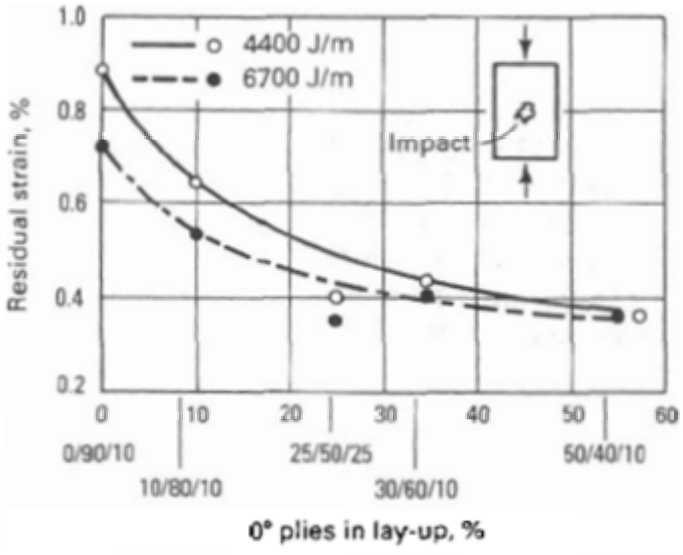

Figure 4-16: Effect of ply lay-up on residual compression strain after impact

The total delamination area, and hence the energy absorbed during impact[314], will be determined by the stacking sequence[315] and the ply-group thicknesses. This is attributable to bending stiffness mismatch between adjacent plies, resulting in cracks between the resin rich areas at the interface, which propagate between the different fibre orientations[143], and not between lamina in the same ply group[152,316,317].

From Table 4-1[314] it can be seen that typically the laminates with ±45° on the outside have the highest compression strength, although the stairwell (0/+/0/-) laminate in the last row of Table 4-1, also has very good overall CAI strength. A relationship exists between the maximum delamination area, and the CAI strength[xxiii], with a larger area producing a lower CAI strength. This is because the CAI strength is determined by stability criterion, which is dependent on the width of the delamination area and the ply stiffness[318]. The total delamination area is the summed area of delamination for all plies in the laminate, and the laminates with surface ±45° plies had the lowest total delamination area. By increasing the number of dissimilar interfaces, particularly when using a stairwell effect where possible[188], and minimising blocked plies, this can increase the energy required to initiate delamination[188,319,320], however the CAI strength seems fairly independent on the number of dissimilar plies, or having ±45° surface plies[314].

Panel	Maximum delamination area (mm²)	Total delamination area (mm²)	Plain compression strength (MPa)	CAI strength (MPa)	Number of dissimilar interfaces
$[(\pm45,0_2)_2]_s$	510 ± 58	1350	880 ± 118	344 ± 35	10
$[(\pm45)_2,0_4]_s$	870 ± 50	1360	881 ± 99	318 ± 64	8
$[(+,0,-,0)_2]_s$	650 ± 21	870	718 ± 35	298 ± 5	14
$[(0_2,\pm45)_2]_s$	765 ± 12	1510	660 ± 11	312 ± 12	10
$[0_4(\pm45)_2]_s$	1620 ± 26	2070	659 ± 92	273 ± 4	8
$[(0,+,0,-)_2]_s$	360 ± 44	2170	724 ± 43	339 ± 11	14

Table 4-1: Carbon fibre/toughened epoxy (T800H/924C) 16 ply panels, 600mm by 300mm

Delamination propagates through the thickness until a preferential ply, nominally the 90° ply[321], is reached, with delamination spreading along the 90° ply interface[322]. Eliminating the preferential interfaces can repress the damage growth[188]. By positioning the 90° plies towards the middle of a substantially thick laminate, delamination should occur deep inside the laminate, creating thicker sub-laminates. Alternatively, for a thinner laminate, it may be preferable to have the 90° towards the outside of the laminate, so that a resultant thicker sub-laminate occurs after impact. This results in a higher ultimate failure load[323,324], as the damaged laminate has higher resistance to buckling and propagation of delamination is reduced.

4.5 Laminate Tapering

To analyse a taper in the laminate, Classical Laminate Theory is no longer relevant, due to a three-dimensional state of stress being present at the termination[325]. Owing to the large number of factors contributing to the design of the tapered laminates, it is necessary that a few simple design rules are determined, albeit design rules are typically specific to a certain case, thus they are not necessarily applicable in the general sense[326]. Furthermore, the margins for

[xxiii] Energy level of 7J with an impact mass of 2kg, impact velocity of 2.5m/s and a 10mm diameter hemispherical tip

safe deviation from these rules of thumb are not well understood. Nevertheless, at the preliminary design stage, design rules should be adequate.

In general, terminating plies will induce a stress concentration that peaks at the terminated ply edge[327,328], resulting in delamination[140], due to the continuous plies diffusing their load into the terminated plies. This will induce both in-plane and out-of-plane (interlaminar) stresses[327], with the interlaminar stresses attributed to a mismatch in the elastic properties between plies. However, the interlaminar stress is very local to the termination, and the in-plane stresses have minimal effect on delamination. The greater the number of terminated plies, i.e. a larger step size, the more exacerbated this issue becomes, whereas the taper angle is not so critical[329]. Hence, trying to minimise the weight, through tailoring the thickness to suit the load, can be negated somewhat by a reduction in laminate strength[327].

Plies should be terminated so that the laminate maintains its symmetry about its mid-plane, although this is hard to achieve, as normally one ply is dropped off at a time, resulting in local asymmetry. However, commercial wing covers have fairly thick skins, thus there is no real difference between a single-ply asymmetric and a symmetric taper in terms of failure mechanisms[330]. It should also remain balanced, thus if a +45° ply is begun or terminated, then the next ply to be begun or terminated should be a –45° ply[296]. The external plies should always be uninterrupted with as much continuity through the laminate to benefit the overall strength and stiffness.

Figure 4-17 illustrates both internally or externally terminated plies. Internally terminated plies are preferred to limit the risk of delamination[331]. Furthermore, the strength of laminates with internal terminations are roughly twice that of externally terminated plies[332], albeit there is still a significant reduction in both tensile and compressive strength[333,334].

Figure 4-17: Basic methods of terminating plies

There are two principal methods of internally terminating plies. The method shown in the top-half of Figure 4-18[335] is termed ‘interleaved’, and is the preferred method[335]. As the size of the resin pocket is a crucial parameter affecting the stress distribution in the taper area[329], then interleaving techniques can be used, where the terminated plies are evenly distributed through the thickness and interleaved between continuous plies, resulting in a diamond pattern. To further enhance this method, plies should be dropped off deep inside the laminate at the beginning and the end of the taper[336]. The other method, shown in the bottom-half of Figure 4-18, is not preferred. However, if this method is adopted, then for every 3 adjacent dropped plies, there should be a covering ply, to minimise delamination[337].

To mitigate interlaminar shear stresses at ply terminations then only 2 plies can be dropped at the same point[336,338]. However, the depth of the step, caused by the termination(s), determines the mean stress to initiate delamination[335], thus it is also dependent on ply thickness. A basic principle for determining the number of plies that can be terminated, is the resultant stress through the taper caused by the stress concentration knockdown, should be less than the allowable stress for the thinner section[327]. Where the laminate is buckling critical, and hence is not limited by the allowable strain, it is more appropriate to drop off many plies, whereas if it is strength driven then it should be more gentle[327]. This is evidenced by experimental data showing that a thicker laminate requires a smaller stress to initiate delamination[321]. Alternatively, a blanket strain limit can be used, such as -4000με[326], to mitigate the effects.

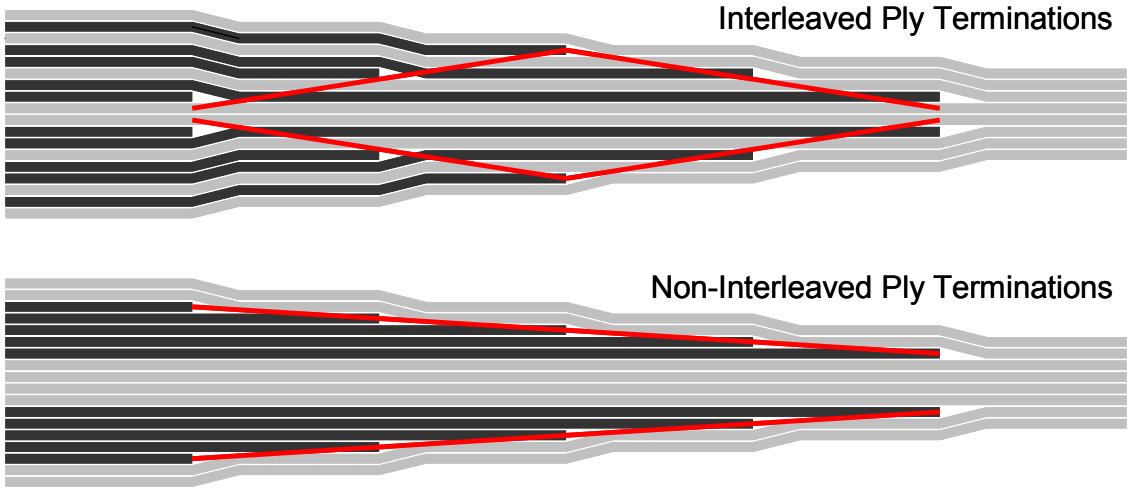

Figure 4-18: Interleaved and non-interleaved ply terminations

With many internal ply terminations, this rapid change in thickness will cause wrinkling of the fibres, which can lead to delamination when reacting load, thus plies should be terminated in small increments[339]. Therefore, a taper ratio ≥ 1:20 for high strain areas, such as in the principal load direction, whereas for lower strain regions, such as normal to the load direction, a steeper ramp-out rate such as 1:5, could be used[336]. Other research has found the previous taper design rules conservative, where taper ratios can be as low as 1:3, albeit for terminating ±45° plies it should ≥ 1:8[327]. There should also be a suitable distance between the end of one taper and the beginning of another, to avoid interaction between the stress concentrations.

Grouping of plies should be avoided in tapered regions, especially those carrying the principal load[326], such as the 0° plies. ±45° plies are also critical as they undergo in-plane shear deformation, which can cause failure of the plies along their length[329]. In general, it is best practice to drop off the 0° plies in areas of lower stress, 90° in areas of high stress and the ±45° plies in between[325,326,336]. Furthermore, dropping a 0° orientation ply onto another 0° ply should also be avoided[326] and a 0° ply onto a 90° ply[340].

In the taper region, structural integrity can be enhanced by either increasing the strength of the interface between the plies; or decreasing the interlaminar stresses[341]. Apart from interleaving, other techniques can be applied such as using a layer of film adhesive in the area at the ply drop to raise the stress required to initiate delamination[331,332,341]. Alternatively, the ply edge at the termination can be chamfered, through abrasion, to reduce the step height[331].

4.5.1 Computational Taper Investigation

For free edge problems, a closed form analytical method can be used to calculate the three-dimensional stresses and ply delamination. However, due to the discontinuity in the stress boundary conditions at the corner of the step, such a method is not applicable to delamination prediction of tapered laminates[335]. ESDU have developed program ESDUpac 9103, which predicts the tensile load at which delamination occurs in a tapered laminate, based on fracture mechanics[335].

ESDUpac 9103 was used to investigate the criticality of terminating either a 0°, ±45°, or 90° plies on the tensile performance of a 4mm thick 10/80/10 laminate, as shown in Figure 4-19. The number of plies terminated at the same position was also investigated, with a ply thickness of 0.25mm. It can be seen quite clearly that the 0° plies are the most critical,

whereas the 90° are the least, and that terminating more plies at the same position is also critical.

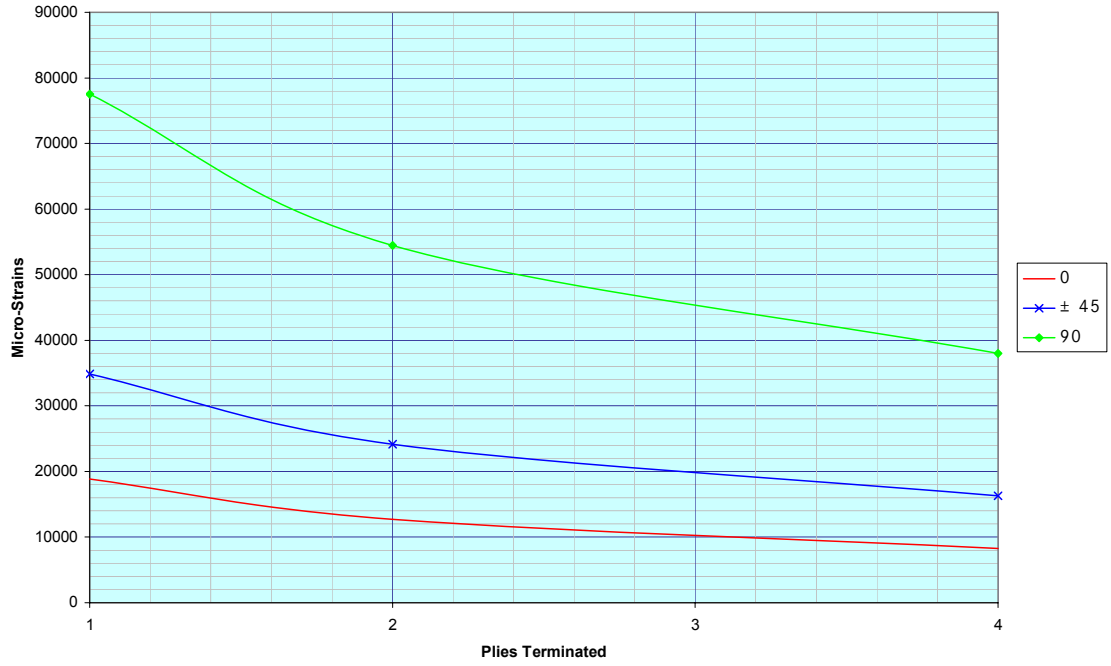

Figure 4-19: Criticality of terminating different ply orientations in 10/80/10 laminate

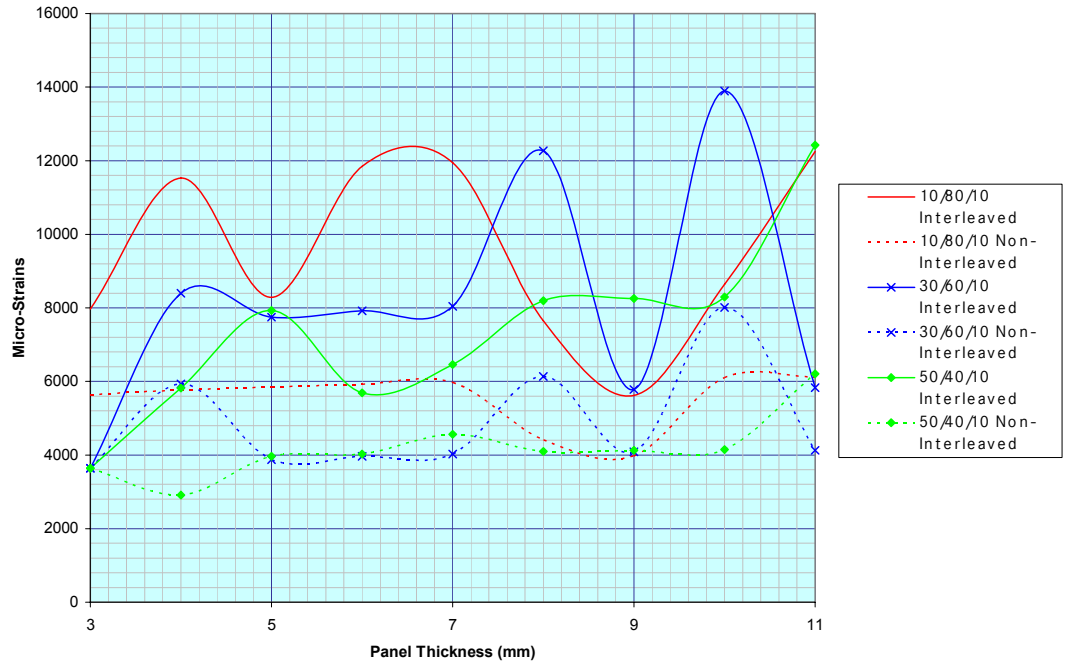

Figure 4-20: Influence of interleaving on different laminates for increasing thickness

This program was further used to perform an investigation on 3 different laminates, namely 10/80/10, 30/60/10, and 50/40/10, as shown in Figure 4-20, to illustrate the advantage of terminating the plies using an interleaved method. The change in laminate thickness was 1mm per taper, thus 4 plies were terminated at the same position. Due to the laminates having different percentages of ply orientations, this means that at each taper a combination of 0°, ±45° and 90° plies could be terminated. From Figure 4-20, it can be seen that, in general, the 50/40/10 laminate is the most critical, with the lowest allowable tensile strain, whereas the

10/80/10 is the least critical. Furthermore, by interleaving the plies this gave a step-improvement in performance of the laminate. However, due to the limitations of ESDUpac 9103, the step-improvement in performance due to the interleaved arrangement is clearly justified, as part of the program input is to identify if the laminate has a configuration that is interleaved or not. If it has, then automatically the performance of the interleaved is increased by a factor. The reasons for the fluctuation in the curves, is due to the sensitivity of either terminating a 0°, ±45°, or 90° ply, with 0° being the most sensitive, hence greater fluctuation, whereas the 90° plies are the least sensitive.

4.6 Ply Blending

Ply blending is the method used to ensure the contiguity of plies across the complete laminate, i.e. at wing skin level, after individual panels, for instance between adjacent ribs and stringers, have been individually optimised. However, to globally optimise a laminate, for the wing skin, the following shortcomings must be resolved:

- The overall panel has sufficient strength and stiffness, through continuity of plies
- The resultant laminate should require little amendment to ensure that it is manufacturable
    - Therefore limitations of the lay-up process have to be inputted as constraints
- All pertinent laminate design rules and design drivers should be respected
    - Therefore design rules have to be inputted as constraints
- Resultant laminate, with its particular stacking sequence, will need to have an estimated allowable strain for strength calculation
- Ensure resultant design has flexibility for change in load
    - Loads are not fully established until the end of the detailed design phase
    - By having a variable stiffness laminate, this will mean the load flow across the laminate will also change
- Joints of plies of different orientations are not recommended[342]

There are three principal approaches in optimising the laminate of the wing skin. The first resolves all the above issues due to its simplicity, although at the risk that the laminate is not optimal, and the last method exacerbates the above issues, whereas the second could be the best compromise:

- Fixed Laminate
    - Such as a 50/40/10, with a predefined stacking sequence, therefore only thickness is a variable
- Guide Laminate
    - Such as 50/40/10, where the percentages of plies are fixed, but the stacking sequence can be optimised
        - So the wing box global stiffness is left fairly impassive to changes in stacking sequence, but local panel buckling performance can be enhanced
- Flexible Laminate
    - The optimum number of plies and their stacking sequence

4.6.1 Genetic Algorithm Application to Flexible Laminates

With the flexible laminate method, the number of plies and the stacking sequence are discrete design variables, entailing a multitude of combinations. For example, if a 3mm symmetric laminate is fabricated from 12 plies, then the panel has 720 (6*!*) possible sequences. This is compounded by having 3 choices of ply orientation, i.e. 0°, ±45° and 90°, resulting in 2160 possible stacking sequences. However, in reality, due to the design rules, the laminate would have the outer plies as [+/-/90/0], therefore only 2 plies can be optimised, due to symmetry, leaving a choice of 6 combinations.

As previously mentioned, GAs are very good at solving the best thickness and stacking sequence for both stability and strength[343], although in order to improve computational efficiency, the panel is typically characterised by a number of parameters that is less than the number of design variables[307]. GAs are also good when the problem has multiple local minima for a given load and panel size, where there may be several stacking sequence permutations that offer similar performance.

Guide based GA reduces the search space by forcing the generation of the individual panel laminates to be completely bounded throughout the optimisation process. A typical individual of a guide based GA is shown in Figure 4-21. Every individual will be made from two strings. The first string is the stacking sequence of the guide, whereas the second string is the number of layers to be retained from the guide for each of the panels that the guide represents. Therefore, the second string of the individual is the same length as the number of panels that the guide represents. The stacking sequence for the first panel is the first n^1 layers of the guide and the second panel has the first n^2 layers of the guide, and so on for each successive panel[344].

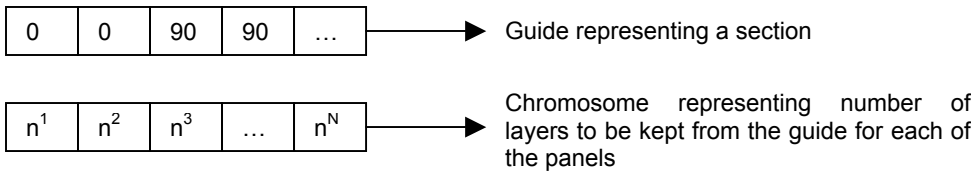

Figure 4-21: Typical individual in guide based GA

The first part of the individual (i.e. the stacking sequence guide) of the initial population is generated randomly. The second part of string is assumed to be equal to the number of plies in the stacking sequence of the guide.

4.6.2 Blending Methodologies

These stacking sequence combinations for the panel can be compared to adjacent panels to analyse the contiguity of plies over the laminate, with continuity constraints applied to minimise ply discontinuity[345]. This process is commonly known as 'blending', which simplifies the overall ply lay-up process and increases the structural integrity[344,346]. The common plies that span across adjacent panels are known as 'global plies'. A measure of continuity can be defined by the ratio of the number of continuous layers to the total number of layers. A ply in one panel's skin laminate is allowed to continue into the adjacent panel's laminate if both layers have the same fibre and orientation, and if they are separated through the thickness by a small number of terminated layers[347], which can be assumed to be a single layer.

Another methodology called OLGA (Optimisation of Laminates using Genetic Algorithms)[348] uses Darwin, which is an advanced commercially available GA computer code. The program calculates for multiple panels, the best stacking sequence, while ensuring a degree of blending, against both stability and strength constraints. The data structure of OLGA contains two principal elements: sub-laminates and design variable zones. The sub-laminates include the stacking sequence parameters (number of plies in the stack, the ply orientations, material types), whereas the design variable zones model geometrical identifiable sections of a structure. By using sub-laminates, the problem can be broken down, which increases the flexibility of blending, which between sub-laminates is easier than with one complete laminate, over various panels. Shown in Figure 4-22[348] are 3 laminates, with each one having a minimum and maximum number of plies, which take into account the minimum needed for panel's individual optimisation, and the maximum needed to ensure blending.

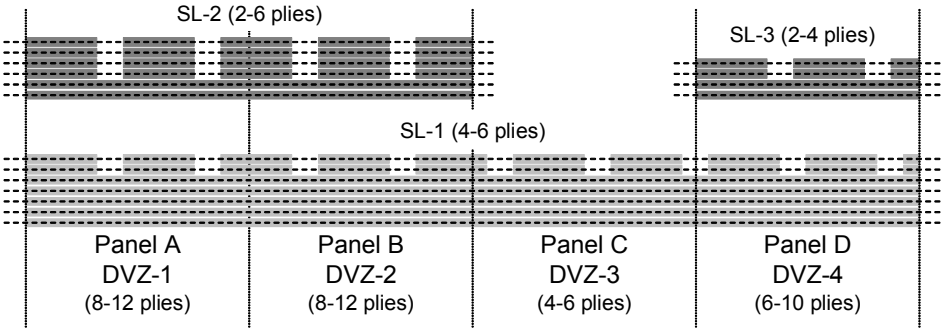

Figure 4-22: Sub-laminate arrangement for blended panel design

A further improvement to the above method is achieved with using an inwardly blending process, where for a simple wing box structure, the Greedy Global/Local with Bounded Implicit Enumeration algorithm[349] solution was 252.73kg in comparison to 255.91kg[344], based on the above process. The weight saving was achieved by ensuring that the outer plies were continuous i.e. inwardly blending, as shown in Figure 4-23[349].

Figure 4-23: Outwardly/inwardly blended

The simplest blending methodology can use the panel with the highest loads (hence thickest) as a guide and using a "greater-than-or-equal-to" blending rule, which allows to continuously drop plies in neighbouring panels[350]. In reality, there may be more than one panel that determines the thickest part, so blending in this case can be done by dividing the panel into overlapping sections, which in Figure 4-24[350] are labelled A to D. If, for each section, the frame of reference is rotated, then the "greater-than-or-equal-to" blending rule can be used again.

Shown in Figure 4-25 and Figure 4-26 is an example of the complicated skin architecture for a theoretical convergence of 3 types of laminates, namely a typical 44/44/11, a 30/60/10 laminate that could be used at the wing tip, and a soft 10/80/10 laminate that could be used along the manhole plank area. As shown in Figure 4-26, the pictorial representation is a single ply of 0.25mm, however, as it is symmetric there will be an opposite ply too. Figure 4-26 is built up by thickness, not necessarily by the individual ply, thus it shows the relative complexity of not having a single laminate type.

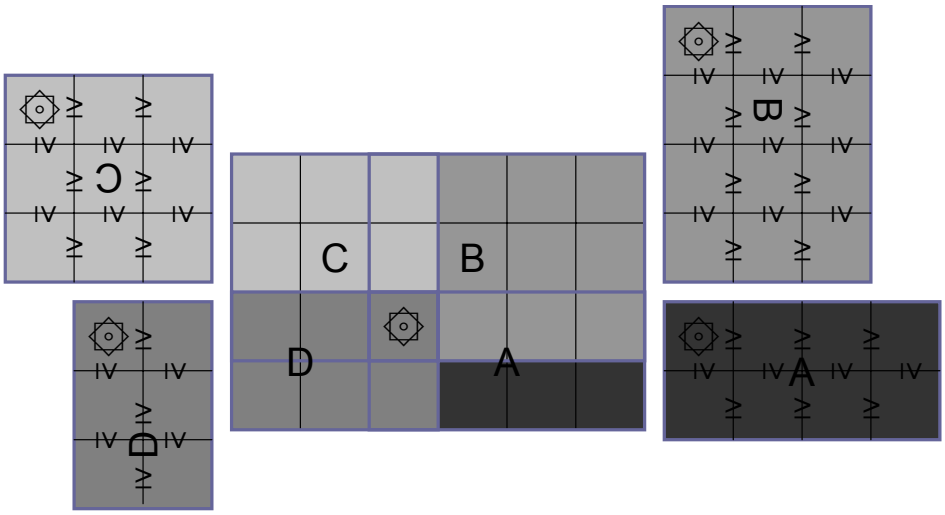

Figure 4-24: Re-orientated sections

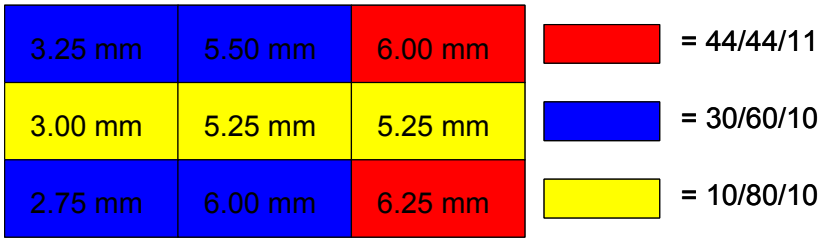

Figure 4-25: Laminate definition and thickness for 3 by 3 panels

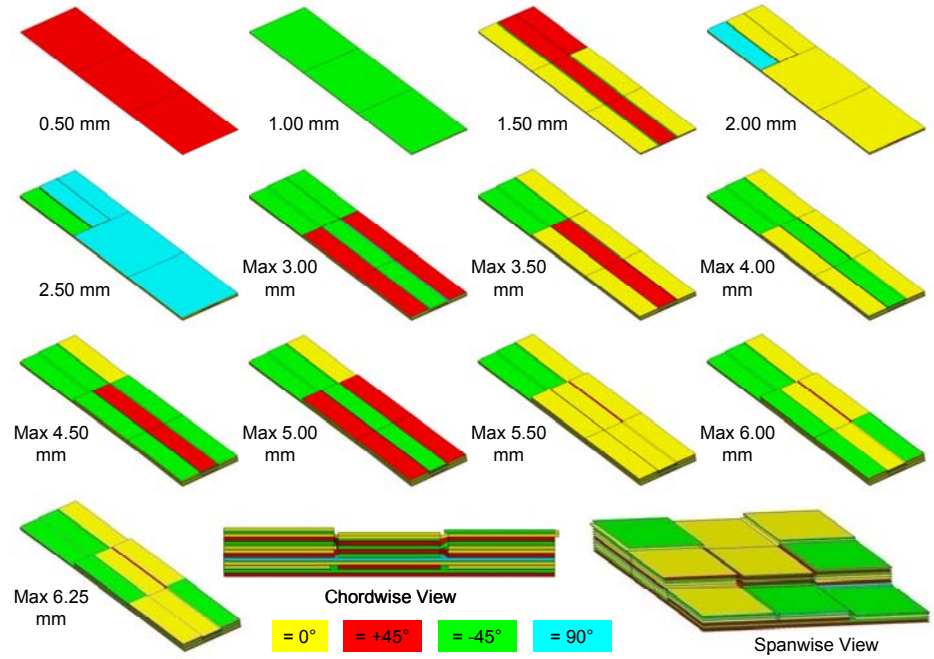

Figure 4-26: Thickness build-up

4.7 Assembly Influence

4.7.1 Bolted Joint

As shown in Figure 4-27, the transition of the bolt load into the laminate will be highest in the 0° plies, and least in the 90° plies.

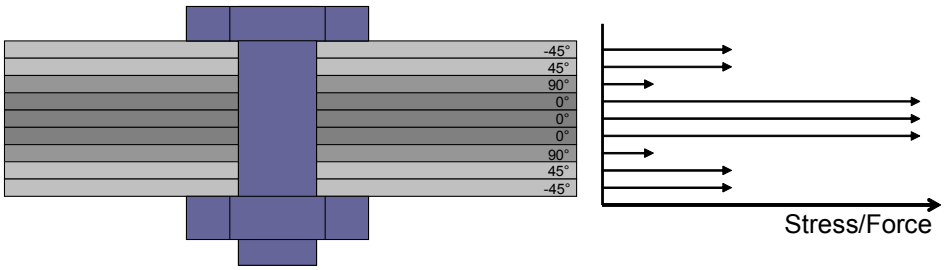

Figure 4-27: Proportion of stress through laminate

The bearing strength can be improved by using all three ply orientations i.e. 0°/±45°/90°[351], such as a quasi-isotropic laminate, which is the laminate used for the Boeing/BAE Systems AV-8B wing skins, to allow for easy field repairs, without the need to consult the manufacturer[233]. It has also been evidenced that for quasi-isotropic laminates, when the 0° and 90° plies are adjacent to each other then this gives a stronger bolted joint, as having these plies together can cause microcracks, which can locally allow the resin to fail and ensures a better load redistribution, which is not possible when the resin is so stiff, that the fibres fail first instead[352].

To enhance the bearing stress a greater percentage of ±45° plies should be added, at the expense of 0° plies[353]. Similarly, the bypass stress can be improved by increasing the percentage of 0° plies, which help to increase the allowable net section stress[354]. The stacking sequence has a large effect on the bearing strength of the joint, with 90° plies on the outside having the highest bearing strength[351,355], which improves the bearing strength between 12-20%, in comparison to a laminate with 0° plies on the outside[356]. To mitigate shear out failure and fastener pull through, the laminate should be designed to be bearing critical, thus at least 40% of ±45° and 10% of 90° plies are required, as these types of failure occur when the laminate is highly orthotropic and lacks bending stiffness.

4.7.2 Bonded Joint

In general, ±45° plies should be placed adjacent to the bondline, as the load is transferred through shear, whereas 0° plies are less favourable and 90° plies should never be placed adjacent to the bondline[357]. However, it is known that by placing 0° plies at the surface can increase the shear load transfer[358]. Furthermore, as 0° plies are the stiffest plies in the laminate, they will have the highest stress, thus having a higher proportion of 0° plies in the laminate as well as locating 0° towards the outside, will reduce the local peel and shear stresses along the bondline, in comparison to the laminate's average stress, thus aiding the bond strength[359].

4.8 Summary

It is seen that designing a laminate is at best a compromise. Having a pair of ±45° as the outer two plies is mandatory, as it maximises buckling performance, reduces coupling effects, is

good for shear transfer between bonded parts, and benefits damage tolerance. It is also known that a 90° ply towards the outside improves buckling performance, particularly under shear, bearing strength, and used with the outer ±45° plies can provide support to the 0° plies to benefit the strength of the laminate. Finally, it is known that the 0° plies are necessary towards the outside of the laminate, to improve global bending stiffness, and to maximise the buckling wavelength, which can increase the rib pitch. In order to maximise the buckling performance of the laminate, as well as the bearing strength, the outer 3 plies will be:

- $[+/-/90]_s$

Thereafter, the laminate will be influenced by the required percentages of each orientation. Independent of this though, the 0° and ±45° plies should be equally banded through the laminate to ensure multiple shear paths, which consequently allows the stair well effect with the additional 90° plies, to ensure that for thicker, hence stiffer, laminates the damage tolerance is optimal through the stacking sequence. Where possible, the 90° plies should be added last to the banded stacking sequence to maximise the thickness of the sub-laminates should delamination occur.

A good laminate will have a varying percentage of the different ply orientations, such that under 8mm, there is a higher percentage of ±45° plies, due to stability, whereas after 8mm there are more 0° plies, due to strength. 0° plies are added to improve the strength in thicker laminates, however it is known that 0° plies should not be terminated in areas of high stress, therefore the number of 0° plies terminating and dropping onto another 0° or 90° should be minimised in this area.

A diamond tapering approach should be used, with the first and last ply of the taper being dropped off deep in the laminate, ±45° plies should be dropped off together, to minimise any imbalance. This approach also allows better selectivity of the plies to be terminated, than when the ply in the laminate's middle is terminated.

A good laminate for a wing skin is a 44/44/11 or 50/40/10 when stability, strength, damage tolerance, and integration of mechanical fasteners are considered.

5 Assembly Techniques

The joining method used for CFRP structures will determine the structural efficiency[360], as the joint generally affects the component strength, thus it will heavily influence the weight and cost of the part. The assembly methods for CFRP wing covers are[148]:

- Mechanically fastened
- Adhesively bonded
    - Co-Cured
    - Co-Bonded
    - Secondary Bonded
- Mechanical and adhesively bonded (hybrid joint)

When comparing a design that minimises the use of mechanical fasteners against a design using fasteners, then it should be on the basis of total cost[361]. Currently, the time required to design a bonded structure is longer than that for a mechanically fastened structure[362].

The de Havilland DH-98 Mosquito was an early example of an aircraft using composite materials. The natural wood was used to carry the in-plane loads, whereas for components such as the landing gear, control surface mounting brackets, and wing-to-fuselage joints, i.e. the out-of-plane loaded components, metal fittings were used. Today with manmade CFRP, where the resin has an even weaker bond than in wood, such a policy is even more relevant[339]. The inadvertent introduction of out-of-plane loads can cause failure in composites; hence bolted joints are often favourable under this loading condition.

Both adhesive and multi-row bolted joints under shear load transfer operate in similar manners, albeit in a bonded joint the load path is far stiffer[363], by as much as 10 times[352], which means they can be very unforgiving. A large difference exists in that a bolted joint can have varying types, number of, and diameter of fasteners depending on the size of the parts to be fitted together and the load going through them, whereas a bonded joint efficiency, which has no voids or porosity, is dependent on the adherends' thicknesses. For this reason, bonding is best applied to thin structures, whereas for thicker parts a bolted joint is more suitable[363].

5.1 Mechanically Fastened Joint

Advantages:

- Positive connection, low initial risk
- Can be disassembled without destruction of the substrate
- No thickness limitations - within reason
- Simple joint configuration
- Simple manufacturing process
- Simple inspection procedure
- The fastener itself is not environmentally sensitive to heat or moisture
- Provides through-thickness reinforcement – not sensitive to peel stresses
- No major residual stress problem
- Good reliability at an economic cost[364]
- Does not require careful surface treatment of the adherend[365]

Disadvantages:

- Plain holes will cause a stress concentration
- Filled holes will concentrate the stress at the bearing surfaces
- Holes can expose fibres to chemicals
- Can be prone to fatigue due to out-of-plane loads[255]
- May require extensive shimming
- Can increase drag due to fastener to skin flushness
- Can cause rework if carried out incorrectly
- Not as strong as a bonded joint or less the joint is thick
    - Thus weight is added and overall joint efficiency is reduced
- Will require secondary sealing due to fuel leakage protection
- Will influence lightning strike mesh design – adding weight and cost
- Time consuming process
- Logistically inferior due to keeping stock of standard and repair fasteners

Typical wing cover laminates are fairly orthotropic, resulting in a joint efficiency that is lower than for metals[233]. However, with an increase in laminate thickness, the load bearing capability will also increase, which then favours the use of a bolted joint. Installation of some mechanical fasteners can cost as much as $100 per fastener, due to the requirements for hole preparation, inspection and the cost of the fastener itself[44].

Both the assembly of composite parts and dissimilar material parts is possible, albeit precautions must be taken when joining dissimilar materials together. A CFRP/metallic joint can cause fretting in the metallic part leading to fatigue cracking. When joining CFRP and aluminium, a 0.1mm thick layer of GFRP is required to act as a barrier between the faying surfaces, as the aluminium would corrode without it, and the fasteners used must be galvanically compatible, and sealed from one of the materials.

Mechanically fastened joints require high dimensional tolerances and shimming to assure a good fit, in order to avoid damage to the CFRP during assembly[44], and induce out-of-plane loads, which can lead to delamination, as found on the Harrier AV-8B wings[135]. Thus, good quality control is essential for the production of CFRP mechanical joints[44].

5.1.1 Fastener Type

The following points should be considered before choosing which type of fastener to use[366]:

- Fastener material
- Corrosion compatibility
- Strength & stiffness
- Head configurations
- Clamp up torque
- Hole fit
- LSP

There are two fastener choices, namely a bolt or a rivet. Bolts are preferred, as they provide the greatest strength[351], as no damage is caused on application, or less over tightened. Standard rivets will typically crush the CFRP or damage the hole, due to the rivet expanding,

whereas percussion riveting is not allowed due to the susceptibility of CFRP to delamination and split out on the reverse side. Furthermore, swaged collar or blind fasteners should be avoided, as when the stem breaks off, the energy dissipated in the CFRP can cause extensive delamination[363].

The standard countersunk fastener has a 100° head[366], however for thin laminates it is possible that knife-edge conditions can occur, thus a limit is set that the countersunk head should be no deeper than one-half to two-thirds of the laminate thickness, depending on the bearing stress on the shank[233]. Typically, countersunk bolts have a lower strength than a protruding bolt head, although with greater thickness the difference is less pronounced[367]. This is because under shear load, the shear force in the bolt is balanced between the contact forces of the parts being joined, hence with the countersunk head, the stress on the reduced shank will be increased[367], which also increases the bearing stress. Figure 5-1 illustrates the differences between bolts designed for tension and for shear. Typically, for thick laminates, tension head bolts should be used as they give the best all-round performance when bolt bending or pull-through is considered[366], however a 130° shear head is also beneficial for pull-through, and is very good for bearing as it maximises the bearing area of the shank[366] for thinner laminates.

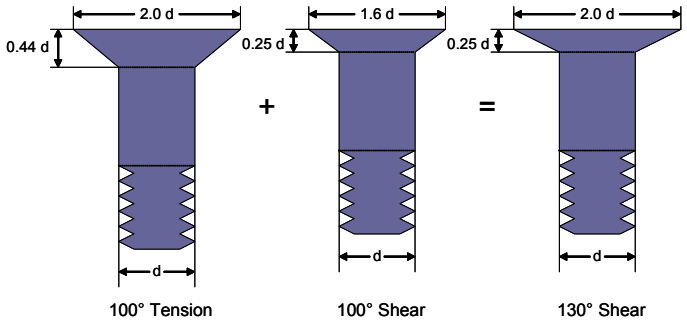

Figure 5-1: Different between tension head and shear bolts

Due to galvanic corrosion issues[xxiv], the practical choice of fastener material for use with CFRP parts is limited to titanium, stainless steel or Inconel[366]. Such fasteners are relatively expensive and heavy, with titanium having the most desirable strength/weight ratio[366]. Ti-6A1-4V is the typical titanium alloy used for fasteners with CFRP, with an ultimate tensile and shear strength of 1100 and 660MPa respectively. When higher strength is deemed necessary then either A286 (1400MPa; 760MPa) or alloy 718 (1515MPa; 860MPa) can be used. For thick structures, which require high shear strength, multiphase alloys that have a shear strength up to 1000MPa can be used. There are also thermoplastic CFRP bolts, which avoid arcing during lightning strike and eliminate any galvanic corrosion problems; however they are expensive and limited by their strength relative to metallic fasteners.

5.1.2 Joint Strength

The design of a CFRP bolted joint is more complex than with metals, due to the resin and fibre type used, the stacking sequence, the complex 3D stress and strain distributions in the joint area, failure modes that do not exist for metal joints, and CFRP bolted joints can fail at loads that cannot be predicted by either perfectly elastic or plastic hypotheses[368].

[xxiv] CFRP acts as a cathode.

Introducing load through mechanical fasteners is difficult to achieve with CFRP, due to the poor interlaminar shear and transverse normal stress properties[369]. The knockdown in strength and fatigue life, due to installation of a fastener, can be as much as 50%, relative to a plain laminate[367]. Furthermore, the free edge effect of the hole will initiate fatigue damage[370], causing crack growth to initiate through two different mechanisms: either in-plane fractures for thin laminates or out-of-plane delamination for thick laminates[371]. There are various parameters that help to determine the static and fatigue strength of the joint[351,360,372,373]:

- Material:
  - Fibre type and form
    - UD or woven fabric
  - Resin type
    - Toughened is beneficial
  - Laminate stacking sequence
  - FVF
  - Fibre surface treatment
- Fastener parameters:
  - Fasteners type
  - Fastener size
  - Clamping force/tightening torque
  - Washer size and bolt/washer clearance
  - Hole tolerance, bolt clearance and chamfer
  - Plain hole or countersunk
- Design parameters:
  - Joint configuration
    - Single shear, doubler shear, single bolt, single bolt row, multi-bolt row
  - Joint geometry
    - Pitch, edge distance, width, hole pattern, laminate thickness and tolerance, etc
  - Loading condition (tension, compression or combined static and/or fatigue loading)
  - Loading rate
  - Failure criterion
- Environmental conditions

By softening the laminate, either by replacing the 0° plies with ±45° plies or glass, this can increase the operating strains. However, this will reduce the laminate's principal modulus, resulting in an efficient joint, but an inefficient structure. Another method to reduce the local stress concentration is to increase the thickness of the structure local to the joint, with a doubler. If the doubler uses primarily ±45° plies, this reduces the stress concentration, relative to the base laminate. However, this leaves the other areas, which have not been softened, with little damage tolerance protection, thus the opportunity for bolted repair is limited. By using a tapered thickness doubler this can improve the efficiency, particularly when a multi-row bolted joint is used[374]. As shown in Figure 5-2[363], if assembled parts have different stiffnesses, due to the part's modulus or thickness, then there will be an imbalance in the load transfer, which can increase the bearing stress on the thinner part[363].

The combined thermal and hygroscopic (effects of moisture content), known as hygrothermal effects, affects the bolted joint strength, due to their influence on the resin system[368]. Moisture absorption will cause plasticisation of the resin system, resulting in a weakening of the fibre/resin interface[364]. This will cause a knockdown in the maximum bearing strength by as

much as 20%[364], as well as the interlaminar shear and compressive strengths. It will also impede the fatigue life[375].

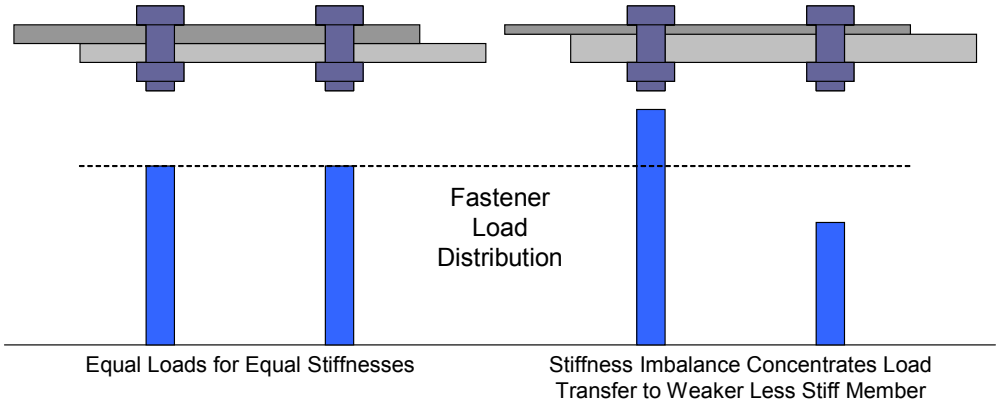

Figure 5-2: Effect of stiffness imbalance on bolt load distributions

5.1.2.1 Interference Fit Fasteners

An interference-fit fastener improves the fatigue life of metal parts, however for composites, due to the low interlaminar strength of CFRP, it has been considered to reduce the overall strength[376]. However, it has been evidenced that a slight interference-fit in thermoset-CFRP could improve the fatigue life of the joint[376]. Typically, net-fit is the maximum interference required, which has an allowance of 0.000 to +0.102mm[377]. Other benefits attained with a slight interference fit are[363,366,376]:

- Increase joint strength through enlarging softened area in laminate local to fastener
- Lower joint deflection
- Equal fastener load sharing
- Reduction of relative fastener flexibility – this causes localised high bearing stresses
- Reduction or delay of hole growth/degradation
- Improved LSP – interference bolts in a sleeve can aid in electrical continuity
- Inhibit fuel leakage
- Provide the necessary reactive torque required for one-sided installation of Hi-Lok fasteners

The amount of interference is fairly easy to control with bolts, and if a sleeve bolt is used, such as the Lockbolt from ALCOA Inc[363], then this should limit the damage to the laminate during installation.

5.1.2.2 Hole Dimensional Tolerance

Tighter tolerances are also necessary with CFRP joints, as if one of the fasteners has a tighter fit, then that bolt will have a higher bearing stress, and due to the lack of ductility in CFRP, load redistribution will only occur after the highest loaded hole has failed. Conversely, with aluminium, inaccuracies in the joint geometry are not as critical, as it will deform plastically and redistribute the load to neighbouring fasteners.

However from a cost perspective, larger tolerance bands are sought after, although bolt hole clearance has a significant effect on bearing strength at 4% hole deformation. This is because with a net fit, load is transferred immediately, but with a clearance fit the load transfer is delayed and is transferred to a smaller area[378]. However, the ultimate bearing strength does not depend on the bolt hole clearance.

5.1.2.3 Torque Tightening

Fasteners that are torque tightened have higher failure loads, as part of the load is transferred by friction and thus delays slippage of the parts, albeit this increases the bearing stress. Clamping pressure is more beneficial for thinner laminates, as this should inhibit localised delamination resulting in local buckling[364]. It is also beneficial, in terms of fatigue life, when used in combination with clearance-fit holes[366]. Countersunk fasteners can provide some clamping force, but far less relative to a protruding head fastener[233].

To ensure the clamping force is effective, the force should be distributed over a large area in order to avoid crushing of the laminate[366], hence a washer can be used. A washer can also improve the joint integrity by suppressing delamination directly under the washer[367] and the micro-buckling of the fibres. The choice of washer diameter is critical, as clamping pressure for a given clamp-up load is inversely proportional to the square of the diameter of the washer, thus a smaller washer will have a higher clamping pressure. Therefore, a smaller washer will lead to a lower tensile strength of the filled hole laminate, with the optimum washer to hole diameter ratio being between 2-3[354].

Laminates with a higher percentage of 0° fibres (>50%), seems to be more sensitive to the clamping effects of the bolt on net-tension strength, which is attributed to the delamination and fibre-matrix splitting[354]. Although fibre-matrix splitting can potentially increase the tensile strength of the filled-hole laminate, it is not desirable as it can propagate under fatigue and also limit the ability of the laminate to react other loads[354].

However, due to the time-dependent nature of composites, there will be relaxation in the clamp-up force, hence the joint will lose some of its strength. For this reason, data accrued for joint performance is based on only 50% of normal fastener installation torque[379]. Furthermore, for a multi-fastener joint, it would take only one under-torqued bolt to significantly inflict a weakening of the joint static strength[233].

5.1.2.4 Multiple Fastener Rows

When more than one fastener is required then a tandem row is preferable[380], as opposed to a parallel row, as shown in Figure 5-3[380]. The distance between the adjacent rows should be greater or equal to 4d. With multiple fastener rows, the fastener holes will typically be subjected to both bearing loads, i.e. the shear load transferred by the fastener, and loads that bypass the hole and carry on through the remaining laminate. This ratio is the bearing load to bypass load and is dependent on the joint stiffness and configuration[381]. This ratio considers the interaction caused by the stress concentration due to the individual fastener, and the further stress concentration due to the diverted load. The maximum stress in the laminate occurs at the edge of the hole due to the bypass loading acting through the area of the narrowest cross-section. As compressive loads can be transmitted through the bolts, whereas

the tensile loads must circumnavigate the bolt through the net section areas, this results in the tensile loads being more critical[233].

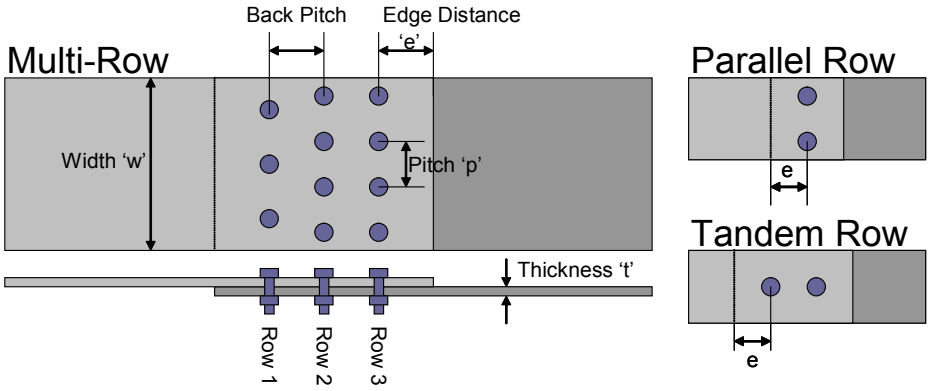

Figure 5-3: Design parameters of the bolted joint

Shown in Figure 5-4 is a bearing-bypass diagram, which can be plotted with the knowledge of the allowable bearing and tension/compression bypass stresses. The tensile through the hole failure is where the load through the hole will cause the laminate to split at the hole, whereas the bypass failure is where there is too much load circumnavigating the hole causing the laminate to fail. For a small width to diameter (w/d) ratio, i.e. a narrow strip, the bearing cut off may not be reached due to the net tension failure. For a large w/d ratio, at high bearing loads, the bearing cut off limit would be achieved. The area enclosed by the dashed line in the diagram represents the safe design area.

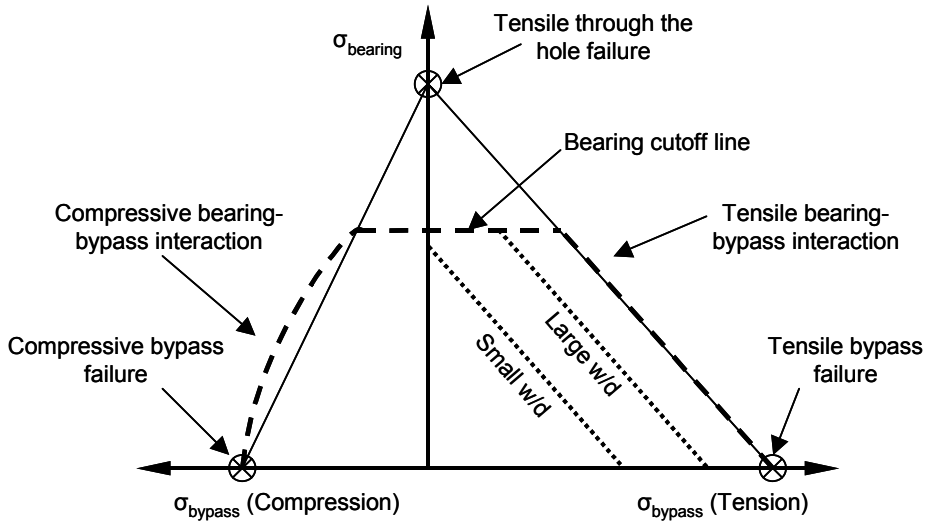

Figure 5-4: Bearing/Bypass diagram

With multi-bolt rows, the outermost rows will have the greatest load transfer, as depicted in Figure 5-5[373], which is similar to the shear stress distribution of an adhesively bonded joint. This provides justification for reducing the number of rows in the joint, albeit to reduce the peak fastener load multiple rows are used[363]. Furthermore, the inner bolt rows of a multi-bolt row joint will restrict the relative motion of the adherends more efficiently than if only one or two rows of bolts were used, thus reducing the joint's susceptibility to fretting fatigue[363].

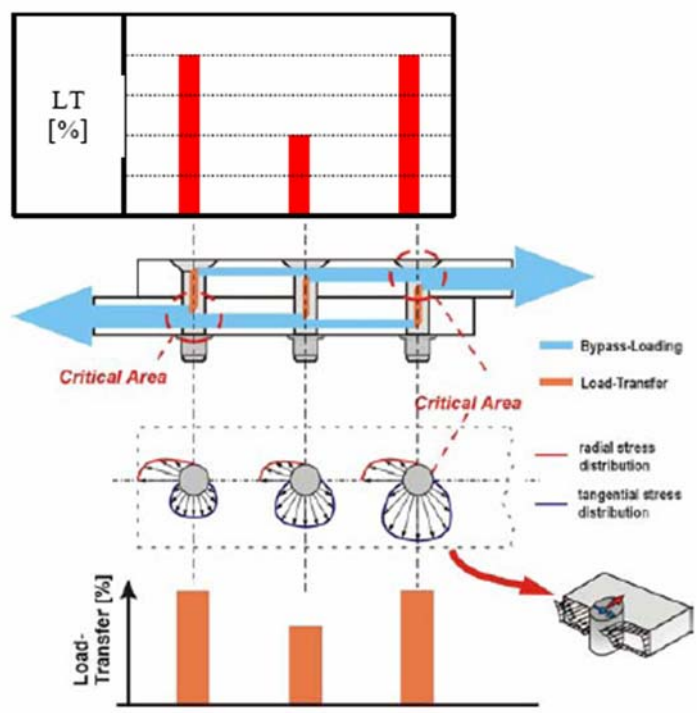

Figure 5-5: Force progression of a single-shear, triple-row joint

5.1.3 Failure Modes

Between 60-85% of failures in composite structures occur at the joints[376], hence it is important to understand the gross failure modes, as shown in Figure 5-6[356]. Due to the local contact between the fastener and the laminate, there will be large strains induced into the laminate, which creates a high stress concentration that can lead to different failure modes[355]. This can then limit the allowable strain to -2500με, whereas without this limitation a strain of -6000με would be possible[382]. In order to relieve the high stress concentrations around the contact edge of the hole, delamination, fibre micro-buckling and matrix cracks occurs[383]. The consequence of this is that the parts fail at a lower load than an isotropic material, such as metal[384], due to the viscoelastic resin properties of CFRP laminates[366]. Therefore, areas where bolting is the design driver, will have a maximum strain limit imposed[307].

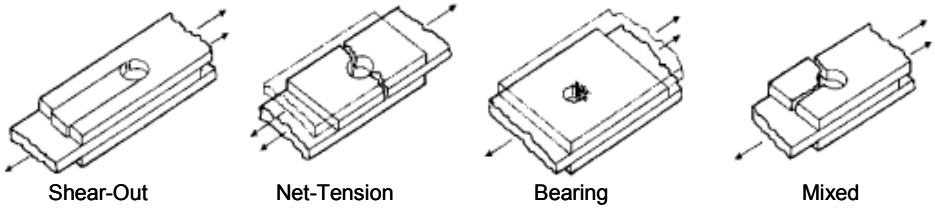

Figure 5-6: Typical failure modes for the pinned-joint configuration

5.1.3.1 Net Section (Net-Tension) Failure

This failure occurs transverse to the direction of the bolt axial load, which results in the laminate breaking between the bolts. This is caused due to the stress concentration[354], which initiates matrix and fibre tension failure. This is principally due to tangential or compressive stresses at the hole-edge, which is a result of bearing-bypass interaction, when the bypass load is too high. This mode of failure is due to narrow fastener spacing, or the w/d is too low.

Net section failure only occurs with the strongest type of laminate for bolted joints i.e. quasi-isotropic, but it is catastrophic as it has the least post-failure strength, and it will be impossible to repair the joint by replacing fasteners in their original position, hence this mode of failure should be avoided. To mitigate this failure, the tensile strength of the fibres and the bearing strength of the laminate[356], should be maximised. The fastener spacing should have a pitch between 4-5d, although this is dependent on the laminate's stacking sequence[367], but it should not be greater than 6d, as this could induce inter-fastener buckling, as well as incur a weight penalty. An edge distance of 3d is required in the direction of the load, but perpendicular to the load, the edge distance can be reduced to 2.5d. Thus the bolting configuration to avoid net section failure should be as shown in Figure 5-7.

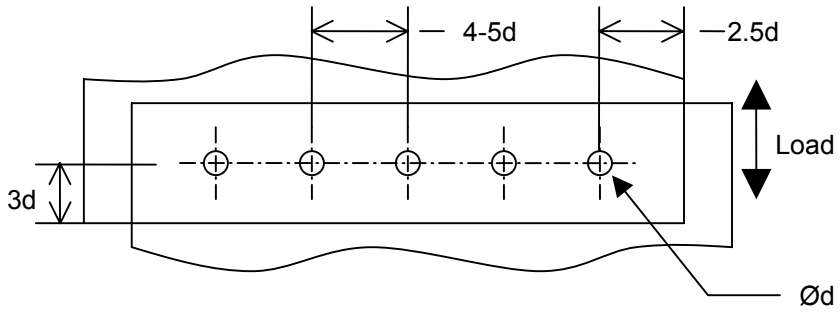

Figure 5-7: Bolt pattern configuration to avoid net section failure

5.1.3.2 Bearing Failure

Bearing strength for bolted joints is typically defined by two values, i.e. the safe and the maximum bearing strengths. The safe bearing strength is when the bearing hole is deformed by 4% of the hole diameter i.e. 0.04D, whereas the maximum bearing strength is the bearing stress at which the fastener hole is deformed to failure[356]. Joints should ideally be bearing critical as this does not necessarily lead to catastrophic failure, and is a relatively strong mode of failure. Only the local area around the hole will be damaged allowing for the hole to be drilled out and the fastener replaced with the next nominal fastener size. Based upon, principally, the joint bolt spacing (d/w), but to a lesser extent the stacking sequence[233], this will determine whether the joint fails in tension or bearing.

This failure occurs when the ratio of d/w is too small, or when the ratio of the bypass load to bearing load is low. To maximise the bearing strength, the joint geometry should have an end distance to hole diameter (e/d) $\geq$ 3-4 and w/d $\geq$ 4[356,385], and if possible it should be designed to fail simultaneously in both shear and tension[351]. For a multiple fastener joint, to minimise the bearing load and maximise the bypass load, the outermost rows should have a w/d =5, using smaller diameter fasteners, whereas the innermost rows have no bypass, therefore a w/d =3 should be used, using large diameter fasteners. A w/d =4 should be used for rows between the innermost and outermost[374].

Without any lateral constraint, the bearing strength is inversely related to the d/t ratio[351], with full bearing strength achieved with a d/t =1, as shown in Figure 5-8[351], albeit as d/t <1, this increases the possibility of pin shear failure[364]. Thus, for double shear the bolted joint should be configured through the thickness as shown in Figure 5-9. For laminates less than 6.35mm, the bolt should be slightly larger, and less for laminates with thicknesses over 19.05mm[233].

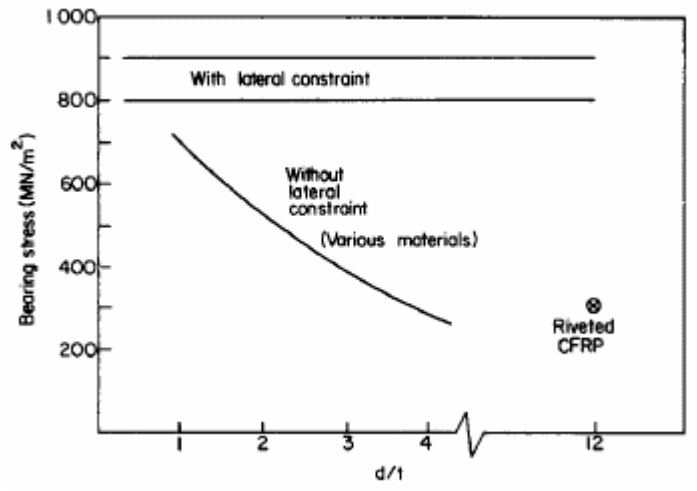

Figure 5-8: The effect of d/t ratio on bearing strength

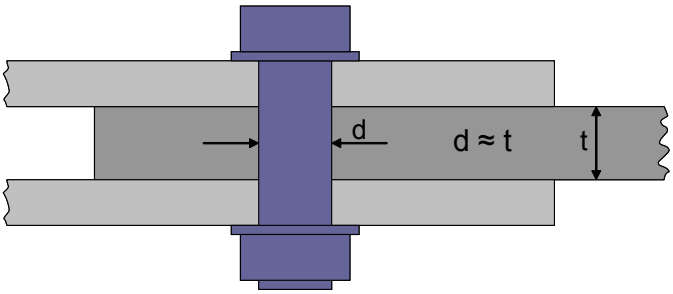

Figure 5-9: Thickness proportioning of bolted joint in proportion to bolt for double shear

Hart-Smith[233] has found that mechanical joints typically use bolt diameters that are less than optimal, due to the lower shear strength of a CFRP laminate in comparison to titanium fasteners. By using a smaller diameter fastener, this will maximise the bearing stress and reduce the cost of the fasteners, however it is more advantageous globally to decrease the bearing stress so that the operating stress of the composite part can be increased[363]. Furthermore, a smaller diameter bolt can bend under shear load, whereas with a larger diameter bolt, the laminate can be loaded more due to the bolt's greater stiffness.

Tension head fasteners with washers are best applied to joints critical with bearing failure, and the bolt hole should be reamed for a close tolerance fit[351]. The bearing strength can also be improved by using a toughened epoxy resin system, due to its greater ductility, which can be further improved if IM instead of HS fibre is used[364].

5.1.3.3 Shear Out Failure

Shear-out failure, just like bearing failure, is principally caused from shear and compression failures of both the fibres and matrix[354]. This is associated with the weakest form of bolted joint, when the laminate has a principally 0° bias, at the expense of the off-axis layers, due to satisfying the in-plane tension requirements[367]. To mitigate shear-out failure an $e/d \geq 3$ is required.

5.1.3.4 Fastener Pull Through

As the through-thickness strength of laminated CFRP is relatively poor, bolt pull-through, as shown in Figure 5-10[386], can be significant under certain load conditions. Furthermore, bolts are designed to carry shear load in-plane of the laminate; hence out-of-plane loading should be avoided[387].

This is a relatively weak mode of failure and is associated with undersize fastener diameters, which bend under load causing uneven bearing stress distribution across the hole's depth. This results in the fastener head rotating and digging into the laminate, and eventually the fastener being pulled through. High tensile strength and high modulus fasteners should be used to minimise the amount of bending, and due to the high reaction load on the fastener head, a tension head fastener should be used. The laminate can be thickened locally, as well as using high strength, low modulus fibres coupled with a toughened resin system[387].

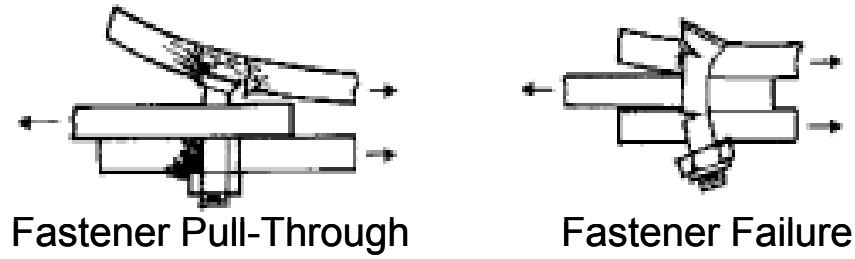

Figure 5-10: Fastener pull-through and fastener failure in composite laminates

5.1.3.5 Bolt Failure

Mechanically fastened joints are used for highly-loaded composite components despite their low bearing stiffness[383], which lead to bolt bending, which in combination with shear stresses could lead to bolt failure[367], as shown in Figure 5-10. To mitigate this, the fastener diameter should be increased, as well as using higher shear strength fasteners.

5.2 Bonded Joint

Advantages:

- Small stress concentration in adherends due to load distribution over large area[146,355]
- High joint efficiency index
- Minimises part count and hence has low cost potential
- Should allow for higher strains to be achieved in comparison to bolted joints[361]
- Reduces necessity for drilling
- Stiff connection
- Excellent fatigue properties
- No fretting problems
- Sealed against corrosion
- Smooth surface contour - can aid laminar flow wing designs on wetted surface
- Damage tolerant

Disadvantages:

- Limits to thickness that can be joined with simple joint configuration
- Inspection, other than for gross flaws, is difficult, thus quality control is more expensive
- Prone to environmental degradation
- Sensitive to peel and through-thickness stresses
- Residual stress problems when joining to metals
- Cannot be disassembled
- May require costly tooling and facilities
- Accurate mating of adherends
- Requires special surface treatment prior to bonding
- Heat and pressure may be required during bonding
- When joining dissimilar materials thermal effects needs to be considered

One of the principal advantages of composite materials is to reduce assembly effort by integrating the constituent parts. The cost of an assembly is directly proportional to the number of parts in the assembly, and assembly costs can account for as much as half the total cost of a finished composite structure[231]. It can also save weight, as attachment flanges, for fastening through, are not required[xxv]. Through the reduction of fasteners, there can be a subsequent extensive reduction in assembly cost and cycle time[388]. This is evidenced from the composite re-design of the Boeing C-17 horizontal tail plane[280] conducted in 1994, which resulted in a 90% parts reduction, 80% fastener reduction, 50% acquisition reduction and a 20% weight reduction, although it is not known what the design constraints were, i.e. was bolted repair considered? Finally, health and safety issues are improved as drilling holes in CFRP requires dust extraction, and less drilling results in a reduction in replacement drill bits as well as general wear on machines.

However, an integrated structure will typically result in a more complex design, requiring greater manufacturing effort, necessitating the use of complicated and expensive tooling[196]. Thus due to the inherent risks involved with integral parts; large parts, such as wing covers, are still typically assembled from discrete parts. In particular, wing covers for large commercial aircraft are both sizeable and complex, and using a one-shot process to manufacture such a composite wing will pose many challenges, and has so far, in terms of serial production, not been achieved[176].

Bonded joints should have better damage tolerance as fibres are not broken, however they are subject to out-of-plane damage due to delamination and debond, because of the relatively weak interlaminar strength of the adhesive joint[389]. Adhesively bonded parts are currently applied to lightly-loaded and non-critical structures, however to maximise their potential, they also need to be applied to highly-loaded structures[390]. Bonding has been applied to critical structure on metallic aircraft, such as the Fokker F-27, which amongst other parts, has wing stringers bonded to the skins, or the Boeing 747 and Lockheed C-5A, both having large areas of bonded structure[391]. This demonstrates that adhesively bonded structures applied to metal aircraft can be designed for durability, with a resulting service life of 30 years or more. Another example is the General Dynamics B-58[xxvi], which used aluminium-bonding techniques for 80% of the complete structure. However, it was purported that it had an

[xxv] The benefit of this is dependent on the structure's overall design and if bolted repair is provisioned for.
[xxvi] Supersonic bomber developed for the USAF in the late 1950s, and retired from service in 1970.

operating cost 3 times greater than the larger Boeing B-52, because of maintenance issues, which can be attributed to the bonded structure[135]. The well established bonding design principles for metallic structures could be applied to CFRP structures, in order to provide a foundation for a certifiable design. However, due to the difference in materials and their design, the bonding design principles may need to be heavily modified to suit CFRP structures[361].

5.2.1 Joint Types

There are many different configurations of bonded joints, as shown Figure 5-11, such as:

- Single strap joints:
  - Simplest bonded joint configuration
  - Highest stress concentration for this joint type at the free ends of the bond
  - The centre of the joint transmits very little load
  - Using a tapered single-lap joints could improve on simple joint behaviour
- Double strap joints:
  - More complex design
  - Eliminates most of the bending and peel stresses
- Stepped lap joints:
  - Difficult to machine
  - Not applicable to thin laminates
  - Produces a harmonised stress distribution
  - Good strength to weight ratio for the joint
- Scarf joints:
  - Similar to stepped lap joints but simpler to machine

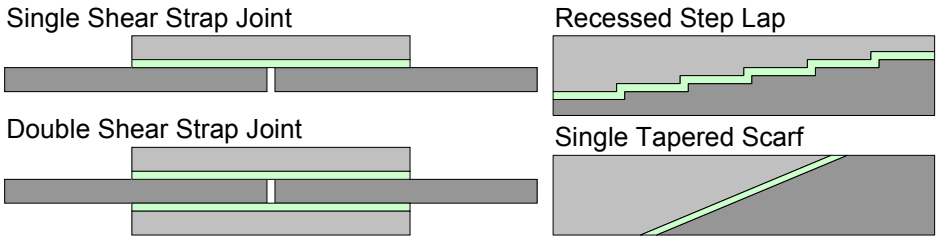

Figure 5-11:Variants of joint types

An alternative joint type is a π-joint, as shown in Figure 5-12[392]. Such a joint can be both co-cured and co-bonded to the skin, and have been applied to an Boeing X-45[xxvii] technology bonded demonstrator wing, which reduced costs by 29% in comparison to the baseline wing[393]. Some of the advantages of a π-joint are[388]:

- The π-joint has two independent bond lines
  - Thus inherent redundancy, and has higher strength than a conventional double lap shear joint
  - Joint works in shear and not tension, which is ideal
- Creates a determinant assembly feature
- Adhesive out-time issues are minimised

[xxvii] An unmanned combat aircraft prototype developed by Boeing

    - Less surface area is exposed to the air before the joint bonds
- Tolerant of inherent defects
    - Thick bond lines
    - Canted blade
    - Blade skewed to one side of the clevis
    - Voids or peel plies that were not removed

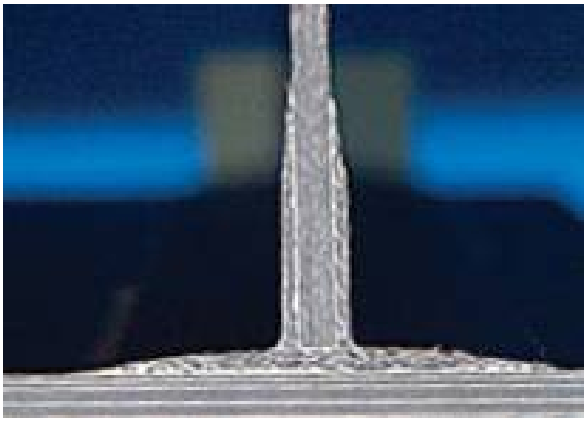

Figure 5-12: π-joint cross-section

5.2.2 Bonding Techniques

There are three principal bonding techniques, namely:

- Co-Curing
    - Uncured parts are cured together, using the resin in the constitutive parts to create the joint
- Co-Bonding
    - A cured and uncured part are cured/joined together to form a joint, using an adhesive between the constitutive parts
- Secondary Bonding.
    - Cured parts are joined using an adhesive between the constitutive parts

5.2.2.1 Co-Curing

The principal advantages of co-curing are[257,394]:

- Principal manufacturing steps are reduced
- Assembly fit-up difficulties are minimised
- Secondary machining operations can be avoided
- Inspection of each individual part is not necessary

The above points are evidenced by the Embrear Super Tucano's co-cured rudder skin panels, which resulted in a part count reduction from 100 to 33 parts, and a weight decrease from 16 to 12kg. This meant that both production costs and through-life-costs[139] could be reduced, in comparison to the hybrid-joint assembly used previously.

However, a major risk with co-curing is that if a deficiency is found in one of the constitutive parts, for example a stringer, after the assembly is co-cured, this may cause costly re-work, or worse still, the part is scrapped. This defect could have been found, at the constituent part level, if the individual parts were first cured, then inspected, and then subsequently assembled. Therefore, the co-curing process must be robust, using precise tooling to ensure repeatability. To achieve this, aspects such as technical risk, cost, schedule, and tool durability must be considered, to avoid issues, such as wrinkling shown in Figure 5-13[339], which can affect co-cured parts. However, if the correct measures are taken, co-curing should provide the highest quality part from all the bonding techniques. Furthermore, due to the relative flexibility of the uncured stringers, there is no need to put any pre-stress into the stringer to ensure they conform to shape, which means the part's mechanical performance can be maximised.

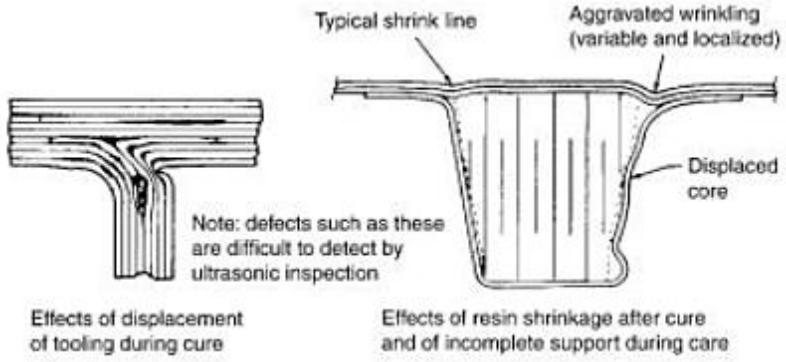

Figure 5-13: Laminate wrinkling of co-cured structures

5.2.2.2 Co-Bonding

Co-bonding techniques have developed from the lack of flexibility of co-curing. Co-bonding is a popular technique as it allows an already cured part to be bonded to an uncured part, using an adhesive ply to create the adhesive layer between the constituent parts. Such a process could be foreseen for wing covers, where either uncured stringers are co-bonded to the cured skin, or vice-versa. Due to the skin geometry and the variation in skin thickness, an uncured stringer that is more conformable, may produce a more compliant solution; however, when risk is considered if the stringers were already cured, then any defects seen in the stringers could be resolved before they are bonded to the cover. Furthermore, a pre-cured stringer design has greater outsourcing potential, as the parts can be made by a supplier, which is geographically separated, as there are no shop-life issues with a cured stringer.

Co-bonding requires a second cure operation, which is often critical, as the autoclave, like most capital equipment, is frequently found to be the bottleneck in the manufacturing process, however this can be minimised dependent on the utilisation of the autoclave or the outsourcing policy used, i.e. the stringers could be manufactured by a supplier.

Co-bonding, as an integral element of an LCM process is not possible. This is because the adhesive curing process requires pressure and heat, whereas resin infusion should not be done under pressure, as this would cause major porosity in the part being infused.

5.2.2.3 Secondary Bonding

The co-cured and co-bonded approach are preferred over secondary bonding[44], primarily due to the amount of effort required to ensure the adherends are clean and match for secondary bonding. Furthermore, if the stringers do not sit perfectly on the cover, then there will be built-in stresses, which will limit the performance of the adhesive, and cause subsequent fatigue life issues due to the in-built out-of-plane loads. Despite this, a further good example set by the de Havilland DH-98 Mosquito was its extensive application of secondary bonding of primary and secondary structures, as opposed to today's malpractice of mechanically fastening thin and lightly-loaded components[339]. Therefore, secondary bonding should be considered, where the baseline solution would be a mechanically fastened joint.

Secondary bonding techniques use either an adhesive paste or film, which means an autoclave is required, as both high pressure and heat is required. Therefore, this bonding process requires the greatest amount of autoclave time.

5.2.2.4 Hybrid Joint

As the wing box is primary structure, it is necessary to reinforce both co-bonded and secondary bonded joints with mechanical fasteners, which creates a hybrid joint[395]. This is due to FAR 23.573 (a)(5), which safeguards against contamination on one or both of the adherends' surfaces prior to bonding. The number and size of the 'chicken fasteners' are determined based on limit load (LL)[44]. This conservative approach is primarily due to the confidence level in the bond, which is attributed to the bond properties, the manufacturing process, and the ability to inspect the bond. This does not apply for well-designed co-cured assemblies, although through-thickness reinforcement from fasteners may be required in areas of high through-thickness stresses, such as Stringer Run Outs (SRO).

For a hybrid joint, the load path through the adhesive bond is far stiffer than through the fasteners, which result in the bolts reacting an insignificant amount of load until the bond fails[363]. In general, a hybrid joint has the following advantages:

- Fasteners provide an alternate in-plane load path
- Fasteners provide through-thickness reinforcement
- Fasteners can contain the propagation of the debond
- Fasteners can be used to reduce peel stresses
- Fasteners can be used as a positioning aid

5.2.2.5 Innovative Methods

Thermoset Composite Welding (TCW) is a process developed by Australia's Cooperative Research Centre for Advanced Composite Structures, using a layer of thermoplastic that is co-cured locally onto the surface of the carbon/epoxy laminate. Such a surface can then be subsequently welded together through heat and low pressure[396]. The purported advantages of such a process over conventional adhesive bonding is that less tooling is required; assembly can be conducted without a clean room, and it saves cost compared to mechanical fastening by as much as 30% for a control surface structure, with even greater savings compared to adhesive bonding.

5.2.3 Bonded Joint Failure

Bonded joints rely primarily on transferring load through lap plates, as shown in Figure 5-14[397]. Such load transfer is best applied to thin sections[255], due to the load being transferred through surface shear tractions between the adherends. Similar to a bolted joint, the thickness and stiffness of the individual adherends will determine the proportion of load between them[352].

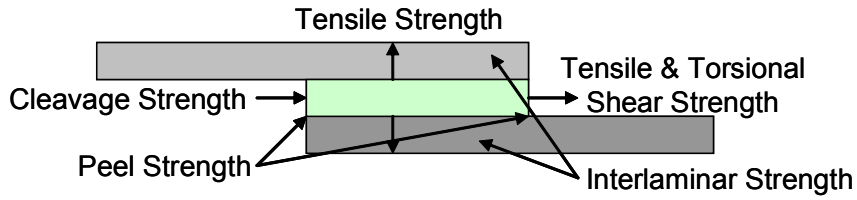

Figure 5-14: Components of bonded joint strength

The potential modes of failure for bonded joints, as shown also in Figure 5-14, are[148]:

- Tensile, compressive, or shear of adherends
- Shear or peel in the adhesive layer
- Shear or peel in the composite near-surface plies
- Shear or peel in the resin-rich layer on the surface of the composite
- Adhesive failure at the metal or composite / adhesive interface

The mode of failure is influenced by the lay-up, stacking sequence and surface plies of the laminate, hence a debond can spread from ply to ply in laminated panels, as shown in Figure 5-15[352]. The normal failure mode of bonded lap joints is delamination between the interface and second ply in one composite adherend, as depicted in Figure 5-15 A, if the bond thickness is thin (0.1-0.5mm)[374]. This is because of the high shear strain at failure of adhesives in comparison to the toughened resin systems of the CFRP parts. Therefore, under static load, the adherend surfaces will fail before the adhesive layer, as well as Hart-Smith[363] stipulating that he has never witnessed failure due to mechanical fatigue of the adhesive layer. Typically, the bond should have far higher strength than the adherend surfaces, so that any flaw in the bond will not grow (unzip) from load redistribution[363], thus making a flaw in the bond tolerable. However, the higher the nominal operating stress relative to the ultimate bond strength, the smaller the tolerable damage size[363]. At the absolute minimum, the shear strength of the bonded joint should be 50% stronger than that of the adherends, in the worst environment, which is typically hot-wet[363].

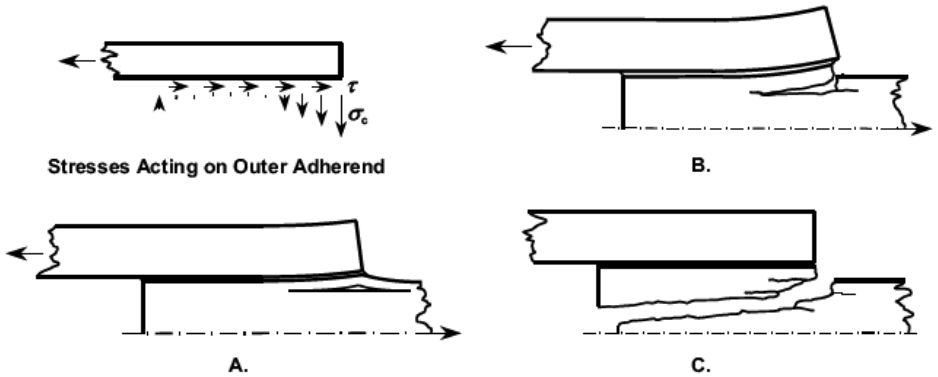

Figure 5-15: Interlaminar delamination in a composite lap joint due to excessive peel stress

Bonding of parts with different thermal expansion coefficients should be avoided, and parts that are bonded should have a maximum Poisson's ratio difference of 0.15[398], to avoid

interface shear issues, caused by the difference in transverse strains in the laminates, which the adhesive has to bridge. An increase in the Poisson's ratio will result in an increase in shear stress.

5.2.4 Adhesive Parameters

Adhesives should encompass the following properties:

- Strain capability
- Cure at the lowest possible temperature
- The coefficient of thermal expansion should be similar to the parts
- Moisture effects must be minimised, otherwise Tg is lowered leading to plasticisation of bond
- Thickness of the adhesive must not be too large

Normally, the bond layer should be between 0.12-0.25mm[399], if the bond layer is either too thin or too thick then it is unsuitable; or less the load is transferred by shear, where thick layers are acceptable[361]. Typically, the bond is stronger than the adherends for thin parts, and the opposite is true for thicker parts[352].

Film adhesive in comparison to paste adhesive is more practical and easier to use as it can be applied like a sheet, hence the amount of adhesive used can be easily controlled, for example it can be cut to the outline of the stringer foot. This can also save a lot of time during production. The film consists of an epoxy layer on a fabric carrier, with the fabric ensuring a minimum bondline thickness as the fabric prevents the adherends contacting each other[190]. Paste adhesives, which cure at room temperature, typically do not have the toughness or durability in comparison to film adhesives with a 121°C curing temperature. This is because they do not have the efficiency of the toughener phase transition during the cure cycle to create the rubber particles which mitigates against crack tip energy[400].

5.2.5 Peel Ply Influence

Principally, there are two methods to prepare the surface of a pre-cured CFRP laminate for bonding: surface abrasion or a peel ply. The peel ply is commonly used as it saves time and produces a more evenly treated surface[401]. A nylon peel ply is common, as it is easy to remove after cure, but it is due to this easy removal that the adherend surface is contaminated with silicone, from the peel ply weaving process, after its removal[402]. Furthermore, for a peel ply to detach without damaging the laminate, the fibres underneath the interface between the peel ply and resin must be totally inert[358]. An activated surface, not an inert one, is required to ensure a good bond, thus the adherend requires higher surface energy than that of the adhesive[358].

Klapprott et al.[401] carried out an investigation, and found that the resultant bond performance when using a nylon peel ply, is dependent on the construction of the peel ply's weave, the toughness, and impregnation ability of the resin used in the peel ply. When the optimum performance was achieved, in this case using a polyester Hysol® EA 9895 peel ply[403], the resultant bond strength had an improvement of 3 times in comparison to a typical nylon peel ply[401].

Therefore, two choices exist: A nylon peel ply is used, and subsequent to its removal, low pressure grit blasting is used to remove all pollutants and the peel ply residue[404], which can inhibit the bonding process[358]. Alternatively, using a polyester peel ply ensures that once the peel ply is removed, there is no need for further abrasion or cleaning[189].

Another issue with using a peel ply, which can particularly affect the adherends at the SRO, is that the texture of a peel ply will leave interlocking grooves on the adherend surface, as shown in Figure 5-16[358]. With a hybrid joint, the adhesive layer may only be subject to pure shear loads, as the separating peel loads have been minimised due to the bolts. Thus the interlocking grooves from the removal of the peel ply can effectively create a load path even if the bond fails[358], thus the adhesive does not need to adhere to allow pure in-plane shear loads to be transmitted.

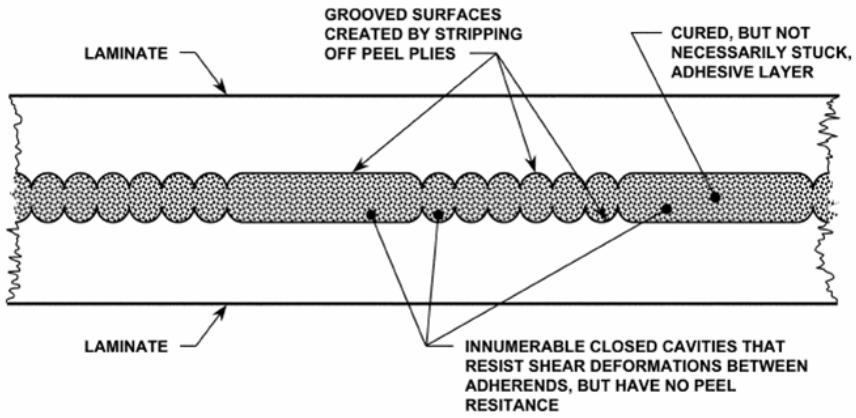

Figure 5-16: Representation of a peel-ply imprint showing orthogonal sets of interlocking grooves

5.2.6 Inspection Techniques for Bonded Joints

Even with a validated and strictly followed bonding process, and with the use of grit blasting or polyester peel plies, due to the deficiencies in the current NDT methods[362] ability to determine a joints' soundness, it is still necessary to include chicken fasteners to create a hybrid joint, for both co-bonded and secondary-bonded joints. However, the US Department of Defence led Composites Affordability Initiative project demonstrated an NDT technique using a high peak-power, short-pulse-length excitation, which generates stress waves that could identify the integrity of the adherends' surfaces, be it a kiss, weak or strong bond[388].

5.3 Stringer to Skin Bond

For a secondary bonded or co-bonded (with hard stringer), then it could be considered to crown the stringer's foot at the edges to improve the fit, in order to increase the thickness of the layer where the load transfer is the most intense, as shown in Figure 5-17[404]. Furthermore, the fillet of the adhesive, which forms at the stringer foot edge and the skin during the curing operation, should be left as this improves the joint strength[190]. This principle is demonstrated on a metal structure, where machining is relatively easy to accomplish, however the same principle could be applied on a CFRP structure, as in any case the stringer profile will be machined.

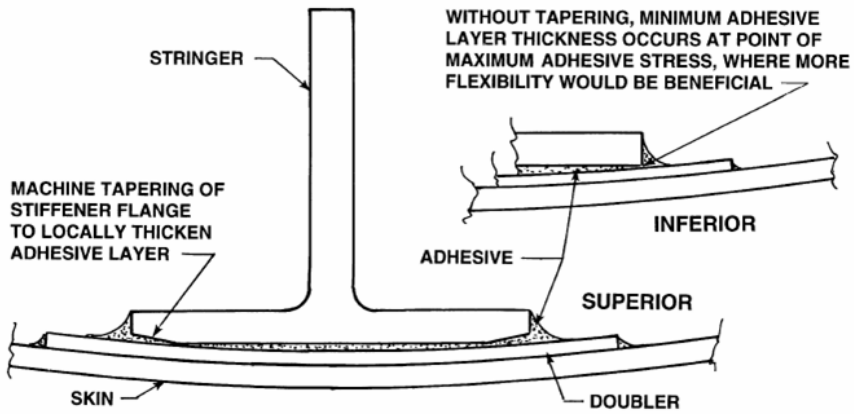

Figure 5-17: Crowning of the metallic T-profile stringer on the SAAB 340 lower wing skins

5.4 Summary

There are a number of integration techniques available, each having advantages and disadvantages in comparison to each other. The requirement to have a hybrid-joint for either co-bonding or secondary-bonding detracts severely from the integration methods, although using an intelligent design, the fasteners required can have a dual-purpose, for example, they can be used to attach the ribs. In any case, as explained later, even a co-cured structure should be designed for a bolted-repair, therefore the influence on the design through integrating bolts, should not penalise too severely a co-bonded or secondary bonded design.

An efficient bonded joint, should be designed to fail first in bearing, thus the d/t should be 1, the e/d should be 3 and 2.5, in load direction and normal to load direction, respectively. Titanium fasteners should be used, as they offer the best solution in terms of weight and cost.

In terms of bonding stringers together, a film adhesive should be used, as this is the most efficient process. In order to prepare for bonding, a polyester peel ply should be used.

6 Damage Tolerance and Repair

Over 81% of all damage on composite structures is because of impact, whereas 10% is attributed to lightning strikes, 7% due to overheating, and the remainder due to delamination[405]. During their manufacture, assembly and service life, CFRP components, will experience impact, with low-energy impact being considered the most perilous, as the damage may not be visible[406]. Designing a highly efficient, lightweight, and cost effective CFRP structure is achievable, however when damage tolerance and repair is considered, this optimum solution is harder to obtain. More specifically, a wing cover can fail due to the following reasons[407]:

- Skin failure:
  - Due to micro-buckling as a result of in-plane stresses in the 0° fibre direction
  - Due to delamination as a result of through-thickness stresses
  - Due to matrix cracking as a result of in-plane tensile stresses perpendicular to the fibre direction and in-plane shear
- Stringer Breakage:
  - Due to delamination
  - Due to buckling
- Skin to Stringer interface failure

To ensure the design is both fail-safe and can sustain large damage, deficiencies should be considered at LL, such as:

- Missing fasteners
- De-bonded stringer
- Large damage due to in-service collision:
  - Hole penetration between stringers
  - Hole penetration through both the stringer and skin
  - Stringer blade damage

6.1 Damage Tolerance

A definition of damage tolerance is: "the ability of a structure to contain representative weakening defects under representative loading and environment without suffering excessive reduction in residual strength, for some stipulated period of service"[408]. Hence safety is the primary objective of damage tolerance, but secondary issues such as minimising weight, as well as curtailing manufacturing, maintenance, and supportability costs[157].

The simplest way to create a damage tolerant design is to reduce the allowable strain by a clear margin below the maximum strain. Thus, once the structure is damaged there will be enough residual strength to resist failure[157]. This philosophy was used for a stringer-stiffened panel, fabricated from UD prepreg, which had a compressive strain allowable of -3600με[409]. The panel was impacted twice and then tested under compressive load, which established that the strain limit was suitable[409]. However, by constraining the design to the lower allowable strain, a weight penalty is incurred if the panel is strength-driven. For this reason, the panel should be designed to be damage tolerant, and the allowable strains should be maximised[157].

For a given impact energy there will be a resultant area of delamination, which will reduce the structure's strength. Damage tolerance allowables are normally based on strain versus delaminated area, or energy level or dent depth. This type of measurement can be used for different materials, thicknesses and loads (compression/tension/shear).

6.1.1 Impact Tolerance

The term "Impact Tolerance" is a combination of impact resistance and impact damage tolerance, dealing with the structure's holistic ability to undergo a given impact with a minimum effect on the structure. Impact resistance is the ability to sustain a given impact for a minimum amount of damage. Impact damage tolerance is the ability to sustain a given level of damage with minimum effect on the performance[188,410], and hence is the structure's ability to retain residual compressive strength. This means that if a structure is impact resistant it does not necessarily mean it is impact damage tolerant, as each aspect is determined by different parameters.

6.1.1.1 Impact Parameters

Impact can be classified into the following categories[411]:

- Low-velocity: contact duration of impact is longer than the time period of the lowest vibrational mode of the structure
- High-velocity: contact duration of impact is much smaller than the time period of the lowest vibrational mode of the structure
- Hyper-velocity: so fast that the local target materials will behave like fluids

Such a classification is required as the energy transfer between the projectile and target, the dissipation of the energy, and the damage propagation mechanisms, are all dependent on the speed[411]. The kinetic energy (KE) of the impactor can be transmitted to the structure, either partly or completely via a number of mechanisms, such as[412]:

- Elastic deformation of the structure
- Vibration of the structure
- Movement of the structure
- Generation of damage

The actual energy-absorbing mechanisms will be dependent on[188]:

- Impactor conditions
  - Shape, energy, mass and velocity
- Material properties
  - Matrix toughness, fibre surface treatment, moisture content, fibre strength and stiffness
- Stacking sequence and thickness
- Overall component geometry

Upon impact, the force on the panel will reach a maximum level, i.e. the peak force, which will then decrease to zero[413]. Depending on the panel and the impactor itself, this will

determine whether or not damage will occur. The peak force is critical in determining whether damage will be initiated, rather than the impact energy itself[414]. There are four principal modes of failure due to transverse impact damage[152,415]:

1. Matrix mode – cracking occurs parallel to the fibres due to compression, tension or shear
2. Delamination mode (critical matrix crack) – produced by interlaminar stresses
3. Fibre mode – in-tension fibre breakage and in-compression fibre breakage
4. Penetration – the impactor completely penetrates the impacted surface

The effects of the above failure modes on the laminate's elastic properties are shown in Table 6-1[416].

No Failure	Matrix Cracking	Fibre Fracture	Fibre Failure
E_{11}	E_{11}	E_{11}	$E_{11} \rightarrow 0$
E_{22}	$E_{22} \rightarrow 0$	E_{22}	$E_{22} \rightarrow 0$
υ_{12}	$\upsilon_{12} \rightarrow 0$	$\upsilon_{12} \rightarrow 0$	$\upsilon_{12} \rightarrow 0$
G_{12}	G_{12}	$G_{12} \rightarrow 0$	$G_{12} \rightarrow 0$
G_{13}	G_{13}	$G_{13} \rightarrow 0$	$G_{13} \rightarrow 0$
G_{23}	G_{23}	G_{23}	$G_{23} \rightarrow 0$

Table 6-1: Influence of damage mechanisms of elastic properties

Due to the out-of plane impact forces, matrix cracks within the plies will occur first, which are caused by through-thickness shear stresses. Matrix cracking is not as problematic as delamination but it can lead to moisture absorption[258]. Subsequent delamination is initiated through opening forces at the matrix cracks[417], which will propagate by mode II interlaminar shear stresses, as shown in Figure 6-1 due to the bending of the laminate upon impact. Delamination damage can affect the strength, stiffness and fatigue of the composite.

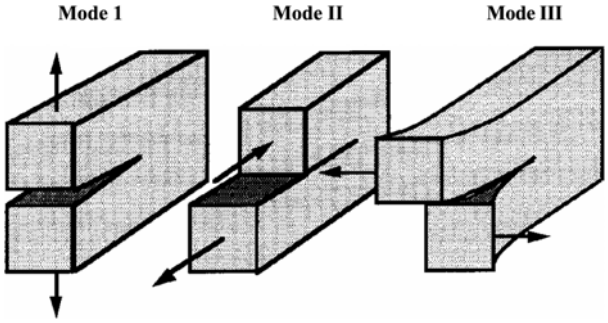

Figure 6-1: Different fracture modes

Fibre fracture, particularly at high-velocity, can absorb much impact energy; however fibre failure is a precursor to catastrophic failure, which occurs later on in the fracture process than either matrix cracking or delamination. Fibre failure occurs under the impactor because of locally high stresses and indentation effects[152]. When fibre failure reaches a critical extent, the impactor can completely penetrate the material. Fibre damage can result in 80% knockdown in strength; however, at a global level, the knockdown is far less due to the toughness of the material[418].

An increase in laminate thickness, will require higher impact energy to cause damage[419], as the critical force to create damage is proportional to laminate thickness[414]. The thickness of the laminate has a dominant effect on where ply delamination occurs through the thickness, with thick laminates having delamination at the impact surface and thin laminates on the back face[410]. The thick laminate will have minimal bending compliance, resulting in delamination

near to the contact face, whereas for thin laminates, due to greater bending compliance and longer contact duration, the delamination is on the back face.

6.1.1.2 Extent of Damage and its Inspection

Despite CFRP laminates having high-energy absorption under gross failure conditions, they have no elasto-plastic energy-absorbing mechanism and hence no obvious visible evidence of permanent indentation[418], which is evidenced by laminates suffering severe delamination, although on the surface there are no witness marks indicating damage. The damage mechanism is dependent on the stiffness of the panel. If a thin laminate is impacted by a large mass, this will cause several millimetres of deflection, resulting in visible damage, whereas for thicker laminates, indentation must be considered more stringently as it may not be visible[418].

Barely Visible Impact Damage (BVID) is a term that encompasses impact damage that requires close inspection to identify it. As BVID is hard to detect, the structure must be designed to withstand ultimate load (UL) for the life of the aircraft with multiple BVID[3], whereas for Visible Impact Damage (VID), LL must be withstood. It is also difficult to predict the knockdown in strength caused by BVID, which leads to a conservative design with a "no-growth" policy between inspection intervals[420] for impact damage during fatigue loading[421]. This is more rigorous than for metallic structure, which allows for some crack growth during the aircraft's life. This policy has led to a compressive allowable strain level, for example of -4000με, being applied for thick-skin primary structure[420].

The United States Air Force (USAF) Damage Tolerance Design Guide for BVID is an indentation depth less than 2.5mm, whereas 0.3mm depth is used for the visibility threshold for the ATR 72 composite wing box[405]. With a higher threshold for the determination of BVID, based on indentation, this will result in a more conservative design, and hence a lower allowable strain level. The effect of BVID on the structural performance is exacerbated by relaxation of the indentation, with reductions in depth of 45% being possible due to viscoelastic effects, cyclic loading, moisture absorption and temperature effects[422,423]. Thus, based upon a visual inspection technique, higher impact energy will be required to produce visible damage after relaxation for certification purposes[405], which would result in even lower allowable design strains. Furthermore, a toughened resin system will require greater impact damage to create a dent depth great enough so it can be seen, which reduces the allowable strains of the toughened systems.

If an alternative technique to visual inspection could be used, then it might be possible to increase the allowable strains, to benefit more from the toughened resin systems. This issue was evidenced by comparing an older CFRP system, Magnamite AS4/Hercules 3501-6, and a tougher system, Magnamite IM7/Cytec's rigidite 5250-4, which showed that the dent depths for the toughened system was between 30-50% smaller, for energies ranging from 14J to over 68J, whereas the C-scan damage sizes were similar between the two systems at lower energies[405]. This clearly illustrates the benefit of using an alternative to visual inspection, in order to maximise the performance advantage offered from toughened resin systems.

6.1.1.3 Impact Energy Thresholds for Wing Covers

Typical impacts on wing covers can include[418]:

- The dropping of tools - fairly low velocity between 4-8m/s and impact energies of up to 50J
- Runway debris - velocity up to 70 m/s and with impact energies of 50J

The impact magnitude and its location, is based on statistical studies of surveys from in-service aircraft. The risk of impact is based on a probability rate per hour at a certain energy level. The internal cover and the external cover will have different impact energy levels, as well as different probabilities. Furthermore, for the external cover, the inner section, typically near to the landing gear will need to consider a higher level of energy, due to greater risk of thrown-up debris, than the outer section. Typically, the internal surface can only be impacted during manufacture and maintenance so internal parts have a low probability of damage, whereas the outer surface can be impacted at any time. VID limits are not established for inner surfaces, as these surfaces cannot be inspected until a scheduled maintenance period, whereas outside surfaces can have regular walk-around inspection.

Due to the differentiation between VID and BVID, which results in impact damage resistance based on LL and UL respectively, there will be different impact energy levels, however, UL requirements is typically the design driver. 35J is the minimum energy, as stipulated by the Airworthiness Authorities, for static requirements which can be applied to the inner skin, at UL for example, whereas a 135J impact is considered highly improbable, which will most likely cause VID[157], and is therefore applied at LL.

6.1.1.4 Particular Risks

As the wing box acts as a fuel tank, the European Aviation Safety Agency (EASA) Certification Specification (CS) section 25.963[424] outlines the certification requirements that must be considered. In section CS 25.963 (d) the following is stated *"Fuel tanks must, so far as it is practicable, be designed, located and installed so that no fuel is released in or near the fuselage or near the engines in quantities sufficient to start a serious fire in otherwise survivable crash conditions"*. Specifically for the Fuel Tank Access Covers (FTAC), sub-section AMC 25.963(g) the following is stated:

3. Impact Resistance
a. All FTACs must be designed to minimise penetration and deformation by tyre fragments, low energy engine debris, or other likely debris, unless the covers are located in an area where service experience analysis indicates a strike is not likely…. The access covers, however, need not be more impact resistant than the contiguous tank structure.
b. In the absence of a more rational method, the following criteria should be used for evaluating access covers for impact resistance.
i.) Covers located within 15° inboard and outboard of the tyre plane of rotation, measured from the centre plane of tyre rotation with oleo strut in the nominal position, should be evaluated. The evaluation should be based on the results of impact tests using tyre tread segments having width and tread equal to the full width of the tread, with thickness of the full tread plus casing. The velocities used in the assessment should be based on the highest speed that the aircraft is likely to use on the ground.

ii.) Covers located within 15° of the front compressor or fan plane measured from the centre of rotation of 15° aft of the rearmost turbine plane measured from the centre of rotation, should be evaluated for impact from small fragments (shrapnel). The covers need not be designed to withstand impact from high-energy engine fragments such as rotor segments.

Therefore, as there are no specific impact requirements or standards for the wing covers but there are for the FTACs, then these standards could be used as well for the wing covers, as shown in Figure 6-2. In terms of the shrapnel, this can cause penetration of the CFRP skin, but the inner section of the wing is thick enough to minimise the likelihood of penetration. The tyre tread will typically have a large mass and a high impact velocity, thus if the skin is impacted by tyre tread, this will result in major delamination.

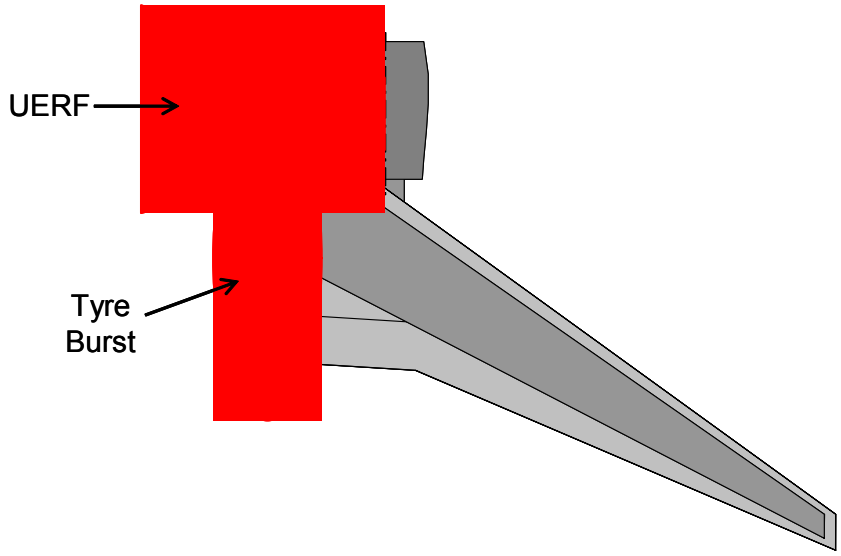

Figure 6-2: Particular risks

6.1.2 Delamination

As shown in Figure 6-3, there are many boundary-layer problems in composite design, where one dimension is relatively longer in comparison to the other two, which cause a three-dimensional stress field. Through-thickness loads, due to impact damage, can cause delamination, which can occur between stringer and skin[xxviii], between sub-laminates or individual plies of the skin, and in sandwich panels between the face-sheets and the core[425]. Delamination will lead to loss of structural integrity, either through complete failure or splits occurring along ply borders, which can cause early buckling, vibration, intrusion of moisture, stiffness degradation, and reduction in fatigue life[410].

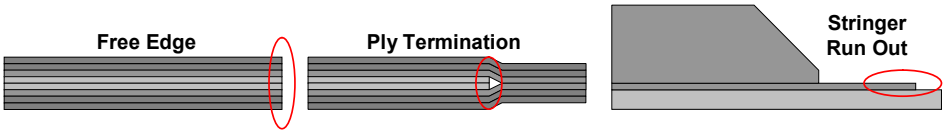

Figure 6-3: Sources of delamination

[xxviii] If co-cured then a stringer detachment from the skin can be termed delamination. However, it can also be termed a 'debond', as to encompass the other attachment methods of the stringers to the skin when an adhesive layer is used.

The growth of delamination is dependent on the interlaminar longitudinal shear stress (σ_{13}) and transverse in-plane stress (σ_{22}) in the layer below the delaminated interface and also by the interlaminar transverse shear stress (σ_{23}) in the layer above the interface[426]. To minimise the occurrence of delamination, a reduction in transverse normal interlaminar stresses must be sought. This can be achieved by optimising the stacking sequence, ensuring well designed ply drop-offs, avoiding tight corner radii, using interleaves i.e. tough thin ductile fibre free layers[410], and limiting the allowable strain limit.

If the laminate is at risk from impact damage, then the laminate's absolute performance is not important, instead it is either CAI[259] or notched performance. CAI relates the extent of the delamination due to the impact, and the subsequent reduction in compressive strength[324,417]. Thinner laminates are affected primarily by CAI, which can lead to over 50% reduction in residual strength[148], which is exacerbated when fatigue is considered, whereas thicker laminates have a higher strain limit[427]. The onset of delamination will create sub-laminates, which result in the global laminate having reduced bending stiffness. This will cause a knockdown in buckling performance, either through local buckling of the sub-laminate or global buckling of the complete laminate. For this reason, impact affects compressive properties far more than tensile properties.

With an increase in laminate thickness, the performance knockdown criticality is less dependent on delamination; instead, it is the notched performance. Under compression load, OHC becomes the limiting factor. By considering the notched effects, which is typically a fastener hole[157] with a 6.35mm diameter, this will cater for small cracks and cuts in the laminate. The reduction in performance due to notched effects is fairly drastic, with a well designed laminate limiting the knockdown in performance by 33%[145]. From a tensile load perspective, notched performance is typically the most critical for all thicknesses of a wing cover, with Filled Hole Tension (FHT) principally being the limiting factor[148], over OHT, as the presence of the fastener in the hole will mean the hole cannot deform freely, hence increasing the notch-sensitivity of the hole. The Tension after Impact (TAI) strength should not limit the performance[420], as tensile strength is not strongly related to delamination, instead it is only affected if there is consequently fibre failure as part of the impact mechanism.

6.1.2.1 Free-Edge Effects

Free-edge delamination is attributed to highly localised interlaminar stresses at the free-edge of the laminate under in-plane loading[320], which is much higher than in the other regions[428]. This is due to each ply behaving independently to each other at the free-edge because of the varying fibre orientations and the mismatch of elastic properties, which result in large stresses to maintain the compatibility of deformations[429]. This has led to an imposed allowable strain limit of approximately -5000με to mitigate free-edge effects[429]. However, consideration should also be given to impact on the free-edge, which could lower this allowable even more.

The simplest solution to mitigate delamination is to use a U-shaped cap on the free-edge[428], although other methods, as shown in Figure 6-4, can also be used, as well as using thinner plies. Another method is to vary the FVF near to the free edge, which minimises the elastic properties difference between the adjacent layers, which then reduces the interlaminar shear, although such a technique can result in a slight loss of in-plane properties[428]. Alternatively, as shown in Figure 6-5, the top free edge of a T-profile stringer can eliminate this issue by using a roll formed fabrication method.

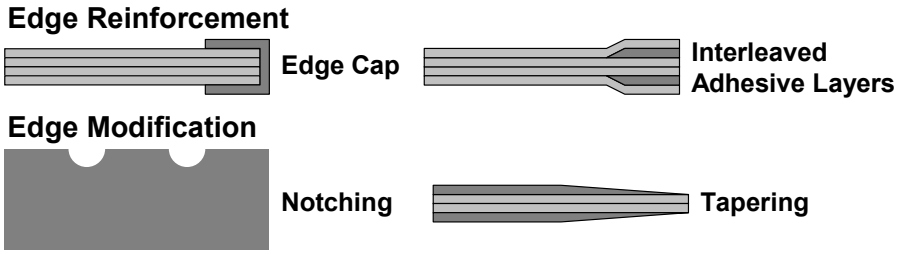

Figure 6-4: Free-edge delamination suppression concepts

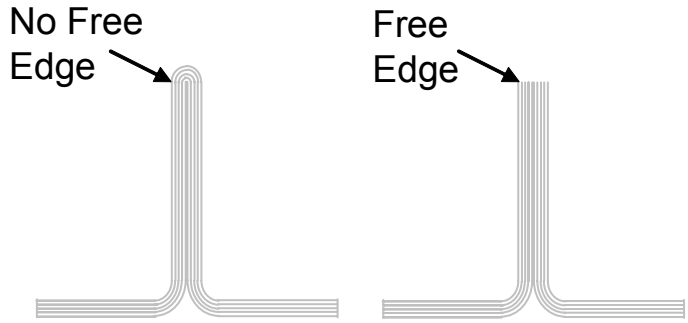

Figure 6-5: Comparison between typical blade stringer and roll-formed stringer

6.1.3 Debonding

Delamination cracks which originate from the edge are known to be the primary cause of damage and failure in bonded joints[430]. Near the free edge of the outer adherend, the interlaminar shear and peel stresses peak can lead to the onset of debonding[328]. When a debond propagates, both G_{IC} and G_{IIC} strain energy release rates increase, leading to an unstable debond growth[425].

Traditional failure mechanism of a stringer-stiffened panel is debonding between the stringer and skin[431]. Stringer to skin debonding can occur due to many parameters such as stringer and skin stiffness and lay-up, which creates a mismatch in the relative Poisson's ratio, the adhesive and the method of assembly, the stringer's geometry and the curvature of the panel[432,433]. There are normally two locations where stringer to skin failure can initiate[434]:

- At the core/noodle region
    - Normally caused by out-of-plane loading on the stringer blade
        - Caused by web attachments in the wing box
- Tip of the stringer foot
    - Caused by large panel deflections which induce local delaminating forces

6.2 Damage Tolerance Enhancement

Damage tolerance resistance can be improved by employing the techniques shown in Table 6-2[188,415].

Concept	Advantages	Disadvantages
Panel Design (overall dimensions and stacking sequence)	Low cost and timescale No need for material re-qualification	Limited improvements imparted
Tougher Matrix	Same architecture as baseline Usually similar cost and timescale Usually same processing route	Reduced fatigue and compression properties Increased sensitivity to processing May require different processing routes May cost more
Plain Woven	Improved drape and manufacturability More elastic response during impact Usually same processing route	Some redesign and re-qualification required Poor undamaged properties Weave needs to be balanced
NCF	Low cost and timescales Environmental benefits Improved manufacturability	Redesign and re-qualification needed Reduced undamaged properties Performance sensitive to processing
Selective Interleaves and Hybrids	Undamaged properties as baseline Similar processing route	May reduce compressive performance Increased thickness may lead to redesign Adds weight and extra cost
3D Composites	Reduced cost Lends itself to design of substructure	Relatively immature concept Can reduce undamaged properties Requires redesign and re-qualification
Stitching	Same processing route Offers fail-safe design	Can reduce undamaged properties Difficult to fabricate with stringers
Z-Pinning	Same processing route Optimisation can limit drop in undamaged properties Offers fail-safe design	High cost Relatively immature concept
Protective Layers	Similar processing route Generally no need for re-qualification	Increased thickness may lead to redesign Adds weight and extra cost

Table 6-2: Advantages and disadvantages of different concepts compared to UD structures

6.2.1 Panel Design

The configuration of the wing box can determine the structure's ability to withstand impact. The wing cover's stringer pitch not only influences the local buckling behaviour of the panel but it also contributes strongly to the damage tolerance of the panel[324]. In terms of impact damage tolerance, it is better to have, for a given allowable strain limit, a greater stringer pitch, as opposed to having a thinner skin[435]. Furthermore, Greenhalgh et al.[412] found that for a stringer-stiffened panel, as the stiffness increased, the deflection decreased. This meant that upon impact, the impactor was arrested quicker, hence the deceleration was higher so the contact force was greater. Thus for a thick skin, there may be significant delamination in the skin, but the internal structure, i.e. the bond between the skin and the stringer, may remain intact. A thin skin will be more flexible under impact, which although it can limit the amount of delamination in the skin, could result in the stringer debonding.

It is known that a 'soft' laminate (e.g. 10/80/10) will have a higher CAI strain than a harder laminate (e.g. 60/30/10))[155], and that the stacking sequence will also affect the laminate's allowable strain[235,314]. Furthermore, the failure mechanism attributable to notched effects, such as OHC, for a soft laminate will be matrix dominated, whereas for a stiff laminate it will be ply kinking/buckling[436].

The thickness of the plies can also alter the damage tolerance of the panel. Thinner plies have higher resistance against matrix cracking[437], and, in general, laminates using thinner plies have greater static and fatigue damage resistance. Conversely, a way of improving residual compressive strength is to increase the ply thickness, as there will be less ply interfaces,

resulting in reduced interfacial weakening[419]. However, it has been statistically argued that a laminate with thicker plies will fail at a lower stress, as it is likelier that the laminate will have more influential defects than a laminate with thinner plies[438]. Furthermore, a doubling of the ply thickness will also double the interlaminar normal stress[439].

6.2.2 Fibre Type

HS fibre is typically more damage tolerant in comparison to IM fibre, as it typically has higher strain to failure, and does not suffer such a severe knockdown due to CAI, as the delamination area after impact is smaller[318]. Furthermore, it suffers less of a knockdown due to OHC. However, conversely it may have a greater knockdown due to FHT[141].

It is possible to create hybrid composites to enhance the damage tolerance of the laminate[235], by mixing carbon with glass or Kevlar, which will have a higher strain to failure, however there are a number of design and manufacturing issues because of the moduli mismatch[152].

6.2.3 Tougher Matrix

Due to the brittleness of CFRP laminates under impact, the energy is absorbed via elastic deformation and damage mechanisms, and not through plastic deformation[152]. This brittleness will then determine the amount of matrix cracking and the interlaminar fracture. Increased G_{IIc}, from using toughened resin systems, helps to restrict the size of delamination, which leads to higher residual compression strength[144]. This improvement in impact tolerance comes at the expense of a reduction in the in-plane properties, and costs at least 3 times more than an untoughened epoxy[169]. Furthermore, improvements made at the resin level are never holistically seen by the complete CFRP system due to the brittleness of the fibres.

A comparison was made between Hexcel's IM prepreg systems of a standard T800/924 and interleaved toughened IMS/M21, with a stacking sequence of $[(\pm 45°/0°/90°)_2]_s$. The OHC strengths were 300MPa and 335MPa respectively[440], and with an impact energy of 7J, the CAI strength was 260MPa and 452MPa respectively, which shows the potential benefit of using a toughened system.

6.2.4 Interleaves and Protective Layers

Resin rich interleaves, which are reinforced with IM fibre, can increase the BVID and FHT strength properties, while only slightly detracting from the hot/wet OHC properties[3]. Protective layers on the surface of the laminate, such as high strain glass fibre, polyethylene, or Kevlar, can be beneficial. Alternatively, thin discrete layers of very tough, high shear strain resin or adhesive can also minimise delamination[441]. However, once the layers are damaged, they provide no further impact resistance[188].

6.2.5 Through-Thickness Reinforcement

Through-thickness reinforcement can improve the damage tolerance performance, but consequently this can decrease some of the in-plane properties and can actually be a cause of delamination initiation[410].

6.2.5.1 Stitching

Military aircraft programs have been using Kevlar stitching to enhance the structural integrity and damage tolerance of thin CFRP structures for many years[25], but thick CFRP structures, as found on transport aircraft wings, have posed a greater challenge, although stitching is more beneficial for thicker laminates[148]. NASA has determined that through-thickness stitching of dry textile preforms is an effective means to enhance damage tolerance[169]. In Figure 6-6[240] the benefit of stitching on CAI performance is clearly seen.

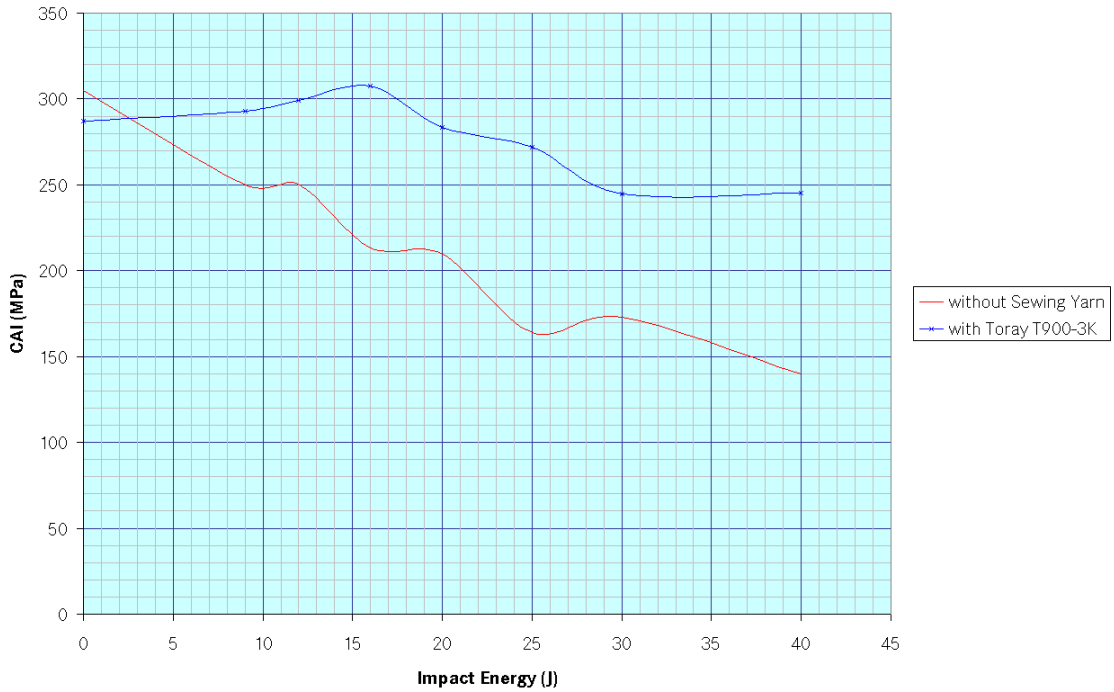

Figure 6-6: Influence of stitching on CAI

Stitching will not eliminate delamination and also does not raise the impact energy threshold that is required to create and propagate delamination, as stitching will not increase the strain energy needed to initiate delamination cracks[164]. However, in particular for post-impact, the stitches suppress buckling under compressive loads, which mitigates the G_{IC} strain energy release rate with respect to the debond length[425], as the stitches provide a bridging action[258]. An example of the bridging action is shown in Figure 6-7[240]. The length of a stitch-bridging zone is dependent on the stitch density, stitch thickness, elastic modulus and tensile strength of the stitch yarn. Furthermore, by bridging the delamination crack, it can resist shear loads better[166].

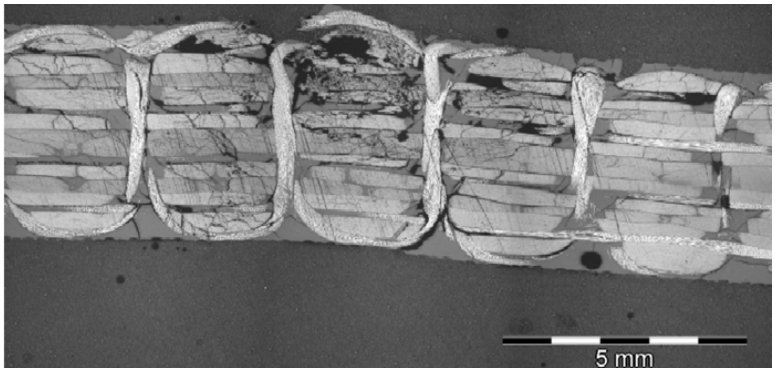

Figure 6-7: Polished cross-section of tested CAI-specimen

A higher stitching density will increase the resistance to impact damage initiation, reducing the delamination area, resulting in an increase in CAI strength[164,175]. However, the stitching density should be optimised, as opposed to a blanket high-density stitching pattern, as this can improve the CAI strength[442], while minimising the damage done to the laminate's in-plane properties. However, an issue with stitching is that once the stitching itself is damaged, it then loses its advantage[409].

6.2.5.2 Z-Pinning

Z-pins can improve both mode I and II fracture toughness, which enhances the impact tolerance[148]. From investigations conducted by Grassi et al.[264], it was found that by adding a 2% volume fraction of z-pins, the through-the-thickness modulus was improved by between 22-35%, although with a consequent reduction of 7-10% in the in-plane direction[264]. Z-pinning is more effective for thicker parts and at higher impact energies, although in general CAI performance can be improved by up to 45%, in comparison to having no through-thickness reinforcement, which could allow for the strain allowable to be increased by 50%[443].

The stringer to skin joint can use z-pins to give better load-bearing properties, in particular the out-of-plane properties benefiting stringer pull-off[148] and resistance to direct impact. The configuration of a typical z-pinned joint is shown in the Figure 6-8, where z-pins are inserted in the blade through the corner radius and the feet, although z-pins inserted through the foot and blade increase the laminate strength[382], it would seem that pins inserted through the radius provide little improvement in strength and might even promote the initiation of delamination[444].

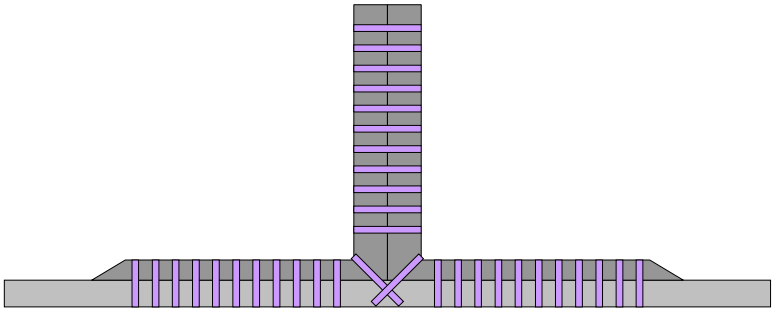

Figure 6-8: Stringer to cover integration using z-pins

A comparison was made between a T-profile stringer-stiffened panel made from Hexcel's T800/924, with CFRP (T300/BMI) z-pins with an areal density of 2%, Hexcel's T800/M21, which is a highly toughened resin system with no z-pins, and T800/M21 with z-pins[445]. The skins were 3.25mm thick with a 30/62/8 laminate and the blade had a thickness of 1.5mm and the foot 0.75mm, with a 50/33/17 laminate. As shown in Figure 6-9[445] (a), the initiation load seems fairly insensitive to the presence of z-pins, or using a toughened resin system, whereas the peak values are improved with a tougher matrix and the presence of z-pins, which both resist the delamination. Referring to Figure 6-9 (b), the strains at initiation are limited by the presence of z-pins, however as would be expected, the increased load carrying ability with the z-pins also means the strains are higher. This means that the z-pinned samples had lower compliance, therefore, if they were constrained by an allowable strain limit, due to damage tolerance, then actually using z-pins would be detrimental[445], although in reality, a different design philosophy would be used. Such a philosophy could be to allow for damage, as opposed to zero damage, and due to the greater damage tolerance afforded by the z-pins, the damage could be withstood. The toughened material also had lower compliance than the conventional T800/924, although the additional toughness does not provide the same level of

benefit at the panel level[445], which could be attributable to the inhomogenity of the toughening agent through the panel.

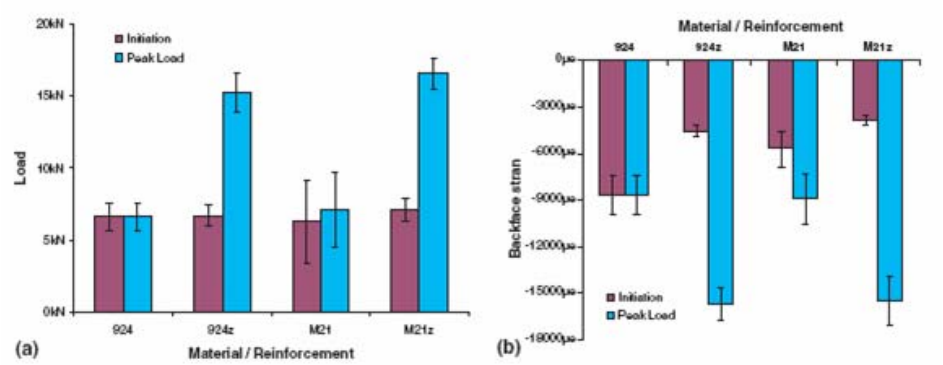

Figure 6-9: Initiation and peak (a) loads and (b) back-face strains, against reinforcement

6.2.6 Stringer to Skin Interface

The Bermuda triangle is created due to the method of stringer fabrication, with a T-profile stringer being made from back-to-back Ls, which when cured together result in a radius between the web and the foot causing a triangular shape. The Bermuda triangle is either filled just with resin during cure or beforehand a noodle[xxix] is placed in this area. However, either way, this area can be the weak point of a conventionally fabricated CFRP stringer, resulting in a crack occurring[446], as shown in Figure 6-10[447]. This issue is improved with thicker structures, as they can react out-of-plane loads better[448].

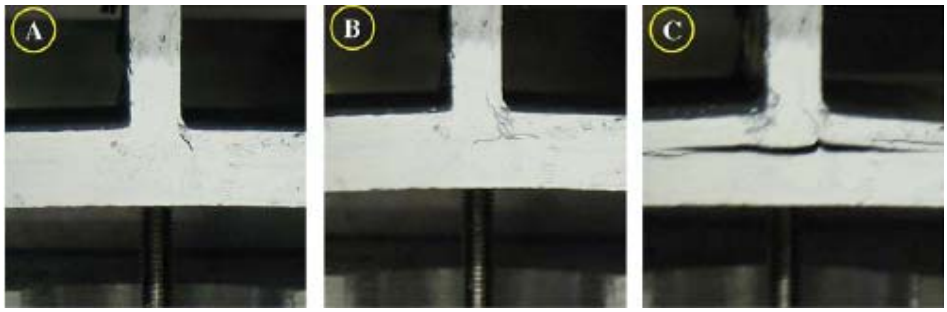

Figure 6-10: Delamination in a UD tape stringer under tensile pull-off test

Shown in Figure 6-11[446], is a 3D braided T-profile stringer which eliminates the noodle zone. However, this current architecture does not include any axial fibre[446], which is necessary for a structurally efficient wing cover.

For a bonded stringer to skin joint, a layer of adhesive film between the stringer foot and the skin will improve the fracture toughness properties K_{IC} and G_{IC}[449], and in particular around the Bermuda triangle area[394]. A further enhancement of this idea is shown in the LHS of Figure 6-12[448], which illustrates a co-bonded (soft stringer) design with two layers of REDUX 319 adhesive, one applied along the spine of the stringer, whereas the other is between the stringer and skin, thus the adhesive layers encompass the Bermuda triangle area. In the RHS of Figure 6-12, a single pair of ±45° plies, create a capping strip, which is located between the

[xxix] The noodle is either a tow preg, a UD split tape spiralled, or a 3D woven triangular filler.

stringer and skin and encompassed between adhesive layers along the stringer's entire length, the purpose of which is to increase the panel's overall longitudinal bending stiffness.

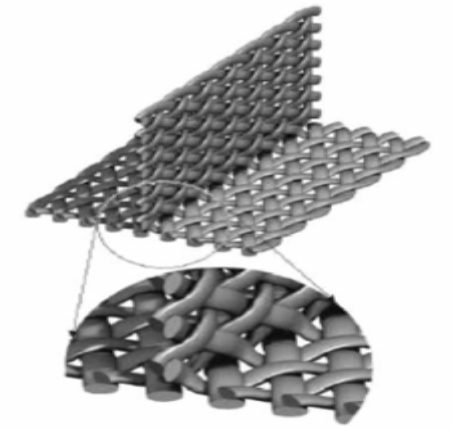

Figure 6-11: 3D-braided T-profile stringer

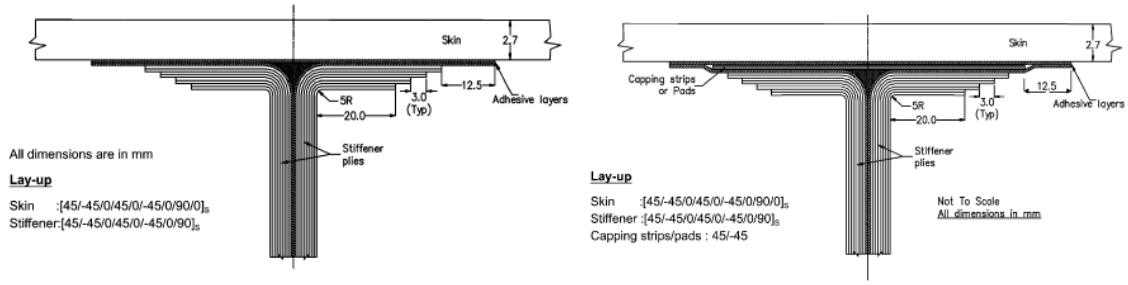

Figure 6-12: Basic T-profile stringer design shown on the LHS and 'padded' on the RHS

Figure 6-13: Location of failure for standard and capping strip design under tensile pull off load

The simple capping strip idea meant that failure occurred between the foot edge and capping plies, and not at the Bermuda triangle, which was the case for the basic configuration, as shown in Figure 6-13[448]. Furthermore, due to the increase in the bending stiffness, based on T-pull off tests, the capping strip design had a failure load 40% higher than the basic configuration[448].

6.3 Stringer Panel Impact

The key material parameters that determine the damage tolerance of a stringer-stiffened panel are[188]:

- Mode I toughness (G_{IC})
  - The driving force for delamination growth is mode I (peel) loading, which is caused by the local buckling of the delaminated plies and sub-laminates. This damage mode influences the global buckling of the panel

- Mode II toughness (G_{IIC})
    - The primary fracture mechanism is mode II (shear) during an impact event, and skin/stringer detachment due to the out-of-plane bending. Impacting close to or underneath a stringer will mean high interlaminar shear forces are induced parallel to the stringer, which generates mode II dominated growth along the stringer. The global panel buckling which can induce twisting at the skin/stringer interface will also create mode II conditions as well
- Bending (D_{11}) and shear (G_{12}) moduli
    - During the impact event, the bending modulus of the laminate, influences the energy absorption process and the area of the panel that responds to the impact event. Furthermore, the bending and shear moduli will help to determine the level of energy at which delamination occurs, its propagation and failure due to buckling. By increasing these moduli, the buckling loads will increase, which will then inhibit damage growth
- Compressive and flexural strength (σ_c and σ_f)
    - A combination of the compressive and flexural strength will determine both the ultimate strength of the panel as well as formation of the impact damage (fibre cracking)

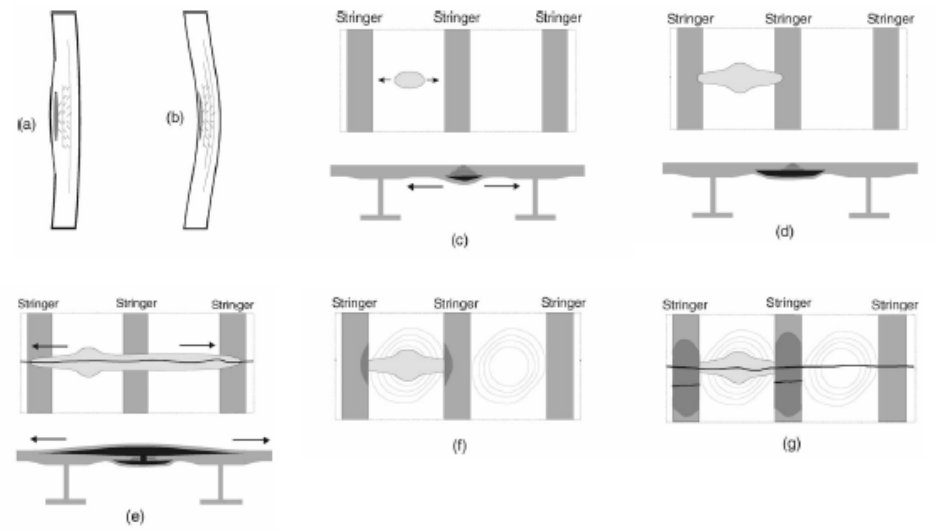

Figure 6-14: General failure process for a damaged stringer-stiffened panel

For stringer-stiffened panels the general failure process is illustrated in Figure 6-14, and is explained as follows[188]: As shown in part (a), upon loading, local buckling of the damaged area occurs, and, as shown in part (b), when the load increases there will be local bending of the delaminated plies and the sub-laminate underneath those delaminated plies. The induced deformation will create mixed-mode delamination forces at the periphery of the damage region and, as shown in part (c), if the local toughness is exceeded then the delamination will propagate. The propagation in delamination may then reach the stringers as shown in part (d), where the out-of-plane constraint of the stringer will inhibit the growth of the delamination. However, on the outer surface if there is delamination, then it will propagate further un-impinged by the internal structure, as shown in part (e). This will lead to catastrophic failure due to excessive bending stresses on the load-bearing layers, which will lead to in-plane failure of the fibres. Alternatively, if the damage growth is limited by the internal structure then the opening forces at the delamination periphery will encourage damage underneath the stringer. This will lead to global buckling, which will create large out-of-plane loads, which further opens up the delamination. This will lead to detachment of the stringer as shown in

part (f), which results in excessive loading of the skin causing cover failure as shown in part (g).

For stringer-stiffened panels, the tolerance to an impact is dependent on its configuration and where the impact occurs[418]. For impact between stringers, the closer the impact is to the stringer centreline, the less compliant the structure is, as it has higher local bending stiffness. Hence, it absorbs more energy elastically, as well as through damage[412], such as delamination of the surface plies or fibre fracture, adjacent to the stringer interface, which can lead to failure due to skin delamination under the edge of the flange[450]. The skin delamination is due to excessive interlaminar tension stress at the stringer/skin interface, which is caused by stringer pull-off load about the blade, and a peel moment applied from the skin[450]. A secondary mode of delamination is at the stringer's blade to foot elbow, due to the lateral moment at the root of the stringer blade[450]. In the middle of the bay, between the stringers, the deflection upon impact is greater whereas the peak force is fairly low, which causes high local curvature and interlaminar stresses[412], resulting in matrix cracking and delamination. This has been evidenced in tests when a series of stringer-stiffened panels were impacted at 15J, either between or beneath the stringers, resulting in the panel strength reducing by 7% and 29%[451], respectively. Alternatively, other I-profile stiffened panels, which were not specifically design for damage tolerance were impacted at 15J and 35J, either between or beneath the stringers, resulting in a damage area of 200mm² and 520mm² at 15J, and 800mm² and 1130mm² at 35J, respectively[421].

The impact energy required to cause BVID reduces significantly the closer the impact proximity is to the stringer. This general prognosis is valid for all stringer types, which is evidenced by further studies using hat- and I-profile stiffened panels[405,412], where at the centre of the stringer the least amount of energy is required to cause detectable damage, whereas in the middle it requires the most. Thus, it is the increased bending stiffness from the stringer that is critical to the amount of damage caused. It has also been shown on the NASA ACT stub wing box test, that BVID at the SROs, i.e. where load distribution is, can lead to early failure[228].

In terms of buckling performance, a mid-bay impact has a larger effect than an impact underneath the stringer foot[324], despite the damage area typically being smaller at the mid-bay. The reason for this is due to the propagation of the delamination from a mid-bay location towards the stringer[323], which will occur earlier and increase in size as it does not have the suppressing influence of the stringer to improve the Mode I displacements. With the delamination underneath the stringer, this will result in stringer-skin debonding.

Therefore, in conclusion, mid-bay impacts, of 35J, should not determine a well designed panel damage resistance, instead the impact under a stringer foot should[322,421]. It is prudent to design a damage resistant panel, as opposed to one without any damage tolerance restrictions, as although this will increase the weight at the panel level, for instance by 16-28% relative to a normal panel[421], this increase will be minimised at the holistic wing cover level.

6.4 Repair

Repair should be considered as an intrinsic part of the overall design process. The type of repair depends on the severity of the damage and the certification requirements[452]. There are several repair philosophies as follows[22,453]:

- If the damage caused is small and provides no negative effect on the structure then it can be simply filled for aesthetic or aerodynamic reasons
- If significant damage has been sustained, and the part cannot be removed from the aircraft, then it will be necessary to perform an in-situ repair
    - Bonded Repair
        - A repair patch that is used in conjunction with relatively low temperatures (<130ºC) and low pressure (<1 bar). This repair will mean that the part will have reduced mechanical properties, as it will have a lower T_g. Furthermore, any moisture trapped can lead to voids in the bond-line
        - Manufacture of a replacement part, as per the original part, and then adhesively bonded. However, the bond can suffer from moisture absorption leading to degradation in the bond-line
    - Bolted repair
        - Local repair, such as a patch to cover a hole, resulting in higher bypass stresses, as all the load does not go through the repair
        - Global repair, will replace a complete section, resulting in higher bearing stresses, as all the load goes through the repair

Currently, for primary and secondary structure, a bolted repair must be applied, which can use patches up to 1×1m, made out of either titanium or composite[23], albeit it is more efficient to use the same base laminate for the repair[454]. However, the bonded composite repair patch is now a recognised repair procedure that has been applied to primary structure on civil aircraft[455]. Advantages of bonded patch repair are:

- Good for thinner laminates
    - Does not require additional holes
- Strong / Light

Disadvantages of a bonded patch repair are:

- Aerodynamic implications
- Surface preparation is critical
- Difficulty in inspecting bond line
- Disassembly of repair impossible without causing more damage
- Not suitable for thick structures due to out-of-plane loading and difficult curing

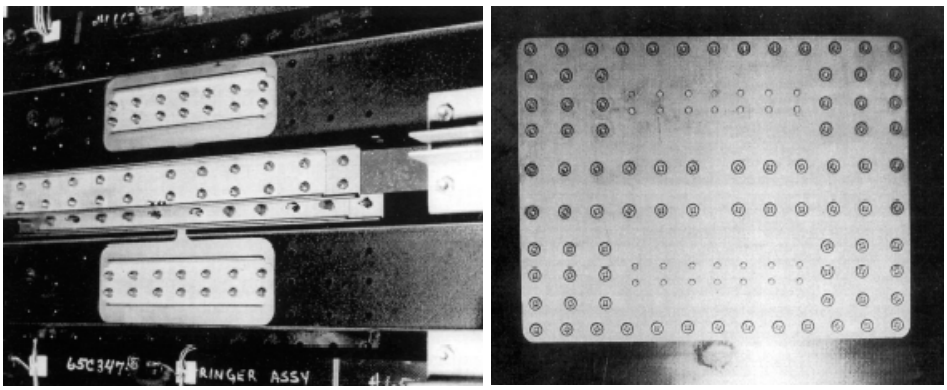

Figure 6-15: Metal repair to CFRP skin panel LHS Inner & RHS Outer Surface

For the skin, a single shear repair joint is used due to the aerodynamic surface, as shown in Figure 6-15[3]. Whereas for the stringers, a double shear repair solution is typically used as

shown in Figure 6-16. For bolted repair, it is necessary to match up both in-plane and bending stiffnesses to mitigate stress concentrations.

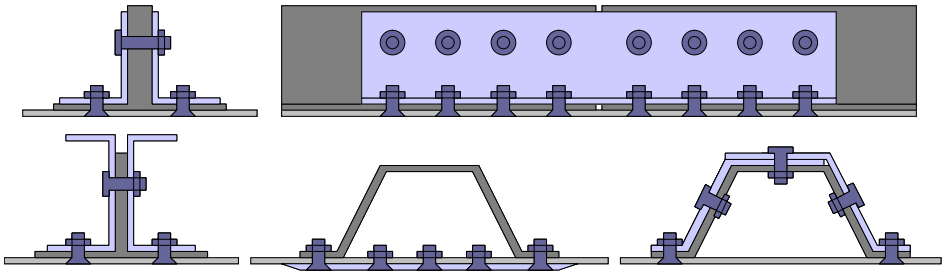

Figure 6-16: Repair concepts for typical wing cover stringers

6.5 Environmental Degradation

During the aircraft's operation, there are a number of ways that composite materials can be degraded or destroyed:

- Moisture
- UV radiation
- Fuels
- Hydraulic fluids
- Chemicals such as paint strippers
- Lightning strike

The typical temperature range for an aircraft is from 82°C when on the ground, and down to -54°C in the air at 30000ft[142]. A temperature beyond the T_g of the material must be avoided, as the structural behaviour will change from elastic to a thermo-viscoelastic, or a thermo-plastic one, with loss of strength and stiffness, which is exacerbated with cycling of the temperature, as this intensifies ageing[456]. The aircraft will also operate in a wide range of humidity conditions, thus the composite could be completely saturated or dry. The tensile properties are affected at low temperatures in dry conditions, whereas the compression and out-of-plane strength are affected at hot temperatures and in a wet environment, as the resin determines these properties.

6.5.1 Lightning Strike Issues

Aircraft are hit by lightning strike (*leader*[xxx]*)* as they offer a particularly attractive medium between the cloud and the ground, furthermore they attract nearby lightning discharges that produce *corona* [xxxi] and *streamer*[xxxii] formations. Typically, commercial passenger aircraft are hit on average between once or twice a year[457]. Therefore, in accordance with CS 25.581, aircraft have to be designed to withstand lightning strike impact, so that they can complete their mission, and also to minimise required maintenance after the event.

[xxx] Leader is the filamentary discharge that propagates from clouds towards earth, and also by-directionally from aircraft (when it goes through the nose for example and out of the tail).
[xxxi] Corona occurs around points of conductors, due to the high electrical potential, the electrical field strength is high enough to breakdown the air, causing a localize discharge.
[xxxii] Streamer is similar to leader but is the part that returns from the ground.

Due to the movement of the aircraft through the air, this leads to the phenomena of a swept stroke, resulting in areas of the aircraft being subject to lightning strike attachment that would not normally be the case if the aircraft were static. Due to the risk and the intensity level between initial strike and re-strike, this has led to the aircraft being zoned, as shown in Figure 6-17[458].

- Zone 1 – Surfaces which have a high probability of initial lightning flash attachment
- Zone 2 – Surfaces which can get a swept re-strike from a Zone 1 point of initial flash attachment
- Zone 3 – Is all other areas, and they should have low probability of direct lightning strike, but may take a high level of lightning current from the entry and exit points

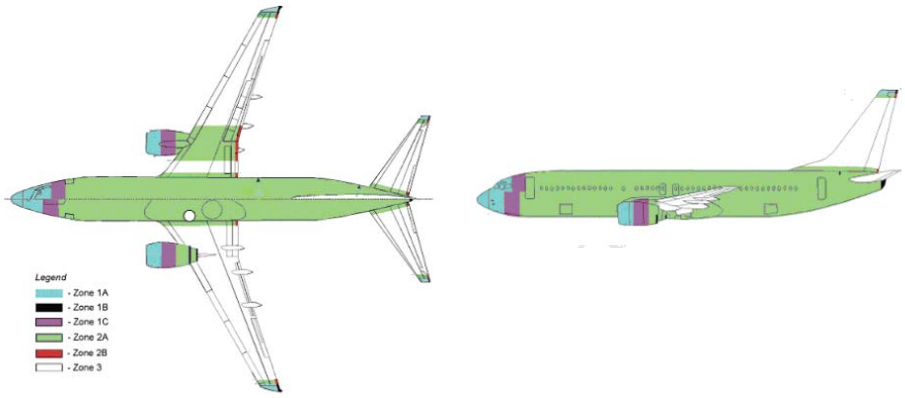

Figure 6-17: ED-91 lightning strike zone of aircraft

In terms of the wing, there are 3 zones, 1A, 2A, and 3. The wing tip and the engine nacelle are designated in Zone 1A, which although has a high probability of lightning flash attachment, does have a low probability of hang on. Just inside from the wing tip and near to the fuselage is Zone 2A, which is a swept zone with low probability of hang on. Zone 3 covers the majority of the wing surface, but has an extremely remote chance of direct swept strokes. Fuel tanks should, preferably, be located in a lightning strike zone 3, however this is often not possible[459].

For a predominantly CFRP wing box, should lightning strike occur, it will seek the path of least resistance; hence it will be attracted to any conductive part in the locality of the attachment, which can lead to damage of the CFRP structure, if not catastrophic failure. This is because carbon fibres and the resin are 1000 and 1,000,000 times more resistant than aluminium, respectively[366]. Carbon by itself could have adequate conductivity, but the dielectric resin reduces the overall conductivity of the laminate severely[460].

A lightning strike can lead to the following direct effects. Upon lightning attachment, a significant amount of energy is transferred, which causes the ionised channel to spread out at supersonic speeds, causing a shockwave. Upon impact to a hard surface, the KE is transformed into a pressure rise, resulting in disintegration of the local structure[460]. Further effects, will occur due to heat transfer, which causes pyrolysis of the laminate, i.e. the interface between resin and fibre is broken down. If gases get entrapped in a substrate an explosive release may occur, which will cause further damage to the structure[460]. The burn-through can be particularly hazardous for wing covers, as it can lead to ignition of the fuel. Therefore, CFRP requires some form of protection to safeguard against the following issues[461]:

- Protection against lightning strike
- Electrostatic Dissipation (ESD)
- EMI – Indirect effects

The issues of CFRP structures are compounded by the latest generation of interleaved toughened CFRP systems, which have been developed as a way to improve the toughness of the laminate. Even without interleaving, the conductive pathway passes through the direction of the fibres, with limited dissipation through the thickness due to the layers of resin. However, this is exacerbated if interleaved tougheners are used as this acts as an insulator. This can lead to the lightning strike discharging into the interleaf, which volatises the resin, leading to large delamination and burn through of the laminate[461].

Some testing has been conducted by Feraboli and Miller[460], who investigated the effect of varying levels of lightning strike intensity on the tensile and compressive strength and modulus on both notched and unnotched CFRP coupons, as shown in Table 6-3[460]. The CFRP was CYCOM/FIBERITE G30-500 12K HTA/7714A, with a 60/30/10 laminate, and a thickness of 2.88mm. In terms of the modulus, an increase in strike amperage, lead to a decrease in modulus. A similar relationship held true for the plain strength samples, as well as the notched compression samples, whereas the notched tensile coupon has an improvement with an induced lightning strike. This is probably due to the damage relieving the stress concentration around the bolt hole, which then improves the strength of the joint.

Strike Amperage (kA)	Modulus (GPa)		Strength (MPa)			
	Plain		Plain		Notched	
	Tension	Compression	Tension	Compression	Tension	Compression
0	90	76	1151	607	565	483
30	83	76	951	517	641	241
50	90	69	896	414	579	172

Table 6-3: Modulus and strength properties for various level of lightning strike intensity

Similar to damage tolerance limitations of VID and BVID, there are different repair scenarios for lightning strike damage, as shown in Table 6-4[460].

Threat	Criteria	Requirement
High Energy Strike	Rare Lightning Strike (50-200 kA)	Striking level in accordance to zoning diagram. Continued safe flight (70% LL) Ready detectable damage
Intermediate Energy Strike	Medium Lightning Strike (30-50 kA)	Repair needed (100% LL)
Low Energy Strike	Nominal Lightning Strike (10-30 kA)	No repair needed (100% UL) Non or barely visible damage

Table 6-4: Typical lightning strike levels and the airframe requirements

6.5.1.1 Current methods of protection

LSP can be used to counter both direct and indirect effects. In terms of the direct effects, adequate conductive paths are required so that the current remains on the exterior of the aircraft and also to eliminate the risk of arcing by ensuring there is a continuous path. Typically, a conductive layer is used as the outermost ply, which first dissipates the intensity of the strike over the surface and is linked to bonding strips, which carries the current through the aircraft to give it a number of routes to exit the aircraft. With such a concept, in the event

of a lightning strike, damage is restricted to the outer surface with the conductive layer being locally vaporised, but with minimal damage to the underlying CFRP laminate[461].

The conductive layer is either an expanded foil or a metal mesh, with the metals used being aluminium, bronze or copper[461]. Although this gives the surface electrical conductivity, they are heavy and look aesthetically inferior due to the poor achievable surface finish. An expanded foil has increased formability and improved adhesion, and is less expensive, as it does not require the costly weaving fabrication process[457]. However it is more fragile, which is an important consideration for a durable manufacturing process. Although aluminium provides a lightweight solution it does suffer from galvanic corrosion with CFRP, whereas copper does not have any galvanic issues, but is instead about three times as heavy as aluminium[457]. Alcore Inc. has developed an expanded aluminium foil that is phosphorically anodised, which should improve its corrosion resistance and thus its compatibility with CFRP[457]. Typically for Zone 3, a 72g/m² mesh can be used[462] but in Zone 2A, for the upper cover, a higher density mesh should be used. An issue with the LSP layer is that the subsequent paint thickness must be controlled, with a thick paint creating a physical barrier, which increases the electrical resistance, resulting in greater damage upon lightning strike[457].

Extra attention is required where fasteners are visible on the outer surface. Shown in Figure 6-18[459], is a strip of copper foil (790g/m²), which is co-bonded along with the skin during cure. This foil runs along all joint lines, in order to diffuse the current into the CFRP. The fastener is then installed through the copper foil that leaves the fastener head exposed. Even though the copper strip will dissipate much of the current, it is still likely that significant current will pass through the fastener. Thus it is necessary that the fastener can tolerate the remaining lightning current. The fastener should be installed exactly and the nut either encapsulated or covered with a polysulfide coating[457]. If there is not intimate contact between the fastener and the laminate, upon lightning strike impact, the immediate heat energy will ionise the air gap which will create an arc plasma that blows out, which can cause serious damage to the laminate[366]. Typically fasteners should not have any protective treatment, as this will diminish its conductivity. However, due to paint adhesion issues, often a phosphate fluoride or a passivated finish is acceptable.

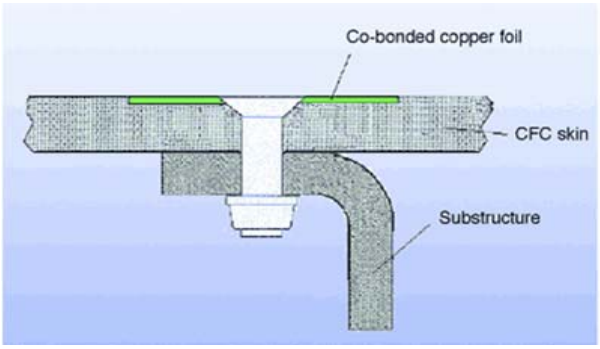

Figure 6-18: Integral copper foil protection

Shown in Figure 6-19[463] is the different mesh densities on a semi-finished A400M lower wing cover, with the higher density mesh, required in zone 2 and along the rib datum's, being identified by the more intensive bronze colour.

Despite the mesh protecting the CFRP, it is still necessary to have a minimum skin thickness of 3.25mm[464], in the fuelled area, to eliminate the potential for burn-through. On the IML, glass fibre will be used to seal edges at areas such as between the ribs to wing cover, in order to inhibit gaps, which could allow upon lightning strike, a phenomenon called "edge glow"[457].

Furthermore, any faying surfaces between metallic and CFRP parts will require one layer of isolating glass fibre to avoid sparking from the connecting bolts, where the glass ply can either be positioned between the two parts or under the nut.

Figure 6-19: Different mesh densities covering the lower cover of the A400M

6.6 Summary

Damage tolerance concerns both the constituent laminates as well as the holistic part. The simplest method of achieving a damage tolerant design is to reduce the allowable strain, so that if damage is sustained there is enough residual strength. However this will lead to a heavy design, therefore the best compromise is to have a limited strain allowable, but also ensure that the design is damage tolerant. The use of toughened resin systems are only beneficial at the laminate level and do not improve the debonding performance of the skin and stringer. This can only be improved by design, through the use of an adhesive, or by using through-thickness reinforcement such as z-pins. The easiest way to ensure that stringer top edge impact does not constrain the design, through limiting the allowable strain, is to enclose it using an edge cap.

Damage from particular risks will be unavoidable, therefore if damage should occur from tyre burst or engine debris, then the aircraft should have enough residual strength to land safely. Lightning strike is also unavoidable, and it would seem the best method to design the aircraft to comply with the regulations is through a protective mesh on the outermost layer.

7 General Wing Box Design

The aim of this chapter is to review, through examples, all aspects of the wing box, from the basic constitution of the box to the complications of laying up stringer profiles. Where necessary analysis will be conducted, using ESDU methods and other validated methods, to verify any statements made. This chapter will help to define the design configurations and the parameters that can be integrated into the optimisation routine.

7.1 General Introduction

The wing box is a torsion box, and as such it can be categorised with other aircraft components, such as the Vertical Tail Plane (VTP), the Horizontal Tail Plane (HTP) and the flaps. The wing box has a variety of functions, which typically include:

- Reacts the flight loads
- Reaction to thrust, vibration, rotational inertia and gyroscopic effects
- Normally carries the engines
- Undercarriage stowage and load introduction
- Control surface attachment and load introduction
- Carries the majority of the fuel

The wing box, as shown in Figure 7-1, has to satisfy the often-conflicting requirements of aerodynamic efficiency over a broad range of flight conditions, aeroelastic issues, as well as structural efficiency. Due to the aerodynamic requirements imposed on the wing, it is necessary that the wing box has significant chordwise and spanwise curvature, as well as overall twist. Furthermore, issues such as ease of manufacture and assembly, inspection and maintenance must be considered.

Figure 7-1: Wing box (dark grey part of wing)

Wing boxes are designed based on a number of load cases, which include flight manoeuvres, gust load conditions, and landing/take-off scenarios. The aerodynamic forces will change in magnitude, direction and location, which means the structure must be able to resist both bending and torsional loads, resulting in tensile, compressive and shear forces. As the wing acts as a beam, all the applied loads are reacted at the wing root joint, hence the bending

moment and shear loads intensify towards the root joint. Internal fuel pressure must also be considered in combination with flight load cases; whereas crash and over-fuelling pressures are considered in isolation.

The constituent members of a wing box are the covers, spars and ribs. The spanwise members will react the bending moment, resulting in normal stresses in both the covers and the spar caps. Due to the tapering of the wing box depth from root to tip, an increase in skin thickness towards the root end is very effective in contributing to bending stiffness due to the depth of the wing. The torsional loads will be reacted by enclosed cells[465] formed by the wing covers, the ribs, and the spar web. Whilst stationary on the ground, the wing structure will be loaded vertically due to the weight of the fuel, the engine and the weight of the structure. Due to the aircraft weight being primarily supported by the MLG, which is typically attached to the wing, this will create large shear forces during ground manoeuvres around the MLG area.

In order to minimise the weight, without risking safety, each constituent structural part of the aircraft will be designed to a Reserve Factor (RF)=1, however, if it is foreseen that future variants of the aircraft will react greater loads, then an RF>1 might be permissible. An RF=1 cannot be obtained typically for all load cases, as there will be one load case, which will size the component. Furthermore, an RF=1 might not be attained, as minimum thickness may be derived from other requirements, such as for lightning strike.

7.1.1 CFRP Influence

A well-designed CFRP wing box should provide the following advantages:

- Higher resistance to buckling loads
- Less mechanical fasteners resulting in reduced excrescence drag
- Better doubler integration
- Improved fatigue performance

However, this is impeded as historically, airframe construction has been evolutionary as opposed to revolutionary, with new technology incorporated with a degree of traditional design[135]. The introduction of CFRP materials to supersede metal parts has been characterised by the term: “Black-Metal” solution, which is basically replicas of metallic designs. The drawbacks of this philosophy are not using fully the directional tailoring of the properties and increasing part integration. However, although employing black-metal designs may not extract the maximum performance from CFRP, it is however not prudent to forget the last 60 years of metal aircraft design. The general structural arrangement for a CFRP component does not need to be any different to an aluminium one, which is clearly seen in Figure 7-2[463], where the A400M wing box uses mechanical fasteners to connect the rib and spars to the covers.

Shown in Figure 7-3 is the Room Temperature (RT)/dry weight estimate for the NASA ACT full-scale wing box[176]. It can be seen that the wing covers are the heaviest items, which is slightly exacerbated as both the intercostals and spar caps, for rib and spar web integration respectively, are incorporated into the cover, which is similar to the A330/340 HTP lower cover shown in Figure 7-4[197]. Furthermore, for this example, it can be seen that the upper

cover is heavier than the lower cover[xxxiii], and that the stringers have a higher proportion of total weight, as the upper cover reacts primarily compressive load, which is more critical for CFRP structures. Furthermore, in comparison to the aluminium baseline wing, the stitched/RFI wing had a weight saving of 28% and 41% for the upper and lower cover, respectively, which illustrates the advantage of applying CFRP to principally tensile loaded parts.

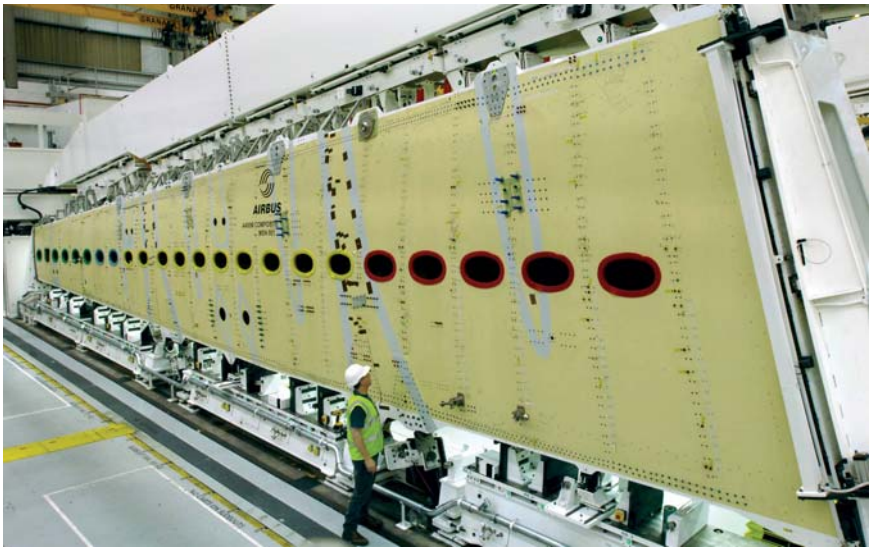

Figure 7-2: Heavy reliance on mechanical fastening through the A400M CFRP wing covers

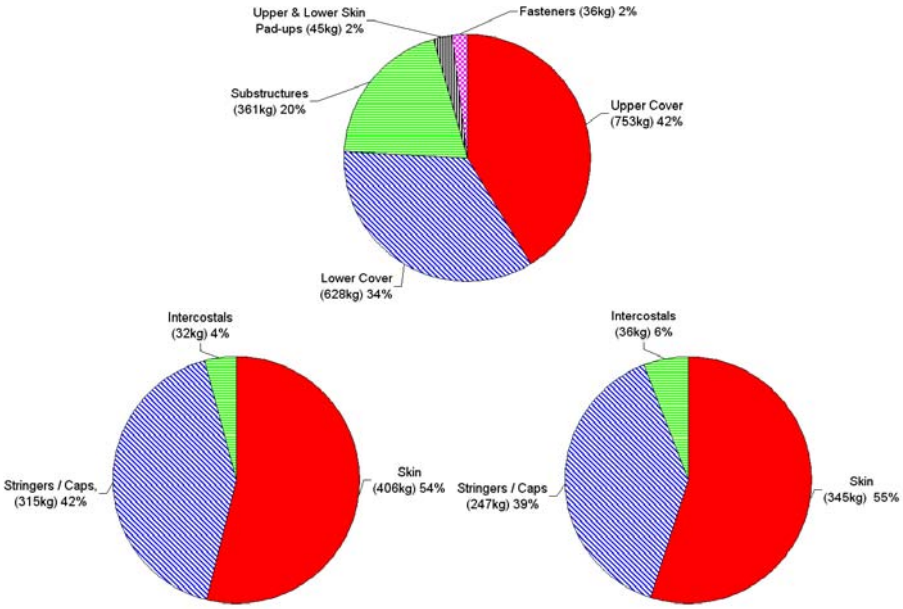

Figure 7-3: Estimated weights for NASA ACT full-scale wing; Wing box breakdown (top); Upper cover breakdown (bottom LHS); and Lower cover breakdown (bottom RHS)

[xxxiii] Typically the lower cover will incorporate a manhole doubler, the expanse of which is dependent on the lower cover size. The incorporation of a manhole doubler can increase the weight of the lower cover above that of the upper cover.

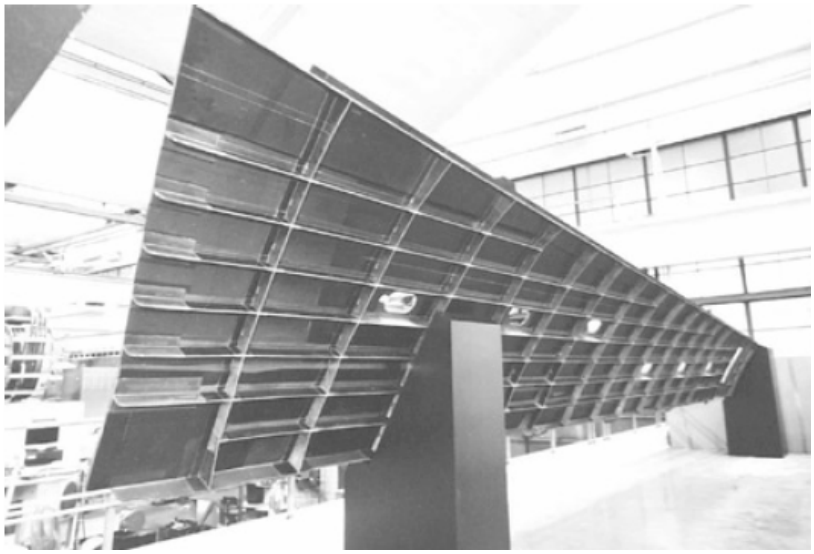

Figure 7-4: Airbus A330/A340 HTP lower skin with stringers, rib shear ties, and spar caps integrated

7.1.2 Functionality of Wing Box Constituent Parts

7.1.2.1 Ribs

The function of ribs are summarised as:

- Maintains the aerodynamic shape of the wing box
- Establishes the column length and provides end restraint for the stringers to increase their column buckling stress
- Provides edge restraint for the skin panels and thereby increase the skin buckling stress
- Provides torsional stiffness and transfers shear load across the chord between top and bottom skins
- Distributes concentrated loads into the structure and redistributes stresses around structural discontinuities
- Act with the skin in resisting the circumferential loads due to pressurisation
- Act as tank boundaries
- Supports fuel, hydraulics, and electrical systems installation

The spanwise orientation of the ribs can be in relation to many references, such as normal to the front spar, rear spar or parallel to flight direction. For ribs that are orientated parallel to the flight direction, they will have a longer chord, and hence for a set number of ribs, this will be the heavier solution.

As the ribs are designed for their in-plane strength and stiffness properties, if they are fabricated from CFRP, due to the influence of shear, the web laminate would be 10/80/10. However, if fuel pressure were a design constraint then a 10/40/50 to 30/40/30 laminate would be more suitable. The rib feet will either have a 25/50/25 or 50/40/10 laminate.

7.1.2.2 Spars

The function of the spars are summarised as:

- Spar caps help to resist the wing bending moment
- Spar webs stabilise the spar caps and balances the shear between the upper and lower cover
- React discrete load inputs attached to the spar
- Form part of the fuel tank boundary

For a conventional separate spar, the web is normally thinner than the caps, which is sized either by the shear load, hence a 10/80/10 would be appropriate, or due to the 9g forward crash case, a 30/40/30 laminate is desirable. The spar caps are mainly resisting axial load, so a higher proportion of 0° plies are required such as a 50/40/10 laminate; however, due to the bolting requirement, a quasi-isotropic 25/50/25 laminate might be more suitable.

7.2 Certification

Design and certification requirements for composite structures are generally more complex and conservative than for metallic structure, as well as requiring higher effort and greater expense[44]. In accordance with CS-25[280], it is specified that at LL, no permanent deformation shall occur in the structure. At 1.5×LL, which is UL, the load shall be sustained for 3s before failure occurs. For most metallic components, plastic deformation will be exhibited before failure occurs, and for composite materials, micro cracking will occur instead. Therefore the factor of safety between LL and UL represents the difference between repeatable, linear, elastic behaviour and structural failure. This safety factor of 1.5 takes into account the following variability[466]:

- Uncertainties in loads
- Inaccuracies in structural analysis
- Variations in material properties
- Deterioration during service life
- Variations in construction quality

For Discrete Source Damage (DSD) (such as when rotor burst failure occurs), then large damage can occur, such as a complete stringer section between adjacent ribs being destroyed, thus it is necessary that the aircraft structure has enough residual strength that it can land safely thereafter. Therefore, the structure has to be designed for DSD at a load level of 70% of LL[467].

7.2.1 For Bonded Structures

In accordance with FAR 23.573 (a)(5) Damage Tolerance and Fatigue Evaluation of Structure: *"In any bonded joint, the failure of which would result in catastrophic loss of the airplane, the LL capacity must be substantiated by one of the following methods:*

i. The maximum disbonds of each bonded joint consistent with the capability to withstand the loads in paragraph (a) (3) [basically LL] of this section must be

determined by analysis, tests, or both. Disbonds of each bonded joint greater than this must be prevented by design features; or

ii. *Proof testing must be conducted on each production article that will apply the critical limit design load to each critical bonded joint; or*

iii. *Repeatable and reliable non-destructive inspection techniques must be established, that ensure the strength of each joint*

Thus for a bonded part, the cover should be designed such that if the stringer debonds between the ribs, then the ribs themselves, which are typically fastened through the skin and stringer feet, act as a design feature to stop the bond unzipping along the complete length of the stringer. Thus, the cover can still react LL when the panel width has effectively doubled. It is only considered that one stringer will debond, between two adjacent intact stringers.

However, this philosophy is questionable. When a skin and stringer is bonded, using a thin layer of film adhesive this may well be capable of transferring the shear load, when there is no discontinuity, however it may be inadequate when damage tolerance is considered[339]. Conversely, a co-cured structure, where the adhesive layer is omitted, and only the resin layer adheres the stringer to the skin, is actually weaker than an adhesively bonded joint, albeit this has been perceived to be treated similar to an integrally stiffened metal structure[339], i.e. it has significantly improved damage tolerance over a bonded structure, using an adhesive. However, an integrally stiffened metallic structure is homogeneous in nature, whereas a co-cured T-profile stringer-stiffened panel is very much inhomogeneous in nature, with only a weak layer of resin connecting the faying stringer surface to the skin. It is most likely that a bonded or co-cured discrete stringer, upon a certain impact level, will debond upon impact, as this is determined principally by the difference in stiffness between the skin and stringer, than between a layer of adhesive, or just the resin. In actual fact, the bonded stringer will probably have better damage tolerance than a co-cured stringer[339].

However, this observation is more appropriate to a co-cured structure where the stringer is still a discrete member, such as a T-profile stringer-stiffened panel, whereas a U-profile stringer uses not just resin but fibre to transfer the load between the skin and stringer. Thus, based on this logic, then it must be the risk of contamination that limits the application of co-bonding and secondary bonding.

Therefore, due to damage tolerance reasons, a bonded stringer will require additional mechanical fasteners to ensure the structure can be certified; however, a well designed (conservative) co-cured panel, with discrete stringer, should also have additional mechanical fasteners, to cater for the advent of a critical impact.

7.3 Wing Cover Design

7.3.1 Layout

In practice, the initial layout is a result of company design experience, history, engineers' intuition, and subsystem integration requirements[40]. The procedure for defining a wing layout is given in Niu's book '*Airframe Structural Design*'[468]. The rib pitch is defined primarily due to panel sizing to maximise the buckling load, but also by hinge locations for flaps and ailerons, as well as reinforced ribs for engine mounting, MLG attachment, and fuel tank boundaries. In terms of the layout and pitch of the stringers, the following should be considered:

- Should reduce the stability performance and take into consideration design constraints
    - Minimise unsupported areas at the SROs, in particular near the spars
- The width of the manhole region should limit the number of stringers that are discontinued
- Stringers should typically be aligned with the 0° direction of the cover laminate and be approximately parallel to the rear spar for the lowest weight solution[xxxiv]
    - Greatest skin thickness allows for easier ply runouts due to parallel offset
- Stringer pitch should ideally be compatible with the fuselage frames and the Centre Wing Box (CWB) stringer pitch[xxxv]
- The upper and lower stringers should be symmetrical as this allows easier system integration and incorporation of stiffeners in the rib webs

Shown in Figure 7-5 are the principal stringer layout alternatives. As previously mentioned, the structurally optimum layout would have the stringers running parallel to the rear spar; this also ensures that there are no SROs in the vicinity of the highly-loaded rear spar, which is structurally efficient. However, the manhole row must be positioned in order to minimise the distance to both the front and rear spars, which typically means the manhole row is aligned to the centreline of the wing box.

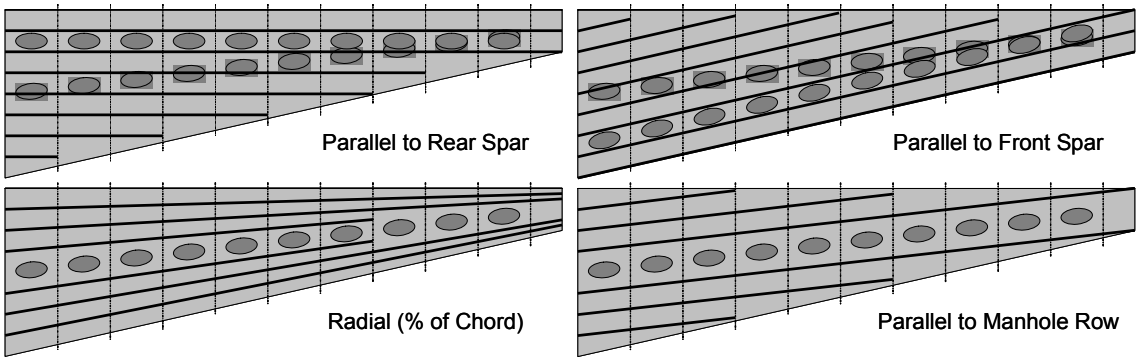

Figure 7-5: Alternative stringer layouts

Referring to Figure 7-5, by orientating the stringers parallel to the rear spar, this limits accessibility via the manholes, and hence is not favourable; furthermore by locating the manholes in the vicinity of the highly-loaded rear spar, this will lead to an inefficient structure, due to the stress raiser caused by the manholes themselves.

Alternatively, the stringers could be orientated parallel to the front spar, however this has the same problem in terms of accessibility via the manholes, and more critically the stringers will run out at the rear spar, which is structurally inefficient. Another alternative is to have a radial layout, which, for a plain cover, has the same number of stringers at the root as at the tip, which can minimise the SRO issue. This solution is also advantageous as at the tip the stringer pitch is smaller than at the root, hence at the tip where the cover is stability critical, the stringer pitch is reduced, whereas at the root, which is typically strength critical, the pitch is wider but will have a thicker cross-sectional area, hence radial stringer could be structurally efficient due to the varying stringer pitch along the span. This solution has, however, a number of disadvantages. Firstly, the lower cover has a number of areas where the stringers have to be terminated, be it for the manhole row, as illustrated in Figure 7-5, or for flap track

[xxxiv] This does not consider the potential influence of aerotailoring.
[xxxv] If a CWB is required, alternative is to butt together the two Lateral Wing Boxes (LWB).

attachments and fuel pumps. This can lead to tapered sections, due to the radial stringer layout, which increases the complexity of integrating such features, and can lead to large areas of skin that are not supported by a stringer. Secondly, the tapering effect can also cause issues, such as with the tooling and ensuring sufficient stringer foot width is available to cater for repair, as towards the tip there will be a greater intensity of stringers, in comparison to the root. Finally, typically the adjacent stringers and ribs define the skin field, which will have a certain thickness based on the load in the skin. By having a tapering section this will increase the ATL effort, and if the taper angle is too shallow, it may not be possible for the ATL to cut the ply to the desired shape.

The last remaining solution is to position the manholes at the centreline of the wing box, and then run the stringers primarily parallel to the manhole. This configuration means that two stringers can run parallel and adjacent to the manhole row, which is structurally good and can facilitate manhole doubler integration. Shown in Figure 7-6[236], is the NASA ACT wing stub box (LHS) and semi-span wing (RHS). It can be seen that the wing stub box did not need to consider the implications of a manhole row running the complete span of the wing, hence the stringers run parallel to the rear spar; whereas for the semi-span wing, the manholes are positioned mid-chord and the stringers run parallel to the manhole row. This is further evidenced by the A400M lower cover shown in Figure 7-7[463], with the manhole row positioned roughly mid-chord of the wing box.

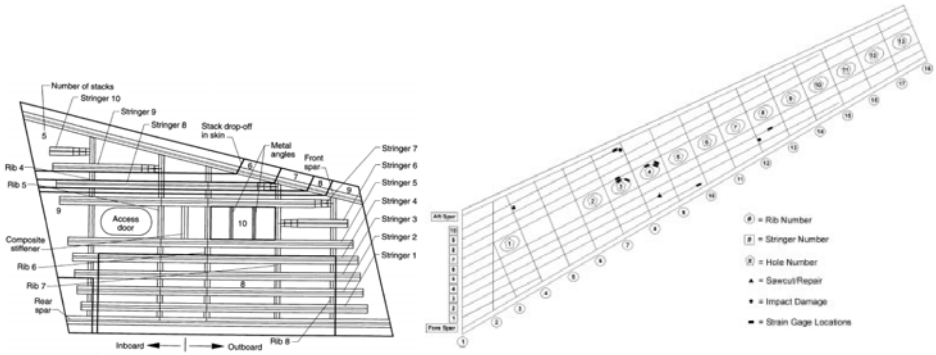

Figure 7-6: Influence of manholes on ideal stringer orientation

Figure 7-7: Manhole row positioned mid-chord on A400M CFRP lower cover

Illustrated in Figure 7-8[176] is a wing box design where CFRP design was considered from the beginning, hence why the engines are mounted to the fuselage, and the rear spar is straight, which is more compliant for CFRP, as opposed to being kinked towards the root joint. The stringers are orientated, one parallel to front spar and the other to the rear spar, to ensure no interference with internal fittings at discrete load locations, e.g. flaps mounting locations[176], whereas all other stringers run parallel to the manhole row.

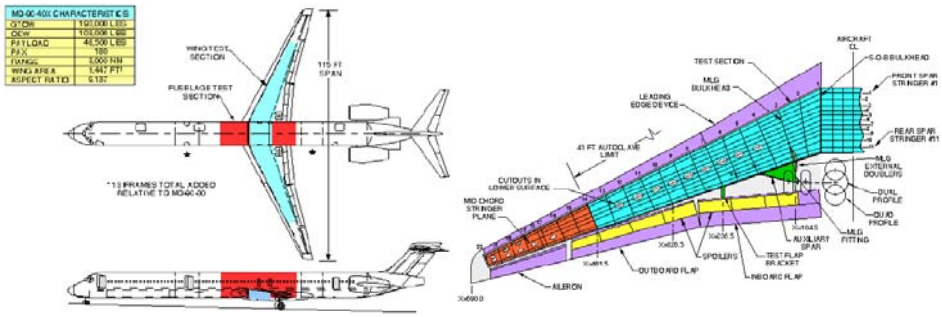

Figure 7-8: MD-90-40X baseline aircraft (LHS) and wing structural arrangement (RHS)

7.3.2 Stringer-Stiffened Panel Stability Characteristics

In order to have a better understanding of this chapter, a short introduction will be given to stability analysis of stringer-stiffened panels. A stringer-stiffened panel has a prismatic cross-section, constructed from flat plates, which are regarded as being rigidly connected to each other, with all degrees of freedom matching at the interface. The panel is supported at regular intervals by ribs, giving rise to a sinusoidal buckling form along its length[469]. When modelling a stringer-stiffened panel, it is implicitly considered as a wide panel with a number of stringers, which are subjected to various loads, including in-plane loads, namely compression, tension, shear, and out-of-plane loads, as shown in Figure 7-9. A combination of these loads could be acting on the stringer-stiffened panel simultaneously. Furthermore, the combined buckling load when reacting both compression and shear load, is always more critical than just compression buckling load[347]. In reality, due to the chordwise profile of the wing cover, the stress required to induce buckling under both compression and shear loads, is increased in comparison to a flat plate with the same dimensions[431]. Therefore, stability calculations performed based on flat panels, will be conservative in comparison to reality.

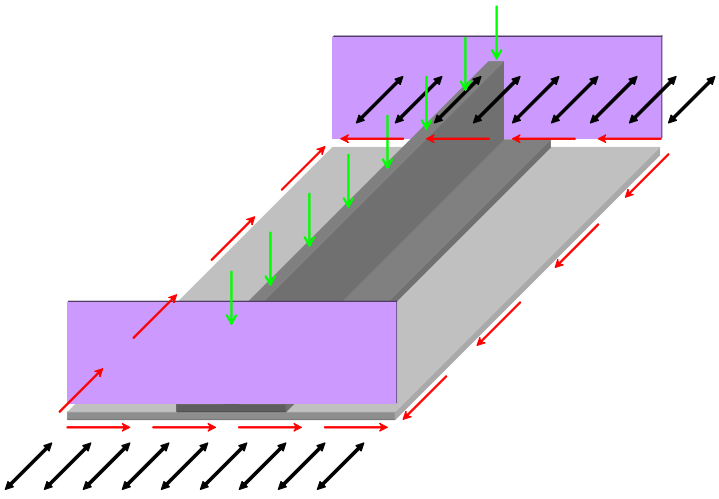

Figure 7-9: Loads on a stringer-stiffened panel

As shown in Figure 7-10[470], there are four principal buckling modes, which are dependent on the buckling half-wavelength, namely:

- Local skin buckling due to compression
- Local stringer buckling due to compression
- Global panel buckling due to compression
- Skin buckling due to shear

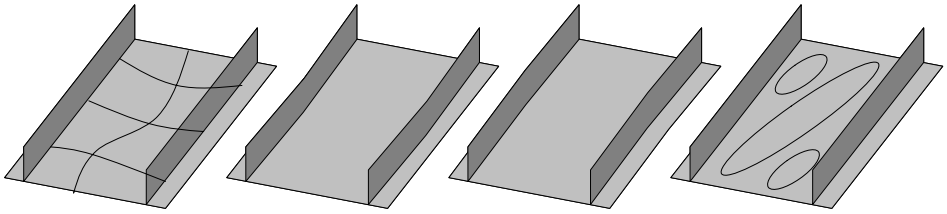

Figure 7-10: Buckling modes

Typically, the half-wavelength for local buckling will occur at a length that is less than the largest dimension of the panel. Local buckling, under compression, occurs as the various plates that constitute the panel have differing levels of resistance to deformation. Hence, deformation takes place between the nodes and typically results in simultaneous warping of both the skin and stringer. Local buckling will lead to a reduction in stiffness, however it will not lead to panel failure, as the material at the nodes is not highly deformed, hence the stresses remain relatively low.

If local buckling occurs in the skin, for a single stringer-stiffened panel, then greater proportion of the load will be reacted by the stringer, due to the reduction in skin stiffness. The same principle can be applied to a multiple stringer-stiffened panel, with varying cross-section. If skin buckling occurs in one bay, then the adjacent stringers and neighbouring skin will have to react a greater load. Distortional buckling occurs between local and global (Euler) buckling with the half-wavelength being typically many times longer than the longest dimension of the panel, with this half-wavelength being heavily dependent on the geometry and loading. The extreme nodes of the member will translate when distorted. Global buckling is a long column failure, where flexural (translation), torsional (rotational), and flexural-torsional deflection occurs at long half-wavelengths, resulting in out-of-plane displacement of the complete cross-section, albeit there will be no distortion in any of the elements[471].

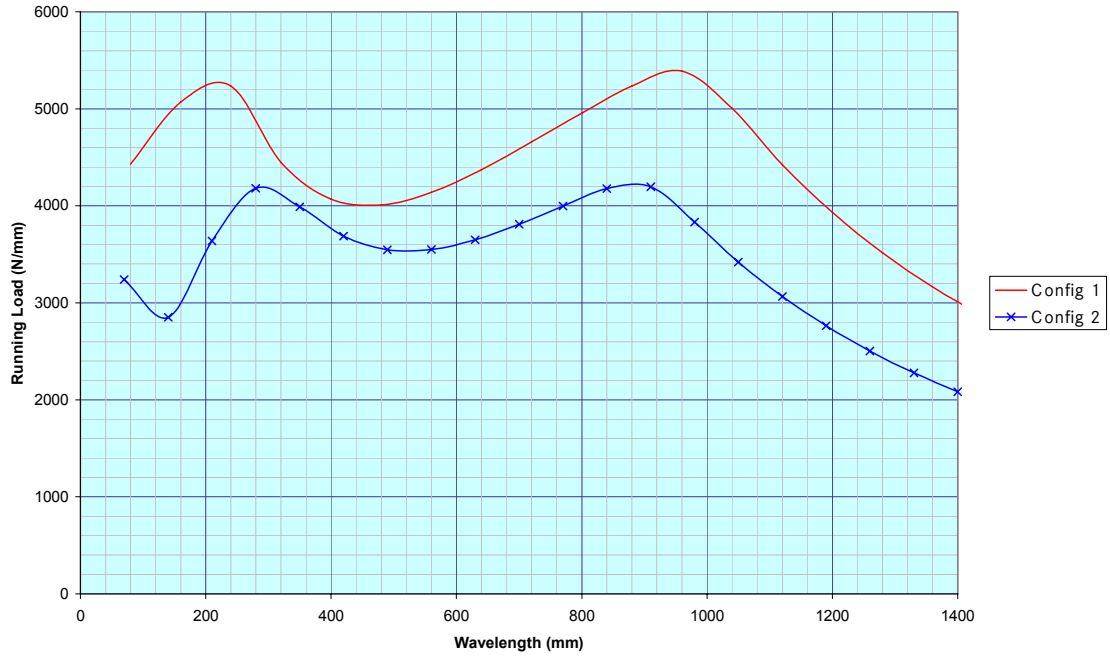

Figure 7-11: P-λ curve for 2 I-stiffened panels

Shown in Figure 7-11[xxxvi] is a Load versus Half-Wavelength (P-λ) curve for two metallic I-profile stiffened panels, with both panels having a stringer pitch of 165mm and a panel length of 1400mm, whereas the differing parameters are shown in Table 7-1.

	Upper Flange		Blade		Lower Flange		Skin
	UFW	UFT	BH	BT	LFW	LFT	ST
Configuration 1	30	8	80	8	70	4	4
Configuration 2	40	6	70	6	60	3	4

Table 7-1: I-stiffened stringer panel parameters

Shown in Figure 7-12 are section cuts of the buckling modes for configuration 1, at different half-wavelengths, with the red line illustrating the unloaded panel, whereas the blue line represents the deformed panel due to buckling. At a half-wavelength of 80mm local skin buckling occurs. At a half-wavelength of 450 and 960mm, distortional buckling occurs in the stringer, which is evidenced, by rotation and transfer of the co-joining nodes attaching the web to the upper flange. At a half-wavelength of 1400mm, the panel is under global buckling, as the whole panel is displaced.

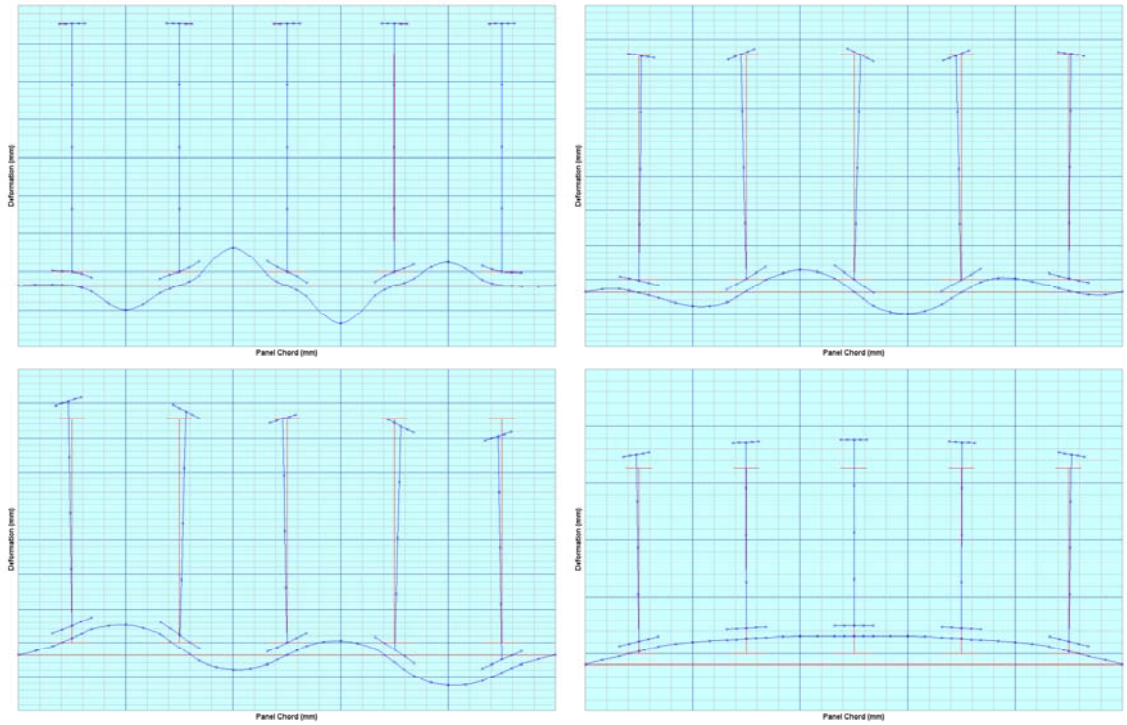

Figure 7-12: Buckling modes for Configuration 1 at half-wavelengths of 80mm (Top LHS), 450mm (Top RHS), 960mm (Bottom LHS) and 1400mm (Bottom RHS)

Figure 7-13 illustrates configuration 2, at a half-wavelength of 135mm, where local buckling occurs both in the skin, but more interestingly in the stringer webs, as the nodes at the extremity of the web remain in their pre-loaded position. At a half-wavelength of 520mm the buckling mode is distortional in the stringer.

[xxxvi] Created using ESDU FSM program, which is explained in Section 8.4.

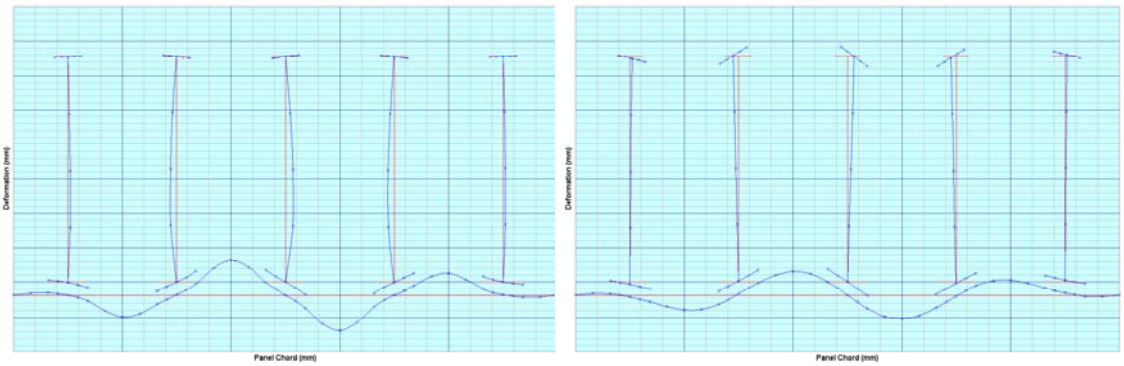

Figure 7-13: Buckling modes for Configuration 2 at half-wavelengths of 135mm (LHS) and 520mm (RHS)

A simple metallic blade stiffened panel was also analysed, as shown in Figure 7-14, with a 165mm stringer pitch and a panel length of 800mm. The blade had a height of 70mm, and a thickness of 6mm. The noteworthy buckling mode from this stiffened panel was at a half-wavelength of 630mm, as shown in Figure 7-15, which illustrates a distortional asymmetric buckling mode in the skin.

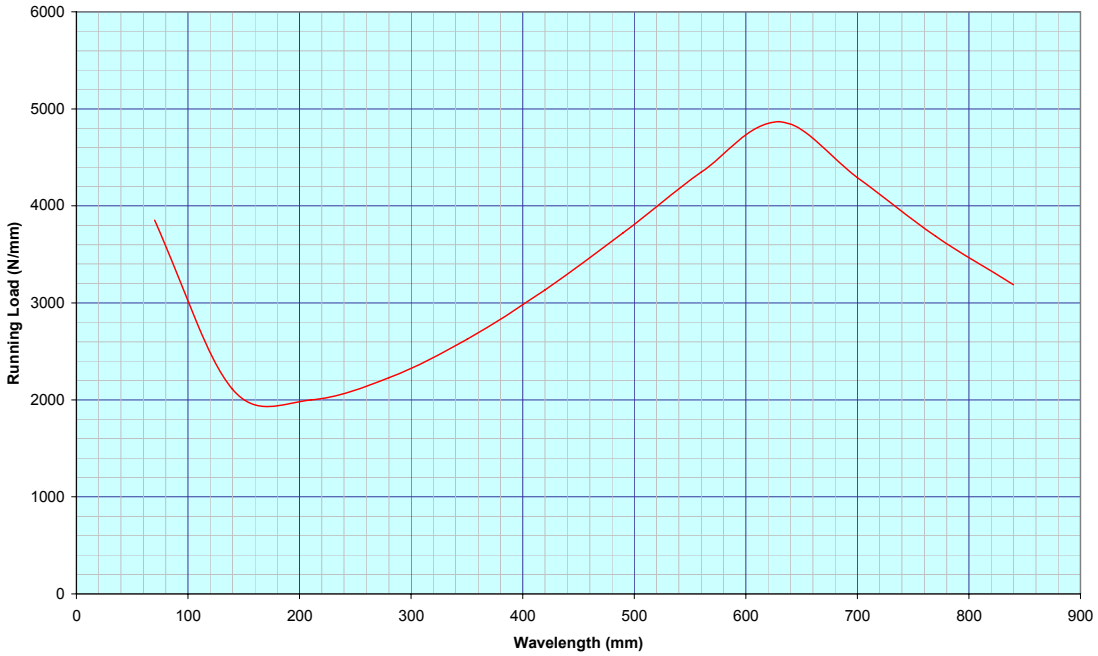

Figure 7-14: P-λ curve for a blade-stiffened panel

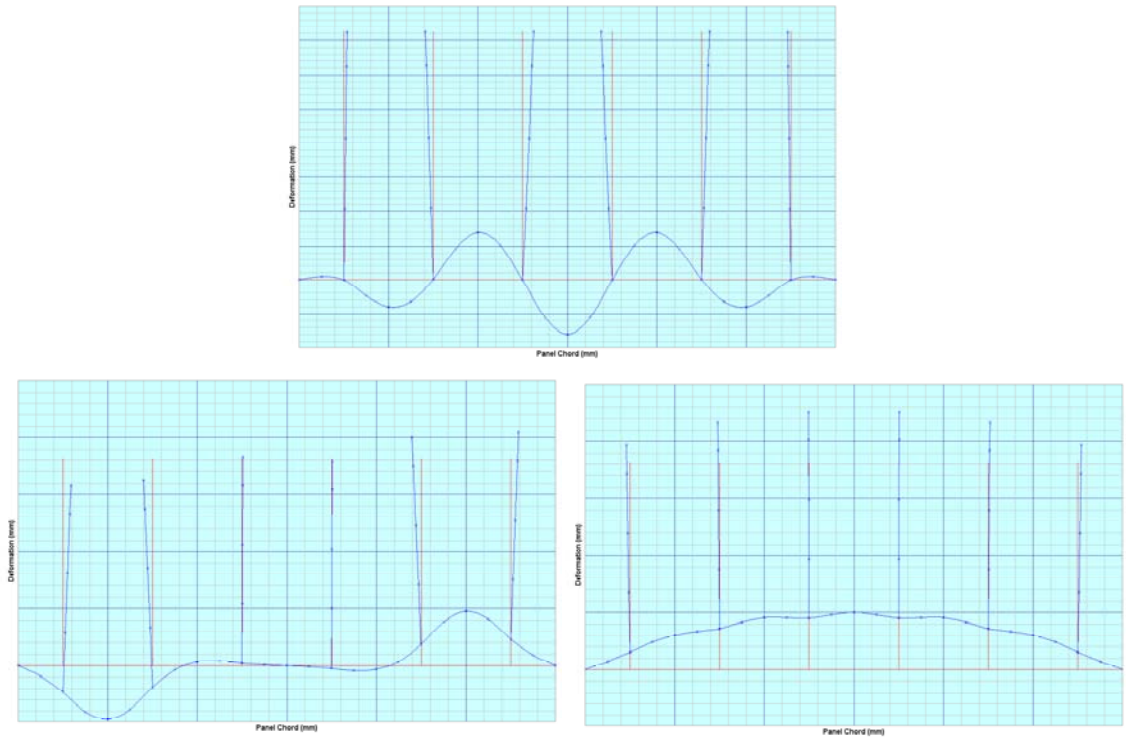

Figure 7-15: Buckling modes at half-wavelengths of 170mm (Top), 630mm (Bottom LHS) and 800mm (Bottom RHS)

7.3.3 Design Considerations

Figure 7-16 illustrates the typical stringer profiles that are suitable for a wing cover. All profiles, except the integral U-profile stringer panel, have discrete stringers that require some form of attachment to connect the stringer to the skin. As the wing covers will have sufficient cross-sectional area to react the shear load due to torsion, this same area can be used to react the tensile load. Both the upper and lower covers will react a combination of shear and compressive loads, which can induce buckling. The stringer-stiffened panel is very efficient, in comparison to just a skin, under in-plane load conditions, with the stringers increasing the buckling resistance and bending stiffness of the panel. As the compressive loads on the upper cover are typically far greater than on the lower cover, the upper cover stringers will be more efficiently designed, using perhaps a more effective stringer shape, such as an I-profile, as opposed to a T-profile.

The distribution of the load into the stringers and the skin will be a function of their respective axial stiffness[431]. Due to this distribution of load, it can be argued that stiffened panels will provide alternative load paths, and thus has a higher residual strength than just a skin[472]. In stringer-stiffened panels, the shear is carried solely by the skin, although if the discrete stringer has a foot, then local to the foot it is possible that the shear is distributed between the skin and stringer foot[xxxvii], or less a closed profile stringer is used, which is evidenced in Figure 7-17 for a U-profile stringer-stiffened panel, based on the following panel:

[xxxvii] ESDUpac A0817 FSM program assumes that local to the stringer foot shear load is proportioned between the stringer foot and skin, the distribution of which is determined by the shear striffness of the constituent parts.

- BH = 30.5mm; BT = varying
- SP = 127mm; ST = varying

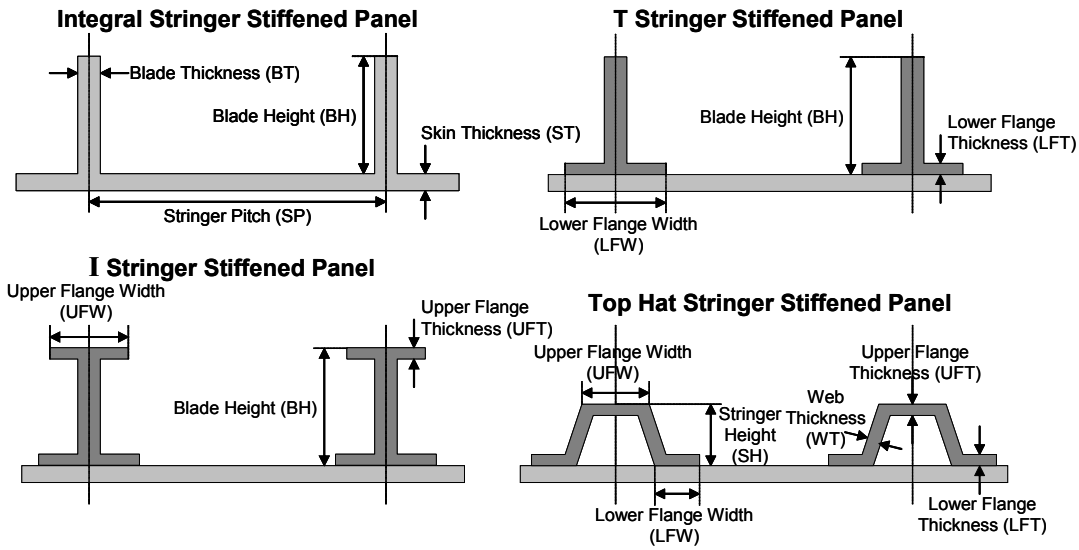

Figure 7-16: Basic parameters of typical stringer-stiffened panels

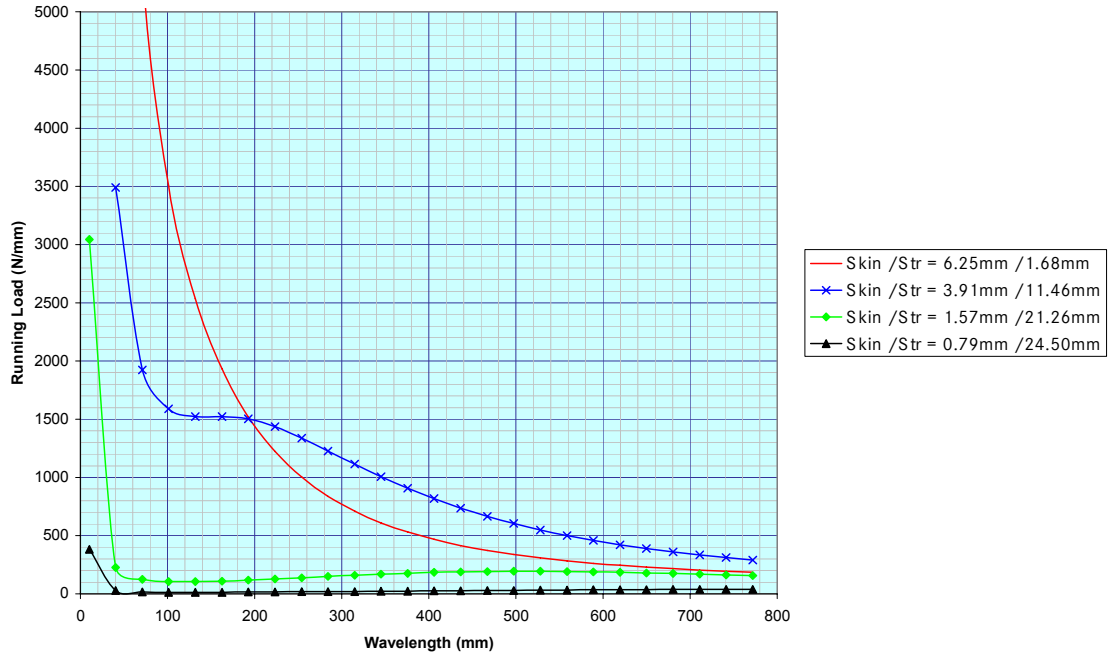

Figure 7-17: Proportioning of thickness in stringer or skin and its influence on shear load

The thickness of the blade and stringer were varied, but the overall cross-sectional area stayed constant, so that the effect on shear performance of the panel could be investigated. It can be seen that the two examples with thin skins fail at a low load level, whereas the panel with a skin thickness of 3.91mm, and a stringer thickness of 11.46mm, performs better due to the thicker skin and the stringer blades having enough inertia to resist the deformation in the skin. Therefore, it would seem that a compromise in the proportioning of cross-sectional area in the skin and the stringer is important, where it would seem that once the skin can take the shear load at a local buckling mode, it is more efficient to increase the area of the stringer in order to limit the amount of deflection in the skin. This is shown in Figure 7-18, for the panel 3.91mm/11.46mm taken from Figure 7-17, with a 10% increase in cross-sectional area either

in the stringer or the skin, resulting in an improvement of 9.3% and 5.1% respectively, over the baseline example.

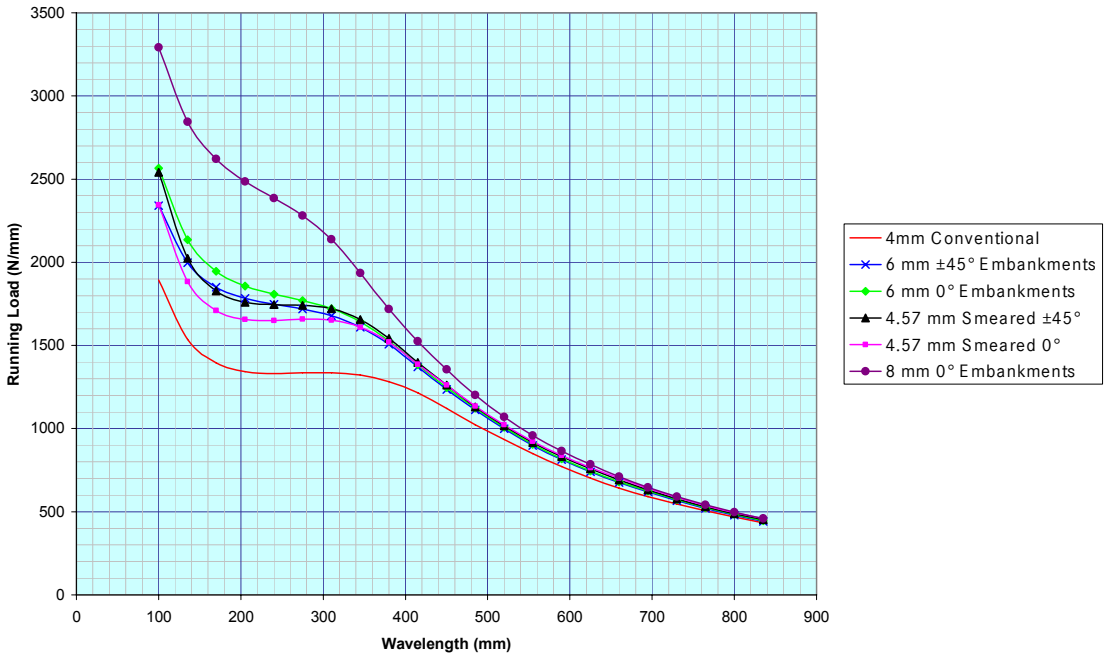

Figure 7-18: Performance improvement due to either 10% more area in stringer or skin

For a commercial aircraft's upper wing cover, the inner section will typically be constrained by the damage tolerance allowables due to the skin's thickness, whereas thinner structure towards the tip will be buckling critical. The MLG, and if required the engine pylon areas, will be bearing driven due to the mechanical fasteners. The lower wing covers performance will be limited also by the above mentioned criteria, however the proportion of the structure sized by either damage tolerance or buckling may be different. This is because the lower cover is subject to greater foreign object damage and has more attachments, such as fuel pumps, engine mounts and manholes, as well as the lower cover having typically greater tensile loading, but lower compressive loading.

The integration of non far-field areas[xxxviii] is critical to the overall efficiency of the wing cover. As advocated by Hart-Smith (1995)[363], when designing with CFRP, it would be appropriate to design first the joints and cut-outs and then the far-field areas. It is important that the design of the far-field areas, and in particular the laminates used, does not compromise the joints, cut-outs and ability to repair the structure. Often the reliance on optimisers creates laminates that are too notch sensitive[363], whereas softening the laminate local to the cut-out is known to be beneficial to the overall compressive strength of the panel[306].

Joints can also cause fatigue issues, due to the high out-of-plane loads, in particular for upper cover bolted joints where the air pressure during flight produces a large sucking force, which in combination with the fuel pressure, results in brazier loads that try to pull the cover off the ribs and spars.

[xxxviii] A far-field area is characterised by being undisturbed by features, for instance the integration of a fuel pump.

7.3.4 Wing Cover Parameters

7.3.4.1 Stringer Pitch

Both weight and cost are a function of the stringer pitch. Once the stringer pitch increases over a certain dimension, the stringer cross-sectional area must substantially increase to ensure that the load in the skin is equal to the bay-buckling load. Due to the increase in stringer cross-sectional area, this will eliminate any weight and cost decrease due to minimising the number of stringers.

An increase in stringer pitch improves the damage resistance of the cover, as it affects both the structure's elastic response and the shear plate thickness[473]. However, a smaller pitch can increase the shear buckling load, whereas with a greater pitch, the stringer will need to have greater stiffness[294]. Furthermore, a more efficient stringer, such as a top-hat-profile stringer under buckling, should have a greater stringer pitch than for a T-profile stringer[464]. By adjusting the pitch based on the stringer profile, this can minimise the difference in RFs for both stability and strength.

The stringer pitch should also allow for easy integration of parts, such as the ribs, which may require adequate landing on a stringer foot for subsequent assembly, thus using a 125mm stringer pitch with a discrete stringer, may not be practicable. Furthermore, integration of systems in the skin, like water drains need to be considered, as well as repair in general.

7.3.4.2 Proportion of Load reacted by Stringer

The proportion of the load reacted by the skin and stringer is determined by their respective stiffnesses and areas. For example, a panel with a thin and soft skin, but with a large and stiff stringer, will react most of the load through the stringer. The ideal proportion of load which is reacted either by the skin or the stringer is not fixed, and is dependent on a number of factors, including the type of stringer profile, stiffness of the laminate, and the associated allowable strains, the sizing criteria, i.e. stability or strength, out-of-plane loads, damage tolerance, and manufacturing constraints. As a general rule, the combined cross-sectional area of the panel should be reduced so as to minimise the weight.

The minimum stiffening ratio between stringer and panel ($AE_{Stringer}/AE_{Skin+Stringer}$) has been defined by Karal[176] as 0.35, to mitigate against crack propagation and to deter DSD from growing beyond the adjacent stringer and causing catastrophic failure. The stringer and skin should have similar stiffnesses to avoid adhesive failure, in particular, under severe impact loads. By increasing the thickness of the skin, the skin's stiffness will increase, and if used with smaller stringers, with similar stiffness, this will diminish any large stiffness difference between the stringer bay area and the area near and underneath the stringers, as evidenced by the damage tolerant stringer panel design by Clarke et al.[409]. However, the upper limit of the stiffening ratio has not previously been defined.

7.3.4.2.1 Sound Stringer-Stiffened Panel

An investigation was carried out to consider the influence of varying the proportion of the load through the stringer using a standard T-profile stringer with a 60/30/10 laminate, and

either a 10/80/10 or 50/40/10 skin, the results of which are shown in Table 7-2 and Table 7-3, respectively. The load in the stringer varied in increments of 10% from 30-70%. The stability calculation was carried out using ESDUpac A0301[474] as only an axial load was considered, and the strength was checked against plain strain, out-of-plane effects, and bearing/bypass in the stringer blade.

Load		Dimensions (mm)							Strength (RF)						Other
N/mm	% in Str	Skin	Stringer				Panel		Tension			Compression			
		Thk	BH	BT	LFW	LFT	Area (mm²)	Low	Plain	OOP	BB	Plain	OOP	BB	ν_{12}
-1000	30	No solution found for sound stringer-stiffened panel													
	40	12.8	40.0	6.7	128.0	3.0	3299	4	4.01	2.06	1.48	4.50	1.75	2.71	0.19
	50	6.7	47.0	6.1	76.0	3.0	1892	3	2.51	1.48	0.81	2.82	1.31	1.43	0.19
	60	4.3	48.0	6.1	64.0	3.0	1362	2	1.98	1.09	0.63	2.23	0.95	1.10	0.19
	70	3.6	63.0	7.0	64.0	3.0	1362	1	2.22	1.93	0.55	2.49	2.00	0.92	0.19
-2000	30	21.5	28.4	6.0	180.0	3.0	5171	5	2.90	1.43	1.39	3.26	1.21	2.86	0.19
	40	16.7	50.0	7.1	166.0	3.0	4311	4	2.62	1.58	0.80	2.95	1.41	1.40	0.19
	50	8.6	58.0	6.5	88.0	3.0	2413	3	1.59	1.04	0.43	1.79	0.95	0.72	0.19
	60	6.3	59.0	6.8	103.0	3.0	2002	2	1.46	0.96	0.39	1.64	0.88	0.65	0.19
	70	4.7	64.0	8.9	80.0	3.0	1762	1	1.43	1.19	0.49	1.60	1.20	0.88	0.19
-3000	30	24.0	37.0	6.0	180.0	3.0	5744	5	2.14	0.96	0.84	2.40	0.79	1.57	0.19
	40	18.8	55.0	7.3	180.0	3.0	4836	4	1.95	1.14	0.66	2.20	1.00	1.18	0.19
	50	10.6	69.0	6.7	116.0	3.0	2998	3	1.33	1.00	0.30	1.49	0.97	0.50	0.19
	60	7.4	64.0	8.2	103.0	3.0	2351	2	1.14	0.80	0.34	1.28	0.75	0.59	0.19
	70	5.3	64.0	10.5	80.0	3.0	1985	1	1.07	0.82	0.41	1.20	0.79	0.77	0.19
-4000	30	25.5	49.0	6.0	180.0	3.0	6128	5	1.72	0.07	0.54	1.93	0.05	0.93	0.19
	40	19.7	64.0	7.3	180.0	3.0	5089	4	1.55	1.04	0.46	1.74	0.97	0.79	0.19
	50	12.3	71.0	7.5	128.0	3.0	3456	3	1.14	0.85	0.31	1.28	0.82	0.53	0.19
	60	8.1	73.0	8.3	105.0	3.0	2583	2	0.94	0.73	0.25	1.06	0.72	0.42	0.19
	70	5.9	67.0	12.0	82.0	3.0	2243	1	0.91	0.69	0.38	1.03	0.67	0.71	0.19

Table 7-2: 10/80/10 Skin & 60/30/10 Stringer

Load		Dimensions (mm)							Strength (RF)						Other
N/mm	% in Str	Skin	Stringer				Panel		Tension			Compression			
		Thk	BH	BT	LFW	LFT	Area (mm²)	Low	Plain	OOP	BB	Plain	OOP	BB	ν_{12}
-1000	30	7.0	46.7	6.0	89.0	3.0	1986	5	3.52	1.92	1.47	2.80	1.18	2.59	0.05
	40	4.85	68.0	6.0	63.0	3.0	1589	3	2.85	2.42	0.85	2.27	1.75	1.41	0.05
	50	4.0	71.1	7.7	65.0	3.0	1553	1	2.82	2.51	0.98	2.25	1.86	1.67	0.05
	60	3.4	81.0	8.8	66.0	3.0	1593	2	2.93	2.70	1.06	2.34	2.04	1.81	0.05
	70	3.25	86.0	9.1	66.0	3.0	1630	4	3.01	2.80	1.04	2.40	2.13	1.75	0.05
-2000	30	9.1	56.0	7.1	102.0	3.0	2578	5	2.28	1.42	0.81	1.82	0.91	1.39	0.05
	40	6.4	76.0	7.1	76.0	3.0	2080	3	1.86	1.60	0.49	1.49	1.16	0.82	0.05
	50	5.4	81.0	9.0	79.0	3.0	2064	1	1.88	1.70	0.67	1.50	1.27	1.15	0.05
	60	4.4	85.0	11.5	68.5	3.0	2065	2	1.90	1.76	0.84	1.52	1.34	1.49	0.05
	70	3.7	87.0	15.2	72.0	3.0	2264	4	2.11	1.98	1.08	1.68	1.51	2.02	0.05
-3000	30	10.2	68.5	6.4	115.0	3.0	2889	5	1.70	1.17	0.50	1.36	0.78	0.84	0.05
	40	7.3	78.0	8.0	91.0	3.0	2394	3	1.43	1.21	0.46	1.14	0.88	0.77	0.05
	50	6.1	82.0	10.8	79.0	3.0	2361	1	1.43	1.29	0.58	1.14	0.96	1.02	0.05
	60	5.0	87.0	12.8	83.0	3.0	2366	2	1.45	1.34	0.63	1.16	1.02	1.11	0.05
	70	4.3	83.0	18.8	75.0	3.0	2625	4	1.63	1.52	1.03	1.30	1.16	2.13	0.05
-4000	30	11.3	73.0	7.0	128.0	3.0	3228	5	1.43	1.01	0.40	1.14	0.68	0.66	0.05
	40	8.0	75.0	9.0	92.0	3.0	2591	2	1.16	0.95	0.45	0.93	0.67	0.78	0.05
	50	6.7	78.0	11.9	95.0	3.0	2573	1	1.17	1.03	0.55	0.93	0.76	1.00	0.05
	60	5.6	86.0	14.6	84.0	3.0	2630	3	1.21	1.11	0.62	0.97	0.84	1.17	0.05
	70	4.7	85.0	20.8	84.0	3.0	2937	4	1.37	1.28	0.89	1.09	0.97	1.88	0.05

Table 7-3: 50/40/10 Skin & 60/30/10 Stringer

As can be seen from Table 7-2, for the 10/80/10 skin laminate, the panel with the lowest cross-sectional area, hence the lightest, had the most load in the stringer. Conversely, the panel with the least load in the stringer had the greatest area, but the highest RF for plain strength, although this panel configuration was highly sensitive to out-of-plane effects due to

the panel's lack of bending stiffness. Finally, due to the amount of load going through the stiff stringer, the RF for bearing/bypass strength was often below unity. In terms of the stiffer panel, with the 50/40/10 skin laminate, as shown in Table 7-3, the lightest solution is when the stringer carries 50% of the load. In general, due to the similar stiffness of the skin and stringer, the panel is less sensitive to the out-of-plane effects, independent of the amount of load in the stringer.

7.3.4.2.2 Damaged Stringer-Stiffened Panel

From Table 7-2 and Table 7-3, it could be considered that for a 10/80/10 and 50/40/10 skin, the maximum stiffening ratio should be 70% and 50% respectively. However, this is when an intact panel is considered. As a single-stringer debond has to be considered, for all bonding procedures except co-curing, and also when a complete stringer section is removed due to discrete damage, then this was investigated.

By amending the .STO file in ESDUpac A0301, it is possible to remove a single adhesive layer connecting the strips between the foot and the adjacent skin, as well as to modify the geometry details of the panel to remove one stringer. The investigation was based on a panel with 6 stringers, with the 3rd stringer amended. The results for both the debonded stringer and the discrete damage are shown in Table 7-4 and Table 7-5, for the 10/80/10 and 50/40/10 skin, respectively.

Load		Sound Panel		Debonded Stringer		Discrete Damage		Critical Case
N/mm	% in Str	Ultimate Load		Limit Load		0.7 × Limit Load		
		Load	RF	Load	RF	Load	RF	
-1000	30	No solution found for sound stringer-stiffened panel						
	40	1340170	1.06	1120270	1.34	1125030	1.92	UL
	50	1329730	1.05	964169	1.15	882760	1.51	UL
	60	1266920	1.00	504497	0.60	453733	0.77	LL
	70	1261700	0.99	439777	0.53	388231	0.66	LL
-2000	30	2674610	1.05	665934	0.40	2590260	2.21	LL
	40	2500210	0.99	1451530	0.87	2131580	1.82	LL
	50	2542840	1.00	1036910	0.62	1699810	1.45	LL
	60	2660200	1.05	1119490	0.67	1364430	1.16	LL
	70	2567660	1.01	955270	0.57	844397	0.72	LL
-3000	30	3814440	1.00	794128	0.32	3720860	2.12	LL
	40	3780210	0.99	881453	0.35	3228040	1.84	LL
	50	3747100	0.98	1173290	0.47	2669940	1.52	LL
	60	3845580	1.01	1575720	0.63	2140120	1.22	LL
	70	3784420	0.99	1271410	0.51	1226920	0.70	LL
-4000	30	5001480	0.99	890065	0.27	4713280	2.01	LL
	40	5217930	1.03	937763	0.28	4354710	1.86	LL
	50	5029570	0.99	1379210	0.41	3637260	1.55	LL
	60	5026090	0.99	1473120	0.44	2726630	1.16	LL
	70	5001660	0.99	1359640	0.41	1680550	0.72	LL

Table 7-4: 10/80/10 Skin & 60/30/10 Stringer RFs for different cases

Based on Equations 4-1 to 4-4, the doubling of the buckling field's width, based on a flat plate, will result in a 75% reduction in buckling load capability. It can be assumed that for both the debonded stringer and the removal of one stringer cases there will be no support given to the skin between the intact stringers, thus under load, local (skin) buckling will typically occur in this area. Thus, as the ability to resist buckling load in the skin is reduced by 75%, but the applied load is reduced by 33% and 53%, respectively, for the single stringer debond and discrete source damage cases, this will result in the damaged stringer-stiffened panels being critical, with the single stringer debond case being the most stringent.

Based on analysis, it would seem that the debonded case results in the lowest RF, except as shown in Table 7-4 for the panels reacting an axial running load of -1000N/mm with 40% and 50% of the load in the stringers. However, these panels were over-dimensioned in order to proportion the load, so they can be ignored. It can be seen from Table 7-5 for the 50/40/10 skin that for the debond case, the highest RF was obtained with the least load in the stringer, and the lowest RF was obtained with the most load in the stringer; whereas for the 10/80/10 skin shown in Table 7-4, there is no such relationship.

Load		Sound Panel		Debonded Stringer		Discrete Damage		Critical Case
N/mm	% in Str	Ultimate Load		Limit Load		0.7 × Limit Load		
		Load	RF	Load	RF	Load	RF	
-1000	30	1240080	0.98	756969	0.90	719144	1.21	LL
	40	1260350	0.99	432159	0.51	402860	0.68	LL
	50	1240370	0.98	378900	0.45	344823	0.58	LL
	60	1242470	0.98	280198	0.33	252260	0.43	LL
	70	1246000	0.98	271365	0.32	243037	0.41	LL
-2000	30	2491790	0.98	1550980	0.92	1474560	1.25	LL
	40	2561370	1.01	979193	0.58	913549	0.77	LL
	50	2487020	0.98	787094	0.47	721765	0.61	LL
	60	2524310	0.99	599841	0.35	539990	0.46	LL
	70	2555210	1.01	509770	0.30	450547	0.38	LL
-3000	30	3768850	0.99	1692540	0.67	2220050	1.25	LL
	40	3739940	0.98	1451790	0.57	1354750	0.76	LL
	50	3731970	0.98	1144710	0.45	1048690	0.59	LL
	60	3737610	0.98	907376	0.36	816784	0.46	LL
	70	3746260	0.98	802964	0.32	709734	0.40	LL
-4000	30	5020780	0.99	2084240	0.62	2939800	1.24	LL
	40	5008160	0.99	1850590	0.55	1729400	0.73	LL
	50	4997480	0.98	1526100	0.45	1399980	0.59	LL
	60	5058850	1.00	1246390	0.37	1122600	0.47	LL
	70	5029070	0.99	1074540	0.32	948787	0.40	LL

Table 7-5: 50/40/10 Skin & 60/30/10 Stringer RFs for different cases

It would seem that the panels with the 10/80/10 skin are more sensitive to the debonded stringer case. This can be explained by comparing the panels sized for a running load of -3000N/mm with 40% of the load in the stringer. The panel axial stiffnesses for the 10/80/10 and 50/40/10 panel are similar, at 1.45×10^{9}N and 1.32×10^{9}N, respectively, whereas the more critical panel bending stiffnesses are 383.3×10^{9}N/mm² and 718.1×10^{9}N/mm², respectively. The strains, at UL due to buckling, are -2665με and -4910με, respectively, however when the adhesive layer is extracted from one stringer foot, then the resultant strains are -819με and -1358με, respectively. Multiplying the residual strain by the bending stiffness gives a stress of 313×10^{6}N/mm² and 3525×10^{6}N/mm², i.e. a factor of 10 difference, between the 10/80/10 and the 50/40/10 respectively. This shows that the 50/40/10 panel has under these circumstances superior damage tolerance.

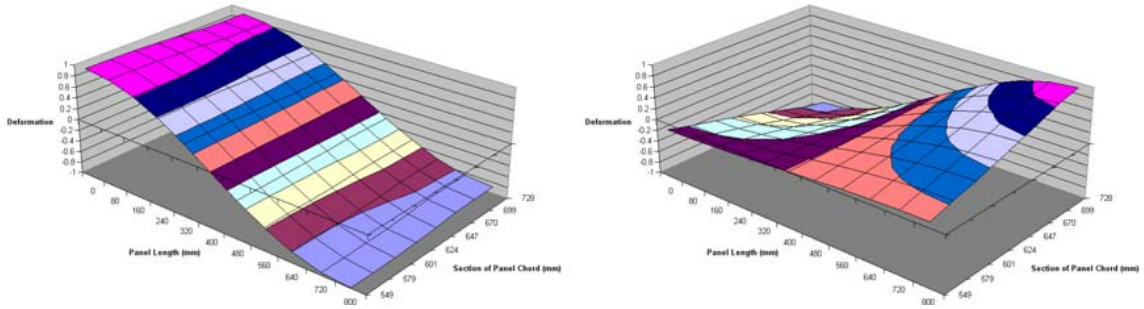

Figure 7-19: Stringer foot & skin deformation for 10/80/10 (LHS) & 50/40/10 (RHS) at UL

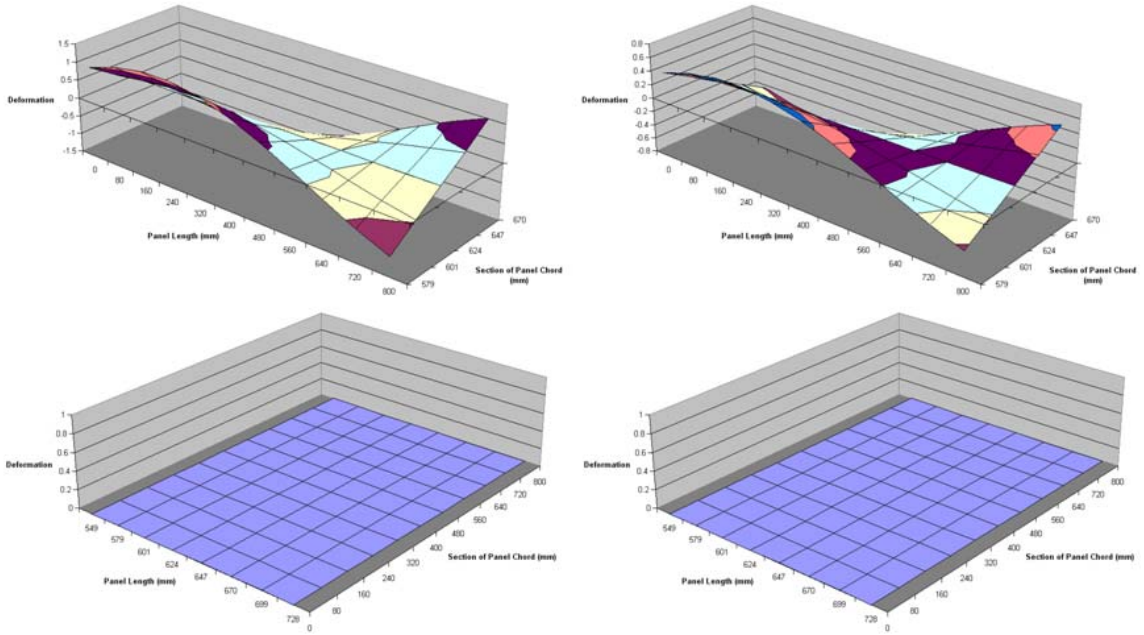

Figure 7-20: Stringer foot (upper) & skin (lower) deformation for 10/80/10 (LHS) & 50/40/10 (RHS) at LL

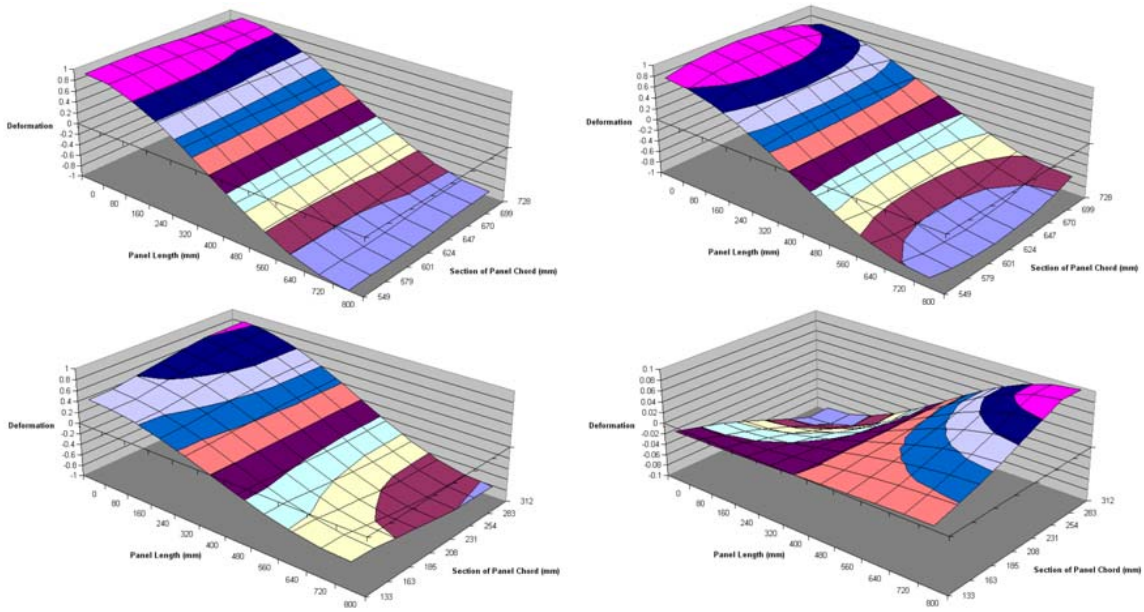

Figure 7-21: Skin without stringer (upper) & skin with stringer in different areas (lower) deformation at 10/80/10 (LHS) & 50/40/10 (RHS) for 0.7 × LL

Shown in Figure 7-19 is a representation of the skin and stringer foot deformation when the panel is sound, the reason for the different form of buckling deformation is because of the orthotropic nature of the laminate, i.e. the 50/40/10 has a θ=1.07, whereas the 10/80/10 has a θ=0.6. The debonded stringer is shown in Figure 7-20, where it can be seen that the debonded stringer has severe deformation in the foot, but the skin has no deformation. Finally Figure 7-21, shows the case for discrete damage, where a comparison is made of the skin without the stringer supporting it, and with the stringer as support. It is seen that the skin deforms more without the stringer as would be expected.

7.3.4.2.3 Damage Mitigated Stringer-Stiffened Panel

The stringer-stiffened panels are re-configured to ensure an RF ≥1, for the debond case, with the results shown in Table 7-6 and Table 7-7, for the 10/80/10 and 50/40/10 skins respectively. It should be noted that the results show the dimensions required to have an RF ≥1 at LL, and hence at UL, with a sound panel the RF would be significantly greater than unity. As shown in Table 7-6 and Table 7-7, the strength RFs are based on UL, to see the improvement over the results shown in Table 7-2 and Table 7-3 for the stringer-stiffened panels designed for UL, but without damage considered. It can be seen that there is a significant benefit in terms of the strength RFs, thus designing the stringer-stiffened panel to mitigate the debond case, can also improve the overall strength of the panel.

Load		Dimensions (mm)							Strength (RF)						Other
N/mm	% in Str	Skin	Stringer				Panel		Tension			Compression			
		Thk	BH	BT	LFW	LFT	Area (mm²)	Low	Plain	OOP	BB	Plain	OOP	BB	ν_{12}
-1000	30	No solution found for sound stringer-stiffened panel													
	40	RF>1 when stringer debonded, thus no need to re-design for debond case													
	50														
	60	6.8	63.0	9.8	64.0	3.0	2197	1	3.24	2.90	1.13	3.64	3.04	2.03	0.19
	70	6.0	71.0	13.0	64.0	3.0	2326	2	3.83	3.54	1.64	4.31	3.78	3.17	0.19
-2000	30	37.0	56.0	12.7	180.0	3.0	8921	5	5.02	4.41	2.35	5.64	4.59	4.74	0.19
	40	18.4	64.0	7.3	166.0	3.0	4777	4	2.92	2.37	0.87	3.29	2.37	1.50	0.19
	50	10.0	63.0	8.4	88.0	3.0	2851	3	1.91	1.58	0.57	2.15	1.60	0.99	0.19
	60	7.1	57.0	9.4	103.0	3.0	2296	1	1.70	1.29	0.64	1.91	1.26	1.18	0.19
	70	7.2	69.0	16.0	80.0	3.0	2796	2	2.31	2.10	1.15	2.59	2.23	2.40	0.19
-3000	30	55.0	83.0	16.0	180.0	3.0	13278	5	4.99	4.65	2.19	5.61	5.01	4.29	0.19
	40	45.0	73.0	25.0	180.0	3.0	11665	4	4.75	4.45	2.75	5.34	4.80	6.79	0.19
	50	17.0	64.0	15.0	116.0	3.0	4805	3	2.13	1.87	1.05	2.39	1.95	2.18	0.19
	60	9.5	66.0	12.5	103.0	3.0	3076	1	1.52	1.30	0.63	1.70	1.34	1.20	0.19
	70	9.0	64.0	22.0	90.0	3.0	3487	2	1.91	1.72	1.14	2.15	1.81	2.94	0.19
-4000	30	72.0	86.0	22.0	180.0	3.0	17366	5	4.89	4.64	2.54	5.49	5.04	5.52	0.19
	40	60.0	73.0	36.0	180.0	3.0	15560	4	4.76	4.52	2.76	5.35	4.92	6.80	0.19
	50	26.0	74.0	22.0	128.0	3.0	7363	3	2.45	2.27	1.38	2.75	2.43	3.24	0.19
	60	13.0	72.0	17.0	105.0	3.0	4196	2	1.55	1.39	0.75	1.74	1.47	1.54	0.19
	70	10.0	60.0	25.0	100.0	3.0	3808	1	1.55	1.35	0.95	1.75	1.39	2.35	0.19

Table 7-6: 10/80/10 Skin & 60/30/10 Stringer

The percentage increase in the panel's area to mitigate the debond case is shown in Table 7-8, for stringer-stiffened panels with both 10/80/10 and 50/40/10 skins. It can be seen for the 10/80/10 skin panels that the least load in stringer results in a larger difference in area, whereas the opposite is true for 50/40/10. There is a larger disparity in area for the 10/80/10 skin panels, which is attributable to the sensitivity of the overall difference in stiffness between the skin and stringers.

As a way to verify that the debond case is the most critical, as opposed to the discrete damage case, the respective RFs are shown also in Table 7-8. It can be seen that whereas the RFs for the debond case are close to unity, their respective RFs for discrete damage is sufficiently greater than unity.

Load		Dimensions (mm)							Strength (RF)						Other
N/mm	% in Str	Skin	Stringer				Panel		Tension			Compression			
		Thk	BH	BT	LFW	LFT	Area (mm²)	Low	Plain	OOP	BB	Plain	OOP	BB	ν_{12}
-1000	30	7.5	45.0	7.5	89.0	3.0	2143	3	3.80	2.32	1.94	3.03	1.47	3.64	0.05
	40	6.1	71.0	8.2	63.0	3.0	2017	1	3.62	3.19	1.26	2.89	2.35	2.14	0.05
	50	5.5	67.0	12.5	65.0	3.0	2141	2	3.89	3.50	2.06	3.10	2.62	3.91	0.05
	60	4.9	76.0	16.0	66.0	3.0	2387	4	4.40	4.08	2.65	3.51	3.10	5.34	0.05
	70	4.4	83.0	20.0	81.0	3.0	2760	5	5.16	4.83	3.39	4.11	3.70	7.25	0.05
-2000	30	9.2	59.0	7.1	102.0	3.0	2620	1	2.32	1.59	0.79	1.85	1.05	1.33	0.05
	40	8.0	79.0	10.0	76.0	3.0	2655	2	2.38	2.13	1.00	1.90	1.58	1.77	0.05
	50	6.8	69.0	15.5	79.0	3.0	2677	3	2.44	2.19	1.47	1.94	1.64	2.97	0.05
	60	6.2	81.0	19.0	77.0	3.0	3005	4	2.77	2.58	1.77	2.21	1.97	3.71	0.05
	70	5.4	84.0	25.0	101.0	3.0	3453	5	3.23	3.03	2.26	2.57	2.33	5.13	0.05
-3000	30	10.8	63.0	8.0	115.0	3.0	3075	2	1.82	1.25	0.70	1.45	0.83	1.22	0.05
	40	8.7	67.0	12.5	91.0	3.0	2885	1	1.73	1.46	0.91	1.38	1.06	1.74	0.05
	50	8.5	76.0	18.4	79.0	3.0	3351	3	2.03	1.86	1.29	1.62	1.40	2.69	0.05
	60	7.1	73.0	24.0	97.0	3.0	3450	4	2.12	1.95	1.58	1.69	1.47	3.90	0.05
	70	6.2	75.0	31.0	125.0	3.0	3899	5	2.43	2.26	1.79	1.94	1.72	4.34	0.05
-4000	30	15.4	74.0	11.8	128.0	3.0	4430	4	1.96	1.65	0.96	1.57	1.19	1.78	0.05
	40	9.7	71.0	13.4	92.0	3.0	3208	1	1.44	1.23	0.79	1.15	0.89	1.53	0.05
	50	8.6	72.0	19.0	95.0	3.0	3388	2	1.54	1.38	1.05	1.23	1.03	2.34	0.05
	60	7.8	78.0	25.0	100.0	3.0	3800	3	1.75	1.62	1.27	1.40	1.23	3.01	0.05
	70	7.4	85.0	34.0	140.0	3.0	4750	5	2.22	2.09	1.55	1.77	1.60	3.48	0.05

Table 7-7: 50/40/10 Skin & 60/30/10 Stringer

Load (N/mm)	% in Str	10/80/10 Skin			50/40/10 Skin		
		% Increase in area to mitigate debond	RF Debond	RF Discrete Damage	% Increase in area to mitigate debond	RF Debond	RF Discrete Damage
-1000	30				8	1.06	1.44
	40				27	1.02	1.35
	50				38	1.03	1.35
	60	61	1.03	2.98	50	1.01	1.29
	70	71	1.00	3.06	69	1.06	1.33
-2000	30	73	1.01	11.24	2	1.04	1.41
	40	11	1.00	3.27	28	1.01	1.50
	50	18	1.00	2.29	30	1.00	1.30
	60	15	1.00	1.62	45	1,01	1.29
	70	59	1.00	2.66	53	1.01	1.27
-3000	30	131	1.01	23.12	6	1.01	1.37
	40	141	1.00	15.38	21	1.00	1.32
	50	60	1.04	3.17	42	1.00	1.62
	60	31	1.00	2.17	46	1.03	1.33
	70	76	1.04	3.31	49	1.02	1.28
-4000	30	183	1.00	38.17	37	1.00	2.26
	40	206	1.00	23.41	24	1.00	1.33
	50	113	1.01	5.07	32	1.00	1.30
	60	67	1.00	2.89	44	1.01	1.30
	70	70	1.03	2.46	62	1.00	1.63

Table 7-8: % increase in area to mitigate debond and RF comparison

The stringer-stiffened panel's area data in Table 7-6 and Table 7-7 is illustrated graphically in Figure 7-22 and Figure 7-23. In general, a very good step trend exists between the data for each case and skin type. For the 10/80/10 skin panel, the most efficient panel will have the highest load concentrated through the stringer for both a sound panel and to mitigate against the debond. Whereas for the 50/40/10 skin panel the most efficient panel has roughly 40-50% of the load concentrated through the stringer. It would also appear that overall the lightest panel is with a 10/80/10 skin and 70% of the load in the stringer for both the sound panel and the panel designed to mitigate the debond. For the sound panel, this is the case when stability performance is considered, strength actually becomes critical, particularly at higher load levels, thus a 50/40/10 skin is likely to be better. However, for the debond case, the 10/80/10

is actually the most efficient, as due to the extra thickness of structure, the strength RFs are sufficiently above unity. Furthermore, the stability efficiency of the 10/80/10 is enhanced, as due to the debonded stringer, stability is more critical, hence a more stability efficient skin is beneficial. However, the benefit of a 10/80/10 skin is marginal over a 50/40/10 skin.

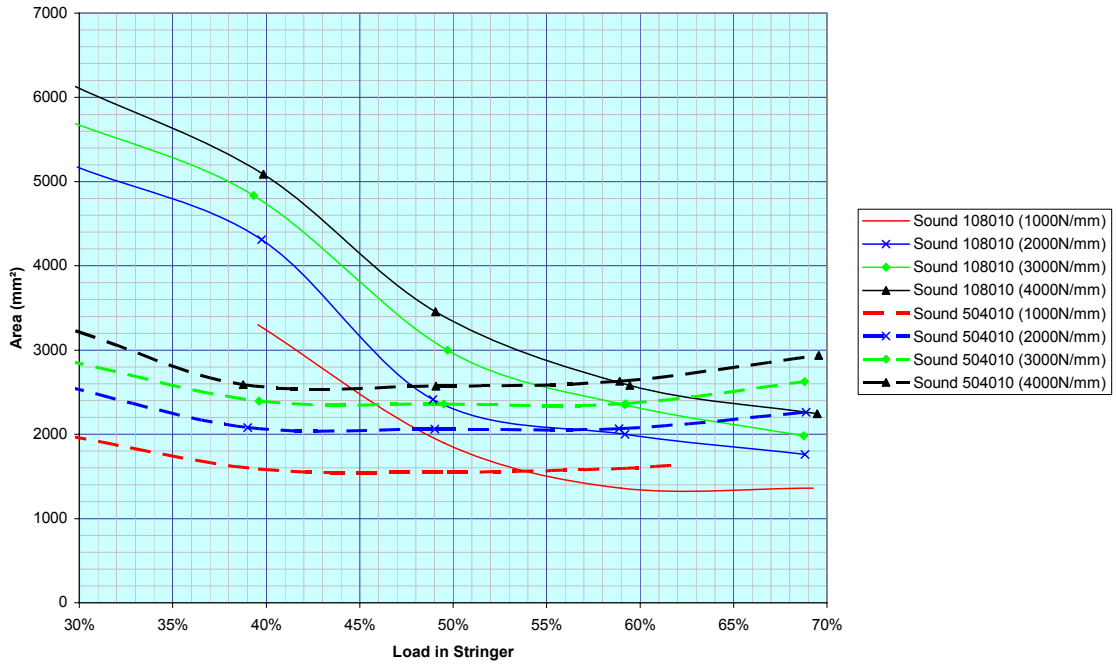

Figure 7-22: Sound stringer-stiffened panel comparison

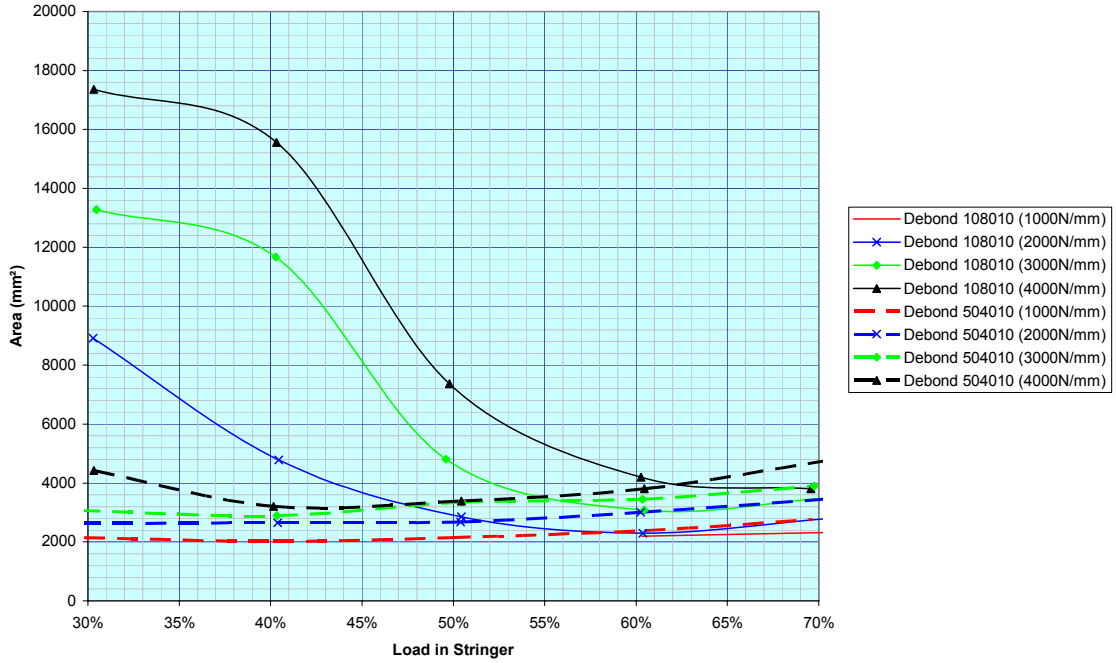

Figure 7-23: Debond mitigated stringer-stiffened panel comparison

Wiggenraad et al. (1998)[473] investigated the optimisation of stringer-stiffened panels for when, debonding, DSD, and a sound panel case were considered together. It was found that between a panel designed for all cases, and one just for the sound panel, there was only a 10% difference in weight, for a running load of -2000N/mm. However, part of the optimisation was to amend the percentage of ±45° plies in the laminate, which was not considered above, and the panel length was just 550mm, whereas for the above examples the panel was 800mm,

which would be a lot more critical for stability. In terms of the strength analysis performed for damaged panels, Wiggenraad et al. (1998) considered that as the panel was already damaged, then the strain allowable due to damage tolerance should not be considered, instead the normal material maximum strain should be considered, in this case -7000με[473].

7.3.4.3 Stringer to Skin Integration

The stringer to skin integration is very critical to the overall panel's damage tolerance and strength. With the advent of toughened resin systems, which has improved the damage tolerance of the laminate, this has had limited success for the skin to stringer foot integration, as shown in Figure 6-9. To reduce the opening forces and restrain damage growth, it is better to have tapered feet, as shown in the LHS of Figure 7-24[188], to remove the through-thickness stress concentration[450,475], or stringer doublers as shown in the middle of Figure 7-24. As shown in the RHS of Figure 7-24 if the stringer foot was embedded this could also be beneficial and may lend itself to dry fibre technology.

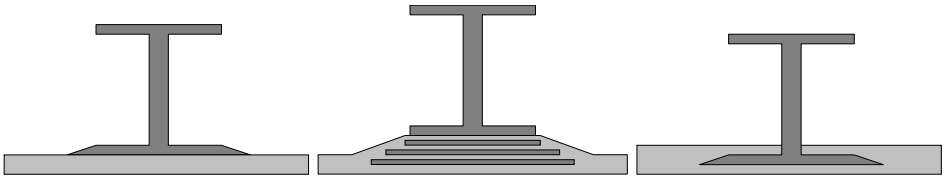

Figure 7-24: Different stringer designs

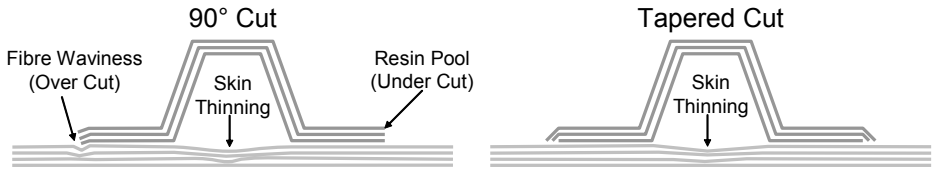

Figure 7-25: Effects of tapering the stringer foot for co-curing

A further benefit of tapering the stringer foot is shown in Figure 7-25[270], as without the tapering, this can induce a bow-wave at the foot termination into the uncured skin, which is not desirable; and would be exacerbated if a co-bonding technique was used with cured stringers. To create this taper for an uncured stringer, the long foot edge can be undercut; alternatively, for a pre-cured stringer the taper can be machined.

7.3.4.3.1 Embankment Design

In terms of overall panel strength, the 0° plies in the skin are critical as they have the highest strains, hence they react a high proportion of the load, therefore these plies typically should fail first. If delamination should exist within the skin, some of the 0° plies may no longer be supported and hence could buckle prematurely, with a resultant load redistribution causing the remaining 0° plies to overload[473], resulting in panel failure. If, however, the propagation of damage is constrained, then this should provide a more damage tolerant design.

A proposed solution, developed by Boeing/NASA[155], to protect the 0° plies in the skin, is shown in Figure 7-26[473], which has a varying stiffness skin using a soft skin laminate, with mainly ±45° and 90° plies. This results in low average axial stiffness across the panel, but with stiffened embankments, with a higher proportion of 0° plies, underneath the stringer foot.

With the 0° plies principally located in the embankment area, this should provide the following advantages[302]:

- Maximises the bending strength requirements in conjunction with skin and stringer column stability
- Increases the local stability requirements with maximum loads concentrated on the smaller elements
- Minimum axial load on the skin element between the stringers
- Load carrying plies in the stringer and embankment, are protected in the thickest part of the cover
- Should the outer 0° plies in the skin buckle; the subsequent eccentricity in load is restrained by the stringer in the embankment area
- Delamination propagation is inhibited, as the 0° plies are isolated, and only connected through compliant ±45° plies, albeit as mentioned in Section 4.4.2, damage tolerance is enhanced by positioning the 0° plies inside of the laminate

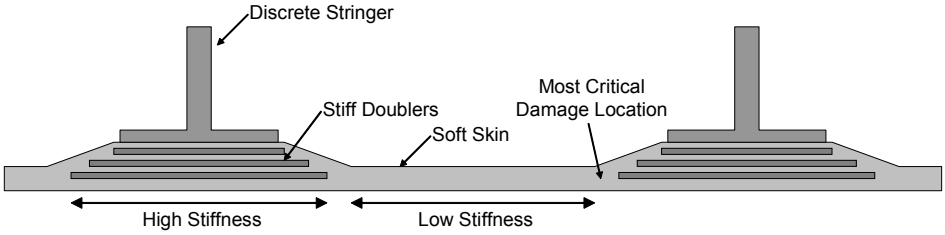

Figure 7-26: Soft skin panel concept

This NASA/Boeing design, after being impacted at between 35J and 50J, both mid-bay and underneath the stringer foot, failed at a strain of -6200με and -7000με, as opposed to -5000με to -5500με for a normal panel[476]. The embankment should be created by a limited number of sub-laminates, as more sub-laminates can cause greater delamination after impact, reducing the ultimate failure load[322].

The Boeing/NASA embankment design[155] was investigated from a stability perspective using ESDUpac A0817. A typical outer wing stringer section was taken with the following details:

- Stringer:
  - Blade: BH = 35mm & BT = 6.256mm
  - Foot: LFW = 50mm & LFT = 2.944mm
  - Laminate (60/30/10)
- Skin:
  - SP = 165mm & ST = 4mm
  - Laminate (44/44/11)

A series of configurations based on this design were investigated, as follows:

- 0° embankment total thickness 6mm
- 45° embankment total thickness 6mm
- 0° smeared into overall skin thickness of 4.57mm
- 45° smeared into overall skin thickness of 4.57mm
- 0° embankment total thickness 8mm

A comparison is shown in Figure 7-27 of the load versus wavelength for the above-mentioned panels. It can be seen that there is a large difference between the conventional panel and the panel with 8mm thick 0° ply embankments, whereas the others are relatively similar. It can also be seen that the main load carrying difference between all the configurations is at a half-wavelength of approximately 240mm, whereas when the buckling mode changes to global from about 500mm onwards, all panels have a very similar performance. The panel's bending stiffness, overall strains and RFs are shown at half-wavelengths of 240mm and 820mm in Table 7-9. As can be seen, at this level of fidelity, the constant thickness panels have a better buckling performance.

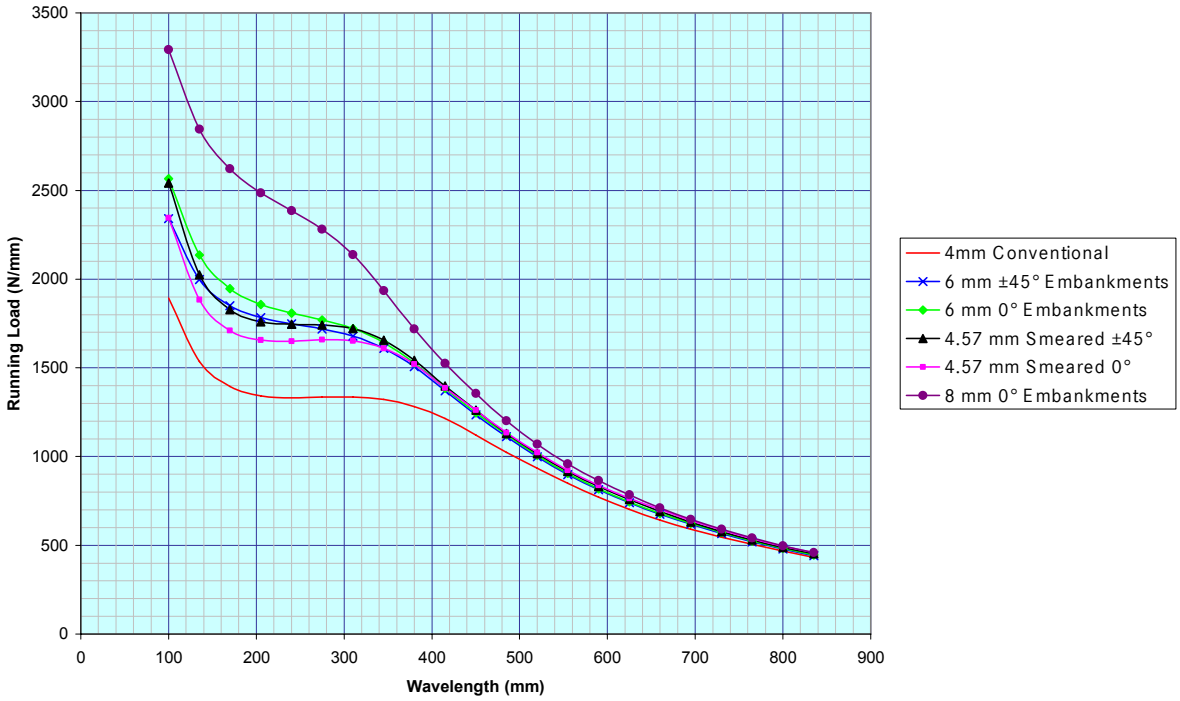

Figure 7-27: P-λ curve comparison of various embankment and smeared thickness configurations

Configuration	Bending Stiffness (GN mm²)	Strain (με)		Reserve Factor	
		240 mm	820 mm	240 mm	820 mm
4 mm Conventional Skin	40.54	2460	888	2.91	0.95
6 mm ±45° Embankments	41.14	3370	882	3.71	0.94
6 mm 0° Embankments	44.24	2890	765	3.86	0.95
4.57 mm ±45° Smeared Skin	41.92	3130	898	3.82	0.99
4.57 mm 0° Smeared Skin	44.24	2560	786	3.61	1.00
8 mm 0° Embankments	46.11	3270	676	5.11	0.98

Table 7-9: Comparison of strains and reserve factors for different configurations for both local and global buckling modes

Although applied to the V22, for the B777 HTP, the embankments have been eliminated, due to the use of toughened resin systems and furthermore they acted like 'speed bumps' for the ATL[477]. Another issue, when applied to wing covers, is that it will result in high amounts of unusable fuel, as the embankments and stringers will act as boundaries. With a normal skin there are passage holes in the stringer blade to allow fuel to flow through, however despite this, due to the height of the holes relative to the skin, some fuel will be unusable. This situation is exacerbated with a stringer integrated on top of an embankment.

Similar concepts to that of the embankment, have been developed by NLR, as shown in Figure 7-28[473], which are purported to be easier to manufacture, whilst maintaining the features of the embankment design, although it is still more complicated to fabricate than a

standard design. Furthermore, due to the simpler IML, it is easier to integrate into the wing box, and with an overall thicker skin in comparison to the embankment design, this will reduce the risk of impact damage between the stringers. Although these designs do not have the increased thickness at the embankment-stringer region, the 0° plies are reinforced by the stringer 0° plies, and these 0° plies are cut off by the soft-skin sub-laminates.

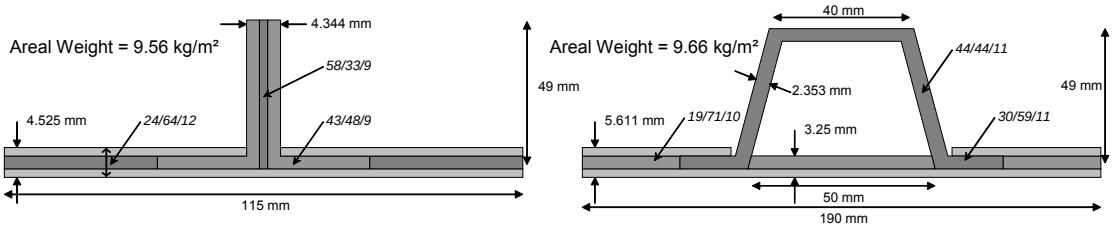

Figure 7-28: So called "Flush Designs" for T-, I- and top-hat-profile stringers

The stringer configurations shown in Figure 7-28 were limited to an allowable strain of -5500με at UL, due to the damage tolerance nature of the design and were sized to react a running load of -2000N/mm. Each design had the following critical constraints[473]:

- T-profile stringer
  - Global buckling load
  - Minimum stringer pitch
- Top-hat-profile stringer
  - Maximum strain
  - Minimum skin width between stringers

From Figure 7-28 it can be seen that due to the damage tolerance constraints, the lightest solution was the T-profile stringer-stiffened panel, despite a top-hat-profile being a more efficient profile under buckling. Physical testing was carried out on the T-profile stringer design shown in Figure 7-28. It was postulated for post-buckling that for the undamaged panels, the discontinuity between the stringer foot and the mid-laminate, could cause a failure mode similar to that from impact damage. This could be somewhat mitigated by lowering the allowable strain limit, but this would lead to an increase in weight, or the stringer foot can be tapered, but this would increase fabrication costs. However, for a wing cover, it is unlikely to advocate post-buckling. A further issue with the discontinuity is the effect this will have on the transfer of shear through the skin.

7.3.4.4 Skin Thickness to Stringer Foot Thickness

The relationship between the stringer foot thickness and skin thickness is important to the panel's overall structural integrity. A thin foot will have greater flexibility, and the pull-off load will peak sharply underneath the blade, and does not disperse much as it tends towards the foot edge, thus failing due to interlaminar tension in the foot to blade elbow region[478]. Whereas, for the thick foot, the stiffness causes pull-off loads to be dispersed to the foot edge, and failure occurs at the edge[450]. Thus thinner feet have lower pull-off potential but higher peel moment capability and hence can be considered to have greater damage tolerance. Once damaged, flexible feet will remain attached to the skin panel after general failure, whereas, very stiff feet may debond from the panel prior to general failure[478].

The peel stresses can be reduced by increasing the bending stiffness of the skin relative to the stringer foot, this is because a flexible foot will attract less load and thus the peel stresses will

be reduced[479]. The difference in interlaminar shear, for a thick (5.3mm) and thin foot (2.65mm), is shown in Figure 7-29[21], where an increase in the stiffness of the foot relative to the skin will increase the maximum shear stresses[479].

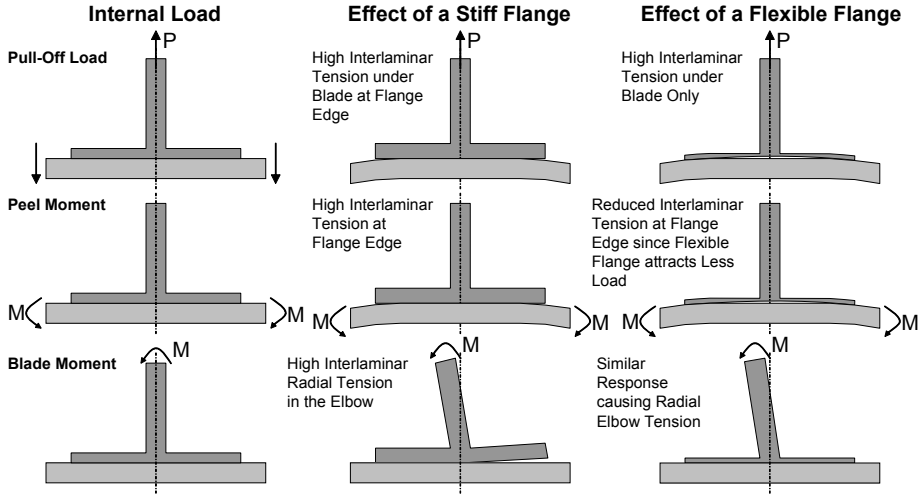

Figure 7-29: Comparison of interlaminar stresses for stiff and flexible lower flanges

The effect of foot thickness on the buckling of a T-profile stringer-stiffened panel was investigated using ESDUpac A0817, for both lightly-loaded and medium-loaded panels. For both panels the skin and stringers had a 44/44/11 and 60/30/10 laminate respectively, with a SP=165 mm, and the following baseline dimensions:

- Lightly-Loaded (N_x=-440N/mm & N_{xy}=194N/mm)
  - Stringer
    - BH=35mm; BT=6.808mm; LFW=50mm
  - Skin
    - ST=4 mm
- Medium-Loaded (N_x=-2580N/mm & N_{xy}=335N/mm)
  - Stringer
    - BH=47mm; BT=6.808mm; LFW=50mm
  - Skin
    - ST=9.75mm

Configuration	Foot Thickness (mm)	RF Improvement	Increase in Area	Specific RF Improvement
Lightly-Loaded	1.7664	1	1	1
	2.9440	0.997	1.052	0.948
	4.1216	1.003	1.104	0.908
	5.2992	1.021	1.157	0.883
	6.4768	1.054	1.209	0.872
	7.6544	1.099	1.261	0.871
Medium-Loaded	2.9440	1	1	1
	4.1216	0.985	1.023	0.963
	5.2992	0.976	1.047	0.933
	6.4768	0.974	1.070	0.911
	7.6544	0.980	1.093	0.896

Table 7-10: Effect of foot thickness on overall performance

The foot thickness was varied, as can be seen in Table 7-10. An increase in foot thickness, hence panel area, caused a reduction in buckling performance for the medium-loaded panels, and for all panels, the specific RF reduced. Thus, the thickness of the foot should be minimised, however, the thickness of the foot should not be too disproportionate to the skin

thickness. For this reason a stringer foot thickness to skin thickness ratio of > than 0.5[176] can be used, as this should help to mitigate against crack propagation.

7.3.5 Skin Laminate Design

The skin performs the following functions:

- Transits the aerodynamic forces to the stringers and ribs by plate and membrane action
- Acts with the stringers to react the tensile loads, but for compressive and shear loads it requires some lateral support from the ribs
- Develops shearing stresses that react the applied torsional moments and shearing forces
- Acts with the ribs in reacting the circumferential load when the structure is pressurised

Wing covers primarily react bending loads, thus the skin laminate will consists of:

- 0° plies to react the axial load (10-55% of total laminate)
- ±45° plies to react the shear load (34-66% of total laminate)
- 90° plies to react bolt bearing, fuel pressure, aerodynamic pressure and transverse loading

Laminates with a high proportion of 0° plies are known as stiff skin designs, which are strain critical, have relatively poor damage tolerance performance, and buckling will occur at a relatively low strain. Alternatively, laminates with a high proportion of ±45° plies, sometimes referred to as 'all bias', have a lower normal stress, hence higher-strain to failure, resulting in a laminate that is less notch-sensitive[307] and has sufficient residual strength after impact to resist failure. As a consequence of the skin's lack of stiffness, the stringers and spar caps will primarily react the principal bending load[395].

The Bell-Boeing V22 Osprey and the BAe Jaguar wing demonstrator[175] used an all bias skin, whereas for a typical high aspect ratio wing, which is required to fly in the transonic speed range, a skin laminate between 44/44/11[21,478] and 50/40/10[456] is a good compromise. This is because structural weight is related primarily to stress rather than strain[157], therefore a laminate with a higher modulus may be able to take a higher stress even though its strain capability is lower. Due to the flutter requirements, which places a limitation on the allowable strain, a skin with a higher axial stiffness is more effective[21]. Furthermore, due to toughened resin systems, it is quite possible that after a certain limited thickness, OHC strength will size the component, and not CAI[155], thus there is no reason to have a principally ±45° laminate. The UD prepreg skin mainly uses 0.25mm thick plies for the following reasons

- Has fairly evenly matched percentages of 0° and ±45° plies, thus desired lay-up is achieved easily with thick plies, while obeying stacking sequence rules
- Skin has typically a large surface and is fairly thick, so thick plies are desirable to reduce deposition time

In terms of the effect of increasing the percentage of 0° plies on the panels buckling characteristics, Nagendra et al. (1991)[306] investigated a series of constant weight T-profile stringer-stiffened panels, as shown in Table 7-11[306], with an applied axial load of -3500N/mm and with 25% shear. It can be seen that the load reacted by the skin improves with a higher

percentage of 0° plies, as the bending stiffness increases, however, the critical local and global buckling loads of the panel remains fairly constant.

Panel	Skin Ply Thickness (mm)		Percentage of 0° Plies	Buckling Load (N/mm)		Skin Load (N/mm)
	0° Plies	45° Plies		Global	Local	Global
1	0.0000	0.59436	0.00	-3816.7	-1432.7	-997.9
2	0.06604	0.56134	5.26	-3824.8	-1419.2	-1185.8
3	0.13208	0.52832	10.53	-3826.7	-1418.9	-1349
4	0.19812	0.4953	15.79	-3812.7	-1384.4	-1484.7
5	0.26416	0.46228	21.05	-3787.8	-1362.7	-1587.4

Table 7-11: Buckling load and skin load variation for change in percentage of 0° plies

The principal direction of the 0° ply is also a very important decision to make, with three possible orientations: parallel to the rear spar; parallel to the front spar; or along the centreline of the cover, which is also typically where the manhole row is. In particular, if an NCF solution was used for the fabrication of the skin, then running the plies parallel to the front spar, or the rear spar if it was straight, could maximise the material utilisation. Another method would be to find the direction of the principal stress vectors, and tailor the 0° plies to follow that.

7.3.6 Stringer Design

The functions of stringers (and spar caps) are as follows:

- Resist bending and axial loads along with the skin
- Carries tensile load, and when supported, compression load
- Divides the skin into smaller segments, which increases the buckling performance
- Transfers aerodynamic loads from the skins to the ribs

The profile of the stringer is a compromise between structural performance and manufacturing issues, such as:

- Strength and stability
- Drainage
- Required space
- Inspectability
- Repairability
- Ease of fabrication
- Removability from mould

The stringer can vary in many ways:

- Profile
- Stringer cross-sectional area
- Stiffness
- Second moment of inertia
- Pitch
- Method of attachment to skin

The stringer can either be discrete or integral, as shown in Figure 7-30, the decision of which will influence both the design and the ease of fabrication. Having an integrated stringer can

increase the fabrication effort and minimise the automation possibilities, reduce the ability to outsource parts, and increase the structural and design optimisation, as they cannot be treated separately.

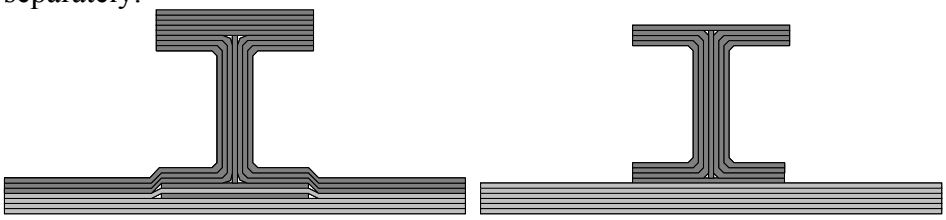

Figure 7-30: Composite panel lay-up geometry for integral and discrete I-profile stringers

Stringers are particularly affected by out-of-plane loads induced by the fuel pressure, which will increase the axial load and hence reduce the structure's overall strength. Therefore, the blade should have sufficient thickness and height to resist the out-of-plane loads, as well as aid bolted repair through the stringer blade. The fuel pressure, in combination with some other out-of-plane load, can be enough to cause interlaminar tension stresses in the bond line[21], thus cleats attached to the stringer blades, for example, should be avoided. However, cleats or intercostals can be used to increase the buckling strength of the blade.

Stringers with higher bending stiffness can resist lateral loading better[464], resulting in a reduction in strain along the stringer top edge, such as an I-profile stringer with its upper flange, or similarly a T-profile stringer with a bulb. I-beams provide nearly all the bending resistance through the flanges, whereas the through-the-thickness shear resistance is reacted by the web[480].

There may be a maximum dimension imposed on the length of the stringer due to manufacturing limitations, and thus the stringers will require a splice to join them. These splices should ideally be located at the ribs[468].

7.3.6.1 Stringer Profile

Shown in Figure 7-31 to Figure 7-35, are typical stringer profiles, ranging from the integrated blade to the top-hat-profile stringer. These figures also demonstrate their integration with castellated ribs. For a given load and application, each stringer will have their relative merits to each other. Stringers that are open-profile are usually easier to inspect and fabricate, but have lower stability efficiency, particularly under compression, in comparison to closed-profile stringers, such as a top-hat-profile stringer[481,482,483].

However, when every aspect is considered, a T-profile stringer offers the best compromise from cost and weight perspective[21], followed by I-profile stringers. Furthermore, despite a top-hat-profile stringer panel having typically a lower cross-sectional area, this will mean that the strain is higher under the same load. Therefore, it is possible that the applied strains will be greater than the allowables strains, thus extra area has to be added in any case. A further issue to consider is the influence the stringer profile has on the rib, particularly if a rib castellation design is used. The castellation in the rib is required to ensure that the rib can be attached directly to the skin, which is probably the most efficient method of transferring the shear due to the wing box torsion. Therefore, the profile and size of the stringer will determine the required castellation size in the rib, which will influence the rib weight; with a larger castellation resulting in a heavier rib due to the required reinforcement.

Stringers, used to stiffen wing skins, are typically symmetric; as asymmetric stringers, such as a Z- or J-profile incur an interaction in buckling modes, with both the translation of the cross-section as well a twist in the stringer, which is known as coupled flexural-twisting, resulting in a lower flexural buckling stress. Closed-profile stringers, have typically higher torsional stiffness, thus they do not suffer from twisting. Furthermore, it is known that open-profile stringers exhibit stringer roll and modal interaction at a lower load level than for a closed-profile stringer[482]. A symmetric open-profile like a T-profile stringer, will have the web placed in the middle of the foot and not at the foot edge, as with a Z-profile stringer, which improves the foot crippling strength, for an equivalent foot width, as the unsupported foot length is half that for the T- than the Z-profile stringer, resulting in a thinner foot for the T-profile stringer[484]. Closed-profile stringers have not been widely used due to their voluminous encroachment on fuel space as well as inspection issues.

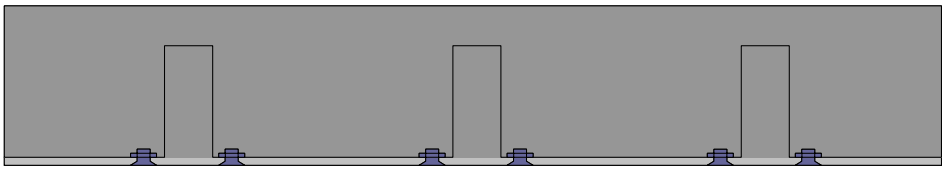

Figure 7-31: Rib integration for U-profile stringer

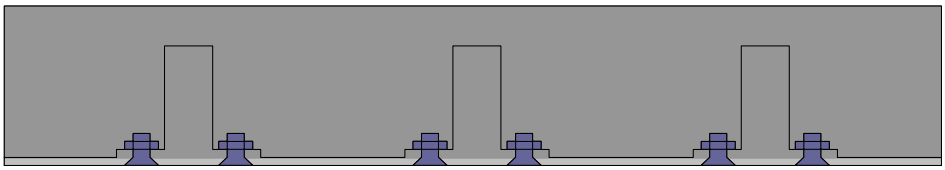

Figure 7-32: Rib integration for discrete T-profile stringer

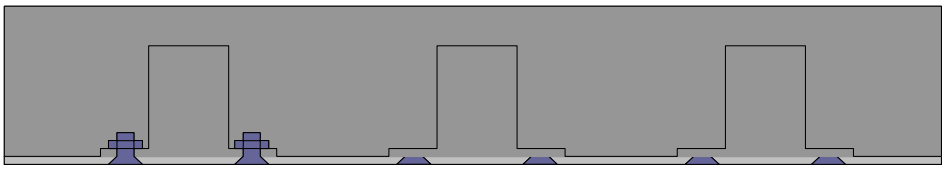

Figure 7-33: Rib integration for discrete I-profile stringer

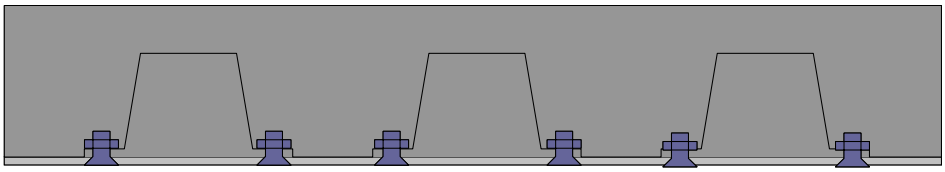

Figure 7-34: Rib integration for top-hat-profile stringer

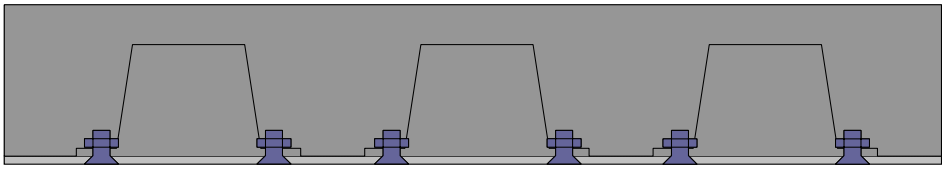

Figure 7-35: Rib integration for top-hat-profile stringer with clearance

7.3.6.1.1 Stringer Profile Down-Selection Example

The initial part of the NASA ACT program investigated a CFRP conversion of the Lockheed C-130 CWB, called the Technology Integration Box Beam. There were three stringer configurations considered for the wing covers, as shown in Figure 7-36[155]. The T-profile stringer-stiffened cover was based on a simplistic manufacturing solution, with pultruded

stringers, which were co-cured to a uniform thickness skin, with a high percentage of ±45° plies due to the non-toughened resin system. The J-profile stringer design had under each stringer a locally thickened skin, with a 0° dominated laminate, which provided superior bending stiffness relative to the conventional T-profile stringer. The top-hat-profile stringer-stiffened cover used high modulus material, in the upper flange and in the skin local to the stringer, to achieve the necessary bending stiffness for buckling. Due to manufacturing limitations, the top-hat-profile stringer was foam filled, to avoid the need for a mandrel to form the stringers. The J-profile stringer-stiffened panel was the lightest, with the T-profile stringer and the top-hat-profile stringer design being heavier, by a factor of 1.08 and 1.37, respectively[155]. It was, however, later realised that when the weight of the cleats and fuel sealing clips were considered, in order to integrate the cover into the wing box, the relative weight factor in comparison to the T-profile stringer panel was only 1.02, and when manufacturability and subsequent assembly was considered the T-profile stringer panel was the most favourable.

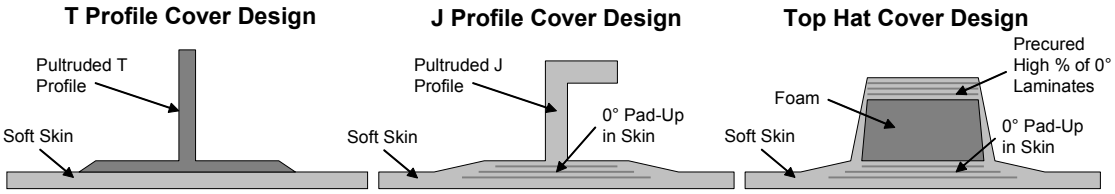

Figure 7-36: Cover designs

7.3.6.1.2 Most Efficient Stringer Profile under Compression Load

Using ESDUpac A0301, different optimised stringer profiles were developed, for a range of running loads, as shown in Figure 7-37 and Figure 7-38, for a stringer pitch of 160mm and 240mm, respectively.

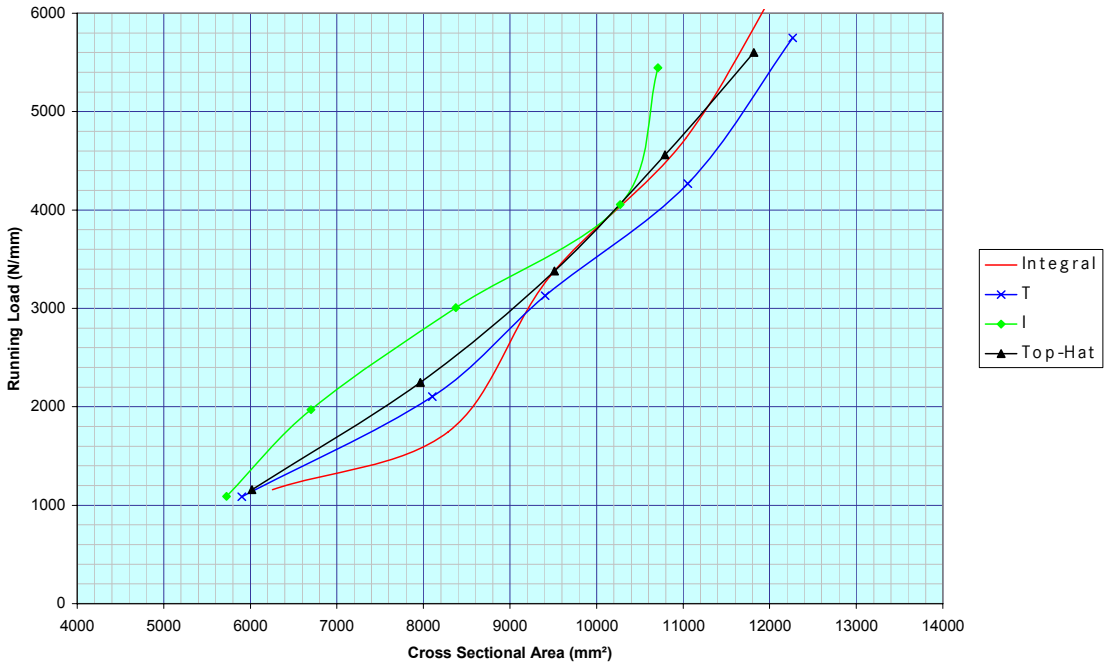

Figure 7-37: Comparison of stringer profiles under axial load for a stringer pitch of 160mm

Using simply-supported conditions along the length of the panel, with constraints on the minimum thicknesses, it was found that the I-profile stringer was the most efficient. However,

these two figures do not consider the limit on allowable strain, which would mean under higher loads, those panels with lower cross sectional area could have an applied strain higher than the allowable strain.

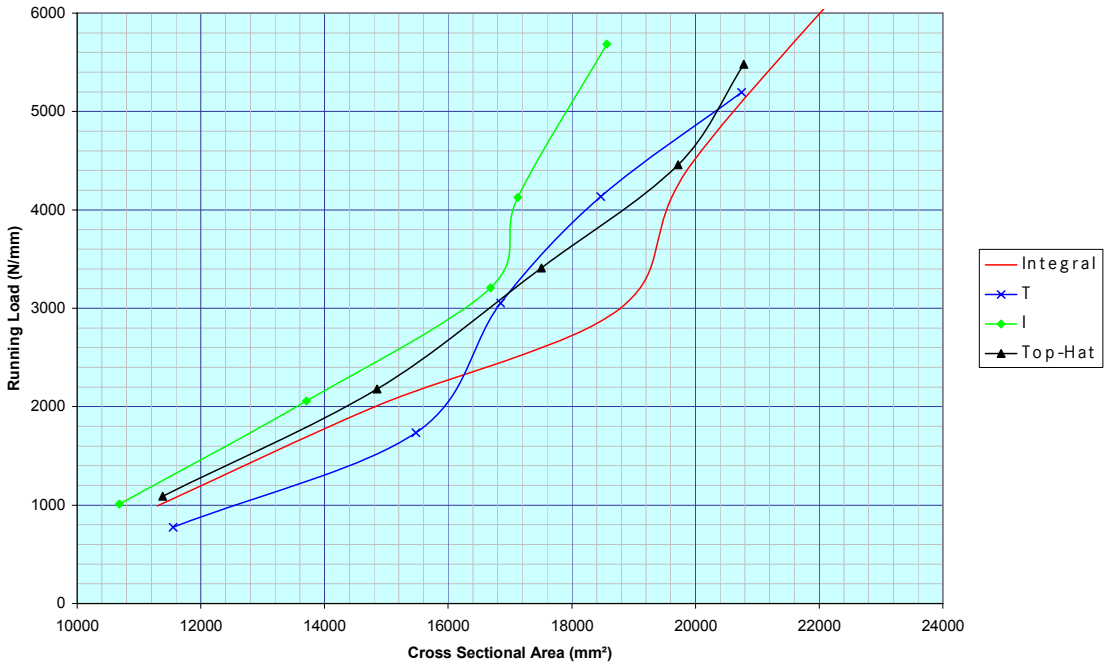

Figure 7-38: Comparison of stringer profiles under axial load for a stringer pitch of 240mm

7.3.6.2 Integral versus Discrete Stringer

The reason for the theoretical greater efficiency of an integral stringer without an attachment flange, in comparison to a discrete stringer with a foot, can be explained by referring to Equation 7-1, which gives the load (N) in the upper and lower covers:

$$N = \frac{M}{b \times h'} \qquad \textbf{7-1}$$

Where ‘h’’ is the distance from the wing box neutral axis to the centre of gravity of the stiffened panel, and ‘M’ is the applied bending moment. Looking at Figure 7-39, it can be seen that the distance h’ for the T-profile stringer is greater than for the U-profile stringer. This means, when everything else is kept the same, then the load per unit length N decreases for the T-profile stringer panel, hence it is less efficient.

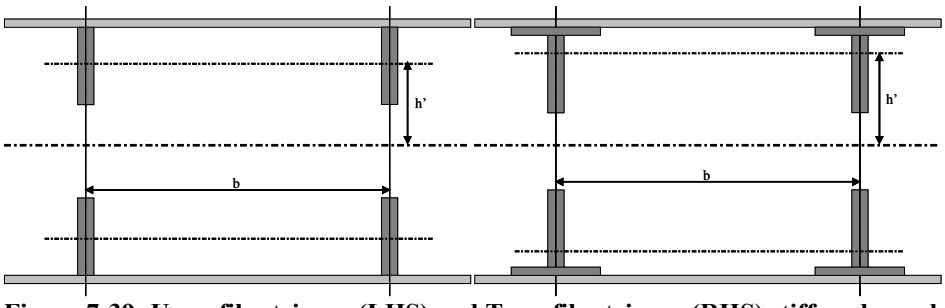

Figure 7-39: U-profile stringer (LHS) and T-profile stringer (RHS) stiffened panel comparison

Furthermore, for a panel driven by strength, the second moment of inertia should be as close to the skin as possible, whereas for buckling the second moment of inertia should be as far away from the skin. Thus, for a T-profile stringer to have the equivalent inertia of a pure blade, then the stringer section must be more substantial. The U-profile stringer configuration can also offer a number of other practical advantages over a discrete stringer-stiffened panel, such as:

- Despite the discrete stringer being bonded to the skin, additional bolting is still required to halt and redistribute load should a debond occur
    - Even if the parts are co-cured it could logically still be considered a discrete stringer[339]
- There are no edge distance problems
    - This can be hugely beneficial at the root joint area
    - No need for grow outs along stringer foot for bolting the ribs to the cover
    - This could then allow a smaller stringer pitch to aid weight reduction for stability driven structures
- Tolerance issues, in particular for thickness, is reduced, which is critical when rib integration is considered
- Minimises unusable fuel, as there is no extra foot

7.3.6.3 U-Profile Stringer Particularities

Co-curing, or co-infusing with an LCM technique, is the only feasible process for a U-profile stringer design. A hard skin with soft stringers could be envisaged but ensuring a good bond is an issue, due to the size of the bonding area. Another issue is that as the stringer constitutes part of the skin, thus curing the skin by itself will mean that the skin laminate is asymmetric, which will cause it to distort during the thermal curing process.

Due to the integral nature of the U-profile stringer panel, as shown in Figure 7-40, the upper skin laminate is both part of the skin and stringer. Furthermore, to respect overall laminate symmetry where there is pure skin, it is necessary for the upper and lower skin laminates to have the same thickness and laminate stacking sequence. The thickness can be varied, either by amending the upper and lower skin laminates, or the mid-skin laminate. It is known that the upper skin laminate should be minimised so that it can be formed into a U-channel, therefore the mid-skin laminate can be relatively thick in comparison to the upper and lower skin laminates. By increasing the thickness of the mid laminate, and not the upper and lower laminates, finer changes in thickness can be accomplished as extra plies can be added to the mid-plane. In terms of shear loading of the panel, due to the discontinuity of the upper skin laminate, in particular in areas of SROs, as shown in Figure 7-41, the shear load can only flow through the lower and mid laminates, therefore this total thickness has to be adequate to take this load.

U-profile stringers are usually applied on parts such as flaps and CWB covers, as they are rectangular in shape, and therefore SROs only occur at the extremities of the covers span. However, a LWB has a tapered planform, thus SROs occur at regular positions along the span, such as shown in Figure 7-41. Due to the issue of the upper skin laminate forming part of the stringer, this leads to a discontinuity in terms of a gap, as shown in the section-cut A-A of Figure 7-41. This can be filled with a suitable roving to ensure that the area does not become accumulated with only resin, and a local doubler can be applied, if required, to reinforce this area.

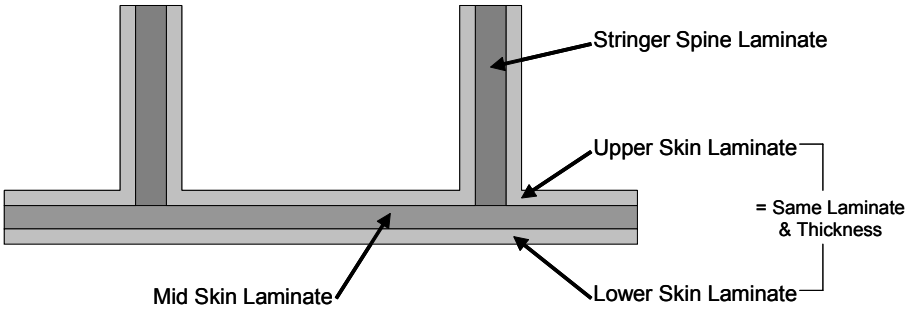

Figure 7-40: U-profile stringer panel laminate constitution

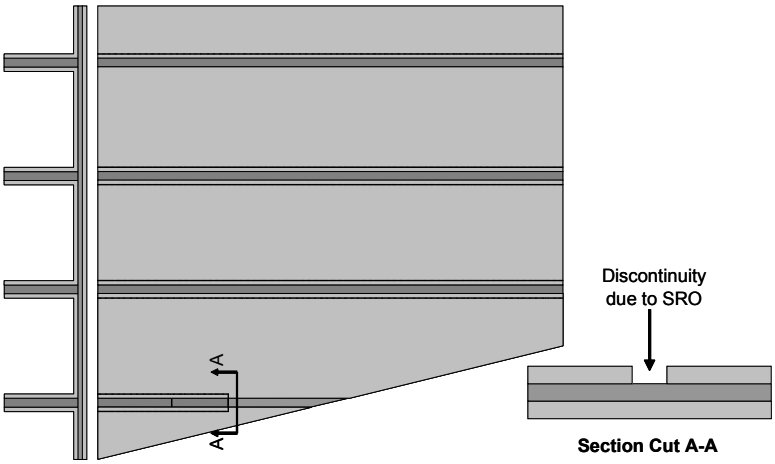

Figure 7-41: Discontinuity in upper-portion of skin laminate due to SRO

7.3.6.3.1 U-Profile Stringer Skin Thickness Proportioning

In order to set the boundaries for optimising a U-profile stringer-stiffened panel, it is necessary to understand how much of the skin's total thickness can be used to form part of the stringer web, this is because the skin carries a proportion of the axial load and all of the shear load, therefore any discontinuity in thickness can be critical. In order to establish the limit, three different laminates were considered, namely 10/80/10, 30/60/10, and 50/40/10.

The strength characteristics were considered with varying amounts of thickness in the U-channel and the amount of shear as a percentage of the applied axial load. Three different thicknesses were considered, with the results shown in Figure 7-42 to Figure 7-47. In order to calculate the panels strength, ESDUpac A8418[310] was deployed, using the strength allowables from Appendix B. The initial tensile and compressive strength axial running loads reacted by the pure laminates, with 0% shear and 100% of the total thicknesses, were:

- 10/80/10
  - 4 mm (N_x =2200 & -1690N/mm)
  - 8 mm (N_x =4276 & -3430N/mm)
  - 12 mm (N_x =5010 & -4460N/mm)
- 30/60/10
  - 4 mm (N_x =4965 & -3016N/mm)
  - 8 mm (N_x =8770 & -5465N/mm)
  - 12 mm (N_x =12491 & -7865N/mm)

- 50/40/10
  - 4 mm (N_x =6360 & -3710N/mm)
  - 8 mm (N_x =12800 & -7465N/mm)
  - 12 mm (N_x =17870 & -10541N/mm)

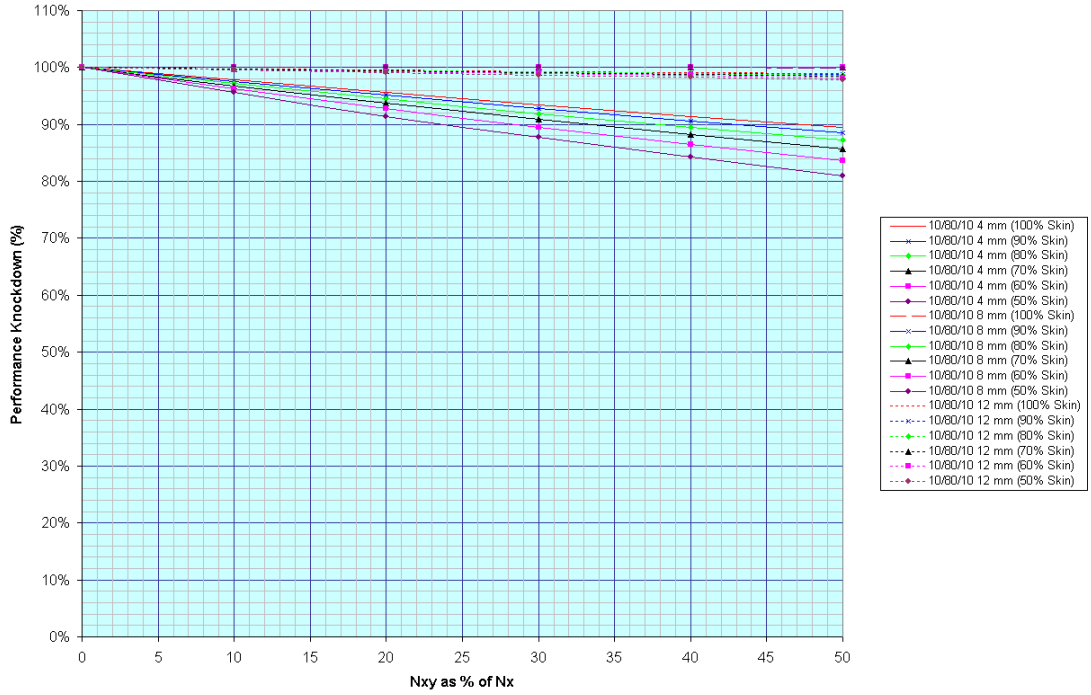

Figure 7-42: Tensile 10/80/10 laminate

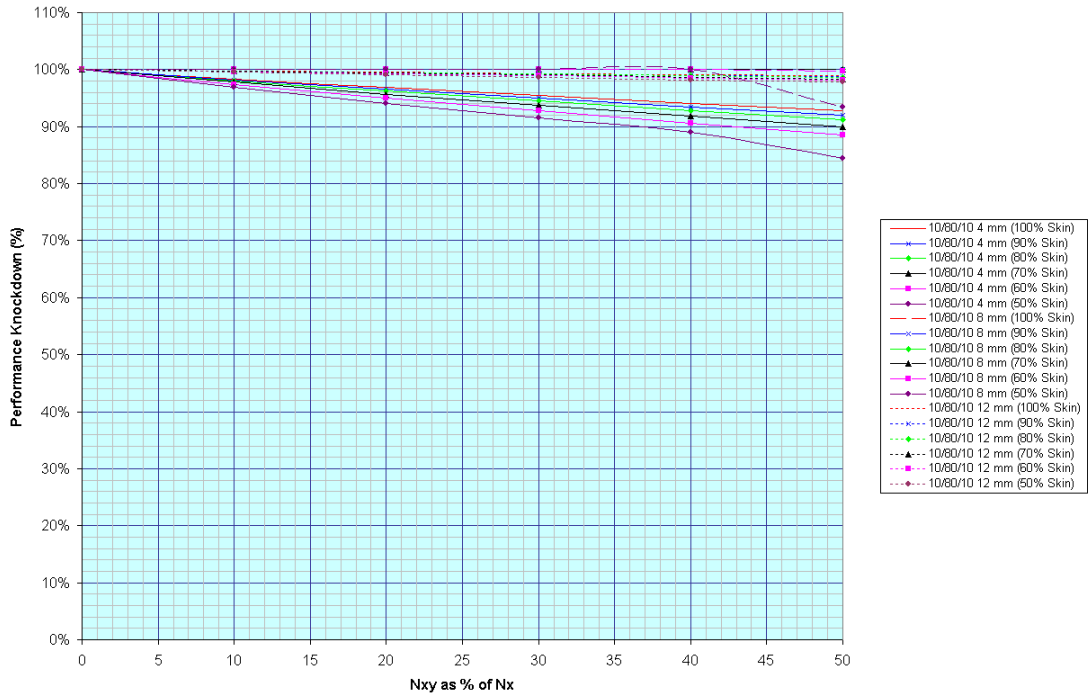

Figure 7-43: Compressive 10/80/10 laminate

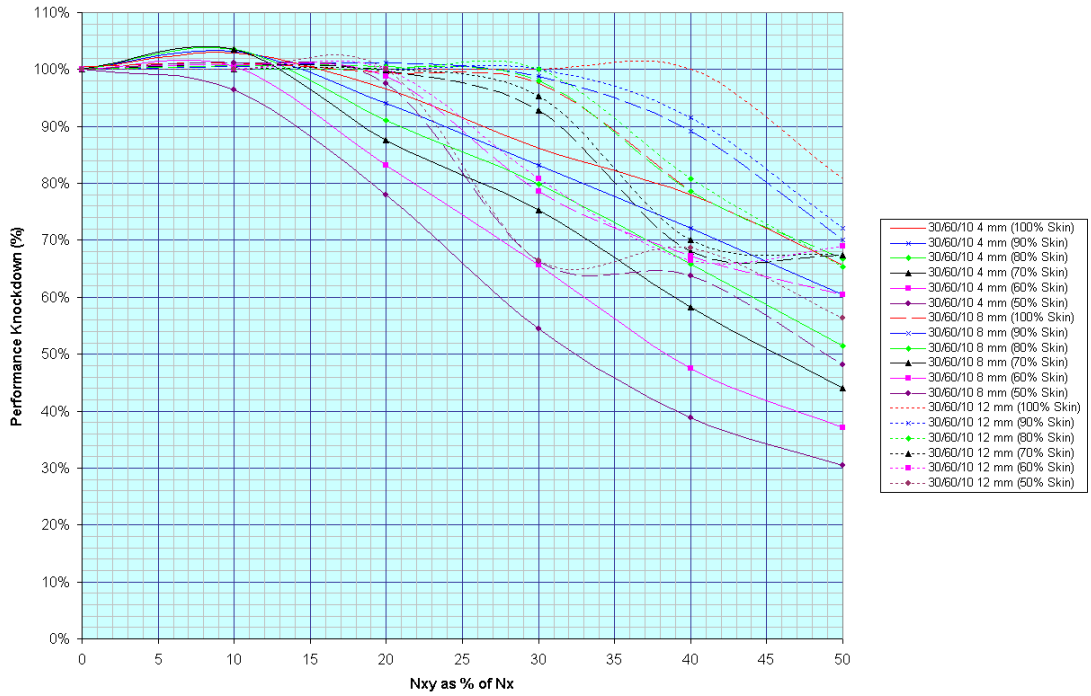

Figure 7-44: Tensile 30/60/10 laminate

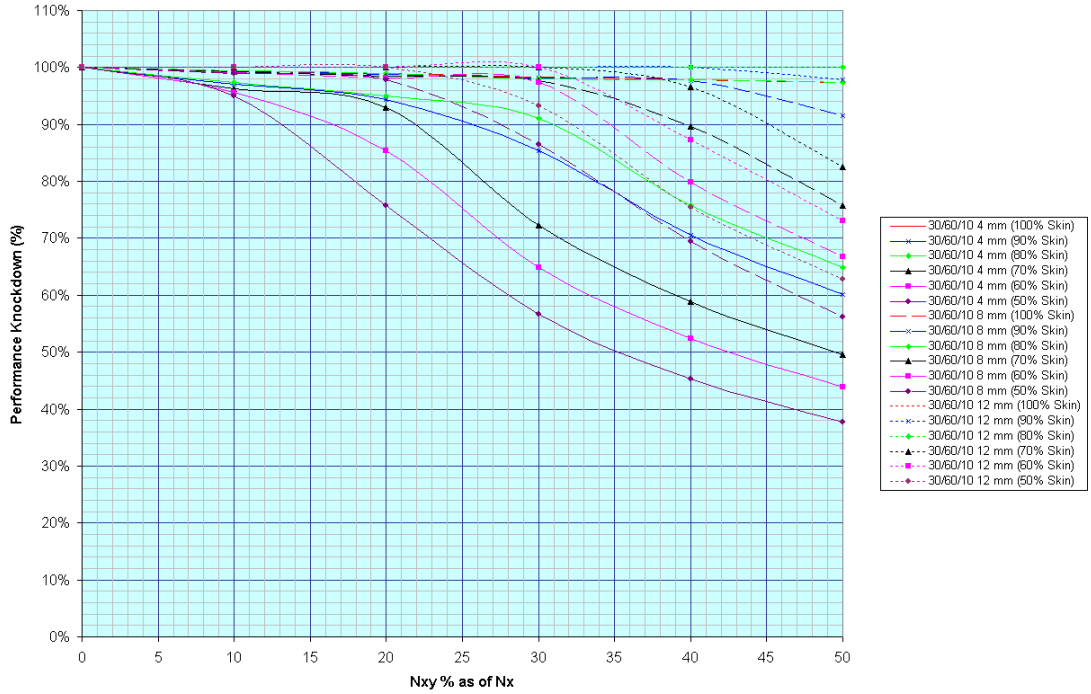

Figure 7-45: Compressive 30/60/10 laminate

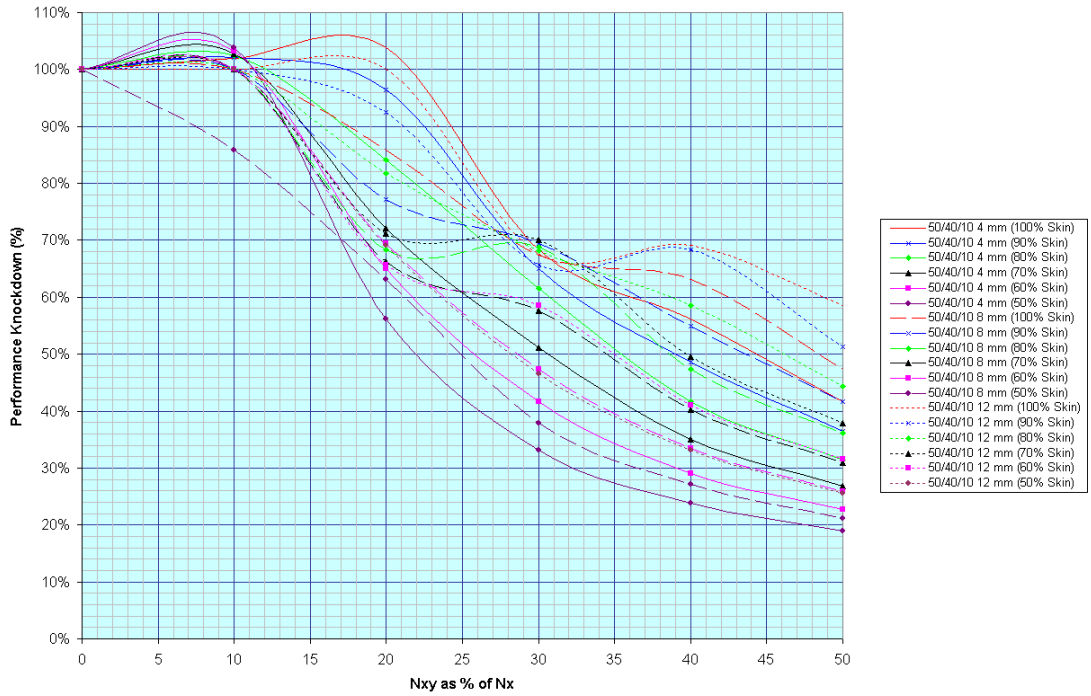

Figure 7-46: Tensile 50/40/10 laminate

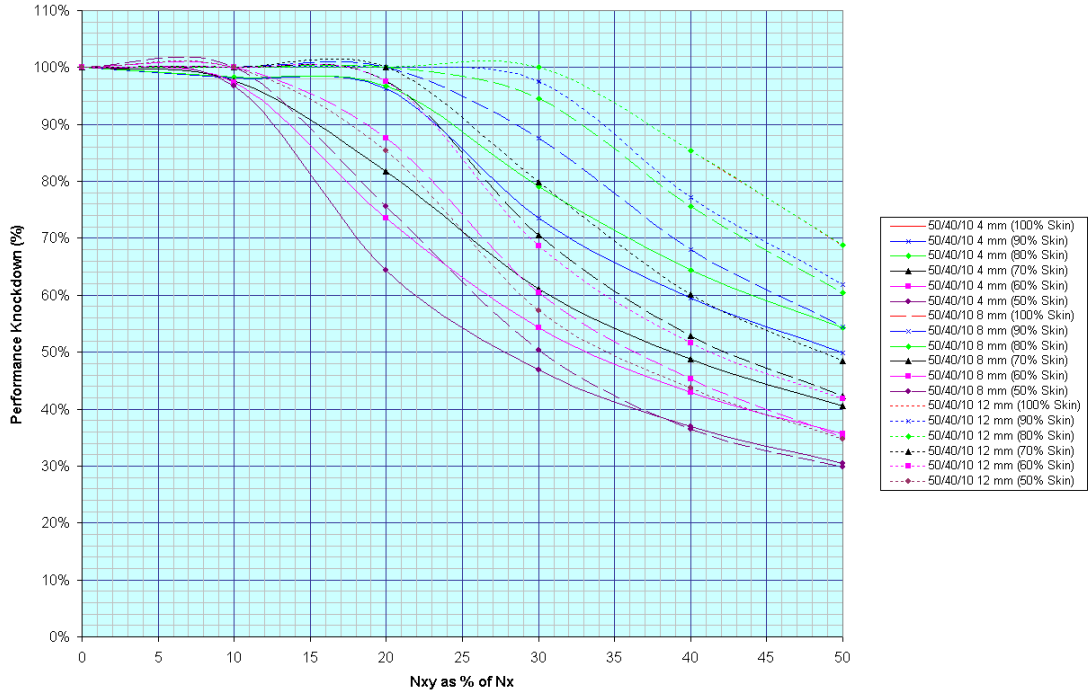

Figure 7-47: Compressive 50/40/10 laminate

The knockdown in the tensile and compressive performance of a 10/80/10 laminate is shown in Figure 7-42 and Figure 7-43. Due to the low axial strength of the laminate, but the high shear strength, the influence of increasing the amount of shear and reducing the amount of skin thickness that can react the shear load has limited effect, resulting in a maximum knockdown factor (KDF) of roughly 0.8 for tensile and 0.84 for compressive, whereas the KDF in performance due to FHT and OHC for a 10/80/10 laminate is 0.6 and 0.65 respectively. Therefore, the proportioning of the skin between the skin and the stringer web for a 10/80/10 skin laminate is not a structural consideration, but instead influenced by design

and manufacturing constraints. Figure 7-44 and Figure 7-45 shows the performance KDF for a 30/60/10 laminate for both tension and compression, respectively. For a 30/60/10 laminate the KDF due to FHT and OHC are 0.5 and 0.6 respectively, therefore a maximum of 30% of the total laminate should be used as part of the stringer web, so that the proportioning of the skin does not become the limiting factor. For a 50/40/10 laminate, the performance KDF under tensile and compressive load is shown in Figure 7-46 and Figure 7-47, respectively. For a 50/40/10 laminate the KDF due to FHT and OHC are 0.4 and 0.55 respectively, hence again a maximum of 30% of the skin laminate should be used to form the stringer web.

7.3.6.3.2 Maximising the U-Profile Stringer's Axial Stiffness

As the stringers need high axial stiffness, it is necessary to maximise the proportion of 0° plies in the total blade. However, if part of the skin laminate is being used to form the angles of the stringer web, then the stringer laminate is partly dependent on the skin laminate. Based on a ratio that the spine thickness can be 2.4 times the thickness of the angle, and that the angle is 30% of the skin thickness, this ensures that the spine thickness is not too great in comparison to the supporting angles. It also enables the total blade thickness to be up to 1.32 ([0.3×ST×2]+[0.3×ST×2.4]) the thickness of the skin, which gives the panel enough optimisation flexibility, as typically the blade thickness is greater than the skin thickness. Three different laminates were investigated, as shown in Table 7-12, namely 50/40/10, 30/60/10 and 10/80/10, with different thicknesses representative for a wing skin. It can be seen that the angles have approximately the same laminate as the skin, as would be expected.

Total Skin Thickness (mm)	Number of 0.25 mm Thick Plies to Constitute 30% of Total Thickness (limit due to strength)	% of 0°/±45°/90° in Angles		
		50/40/10	30/60/10	10/80/10
3	3	0/66/34	0/66/34	0/100/0
7	8	50/38/12	38/50/12	12/76/12
11	13	46/38/16	31/61/8	8/77/15
15	18	50/39/11	33/56/11	22/77/11
19	22	50/41/9	32/59/9	9/82/9

Table 7-12: Laminate constitution in angles for blade for 3 different skin laminates

Total Skin Thickness (mm)	50/40/10	30/60/10	10/80/10
3	22/52/26	22/52/26	21/69/10
7	52/34/14	47/40/13	35/51/14
11	52/35/13	45/46/9	35/53/12
15	55/35/10	47/42/11	37/52/11
19	54/36/10	46/44/10	36/54/10

Table 7-13: Achievable holistic blade laminate with 0.184 mm 60/30/10 spine

Total Skin Thickness (mm)	50/40/10	30/60/10	10/80/10
3	17/55/28	17/55/28	17/71/12
7	55/35/10	50/40/10	38/52/10
11	56/32/12	49/42/9	38/49/13
15	59/31/10	51/39/10	41/48/11
19	59/31/9	51/39/10	40/50/10

Table 7-14: Achievable holistic blade laminate with 0.25 mm for 0° plies and 0.184 mm for ±45° and 90° plies

However, the target laminate for the total blade should be approximately 60/30/10, thus the spine should have as high a proportion of 0° plies as possible, while respecting the stacking sequence guidelines. A comparison has been conducted using a conventional 60/30/10 spine with 0.184mm thick plies for all orientations, and a targeted 70/20/10 laminate using a 0.25mm thick ply for the 0° ply and 0.184 mm for the off axis plies. Remembering that the

skin laminate and hence the angles use 0.25 mm thick plies, then the resultant blade laminates obtained, are shown in Table 7-13 and Table 7-14.

From Table 7-13 the 50/40/10 skin laminate with a skin thickness of 7mm can obtain a fairly stiff stringer laminate with over 50% 0° plies, however this is improved with Table 7-14 with the 11mm laminate having almost a 60/30/10 laminate. The 30/60/10, improves somewhat the amount of 0° plies in the blade, in particular with the 0.25mm 0° plies; whereas 10/80/10 never reaches a high proportion of 0° i.e. there are always more ±45° plies.

In order to improve the amount of 0° plies in the blade still further for the 30/60/10 and 10/80/10 skin laminates, the laminates' stacking sequence can be amended to maximise the amount of 0° plies in the outermost 30% of the laminate. Shown below is an example for a 19mm laminate, where the laminate enclosed in parentheses () identifies the part of it that has been amended:

- For 10/80/10
  - Original
    - $[(+/-/+/90/-/0/+/-/+/-/90/+/-/0/+/-/+/-/+/-/+/-)/90/+/0/-/+/-/+/-/+/-/+/90/-/0/+/-]_s$
  - New
    - $[(+/-/+/90/-/0/+/0/-/0/+/0/-/90/+/-/+/-/+/-/+/-)/+/-/90/+/-/+/-/+/-/+/-/+/-/90/+/-]_s$

- For 30/60/10
  - Original
    - $[(+/-/90/0/0/+/-/0/+/-/0/+/-/90/0/+/-/0/+/-/0/+)/-/90/+/-/0/+/-/0/+/-/0/+/-/90/0/+]_s$
  - New
    - $[(+/-/90/0/0/+/0/0/-/0/0/+/90/-/0/0/+/0/0/-/0/+)/-/90/+/-/+/-/+/-/+/-/+/-/+/-/90/+]_s$

This results in the following blade laminates:

- 10/80/10
  - Original
    - Pure 0.184mm for all orientations = 36/54/10
    - 0.25 mm for 0°, all other 0.184 mm = 40/50/10
  - New
    - Pure 0.184mm for all orientations = 40/50/10
    - 0.25 mm for 0°, all other 0.184 mm = 44/46/9
- 30/60/10
  - Original
    - Pure 0.184mm for all orientations = 46/44/10
    - 0.25 mm for 0°, all other 0.184 mm = 54/36/10
  - New
    - Pure 0.184mm for all orientations = 51/39/10
    - 0.25 mm for 0°, all other 0.184 mm = 59/31/10

Thus, by doing this, the axial stiffness of both the 10/80/10 and the 30/60/10 skin are improved, however, the 10/80/10 is still some way off the target of a 60/30/10 stringer. By increasing the proportion of 0° plies towards the outside of the laminate, this will decrease

both the damage tolerance and stability performance of the skin, thus negating any benefit of using a softer skin. Therefore, such an approach is not beneficial.

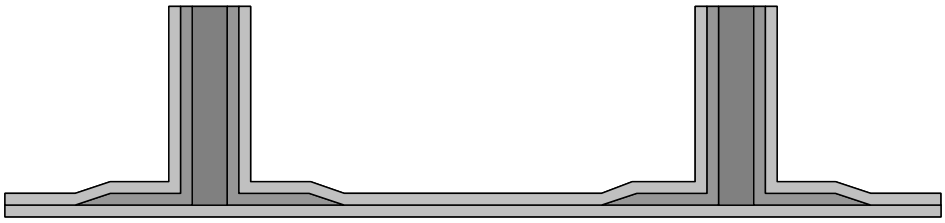

Figure 7-48: U-profile stringer concept

Another approach to resolving this issue is to use an intermediate angle, as shown in Figure 7-48. Not only can this be used to improve the amount of 0° plies in the overall stringer blade, it can also improve the damage tolerance of the design. Furthermore, it minimises the amount of skin laminate needed to create the angle, which is good from a strength perspective, allows better draping, and could be more beneficial for thinner sections. However, shear flow through the skin would be an even greater consideration, as only the lower part of the skin is continuous.

7.3.6.4 Top-Hat Particularities

The width of the top-hat upper flange can vary in width over a large range with little effect on the structural efficiency[485], and can thus be exploited for design or manufacturing reasons. Due to the interaction of shear flow between the skin and the stringer for a given weight, by increasing the compressive stiffness, this will cause a knockdown in the shear stiffness, as the extensional stiffness is increased with a greater proportion of 0° plies, whereas the shear stiffness is increased with a greater proportion of ±45° plies[485]. Furthermore, the weight increase is more substantial for increasing the shear stiffness than it is for the extensional stiffness[485]. A further observation is that the pitch of the stringer (in this case the space without an enclosed area above it) has a larger effect on the weight, than the width of the top element.

Due to the closed-profile nature of a top-hat-profile stringer, it can be used as a vent passage on the upper cover, thus the part has a dual purpose. Furthermore, as the structure is CFRP, the corrosion issues that have blighted such a dual-purpose design on aluminium wing covers, is removed. However, a vent pipe requires a minimum area, which has to run almost the whole span of the wing cover. Regardless of the overall fuel tank volume, it will be assumed that the vent pipe has to have a cross-sectional area of 4500mm². Based purely on the structural requirements, the enclosed area of the top-hat-profile stringer, inboard, may be sufficient, however toward the mid-span and further, the volume will decrease, which may be insufficient for venting. There are two choices; either using two top-hat-profile stringers to act as the vent stringers, which may complicate the fuel system architecture, or have a non-structurally optimised top-hat-profile stringer, for the sake of the fuel system.

For a top-hat-profile stringer it is important that the foot attachment to the skin not only has the outwardly formed foot, but there is also some reinforcement on the inside of the closed profile, as shown in the RHS of Figure 7-49. This is because this radius from the web to the skin is critical for the strength of the stringer, particularly when the upper flange has high stiffness or the stringer webs are tall. Therefore, it is necessary to have some kind of inner stiffness to this radius.

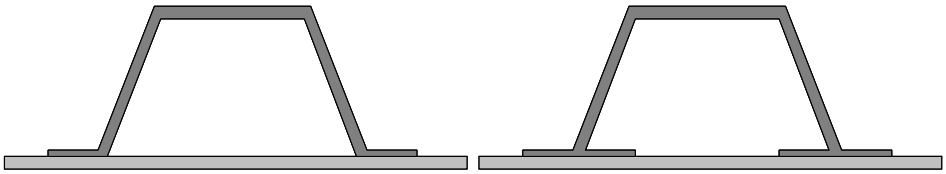

Figure 7-49: Conventional discrete (LHS) and damage tolerant top-hat-profile stringer (RHS)

7.3.6.4.1 Overall Laminate for Top-Hat-Profile Stringers

Top-hat-profile stringers applicable to both inboard and outboard positions were investigated with the following dimensions:

- Lightly-Loaded
  - Stringer
    - Lower flange (LFW=20mm; LFT=1.5mm)
    - Web (SH=40mm; WT=2.0mm)
    - Upper flange (UFW=39mm; UFT=2.0mm)
    - Pitch between webs =60mm
  - Skin
    - ST=4.0mm, SP=160mm
- Heavily-Loaded
  - Stringer
    - Lower Flange (LFW=28mm; LFT=3.0mm)
    - Web (SH=70mm; WT=4.0mm)
    - Upper Flange (UFW=51mm; UFT=4.0mm)
    - Pitch between webs =73mm
  - Skin
    - ST=10.0mm, SP=240mm

	Inboard		Outboard	
Load Case	Nx (N/mm)	Nxy (N/mm)	Nx (N/mm)	Nxy (N/mm)
1	-4600	0	-900	0
2	-4600	1150	-900	225
3	-4600	2300	-900	450
4	-4600	3450	-900	675
5	-4600	4600	-900	900
6	0	4600	0	900

Table 7-15: Load cases for inboard and outboard positions

Stringer Laminate	60/30/10			
Skin Laminate	50/40/10		10/80/10	
Performance	Reserve Factor		Reserve Factor	
Load Case	Inb.	Out.	Inb.	Out.
1	0.94	1.09	0.85	0.95
2	0.86	0.95	0.78	0.84
3	0.64	0.69	0.61	0.65
4	0.49	0.53	0.48	0.51
5	0.40	0.42	0.40	0.42
6	0.51	0.53	0.53	0.54

Table 7-16: RF's for baseline 60/30/10 stringer laminate with hard and soft skin for different load cases

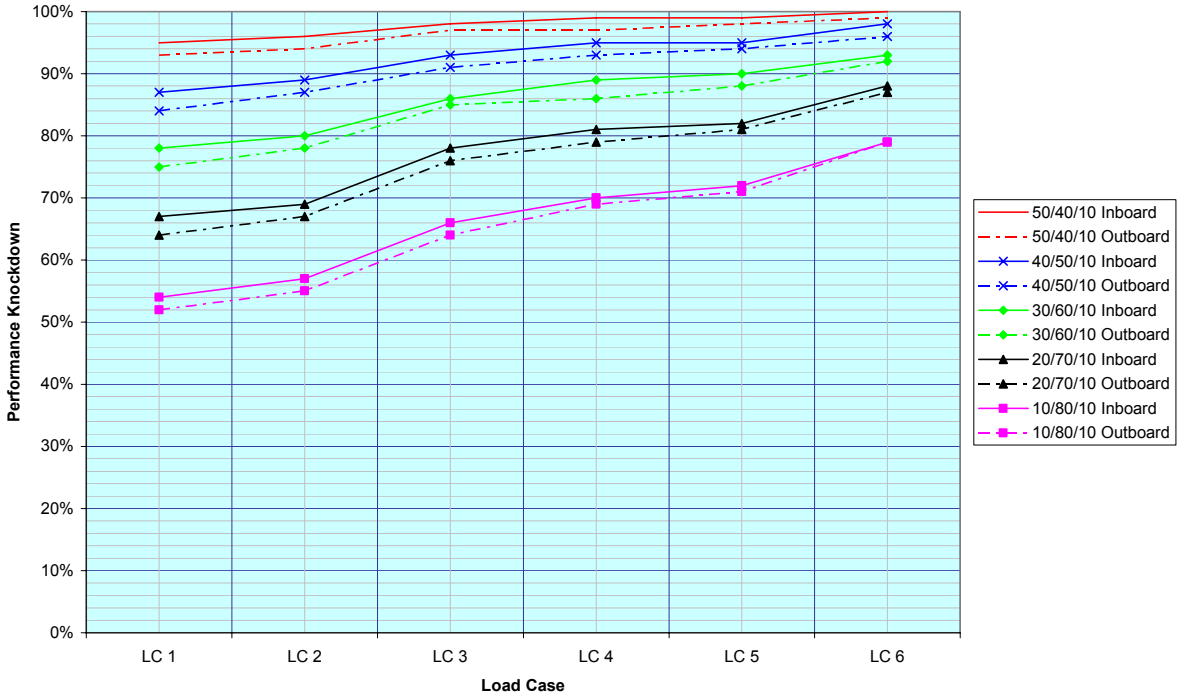

Figure 7-50: Knockdown in performance for 50/40/10 skin laminate with different stringer laminates

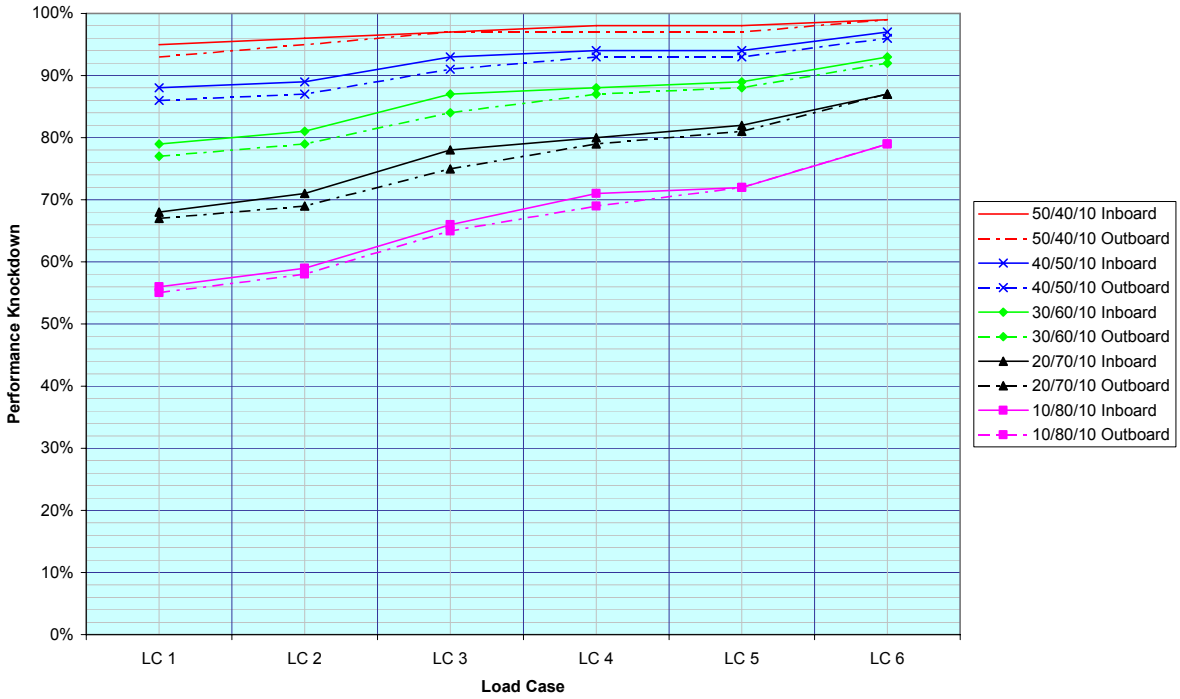

Figure 7-51: Knockdown in performance for 10/80/10 skin laminate with different stringer laminates

The load cases for the stringer are shown in Table 7-15, where 'Load Case 1' is a pure axial load, whereas 'Load Case 6' is a pure shear load. The laminates of the stringers varied from an axially stiff 60/30/10 laminate to a softer 10/80/10, in increments of 10% in terms of the percentage of 0° plies. The skin laminate was either 50/40/10 or 10/80/10, as shown in Table 7-16, with the actual RF's for the different load cases.

Stringer-stiffened panels with a 50/40/10 and 10/80/10 skin laminate are shown in Figure 7-50 and Figure 7-51, respectively. These figures illustrate the performance knockdown due to changing the stringer laminate, relative to the 60/30/10 baseline stringer laminate. Comparing the panel with a 50/40/10 and a 10/80/10 skin laminate in Table 7-16, it can be seen that when the load is primarily axial, a 50/40/10 laminate has a higher performance, whereas for increasing shear this advantage is diminished in particular with pure shear, where a 10/80/10 laminate is preferable. This trend also occurs with the stringers as shown in Figure 7-50 and Figure 7-51. The 60/30/10 stringers, in general, have the higher performance, regardless of the load case, however with increasing shear the advantage of a 60/30/10 is slightly diminished. Although, in conclusion, the stiffer 60/30/10 stringers provide the highest stiffness to the skin and hence a 60/30/10 stringer would, overall, seem optimum.

7.3.6.4.2 Change in Top-Hat Upper Flange Width

Shown in Table 7-17 is the increase in performance of the overall panel if the width of the upper flange is changed. For the lightly-loaded panel, the upper flange width was increased and decreased by 10mm, whereas for the heavily-loaded panel the upper flange width was increased and decreased by 20mm. It is clear to see that by increasing the width, and hence decreasing the angle of the vertical flanges, that the performance is increased, in particular, when the panel is dominated by axial load. The reason for this is that by increasing the area away from the panel's neutral axis, the panel's ability to resist buckling is enhanced.

Skin Laminate	50/40/10											
Stringer Laminate	60/30/10						10/80/10					
Upper Flange Width	Baseline		Wider		Narrower		Baseline		Wider		Narrower	
Performance	Reserve Factor		% Relative to Orig.		% Relative to Orig.		Reserve Factor		% Relative to Orig.		% Relative to Orig.	
Load Case	Inb.	Out.	Inb.	Out.	Inb.	Out.	Inb.	Out.	Inb.	Out.	Inb.	Out.
1	0.94	1.09	113%	110%	85%	89%	0.51	0.56	115%	111%	84%	89%
2	0.86	0.95	109%	108%	87%	90%	0.49	0.52	114%	110%	84%	89%
3	0.64	0.69	106%	106%	88%	91%	0.42	0.44	108%	108%	86%	90%
4	0.49	0.53	105%	105%	89%	92%	0.34	0.36	105%	106%	89%	91%
5	0.40	0.42	105%	105%	90%	92%	0.29	0.30	105%	104%	90%	93%
6	0.51	0.53	103%	104%	91%	93%	0.41	0.42	101%	103%	92%	94%

Table 7-17: Effect of change in upper flange width

7.3.6.4.3 Change in Top-Hat Overall Height

The overall height of the top-hat-profile stringer was varied as shown in Table 7-18, with the inboard stringers height varied from its baseline of 70mm to either 60mm or 80mm; and the outboard stringer's height varied from its baseline of 40mm, to either 30mm or 50mm. In order to limit the number of variables, despite the height increasing, the area enclosed by the stringer was kept constant, thus the stringer's width at it's base changed. As would be expected, a taller stringer has vastly improved performance, which is further evidenced by the work carried out by Mittelstedt and Beerhorst[486].

Skin Laminate	50/40/10											
Stringer Laminate	60/30/10						10/80/10					
Upper Flange Width	Baseline		Taller		Shorter		Baseline		Taller		Shorter	
Performance	Reserve Factor		% Relative to Orig.		% Relative to Orig.		Reserve Factor		% Relative to Orig.		% Relative to Orig.	
Load Case	Inb.	Out.	Inb.	Out.	Inb.	Out.	Inb.	Out.	Inb.	Out.	Inb.	Out.
1	0.94	1.09	146%	162%	79%	53%	0.51	0.56	150%	162%	84%	56%
2	0.86	0.95	136%	145%	82%	56%	0.49	0.52	147%	154%	84%	58%
3	0.64	0.69	130%	136%	87%	65%	0.42	0.44	135%	139%	86%	62%
4	0.49	0.53	128%	133%	89%	67%	0.34	0.36	131%	131%	89%	66%
5	0.40	0.42	127%	131%	90%	69%	0.29	0.30	129%	128%	90%	69%
6	0.51	0.53	123%	125%	93%	74%	0.41	0.42	122%	119%	92%	82%

Table 7-18: Effect of change in height of stringer (constant enclosed area)

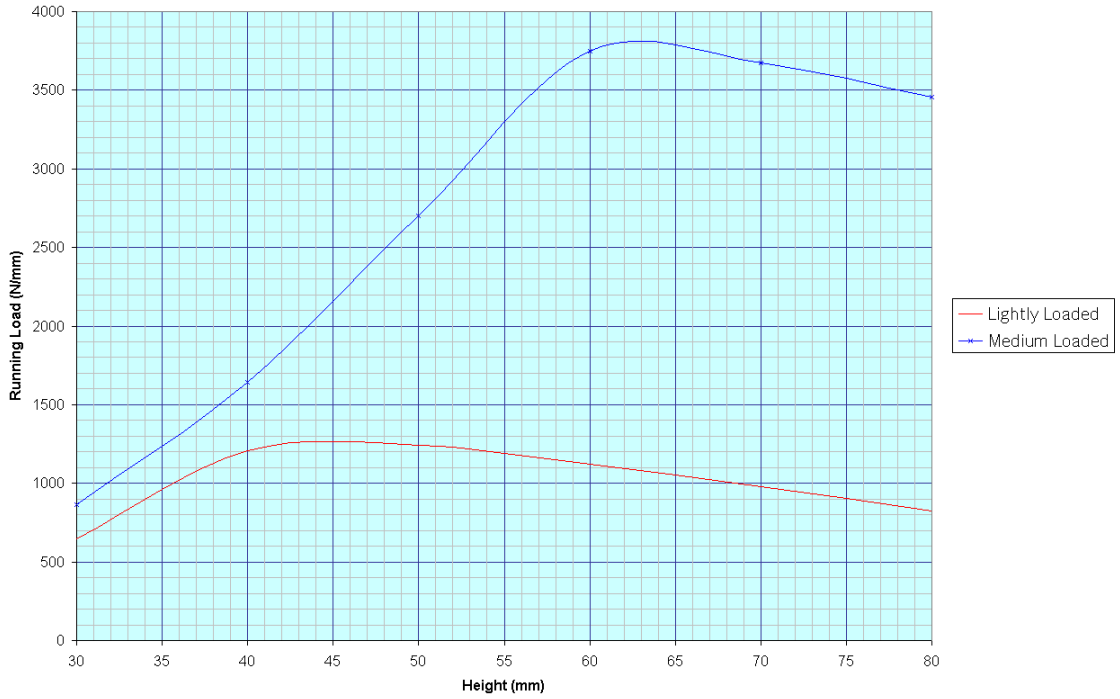

Figure 7-52: Influence of height on top-hat axial performance

However, there is a limit to this effect, as shown by the following example. Using the baseline top-hat-profile stringer panel, with a 44/44/11 skin and a 60/30/10 stringer:

- Lightly-Loaded
  - Stringer
    - Lower flange (LFW=20mm; LFT=1.472mm)
    - Web (SH=Varying; WT=1.84mm)
    - Upper flange (UFW=60mm; UFT=1.84mm)
  - Skin
    - ST=4mm, SP=160mm
- Medium-Loaded
  - Stringer

        - Lower flange (LFW=24mm; LFT=2.944mm)
        - Web (SH=Varying; WT=3.312mm)
        - Upper flange (UFW=74mm; UFT=2.944mm)
    - Skin
        - ST=8mm, SP=200mm

Referring to Figure 7-52, it can be seen that height has a strong influence on the buckling load, where after a certain height, the instability of the vertical flanges becomes critical, resulting in a reduction in buckling load. Therefore, it is a compromise between second moment of inertia and local buckling of the stringer's webs.

7.3.6.4.4 Upper Flange Laminate

The effect of changing the upper flange laminate was investigated using a baseline top-hat-profile stringer panel, with the following dimensions for a lightly- and medium-loaded panel, with a 44/44/11 skin and a 60/30/10 stringer:

- Lightly-Loaded (N_x = -1010N/mm)
    - Stringer
        - Lower flange (LFW=20mm; LFT=1.472mm)
        - Web (SH=40mm; WT=1.84mm)
        - Upper flange (UFW=39mm; UFT=1.84mm)
        - Pitch between webs=60mm
    - Skin
        - ST=4.5mm, SP=160mm
- Medium-Loaded (N_x = -2776N/mm)
    - Stringer
        - Lower flange (LFW=24mm; LFT=2.944mm)
        - Web (SH=56.5mm; WT=3.312mm)
        - Upper flange (UFW=48mm; UFT=2.944mm)
        - Pitch between webs=74mm
    - Skin
        - ST=8mm, SP=200mm

The effect of having a pure 0°, ±45° or 90° laminate in the upper flange in comparison to the baseline solution is shown in Table 7-19. Clearly, having a highly stiff laminate in the direction of the load is beneficial, as this will maximise the column stiffness; in particular, if the skin local to the stringer also has a high percentage of 0° plies. If the vertical webs use a primarily ±45° laminate, this will give good shear stiffness to maximise column transverse shearing deformation. Such a design should be highly efficient, however the design and fabrication is challenging, and the resultant laminate would not conform to the laminate design rules, leading to shear stress issues due to different thermal expansion rates.

	Lightly-Loaded	Medium-Loaded
100/0/0	118%	112%
0/100/0	60%	67%
0/0/100	54%	62%

Table 7-19: Influence of upper flange laminate on top-hat axial performance

The fabrication cost of top-hat-profile stringer could be reduced by using prefabricated pultruded rods, of unidirectional carbon-epoxy material, embedded in syntactic film adhesive,

as shown in Figure 7-53[487]. These rods have higher stiffness and strength in comparison to UD tape, as the fibres have far less crimp, and are packed together in the cap and at the base of the top-hat-profile stringer to create high stiffness regions. However, a perceived limitation of such a design is that it may be difficult and inefficient to transfer load into and out of the rod members at a joint, and repair is also problematic.

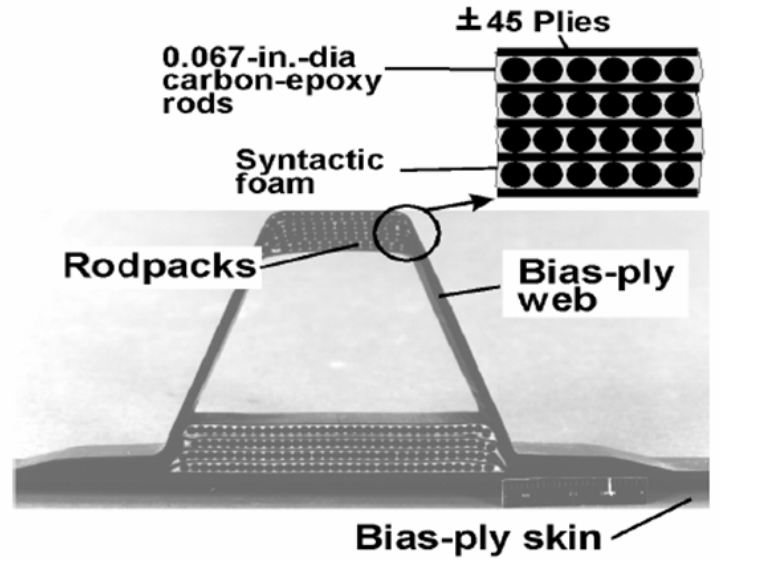

Figure 7-53: Rod-reinforced top-hat-profile stringer

7.3.6.4.5 Summary for Top-Hat-Profile Stringer

Despite the theoretical advantages of a top-hat-profile stringer panel, when under the constraints of buckling, and also the possibility to use the closed-profile as part of the tank venting system, there are a number of drawbacks, which can be summarised as follows:

- The manufacture of the closed-profile is difficult for either a co-curing or co-bonding (uncured stringer):
    - Metal mandrels can be used, but there can be no locking features, caused by a change in cross-section, otherwise the mandrel cannot be extracted
        - This can limit optimisation of the skin, thus is not acceptable
    - ROHACELL, with a density of 50-70 kg/m³, can be used to create a mandrel
        - Can be machined out after cure, which is wasteful
        - If left, this will then mean that the closed-profile cannot be used for venting
            - Could increase the weight, or be beneficial to the structures stability performance
    - The manufacture of the laminate itself can be fairly difficult due to the tapering section, and the different thicknesses needed for the foot, web and upper flange
    - With change in thickness for the feet, webs and upper flange, this can lead to consolidation issues at the radii, as it is here that the thickness changes
    - Reinforcement needed internally to support the web against pull-off loads
- A pre-cured stringer to be used either with a co-bonding (cured stringer) or secondary bonding technique, will still need a mandrel to ensure it does not deform during cure
- Ribs will typically be heavier due to the larger castellations required
- Attachment of brackets to stringer is more difficult due to access

- SROs are more difficult to design due to the closed-profile
    - Cannot simply taper the stringer blade
    - These issues are exacerbated on wing covers due to tapering section, and integration of parts attached to the covers, such as flap tracks, MLG, etc.
- Fuel volume is reduced due to the closed-profile, and fuel can get trapped inside the enclosed space
    - The functionality of the passage holes are compromised, as shown in Figure 7-54, with Rohacell, shown in the top view, requiring a continuous sealed passage through both webs, whereas without a core, the stringer can act as a fuel trap

Thus, for these reasons and evidence from other programs, top-hat-profile stringers will not be investigated further for application on heavily loaded wing structures.

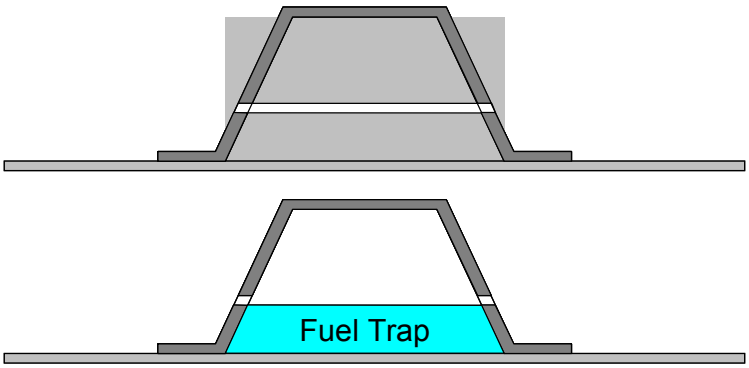

Figure 7-54: Passage hole integration into top-hat-profile stringer (top with Rohacell core/bottom without)

7.3.6.5 I-Profile Stringer Particularities

Two I-profile stringer-stiffened panels, with a 44/44/11 skin laminate and 60/30/10 stringer laminate were investigated to see the effect of upper flange width on the panel's overall performance. The panels had the following dimensions:

- Lightly-Loaded (N_x=-940N/mm and N_{xy}=235N/mm)
    - Stringer
        - Lower flange (LFW=60mm; LFT=1.104mm)
        - Blade (BH=50mm; BT=1.84mm)
        - Upper Flange (UFW=varying; UFT=1.104mm)
    - Skin
        - ST=5.00mm; SP=160mm

- Heavily-Loaded (N_x=-4780N/mm and N_{xy}=720N/mm)
    - Stringer
        - Lower flange (LFW=65mm; LFT=5.520mm)
        - Blade (BH=66mm; BT=2.576mm)
        - Upper Flange (UFW=varying; UFT=2.576mm)
    - Skin
        - ST=10.50mm; SP=240mm

Shown in Figure 7-55 is the increase in performance of the panel normalised with respect to the weight of the panel, due to the increase in upper flange width, in comparison to the

standard I-profile stringer panels i.e. with an upper flange width of 32mm and 37mm for the 160mm and 240mm stringer pitch, respectively. For the 160mm pitch, the optimal width of the upper flange was roughly 40mm, whereas for the 240mm, it was 70mm. At a certain upper flange width, the panel's overall performance decreases, as the upper flange buckles early on, as can be seen in the RF versus wavelength curves shown in Figure 7-56, for 'Lightly Loaded 47' and 'Heavily Loaded 87'.

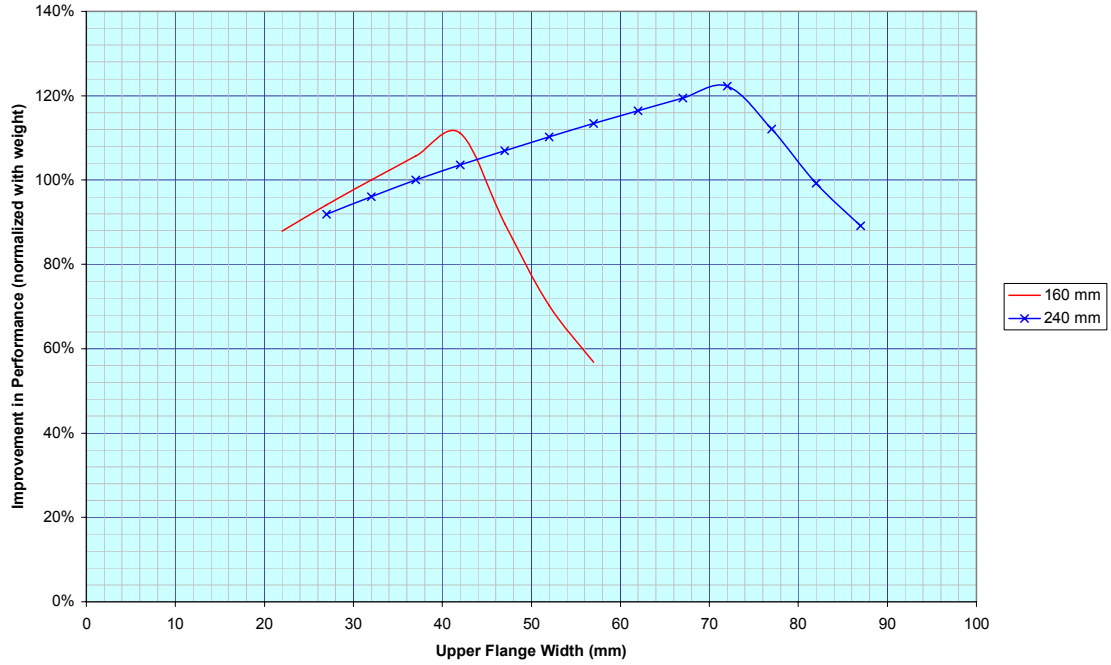

Figure 7-55: Improvement in performance with change in upper flange width at two load levels

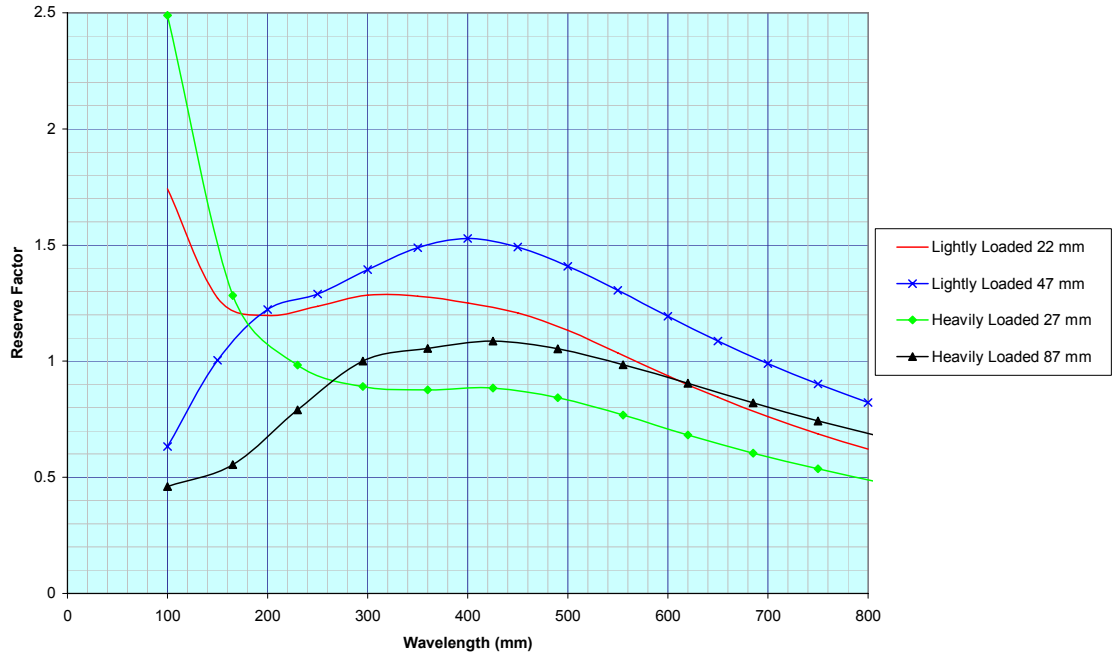

Figure 7-56: RF-L curves for selected examples

7.3.6.6 T-Profile Stringer Improvement with Bulb

One way to improve the bending stiffness of a standard T-profile stringer to enhance its out-of-plane performance, is to have a bulb on the free-edge of the stringer blade, as shown in Figure 7-57.

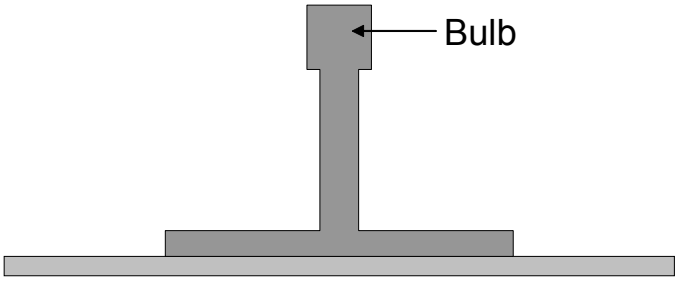

Figure 7-57: T-profile stringer with bulb

For a bulb to be effective, it must have sufficient stiffness to provide simply supported conditions to the web. This can be calculated using Equation 7-2[488]:

$$2.73 \times \frac{I_b}{BH \times BT^3} - \frac{A_b}{BF \times BT} \geq 5 \qquad \textbf{7-2}$$

Where A_b = area of bulb and I_b = bulb's second moment of inertia, which is given by Equation 7-3, where d_b = the bulb's diameter.

$$I_b = \frac{\pi \times d_b^{\,4}}{64} + \left(\frac{\pi \times d_b^{\,2}}{4} \times \left(\frac{d_b - BT}{2} \right)^2 \right) \qquad \textbf{7-3}$$

It is necessary that the buckling stress of the bulb is greater or equal to the buckling stress of the blade, therefore:

$$\left(\frac{\pi^2 \times k_c \times E}{12(1-\nu_e)^2} \times \left(\frac{t}{h} \right)^2 \right)_{bulb} \geq \left(\frac{\pi^2 \times k_c \times E}{12(1-\nu_e)^2} \times \left(\frac{t}{h} \right)^2 \right)_{blade} \qquad \textbf{7-4}$$

$$\left(k_c \times E \times \left(\frac{t}{h} \right)^2 \right)_{bulb} \geq \left(k_c \times E \times \left(\frac{t}{h} \right)^2 \right)_{blade} \qquad \textbf{7-5}$$

Where k_c = buckling coefficient, E = modulus, υ_e = elastic Poisson's ratio, t = thickness, h = height of element. Thus (for derivation refer to Bruhn, "Analysis & Design of Flight Vehicle Structures"[488]):

$$\left(\frac{d_b}{BT} \right)^4 - 1.6 \left(\frac{d_b}{BT} \right)^3 - 0.374 \left(\frac{d_b}{BT} \right)^2 = 7.44 \frac{BH}{BT} \qquad \textbf{7-6}$$

From Equation 7-6, the optimum bulb diameter to blade thickness (d_b/BT) was calculated based on a given blade height to blade thickness (BH/BT), and plotted in Figure 7-58. Therefore, the bulb diameter for normal ratios of (BH/BT) should be 2-4.

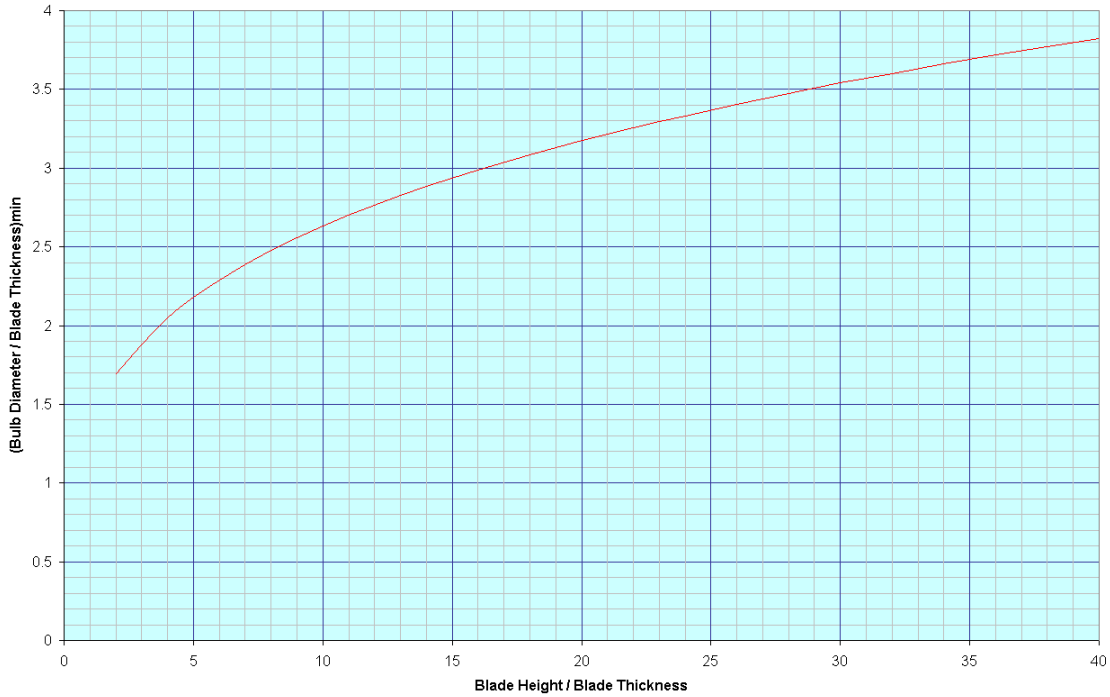

Figure 7-58: Minimum bulb dimensions required for buckling as simply supported plate

Two standard T-profile stringer-stiffened panels, with a 44/44/11 skin laminate and a 60/30/10 stringer laminate were adapted with bulbs; the details of the panels are given below:

- Lightly-Loaded (N_x=-414N/mm and N_{xy}=184N/mm)
  - Stringer
    - Lower flange (LFW=50mm; LFT=2.944mm)
    - Blade (BH=35/50mm; BT=6.808mm)
    - Bulb Diameter=15mm
  - Skin
    - ST=4.00mm; SP=165mm

- Highly-Loaded (N_x=-1935N/mm and N_{xy}=288N/mm)
  - Stringer
    - Lower flange (LFW=68mm; LFT=2.944mm)
    - Blade (BH=50/75mm; BT=10.304mm)
    - Bulb Diameter=25mm
  - Skin
    - ST=6.00mm; SP=165mm

For the lightly-loaded panel, the RF increased by 3 times for a 21% increase in cross-sectional area. Similarly, for the heavily-loaded panel, the RF increased by 3.3 times for a 35% increase in cross-sectional area. Thus, the bulb design is very beneficial. Furthermore, the structure's ability to withstand the out-of-plane loading effects is also improved by 3 times under tension and between 1.5-2 under compression.

7.3.6.7 Stringer Laminate

A typical stringer laminate is $60/30/10^{456}$, as a high percentage of 0° plies are required to react the axial load, as well as a minimum of 10% 90° plies due to laminate design rules. A fairly substantial percentage of ±45° plies are also required for the following reasons:

- Damage tolerance
- Repair
- Bolt bearing
- Shear along blade due to bending
- Transfer of rib shear into cover via the stringer foot first
- Provides blade with better twisting resistance after a certain height

The stringer typically uses 0.184mm thick plies for the following reasons:

- As there are twice as many 0° plies as ±45° plies (60/30/10), in order to attain the desired lay-up for a thinner section, while obeying the stacking sequence rules, thinner plies are necessary
- Due to the high-stiffness of stringers, finer changes in thickness are considered necessary to reduce overall weight

7.3.6.7.1 Fibre-Metal Laminate

Due to the high percentage of 0° plies in the stringer blade, the bearing performance of the stringer can be poor, which can constrain the design when repair is considered. As highlighted previously, this can be improved through applying an FML in critical areas. The benefit of using an FML has been demonstrated on the following stringer-stiffened panel, with a 50/40/10 skin and 60/30/10 stringer, designed to react a nominal axial load of -3000N/mm:

- Stringer
  - Lower flange (LFW=91mm; LFT=3.0mm)
  - Blade (BH=78mm; BT=8.0mm)
- Skin
  - ST=7.3mm; SP=208mm

Using data established in Appendix B for the FML, Table 7-20 was obtained. It can be seen that based on an assumed 4 bolt row, with the first bolt taking 35% of the applied load through the blade, then the bearing/bypass performance improves with an increasing percentage of titanium in the stringer blade. As a direct effect of the increase in titanium, the stiffness of the blade is increased, as the least stiff plies are replaced by the titanium, i.e. first the 90° plies followed by the ±45° plies, and hence the amount of load attracted also increases. Although the FML is favourable, its overall benefit is hindered by a higher amount of load passing through the joint.

Another issue is that by maintaining the cross-section of the panel but increasing the percentage of titanium, there is a consequential increase in weight. Therefore, the application of an FML, to improve the bearing/bypass interaction in area of a joint, must be correctly justified and designed.

Stringer Blade Laminate	% of load in Stringer	Reserve Factors			% Weight Increase
		Stability	Bearing/Bypass T	Bearing/Bypass C	
60/30/10 [0]	40	0.98	0.46	0.80	100
60/20/0 [20]	42	1.05	0.55	0.91	109
60/0/0 [40]	45	1.09	0.61	1.01	118

Table 7-20: Influence of amount of titanium in stringer blade on performance

7.3.6.8 Stringer Type and Fabrication Methods

7.3.6.8.1 General Fabrication

There are different ways of manufacturing a stringer. The most simple method is to use back-to-back L's, as shown in Figure 7-59(a). However, as the blade thickness is constant at a given section and not tapered in thickness, this means that the thickness of the blade is dependent on the thickness of the foot, which can limit optimisation flexibility. A further weakness with this concept, especially if the stringer is to be pre-cured, is that the Bermuda triangle formed at the bottom of the back-to-back L's would either remain an unfilled cavity, or more typically, would be filled with resin, which is not structurally acceptable. This can be improved by using a capping plate as shown in Figure 7-59(b). Furthermore, by adding a spine to the web, as shown in Figure 7-59(c), it allows the thickness of the blade to be independent from the foot, and as it can minimise the thickness of the back-to-back L's in order to ensure that the L's have a more quasi-isotropic laminate, while the total blade has a higher proportion of 0° plies. It can also ensure that the radius between the blade and foot is minimised, which can reduce the size of the Bermuda triangle at the base of the blade. In terms of the blade, any spine used to make up the channel sections should be less than 60% of the total blade thickness.

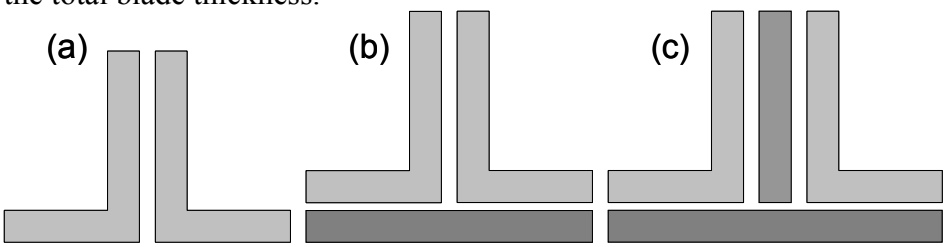

Figure 7-59: Different ways of fabricating a T-profile stringer, similar for I-profile stringer

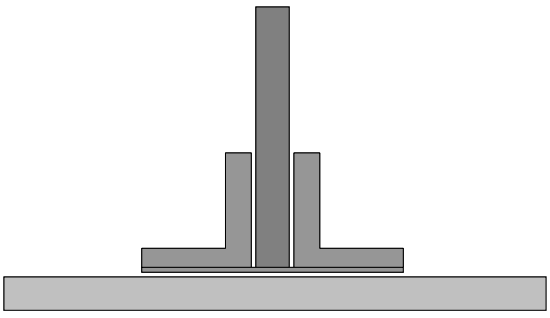

Figure 7-60: π -Joint to aid efficient stringer integration

Often wing covers have fairly pronounced spanwise curvature, which means the stringers need to have good conformability, which is aided by having less 0° plies in the stringer preform. A solution that ensures structural efficiency and conformability is to use the concept of an enlarged π-joint, where the π-shape is fabricated with uncured prepreg or dry fibre, which has principally bias plies to aid drapeability. Inside the π-joint, a pre-cured spine, with a principally 0° laminate, can be inserted and co-bonded, as shown in Figure 7-60.

7.3.6.8.2 Asymmetry due to Discrete Stringer Fabrication

The T-profile stringer, and similarly an I-profile stringer, can be fabricated by one of the following methods as shown in Figure 7-61. If the stringer is fabricated using roll-forming then there will be asymmetry in the blade, as shown on the LHS; whereas on the RHS the back-to-back L's are symmetric, but if a capping laminate is used then on one side, in this case the LHS, there will be asymmetry.

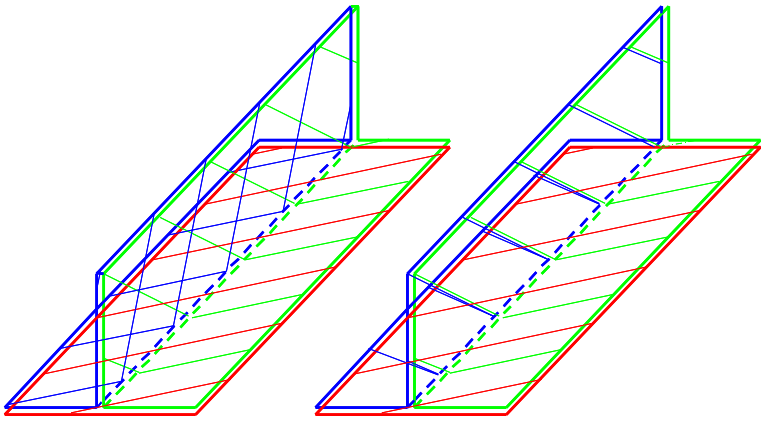

Figure 7-61: Asymmetry of stringer fabrication with UD plies

Using ESDUpac 8147[489], the buckling load for a stringer blade 5.888mm thick (32 plies of 0.184mm), 90mm high and 800mm long, was calculated for the following 62.5/25/12.5 laminates:

- Symmetric
  - $[+/0/0/-/0/0/90/0/0/90/0/0/-/0/0/+]_s$
    - N_x=-8940N/mm; N_{xy}=8950N/mm
- Asymmetric
  - [-/0/0/+/0/0/90/0/0/90/0/0/+/0/0/-/+/0/0/-/0/0/90/0/0/90/0/0/-/0/0/+]
    - N_x=-8920N/mm; N_{xy}=8930N/mm

Similarly, for a 37.5/50/12.5 laminate:

- Symmetric
  - $[+/-/+/-/0/0/90/0/0/90/0/0/-/+/-/+]_s$
    - N_x=11400N/mm; N_{xy}=11500N/mm
- Asymmetric
  - [-/+/-/+/0/0/90/0/0/90/0/0/+/-/+/-/+/-/+/-/0/0/90/0/0/90/0/0/-/+/-/+]
    - N_x=11400N/mm; N_{xy}=11500N/mm

There is very little difference between a symmetric and asymmetric laminate in terms of the critical buckling load. However, asymmetric laminates have more couplings, which are exacerbated for thinner laminates[480], resulting in convoluted structural analysis. As the foot thickness is generally thinner than the blade, then the foot should be more critical concerning the coupling effects. However, the foot is attached to the skin, thus it is constrained by the skin, and hence the coupling effects are more critical for the free web, i.e. the blade.

7.3.6.8.3 Asymmetry due to U-Profile Stringer Fabrication

The forming of U-channels that are cured to an underlying skin creates an asymmetric global skin laminate, as shown in Figure 7-62. An investigation was carried out using ESDUpac 8147[xxxix] to see the effects that this had.

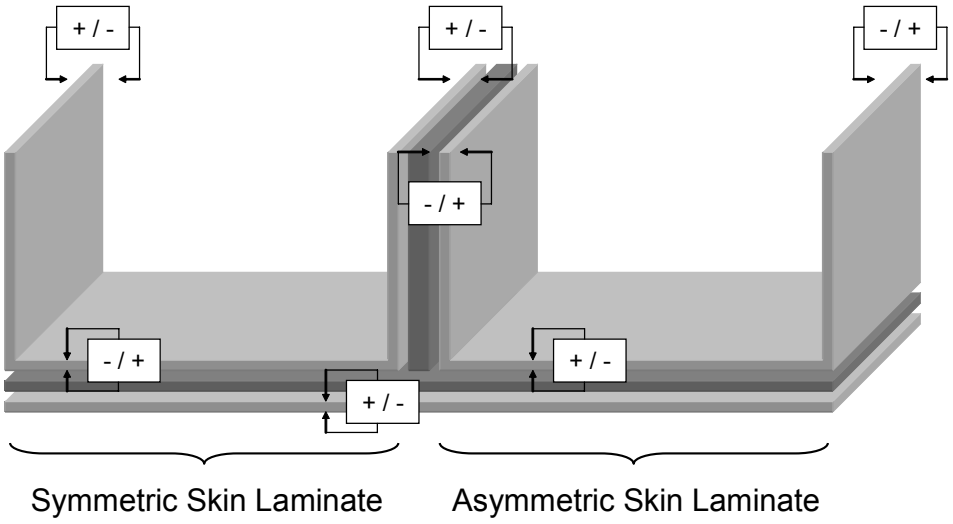

Figure 7-62: Asymmetric situation with U-profile stringers

To investigate the effect on the stringer, 3 skin laminates were investigated, namely 10/80/10; 30/60/10; and 50/40/10. From 7.3.6.3.1, it was decided that 30% of the total skin laminate would constitute as part of the blade, thus for laminate thicknesses of 4mm, 8mm, and 12mm, this meant that the bias plies in parentheses () are reversed, as shown for the 50/40/10 example:

- 4mm
  - Symmetric
    - $[+/-/90/0/0/+/0/0]_s$
  - Asymmetric
    - $[(-/+)/90/0/0/+/0/0]_s$
- 8mm
  - Symmetric
    - $[+/-/90/0/0/+/0/0/-/0/0/+/90/-/0/0]_s$
  - Asymmetric
    - $[(-/+/90/0/0/-/0/0/+)/0/0/+/90/-/0/0]_s$
- 12mm
  - Symmetric
    - $[+/-/90/0/0/+/0/0/-/0/0/+/90/-/0/0/+/0/0/-/0/+/90/-]_s$
  - Asymmetric
    - $[(-/+/90/0/0/-/0/0/+/0/0/-/90/+)/0/0/+/0/0/-/0/+/90/-]_s$

This was similarly carried out for 30/60/10 and 10/80/10 laminates. The load carrying ability under axial and shear load is shown in Table 7-21. In order to verify the results from the

[xxxix] Validated with ESDUpac A9406[641], to check the applicability for use with asymmetric laminates, as ESDUpac A9406 cannot check symmetric laminate, as they have non-compatible D13/D23 terms, however between the two programs there is only a 0.8% difference in accuracy for an asymmetric laminate

ESDU program, the closed form equations, as shown in Appendix D, and used by Weaver (2004)[490] were used, as shown in the columns identified as "CLF", i.e. closed-form equation. In general, there is acceptable coloration, although divergence in the results occurs, with an increase in thickness and a larger proportion of bias plies. However, there is no significant knockdown in buckling performance due to the asymmetry of the skin laminate.

Thickness (mm)	Loading (N/mm)	10/80/10			30/60/10			50/40/10		
		ESDU	ESDU	CLF	ESDU	ESDU	CLF	ESDU	ESDU	CLF
		Sym.	Asym.		Sym.	Asym.		Sym.	Asym.	
4	Nx	541	541	556	492	491	503	488	488	501
	Nxy	691	691	692	637	636	630	636	629	626
8	Nx	3900	3870	4329	3580	3580	3887	3410	3400	3645
	Nxy	4790	4790	5395	4220	4220	4602	3930	3920	4259
12	Nx	11600	11600	14554	10900	10900	13080	10300	10300	11896
	Nxy	13600	13600	18066	12100	12100	15303	11100	11100	13550

Table 7-21: Skin laminate investigation for U-profile stringer

7.3.6.9 Foot Width

The consequence of the rib foot being mechanically attached through the stringer and skin is that at every rib datum, the stringer foot is grown out to accommodate the landing of the rib foot, as shown in Figure 7-63. This is governed by the size of the castellation in the rib required to allow fuel to flow through, the tolerance float on assembly, and the number and size of bolts. Furthermore, the stringer width could further increase due to the root joint design, where the stringer feet are sometimes grown out to allow the integration of the root joint.

The stringer foot width can also be determined by other factors that affect the wing cover's overall performance. Based on work carried out by Wiggenraad et al. (2002)[421] a more damage tolerant cover design has a wider stringer foot, in this case from the original 40mm to 80mm. Consequently, a wider foot will decrease the effective buckling area of the panel and minimise the peel stress between the stringer and skin[491]. Furthermore, the foot width is a factor of the bonding capability at the intersection of the stringer blade and skin[394]. When the width is too small then the tensile pull-off strength is reduced, whereas if it is too wide, then it will add too much weight. However, in terms of the strength, under pull-off load, when the width of the foot increases the panel's strength reduces[479]. Under bending, the ratio of the bending stiffness (D_{22skin}/ $D_{22stringer}$) has an effect on the panel's strength[479], with a stiffer skin being beneficial, which helps to reduce the peel stresses in the bond. Under transverse loading, the panels strength can be increased by ensuring the skins lateral stiffness i.e. E_yA, is greater than the stringer foot's[479]. This should always be the case as the skin has a greater E_{22} as the skin has more ±45° plies, plus the thickness of the skin is typically greater.

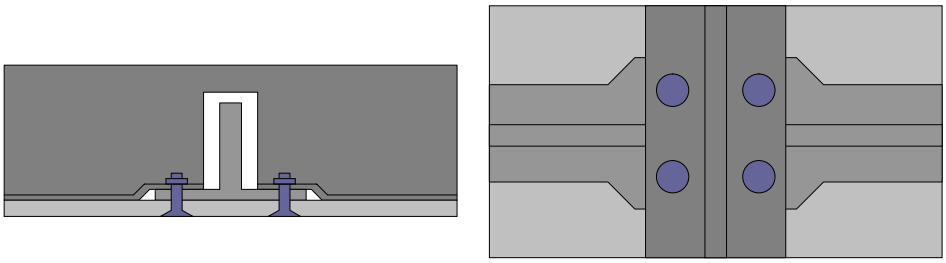

Figure 7-63: Stringer grow-out for rib integration

An investigation was carried out using ESDUpac A0817 to investigate the effect of foot width on the buckling performance of a T-profile stringer-stiffened panel. Two different panels were used to represent a lightly-loaded and medium-loaded panel. For both panels the skin and stringers had 44/44/11 and 60/30/10 laminates, respectively, with a stringer pitch of 165 mm, and the following dimensions:

- Lightly-Loaded (N_x=-440N/mm and N_{xy}=194N/mm)
  - Stringer
    - BH=35mm; BT=6.808mm; LFT=2.944mm
  - Skin
    - ST=4mm
- Medium-Loaded (N_x=-2580N/mm & N_{xy}=335N/mm)
  - Stringer
    - BH=47mm; BT=8.096mm; LFT=2.944mm
  - Skin
    - ST=9.75mm

The foot width for the lightly-loaded panel was varied in increments of 20mm, from 30mm to 130mm, and from 50mm to 130mm, for the medium-loaded panel. The results are shown in Table 7-22. In general, it can be seen that by increasing the foot width, the panels performance does increase, as would be expected; however, if the increase in RF is normalised with respect to the weight, it is seen that for the lightly-loaded panels the performance decreases; whereas for the medium-loaded panels there is no advantage.

Configuration	Foot Width (mm)	RF Improvement	Area Increase	Specific RF Improvement
Lightly-Loaded	30	1	1	1
	50	1.040	1.061	0.980
	70	1.084	1.122	0.966
	90	1.135	1.828	0.960
	110	1.196	1.244	0.962
	130	1.272	1.305	0.975
	90*	0.908	1.012	0.897
Medium-Loaded	50	1	1	1
	70	1.030	1.028	1.002
	90	1.057	1.056	1.001
	110	1.084	1.084	1.000
	130	1.109	1.111	0.998
	130*	0.959	0.800	1.200

Table 7-22: Effect of foot width on overall performance

For the lightly-loaded panels, a direct comparison between increasing the width of the foot at the expense of decreasing the skin thickness by 1mm is shown in the "90*" row, in comparison to "30"[xl]. This illustrates that area added to the skin is more effective than in the foot. For the medium-loaded panels, the panel in the last row "130*" has a skin thickness of 5.75mm and a foot width of 130mm. This panel reacts almost the same axial load as the baseline panel with a foot width of 50mm, but achieves a weight saving of 25% over the baseline panel. In terms of strength, the thinner panel has an overall RF=1.85, whereas the thicker skinned panel has an RF=2.19. Therefore, the broad conclusion is that the foot width should be governed by the necessity to repair the stringer via a bolted repair.

[xl] $(90 - 30) \times 2.944 \approx 165 \times 1$.

7.3.6.10 Stringer Radius Size

The radius between the foot and web influences the strength of the bond, with the radius being a factor of manufacturing quality[394]. An investigation was conducted by Huang (2003)[394] into the optimal radius for a co-cured part, with a flange width of 50mm under tensile pull off load. It was found a radius of 3-6mm[394] was optimal for this configuration, which had a blade thickness of only 2.286mm and a foot thickness of 1.143mm, which is relatively thin compared to a stringer designed for a wing cover. When the radius is too large, then fibre twist occurs and resin gets trapped in the corners of the back-to-back L's, therefore the strength of the structure is strongly dependent on having uniform fibre distribution. Conversely, too small a radius with a small cross-section would lead to a sharp corner, which could break off easily, under an external force[394]. Thus a compromise is required in terms of the cross-sectional area and the radius. The radius size is critical, as a larger radius will result in a weight increase, and furthermore, increase the size of the Bermuda triangle area, where for a 3mm and 6mm radius the resulting Bermuda triangle area is 3.86mm² and 15.45mm², respectively.

7.3.6.11 Stringer Run Outs

The termination of a stringer, commonly termed SRO, is extremely critical to the overall panel's structural integrity. The termination of a stringer is due to:

- Taper of the wing box
- Connection of a discrete load, such as the engine pylon or flap track attachment
- Cut-out in the skin such as the manholes or pump-holes

In order to analyse the complex in-plane and out-of-plane stresses local to the SRO, Finite Element Methods (FEM) or testing is required. However, at the preliminary design phase, such methods are not appropriate, therefore design principles must be established and used at this phase[492].

As the stringers are attached to the skin along their length, the principal strain will be the same in both components. Thus the SRO must be designed in such a way that the load is gradually dispersed from the stringer into the skin. A common aspect of the SRO is a decrease in the cross-sectional area of the stringer local to the termination in order to reduce its stiffness, which mitigates the high through-thickness stress at the interface[493]. The effect of this is to reduce the relative deflection between the stringer and skin, which consequently decreases the interface peel stress, interlaminar shear stresses and local buckling[494]. Without this gradual decrease in cross-sectional area, a sharp change in section can overload the interface between the SRO and the skin.

Decreasing the cross-sectional area can be achieved by tapering the blade height, the foot width or blade thickness, or a combination of all three. Other beneficial enhancements to the SRO are anti-peel bolts[xli] through the foot, the stringer foot being fish tailed, and increase in skin thickness at the SRO to deter local skin buckling, as shown in Figure 7-64. By increasing the thickness locally in the skin, this can cause a number of manufacturing issues, in particular extra effort for the ATL, as well as the stringer conforming to the skin contour. A similar

[xli] As the bond is designed for UL, then the anti-peel bolts need to be designed for LL.

benefit, which is easier to integrate, is to have a local doubler in the area of the SRO, as shown in the bottom left of Figure 7-64.

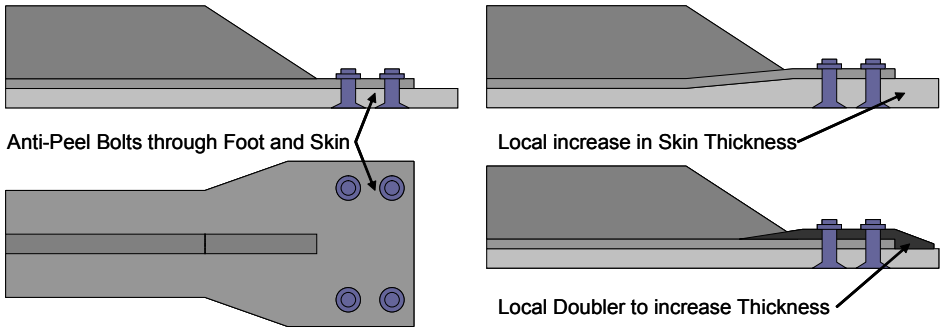

Figure 7-64: Typical methods to improve the SRO area

Stitching can also be used to increase the through-thickness strength, which increases the UL of the panel[491]. Furthermore, if the SRO terminates at the rib, the rib bolting will minimise the local bending induced by a considerable factor. However, these design principles do not necessarily ensure that unstable crack propagation cannot occur between the skin and stringer[493]. Impact damage at the SRO can have a particular influence, inducing significant local stress gradients[495].

A substantial SRO investigation was conducted as part of the NASA ACT program. The panels were fabricated from NCF material with a $[+/-/0_2/90/0_2/-/+]_{Textile}$ lay-up, a resultant textile thickness of 1.47mm, using the Hercules resin system 3501-6[495]. The stringers were fabricated from back-to-back L's with no capping plate, which had typically a thickness of 11.8mm, although for panels with a tapered stringer, the stringer blade thickness decreased down to 3mm local to the SRO. Two different skin thicknesses were investigated; one configuration had a constant thickness of 7.4mm, whereas the second had a varying thickness from 7.4-11.8mm. It was found that for the thin panels, interlaminar stresses and bending were considered to predict the failure, whereas for thick panels, interlaminar shear stresses and axial strain were influential[495].

In general, it was found that a SRO should have either a reduction in blade thickness or height, or both[495]. However, with a reduction in blade thickness, this caused greater shear stress between the stringer foot and skin, which can be explained, as a reduction in blade thickness also results in a reduction in foot thickness; whereas by reducing the height, with a taper ratio of 6° with reference to the stringer foot, this issue is minimised[495]. It was also found that by increasing the foot length, this reduced the interlaminar shear forces between the stringer foot and the skin, as well as reducing bending in the SRO area[496].

Another extensive SRO investigation was carried out by Falzon and Davies[493], investigating panels, with a skin thickness from 8-19.5mm, using the prepreg system AS4/8552. The stringers were fabricated from back-to-back L's with a capping plate, having a blade thickness of 10-14mm, and a foot thickness of 6-7.5mm. The blade taper design was also investigated, with either a complete taper right down to the foot or with a 10mm step remaining, as shown in Figure 7-65, to aid manufacturing[493]. The blade taper, with respect to the foot, was 15°. Furthermore, for some panels, the skin thickness local to the SRO was increased, as previously illustrated in Figure 7-64.

The completely tapered blade offered no advantage over the design with a 10mm step. Instead it was beneficial, as a complete taper caused a reduction in the integrity of the back-to-back L's, which induced a higher peel and interlaminar shear stress[493]. For thinner skins <8mm, an

increase in skin thickness local to the SRO is advantageous, as it reduces the local bending and hence the mismatch in strains on the IML and OML; however, it is not advantageous for thicker panels[493]. Finally, it was found that a 45°/45° interface between the skin and stringer adherend plies was superior to a 0°/90°[493]. This is due to a 0°/90° interface leading to a highly unstable Mode II crack growth at the SRO, resulting in an unzipping effect of the bond, which increases the load in the skin. This leads to skin and then global buckling, which increases the Mode I failure[493]. Whereas, for a 45°/45° interface, after initial unstable crack propagation, this will be followed by stable crack propagation between the stringer and skin.

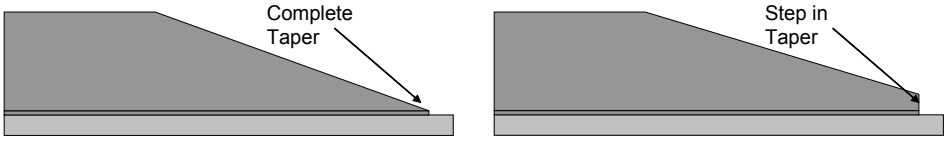

Figure 7-65: Taper of blade

Finally, the thermal effects of curing can influence the SRO design. It is known that delamination/debonding can occur due to residual thermal stresses caused by mismatch in thermal expansion and Poisson's ratio[497]. For this reason, a 50/40/10 skin and 60/30/10 stringer should mitigate these issues better than if a 10/80/10 skin is used in combination with a 60/30/10 stringer. This can be exacerbated in the area of the SRO due to the change in section and the local load flow.

7.3.6.12 Stringer Repair

The minimum width and height of the stringer foot and blade, as shown in Figure 7-66, are defined by Equations 7-7 and 7-8 respectively.

$$LFW \geq \left(2 \times \left(1.5 + 2.5\right) \times d\right) + \left(2 \times r\right) + BT \quad \textbf{7-7}$$

$$BH \geq \left(\left(1.5 + 2.5\right) \times d\right) + r + LFT \quad \textbf{7-8}$$

It should be noted that for an I-profile stringer, the minimum blade height requirement is the same as for a T-profile stringer, despite there being no edge to the blade for an intact I-profile stringer. However, if the upper flange is removed, due to repair, then the blade will have an edge, hence why the T-profile stringer requirement is relevant to the I-profile stringer. In terms of the upper flange, as shown previously in Figure 6-16, there is no need for a bolted repair solution, as usually this would be replaced with an integrated flange from angles bolted to the stringer blade. However, due to manufacturing requirements, the minimum width is given by Equation 7-9.

$$UFW \geq BT + \left(2 \times \left(r + 5\right)\right) \quad \textbf{7-9}$$

Where 5mm is a manufacturing constraint for tooling.

For the integral U-profile stringer, as there is no discrete foot, the only bolted repair requirement will be for the blade, which will be the same as Equation 7-8.

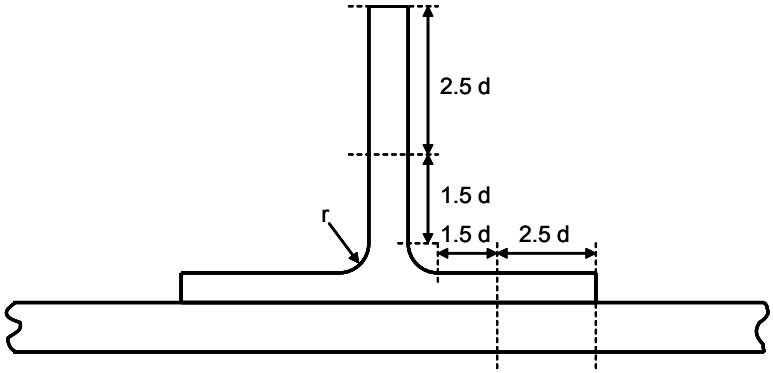

Figure 7-66: Stringer bolted joint edge distance requirements

7.3.6.13 Stringer Families

Emphasis is put on creating a family of parts for items such as electrical brackets, which are ubiquitously found on wings and fuselage. If these parts could be made into families, their design would be easier and greater batch quantities could be manufactured, helping to reduce both NRC and RC costs respectively. However, can this principle be applied to stringers? A typical wing cover will have, in the root joint area, between 12 to 40 stringers across the chord, and these stringers could be grouped into families based on certain characteristics. Families of stringers could be based on physical size, such as the number of plies required to make the blade and the foot; therefore, a number of stringers would use the same basic preform; or alternatively for pre-cured stringers, the average spanwise profile (radius) of the stringer due to the IML surface, could be used to determine a family of stringers, so that a number of stringers can share the same stringer form tool.

The benefits of stringer families must be established. By imposing such a limitation on the optimisation of the cover will mean that a weight increase will be caused, the severity of which will be dependent on a number of factors. For a long-range aircraft, where weight optimisation is of primary importance, it might be hard to justify stringer families. For a short-range aircraft, where the trade-off between weight and cost may substantiate the justification of stringer families, the manufacturing rate may mean that per stringer one tool is required to maintain the build rate. Therefore, apart from a slightly higher NRC due to tooling design, and the lack of flexibility of having stringers that cannot be used in more than one place, it would again seem that stringer families cannot be justified.

7.3.7 Doublers

Doublers are required, principally, due to an attachment, which induces an out-of-plane load, or due to a hole in the part. It is advisable that the doubler laminate itself is both symmetric and balanced, as well as the complete laminate, when the doubler is integrated. However, with a discrete doubler, which is not integrated into the mid-plane of the laminate, this will typically lead to asymmetry of the total laminate, therefore the doubler and the skin has to be designed in such a way as to minimise this.

7.3.7.1 Doubler Integration

There are a number of methods to integrate a doubler:

- Interleaved ply by ply
  - Good mechanical performance and superior interlaminar properties
  - Complex ATL process
- Interleaved stack in neutral axis
  - Fairly good mechanical performance and good interlaminar properties
  - ATL defines the ramp rate of the doubler and slows down the ATL deposition rate
- Co-cured doubler stack
  - Good mechanical properties and interlaminar properties
  - Adaptable for load changes
  - Could induce large peel stresses depending on its depth due to single line of load transfer
- Cured doubler co-bonded
  - Fairly good mechanical properties and interlaminar properties
  - Very flexible for load changes
  - Can be manufactured separately
  - Could be made from different fibre type to improve bearing/bypass ability
  - Would need local NDT
- Cured doubler secondary bonded on cured skin
  - Fairly good mechanical properties and interlaminar properties
  - Very flexible for load changes
  - Can be manufactured separately
  - Could be made from different fibre type to improve bearing/bypass ability
  - Would need local NDT

7.3.7.1.1 Interleaved

An interleaved doubler seamlessly incorporates the doubler into the basic laminate, and in this respect it is the most structurally efficient. However, if the doubler has a substantial thickness, then due to the necessary ramp rates, the influence of the doubler can extend far beyond the area where the doubler is needed. This can then increase the weight in comparison to a discrete doubler and also increase integration issues with other parts of the cover. Such an interleaved concept could be beneficial to act as the complete or partial doubler for the manhole, MLG, engine pylon, and areas that are bearing/bypass driven such as the spar and the root joint.

7.3.7.1.2 Embedded

An embedded doubler concept integrates the required extra thickness into one sub-panel, which is then integrated into the mid-plane of the skin laminate. This should make the doubler more discrete, i.e. more localised. The integration of the laminate would involve laying the base skin laminate until the mid-plane and then laying the doublers onto the skin, and the ATL would then lay the remaining skin laminate. Thus the permissible ramp rate of the integrated doubler will be restricted by the limitations of the ATL, which in reality can

severely limit thick doublers. Furthermore, the mechanical performance of the doubler is not as good as the interleaved concept.

7.3.7.1.3 External

An external doubler will typically be bonded and bolted to the cover, either on the inside or outside surface, depending on the application. An external doubler might be the only option available, due to the thickness needed, such as for the MLG and engine doublers. For small items, such as water drains, it is possible to have a doubler in between the stringers; whereas for larger items, such as fuel pumps, it may be necessary that one or two stringers are terminated to accommodate the doubler, although this is dependent on the stringer pitch and the fuel pump size.

7.3.7.2 Manhole Doubler Integration

It is necessary to have manholes integrated into the wing box in order to comply to CS 25.963(c)[424], which states *"Integral fuel tanks must have facilities for inspection and repair"*. Furthermore, manholes are required for general inspection and for the assembly of the wing box. The manhole covers are typically positioned in the lower skin, due to:

- Improved access
- The aerodynamic requirements concerning steps and gaps are less severe for the lower cover

Normally a manhole is located in every rib bay to allow access, however, if the wing has sufficient depth, then climb-through manholes can be integrated into the ribs. Even so, it is still necessary to have a manhole integrated in the lower cover, in every second rib bay, due to health and safety reasons. It is, however, preferable from a maintenance perspective, to have the manholes in the lower cover, as this is the easiest option for access. The trade-off between having a few ribs with manholes, and having a manhole in every rib bay will also be heavily influenced by the overall weight penalty of each option.

The manholes are normally of a common shape to reduce costs, and the FTACs that are installed into the manhole are mainly non-load carrying, thus they are typically clamped to the wing skin, as shown in Figure 7-67. Alternatively, as trialled in the NASA ACT wing stub box, the single FTAC was bolted directly to the upper cover. It was found, upon testing, that the strains at the corners of the slotted manhole were much higher than at the sides of the manhole, with the strains at the edges exhibiting non-linearity[236]. Furthermore, the interaction between the manhole, and the satellite bolt holes led to very high strains at the periphery of the manhole[236]. Thus, having a clamped solution should result in a thinner skin local to the manhole, as the stress concentration is only due to the manhole and not due to the additional satellite holes required for bolting the FTAC to the skin. The FTAC itself will be designed to withstand all pressure and mechanical loads, while the adjoining structure will be designed to ensure that the FTAC is not subjected to any load[21].

Weight saving and reduction in manufacturing/assembly effort can be sought if the laminate around the manholes is softened. This should allow for a gentler change in thickness chordwise, in comparison to a typical manhole area, which has a doubler nominally twice as thick as the surrounding skin. The softening is achieved by using a laminate with a heavy bias

of off-axis plies, such as a 10/80/10 laminate. Through the softening of the laminate, the allowable stiffness is reduced, as shown in Table 7-23, and hence the load carrying ability is diminished. This means that the load will be redistributed into the surrounding areas of the cover, and hence this part of the skin will be slightly thicker than if the whole skin had a stiff 50/40/10 laminate.

Figure 7-67: Section-cut through manhole showing clamped FTAC design

	E_{11}	E_{22}	G_{12}	ν_{12}
10/80/10	34977	34977	30666	0.56
50/40/10	84502	34347	17683	0.43
60/30/10	96554	32005	14437	0.37

Table 7-23: Moduli for IM laminates

Shown in Figure 7-68 is a stress plot chordwise across the rib bay, which compares directly the stresses attained by both the normal skin laminate (50/40/10), and the locally softened (50/40/10 across the rib bay except around manhole area it is 10/80/10). The chordwise width of the 10/80/10 area in this example is 460mm. It can be seen that for the normal skin laminate, the stress rises to a maximum value around the manhole edge of over 600N/mm², with a rapid increase due to the proximity of the manhole edge. For the locally softened example, the transition from a 50/40/10 laminate to a 10/80/10 laminate is evidenced by a large and distinct decrease in stress, which then increases to about 250N/mm² due to the influence of the manhole edge. It can be seen that for the softened configuration, the stress is higher across the 50/40/10 laminate, reflecting the increased load going through this region.

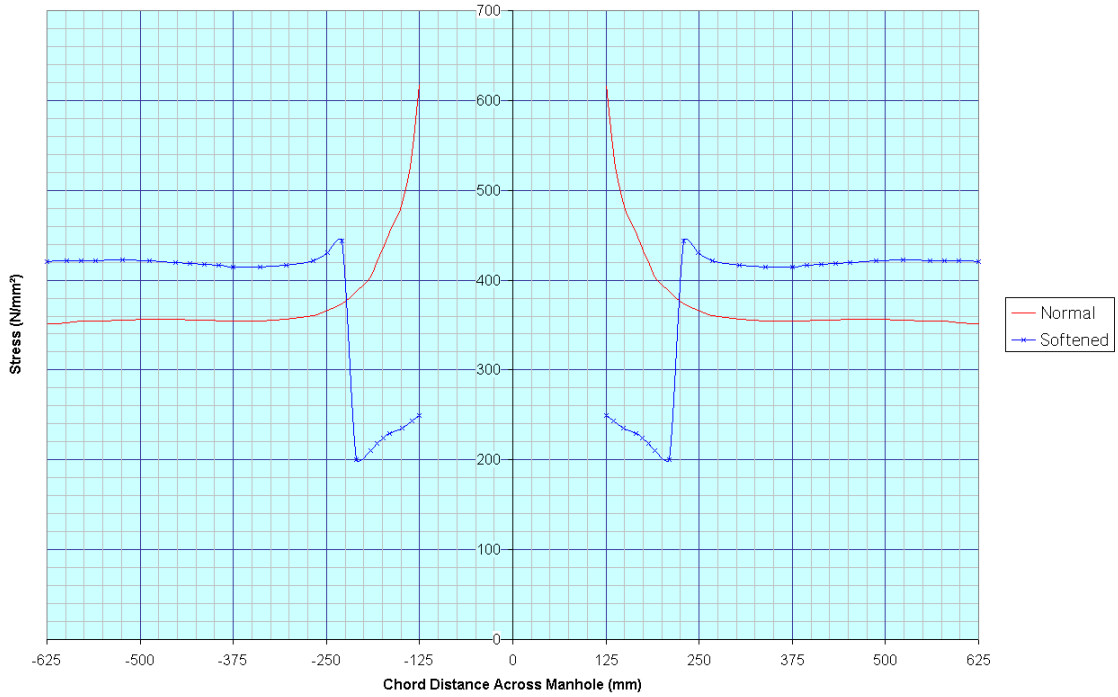

Figure 7-68: Stress plot across the manhole's chord centreline

Figure 7-69 represents the same configuration, but instead strain is plotted. As can be seen, for both configurations the strains rapidly increase with closer proximity to the manhole edge. However, despite the softened laminate having similar peak applied strains to the hard

laminate, the soft laminate has a far higher allowable strain, hence the hard laminate will have an RF<1, whereas the soft laminate will have an RF>1.

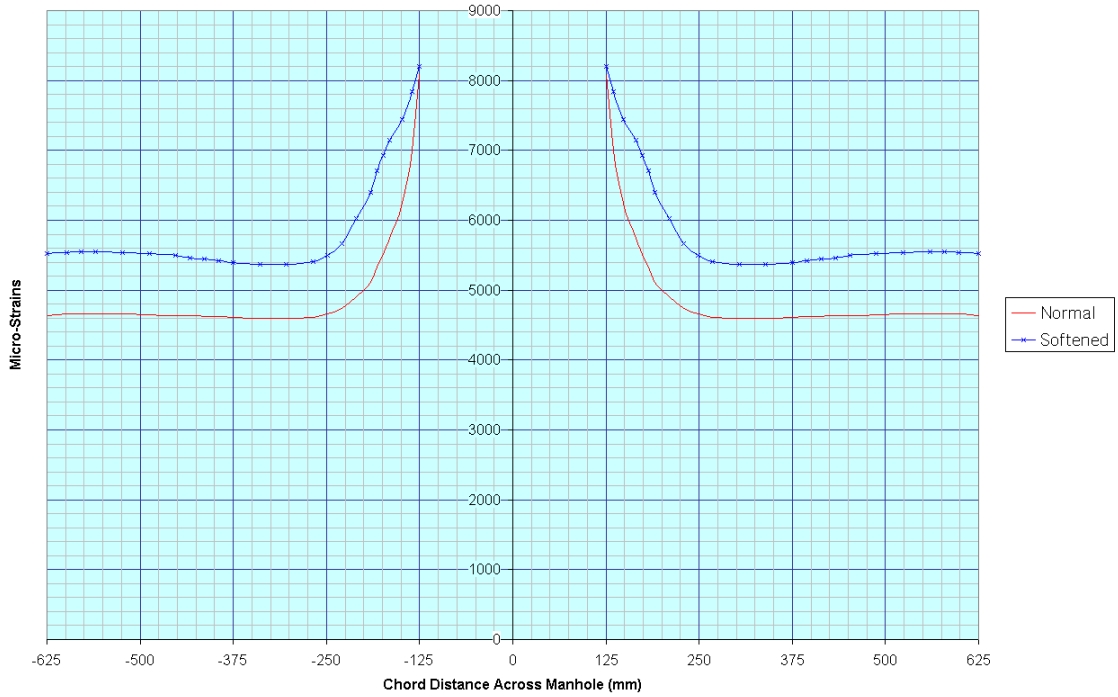

Figure 7-69: Strain plot across the manhole's chord centreline

As the load carrying ability of the softened manhole is reduced, the chordwise width of the softened area should be minimised so that it has sufficient width to perform its task of lowering the stress around the manhole, but also the load carrying 50/40/10 laminate is maximised, so that the optimum global solution can be sought with respect to weight.

7.3.8 Spar Integration

A conventional discrete C-channel spar, which is mechanically fastened to the skin, will influence the thickness of the skin underneath the spar flange, due to the bearing/bypass interaction. Furthermore, the bolting pattern will influence the chordwise width of the spar flange.

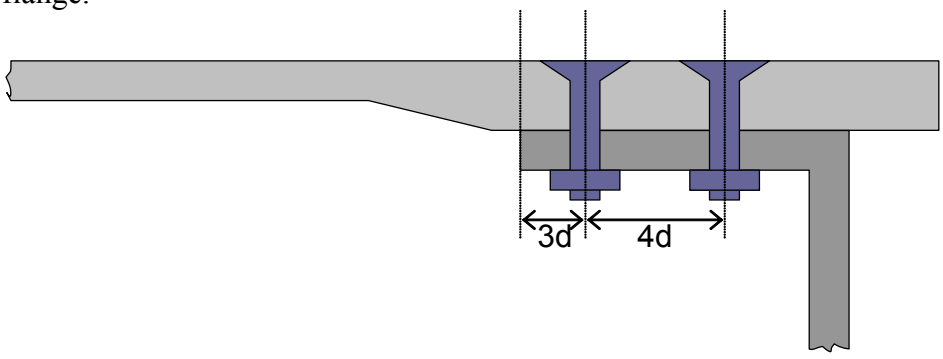

Figure 7-70: Spar to skin landing

As shown in Figure 7-70, a good edge distance at the spar is 3d. Typically, the bolt pitch should be 4d to ensure that if failure should occur then it is in bearing, whereas 6d is the maximum, due to fuel sealing requirements. Often, due to the load, the bolting configuration

has to be either staggered or a double row, with a separation between rows of 4d. A staggered row can be better when fuel sealing is considered, with a single row at the tip.

7.4 Tolerances

Typically single sided tooling is used for wing covers to define the OML, whereas the IML is the bagged surface. The reasons for this are:

- The aerodynamic surface is critical to the aircraft's aerodynamic performance, so it needs to be well defined
- The tooling design and fabrication is simpler using the smooth OML
- As the tooling is a long-lead item, it is beneficial that the OML is defined early on in the program, whereas the IML is defined very late in the program
- If changes occur to the IML due to design alterations, this does not affect the skin tool

However, due to the single sided tooling philosophy, and the anomalies of the curing process, this can result in a variance in the parts thickness. This variance is because of the deviation from the targeted FVF, which can fluctuate across the laminate, due to issues such as resin content and the curing parameters, e.g. the applied pressure. This can be exacerbated for prepregs with higher initial resin content and for LCM techniques, where resin content is harder to control. This issue is extremely critical due to the precursors of structural analysis for CFRP versus metal. The structural analysis for metal parts is determined by the thickness of the part, whereas for CFRP parts, it is not only the thickness that is critical, but also the FVF, as within limits, this determines the strength of the part. Therefore, if a metallic part is too thick, it can be fettled to the 'should be' thickness. However, this cannot be done with a composite part.

Spring-back can also occur due to the thermal curing process, which can cause the component to spring-back when released from the mould tool, although this should be minimised by correct tool design and using Invar® steel for the tool.

Due to this variance in thickness, it can be difficult to ensure that parts on assembly fit together well. Areas on the covers that require special attention, due to tolerances, are:

- At rib to skin locations
- Hard points, i.e. flap tracks
- Manhole plank – due to installation of manhole covers
- Wing tip
- Fuel pump area
- Root joint

With aluminium wings, it is possible that the covers can be pulled to shape through the attachment to the ribs and spars. However, with CFRP wing covers, due to their higher stiffness (although this is dependent on the directional stiffness of the laminate) and the lack of ductility in CFRP, there is a very small limit margin for built-in strains, i.e. strains induced due to assembly. There are two methodologies to alleviate this issue; either the IML, at critical interfaces, will require well-defined tolerances, so that a metallic inside-out wing box can be used, or an outside-in assembly methodology is used.

7.4.1 Inside-Out Build Philosophy

There are two methods to ensure that critical interface surfaces on the cover are well defined:

- Machine all critical interfaces after cure
- Use tooling to control, at least, the critical surfaces

To machine the interfaces, this will require adequate provision of sacrificial plies to ensure that load bearing plies are not machined, as shown in Figure 7-71. The required total thickness of the sacrificial plies is determined by the variance in thickness of the CFRP part, which itself is dependent on the thickness of the part in that area, the degree of spring-back for instance of the stringer feet[xlii], and the tolerance of the milling machine. The sacrificial plies, used in areas of joints, will be carbon, as they will be load-bearing plies due to the bolted attachment. This will add in both weight and cost to the structure, as these patches will have to be positioned by hand due to their size, and once cured and machined, will require a glass ply to be applied, again by hand, and then cured in the autoclave for a second time, due to galvanic corrosion issues with the rib[xliii]. Such a process is not conducive to a lean methodology.

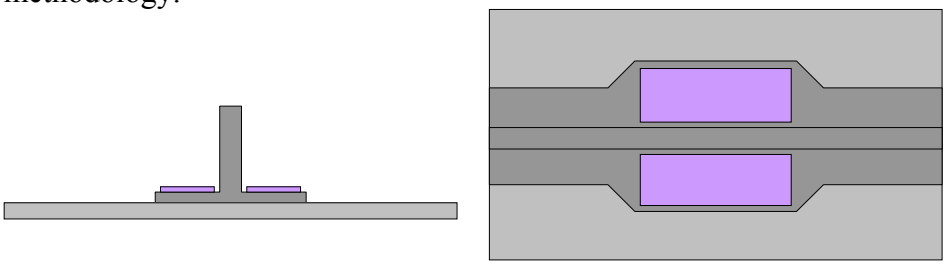

Figure 7-71: Sacrificial ply tabs added to stringer foot in areas of rib integration

Alternatively, sacrificial plies could be added to the spars and ribs, if they are made from CFRP. Conversely, if the ribs are made from aluminium, the rib can be machined to the required dimensions, except for the feet that have excess thickness. As part of a lean manufacturing philosophy, the supplier of the ribs can wait until a thickness tolerance analysis has been carried out on the longer lead-time wing cover, to determine the required thickness of the rib feet. The rib feet can then be post-machined and delivered to the assembly line.

Closed mould tooling could be considered to ensure good tolerances on the IML, however due to the size of the component, it is probably technically infeasible. Closed mould tooling is also problematic when design changes are considered. Alternatively, an IML defined tool could be used and the outer OML profile is defined using large caul plates, as has been used for the Boeing F/A-18 wing skins[404]. It is questionable whether or not caul plates are sufficient to maintain the tolerances required for the OML, and they can leave witness marks. The problems with design changes affecting the IML will be as problematic as for the closed-mould concept. A plausible option could be for a conventional OML tool with local IML tooling at the critical interfaces such as at the rib locations.

[xlii] Presumption is that the stringer is pre-cured prior to assembly.
[xliii] This assumes that the rib will be aluminium.

7.4.2 Outside-In Build Philosophy

If the reference face for the wing box assembly was the OML, then it would be possible to assemble the box independently of the constituent part's thickness tolerance. To realise this, the parts that separate the covers, i.e. the ribs and spars, must be allowed to float. This is achieved by using ribs, as shown in Figure 7-72, and spars that are differential i.e. the attachment flanges are separate, or the flanges are integrated into the covers. With separate feet for the ribs, this will mean that a joint is required both conventionally in the stringer-skin area as well as through the rib web. This will increase the assembly effort considerably, which will be mainly carried out through manual work. There will also be a weight impact, as the joints will typically require extra thickness.

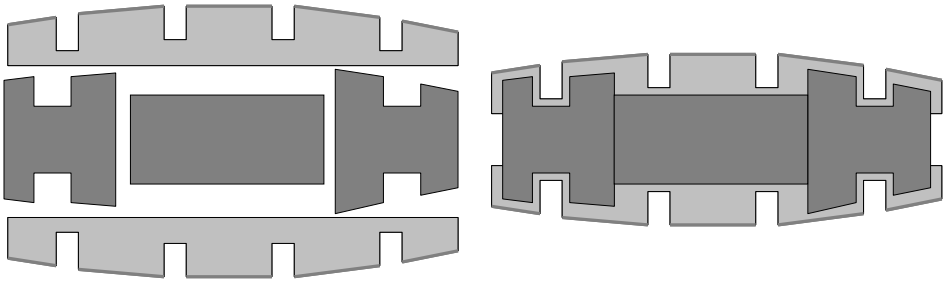

Figure 7-72: Differential rib design

The spar for this assembly philosophy is likely to be heavier, as the spar web, in particular the rear spar is heavily-loaded in shear, and the front spar must withstand the 9g forward crash case[424], therefore having a joint in the web is not optimal. The spar often has penetrations due to the slat tracks and there are many pneumatic, hydraulic and electrical attachment points on the spar web. Therefore, a large joint running along the span is not conducive to this.

Alternatively, the cover could integrate the attachment flanges for the ribs and also the spar if deemed necessary. Intercostals can be integrated between the stringers for rib attachment, as shown in Figure 7-73. The intercostals could also influence the structural behaviour of the cover by supporting the stringer blade to increase the critical Euler buckling load of the blade. The more integrated cover concept could be further enhanced through an integrated spar cap, where effectively a large stringer, which might be interleaved into the cover, is used as the attachment flange for the spar web.

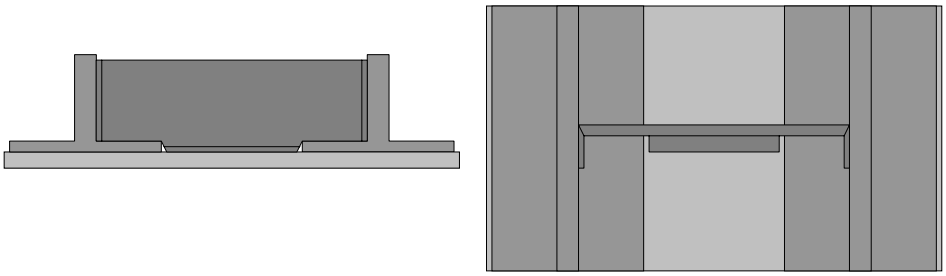

Figure 7-73: Intercostal between stringers

By making the cover a more integrated component, and mitigating against the thickness tolerances, it is limiting the flexibility to counter build tolerances in both the chordwise and spanwise directions. This would mean very tight positional tolerances on the cover features during the cover manufacture, as well as exact positioning of the covers relative to each other during wing box assembly.

It is possible that a compromise could be found where the upper cover has integrated intercostals and the lower cover has conventional flanges bolted to the skin. This can negate against thickness and positional tolerance problems, as well as improve the outer surface quality of the aerodynamically critical upper cover.

7.4.3 Shimming

Gaps up to 0.13mm can be left unshimmed, whereas gaps from 0.15-0.76mm may be filled with liquid shim, or a combination of liquid shim and flat solid shim[498]. However, shimming should only be considered as an ancillary assembly step, not as an implicit step, as it is a time consuming process, and gaps should be minimised through good design and manufacturing.

7.4.4 General Issues

During the early 1990s, when air traffic volume rose, the airline operators conveyed to the aircraft manufacturers that further growth in air traffic will be impeded by the high acquisition cost of the aircraft. One of the reasons for this high acquisition cost is due to the cost of manufacture, and therefore efforts can be made to reduce this. Tolerances are one of the functions of the manufacturing cost of the aircraft and with tighter tolerancing, this results in higher manufacturing costs. Due to the tight manufacturing tolerances, excrescence drag, i.e. drag due to the deviation from a smooth sealed aerodynamic surface, is relatively low, accounting for about 2-4% of the aircraft parasite drag at cruise condition[499,500]. The main features contributing to excrescence drag in the forming of metal/composites are[501]:

- Control of leading-edge profile and surface panel profiles (wings/flaps/empennage, etc)
- Fasteners' flushness for skin joints
- Component surface geometry, subassembly joints, and access panel fitment mismatches

There is little data pertaining to the cost implications of maintaining the tight tolerances specified by the aerodynamicists[501]. Using a multidisciplinary approach, a trade-off could be foreseen between the effect that a change in parasitic drag has on the manufacturing cost. However, as tolerances are relaxed, there will be a subsequent increase in excrescence drag. To put this into perspective, based on full utilisation, a 1% increase in total drag will mean that an extra 100000 and 15000 gallons of fuel is consumed every year, for a Boeing 747 and 737 respectively[500]. Furthermore, it is not just the extra fuel burn that must be considered, but the other cascading issues from this:

- Additional fuel must be carried to meet the payload range
- Reinforcement of related structures is required
- The aircraft cost would increase as more material is used

7.5 System Influence

As the wing box is the primary volume where fuel is held, it is important that this volume is both maximised, to increase range, but also all the available fuel can be used, otherwise this is

just dead weight. This can be achieved using a network of pipes connecting remote pickup points to the fuel pump; however, this will mean a more complicated system architecture, increasing both cost and weight. Furthermore, the fuel pump will no longer be direct feed, therefore the pump will have to be more powerful due to the remote pickups. Alternatively a compliant IML architecture can be sought, to minimise the number of puddles[xliv] formed. Passage holes are also required in the stringer blade to allow fuel to flow through them; otherwise, the blade will act as a local fuel boundary, as shown in Figure 7-74.

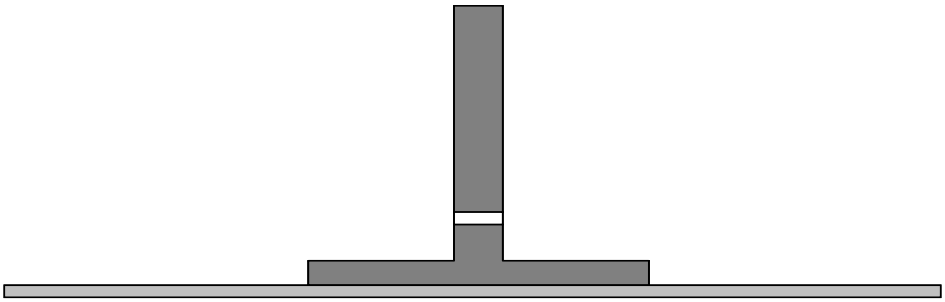

Figure 7-74: Passage hole through stringer blade

Due to the presence of water in the tank[xlv], these puddles will be first filled with water, as water is heavier than fuel. Therefore, in these locations, on the lower cover, water drains will be required, again adding cost and weight to the structure. Water drains are periodically manually used to drain away the water. Water drains could be eliminated if the water could be scavenged away as part of the fuel and burnt in the engine. This procedure may well, serendipitously, solve another issue, in that water will no longer collect in the wing box, which could act as an electrolyte between the CFRP wing covers and metallic ribs, resulting in corrosion of the ribs.

7.5.1 Fuel Tank Painting

As aviation fuels typically contains elements that may be corrosive, it is necessary to paint the internal surface using either epoxy or polyurethane paint[225]. A further benefit, by painting the internal surface with an epoxy-primer, which is typically a yellow-green colour, is that deficiencies, such as cracks, are easier to identify in the constituent parts.

7.5.2 Fuel Tank Sealing

Sealing is required, due to corrosion protection, to inhibit water ingression, and to ensure the integrity of the fuel tank. Polysulfide sealing compounds are typically used, which are available in a range of ways to apply them, with different viscosities and cure times. Fasteners that go through an outer surface are typically "wet" installed through the application of sealant to the fastener prior to installation. For the integration of an aluminium inner structure to a CFRP skin, a glass ply will be required between the two parts as shown in Figure 7-75[190], as well as an interfay sealant. The glass-fibre barrier is extended by 6.35mm greater than the metallic part's footprint[502].

[xliv] This is where fuel would collect due to the architecture of the cover, which effectively cannot be used as it is trapped. This is based on the aircraft being straight and level.
[xlv] Water is always present in fuel, as well as the wing box tank is vented to atmosphere.

For the co-cured, co-bonded and secondary-bonded CFRP to CFRP joints, the adhesive or resin bond itself will form the interfay sealant and fillet seal. Furthermore, there is no need for a glass ply to separate the part, as there are no corrosion issues. Therefore, a pure CFRP joint is far more compliant and thus requires less sealing.

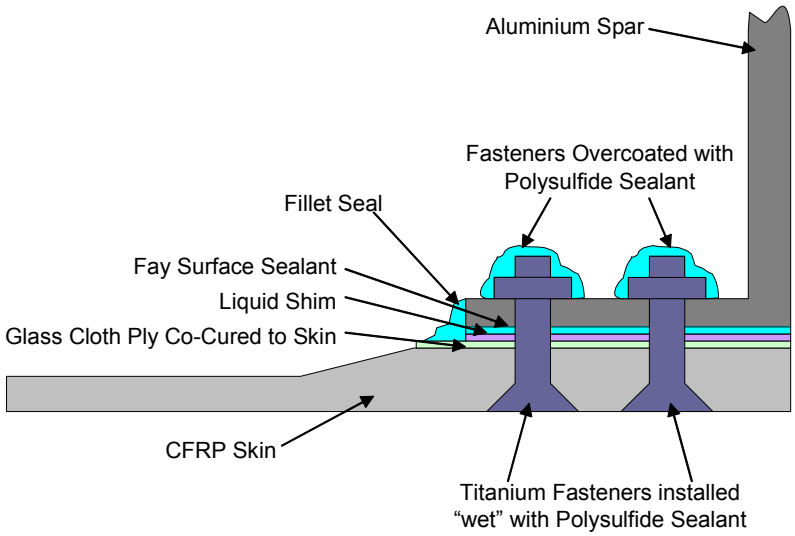

Figure 7-75: Typical wing fuel tank sealing

7.6 Post Buckling Design

In order to maximise the performance of CFRP wing covers from a weight perspective, in particular in comparison to aluminium design, the cover should be designed to work in the post-buckling range[503]. From experienced gained with aluminium post-buckling structures, if the stringers are correctly designed relative to the cover, the skin can buckle but the complete structure can take a load several times higher than at which the first buckling mode occurs in the skin[503]. Thus, the upper limit of the post-buckling range is the compressive strength of the material[504]. However, post-buckling can cause a reduction in torsional stiffness of the complete box[465]. Further issues that impinge on a CFRP post-buckling design, is a smaller margin between the strain at which local buckling occurs, and the allowable strain.

Due to the buckling of the skin, this will result in large out-of-plane forces, which are poorly reacted by laminated structures[475]. This will also induce large out-of-plane forces into the stringers, which can lead to the stringers being pulled off the skin, as the stringer not only has to react the greater in-plane loads but also the out-of-plane loads. This can be improved by reducing the relative difference in flexural (torsional and bending) stiffness of the stringer foot and the skin[431,478], which is determined by the number of ±45° plies in the stringer foot. This, however then limits the ability to optimise the structure for its in-plane loads. Furthermore, co-curing should be considered, to minimise the risk of defects in the bondline[505], as well as Z-pinning to enhance the strength of the joint[445].

Other issues also include the aerodynamic constraints imposed on the wing's profile, which means that skin buckling should not occur. Furthermore, the minimum wing skin thickness may not be determined by stability requirements, but instead by lightning strike requirements. Therefore, the structure might be too thick to be used for post-buckling.

Finally, post-buckling of CFRP structures is very complex, as its prediction is both difficult and design procedures are inadequate[503,506]. CFRP structures that are designed for post-

buckling are based on detailed FE analysis, which are verified by thorough experimental tests. This creates a continuous and expensive interaction between numerical analysis and experiments to create a validated design[503].

7.7 Aeroelastic Tailoring

A good definition for aeroelastic tailoring is[507]: "Aeroelastic tailoring is the embodiment of directional stiffness into an aircraft structural design to control aeroelastic deformation, static or dynamic, in such a fashion as to affect the aerodynamic and structural performance of that aircraft in a beneficial way."

The optimal shape of the wing is dependent on the particular stage of flight; hence the necessity for discrete moveable surfaces, attached to the leading and trailing edges, to vary the camber and angle of attack of the wing during flight. The standard wing shape is optimised for a particular flight condition, which is usually cruise condition. High-lift devices can be quite sophisticated on large transport aircraft, with leading edge slats and trailing edge multi-element flaps. Such devices add both weight and complexity to the wing, hence the reason for trying to encompass aeroelasticity into the wing design to lessen the dependency on complex high-lift devices.

When a wing box is subjected to a typical flight load, the lower cover will be subject to tensile loads, while the upper cover will be in compression. The forces will cause opposite extension in each cover panel, and with the extension-shear coupling, this causes opposite shear deformation, as illustrated in the LHS of Figure 7-76[508]. The deformation in the upper and lower covers will induce a torque, which causes the complete box to twist, as shown in the RHS of Figure 7-76.

The aeroelastic advantages of CFRP material is well known, with unbalanced laminates providing opportunities for aeroelastic tailoring, creating coupling between the bending and twisting behaviour of the laminate, as well as between the in-plane stretching and shearing[509]. The magnitude of the shear-extension and bend-twist coupling terms, will be dependent on the number of plies and the stacking sequence. As the number of plies increase, the coupling terms tend to diminish.

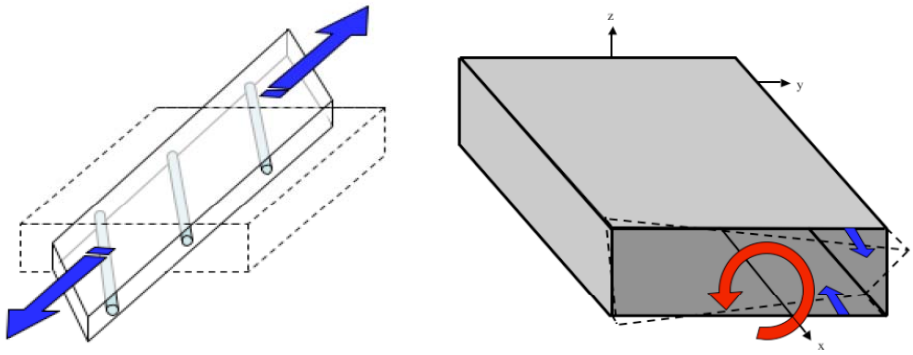

Figure 7-76: Box bend-twist coupling caused by laminate shear-extension coupling

By taking advantage of aeroelasticity, this can lead to both direct and indirect benefits. By tailoring the laminate stiffnesses, the wing box can predictably deform under an applied load so that it is directly beneficial to the aircraft performance, as shown in Figure 7-77. This can be beneficial in controlling the torsional deformation of the wing box, to maintain structural wing wash-out. Wing wash-out is a desirable characteristic as it lowers the wing tip's angle of

attack relative to the root. This ensures that if the wing should stall, then this occurs first at the root, which improves the handling characteristics of the aircraft. Likewise, aeroelastic tailoring can be used to mitigate wash-in, which is not desirable. Thus, aeroelastic tailoring can indirectly lead to the ailerons requiring less deflection to trim the wing, which in-turn reduces the actuator power and its weight[510].

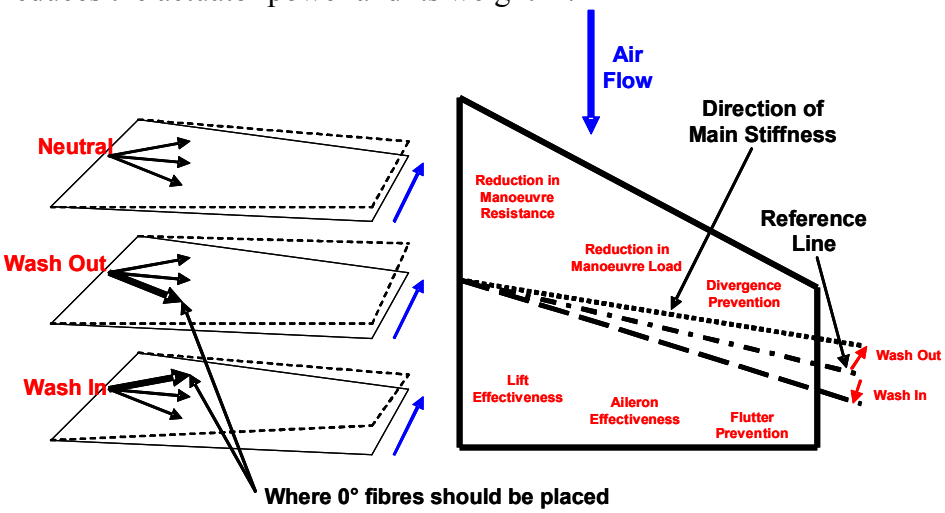

Figure 7-77: Wing tailoring

As shown in Figure 7-78, an alternative to an asymmetric laminate is to tailor a balanced laminates, using either[508]:

- Laminate Rotation
- Angle Ply Rotation

The laminate rotation uses an orthotropic laminate, whose principal material axes are not aligned with the structural natural axes. The angle ply rotation technique, which has unbalanced angle plies i.e. no counterbalancing –θ° plies for every +θ° plies, with the 0° and 90° plies to provide directional stiffness. The angle ply rotation technique can be advantageous in comparison to the laminate rotation technique, as all plies make a contribution towards the desired behaviour[508]. Both techniques do not necessarily create asymmetrical stacking sequences about the mid-plane.

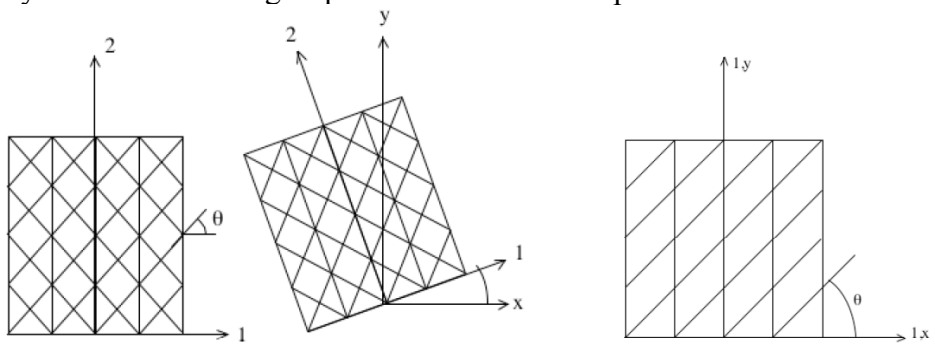

Figure 7-78: Laminate rotation (LHS) and angle ply rotation (RHS)

An investigation was conducted with ESDUpac A0817 and max strain theory to investigate the effects of rotating the skin laminate's principal orientations. Five different laminates were investigated as shown in Figure 7-79. Laminate A was conventionally orientated, whereas Laminate B rotates all 3 orientations 15° clockwise, whereas Laminate C, D and E, rotates individually the 0°, 45° and 90° orientations 15°, respectively. These laminates were applied

to 4 different realistic stringer-stiffened panels, with dimension as shown in Table 7-24, with the basic laminates for the skin and stringers being 44/44/11 and 60/30/10, respectively.

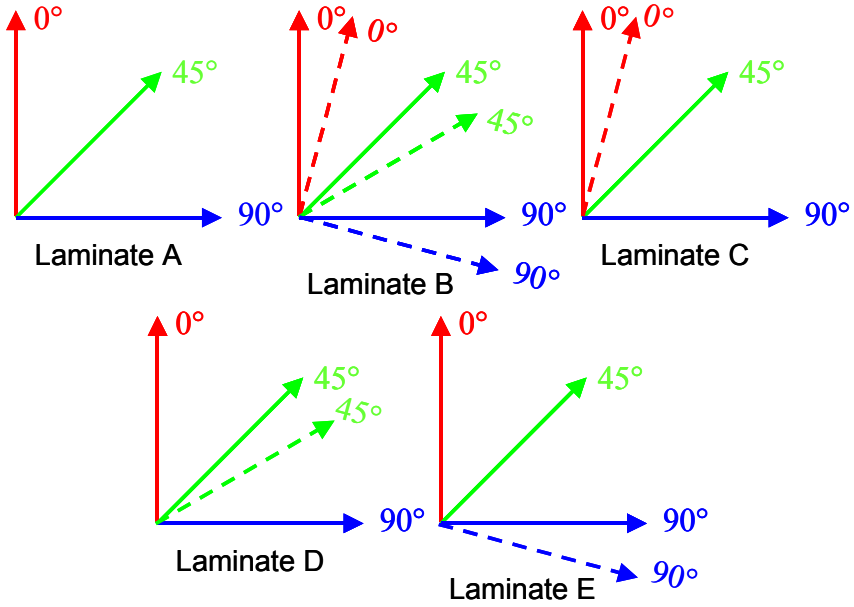

Figure 7-79: Laminates types and orientations

Elements	Config. A (mm)	Config. B (mm)	Config. C (mm)	Config. D (mm)
BH	35	35	50	47
BT	6.808	6.624	10.304	8.096
LFW	50	50	68	68
LFT	2.944	2.944	2.944	2.944
SP	165	165	165	165
ST	4	5.75	6	9.75

Table 7-24: Basic dimensions

		Running Load (N/mm)				Panel Checks		Performance Improvement	
		Nx	Ny	Nxy	Nxy as % of Nx	EAstr (%)	v	Stability (%)	Strength (%)
Config. A	Laminate A	-440	7	195	44	40	0.07	100	100
	Laminate B	-440	7	195	44	46	0.00	105	105
	Laminate C	-440	7	195	44	44	0.17	100	115
	Laminate D	-440	7	195	44	42	0.10	106	83
	Laminate E	-440	7	195	44	41	0.12	99	105
Config. B	Laminate A	-385	1	-160	42	34	0.18	100	100
	Laminate B	-385	1	-160	42	40	0.04	104	96
	Laminate C	-385	1	-160	42	38	0.27	101	104
	Laminate D	-385	1	-160	42	36	0.07	101	85
	Laminate E	-385	1	-160	42	35	0.22	101	102
Config. C	Laminate A	-2095	-62	312	15	49	0.19	100	100
	Laminate B	-2095	-62	312	15	56	0.01	101	91
	Laminate C	-2095	-62	312	15	53	0.28	99	96
	Laminate D	-2095	-62	312	15	52	0.07	103	91
	Laminate E	-2095	-62	312	15	50	0.24	99	100
Config. D	Laminate A	-2576	-41	-347	13	41	0.14	100	100
	Laminate B	-2576	-41	-347	13	37	0.00	99	86
	Laminate C	-2576	-41	-347	13	35	0.23	100	93
	Laminate D	-2576	-41	-347	13	34	0.08	98	91
	Laminate E	-2576	-41	-347	13	32	0.19	100	100

Table 7-25: Effect of skin laminate rotation on stringer-stiffened panel

From Table 7-25 it can be seen that configurations A and B have a fairly low axial load, but a relatively high proportion of shear load, whereas configurations C and D have higher compressive axial load, but a lower proportion of shear in comparison to axial load. It can also be seen from Table 7-24 that for configurations A and B, the skin is fairly thin and

therefore the structure should be stability critical, whereas configuration C and D have a fairly substantial structure, therefore it should be more strength critical. As shown in Table 7-25, for the thinner panels, in general, by rotating the entire laminate by 15%, this can benefit both stability and strength performance. However, for thicker panels, there is no benefit. It would also seem that from every configuration, by rotating just the whole laminate by 15°, this reduces the Poisson's ratio down to almost 0.

7.8 Summary

This chapter has brought together all issues that affect the design of a CFRP wing box, and in particular, the wing cover. Only a few of the topics previously discussed can be incorporated into an optimisation program at the preliminary design phase, however it is crucial to a well designed wing cover that all the above topics are considered. For instance, the SRO issue can only be incorporated into the optimisation routine in that the stringers are terminated at the ribs and that they are designed in such a way that they do not pose a constraint on the global cover, such as a poor design could limit the allowable strains.

In general a CFRP cover will have a similar configuration to a traditional metallic cover, although a well designed CFRP cover should be lighter. The lower cover heavily influences the stringer layout, with the manholes typically being placed mid-chord of the wing box with the stringers running parallel to manhole row and each other.

This chapter has also highlighted that the heaviest parts of the wing box are the wing covers, and thus they should be well optimised. Only 3 stringer profiles will be considered for the optimisation, namely the U-, T- and I-profiles. Despite the top-hat-profile potentially being more efficient for stability critical structures, often this increased efficiency cannot be used, as the resultant strain in the structure is higher than the allowable strain. Furthermore, there are a number of other issues with a top-hat-profile stringer. When optimising a stringer-stiffened panel it is necessary to consider compression, shear and OOP loads. The proportion of cross sectional area between the stringer and the skin is dependent on the loading, although to resist OOP loads a substantially thick blade is required. Furthermore, for a discrete stringer, the stringer foot thickness to skin thickness is critical to the damage tolerance of the cover.

The stringer itself should be fairly straightforward to optimise, as for all stringers it is really only the blade that can be optimised, except for the I-profile stringer, where the upper flange width can also be varied. All other dimensions are dependent on other factors, such as bolted repair, or ratios governing the skin thickness to stringer foot thickness. The fabrication of stringers can result in asymmetry, however the affect of this has been shown to be limited. The stringer pitch is dependent on the fuselage frames, due to overall aircraft integration issues, whereas the minimum stringer pitch is limited for discrete stringers due to the minimum width of the stringer foot. In general the U-profile stringer-stiffened panel should be the most efficient, however due to stacking sequence rules and transfer of shear through the skin, the ability to optimise an integral panel is restricted.

The certification requirements impose a large constraint on the wing cover; hence, this must be built into the optimisation routine, which can impose limitations on the amount of load that the stringer should react. Typically the damaged panel state is considered the most stringent.

8 Optimisation Procedure

8.1 Introduction

Today's aircraft have a very high standard of technical prowess, which has been made partly possible through the use of numerical analysis tools and automated optimisation routines that continue to improve in their applicability and accuracy. The founders of structural optimisation are Maxwell and Mitchell[511], whose work dates back to 1904. The premise of structural optimisation is to find a solution with the optimum performance while satisfying all design criteria. An optimiser is a computational approach, used to automate an iterative mathematical process to search for the best solution, the accuracy of which is dependent on the level of discretisation. Through employing optimisation techniques, it is possible to explore the design space more thoroughly, allowing greater trade-offs to be performed between different designs.

The benefit of employing optimisation tools should be quantified in terms of the cost of implementation with respect to the number of person years that it can save. However, it has been evidenced by Vanderplaats (1999)[511] that optimisation tools never reduce engineering costs as the engineering community will still use all available time and budget to achieve the result. Therefore, the aim of using optimisation tools should be either to produce a better design in the original time frame, or better still reduce the design cycle and then move onto the next project. However, despite the widespread application of optimisation programs, they should not be considered a principal design tool[512], instead they should be considered as an aid to relieve valuable engineering resources.

An optimisation problem is expressed as an objective function of a number of variables, which are to be minimised and maximised, when subjected to a number of constraints, for example[511]:

$$Minimise \quad F(X) \tag{8-1}$$

When subjected to:

$$g_j(X) \le 0, \qquad j = 1, m \tag{8-2}$$

$$X_i^L \le X_i \le X_i^U, \qquad i = 1, n \tag{8-3}$$

Where $F(X)$ is the objective function, which is dependent on the values of the design variables X, which themselves include member dimensional or shape variables of a structure. Equation 8-2, states the constraints, which provide the boundaries on various response quantities. A strain limit is typically used to constrain a CFRP structure, therefore, if $\bar{\varepsilon}$ is the maximum allowed stress, then the constraint function can be written as[511]:

$$\left(\varepsilon_{ijk} / \bar{\varepsilon}\right) - 1 \le 0 \tag{8-4}$$

Where i = element, j = stress component, and k = load condition.

The limits on the design variables in Equation 8-3 are known as side constraints, and these limit the region of search for the optimisation. An example of this would be for the thickness of a part being set between allowable limits.

8.1.1 Optimisation Methods

There are several advantages of numerical optimisation methods, such as[513]: reduction in design time; improvement in design quality; can deal with many variables and constraints; and systematised logical design procedures. However, there are also some limitations to this type of optimisation, such as[513]: the technique is limited to the rules/methods of the optimiser; incomplete problem formulation, i.e. when a constraint is ignored, can lead to meaningless results; and the computational power will limit the number of variables and constraints etc. Optimisation tools fall loosely into two categories[512], albeit they can be interrelated:

- Computational Based – such as Multidisciplinary Optimisation
    - Relies on a predetermined set of existing computational tools and geometric models to generate data and information that is interpreted by computer and to a lesser extent by the engineer
    - The interpretation is in isolation of the historical database and is based solely in the context of the existing design activity
    - The main assumption is that an optimum design can be found. This implies that within the tool the optimum design process and knowledge is fully modelled and that the computer can converge to an optimum solution
    - The motivation for this approach is:
        - A computer is more efficient and accurate than a human
        - Total system costs are lower than a human
    - However, this method is limited because:
        - It is bounded by a set of pre-existing data and information
        - It is restricted to only explicit knowledge
        - It fails to use tacit and intuitive knowledge

- Knowledge Based Engineering (KBE) – such as decision-based design
    - An activity that requires all knowledge to find the optimum design
    - Is based on human knowledge that grows and can be used to guide a design
    - The data, information and knowledge generated in the design activity are explicitly and implicitly integrated into the design knowledge base, and then the full knowledge base is interpreted in the context of all relevant data, information, and knowledge

		TO	
		TACIT	*EXPLICIT*
FROM	*TACIT*	Socialisation (Brainstorming)	Externalisation (Writing)
	EXPLICIT	Internalisation (Learn by Doing)	Combination (Meetings)

Figure 8-1: Four modes of knowledge creation

To design an optimum part, it will require a cognitive awareness of all knowledge relative to a desire[512]. An engineer is a passionate and knowledgeable decision maker who utilises critical and intuitive skills; whereas the design of a product is a creative practice that simulates and is learned through the acquisition of knowledge[512]. Shown in Figure 8-1[514] are the four modes of knowledge creation, where information can be both tacit and explicit. Computational based methods only use two modes; tacit to explicit and explicit to explicit knowledge steps, whereas KBE uses all four modes[512].

Optimisation tools, particularly Computational-Based, are most useful at the conceptual and early detailed design phase of the product design cycle, and this is where they are applied today. KBE optimisation approach can be used when the design is iterative; however, for unconventional designs where little information exists, Computational-Based analytical tools are more suitable[515].

8.1.1.1 Computation-Based Approach

Computational-based approach to structural optimisation can be sub-categorised into two groups:

- Analytical Methods
  - Based on the mathematical theory of calculus, variational methods for studies of optimal layouts etc
- Numerical Methods
  - Mathematical programming, where a near optimal design is automatically generated in an iterative manner. Often it is better to provide an initial guess so that a good starting point can be provided

8.1.1.2 Knowledge Based Engineering

To create competitive advantage it is necessary to be innovative[516]. Innovation can be in both the products manufactured as well as the processes within the organisation, and they can be either radical or progressive[129]. People are vital to innovation due to the tacit knowledge held within the person, and their interaction inside and across organisations[516]. For this very reason, Knowledge Management (KM) is crucial to the competitive advantage of the firm. The effective management of knowledge has shown to be beneficial in terms of reducing project duration, enhancing quality and customer satisfaction[517]. If knowledge is not captured then this can lead to blighted project performance due to duplication. Knowledge that can be converted to create value and profit can be defined as intellectual capital. Knowledge is taken from three sources:

- Design Object Knowledge
  - Depicts the objects structure, its components, and how they are related
- Design Cases
  - Records a design problem and how it was decomposed into sub-problems
- Functional Knowledge
  - Shows the connectivity between functional descriptions and the design objects

As shown in Figure 8-2[512], the opportunities to impact on performance or the cost of the design are influenced heavily at the conceptual stage. If it would be possible for more information to be available at the conceptual stage, then greater cost and performance benefits could be achieved. This can be accomplished by using KBE.

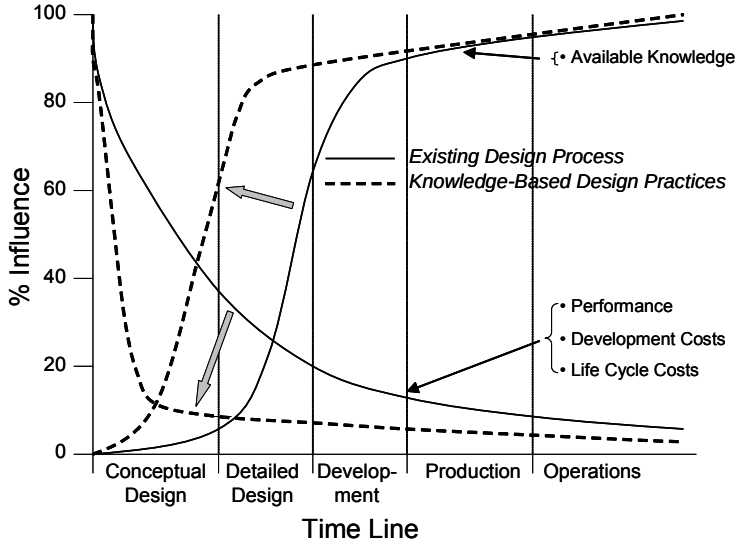

Figure 8-2: Influence of knowledge on performance and cost in design

8.1.2 Multi-Disciplinary Optimisation

Complex engineering systems, consisting of different sub-systems, can no longer be designed in isolation. This can be achieved using a synergistic design process, which then stipulates that a more comprehensive strategy is required[518]. This can be encompassed in an MDO methodology, which should promote collaboration and replace the typical un-quantified, politically biased, trade-offs between the different disciplines. MDO is an optimisation problem where the constraints and/or objective functions are derived from more than one discipline, and where it can find a holistic optimal solution for sometimes conflicting requirements. It also ensures interdisciplinary, instead of sequential, interaction.

MDO is defined as "A methodology for design of complex engineering systems that are governed by mutually interacting physical phenomena and made up of distinct interacting subsystems in their design, everything influences everything else"[519]. MDO methods have been developed since the 1980s, which is also the same time period where computational power has increased dramatically, hence its ability to handle large amounts of data. Formal MDO can provide enormous capabilities to a design team[40]. MDO can assist in introducing new technologies by holistically considering the interaction between different disciplines and controlling the resultant complexity in the design process[520]. The ultimate aim of MDO will be to incorporate as many disciplines into the optimisation framework, which will result in an increase in the number of different design variables and constraints within the problem.

Traditional MDO has, however, overlooked the issues of cost, and instead focused primarily on system performance. If cost was included at all, then it was based solely on the weight of the product[521], which is both inadequate and even misleading. The Defense Manufacturing Council has requested that cost should be given equal parity to weight, as a design variable[32]. It is known today that from the early stages of aircraft development, design decisions should

be based upon the aircraft's operating cost[522] and not just on it's weight, which can then lead to the creation of overall feasible designs[523].

The MDO optimisation is an evolutionary process, and for this reason, the infrastructure of the MDO must be created so that it can be easily developed further[54]. An MDO tool, which is a 'black box' that requires no interaction or understanding of the process, could result in misinterpretation of the analysis results. It is very important that the human interface must be able to aid the engineer in understanding and directing the MDO process[524].

8.1.2.1 Previous Cranfield MDO Work

Previous Cranfield endeavours into this field were carried out by Gantois[54], who worked within a European funded project and investigated the application of MDO to the design of the A3XX (A380) wing, by considering factors such as weight, drag and manufacturing costs. The objectives of the MDO, was to provide the various European partners, the ability to use their own in-house analysis tools but within the control of an MDO. This required all disciplines to submit their analysis tools, and use a language such as FORTRAN or ASCII to link them.

Gantois investigated the initial conceptual stage of the design process, with geometric design parameters such as wing sweep angle, aspect ratio, planform area, spar position, wing depth and twist. Secondarily, the internal layout of the wing was considered such as the number of ribs and stringers[54]. Manufacturing cost was conducted at a sub-level in the optimisation, which meant that the recurring cost did not affect the final assessment of DOC, which was not an optimum procedure[54].

8.1.3 Optimisation Algorithms

Deterministic procedures create an objectively robust optimum design through measuring analytically the robustness of an alternative design with its first-order derivative or other non-statistical concepts to ascertain and then incorporate those measures into the procedure[525]. Deterministic gradient-based optimisation techniques can be used if there are only a few thousand design variables and the gradient information is available[518]. However, where there is a mix of continuous, discrete, and integer type design variables then gradient-based approaches are not optimum. If the problem is multi-modal, requires approximations, is non-differentiable, or comprises of multiple objectives techniques, an Evolutionary Algorithm (EA) is required[526].

EAs require no derivatives or gradients of the objective function, can search for the globally optimum solution within many local optima, be executed in parallel and can be used with arbitrary solver codes without major modification[526]. EAs can also solve multi-objective problems directly. Alternatively, a GA is an elitist reproduction strategy based on the Darwinian principle of the survival of the fittest, with chromosomal representation of design evolved using random actions encompassed in operations like crossover and mutation, with bias to those that are deemed to be more fit at any stage of the evolution process. The optimum design is then improved by creating successive generations. However, non-gradient methods may require far greater computational resource to find the global solution in comparison to gradient methods[527], due to the many searches that they have to perform.

8.2 Previous Optimisation Research

8.2.1 CFRP Skin Optimisation

Various research has been carried out into CFRP skin optimisation, such as Adams (2005)[349], Soremekun et al.[348], Le Riche et al.[528] and Liu (2001)[347], typically, using a GA to find the optimum laminate under the constraints of stability and strength. Liu incorporated a penalty function, for laminates that had more than 4 contiguous plies of the same orientation, so that laminate design rules could be considered[347]. Similarly, Todoroki and Haftka[529] introduced a recessive repair based on the Baldwinian techniques for the contiguity constraints. The principal idea of Baldwinian repair is that the stacking sequence is repaired and not the chromosome, thus if there are more than 4 plies of the same orientation, then those plies in error are moved in the stacking sequence, such as $[0_2/0_2/90_2/90_2/90_2/\pm45]_s$ changes to $[0_2/0_2/90_2/90_2/\pm45/90_2]_s$.

8.2.2 Stiffened Panel Optimisation

The optimisation of stringer-stiffened panels has been a field of endeavour since the beginning of monocoque aircraft design in the 1930s. At the preliminary design stage, basic structural efficiency is sought, thus parametric studies of stiffened panels are conducted which, amongst other aspects, optimise the stringer type and the proportioning of the thickness in the stringer elements and the skin. These studies are performed afresh for every new design, as the loading intensity and distribution may be different, more advanced materials are available, lessons have been learnt from previous optimisations, and the mission requirements could be different. Furthermore, the manufacturing techniques chosen can determine the choice of stringer type and the ability to tailor the structure.

There are many different stringer types; however, experience should be taken into consideration and only the stringer configurations that are deemed applicable should be down selected for optimisation. Even for a relatively simple T-profile stringer-stiffened panel, there are many dimensional variables to consider, such as: stringer pitch, skin thickness, stringer blade height and thickness, and stringer foot width and thickness.

Due to the isotropic nature of metallic structures, it is possible to derive equations to help determine geometry of stiffened panels for various stringer profiles. With reference to Niu's book '*Airframe Stress Analysis and Sizing*'[530], there are a number of different metallic stringer-stiffened panels listed, with efficiency ratings. These efficiency ratings were taken from work conducted by Emero and Spunt[531,532], who developed a series of equations to assist, at the preliminary design phase, the sizing of stringer-stiffened panels. The equations were implemented in a simple spreadsheet, to calculate the required dimensions for the four different stringer-stiffened panels, at different load levels. The dimensions for the "Integral Blade", "Integral I", "Zee" and "top-hat" stiffened, are shown in Table 8-1 to Table 8-4.

These dimensions were compared against ESDUpac A9816[533] and ESDU data sheet 73007[534], as shown in the bottom two rows of Table 8-1 to Table 8-4. It can be seen that the simple "Integral Blade" shows good correlation between the given geometry from the papers, and the critical load from the ESDU methods, whereas the other stringer types show reasonable

correlation. These values were further checked against another unreleased ESDU program[xlvi] for metallic stringer-stiffened panels, which can investigate both elastic and plastic behaviour, by adding in the reference stress (f_n) and the material characteristic. This program gave very similar results to ESDUpac A9816.

Nx as input into equations (N/mm)	-1000	-2000	-3000	-4000	-5000	-6000
SP (mm)	68.51	81.47	90.17	96.89	102.45	107.23
ST (mm)	1.66	2.35	2.87	3.32	3.71	4.07
BH (mm)	44.53	52.96	58.61	62.98	66.59	69.70
BT (mm)	3.73	5.28	6.47	7.47	8.35	9.15
BH / SP	0.65	0.65	0.65	0.65	0.65	0.65
BT / ST	2.25	2.25	2.25	2.25	2.25	2.25
Critical Nx from ESDU 98016 (N/mm)	-995	-1946	-2973	-3961	-4574	-5787
Critical Nx from ESDU 73007 (N/mm)	-971	-1943	-2905	-3873	-4831	-5802

Table 8-1: Dimensions and critical running loads for integral blade

Nx as input into equations (N/mm)	-1000	-2000	-3000	-4000	-5000	-6000
SP (mm)	49.66	59.06	65.36	70.23	74.26	77.72
ST (mm)	1.75	2.47	3.02	3.49	3.90	4.28
BH (mm)	39.73	47.24	52.28	56.18	59.41	62.18
BT (mm)	1.22	1.73	2.12	2.44	2.73	2.99
UFW (mm)	23.84	28.35	31.37	33.71	35.64	37.31
UFT (mm)	1.22	1.73	2.12	2.44	2.73	2.99
BH / SP	0.80	0.80	0.80	0.80	0.80	0.80
BT / ST	0.70	0.70	0.70	0.70	0.70	0.70
Critical Nx from ESDU 98016 (N/mm)	-1024	-2011	-2729	-3358	-3968	-4564
Critical Nx from ESDU 73007 (N/mm)	-1045	-2093	-3135	-4172	-5218	-6284

Table 8-2: Dimensions and critical running loads for integral I

Nx as input into equations (N/mm)	-1000	-2000	-3000	-4000	-5000	-6000
SP (mm)	81.96	97.47	107.87	115.92	122.57	128.28
ST (mm)	1.36	1.93	2.36	2.72	3.05	3.34
SH (mm)	40.98	48.74	53.94	57.96	61.28	64.14
WT (mm)	1.26	1.78	2.18	2.51	2.81	3.08
LFW (mm)	12.29	14.62	16.18	17.39	18.38	19.24
LFT (mm)	1.26	1.78	2.18	2.51	2.81	3.08
UFW (mm)	28.69	34.12	37.76	40.57	42.90	44.90
UFT (mm)	1.26	1.78	2.18	2.51	2.81	3.08
SH / SP	0.50	0.50	0.50	0.50	0.50	0.50
WT / ST	0.92	0.92	0.92	0.92	0.92	0.92
Critical Nx from ESDU 98016 (N/mm)	-917	-1818	-2702	-3558	-4351	-5335
Critical Nx from ESDU 73007 (N/mm)	-619	-1237	-1839	-2425	-3044	-3640

Table 8-3: Dimensions and critical running loads for top-hat

[xlvi] ESDUpac AS770v1.0 "advanced copy" received directly from ESDU Organisation.

Nx as input into equations (N/mm)	-1000	-2000	-3000	-4000	-5000	-6000
SP (mm)	47.98	57.06	63.14	67.85	71.75	75.09
ST (mm)	1.40	1.98	2.43	2.80	3.13	3.43
BH (mm)	41.74	49.64	54.93	59.03	62.42	65.33
BT (mm)	1.49	2.10	2.57	2.97	3.32	3.64
Skin Flange Width (mm)	14.01	16.99	19.05	20.68	22.05	23.24
Skin Flange Thickness (mm)	1.49	2.10	2.57	2.97	3.32	3.64
Free Flange Width (mm)	14.01	16.99	19.05	20.68	22.05	23.24
Free Flange Thickness (mm)	1.49	2.10	2.57	2.97	3.32	3.64
BH / SP	0.87	0.87	0.87	0.87	0.87	0.87
BT / ST	1.06	1.06	1.06	1.06	1.06	1.06
Critical Nx from ESDU 98016 (N/mm)	-952	-1743	-2409	-3041	-3611	-4169
Critical Nx from ESDU 73007 (N/mm)	-969	-1930	-2904	-3863	-4833	-5804

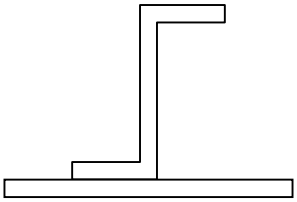

Table 8-4: Dimensions and critical running loads for zee

At a load level of 4000N/mm, the load versus wavelength, using ESDUpac A9816, is shown in Figure 8-3. The curves for the "Integral I" and "Zee" are similar, due to both types having an upper flange. For the "top-hat", there is a distinctive peak in load capability; thereafter, it goes into a global buckling mode, whereas the "Integral Blade" seems fairly insensitive to load over the wavelength.

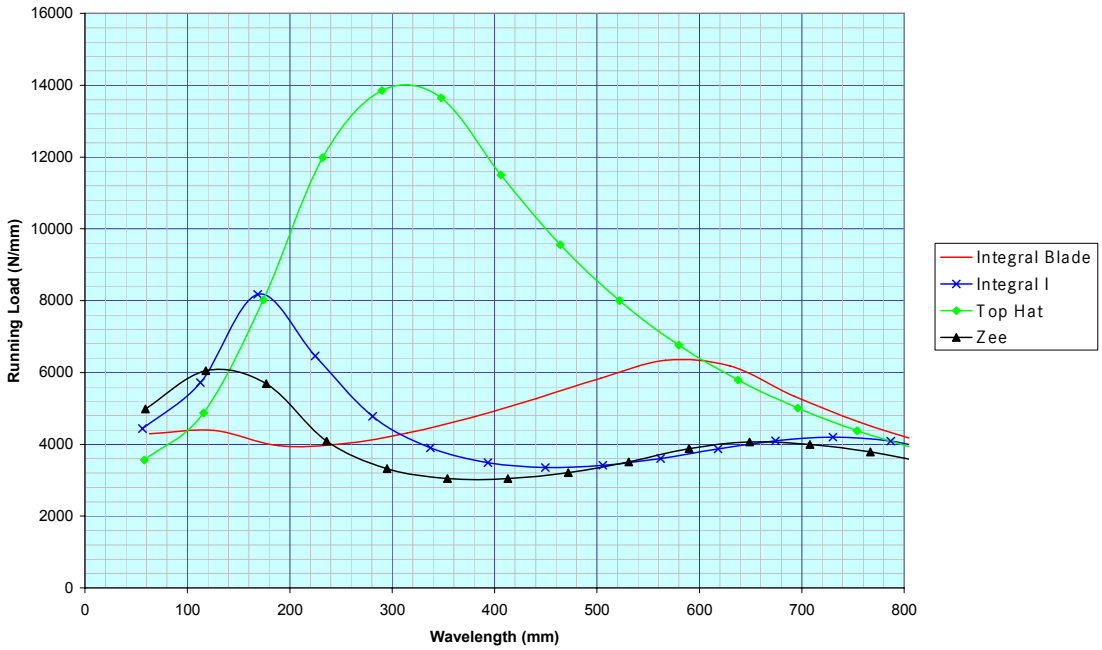

Figure 8-3: Comparison of P-λ curves for different stringer sections at 4000N/mm

To ensure the determined stringer dimensions were optimal, the dimensions of the panels were varied, while maintaining the equivalent effective area. Typically, a higher critical running load could not be achieved by varying the proportioning of area, thus such simple formulae are very efficient at sizing metallic stringer-stiffened panels.

8.2.2.1 Laminated Stiffened-Panels Specific Tools

In comparison to metallic structures, designing with composites has a larger number of variables and is nonlinear, thus simple linear equations[531], or design curves[534], are not applicable. The first automated optimisation methodologies were developed in the 1970s,

such as by Stroud and Agranoff (1976)[485]. They used a program based on non-linear mathematical techniques to optimise hat-stiffened and corrugated panels, using simplified buckling equations as constraints. The design variables were the width and thickness of the individual elements of the panel. It was assumed that the laminates were orthotropic; therefore possible flexural anisotropy was not considered. Subsequently, the importance of flexural anisotropy, and under which circumstances it should be considered, has been characterised by Nemeth[535]. This has also been incorporated into recent work performed by Weaver (2006)[536]. Venkataraman et al.[537] have reviewed some of the major programs developed to optimise stringer-stiffened panels, such as:

- PANel Design Analysis (PANDA & PANDA2)
- STructural Analysis of General Shells (STAGS) [Nonlinear shell FE analysis]

Particular mention is given to VIPASA (Vibration and Instability of Plate Assemblies including Shear and Anisotropy) and programs based on this. VIPASA is a general algorithm for determining the buckling loads of structures, based on an assembly of prismatic panel components, using 'exact FSM', where the field equation is solved using the exact solution of governing differential equations[464]. VIPASA was developed further by NASA[538], which became part of Panel Analysis and Sizing COde (PASCO)[539], combining VIPASA with an optimisation methodology called CONstrained function MINimisation (CONMIN)[540].

As VIPASA underestimated the buckling load under shear load[541], due to the inexact matching of boundary conditions under shear loading, the program VIPASA with Constraints (VICON)[542] was developed and subsequently incorporated into the VIPASA with Constraints and Optimisation (VICONOPT)[543] program. VICON is based on an approximate method for panels with finite length, with simply supported boundary conditions at the panel's ends. The boundary conditions are implemented by representing a buckling mode corresponding to a general applied load with a series of complex sinusoidal terms of various half-wavelengths[542]. However, a limitation of this method is that the compatibility of the structure with the end conditions is not continuous, instead it is enforced at a set of collocation points using the Lagrange multiplier technique[544]. VICONOPT can also take into consideration lateral pressures and global imperfections, using a rational method, instead of just applying a knockdown factor[469]. Liu et al. (2006)[545] compared the results of VICONOPT against those of both linear and non-linear ABAQUS FE as well as experimental testing. Table 8-5[545] shows that VICONOPT, which is based on an FSM method, has very similar results to the linear FE results, as well as the experimental results.

Panels	Results	VICONOPT	ABAQUS		Experiment
			Linear	Nonlinear[xlvii]	
3-Blade	Initial Buckling Load (kN)	1397	1396	1362	1378
	Initial Buckling Strain (με)	4482		4330	4400
2-Balde	Initial Buckling Load (kN)	1259	1205	1150	1160
	Initial Buckling Strain (με)	5331		4649	4528

Table 8-5: Summary of initial buckling results for T-profile stringer-stiffened panel

[xlvii] Nonlinear results calculated with a full cosine-wave imperfection over the length of the panel of amplitude 0.5 mm causing increased compression in the stiffener at the panel centre.

8.2.2.1.1 Closed-Form Equations

PANDA 2[546] uses closed-form formulae to calculate the local and global buckling of various stringer-stiffened structures, which can be loaded with up to 5 combinations of in-plane loads, edge moments, normal pressure, and temperature[547]. Using closed-form formulae is the simplest method of stability analysis for CFRP structures. Such formula were first developed by Timoshenko & Gere[548] and Lekhnitskii[285] for isotropic and orthotropic laminates. For local buckling analysis it is necessary to consider each element of the stiffened panel separately, e.g. for a discrete T-profile stringer, the skin, foot and blade must be individually calculated. Whereas, to analyse the global buckling the whole section has to be considered. Furthermore, the axial and shear loads are calculated separately, with their cumulative effect considered using an interaction formula.

However, there are a number of shortcomings with closed-form formulae. The first issue is that laminates typically have some form of anisotropy, which makes the analysis using these simple formulae inaccurate[536]. Furthermore, despite closed-form formulae being adequate for the analysis of closed-profiles, they are inadequate for open-profiles[549]. This is because open-profile stringers have a more complicated stringer twisting behaviour, which includes both overall stringer torsion, coupled with local bending of the stringer web. As the two modes are interdependent, and a pronounced interaction between the two can occur, this can result in large errors. Programs such as STAGS and VIPASA give exact solutions for buckling modes of open-profile stringers, as they satisfy the conditions of the problem within the limits of linear elastic, Kirchhoff thin-plate theory. However, despite this, the exact theories also differ to experimental results due to lack of provision for initial imperfections, or due to transverse shear deformations through the thickness[549].

Finally, basic closed-form formulae do not estimate correctly the local and global buckling, as the influence that the stringer stiffness has on supporting the skin is ignored[469,550]. Typically, when a local buckling mode occurs, both the stringer and skin will have the same number of longitudinal half-wavelengths[551], which normally results in a lower energy state than would occur when the constituent parts work in isolation. The interaction is further compounded by the fact that the stringer foot acts as reinforcement to the skin. For this reason, closed form solutions typically predict lower buckling loads. It is possible to take into account the stringer foot stiffness influence on the skin by applying a factor, which can be derived from charts and are based on the ratio of foot width to skin pitch, or foot thickness to skin thickness[398]. Such charts have been deduced by HSB in reports 45130-01/-02[552].

8.2.2.1.2 FEM Optimisation

The use of FEM to optimise stiffened panels requires frequent remeshing, to update the model's geometry and stiffnesses, so that the load distribution is correct. Bisagni and Lunzi[506] used FEM in combination with neural networks to optimise a post-buckling stringer-stiffened panel using woven cloth. However, UD is used typically for such structures, which is harder to optimise computationally than woven fabric. Therefore, such methods require relatively higher computational resources, especially when considering genetic searching, fitness selection, and FE calculation[545]. Furthermore, FEM is not as efficient as specific optimisers for the design of stringer-stiffened panels[553].

8.2.2.1.3 Genetic Algorithm Assisted Optimisation

A GA was initially used by Le Riche et al.[528] followed by Nagendra et al. (1993/1996)[307,554], to search for the optimal laminate stacking sequence and overall thickness for a given panel (i.e. a given load and panel aspect ratio). A GA was used to optimise the design of a stiffened panel with four T-profile stringers, with a hole located in the centre of the panel[307]. It was found that the results obtained using the GA had higher performance than with a continuous laminate[307].

Liu et al. (2006)[545] used a two-level approach, where baseline laminates of 50/40/10 and 60/30/10 were used for the skin and stringer laminates respectively. The elastic moduli for these laminates were derived from 10mm thick laminates, as at this thickness the elastic moduli values become fairly constant, due to the integer nature of the plies. The moduli were inputted into VICONOPT to perform the first level optimisation, which basically only used two discrete variables, the thickness of the skin and the stringer, to increase the speed of the optimisation. Once the correct thicknesses were found, the stacking sequence was optimised as part of the second level, to see if the thickness could be decreased.

Liu and Haftka[555] used flexural lamination parameters for the optimisation of un-stiffened orthotropic wing covers in a wing box, using a single-level weight minimisation approach. Under the constraints of stability, strength, and the flexural lamination parameters, the wing box was optimised. Comparing their results to a two-level approach using GAs, it was found that single-level was very competitive.

However, at the preliminary design phase, using GAs has the following drawbacks:

- They are computational inefficient for realistic design at this phase[464]
- A highly specific stacking sequence is not recommended at this phase[537]
- Overall laminate design needs to be verified with the manufacturing department, therefore at this design phase, pre-verified laminates should be used
- They have difficulty considering the laminate design guidelines[343]
- Must be certain that the global laminate has sufficient strength and stiffness

Emphasising on the second point further, it is known that composites have failure modes that are difficult, or computationally expensive, to solve at the preliminary design phase. Specific stacking sequence for each panel may lead to a globally weak structure, which is hard to justify at this level of optimisation. Furthermore, if using an allowable strain level to constrain the design, then it will be necessary to have a strain limit based on every laminate permutation used in the optimisation. However, even at the detailed design phase such data is not likely to be available. Finally, at this design phase only the most critical load cases are analysed, whereas in the subsequent design phases a greater number of load cases will be considered, as well as the loads will change during the design phases due to load maturity. Thus, it is fairly pointless to have highly specific laminates at the preliminary design phase, as they will change anyway throughout the subsequent design phases. Therefore, it is more prudent to use pre-defined continuous laminates, with defined strain allowables.

8.2.2.2 Incorporating Cost

Kassapoglou (1997)[484] investigated the cost and weight of a stringer-stiffened panel using both T- and J-profile stringers. The structural calculations were carried out using simplified closed-form equations, hence why under local buckling there was no interaction considered between the skin and stringer. Costs were based on mainly linear relationships for manual labour for hand lay-up and bagging and debagging, which are considered the most labour intensive operations[484]. Manufacturing constraints were also included such as minimum stringer spacing; hence this optimisation methodology considered stringer pitch as a discrete variable.

This optimisation procedure can only be used to determine either the lowest weight or lowest cost. Normally, the lowest weight option will not have the least cost. By changing the stringer cross-sectional area between the two configurations for lowest cost and weight, the boundary of 'near-optimum' configurations (the Pareto set) is obtained in cost-weight space. A penalty function is established as the sum of the percentage difference of the weight and cost of specific configurations from the individual minimum weight and cost points. A search is conducted among the configurations in this Pareto set to determine for which one the penalty function is minimised. This corresponds to the optimum configuration.

Edwards et al.[556] used a cost model in conjunction with VICONOPT to investigate the cost of stringer-stiffened panels, using both I- and T-profile stringers. The cost model summed the cost of the material cost, the fabrication cost, the curing cost and the NDT cost. As the stringer pitch was a variable that could be optimised, it was found that an increase in stringers, i.e. an increase in parts, lead to an increase in overall cost, despite the material cost being lower because of the increased structural efficiency of having more, but smaller, stringers. Therefore, this costing method only considered the cost of the material directly used, i.e. based on the weight, it took no consideration of resultant scrap from the panel fabrication.

8.2.2.3 Incorporating Manufacturing

Park et al. (2004) considered an RTM process, where it is necessary to optimise the location of the injection gates and the stacking sequence to improve the resin flow[557]. However, the stacking sequence also determines the performance of the part, thus if first the structural design is optimised and then the manufacturing process, this is known as separate optimisation, whereas when the product is optimised for both, this is known as simultaneous optimisation[557]. In this case, the single-objective function is when both the mechanical performance and reduction in mould filling time is enhanced.

Henderson et al.[558] investigated the optimisation of a stringer-stiffened panel for weight and manufacturing cost. The RFI process is modelled based on Darcy's law[xlviii], whereas the single T-profile stringer-stiffened panel can vary in terms of geometry and layup[558]. The least cost option, i.e. the panel with the quickest infiltration time, was with a pure skin with no stringer, whereas the structural optimum had the highest infiltration time but the lowest weight. It was also found that by having 90° plies in the stringer blade improved the infiltration time by 28%, albeit the consequence of which was a loss of stiffness, which was

[xlviii] Darcy's law is an equation that describes the flow of fluid through a porous medium.

compensated for with a 5% increase in blade height, resulting in a weight increase of 4%[558]. This optimisation routine does not however consider the laminate design guidelines.

Finally, Kaufmann (2008)[559], investigated the cost implication of inspection in his cost/weight optimisation methodology, considering the effects of defects.

8.3 Optimisation Methodology

When structurally optimising a wing box, the bending and in-plane effects of the laminates should be decoupled[344]. From a physical perspective, the thickness of the upper and lower covers is small when compared to the depth of the wing box[xlix]; the contribution to the overall stiffness of the structure is primarily due to the in-plane stiffness of the covers, which is dependent on the percentage of each ply orientation in the laminate and their overall thickness. Thus, the depth between the wing covers is the main stiffness contribution to the wing box. The laminates local buckling performance is, however, dependent on the stacking sequence. Therefore, by decoupling the two, it is possible to maximise the local buckling performance of the panel, without affecting the overall stiffness of the wing box. To quantify the benefit of being able to alter the stacking sequence to help the local buckling performance, a T-profile stringer-stiffened panel with the following parameters were investigated using ESDUpac A0817:

- Skin
  - Panel size =770×165mm
  - ST =6mm (nominally a 44/44/11 laminate)
- Stringer
  - BH =50mm & BT =10.304mm
  - LFW =68mm & LFT =2.944mm
  - Nominally a 60/30/10 laminate

Four different stacking sequences were investigated:

- Configuration A $[+/-/90/+/-/0/0/0/+/-/0/0]_s$
- Configuration B $[+/-/90/0/+/0/-/0/+/0/-/0]_s$
- Configuration C $[+/-/+/-/+/-/0/0/0/90/0/0]_s$
- Configuration D $[+/-/0/0/0/+/0/0/-/90/+/-]_s$

All 4 configurations had an axial stiffness of 7.97×10^8N, and a panel bending stiffness of 1.93×10^{11}Nmm^2, as the laminates had the same number of plies and percentage of different orientations. However, based on the following applied loads: N_x=1935N/mm, N_y=62N/mm, and N_{xy}=288N/mm, which is a typical upper cover load where buckling is still critical, the following RFs were obtained:

- Configuration A = 0.980
- Configuration B = 0.968
- Configuration C = 0.965
- Configuration D = 0.906

[xlix] For a conventional commercial transport aircraft.

This illustrates that the stacking sequence has a strong influence on the buckling load, but more importantly, it emphasises what has been said in previous sections. A well designed laminate, with the outermost plies being ±45°, followed by a 90° ply, then with uniformly banded 0° and ±45°, such as configuration A or B, can be used at the preliminary design phase, which simplifies the optimisation process, when compared to using a GA to find the optimum stacking sequence. Therefore, at the preliminary design phase, having a set stacking sequence ensures contiguity of plies, which can globally save weight, and if the laminate is well designed then this will minimise any weight disadvantage against a GA optimised stacking sequence.

8.3.1 Panel Discretisation

Single-level optimisation is computationally inefficient for a complete wing cover, where all the panels are optimised simultaneously[346]. Therefore, it is necessary to divide the cover into individual panels, which are typically defined by the rib planes and a half-stringer pitch, each side of the stringer datum, as shown in Figure 8-4. This is necessary as the load intensity varies across the cover; hence, this is a way of proportioning the load, resulting in a more tractable optimisation problem, as the local panel can be designed for the local loads. The load is idealised, as being constant over the local panel, hence, there should be no change of section across the panel. However, across the global panel changes in section will occur due to the change in load intensity. It could be envisaged that the local panels are divided still further spanwise, to have a finer distribution of load, which should result in a more optimised structure. However, this will double the optimisation time, would complicate manufacturing, and, at the preliminary design phase, would not be significantly beneficial.

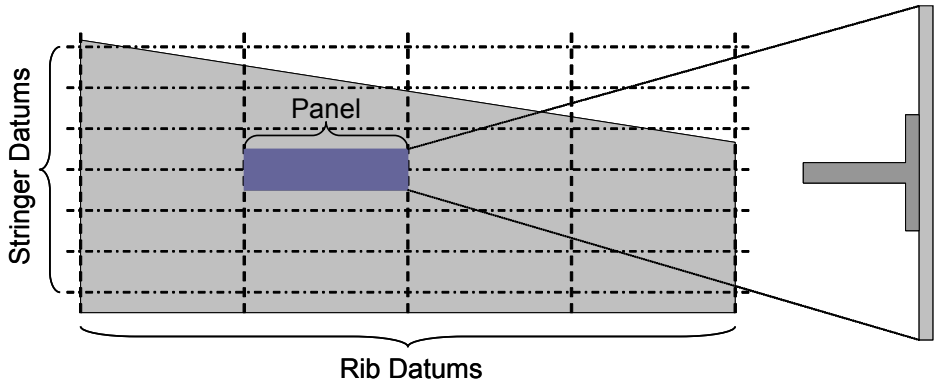

Figure 8-4: Panel basis

Shown in Figure 8-5 is the input format for the load data and the information pertaining to the out-of-plane effects. Each stringer and rib bay intersection can have different in-plane loads, which include both axial (N_x) compressive and tensile loads, as well as shear (N_{xy}). Due to this level of analysis being conducted at the preliminary design phase, the information required to calculate the out-of-plane strength effects will be considered for each rib bay. In any case, fuel pressure should be fairly constant over the whole cover, the curvature of the cover can be considered similar within the confines of adjacent ribs, as well as the eccentricity of the loads through the stringer-stiffened panel section.

The loads will be generated from a FEM, as this is the most reliable method to model the load distribution over a complex item such as a wing cover, where there are many load inputs. However, in order to minimise the dependency on FEM, a multi-level load-flow approach[560] should be used[561]:

- Global load-flow level: minimise total structural weight subject to the system level constraints e.g. stability and strength
- Local load-flow level: minimise the change in equivalent system stiffness subject to local strength and buckling requirements so that global load redistribution is reduced

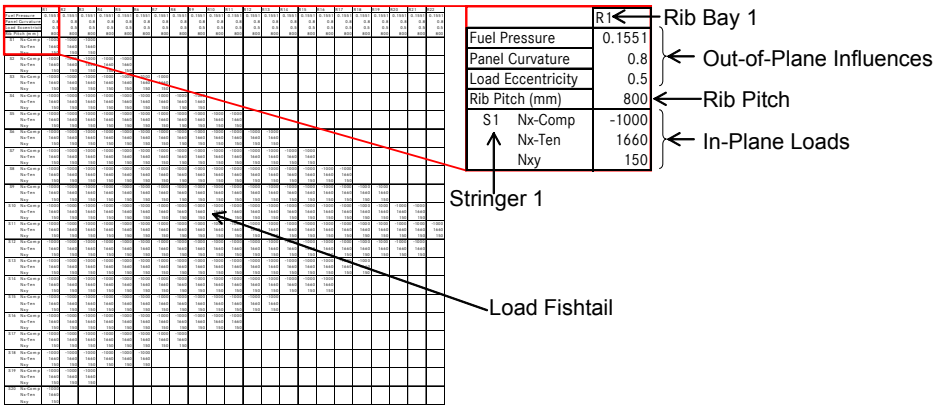

Figure 8-5: Wing cover load fishtail input

When optimising each individual local panel, the assumption is that the load flow across the complete wing cover is independent of the local panel designs. Hence, the global wing cover loading is not altered as the local panel stiffness changes. In reality, this will not be the case, therefore, once the individual panels have been optimised, the global FEM must be updated, with the new dimensions and stiffnesses inputted, the FEM run to obtain the new load flow, which will be inputted for subsequent optimisation runs. It is important that sudden large changes in stiffness do not occur at the local level, as this will have a large consequence at the global level[347]. The whole optimisation process is repeated until the change in local panel loads is negligible.

Typically, there are several load cases derived for the aircraft's wing. Each one will have different load flows and intensities, depending on the type of manoeuvre. For preliminary design, the input load plot is derived from the most extreme loads from the various cases. It could be that this is too conservative an approach, as the sum of the individual panels is considered and not the total wing cover as a whole. However, at this level of optimisation, this can be considered best practice. It would also be possible to run a number of load cases, i.e. using multiple load cases, if deemed more appropriate, and then compare the results to compile the best thickness distribution across the cover.

8.3.2 Optimisation Routine

The basic goal of the optimisation methodology is to minimise weight, based on the pre-defined manufacturing and fabrication process, which is defined in Chapter 9, and then calculate the manufacturing cost based on the resultant wing cover. The reality is that the lowest weight solution will always be sought, based on the constraints imposed on the cover, thus trying to search for a solution that finds a compromise between weight and cost, with the least penalty, will not be sought. Shown in Figure 8-6 is a multiple-level/-fidelity hierarchical optimisation methodology, based on the work conducted by Moore et al.[56]:

- Global level
  - Edge of Part (EOP), stringer and rib layout (carried out by the engineer)
- Intermediate level
  - Stringer profile and skin laminate type
- Local level
  - Minimise panel cross-section

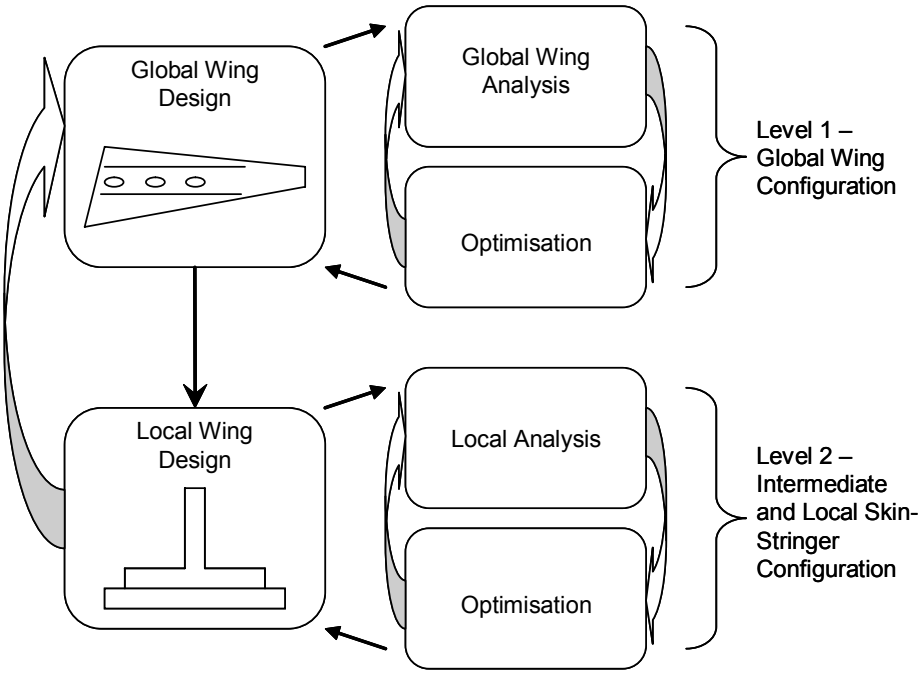

Figure 8-6: Optimisation architecture

The structural optimisation is controlled through the Input/Output spreadsheet as shown in Appendix D. An integral part of this spreadsheet is to decide on the panel configuration, which is determined by selecting from the following options (these points will be discussed in greater detail in the following text):

1. Integration
2. Stringer Profile
3. Skin Laminate
4. Skin Material
5. Stringer Material
6. Stringer Fibre Type
7. Skin Fibre Type
8. Fuselage Material
9. Stringer Pitch

Some optimisation procedures have included stringer and rib pitch as part of the discrete variables[56]. However, due to sound structural design principles, the upper cover stringers, where possible, should converge with the fuselage frames. As the fuselage frame pitch is typically larger than an ideal wing cover stringer pitch, the stringer pitch is instead an integer division of the fuselage frame pitch. Furthermore, due to rib requirements, the lower cover stringer pitch and layout is typically similar to the upper cover. It has been shown that for a metallic aircraft, the fuselage frame pitch is ideally 19.5" (495mm)[562]. Ignoring the sweep of the wing, a typical stringer pitch for metallic wing covers was 165mm[176] (495/3), whereas for

the NASA ACT semi-span CFRP wing covers, the optimum stringer pitch was 193mm[176]. For CFRP fuselages, the frame pitch can be increased to 25" (≈625mm)[562]. The rib pitch is defined by the engineer, due to the reasons mentioned in section 7.3.1.

Fuselage Frame Pitch	Stringer Pitch (mm)			
	/2	/3	/4	/5
Metallic (19.5" [495mm])	247.5	165	123.75	NA
Composite (25" [625mm])	312.5	208.3	156.25	125

Table 8-6: Possible stringer pitches

Shown in Table 8-6 are the choices of stringer pitch for the wing cover, with the pitches highlighted in light orange only possible for a U-profile stringer-stiffened panel. As previously mentioned, for a discrete stringer the stringer pitch should be greater than 125mm. This can be justified by considering the following example: If the skin is 20mm thick, then the stringer lower flange thickness is half the skin thickness, i.e. it is 10mm thick. As the lower flange thickness is 10mm, due to a d/t of 1, then the repair bolt must be 9.53mm diameter. Furthermore, the radius between the foot and blade is assumed to be 5mm. If the skin thickness is 20mm, then the blade thickness could be up to 30mm. Thus based on Equation 7-7 the stringer's foot width would be 123mm. Taking into account both dimensional and positional tolerances then it is easy to see that a stringer pitch greater than 125mm should be used for discrete stringers. Conversely, a stringer pitch equal to the frame pitch would lead to poor stability performance of the structure, hence why the minimum stringer pitch is half the frame pitch.

There are, principally, two elements to the optimisation, namely stability and strength analysis. It is first of all necessary to design the stringer-stiffened panel due to the stability constraints, and then to verify against strength. For stability analysis, a panel with 5 identical stringers will be analysed with ESDUpac A0817 FSM, in order to minimise the effects of boundary conditions[1] and to be able to model defects. To verify the decision to use a 5 stringer panel, a comparison of a lightly-loaded and heavily-loaded stringer-stiffened panel, with 50/40/10 skin and 60/30/10 stringers, with constant stringer pitch but varying number of stringers was carried out. Both a sound panel and a panel with a single stringer debond was analysed, as shown in Table 8-7. It can be seen that the knockdown in performance due to the debond is fairly insensitive to the number of stringers. Furthermore, Figure 8-25 illustrates that with more than 5 stringers, there is little benefit in using more stringers to analyse the panel. Therefore, in the interest of saving computational effort and to be representative of the wing cover, a 5-stringer panel will be used for all calculations.

Number of Stringers	Lightly-Loaded			Heavily-Loaded		
	Panel Load (N)		KD	Panel Load (N)		KD
	Sound	Debond		Sound	Debond	
3	685431	173533	25%	2777910	786966	28%
5	1049660	282792	27%	4237460	1275350	30%
6	1240370	339081	27%	4997480	1526100	31%
7	1430010	395300	28%	5744740	1776840	31%

Table 8-7: Comparison of sensitivity in knockdown with respect to number of stringers

The global optimisation process is dependent on the method of panel integration, as shown in Figure 8-7. For a co-cured panel, it is not necessary to consider a single stringer debond, but instead only DSD, where one stringer is completely removed. Thus for co-curing, a 5 stringer

[1] For a typical wing cover, each rib bay will have multiple stringers, thus it is more accurate to analyse a multi-stringer panel as opposed to a single-stringer panel.

panel with the middle stringer removed will be optimised, based on 0.7×LL, and then the panel is verified with an intact 5 stringer panel, based on UL, as shown in Figure 8-8. It is known from previous investigations, that the panel with DSD will determine the stability design, however if the resultant RF <1, when verifying the design against the intact panel, then it can be re-optimised using the panel designed for the DSD as baseline. If the panel does require to be optimised for the intact stringer panel, then the new design should be verified for DSD. It is considered that there will always be one case that sizes the panel, i.e. the situation will not occur that a panel that has been subsequently re-optimised, has an RF <1 for the original case.

For a co-bonded or secondary bonded panel, a similar process is followed, as shown in Figure 8-7. However, in this case, the optimisation routine begins initially with the debonded stringer case with the single debonded stringer, as shown in Figure 8-8.

The methodology of using ESDUpac A0817 FSM to analyse a sound panel, a panel with a debonded stringer, and a panel with a complete stringer removed, appears to suitably represent the knockdown in performance due to the different levels of damage that can be inflicted on a stringer-stiffened panel, as proven in sub-chapter 7.3.4.2. For the sound panel, the panel must react UL, where the applied axial load is apportioned between the stringers and skin based on the stiffness of each element, whereas the shear load is distributed between the skin and the stringer's bonded lower flange. In terms of the debonded panel, the distribution of the axial load, in this case LL, between the 5 stringers and skin, is the same as for the sound panel, whereas the shear load local to the debonded stringer is transferred only through the skin, as without the bond there is no means to transfer the load into the stringer's lower flange. For the remaining 4 stringers, the shear load will be conventionally apportioned between the skin and stringer's lower flange. For the damaged panel with the middle stringer removed, the 70% of LL will be distributed between the 4 remaining stringers and the skin.

When using the executable ESDUpac A0817 FSM program, the geometry file, i.e. the .STO file, is defined by the .PGD, which is the general input file for stringer profile, geometry, and loads. This assumes a sound panel; therefore it is necessary to amend the .STO file. Manually amending the .STO file to represent either a debonded or a removed stringer requires some effort, in particular for the removed stringer, as all the nodes and strip-elements must be amended. For this reason, .STO templates are setup in a spreadsheet for the 3 different stringer panels, as well as the different levels of damage to the panel, which can be automatically updated based on the geometry of the panel as well as the applied loads, obtained from the Input/Output spreadsheet, as shown in Appendix D. This data can then be exported into a WordPad file, which is the format required for ESDUpac A0817.

Shown in Figure 8-9 is the optimisation methodology, which can be considered to be at a Local Level, with reference to Figure 8-6. The optimiser's objective is to maximise stability performance per panel while minimising the complete cross-sectional area, and maintaining the strength requirements. The variable parameters will control the cross-sectional area of the stringer-stiffened panel.

The optimisation process shown in Figure 8-9 is principally for either a U-profile or T-profile stringer panel, as only the stringer blade (BH & BT) and skin thickness (ST) are variables that can be altered. For the I-profile stringer panel, the stringer's upper flange width (UFW) can vary. Limits will be set on the minimum dimensions for the elements that constitute the stringer-stiffened panel, which have been previously mentioned, and are summarised as:

- Stringer elements widths given by Equations 7-7, 7-8, and 7-9, for the LFW, BH, and UFW respectively
    - The radius 'r' is 0.5 × LFT, due to the fabrication method of the stringer
    - The diameter 'd' of the repair bolt is related to the thickness of the laminate, as shown in Appendix D
- Stringer's lower flange is constrained to:
    - LFT_{min} = 3.312mm (UD) / 3.7mm (NCF) / 3.2mm (Braid)
    - LFT/ST > 0.5
        - The exact relationship between ST and LFT is given in the stringer tables in Appendix C
- Minimum BT_{min} = LFT = UFT
    - For an I-profile stringer, UFT is always the same as the LFT
- Minimum skin thickness of 3.25mm

With respect to Figure 8-9, the stability analysis is simply calculated using the ESDU FSM program, while ensuring that the correct allowables are used, as given in Appendix B, and for a given thickness, the correct laminate stacking sequence is inputted, which are illustrated in Appendix C. Once an RF ≥1 is reached, based on the lightest solution then the optimisation for stability is completed.

In terms of the strength verification, both in-plane strength can be considered, as well as the influence of out-of-plane effects. The panel's strength is dependent on the configuration, in terms of the skin laminate (% of ±45° plies), the skin fibre type, the skin thickness, and the stringer pitch, as discussed in Appendix B, which constrains the allowable strain.

Ignoring the out-of-plane effects, the strength RF is simply checked using the maximum strain criteria approach, for each individual element of the stringer-stiffened panel, ensuring that the force has been apportioned correctly, based on the individual stiffnesses and areas of each element, as shown in Appendix D. The resultant applied strains should be the same for each element of the stringer-stiffened panel. If the RF ≥1, then the solution is deemed ok, if however the RF <1, then the thickness of the individual elements will need to be increased. This is carried out automatically within the Input/Output spreadsheet.

When it is deemed appropriate to also consider the out-of-plane effects, then the calculative process is slightly more complicated, although as it is setup in an Input/Output spreadsheet it is fairly straightforward. However, a well designed wing cover should not be too sensitive to out-of-plane effects, as shown in Table 7-3, hence why the strength optimisation function will only consider normal in-plane strength, and not the out-of-plane effects. As out-of-plane effects will cause bending of the section, it is necessary to consider the inertia of each element that constitutes the stringer-stiffened panel, which is inputted into equations that consider the effects of fuel pressure, geometric imperfections, and load eccentricities. These equations are given in Appendix D.

There are three final verifications of the panel conducted. The first is a check on bearing/bypass strength for the stringer blade, lower flange, and the skin, when bolted repair is considered. Bearing/bypass interaction has too many variables to make it a part of the optimisation routine at the preliminary design phase, as the number of bolts, the number of rows, and the bolt size can all be altered to benefit this. Therefore it is only incorporated for information, to inform the user of issues.

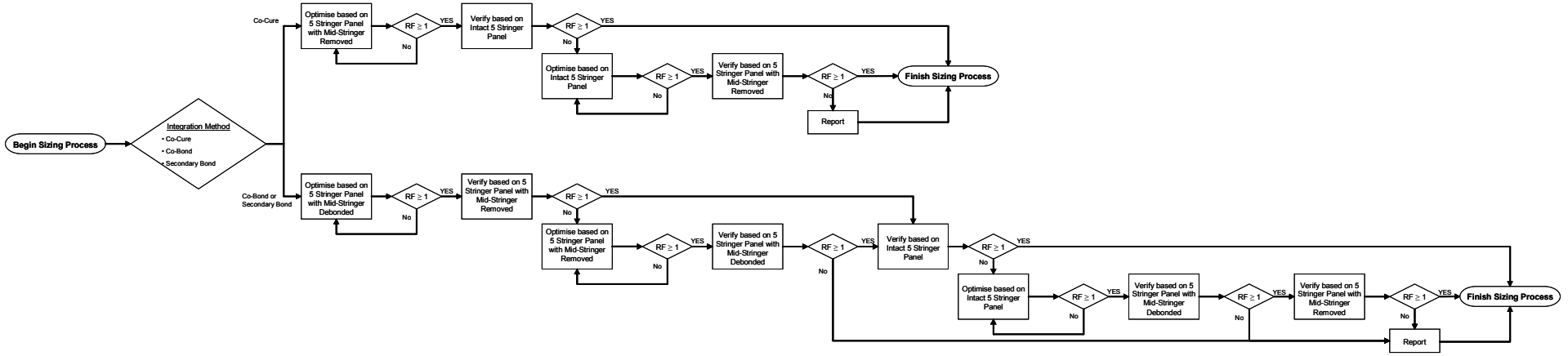

Figure 8-7: Global optimisation process

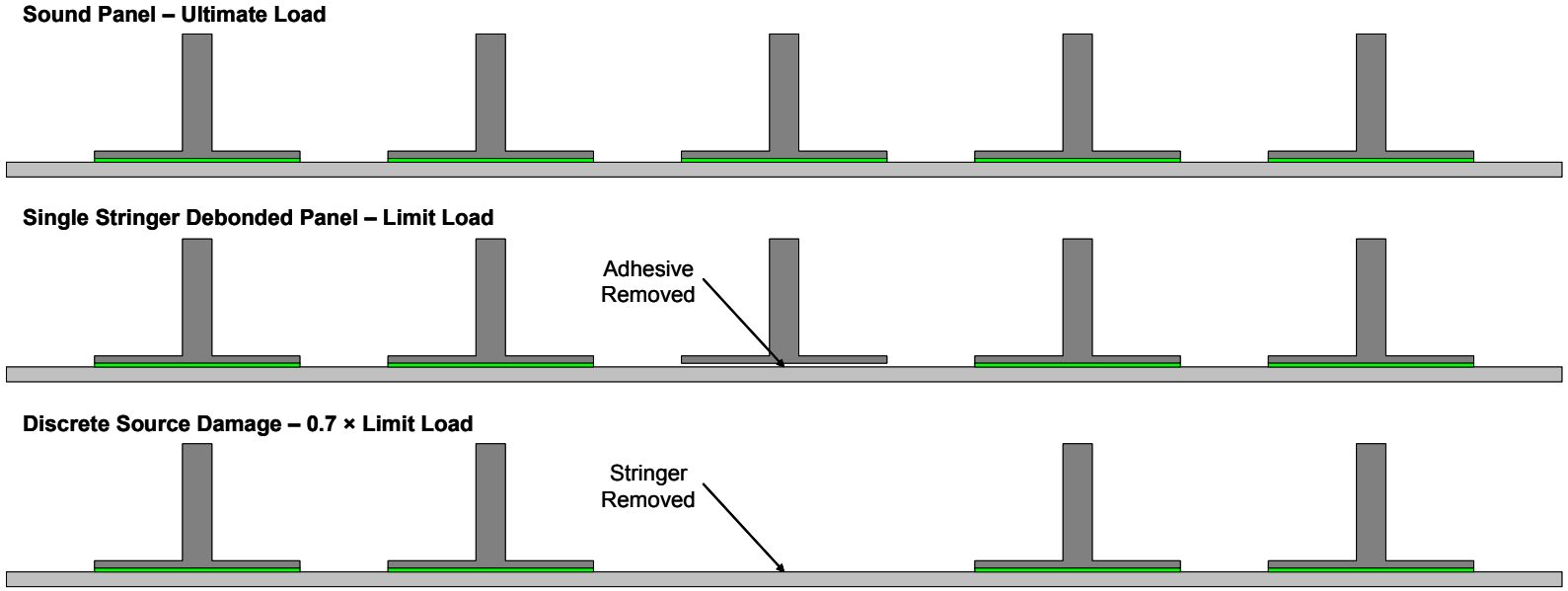

Figure 8-8: Stringer panel configuration for different level of damage

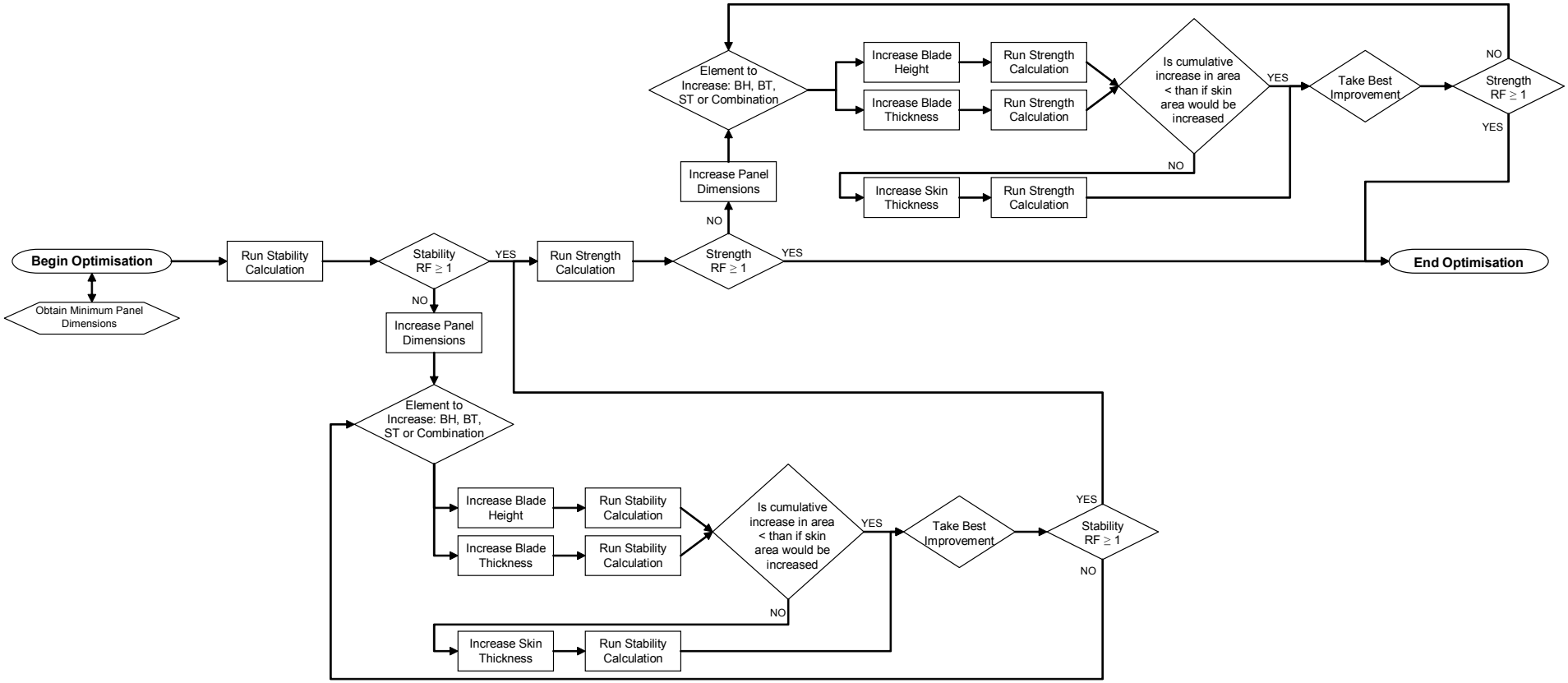

Figure 8-9: Principal optimisation process for stability and strength

The second verification is in terms of the stiffness ratio between the skin and the stringer, which should not be below 35%; however this is purely a guideline, and therefore is only for information.

The final verification is the Poisson's ratio for a bonded joint. As previously mentioned, parts that are bonded together should have a maximum Poisson's ratio difference of 0.15[398] between the parts. In order to ensure that this is respected during the optimisation process, without causing principal issues during the optimisation of the wing cover, the combinations of different skin laminates to the 60/30/10 stringer laminate must be verified in terms of difference in Poisson's ratio. This is shown in Table 8-8, where it can be seen that for both 10/80/10 and 30/60/10 skin laminates, for different skin thicknesses and stringer foot thicknesses, that often the allowable limit of 0.15 is surpassed. Therefore, based on Table 8-8, 10/80/10 and 30/60/10 laminates can only be used with a co-curing process. Conversely, the 50/40/10 and Tailored laminate never exceeds the Poisson's ratio limit, thus they can be used in combination with bonding, i.e. for co-bonding and secondary bonding, as well as for co-cure.

Skin		Stringer (60/30/10)						
		3 mm	6 mm	9 mm	12 mm	15 mm	18 mm	21 mm
10/80/10	3 mm	0.06	0.13	0.06	0.11	0.07	0.10	0.07
	6 mm	0.08	0.15	0.09	0.13	0.09	0.12	0.09
	12 mm	0.14	0.21	0.15	0.19	0.15	0.18	0.15
	24 mm	0.17	0.24	0.18	0.22	0.18	0.21	0.18
30/60/10	3 mm	0.00	0.07	0.01	0.05	0.01	0.04	0.01
	6 mm	0.14	0.22	0.15	0.19	0.15	0.18	0.15
	12 mm	0.08	0.15	0.09	0.13	0.09	0.12	0.09
	24 mm	0.12	0.19	0.12	0.16	0.13	0.15	0.13
50/40/10	3 mm	0.00	0.07	0.01	0.05	0.01	0.04	0.01
	6 mm	0.08	0.15	0.09	0.13	0.09	0.12	0.09
	12 mm	0.01	0.09	0.02	0.06	0.02	0.05	0.02
	24 mm	0.03	0.11	0.04	0.08	0.04	0.07	0.04
Tailored	3 mm	0.06	0.13	0.06	0.11	0.07	0.10	0.07
	6 mm	0.06	0.13	0.06	0.11	0.07	0.10	0.07
	12 mm	0.03	0.10	0.04	0.08	0.04	0.07	0.04
	24 mm	0.02	0.10	0.03	0.07	0.03	0.06	0.03

Table 8-8: Poisson's ratio difference between skin and stringer foot

An example of the spreadsheet, where all input and output data pertaining to the stability and strength calculations, is shown in Appendix D.

8.4 Finite Strip Method

As FSM is used to calculate the stability performance of the stringer-stiffened panel, and thus forms a major part of the structural optimisation analysis, it is deemed appropriate to discuss FSM in some detail.

FSM was originally developed by Cheung, whose book titled '*Finite Strip Method in Structural Analysis*'[563] provides a good explanation of the method, or more recently, the work by Loughlan[294]. FSM can provide an effective and convenient method to analyse elastic buckling of structures. FSM, like FEM, is a multi-field form of the traditional single-field Rayleigh-Ritz method. The buckling behaviour of stringer-stiffened panels can be determined easily with FSM, and is very competitive with FEM[564,565], particularly as it can take into consideration the interaction between skin and stringer. Using FSM as opposed to FEM, will reduce the computational effort for solving the Eigen value type problem of predicting the

stress at which buckling occurs[565], due to the problem being represented only by the degrees of freedom at the plate junctions of a single cross-section[469]. The accuracy of FSM is dependent on the number of strips and on their structural location[564].

FSM assumes the prismatic structure consists of a number of strips, as illustrated in Figure 8-10. As with FEM, FSM uses shape functions to define the displacement field in terms of nodal degrees of freedom. For single-term FSM (sometimes referred to as semi-analytical FSM[565]) continuously differentiable functions are used to portray the sinusoidal displacement variation along the strip length[294], with nodal lines both straight and parallel to the ends in any mode of buckling[566], whereas the displacement state across the strip is based on algebraically simple polynomial shape functions, which have an associated nodal line displacement parameter. When the mode shape of the buckling is purely a longitudinal sinusoidal form then this conforms to plane stress theory and classical plate theory[544]. Therefore, strain is defined by the nodal degrees of freedom as it is a function of the displacement field, and the strain is used in conjunction with a stress-strain relationship to calculate the stiffness coefficients for the nodal degrees of freedom[567].

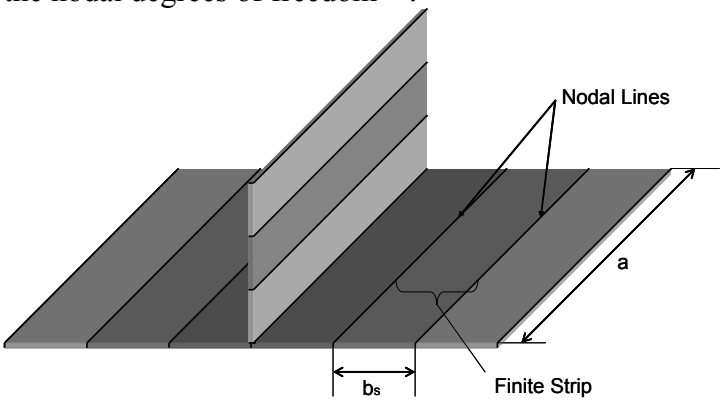

Figure 8-10: Composite prismatic section discretised by finite strips

8.4.1 Incorporation of Shear

The x, y, and z-axes define the longitudinal, transverse and lateral direction, respectively with the buckling displacements being termed u, v, and w. The buckling displacement w is given by Equation 8-5[541]:

$$w = f_1(y)\cos\frac{\pi x}{\lambda} - f_2(y)\sin\frac{\pi x}{\lambda} \qquad \textbf{8-5}$$

Thus, if the panel and loading is uniform in the x-direction then the solution will be exact. The functions $f_1(y)$ and $f_2(y)$ allow various boundary conditions to be defined on the panel edges i.e. parallel to stringers, however, these cannot be defined at the ends of the panel. For a specially-orthotropic panel with no shear, the solution from Equation 8-5 for 'w' involves a series of node lines that are both straight and perpendicular to the panel ends, and spaced λ apart, as shown in the LHS of Figure 8-11. Along each node line, the buckling displacement satisfies simply supported conditions; hence it gives an exact solution.

This has been verified with the specially-orthotropic T-profile stringer-stiffened panel with 8 stringers, having the following dimensions: BH=70mm, LFW=80mm, SP=260mm, a=1020mm, BT&LFT=6mm, ST=10mm, and t_{ply}=0.5mm:

- Stringer $[+/-/-/0/+/0]_s$
- Skin $[+/0/-/-/0/0/0/+/+/-]_s$

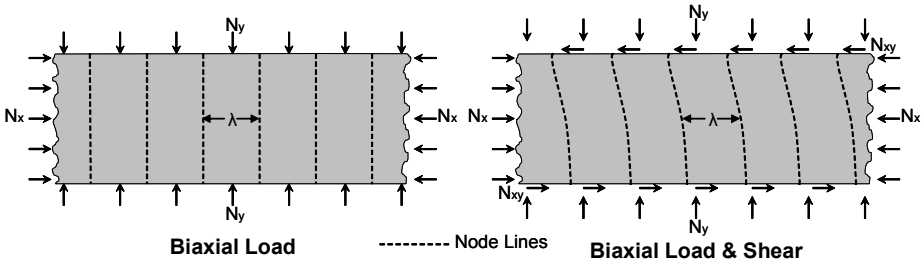

Figure 8-11: Nodal line distribution for panel under biaxial load (LHS) and biaxial & shear load (RHS)

A back-to-back comparison between the FSM program ESDUpac A0817 and SAMCEF, an FEM package, for a panel reacting a biaxial load of N_x=-2000N/mm and N_y=-100N/mm, resulted in an RF of 1.38 and 1.28, respectively. As shown in Figure 8-12, the illustrated buckling modes are very similar, as are their respective RFs.

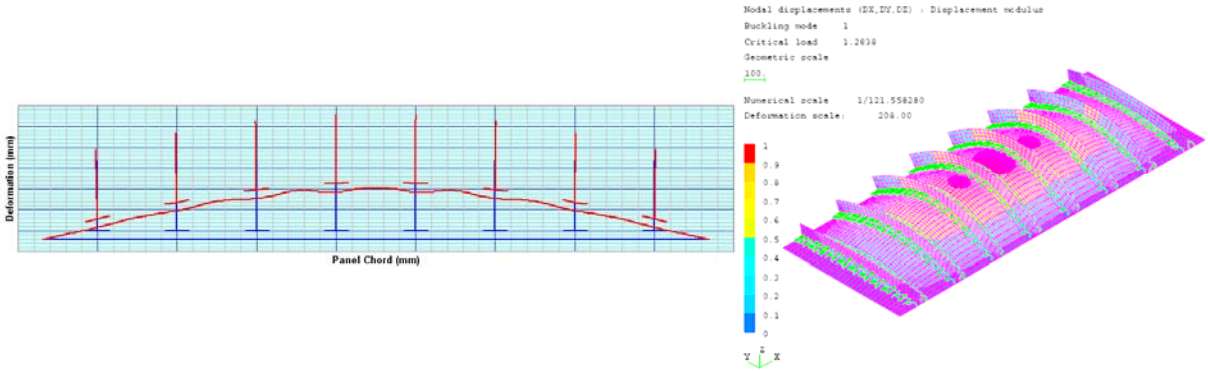

Figure 8-12: FSM (LHS) and FEM (RHS) global buckling mode

A panel loaded under shear, or with an anisotropic laminate, will have skewed node lines, as shown in the RHS of Figure 8-11, which cannot coincide with the panel ends. Hence, the solution from single-term FSM is only accurate when many multiple wavelengths form along the panel length[544], as under these circumstances, the boundary conditions at the panel ends are not relevant. As λ approaches the panel length, the buckling load will typically be underestimated, as the boundary conditions at the panel ends influence the loading, albeit if $\lambda<1/3\times a$ it is generally accurate[541]. Conversely, if boundary conditions were imposed, it would force the nodal lines to coincide with the panel ends, resulting in a higher buckling load. This issue is demonstrated, by applying an additional shear load of N_{xy}=200N/mm to the previous example of a specially-orthotropic T-profile stringer-stiffened panel. The P-λ curve extracted from the FSM program is shown in Figure 8-13, which illustrates a local buckling mode at a half-wavelength (panel length) of 400mm.

At a half-wavelength of 400mm, the RF for FSM was 2.66, while with the more accurate FEM it was 1.99, with the mode for both methods shown in Figure 8-14. At a half-wavelength of 730mm, the RF for FSM and FEM was 1.43, with the mode shown in Figure 8-15. Finally, at a half-wavelength of 1020mm, the RF for FSM was 0.81, while with FEM it was 0.82, with the mode shown in Figure 8-16. This highlights the methods limited applicability when shear is applied, at lower half-wavelengths, i.e. when λ approaches the panel length.

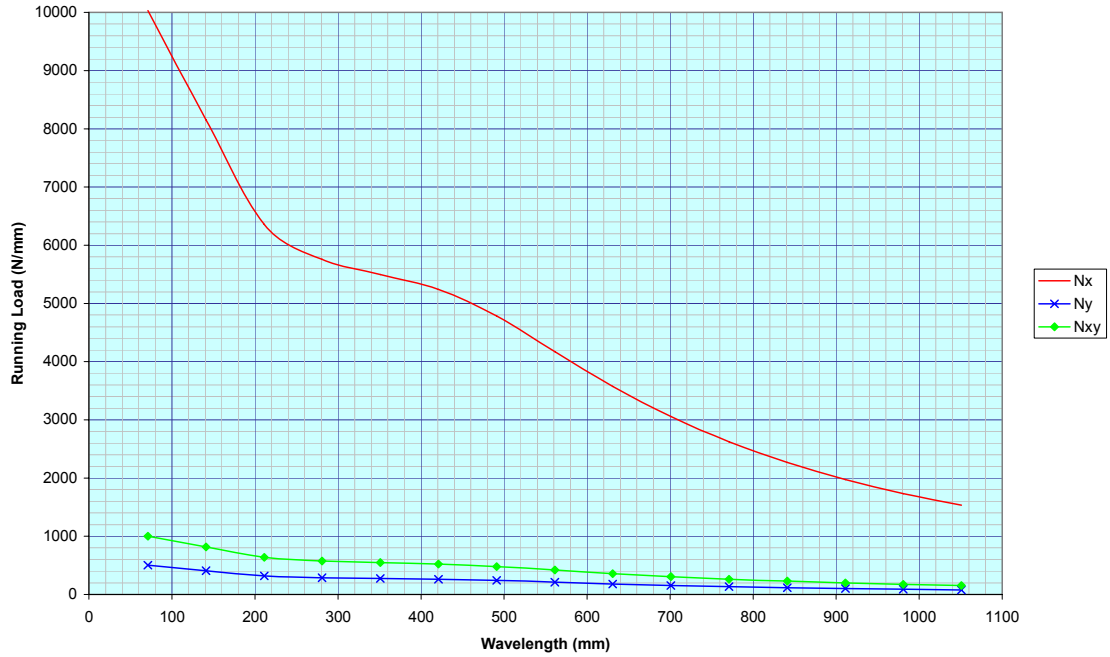

Figure 8-13: P-λ curve for specially-orthotropic T-profile stiffened stringer panel

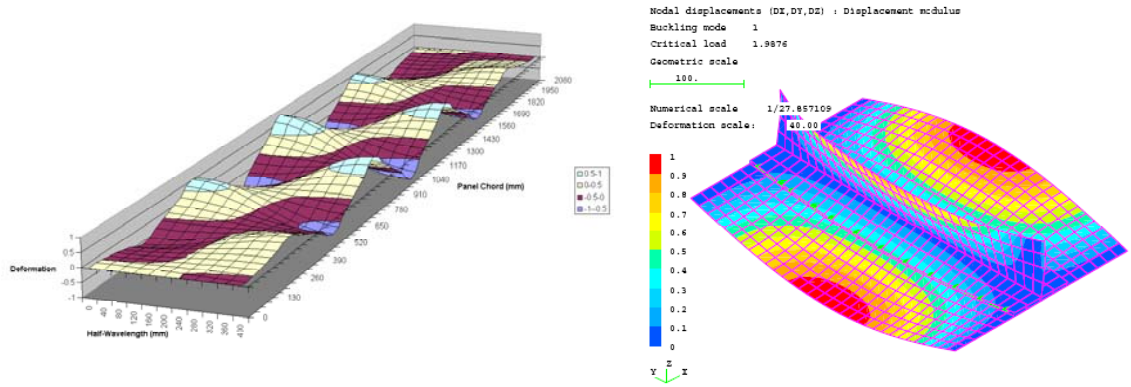

Figure 8-14: Comparison of methods with shear at half-wavelength of 400mm (LHS is FSM)[li]

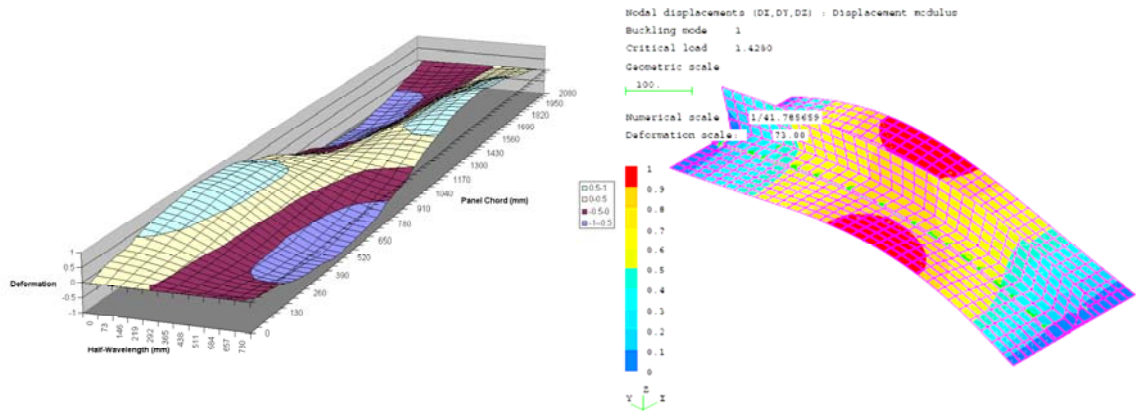

Figure 8-15: Comparison of methods with shear at half-wavelength of 730mm (LHS is FSM)[li]

[li] Note that FSM models 8 stringer panel, whereas the FEM models only 1.

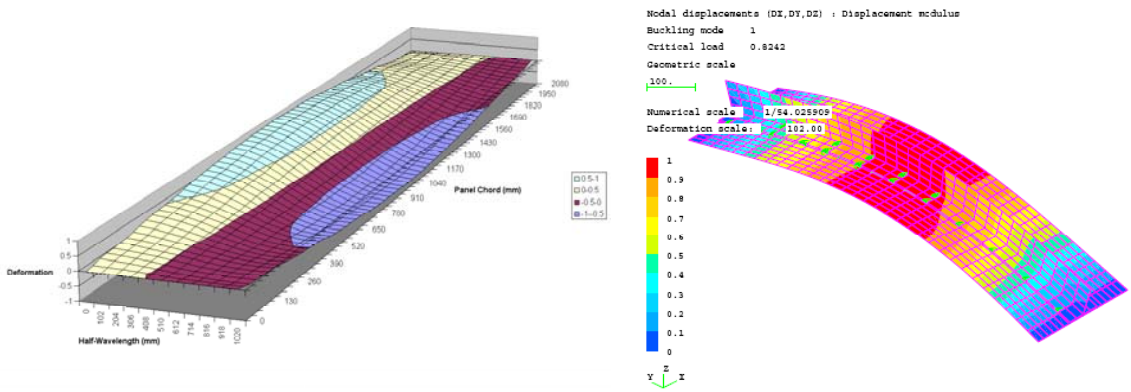

Figure 8-16: Comparisons of method with shear at half-wavelength of 1020mm (LHS is FSM)[li]

Further comparisons were made as shown in Table 8-9 for various T-profile stiffened-stringer panels, using a 44/44/11 laminate for the skin and a 60/30/10 laminate for the stringers, with varying geometry and load intensity. It can be seen that, in general, the buckling load RF with FSM is very similar to FEM.

Loading			Rib Pitch	Skin		Blade		Foot		Reserve Factor	
Axial (N/mm)	Transverse (N/mm)	Shear (N/mm)	a (mm)	SP (mm)	ST (mm)	BH (mm)	BT (mm)	LFW (mm)	LFT (mm)	SAMCEF	ESDU pac A0817
2094.6	62.3	311.8	770	165	6.000	50	10.304	68	2.944	1.070	1.182
2316.3	162.9	169.5	740	165	6.000	50	9.200	68	2.944	1.000	1.083
2318.3	135.7	228.5	715	165	5.750	48	9.016	68	2.944	0.910	0.980
2575.6	41.4	347.1	690	165	9.750	47	8.096	68	2.944	1.100	1.290
2020.2	29.6	232.6	760	165	6.250	48	8.464	68	2.944	1.000	1.107
1911.9	79.3	80.2	770	165	5.000	48	8.464	68	2.944	0.970	1.103
1154.1	7.5	432.7	770	165	5.000	48	8.280	68	2.944	1.000	0.975
2034.4	4.0	318.1	770	165	7.750	47	8.832	68	2.944	1.050	1.166
439.2	7.3	194.9	820	165	4.000	35	6.808	50	2.944	0.960	0.894
433.3	3.8	87.8	820	165	4.000	35	6.256	50	2.944	1.180	1.181
384.8	1.2	159.8	820	165	5.750	35	6.624	50	2.944	1.530	1.454
									Average	1.070	1.129

Table 8-9: Comparison of FSM with ESDUpac A0817 for various T-profile stringer-stiffened panels

The author spent much time validating the development versions of ESDUpac A0817, which is similar to ESDUpac A0301 that was released in December 2003[474], but with the ability to calculate the buckling load when the panel is under shear and/or any combination of biaxial load, as opposed to just axial load. The author found many issues by comparing FE results with the results from the development versions, but through various E-mail communications and telephone calls, these issues have now been resolved, with the new ESDUpac A0817 scheduled to be released sometime in 2009. Adam Quilter from ESDU has expressed his gratitude for the author's effort, as shown in Appendix D.6.

The limitation of single-term FSM has been evidenced by the work conducted by Stroud et al.[541], where they investigated the influence that increasing shear had on a blade- and hat-profile stiffened panels (with nominal dimensions of SP = 127mm and a = 762mm), and the results obtained by using different methods to calculate the buckling loads; the results of which are shown in Table 8-10 and Table 8-11[541]. In the tables, 'd' and 's' notate discrete

stringers and smeared stringers respectively. With a smeared stringer, the local deformations are lost, which can affect the overall buckling mode, leading to a predicted buckling load higher than the real buckling load[541]. This is also similar to modelling the stringers with bending (EI) and torsional (GJ) stiffnesses, to represent the stringers[541]. Under most circumstances such a method is sufficiently accurate to predict structural efficiencies and design trends[485]. Whereas, the '0' and '90' in the tables signify that the stringers are orientated either along the 0° direction of the panel or the 90°, respectively. The reason why the stringers are orientated 90° to the panel is to synthesise an infinitely wide panel.

A comparison in the tables shows that the FSM programs, PASCO and ESDUpac A0817, have good correlation; however, between FSM and the FEM program Engineering Analysis Language (EAL) the correlation is fairly poor, which is exacerbated with increasing shear. Only under pure axial load are the results similar. The difference between having discrete or smeared stringers is fairly inconsequential, however, with the stringers orientated at 90° to the axial load, this improves the accuracy of the FSM dramatically.

Taken from NASA TM 83194 Example 1 CFRP Blade Stiffened Panel							
Loading		Factor					
Nx	Nxy	FSM					FEM
kN/m	kN/m	PASCO Fd.0	PASCO Fs.0	ESDU	PASCO Fs.90	PASCO Fd.90	EAL
0	175	0.57	0.56	0.56	1.47	1.50	1.55
35	175	0.54	0.52	0.52	1.31	1.34	1.40
87.6	175	0.49	0.48	0.47	1.12	1.15	1.21
175.1	175	0.42	0.41	0.40	0.82	0.84	0.84
350.3	175	0.32	0.32	0.30	0.47	0.48	0.48
175.1	0	1.00	1.00	0.93	1.00	1.00	1.00

Table 8-10: Blade-profile stiffened panel – comparison of results between different methods

Taken from NASA TM 83194 Example 5 CFRP top-hat Stiffened Panel							
Loading		Factor					
Nx	Nxy	FSM					FEM
kN/m	kN/m	PASCO Fd,0	PASCO Fs,0	ESDU	PASCO Fs,90	PASCO Fd,90	EAL
0	175	1.30	1.15	1.30	3.57	4.04	3.19
52.5	175	1.21	1.08	1.21	3.20	3.57	2.93
105.1	175	1.13	1.02	1.13	2.88	3.20	2.68
175.1	175	1.03	0.94	1.03	2.42	2.66	2.33
350.3	175	0.89	0.78	0.84	1.43	1.53	1.41
175.1	0	2.99	3.04	3.03	3.04	3.00	3.00

Table 8-11: Hat-profile stiffened panel – comparison of results between different methods

8.4.1.1 Multi-Term FSM

Two multi-term FSM programs were developed by Dawe and Peshkam[544,568] called BAVAMPAS (Buckling And Vibration Analysis of Multi-term Plate Assemblies using SDPT [Shear Deformation Plate Theory]) and BAVAMPAC (Buckling And Vibration Analysis of Multi-term Plate Assemblies using CPT [Classical Plate Theory])[568]. Using these programs it was found that upon the 5th harmonic term, an answer within 1% of that from EAL, as shown in Table 8-10 and Table 8-11, was given. This validates that at least multi-term FSM is very

competitive in comparison to FEM, for calculating the buckling load of stringer-stiffened panels when reacting shear load and with laminates other than specially orthotropic. This is despite the fact that highly accurate results can be obtained when only a single-strip is used for each component flat[568].

For multi-term FSM (sometimes referred to as spline FSM[565]), the formulation of the strip for each displacement-type component is represented by a finite series of products of longitudinal trigonometric functions and crosswise polynomial functions[544]. This method is more flexible when shear, anisotropy and different boundary conditions other than simply-supported, are considered[565]. However, multi-term FSM is an order of magnitude slower than single-term FSM, therefore the trade-off is between accuracy and speed.

8.4.2 Strip Discretisation

Based on the blade-stiffened stringer design from Stroud et al.[541], with the standard results shown in Table 8-10, a comparison was conducted into the sensitivity of the number of strips used to discretise the panel flats, namely the skin between the stringers and the stringers themselves.

From Figure 8-17[474], it can be seen that the standard integral (U-profile) stringer model consists of 5 nodes and 4 strips for both the stringer and skin. The number of strips were doubled and halved by modifying the .STO file. The effect on the P-λ curve can be seen in Figure 8-18, although the effect is very small. In general, by doubling the number of strips, there was roughly a 0.3% overall change in results, whereas halving the number of strips resulted in a near 2% change. Hence, the standard number of strips should be used.

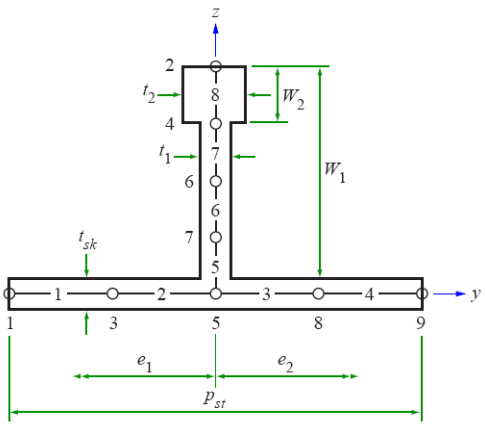

Figure 8-17: ESDUpac integral stringer

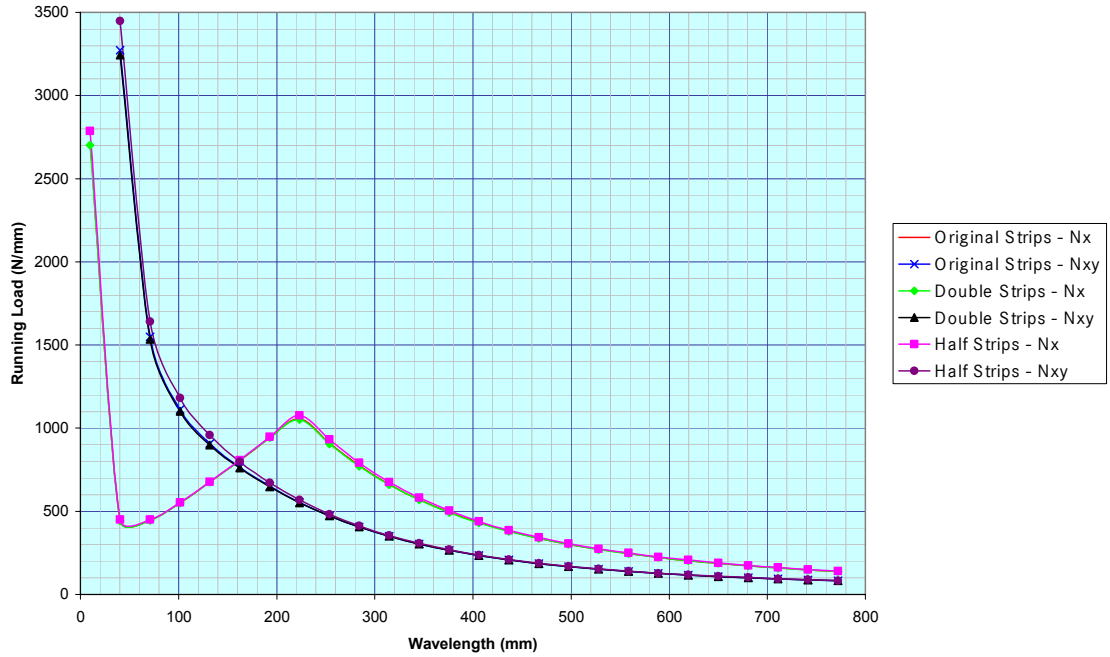

Figure 8-18: Comparison of the number of strips to discretise the stringer panel

8.4.3 Input Data for ESDUpac A0817

A minimum of 2 input files are required, namely the .pgd file, and the .lam file, as shown in Figure 8-19 and Figure 8-20 respectively. The .pgd file details the geometry and loading details of the panel, as well as the boundary conditions. The .lam file, in the format shown in Figure 8-20, details the principal elastic constants of the ply, and the stacking sequences for the chosen laminates.

omegad01.pgd - Editor

Datei Bearbeiten Format ?

```
A
Omega 6 stringers
omegad01.pgd

omegad01.lam
N
mm
9           6
390         1020        0.13
0.0         0.0         0.0
20.00       1.472       2
40.00       1.840       3
39.00       1.840       3
60.00       4.500       1
160.0       4.500       1
80.0        1
80.0        1
800.0       10.0        5.00
2           1
1                                [ NRLCS
1   4       -240000.0   0.0   -960000.0    [ LcNr    LcId    PXX     PYY     PXY
```

Figure 8-19: Typical .pgd file for ESDUpac A0817

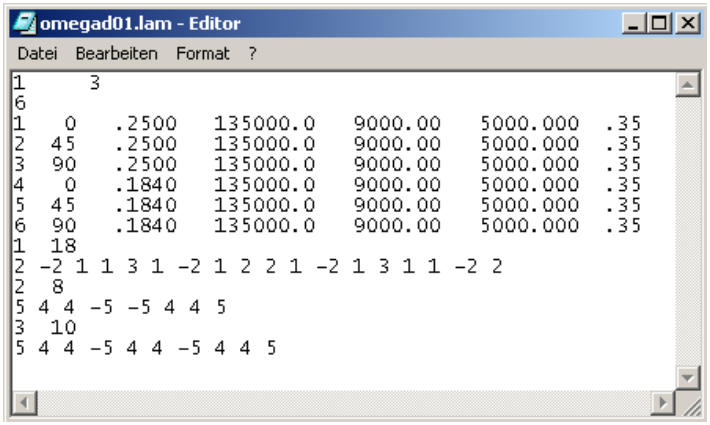

Figure 8-20: Typical .lam file for ESDUpac A0817

8.4.4 Output Data from ESDUpac A0817

Apart from the basic buckling load and the P-λ curve, which was illustrated in Section 7.3.2, it is also possible to show a topographical deformation of the skin part of the stringer-stiffened panel, as shown in Figure 8-21 and Figure 8-22, which compares local and global buckling modes respectively, for both compression and shear dominated loaded panels.

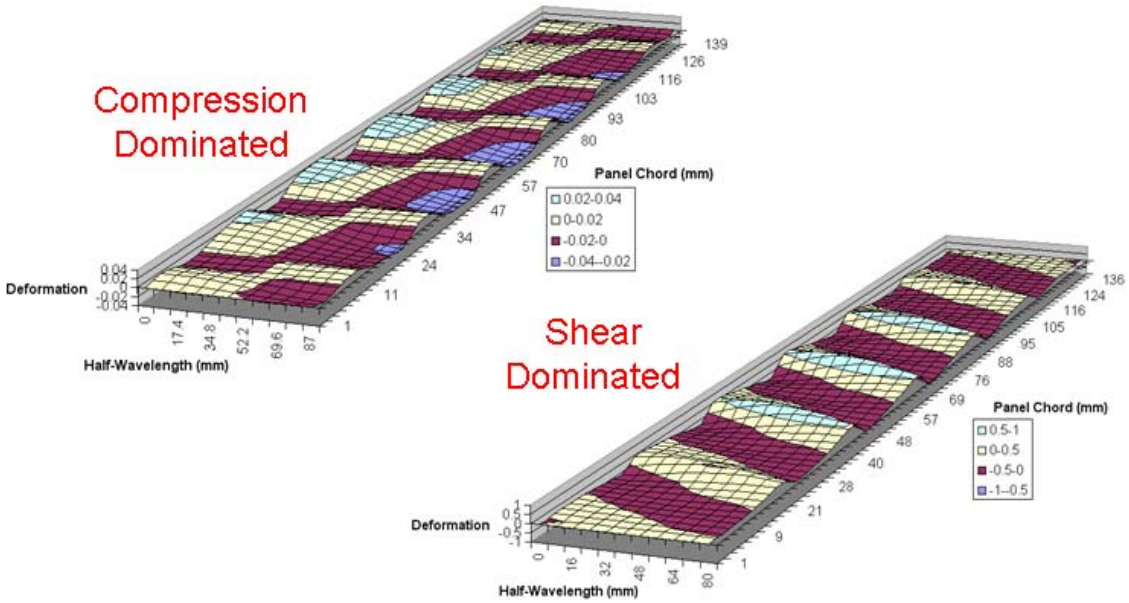

Figure 8-21: Local buckling modes for compression and shear dominated panels

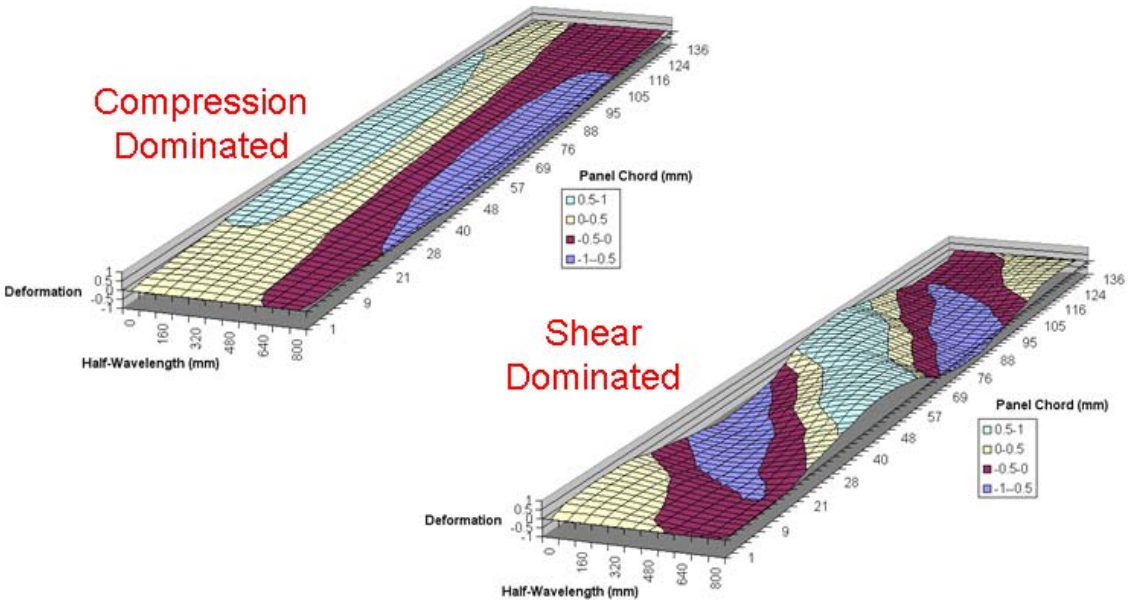

Figure 8-22: Global buckling modes for compression and shear dominated panels

8.4.5 Parametric Investigation into Basic Panel Setup

To demonstrate certain setup parameters within ESDUpac A0817, a basic T-profile stringer-stiffened panel, subjected to a running load of N_x=-3200N/mm and a N_y=-127.5N/mm, using a specially-orthotropic laminate for all elements, was investigated. By employing such a laminate, the special-stringer feature in ESDUpac A0817 could be used. The panel has the following basic dimensions:

- Stringer
  - Lower flange (LFW=80mm; LFT=4.0mm $[90_2/0_2]_s$)
  - Web (SH=70mm; WT=4.0mm $[90_8]$)
- Skin
  - ST=4.0mm $[0_8]$, SP=260mm

The edge constraints of the panel, along the span edges, can be idealised in the FSM program:

- Free (F) – can deflect and rotate
- Simply Supported (SS) – cannot deflect but can rotate
- Clamped (C) – fixed, cannot deflect or rotate

It has been shown that the effects of clamping has greater effect on compressive buckling than on shear buckling[569]. As shown in Figure 8-23, when considering the P-λ curve for a single stringer, it can be seen that the stringer with no lateral edge support (1 Stringer F) reacts the least load, whereas the stringer with clamped edges (1 Stringer C) can react the most load, with the simply-supported stringer (1 Stringer SS) in the middle. For a stringer-stiffened panel with 6 stringers, as shown in Figure 8-24, the simply supported and clamped panels exhibit exactly the same behaviour, hence why the red curve is hidden beneath the green curve, whereas the free panel with no lateral edge support has the lowest performance.

Shown in Figure 8-25, is a comparison of the panels' performance, in terms of maximum running load, in relation to the number of stringers on the panel. It can be seen that after about 5-6 stringers, there is a very small difference in the total running load that can be reacted by

the panel. With reference to Figure 8-26, it can be seen that the super-stringer has a very similar P-λ curve to a 6-stringer panel. Therefore, a 5-stringer panel should be used to model the stringer-stiffened panel, as well as using simply-supported conditions along the lateral edges of the panel.

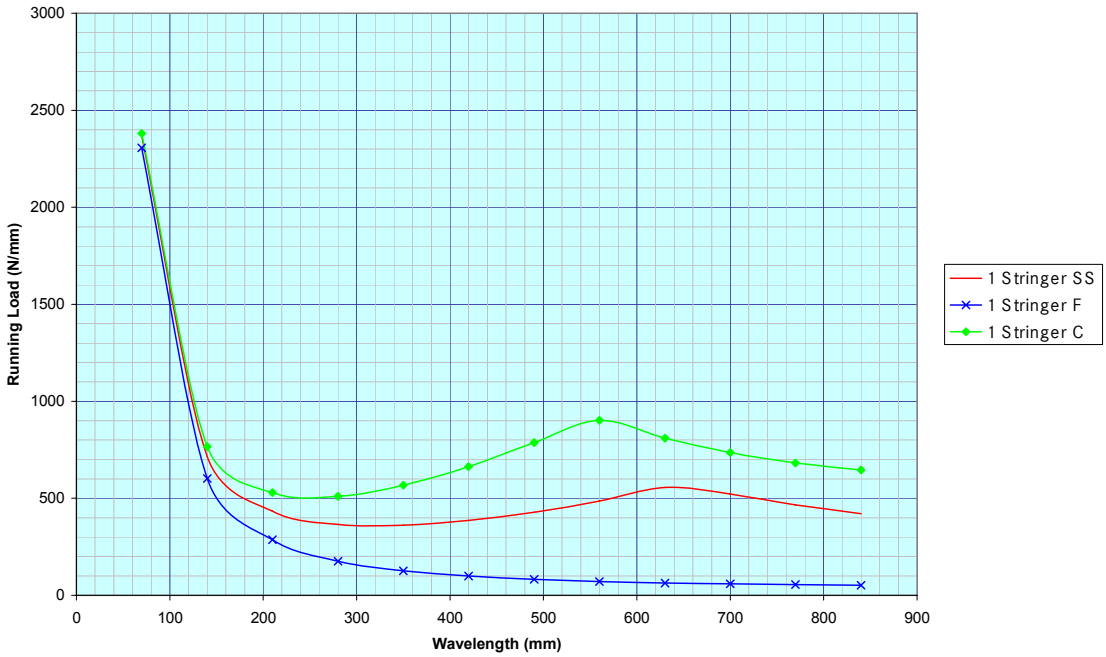

Figure 8-23: Comparison of edge boundary conditions for single stringer-stiffened panel

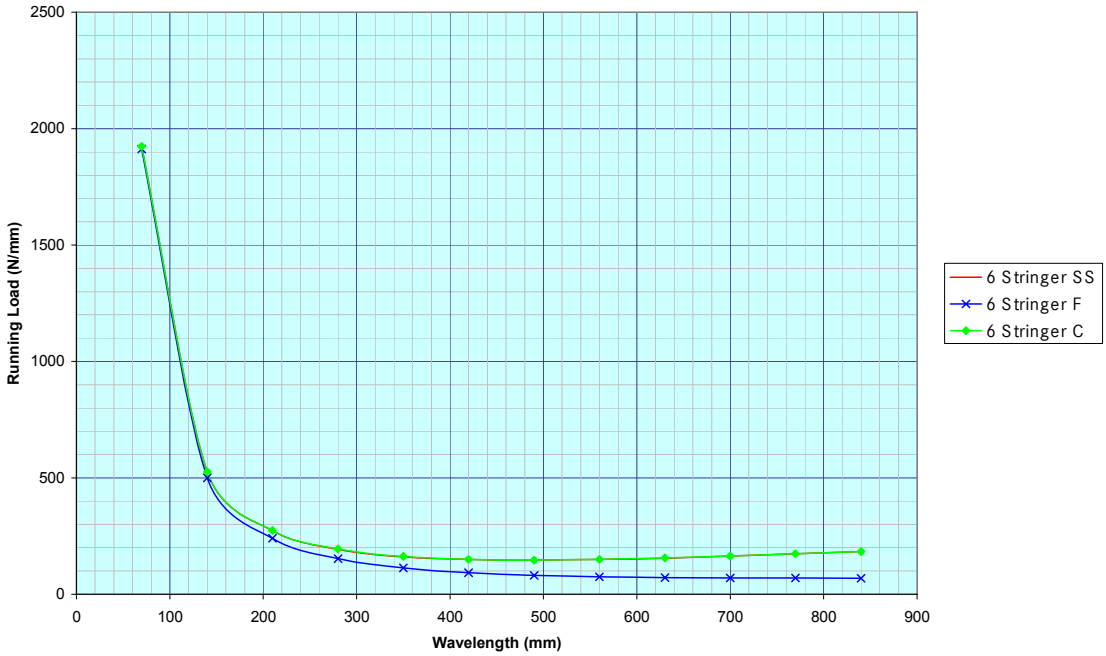

Figure 8-24: Comparison of edge boundary conditions for 6-stringer-stiffened panel

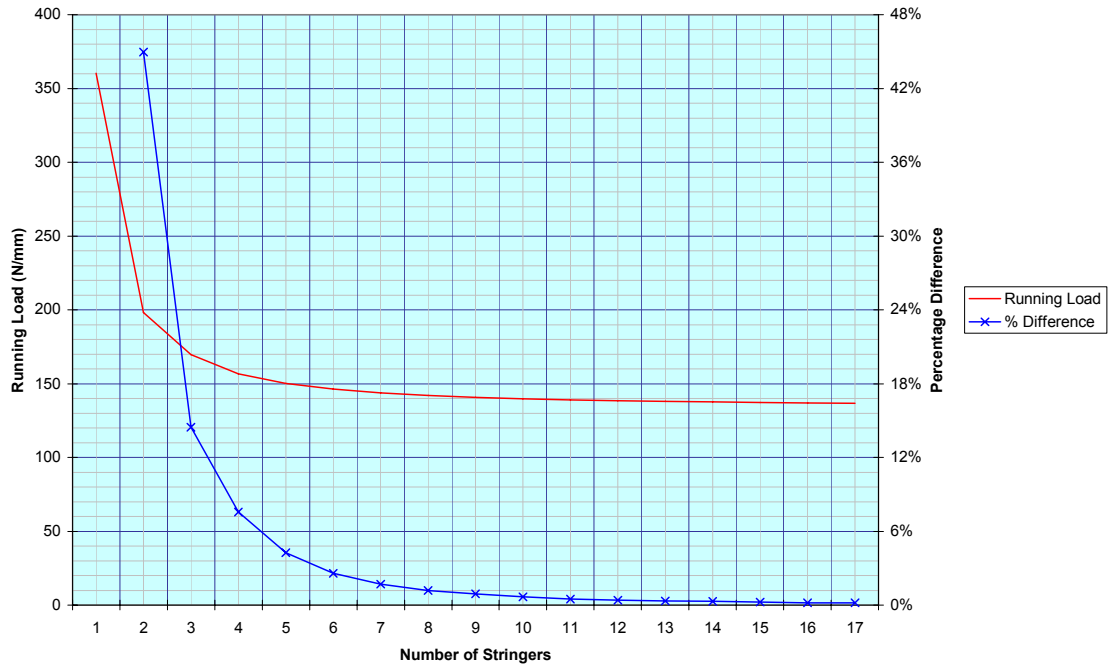

Figure 8-25: Sensitivity study of varying the number of stringers

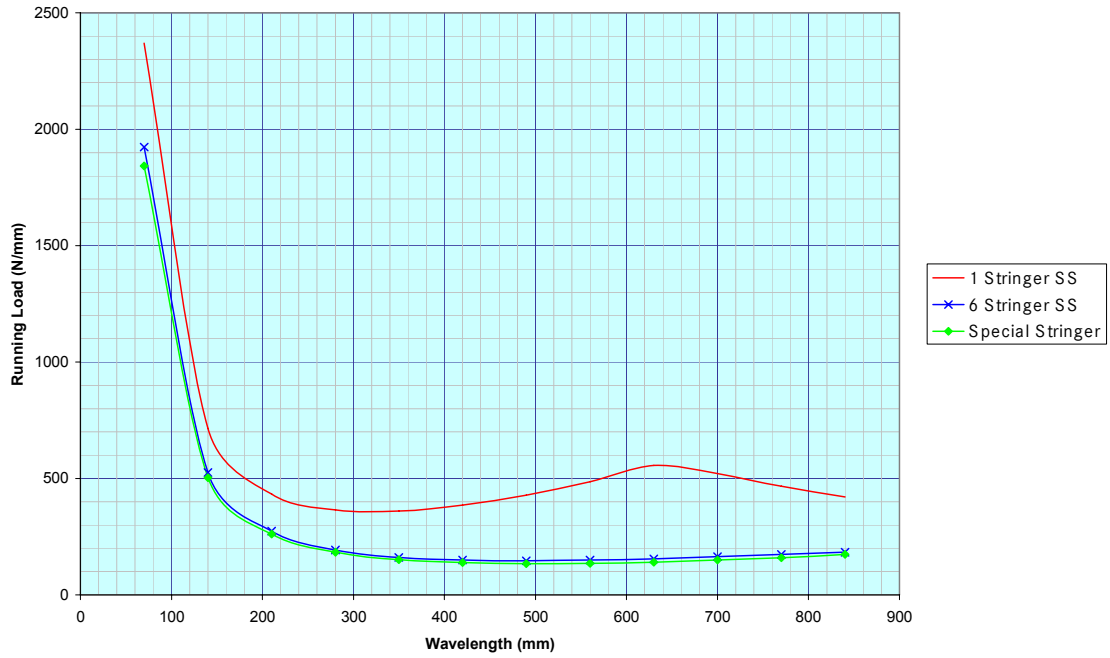

Figure 8-26: Comparison between a special-stringer and a panel with 1 or 6 stringers

8.4.5.1 Adhesive Layer

In the ESDU FSM programs, an adhesive layer is included for all discrete stringers, i.e. the stringer has a flange that attaches to the skin. The adhesive layer is modelled with elements, which improves the discretisation of the problem, with the layer itself based on a simplified strain-displacement relationship. As a film adhesive is normally used then the properties for FM300, which is a typical film adhesive used in the aerospace industry, will be used for all calculations[570]:

- Nominal ply thickness =0.13mm
- Elastic modulus =1.02GPa
- Shear modulus =0.39GPa
- Poisson's ratio =0.3

In order to justify the use of these properties, the specially-orthotropic T-profile stringer-stiffened panel example, as illustrated in Figure 8-16, was investigated. With these properties for FM300 applied the RF=0.55, whereas, with the adhesive properties set to zero, the RF=0.06. Finally, by doubling the moduli of the resin, this only provided a 0.001% improvement in the performance. Therefore, the adhesive properties seem to be applicable to use in combination with the ESDUpac A0817.

8.5 Output Data

The resultant output dimensions are inputted into a fishtail plot, an example of which is shown in Figure 8-27, for an I-profile stringer-stiffened panel. This data can be used to calculate the weight of the wing cover and work out its manufacturing cost.

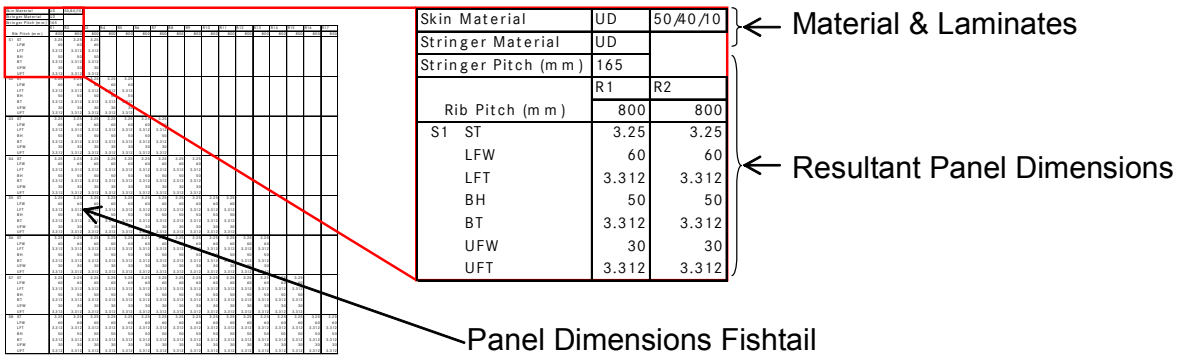

Figure 8-27: Output fishtail plot of resultant wing cover dimensions

8.5.1 Weight Estimation

From the resultant dimensions, it is possible to work out the weight for the wing cover. This weight information is important, not just because weight is critical to the aircraft's overall performance, but also so that different wing cover solutions can be compared. However, the fidelity of the weight estimation must also be considered. For comparison purposes, this is not a major consideration, as it is relative. However, at this level of optimisation it is also necessary that the weight estimation is accurate enough to compare with the given weight target for the product. It is known that this weight will be different to the weight obtained based on the panel dimensions, due to the following reasons:

- Actual structure differs to the theoretical optimum structure due to design and manufacturing constraints
  - Tapering of plies due to change in thickness
  - Constraints due to the ATL
- Theoretical structures do not include items such as
  - Fasteners
  - Lightning strike mesh
  - Tolerance mitigating features

Therefore, it is necessary to use a reality factor, Φ, to obtain a realistic weight (W_{real}) based on the theoretical weight (W_{theor}), as given by Equation 8-6.

$$W_{real} = W_{theor} \times \Phi \qquad \textbf{8-6}$$

For a simple part, like a stringer, the value of Φ will be close to unity, whereas for a complete wing cover, it will be higher[40]. It is judged that a value of 1.15 for Φ is realistic for converting the weight estimated at this level of optimisation, to a realistic end weight. For a complete wing cover, however, this can be very sensitive to the assumptions that Φ is based upon.

9 Cost

9.1 Introduction to Cost Engineering

Due to increased global market competition, cost analysis within engineering projects is now a necessity and not just a 'nice to have'. This has led to cost engineering, which can be defined as "the application of scientific and engineering principles and techniques to problems of cost estimation, cost control, business planning and management science"[571]. Cost modelling is hard to assess as a scientific theory, as it is seen as an attribute of design, manufacturing, or the product itself[5].

Typically, barriers exist between the finance, engineering and production departments, which result in little similarity between the systems that they use for costing activities[572]. This results in difficulties in determining the real costs, as procurement know the real cost of the material, production are aware of how much they really use, and engineering normally have to make a judgment based on their limited information. This lack of integration results in information-islands scattered everywhere, which duplicates effort and is hard to keep accurate[572].

In large firms, there are departments that are responsible for working out the costs for particular designs; however, there is usually a long delay in receiving an estimate, as the department has not been directly involved with the design, thus they do not understand the intricacies of the design, resulting in lengthy discussion required between the designer and the cost estimator. Another cause of frustration is that only a small budget may be available to carry out a formal cost estimation, within a project, as it is still not considered an intrinsic part of the concurrent engineering philosophy. These issues push for an automated cost estimation as part of the design function.

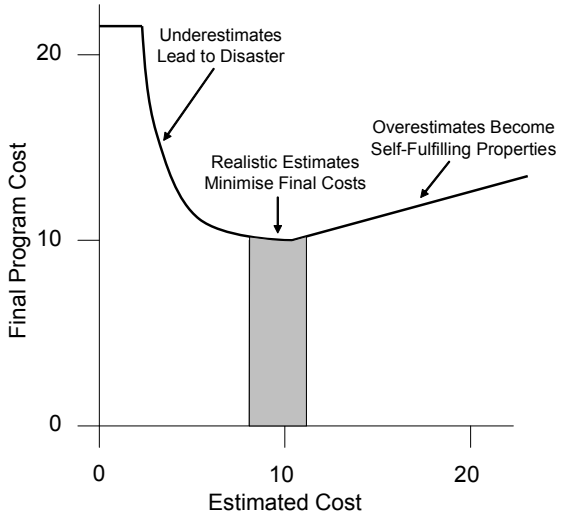

Figure 9-1: The Freiman curve

Another issue concerning cost estimates is the product perceived initially is far different to the end result, and hence the cost estimate will not be accurate. This phenomenon is represented by the Freiman curve[573], shown in Figure 9-1[574], which represents the link between cost growth to the ratio of the actual estimate. The curve has a bathtub shape, which illustrates that underestimates can lead to large cost growth over what the actual cost should be. This inaccuracy can affect the firm's performance, as an overestimation can lead to losing goodwill in the market, whereas underestimation could lead towards financial disaster.

Figure 9-2[575] illustrates the various levels of accuracy needed at different stages of the design cycle. At the conceptual stage, it must be rapid and simple to use, which can provide direction to make relativistic trade-off studies[575], thus an accuracy of ±20% is acceptable.

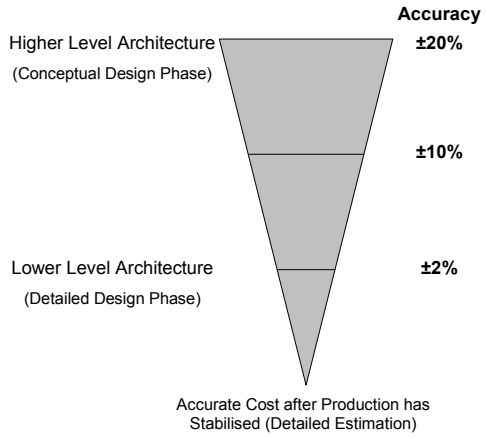

Figure 9-2: Requirements for cost estimation

9.1.1 Cost Methodologies

There are a number of methodologies for cost estimation[522]:

- Design to Cost
  - Manufacturer's cost; does not include the cost of operating
- Design for Cost
  - Manufacturer's cost; does not include the cost of operating
- Cost of Ownership
  - Airliner's cost, but requires a high level of information
- Life Cycle Cost
  - Manufacturer's and airliner's cost, but requires a high level of information
- Direct Operating Cost
  - Airliner's cost, considering the holistic running cost

Design to Cost is a management process, similar to target costing, which derives: "The maximum manufactured cost for a given product; a cost that will allow an expected return to be earned within a given market niche and also allow the product to gain market share"[576]. In other words, the design to cost methodology, attempts to restrain the cost while creating a product that satisfies the requirements[577]. The cost may not be the initial production cost, instead it may be, once the production has progressed someway up the learning curve[578]. However, Design to Cost is not an effective philosophy, as it typically results in an inferior design, and one that overshoots the poorly estimated targets[579]. Design for Cost is an alternative, which makes continuous use of engineering process information during design, and thus is part of the concurrent engineering philosophy[580].

9.1.1.1 Life Cycle Costs

LCC analysis became popular in the 1960s, when the U.S. government agencies required a method to improve the cost effectiveness of equipment procurement[581]. The identification of the design and production process alternatives, which meet minimum performance requirements, both at the lowest average unit production cost, and at the lowest operation and support cost per operating hour[582], are the two principal aims for an LCC trade study. Or in other words LCC estimates the total cost from 'womb to tomb' or 'cradle to grave'[5]. LCC has been mainly used for military aircraft, as the complete cost of the aircraft, i.e. its development, operation and disposal costs, were paid for by one customer. By including LCC in the optimisation process, it is possible to specify LCC, acquisition cost, or DOC as the parameter to be optimised. For an aircraft wing, the LCC can be expressed as given in Equation 9-1[31]:

$$LCC = C_{RDTE} + C_{MAN} + C_{OPS} + C_{DIS} \quad \textbf{9-1}$$

Where C_{RDTE} = research, design, testing and evaluation cost, C_{MAN} = acquisition cost of wing C_{OPS} = operation cost associated with wing, and C_{DIS} = disposal cost of wing. Where[31]:

- RDTE entails: Design; Manufacturing Engineering; Testing; Structure Analysis; System Integration; etc
- Manufacturing entails: Manufacturing; Manufacturing Engineering; Tooling; Quality Assurance; etc
- Operation entails: Maintenance; Overhaul; Repair; Flying; Depreciation; etc
- Disposal entails: Disassembly; Recycling; Disposal; etc

9.1.1.2 Direct Operating Costs

DOC can be used to calculate the cost to fly a passenger over a certain distance, in the most cost effective manner, and hence this metric is popularly used by the commercial sector. This means that acquisition cost, performance, and reliability are important to the aircraft's cost effectiveness[3,575]. Provided by the AEA, the DOC can be calculated with Equation 9-2[575]:

$$\text{DOC} = \text{Fixed Costs} + \text{Trip Costs} \quad \textbf{9-2}$$

Fixed costs include[30,583]: Acquisition; Operation; Maintenance; Interest; Depreciation; Insurance Premium; and Crew. Whereas, trip costs are: Fuel; Navigation; Landing; and Maintenance (repair).

DOC is a good criterion on which to base a cost/weight optimisation, as this can judge, over the operational lifetime of the aircraft, the penalty in terms of cost in fuel burn of carrying extra weight, the effect of the acquisition cost and the maintenance required. As the insurance cost is very small, it can be ignored, and as the cockpit crew cost is not influenced by design, this, too, can be overlooked[522]. Maintenance costs, in particular the direct maintenance costs, are hard to estimate and require insight into airline practices[522], thus this influence can be removed from the cost analysis. The salary cost of the crew and navigation/landing charges are aircraft weight dependent; however they can be considered to be a second order aircraft price dependent contribution to the DOC[575], hence these cost factors are ignored. Therefore, a simplified method to work out DOC at the preliminary design phase is given by Equation 9-3:

$$DOC = FB + AC = FB + n \times MC \quad \text{9-3}$$

Where *FB* is fuel burn and *AC* is acquisition cost. For this level of abstraction, the acquisition cost is assumed to be the manufacturing cost (MC) multiplied by a weighting factor (n), to cater for the desired profit level[583].

9.1.1.3 LCC versus DOC

In simple terms LCC and DOC are very similar, with DOC being encompassed within LCC. The only real difference is that with DOC, the acquisition cost is the price of the aircraft, whereas LCC includes the costs incurred by the manufacturer for developing and manufacturing the aircraft, as well as the cost of disposal of the aircraft. However, today, the manufacturer should be able to better predict these costs; thus the cost to develop, manufacture and earn a profit, should be incorporated within the acquisition price. For this reason, LCC and DOC can be treated, in today's financially regulated environment, similarly.

9.1.2 Cost Categories

Cost can be split into 3 categories:

- RC
- Capital Cost
- NRC

RCs vary as a function of production, hence they are similar to variable costs. A RC is an ongoing/repetitive cost, such as the material and labour required to fabricate the product. Other types of recurring costs are:

- Recurring Engineering: This is for minor engineering changes during manufacturing to improve production
- Recurring Tooling: This is for all labour associated with tool care, maintenance, modification and replacement
- Recurring Manufacturing: This is for all hours spent on scheduling, fabrication, assembly, reworking, etc
- Recurring Quality Assurance: Hours required to inspect the parts as well as the tooling etc

Capital costs are the costs incurred for the purchase of facilities, such as buildings and machines. NRCs, are similar to fixed costs, which are only incurred once during the product's life cycle, and normally occur before production starts, such as:

- Nonrecurring Engineering: This is the engineering hours required to develop the part, which is ongoing until the end of the program, as design changes occur throughout the production lifetime
- Nonrecurring Tooling: These are the tools used specifically for producing the part. The hours spent planning and establishing this is known as nonrecurring tooling hours.

These costs can also be incurred during manufacture, for example if there are changes to the design or if the rate increases and more tools need to be produced

In order to allocate cost properly, the distinction needs to be made between:

- Direct Cost - directly attributed to a product and adds value to the product
  - Direct material, inspection or design costs
- Indirect Cost - not directly attributed to a product and is non value adding i.e. overheads
  - Administration or support costs

9.1.3 Cost Models

Ideally, the cost model should be capable of estimating, early on in the design process, the costs of each step, so that the total LCC can be estimated[521]. Cost models should be developed in partnership with engineers, so the scope of the design possibilities can be comprehended, which entails how flexible the cost model needs to be[584]. Cost models have to be easy to audit and rationalise, should be able to be used by geographically dispersed users, and must integrate with available design and optimisations tools[584].

Cost models can be categorised as either quantitative or qualitative, with the quantitative methods using detailed analysis of a product design, such as its features and the manufacturing process; whereas the qualitative methods compare a new product to a similar existing one. A quantitative method may well be more accurate, however it requires greater effort to construct, and may only offer greater accuracy in comparison to a qualitative approach, once all the design and manufacturing details are established.

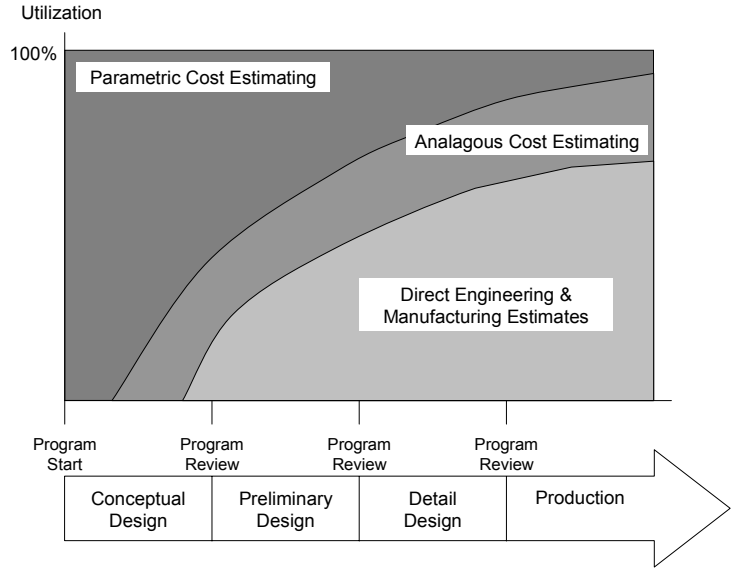

Figure 9-3: Estimating methods versus phase

The compatibility of cost models to the different phases of the design process is illustrated in Figure 9-3[585]. At the conceptual level the model will be based on parametric attributes or weight/complexity-based models[32]. The highest level will include the allocation of RCs and NRCs, as well as the operation and support cost for the entire life cycle of the aircraft[32].

9.1.3.1 Parametric Estimating

Parametric cost modelling, is a commonly used practice, where historical data is used to relate the weight of the product to its cost[586]. The creation of a cost model is fairly easy, but the accuracy of it depends on the exactness of the historical cost data. The costs associated with the complete program can be broken down into separate cost estimating relationships for engineering, material, labour, etc.

Most parametric based models are centred on metallic designs, albeit they can be adapted for composite designs using modifying factors[572]. Metal cost tools are typically based on the principle that less weight will also mean less cost, however, for a composite part this might not be the case. For example, a part could be either fabricated from CFRP or GFRP; the lighter but by far the most expensive, would be the CFRP solution. A further issue is parametric tools do not necessarily consider the advantages of greater part integration potential with composites, which can reduce the cost of the product. Examples of parametric models are DAPCA IV model developed by Rand Corporation[587], and Roskam's book '*Airplane Design: Part V: Component Weight Estimisation*'[588].

9.1.3.2 Analogous and Case Based Reasoning

These methods primarily depend on the similarity and differentiation of like-products, so that the cost estimate is comparable to a previous one[589]. Through differentiation, the like-product's historical cost needs to be adjusted to account for any variation in design, etc. However, such estimation is dependent on the similarity between the parts and the time gap between, although this should not be too significant as aircraft design is fairly iterative. The difficulty is with the definition of analogies. The approach taken by Eaglesham[572] used actual process times for the same or similar products, through looking at previous manufacturing production job cards.

9.1.3.3 Detailed Estimating

A top-down or bottom-up method can be applied to all estimation methods. Top-down will involve the creation of an overall estimate to represent the completed project, which can then be broken down into subcomponents of cost. Bottom-up, on the other hand, will create sub-level and component costs initially, which can then be added together to attain a complete cost estimate.

This technique entails the posthumous collation of the complete cost information that is directly related to the part, which is derived from the functional Work Breakdown Structure (WBS) to give an appraisal of material, fabrication, and assembly. Such an approach is difficult to manage and maintain[7]; as it requires various detailed inputs that can only be obtained after the part has been defined. However, if the level of abstraction could be chosen, then this can determine the level of detail required; after all, when trying to obtain the cost of manufacturing and assembling a wing box, it is not really necessary to model the cost of the fasteners that attach an electrical bracket to a rib.

9.1.3.4 Activity Based Costing

The traditional method of cost accounting would allocate the overhead costs attributable to the part based on volume. Such a method was pertinent when volume bases could be related easily to cost consumption. However, due to the higher proportion of automation found in today's manufacturing, the proportioning of costs between direct material and labour costs, and production overhead cost has changed[583,590], with the latter being dominant[5]. As the traditional accounting systems are not an efficient method to allocate overhead charges, due to its inability to breakdown non-value adding activities, Activity-Based Costing (ABC) has been developed, to overcome some of these shortcomings. ABC is a methodology that measures the cost and performance of activities, resources, and cost objects. Resources are allocated to activities, then activities are assigned to cost objects based on their use. The cost elements include:

- Factory overheads
    - Includes all the costs to be attributed to the final product including general and administrative costs
- Production overheads
    - Includes cost items such as depreciation, transport, storage etc

ABC is preferred in composite material manufacture as it can evaluate the overhead costs more accurately[591], as well as being applicable to all activities involved, such as: design and engineering, production planning, material procurement, fabrication processing, and delivery to customer[572]. ABC relies on historical data and thus is not capable to determine the impact of production, design, or material changes[196], which is exacerbated when novel design or manufacturing processes are used. Furthermore, not every company has the resources to use this technique[572]. However, at the preliminary design, a simplified ABC method that utilises the main features of the design and a simplified process plan, could provide adequate cost estimates[35].

9.1.3.5 Genetic Causal Method

Certain key attributes of a product are causal; a tool to estimate cost could be based on high-level influential manufacturing drivers that relate to fabrication and assembly cost. This is an ideal method at the preliminary design stage, as it avoids in-depth manufacturing calculations. Such a model can look at the cost factors through the material transformation route, which can allow easier integration of bought-in or semi-finished components, such as preforms. A genetic-causal method is achieved by[592]:

- Classifying the generic cost elements that are linked to a particular (genetic) design (product) attribute
- Developing causal parametric relations that link those genetic attributes to the resultant manufacturing (or life cycle) costs

The Genetic Causal Costing Model categorises and incorporates the scientific requirement of utilising causal relations. The generic methodology has the following principles[7]:

- Genetic principle: cost is classified into families according to product and process, to identify likely commonality through shared cost drivers

- Causality principle: cost is formulated into a relation as a function of the design attributes which gives rise to a cost potential, using: weight, geometric size and shape, material selection, part count, fastener count, etc

The costs can be split into: Materials, Fabrication Processes, and Assembly. Other costs can be then split into: Support, Quality, Inspection, and General Factory Overheads. Furthermore, jigs and tools can be considered, whereas machine costs can be amortised with a utilisation factor over a certain period. However, the main point to understand is that any cost that is genetically inherited and comes from the engineering definition is a dependent cost.

9.1.3.6 Process Based Cost Model

A Process Based Cost Model (PBCM) is related to the acquisition cost of the product being modelled[521]. The basic ideals of a PBCM are[593]:

- Predict fabrication costs for designs and processes for which production data are available
- Predict fabrication costs for advanced technology designs and processes for which directly applicable production data are not available
- Evaluate a range of advanced designs based on modifying variables normally specified on engineering drawings
- To be refined over the course of the structural development effort

Figure 9-4[196] outlines the steps required to develop a consistent cost model. It is necessary to consider the objective of the cost estimation, i.e. is it purely the manufacturing cost required, or should overhead charges be included, etc.

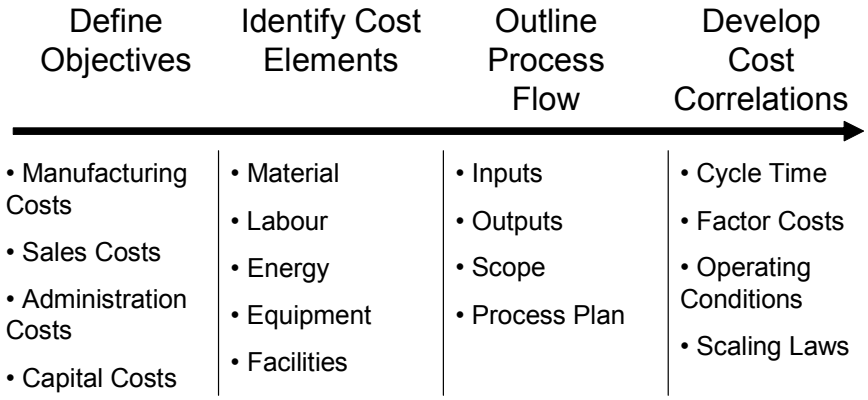

Figure 9-4: Process based cost model

A detailed manufacturing cost estimating process can be created, once the following premises are established[593]:

1. Identify a design
2. Prepare a manufacturing plan
3. Make estimates for each process step in the manufacturing plan
4. Sum up the costs for each process step in the manufacturing plan

The inputs must consider the design of the production facility (equipment layout, machine processing and failure rates, machine capacity), the operational conditions (flow of materials

and work-in-progress, arrival schedule of parts), and the operational policy (last-in-first-out, batch size). The development of the factory will begin by identifying the major process cells to be used for a particular design, where a process cell is an area within which a sequence of related process steps is conducted.

By automating formulated equations for each manufacturing step, this can allow the identification of parameters that control the part cost, as well as being the optimum format to be integrated into an MDO algorithm[593]. The process steps should be able to be modelled at different levels of fidelity, due to the availability of information. The reason for this is if a new process is to be used, then initially it should be simply formulated, but later the process steps can be more detailed. To acquire information to construct a PBCM, this will require various sources to be investigated[33].

NRCs, such as capital equipment and tooling, can be allocated based on the time it is used. The cost for an autoclave, for example, can be related to an hourly charging rate, which is based on the purchase price, the interest rate, use factors, maintenance, scrap rate costs etc. If there already exists capital equipment and it is not fully utilised, then it can be argued that capital cost should not be included at this level of abstraction. If NRCs are incurred, the engineer can only minimise these costs through maximising the utilisation. For example, if only one ATL is used, the production rate might not be met, but if two ATLs were purchased, then the rate is met but it could mean one of the ATLs is then underutilised. Equation 9-4 is the basic equation for estimating the manufacturing cost of a process step.

$$MC = PT \times PC \qquad \textbf{9-4}$$

Where PT is process time and PC is process cost. Costs that cannot be determined through time can instead be determined through a physical parameter such as area, which determines the amount of the resource being consumed. For example, cleaning a tool can be based on the tool's surface area; however, for the laying up of a part, not only area but also distribution of thickness is important.

A correctly established PBCM should have better accuracy than qualitative methods based on empirical formulae[521]. However, a PBCM takes an engineering perspective to cost modelling; hence it ignores the accounting basis of the information[572]. Due to the lack of a standard database, and because of the proprietary nature of cost information, little work has been conducted in the field of PBCM[146]. Furthermore, PBCMs that have been developed by a company, will be specific to the company, therefore its applicability to other companies is limited[572]. It should be noted that previous successful PBCM required three or more highly skilled academics to develop it for each manufacturing case; therefore in practice a PBCM would be very expensive to establish[572]. At least three PBCM tools exist, namely[572,591,594,595]:

- Northrop's Advanced Composite Cost Estimating Model (ACCEM)
- Manufacturing Cost Model for Composites (MCMC)
- MIT and Boeing developed Composite Optimisation Software for Transport Aircraft Design Evaluation (COSTADE)

9.1.3.6.1 ACCEM

ACCEM was developed by Northrop Corporation for the USAF and was originally published in 1976. The complete process is modelled as individual primitive steps, based on power-

laws, which accumulate to give the total fabrication cost. Such a model is good for processes that are either additive (tape-laying) or subtractive (machining) in nature; however, it can become a very complicated model[596].

9.1.3.6.2 COSTADE

COSTADE combines a truly multidisciplinary formulation with design, stress, manufacturing, weight, and cost modules[597]. COSTADE can be used at the preliminary design phase, to analyse trade-offs between cost and weight on composite structures[593]. COSTADE considers a number of manufacturing processes, including automated and manual operations[558]. COSTADE's cost estimates are based on resource cost and manufacturing time relations that utilise a number of ground rules for RC and NRC[558].

COSTADE uses size and complexity scaling laws to offer simple and physical interpretations of the most important effects of part size and complexity respectively, when estimating the times for each of the individual process steps. Developing general scaling laws, that are both simple and offer physical interpretation, can be a way to avoid using detailed empirically based models, which are particularly beneficial for novel processes[598]. The size scaling laws assumes that manufacturing operations (humans and machines) can be represented as dynamic systems with first order velocity response. Thus, a general relationship can be derived which relates the time of an operation and some extensive (size) measure of the operation, such as length, area, volume, and weight. Size effects can be derived from data, but for automated processes, it is possible to use equipment specification to estimate the time.

9.1.3.7 Commercially available Costing Tools

Commercial cost models, such as PRICE-H and SEER-MFG, have pre-programmed cost frameworks, which can be tailored to a specific need by using a firm's cost data[58].

9.1.4 Secondary Considerations

9.1.4.1 Learning Curve Effects

The "learning curve" or "progress function" dates back to 1936 in the paper "Factors Affecting the Cost of Airplanes" by T.P. Wright[599], who found the premise that the cost required to fabricate a part decreases as production volume increases. This is because humans learn and get better at doing repetitive jobs, as well as there being economies of scale for large production quantities[33]. The reasons for improvement include: an increase in employee's skill level; improved production methods; better management practices – such as production planning; implementation of quality policies; standardisation of the product and process; better worker and management relationship; etc[146].

Learning curve effects are dependent on the size and complexity of the product. If it is fairly complex and takes a longer time to make, then the amount of improvement occurs over a longer time period[146]. One pertinent factor is organisational learning which inflicted the Lockheed L-1011 Tri-Star program in the 1970s. Lockheed lost over $1 billion, as the program did not follow the typical learning curve pattern. Cut backs in production led to knowledge depreciation, which caused a shift in the learning curve. This meant financial disaster for the program, as the unit production cost was greater than the selling price[32]. This

trend continued throughout production. Therefore, a new aircraft will require a substantial order book, to ensure the production run is long enough, and the initial orders are sufficient to guarantee that learning can be accrued quickly. This makes it even more important to get the design right first time to ensure the greatest learning.

9.1.5 Use of Spreadsheets

As reported by Kendall et al.[600], cost models are typically built using computer based spreadsheet programs. A spreadsheet is parametric in nature and can therefore offer great flexibility in change as well as easy manipulation of process and/or economic parameters for sensitivity studies. The format of a spreadsheet is also familiar to all disciplines, including engineering and accountancy. However, spreadsheets are not without their issues. Spreadsheets can become quite complicated and are difficult to decipher by other users, which means they are hard to audit. This is exacerbated by having hidden sheets or cells, which form an intrinsic part of the spreadsheet, although the input sheet is fairly simple. This means, if a third party wants to develop it, it is often easier to start from the beginning again.

9.1.6 Summary

A PBCM will be used as this can most accurately model the cost. However, as a PBCM requires fairly detailed information on the process steps, only established processes will be used, as novel manufacturing processes may require many years of data collection to ensure accurate cost estimations[33]. The reasons for not using a commercially available code model, such as SEER-MFG for this work, are:

- By developing a cost model, the methodology and assumptions are known
- Not to be dependent on the software supplier
- A heavy financial cost would be incurred if using 3rd party software
- The work entailed in the thesis would only use a small portion of the program's functionality

9.2 Creating the Cost Model

9.2.1 Basic Methodology Premise

There are essentially three elements to the cost methodology; the first part is a way of comparing different designs, based on the financial benefit of reducing the weight, whereas the second part calculates the actual manufacturing cost of the product, and the third part estimates the disposal costs.

9.2.1.1 Economic Value of Weight Saving

The benefits of a lighter weight structure must be justified, particularly when the decrease in weight results in an increase in cost. One method of doing this is to compare them directly, by using the cost premium Equation 9-5:

$$C_P = (c_{alt} - c_{base})/(m_{base} - m_{alt}) \quad \textbf{9-5}$$

Where C_p is the cost premium in order to save the weight difference between the two designs, m is the mass and c is the cost, whereas subscripts '*base*' and '*alt*' are the baseline and alternative designs respectively. The cost required to save 1kg of weight can be simply calculated by Equation 9-6:

$$C_P = (c_{alt} - c_{base})/(m_{base} - m_{alt})^2 \quad \textbf{9-6}$$

An alternative method as proposed by Ashby[601], is to use a value function as an exchange constant. The exchange constant is the Economic Value of Weight Saving (EVWS) for every 1kg saved. The value function V is given by Equation 9-7:

$$V = EVWS \times m - c \quad \textbf{9-7}$$

A simple calculation to see if one design is more cost effective than the other, based on a weight penalty and EVWS, is given by Equation 9-8[150]:

$$Benefit = \frac{c_{base} + (m_{base} - m_{alt})EVWS - c_{alt}}{c_{base}} \quad \textbf{9-8}$$

If the equation results in a value greater or equal to 0 then there is a benefit in using the comparative system.

9.2.1.2 Establishing a value for EVWS

A number of values for EVWS have been defined previously; for example, Bader (2002)[160] used a value of \$1000/kg for general commercial aircraft; whereas Castagne et al. (2004)[52] used a value of \$300/kg for regional aircraft; and Edwards et al. (1998)[556] recommended a value of \$150/kg. However, this value should be dependent on the price of fuel, the fuel efficiency of the engines, as well as the range of the aircraft. These factors are incorporated into Equation 9-9[602]:

$$EVWS = \left(\Delta W_A \times \left(e^{\frac{ctg}{r}} - 1 \right) \right) \times FC \times FP \quad \textbf{9-9}$$

Where, ΔW_{FO}=extra weight of fuel (kg) used to fly range R, ΔW_A=extra structural weight (kg), c=specific fuel consumption ($kg \cdot s^{-1} \cdot N^{-1}$), g=gravity ($m/s^2$), t=time taken to cover the range R (s), r=the lift to drag ratio, FC=flight cycles, and FP=fuel price (\$/kg). For an A320 type and A340 type of aircraft the EVWS, based on a fuel price of \$0.75/gallon, was \$513/kg and \$1038/kg, respectively. For the derivation of these values, and derivation of the Equation 9-9, D.6 should be referred to.

9.2.2 Manufacturing Cost Calculator

9.2.2.1 Premises for Calculation

- Principal Manufacturing Steps and Factory Layout
- Material Costs
- Capital Equipment and Tooling
- Labour Rates
- Production Rates
- Outsourcing Policy

9.2.2.1.1 Principal Manufacturing Steps and Factory Layout

Although there are many fabrication and integration techniques possible, resulting in a great number of different permutation for methods to manufacture a wing cover, only the principal combinations, shown in Figure 9-5, will be considered further. In terms of the integration: COCU = co-cured, CBSK = co-bonded (pre-cured skin), CBST = co-bonded (pre-cured stringer), and SEBO = secondary bonding. For the stringer profile: USTR = U-profile stringer, TSTR = T-profile stringer, and ISTR = I-profile stringer. For the skin laminate: LTLD = laminate tailored, L541 = laminate with a 50/40/10 distribution, L361 = laminate with a 30/60/10 distribution, and L181 = laminate with a 10/80/10 distribution. For the skin material, there are the following options: SKUD = skin fabricated from UD and SKNF = skin fabricated from NCF. Similarly for the stringer material: STUD = stringers fabricated from UD, STNF = stringer fabricated from NCF, and STBD = stringer fabricated from braids. For the stringer (ST) and skin (SK) the fibre type options are: **HS= HS fibre, **IM = IM fibre, and **HY = a hybrid laminate of IM and HS fibre.

The choices available for the different integration processes illustrated in Figure 9-5, have been explained in the previous chapters, however a short review behind the reasoning is nonetheless pertinent. Co-curing is the only integration process that can use all stringer profiles, as using a co-bonding or secondary bonding technique for a U-profile stringer panel is not possible. Furthermore, as co-curing uses the resin to bond the discrete parts together, and not an adhesive, it is also possible to use all skin laminate types. For co-bonding or secondary bonding, only the tailored or 50/40/10 laminate can be used, due to the Poisson's ratio constraint between the stringer foot and skin.

Co-bonding techniques can only principally be used with UD prepreg, as co-bonding requires both external heat and pressure for the film adhesive to activate, whereas a VARTM/MVI process, which is used to infuse the dry NCF, requires only heat, thus the co-bonding process is incompatible with infusing an NCF part. However, despite it being theoretically possible to co-bond a dry fibre stringer to a hard skin, using an LCM process, it would require complicated tooling to ensure that resin does not escape from the stringer local mould tooling, therefore it is discounted here. Furthermore, co-bonding of an NCF or braided cured stringer, with a uncured prepreg skin is foreseeable, as identified in Figure 9-5 by the boxes being coloured green, although the resin systems should be compatible, such as Cytec's 977-2 resin system for prepreg and 977-20 for liquid resin.

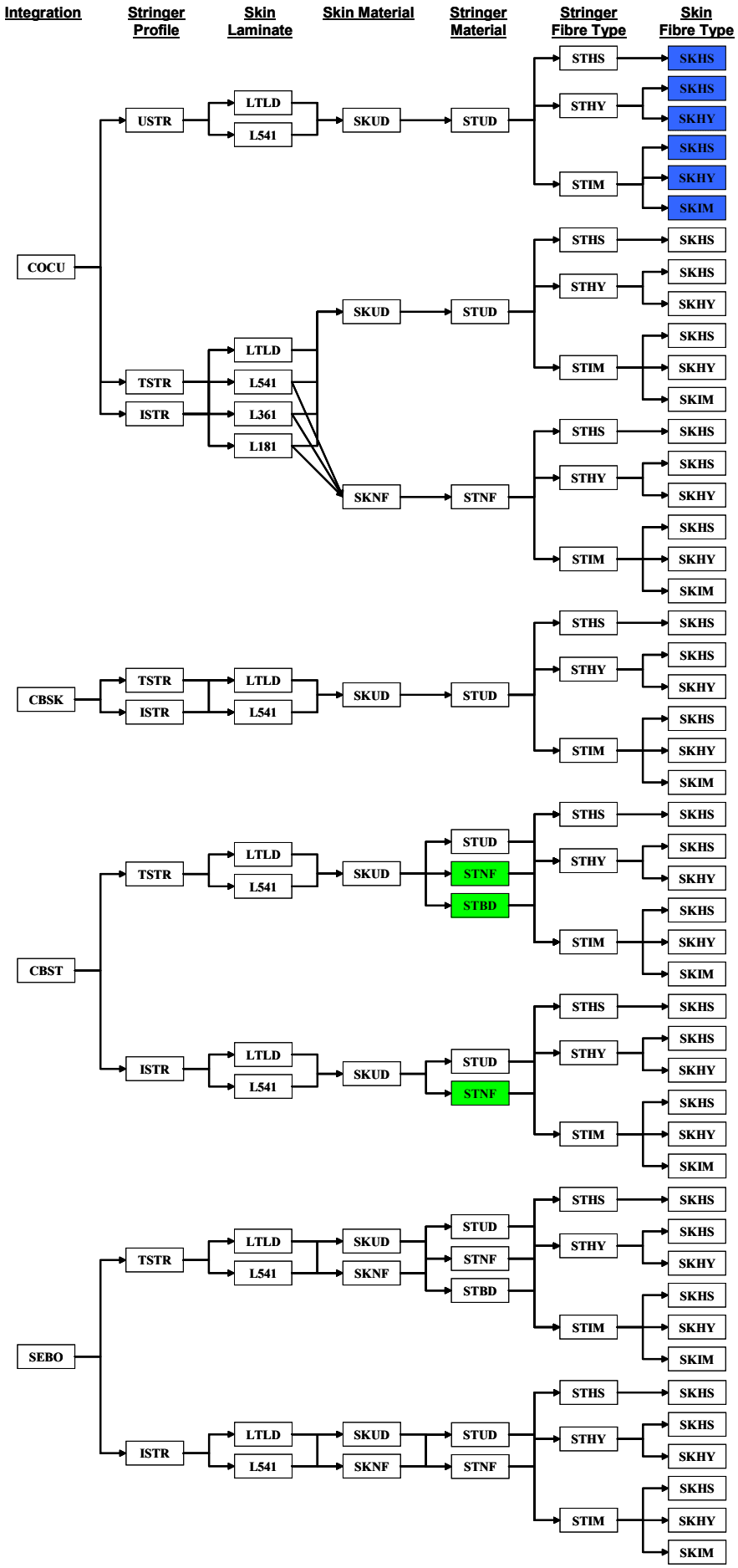

Figure 9-5: Global integration processes for wing cover

Stringers fabricated from braids are only applicable to pre-cured T-profile stringers, as the braids considered here have a constant diameter. Thus for a dry preformed stringer, the resultant braid sock will have to be cut along its length, which can lead to the braid disintegrating. This problem is exacerbated for an I-profile stringer, where the blade height needs to vary along the length, thus making the stringer spine for a braided I-profile stringer is not feasible, regardless of the cover integration technique.

In terms of the combination of fibre types between the skin and the stringer, it is nonsensical to use an IM skin with either HS or hybrid stringers, as the IM skin has the lowest strain allowable, relative to the HS and hybrid skins, whereas the stringers should be as efficient as possible, thus using HS and hybrid stringers in combination with an IM skin, would lead to an expensive yet relatively inefficient combination.

Finally, the blue coloured boxes highlight that a stringer pitch less than 125mm can be used, for the U-profile panel, whereas for the other panel types the minimum stringer pitch must be greater than 125mm.

In Appendix E the principal process steps are detailed for each different method of cover manufacture. As can be seen from Appendix E, the different process steps have been rationalized in order to make the issue of calculating the manufacturing cost tractable. There are many process steps that are not only repeated within the manufacturing process, such as the application of a vacuum bag, but that they are common process steps across all methods of cover manufacture.

The fidelity of the process steps to attain the manufacturing cost is considered suitable for the preliminary design phase. Shown in Table 9-1 are the principal steps required to deposit UD tape using an ATL. The steps in italics, at this level of fidelity, are considered not necessary for the manufacturing cost calculation. For instance "Take Roll Out of Freezer", "Insert Roll into Machine" and "Position Tooling to Machine" requires so little time relative to "Carbon Fibre Deposition" that they can be ignored. Furthermore, the operation "Thaw Roll" is a step that can be conducted off-line, i.e. the roll can be thawed outside the intrinsic process flow. Therefore the only three processes that are of importance are those in bold type face shown in Table 9-1.

Take Roll Out of Freezer	*Time*	*NA*	*0.05 hrs*
Thaw Roll	*Time*	*NA*	*8 hr*
Insert Roll into Machine	*Time*	*NA*	*0.15 hrs*
Position Tooling to Machine	*Time*	*NA*	*0.05 hrs*
Carbon Fibre Deposition	**Volume**	**NA**	**Use Calculator**
UD Deposition	**Piece**	**NA**	**0.02 hr**
Edge of Part Ultrasonic Cutting	**Perimeter**	**NA**	**50 m/hr**

Table 9-1: Process steps for ATL UD deposition

The process times will depend on material characteristics, automation, tooling aids, and factory layout[33]. It was not possible to conduct time and motion studies for the different process steps, therefore the author estimated the durations based on his experience. To reduce the risk of amplifying inaccuracies the cost model concentrates purely on the manufacture of the CFRP cover manufacture. Therefore no drilling or subsequent bolting will be considered, such as at the SRO positions, or as a debonding stopper, as the drilling operations are assumed to occur in the drill jig for wing box assembly.

9.2.2.1.2 Material Costs

When material cost is taken into account, it is principally the CFRP used to fabricate the part, which is considered. However, during the different processes that are used to produce the resultant wing cover a number of secondary and tertiary materials are used. Examples of secondary material would be lightning strike mesh and adhesive film, whereas tertiary materials could be tool cleaning or release agent, and breather material or the vacuum bag. Therefore, for each process step the materials used needs to be understood, in order to gain a more accurate manufacturing cost estimate.

Obtaining realistic CFRP cost data is difficult. One of the reasons for this is that the price of the material is very much dependent on the amount of material purchased. For instance, when purchasing 25,000kg of CFRP, the price could be \$265/kg[lii], whereas a larger purchase of over 112,500 kg, could reduce the price to \$199/kg[603]. This is perhaps another reason why single sourcing and one type of CFRP is used for the complete aircraft, in order to maximise the amount of material purchased, and hence reduce the cost.

In Appendix E all pertinent material costs are listed as well as the primitive disposal costs for CFRP during manufacture and at the end of the aircraft's life cycle.

9.2.2.1.3 Capital Equipment and Tooling

The cost per hour for all significant capital equipment is given in Appendix E. All capital equipment will have straight-line depreciation. There will be sufficient capital equipment to support the monthly rate, which will be calculated based on the process duration. It is assumed that any excess capacity can be utilized by other projects

Similarly, there will be sufficient tooling to support the monthly rate, however as tooling is specific to the individual project, then if under utilization occurs then this cannot be mitigated. Thus the cost of the tooling is simply the number of tools required multiplied by the cost of the tooling, amortised over the total production rate.

9.2.2.1.4 Labour Rates

Labour is related to tooling and equipment, as well as floor space required to meet production rates, which is dependent on process times. Labour costs for a given process are generally a function of [33]:

- The required team size
- Labour rates (cost/unit time) for a given skill level
- Burden rates (e.g. employee medical and retirement benefits) for a give job description
- Overhead rates that depend on a company's accounting practices

The cost for direct labour cost will be \$100/hr[196], which includes overhead and benefit charges. Direct labour can be redeployed to other tasks, be it another task within the manufacture of the wing cover, or on another project within the firm.

[lii] Based on fiscal year 2000.

9.2.2.1.5 Production Rate

The production rates (number of products required per month), total production run, as well as the process step times, will have a strong effect on the NRC assessments. Shown in Table 9-2 is a summary of production rates for various categories of aircraft based on the market analysis carried out in Appendix E. Furthermore, the number of suppliers in the market is included in Table 9-2, which then defines the expected yearly rate. Currently, there are two Primary Manufacturers serving the regional aircraft market, namely Bombardier and Embrear, whereas for the conventional commercial aircraft, there is currently also a duopoly market, with Airbus and Boeing. It is assumed that for the regional aircraft market there could be up to 6 suppliers, whereas for the more capital-intensive larger commercial aircraft market there could be 3-4 suppliers. It will be assumed that all programs will have a production span of 15 years.

	Regional Aircraft			**Commercial Aircraft**		
	20-60 Seater	**61-90 Seater**	**91-120 Seater**	**SA**	**WB**	**VLA**
2 Suppliers	24	96	96	348	156	24
3 Suppliers	12	60	60	228	108	12
4 Suppliers	NA	48	48	180	NA	NA
5 Suppliers	NA	36	36	NA	NA	NA
6 Suppliers	NA	24	24	NA	NA	NA

Table 9-2: Predicted manufacturing rate for various aircraft types per year

Production will be based on a ((52×5)-25)=235 days of production per year, with 85% uptime, with two 8 hour shifts[196].

9.2.2.1.6 Outsourcing Policy

Outsourcing can be considered as an external supplier manufacturing parts, who contributes to the overall assembly of the wing cover. There are different possibilities for outsourcing, which is dependent both on the outsourcing strategy and on the location of the supplier. The premise of this study is that the assembly (integration) of the wing cover is of strategic importance to the prime contractor; hence this will not be outsourced.

The outsourcing of the stringers, and even the skin, could be foreseen, however this is very much dependent on the method of integration of the stringers to the skin, i.e. co-cure, co-bond, or secondary bond. It is unlikely that just the cured skin would be outsourced, particularly for the larger wing skins, as they would be cumbersome to transport, and as the cost of transportation, for just the skin, or for the cover with the stringers integrated, would be about the same, then this would typically not be pursued. Furthermore, an NCF preform for the skin would have the same problems, as due to the thickness and both the spanwise and chordwise curvature, it would be necessary to ensure the preform is fabricated in its required form, thus it is unlikely afterwards that it could be rolled up, to ease transportation. However again this is dependent on the size of the skin.

If the supplier could be in the immediate vicinity of the prime contractor, this would allow the supply of uncured parts to the prime-contractor, however this would not be possible if the supplier is located away from the prime contractor's site, due to the shop-life of uncured prepreg. As shown in Table 9-3, there are many outsourcing permutations. However, in terms of the manufacturing cost calculator, at this level of abstraction, there will be no direct influence if an outsourcing strategy was pursued or if it is made in-house.

		Co-Cure		Co-Bond (Hard Str/Soft Skin)		Co-Bond (Soft Str/Hard Skin)		Secondary Bond	
Outsource		**Prepreg**	**NCF**	**Prepreg**	**NCF**	**Prepreg**	**NCF**	**Prepreg**	**NCF**
Off-Site	Skin		Preform		NA	Cured	Cured	Cured	Preform / Cured
	Stringer		Preform	Cured			NA	Cured	Preform / Cured
On-Site	Skin	Uncured	Preform	Uncured		Uncured / Cured	Cured	Uncured / Cured	Preform / Cured
	Stringer	Uncured	Preform	Uncured / Cured		Uncured	NA	Uncured / Cured	Preform / Cured

Table 9-3: Outsourcing possibilities

9.3 Economic Model Premises

The overall cost is given in Equation 9-10:

$$\text{Overall Cost} = \text{Manufacturing Cost} + \text{Disposal Cost} \qquad \textbf{9-10}$$

The overall cost does differ from the stated LCC, as it does not include a cost for research, design, testing and evaluation. This is because this cost is complicated to predict, as it is dependent on the strategy taken in developing the aircraft, in terms of its novelty, how the development will be carried out, i.e. globally dispersed teams due to strategic reasons, or carried out within the confines of the Primary Manufacturer.

It will be assumed that 0% scrap will occur, i.e. the manufacturing process is robust enough to ensure that all parts produced are fit for purpose. This is probably not realistic as scrap parts will occur, but as the results will be used relative to each other, then as they are based on the same assumptions then this assumption is tolerable.

A discount rate could be applied to account for inflation over the assumed 15 years of production, however due to primitive nature of the manufacturing cost calculator, and that the different solutions will be compared relative to each other than a discount rate is not necessary.

Overhead costs will be ignored, thus support functions such as maintenance, part and material distribution and administration/management will be ignored. Furthermore, energy costs have been ignored, which could be a significant cost for equipment such as an autoclave. There will also be no allowance for learning curve effects.

The Pareto 80:20 rule will be applied to the process times and hence this will also proportionally increase the labour and capital equipment costs, however the material costs will not be amended. This is because the material costs, in particular for the CFRP material, already consider issues such as off-cut material. There will be also be a 80% utilization rate applied to the process time to reflect the efficiency of the production procedure.

10 Results

10.1 Structural Optimisation

The optimisation process was verified based on a fairly simple, but representative, cover with overall dimensions of 625×2400mm. Despite the overall cover dimensions remaining constant, the stringer pitch varies, as shown in Figure 10-1, thus the load distribution changes[liii]. The exact configuration of each cover is shown in Table 10-1, which highlights that three different stringer pitches and stringer profile types were evaluated, as well as different CFRP materials and laminates. The weight of each configuration is illustrated in Figure 10-2 and detailed in Table 10-1.

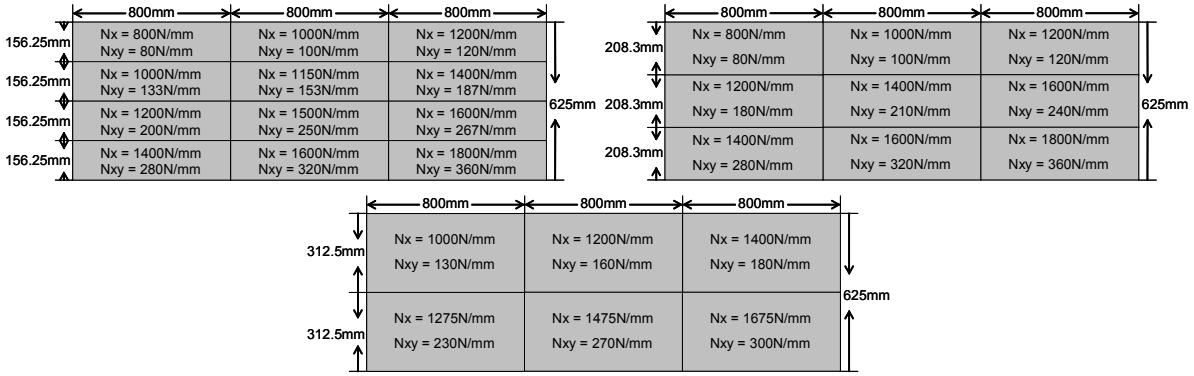

Figure 10-1: Load distribution for covers with varying stringer pitch (overall 625×2400mm)

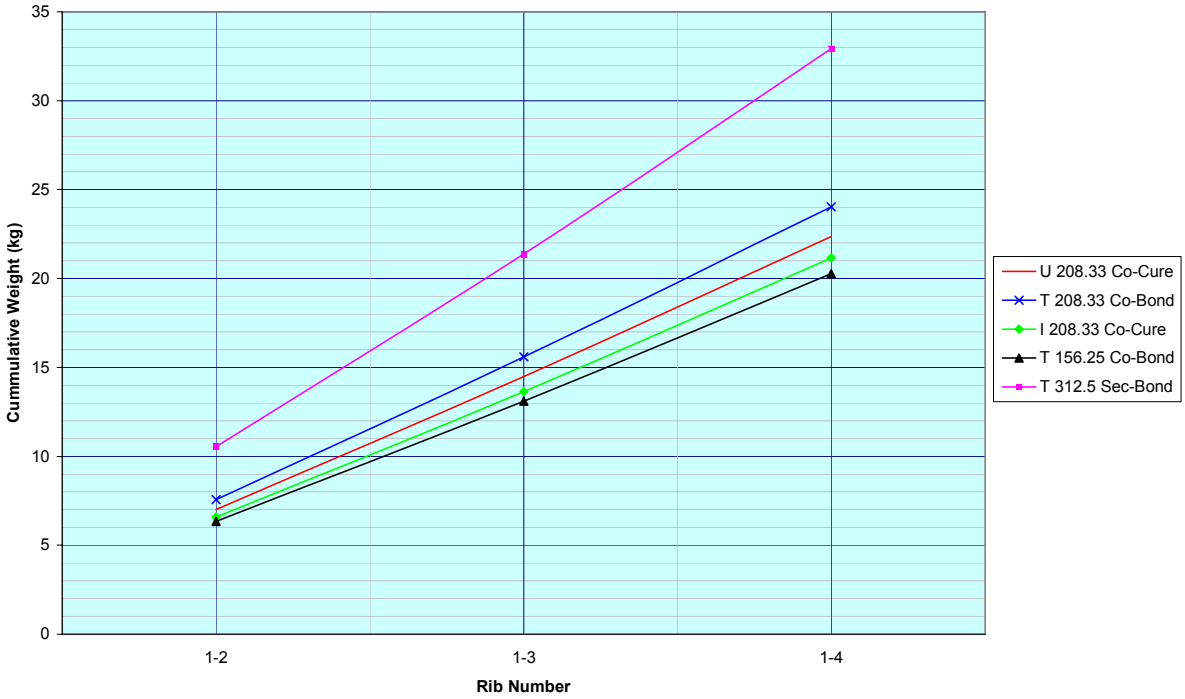

Figure 10-2: Cumulative weights for optimisation examples

[liii] The disparity in total load across the three different panels is within 3%.

The results show clearly that for a stability critical stringer-stiffened cover, a reduced stringer pitch, with a more efficient stringer shape, i.e. an I-profile, a skin laminate with a higher proportion of ±45° plies, i.e. 30/60/10, and higher performance IM fibres are all advantageous. These results correspond well with the theory.

Using the heaviest solution as baseline, it is possible to calculate the EVWS for both a short and long range aircraft, at a low and high fuel price level, as shown in Table 10-1.

Str Type	Int Met-hod	Str Pitch	Skin Config			Str Config		Weight	Single-Aisle		Wide-Body	
			Mat'l	Laminate	Fibre	Mat'l	Fibre		$0.24 /kg	$0.84 /kg	$0.24 /kg	$0.84 /kg
								(kg)	($)	($)	($)	($)
U	Co-Cure	208.33	UD PP	50/40/10	HS	UD PP	HS	22.35	5482	19014	10983	38441
T	Co-Bond	208.33	UD PP	50/40/10	IM	UD PP	IM	24.04	4562	15979	9230	32305
I	Co-Cure	208.33	NCF	30/60/10	Hyb	NCF	IM	21.16	6038	21149	12216	42757
T	Co-Bond	156.25	UD PP	50/40/10	IM	UD PP	IM	20.27	6495	22753	13143	45999
T	Sec-Bond	312.5	NCF	50/40/10	HS	Braid	HS	32.93	-	-	-	-

Table 10-1: Weight and respective EVWS for various covers

10.2 Manufacturing Cost Calculation

The next step is to calculate the manufacturing cost. As the examples above are being considered for both short and long range markets, then the production rates of 348 and 24, respectively, will be considered. The manufacturing cost breakdown, including the recycling cost over the life cycle of the aircraft, attained from the manufacturing cost calculator process, is illustrated in Figure 10-3 and Figure 10-4 for both high and low manufacturing rates, respectively. In general it would seem that the results comply with the theory, which has been discussed throughout this thesis.

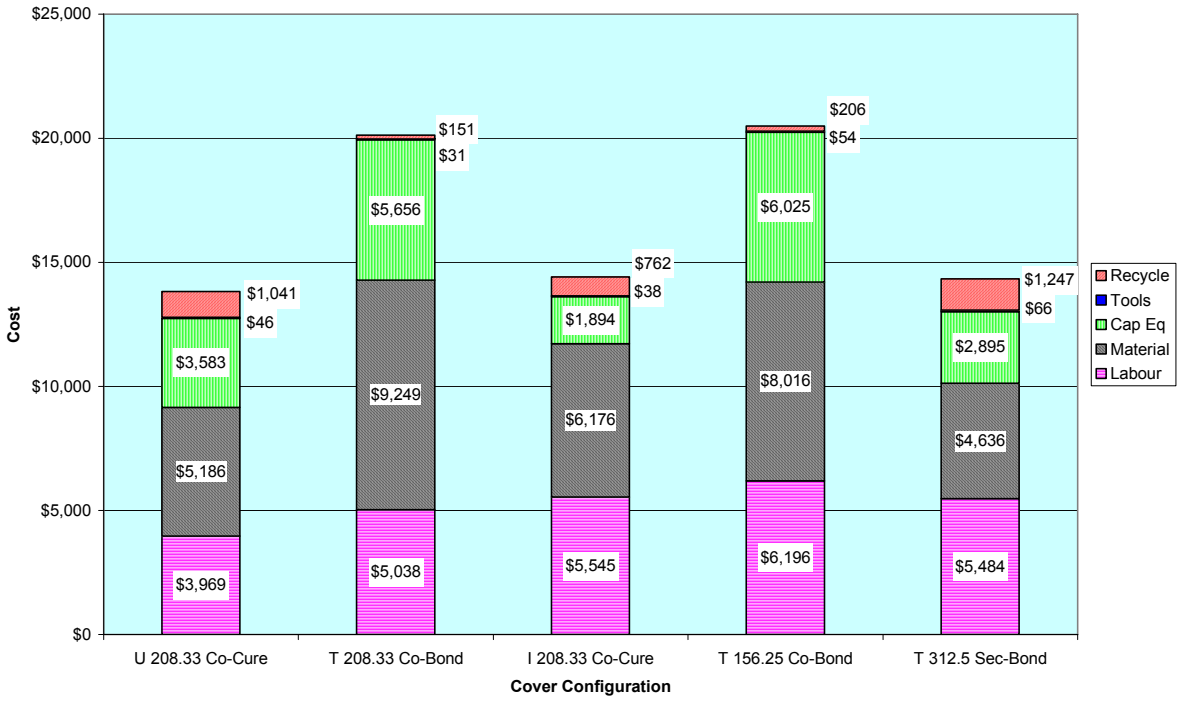

Figure 10-3: High rate cost breakdown for different cover configurations

Overall the manufacturing cost per cover is higher for the low manufacturing rate, as the tooling is amortised over less production cycles, and the nesting of parts is less efficient, resulting in higher material use, thus greater off-cut material. In general the tooling is more expensive for the co-bonding and secondary bonding processes. This is due to the significantly more expensive skin tool being utilised for a longer duration than the stringer tooling. Thus, more tools are required to support the production rate. This is demonstrated by the secondary bonded example, which despite only having 2 stringers, still has the highest tooling costs. In terms of the stringer tooling, the mandrels required for the U-profile stringer-stiffened panel is considerably more expensive than the conventional T-profile stringers, whereas the I-profile stringers is more expensive than the simple T-profile stringers. This can be easily appreciated by looking at the cost breakdown for the low production rate, where only 1 skin tool is required to support the production rate for all variants, but the tooling cost is the highest for the U-profile stringer-stiffened panel.

A further observation from Figure 10-3 and Figure 10-4 is that the pure IM fibre stringer-stiffened covers, which coincidentally are also the only co-bonded examples, are the most expensive. This can be easily explained as the material cost contributes to over 40% of the total cost, thus as the IM fibre costs twice that of HS fibre, then the covers fabricated from IM fibre will be significantly more expensive than a similar HS fibre fabricated cover. As a percentage, the CFRP material and noodle filler constitutes between 89-92% of the total material cost for all variants, which illustrates the insignificance, at least based on the small examples, of including secondary materials in the manufacturing cost calculation. Finally, co-curing operations have a significantly reduced capital equipment cost, which is principally due to only one autoclave cycle being required, albeit the secondary bonded variant also has low capital equipments costs due to the use of an oven instead of the autoclave.

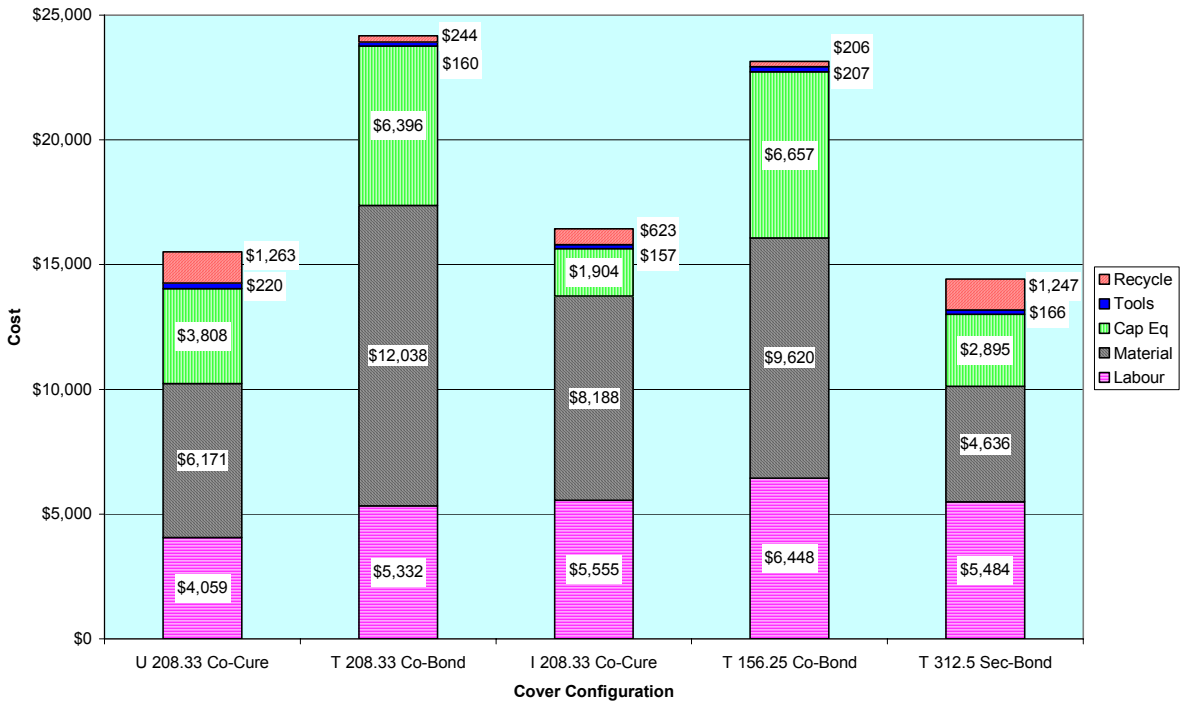

Figure 10-4: Low rate cost breakdown for different cover configurations

Between the conventional UD prepreg and the NCF variants it is clear to see, in particular when the "T 208.33 Co-Bond" using IM fibre UD prepreg and "I 208.33 Co-Cure" using IM fibre NCF are directly compared, that an LCM process can significantly reduce the

manufacturing cost. The major cost savings are incurred from the categories material and capital equipment. The material saving is principally due to the NCF skin being supplied directly to the desired contour, hence there is no off-cut material. The capital equipment savings is due to the lower cost NCF depositor and oven being used, as opposed to an ATL and autoclave.

Finally, the difference in cost between co-curing, co-bonding and secondary bonding is due to the tooling, as previously mentioned, as well as the capital equipment. In general it can be seen that co-bonding is the most expensive integration method based on these examples, although this does not factor in the risk aspect of an all-in-one process. Co-bonding requires a second autoclave cycle, which due to the high charging rate of the autoclave will mean the manufacturing cost is substantially increased.

The manufacturing cost estimates are very much dependent on the various assumptions made, a good example of which is the cost of recycling. With reference to Figure 10-3 and Figure 10-4, the recycling costs for the stringer-stiffened covers using IM material are minimal in comparison to the other solutions. This is due to the disposal cost of uncured IM prepreg being cost neutral and the cost of recycling cured IM being only $-10/kg. Thus, despite the potential for off-cut material during production, this does not affect the recycling cost. Albeit there will be an increase in the raw material cost due to the higher amount of material required. The efficiency of material utilization, i.e. the amount of off-cut material, is reflected in the buy-to-fly ratio, which is shown in Table 10-2, for both high and low production rates.

Table 10-2 clearly shows the increase in off-cut material for the low production rate, due to the smaller laminate sizes required to nest the stringer parts, which results in more off-cut material as a percentage of the required area. For the "T-Profile 208.33 Co-Bond" configuration, the recycling cost (for all cases shown in Table 10-2, the recycling cost is only incurred during the manufacture, i.e. the cost for recycling the part at the end of its life is omitted) stays the same, despite the buy-to-fly increasing from 1.37 to 1 to 1.86 to 1, although the raw material price increases from $9,249 to $12,038. Furthermore, the configuration "I-Profile 208.33 Co-Cure", has a positive recycling cost value, as 0% scrap is assumed for the hybrid laminate skin, and the off-cut IM material for the stringer has a recycle value of $27/kg.

Aircraft Type	Single-Aisle (High Production Rate)			Wide-Body (Low Production Rate)		
	Manu. Cost	Recyc. Cost	Buy-to-Fly	Manu. Cost	Recyc. Cost	Buy-to-Fly
U-Profile 208.33mm Co-Cure	$13,824	$-214.27	1.35 to 1	$15,520	$-435.92	1.72 to 1
T-Profile 208.33mm Co-Bond	$20,125	$-3.15	1.37 to 1	$24,170	$-3.15	1.86 to 1
I-Profile 208.33mm Co-Cure	$14,412	$21.03	1.06 to 1	$16,406	$159.90	1.30 to 1
T-Profile 156.25mm Co-Bond	$20,498	$-3.52	1.37 to 1	$23,139	$-3.52	1.70 to 1
T-Profile 312.5mm Sec-Bond	$14,327	$-28.11	1.02 to 1	$14,427	$-28.11	1.02 to 1

Table 10-2: Comparison of recycling cost (ignoring end of life scrap cost) and buy-to-fly ratio

10.3 Life Cycle Cost Analysis

In order to rationalise the cost and weights, the EVWS must be factored in, as without this, for these examples, the lightest solution is the most expensive, and the heaviest solution is the

least expensive. Shown in Table 10-3 are the EVWS manufacturing costs, for both high and low production rates, and low and high fuel prices.

Aircraft Type	Single-Aisle (High Production Rate)					Wide-Body (Low Production Rate)				
Fuel Price		$0.24/kg		$0.84/kg			$0.24/kg		$0.84/kg	
Costing Index	Org. Cost	Adj. Cost	Ra-nk	Adj. Cost	Ra-nk	Org. Cost	Adj. Cost	Ra-nk	Adj. Cost	Ra-nk
U-Profile 208.33mm Co-Cure	$13,824	$8,396	2	$-5,190	2	$15,520	$4,537	2	$-22,920	2
T-Profile 208.33mm Co-Bond	$20,125	$15,563	5	$4,146	4	$24,170	$14,940	5	$-8,135	4
I-Profile 208.33mm Co-Cure	$14,414	$8,377	1	$-6,735	1	$16,427	$4,210	1	$-26,330	1
T-Profile 156.25mm Co-Bond	$20,498	$14,002	3	$-2,255	3	$23,139	$9,996	3	$-22,861	3
T-Profile 312.5mm Sec-Bond	$14,327	$14,327	4	$14,327	5	$14,427	$14,427	4	$14,427	5

Table 10-3: Original and EVWS-factored manufacturing cost

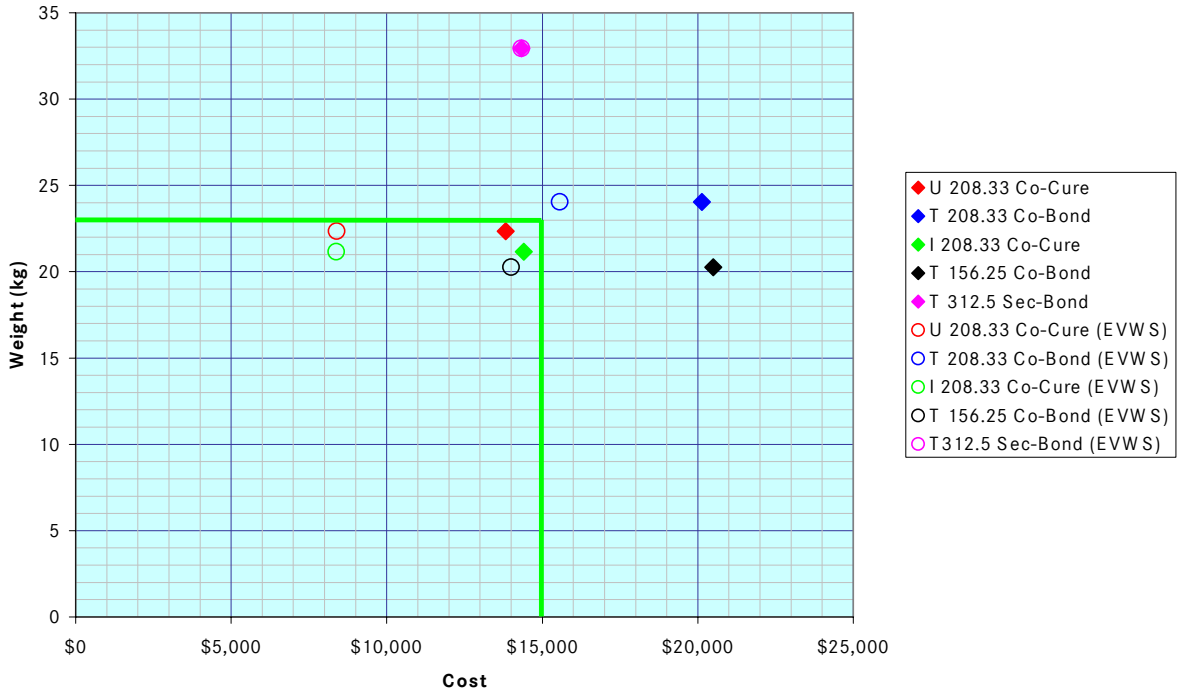

Figure 10-5: Cost vs. weight comparison for high rate at low fuel price

Table 10-3 also ranks the different cover configurations based on cost, with the least expensive solution rated '1'. For every scenario the least expensive option is the I-profile stringer-stiffened cover, using an NCF hybrid skin and NCF IM stringers. The most expensive option, is dependent on the price of fuel, but is either the heaviest solution, i.e. the T-profile stringer-stiffened cover, with a stringer pitch of 312.5mm, or the second heaviest solution i.e. the T-profile stringer-stiffened cover, with a stringer pitch of 208.33mm. A comparison of the different configurations, based on the high production rate with the low fuel price is illustrated in Figure 10-5. As the EVWS is referenced to the heaviest (baseline) solution, then both points for the heaviest solutions are coincident, as the EVWS for this solution is $0. For all other solutions, it can be seen that the EVWS factored manufacturing costs are, by some

margin, to the left of the pure manufacturing costs. Typically, there will be a target weight and cost that has to be achieved, which is illustrated in Figure 10-5 with the green border. Thus, any solution within the green border reaches the weight and cost targets. From the example shown in Figure 10-5, there are 3 possible cover configurations that could be used. The least cost solution would be “I 208.33 Co-Cure”, however if weight is of premium importance then the “T 156.25 Co-Bond” could be considered.

10.4 Summary

The structural optimisation procedure, the manufacturing cost calculator, and the EVWS factor, seems to work, as the results correspond well to the prognosis from this thesis. The weight reality factor could have been applied to these weights, as mentioned in section 8.5.1, in order to obtain a realistic weight, however as the comparison in this context is relative, it does not need to be included.

The many assumptions and costs used for the manufacturing cost calculator can be questioned, however with limited information available, it is deemed satisfactory. The basis for the recycling costs, or the value of scrap, needs to be improved, as these costs have the least foundation. However, obtaining these costs currently is difficult, although it is hoped in the future such costs will become available. The material costs have been obtained from different references, either directly from suppliers for the secondary materials, or from scientific papers for the CFRP costs. These costs are blanket costs and do not factor in the opportunities to obtain a discount through single supplier sourcing over a long period, which would better represent reality.

The PBCM itself does not represent every operation required for the complete process, such as transportation, although this has been considered by factoring in the Pareto 80:20 rule. By including more processes, or greater detail of sub-processes, this should provide a resultant higher fidelity manufacturing cost. However, the ability to extract that knowledge and integrate it into a PBCM is likely to be difficult, due to the proprietary nature of the information; and incorporating it into formulae within a spreadsheet. Alternatively, some of the process steps included could be removed, such as tool cleaning, if required, however as these process steps are easily integrated into a spreadsheet then they should be left due to the increased integrity it provides. Finally, the rates used, such as the tooling area that one person can clean within an area, have been estimated. These rates should be improved by carrying out time and motion studies, which can be done even at University level.

The assumption that the NCF skin laminate results in 0% scrap during manufacturing as the skin textiles are delivered pre-cut is a reasonable assumption. However, not paying a surcharge for having the textiles delivered in this way could be questionable. Nevertheless, factoring in this surcharge on an already assumed cost for the NCF could diffuse the cost assumptions even further, hence why it has not been factored in. The process reliability could also be factored in, such as a greater chance of major porosity occurring when employing a LCM in comparison to a conventional prepreg/autoclave process. However, when manufacturing a valuable product, such as a wing cover, the process would be validated before serial production, thus such risks are mitigated, and hence do not need to be considered.

11 Discussion

In general there are two principal discussion points: the first being the future potential to ensure a step change reduction in LCC of CFRP wing covers/wing boxes; the second discussion point is the optimisation methodology and cost calculator developed as part of this thesis, i.e. the LCC estimator. A final point for discussion is the novelty of this thesis.

11.1 LCC Reduction

As shown in Figure 11-1, a large reduction in LCC can only be accomplished with a holistic change in mindset to the application of composites materials to wing structure by considering the highlighted pertinent factors. These factors must be developed further, and appraised thoroughly via LCC estimation techniques, to ensure a positive outcome.

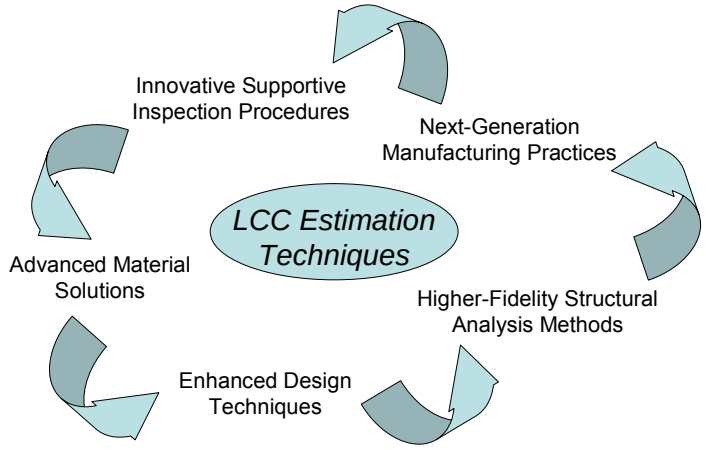

Figure 11-1: Holistic and integrated factors to create step change in CFRP wing cover efficiency

11.1.1 Design Drivers

The features and dependent design considerations for composite wing covers are shown in Figure 11-2. The CFRP material is critical to all design considerations, and only through improved material systems, both in terms of performance and cost, as well as enhanced design methods in combination with a new inspection philosophy, can the enhanced performance of CFRP be realised. However, the adaptation of CFRP material by the aerospace industry has occurred during a time period when only large and mature firms exist, hence they are conservative. Concurrently external regulations appropriately constrain the design freedom of these firms to ensure a high level of safety. This has resulted in the performance advantage of CFRP not being fully realised.

The stiffness and strength of the structure is very much dependent on the physical properties of the material itself, the constitution of the laminate, the cover configuration, as this helps determine the panels global stiffness, as well as the integration method, as this too can determine the overall global stiffness, i.e. if a stringer debond must be considered. The damage tolerance is primarily affected by the same feature for similar reasons.

In terms of maintainability, it is necessary to consider the constraint on the local laminate, i.e. if the structure is constrained by strength then extra provision needs to be made for a bolted

repair, whereas if the structure is sized due to stability, then there should be enough residual strain to ensure extra provision is not required. This rational is essentially the same for non far-field areas such as cut-outs and doublers.

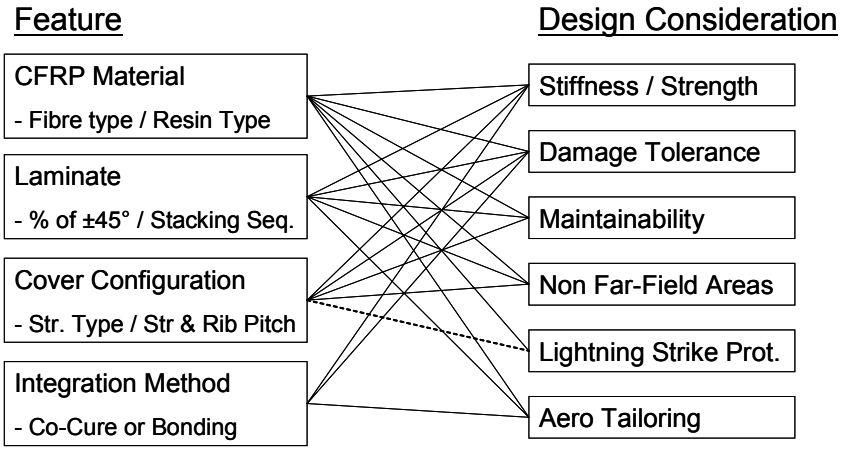

Figure 11-2: Composite wing design considerations

From an LSP perspective, the homogeneity of the laminate is critical, as layers of toughener can act as a dielectric, which is not desirable. Furthermore, as shown in Figure 11-2, the cover configuration can have a secondary effect, hence the dashed line, as if the stringers and ribs are bolted through the cover, then extra LSP mesh will be required on the outer surface.

For aero-tailoring, it is preferable to have a higher strain material and that a good joint exists between the skin and the stringers, so that the wing cover does not suffer from loss of integrity. Finally, the laminate stacking sequence is very important, as it is primarily through the laminate that aero tailoring can occur.

It has been evidenced in this thesis that the most efficient and least cost option is to use a co-curing/co-infusing integration method, as single-stringer debond does not need to be considered from a certification perspective, and it reduces the number of autoclave cycles to just one. However, for large wing covers there is an inherent risk in co-curing, as a failure can be costly to repair, and the limited shop-life of prepreg CFRP constrains fabrication flexibility, thus the risk of failure has to be balanced with the potential advantages. For this reason co-bonding techniques are often used in reality. There also needs to be a greater push to ensure that should damage occur then a bonded repair can be used, so that the detrimental influence of a laminate's notch-sensitivity can be banished.

11.1.2 Manufacturing Cost Drivers

The application of CFRP to aircraft structure has increased over the years, and in particular over the last decade, with CFRP being applied to both the fuselage and wing box. It is necessary that the application of CFRP is based primarily on technical reasons, and not due to market pressure. Despite many contemporary aircraft development programs applying CFRP to wing boxes, Mitsubishi Aircraft Corp. have taken the decision to redesign their proposed Regional Jet, and have replaced the planned CFRP wing box with an aluminium design, sighting shorter lead times for structural changes as the reason for this decision[604]. This decision could have been influenced by Mitsubishi's experience with the problematic Boeing 787 wing box. However, only time will tell if this decision was the correct one.

Shown in Figure 11-3[605] is the cost reduction prognosis, from Japan's Aerospace Exploration Agency low cost composite program, for a wing box manufactured using an RTM process in comparison to the conventional UD-prepreg/autoclave process. It can be seen that a 20% RC saving is deemed plausible due to, principally, a reduction in part fabrication and the curing effort. However, the assembly effort remains the same, thus separate pieces are still used for each constitutive part, i.e. covers, spars and ribs, instead of a more integral wing box concept, such as with integral spars, which could be foreseeable with an LCM process. Furthermore, as Figure 11-3 does not include NRCs, the extra cost for high-tolerance double-sided closed tooling has not been factored in. Furthermore, with double-sided tooling the ability to alter the design is constrained. If these factors were to be included, then this would surely offset some of the cost advantage portrayed.

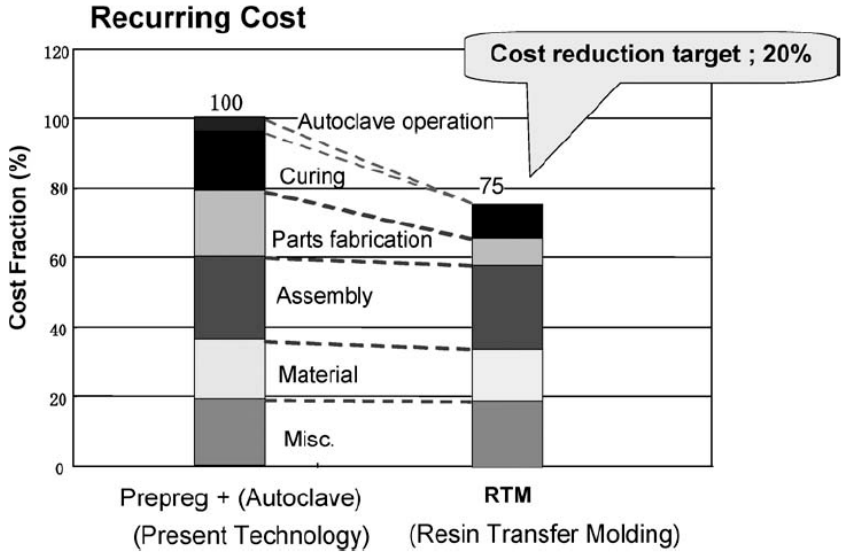

Figure 11-3: Cost reduction target for JAXA's low cost composite program

The ideal material for wing covers manufactured using RTM would be NCF, such as used in the optimization process with the MVI process. However, NCF applied to wing covers is currently not competitive against UD-prepreg, as despite a higher deposition rate, the raw material (fibre, toughener and resin) has a similar cost to that of UD-prepreg, the amount of off-cut material is a lot higher, and the ability to finely tailor the thickness is restricted. A further issue, is that there is not significant investment in the R&D of next-generation NCFs, as there are for UD-prepregs, which means NCF will likely remain one step behind UD-prepreg in terms of material properties.

The higher raw material costs of CFRP in comparison to standard aluminium alloys, can be offset by principally reducing the individual part fabrication cost and the assembly cost. This leads to increasing part integration, through the use of larger and more complex preforms. However, an issue with increasing part integration is that it is harder to optimise the larger parts, due to the limitation of manufacturing processes, inadequate structural analysis methods, and issues of repair. Furthermore, when processing a larger part, the cost of failure is more critical.

The manufacture of large integral preforms could be sourced from suppliers. This would allow the Primary Manufacturer to carry out the value adding process of system integration, whereas the supplier can move up the supply-chain by increasing the degree of product transformation and adding greater value. A suitable supplier could specialise in the fabrication of preforms, which should ensure the overhead costs are reduced. Furthermore, if the

company concentrates only on preform fabrication it should be more efficient at this; hence the cost of manufacture should be lower. Another benefit is that the supplier may be able to obtain the raw material at a lower price as they purchase larger quantities of rovings to fabricate the perform. Alternatively, the preforms could be fabricated directly at the material suppliers, thus leftover material can be re-used or recycled at source. Furthermore, if based on a fixed cost contract, the preform supplier would want to use the material more efficiently, and therefore it is in the supplier's interest to ensure the minimum amount of material is wasted. The opposite is true, if the material supplier just supplies the material, in this case, the more carbon fibre that they can sell, the better.

An intrinsic issue with integrated parts is that less parts are needed, however they are both larger and more complex. Such parts could only be manufactured by suppliers who have both financial strength as well as knowledge and the correct facilities, thus suppliers will become more concentrated. Under these circumstances, the supply chain may be reconfigured from a part based to a process based supply chain, where each supplier is world-class in a single manufacturing process. This could also force the suppliers to concentrate around the aerospace hubs, in order to minimise the risk of global supply chains, such as Toyota's business model is built upon. However, in order to create competition, a wide choice of suppliers should be available, not just a concentrated number of powerful suppliers, and this can only be achieved by reducing barriers to entry, which can be partly achieved through reducing the need for specialised equipment. Furthermore, a large benefit of global outsourcing is the financial support obtained from local governments. It is unlikely that foreign governments would financially assist indigenous firms that are set solely around an aerospace hub in a foreign (western) country.

For a conventional differential concept the assembly effort can be reduced by relying more on bonded joints for the attachment of the principal parts. The π-joint can offer a reliable joint, however integrating this joint into the design can lead to tolerance issues. For instance, a π-joint could be ideal for the spar integration, with the π-joint preform being attached along the span of the wing cover, however tooling will be required to ensure it maintains its position. Despite the tooling, having such a long joint means that even with a slight error, manufacturing issues can occur, such as maintaining the gap in the groove for the tongue, i.e. the spar web. The final issue is the reliability of the bonded joint, and whether the bonding process and inspection techniques can support the in-service application of purely bonded joints.

Alternatively, if bolted joints must be provisioned for, then this should be automated as far as possible, however in order to achieve this, access from both sides is normally required. This would be best achieved with a differential concept, as opposed to an integral concept, due to accessibility reasons.

A further observation from Figure 11-3 is the raw material price remains similar, regardless of the manufacturing process used. It is unlikely in the future that the material price will reduce to such an extent that a clear step change will occur. In actual fact, the material price is likely to remain high due to the limited amounts purchased of the highly qualified aerospace material. This will be exacerbated with newer materials coming onto the market, which because of the increased performance, will be more expensive than the contemporary materials. Thus it is necessary to ensure that the material is efficiently used.

The preparation for curing and curing itself has been heavily reduced in Figure 11-3 as an RTM process was used. It should be possible in the future to make great strides into reducing

the cost of curing the part, as new technology is being introduced that imparts the heat directly into the part, reducing direct costs and time. Furthermore, improved techniques for preparing the component for curing, for example automated vacuum bagging, should reduce the need for manual work, which is a high cost item.

11.1.3 Outsourcing Strategy

Another approach to minimise the LCC is to reduce the acquisition cost though an efficient supply chain management strategy. There are two forms of outsourcing, namely global outsourcing to reduce and spread the financial risk of a new aircraft development program, and local outsourcing where the best suppliers should be sought. These two forms of outsourcing are not necessarily mutually exclusive from one another.

In order to reduce both lead time and inventory, while using a supply chain, it is beneficial to have suppliers concentrated geographically close to the Primary Manufacturer, such as the "Toyota Plant" model, which is similar to the existing aerospace hubs, such as Toulouse, in France. However, through employing a global outsourcing strategy to reduce the financial cost for the Primary Manufacturer, a stipulation is likely to be that engineering and production work will be conducted within the local country, and not where the Primary Manufacturer is based. This creates a dilemma, in that global outsourcing has to be employed, to some degree, to help finance the program, however it is more efficient to have suppliers local to the Primary Manufacturer.

It is known that the most favourable type of part to outsource is a decomposed sub-system. When considering the wing, a sub-system can be considered to be a flap or a wing box. By outsourcing larger sub-systems or sub-assembles this can also help to reduce lead time and inventory levels, as only major components are delivered to the Primary Manufacturer. This is a similar approach to Boeing's, with the 787, where the wing box is manufactured completely in Japan. By employing this strategy all interfaces within the sub-system are handled by the supplier, which should increase developmental efficiency, although this is based on the assumption that the supplier is competent, i.e. they have a core-competence for that particular sub-system. However this is the key point, global outsourcing typically occurs in countries that are developing their understanding of aircraft design and manufacture, hence why they offer some form of subsidy, thus the supplier is not necessarily the most competent, instead, in simple terms, they are the cheapest. This was the original relationship between Boeing and the heavy industries in Japan, and now it needs to be questioned who has the core knowledge on wing design and manufacture, Boeing or the Japanese Heavies? The integrator or the designer/manufacture?

Local outsourcing should be concerned with finding the best suppliers in the business, and not just the cheapest. Close relationships should be built up with suppliers so that the engineering development and the manufacturing are conducted in the most efficient way possible. This can only be achieved by both the Primary Manufacturer, or system integrator, and the suppliers being not just competent, but the best in their field. Furthermore, the relationship has to be established and built upon to build trust; this is the only way that the supplier will be willing to carry out R&D, without contractual guarantees. However, such a close relationship can lead to moral hazard and increase the switching costs to an alternative supplier.

There is no easy solution to an appropriate outsourcing to help reduce the LCC of the aircraft, however if the Primary Manufacturer pursues a system integrator strategy then their principal core-competence must be outsourcing management itself.

11.2 Optimisation Methodology and LCC Calculator

The primary objective of the optimisation methodology is to minimise weight, based on a given cover configuration (rib and stringer pitch, material type, and stringer profile) that will help to determine the manufacturing cost, while being constrained by an allowable strain. From a structural perspective this is pertinent; however from a program viewpoint, the objective of optimisation can change through the different design phases because of commercial pressures. Typically, an aircraft program is concerned with reaching the performance goals and then to deliver within the promised timeframe. Therefore, under this commercial pressure, a theoretical EVWS may not hold enough influence, when the consequence of not achieving the weight target could be a lack of sales, or selling at a lower cost. Under these circumstances, caution could be thrown to the wind and major decisions taken in order to try and reach the weight target, such as changing from HS to IM fibre, despite IM fibre costing significantly more, with the misguided hope that later the cost can be reduced, so that a profit can still be made, through slight design or manufacturing improvements. Therefore, it is even more necessary when using an EVWS, to justify the extra expenditure to achieve a weight saving; that better methods to predict product performance and the resources required to achieve this aim, are available.

In terms of the structural optimisation process developed, the approach taken may seem fairly simplistic when compared to methods using GAs to optimise the stacking sequence. However, at the preliminary stage using such techniques are excessive; it is far better to have a good firm foundation at this stage, so the influencing factors can be analysed. GA techniques are best applied at the detailed design phase, when the skin is being designed in isolation, and the IPT can analyse the design together. At the preliminary design phase, there is not enough codified information available to be able to understand the consequences of multiple ply terminations and butting plies of different orientations together. This can only be determined when the modelling fidelity is far higher, so stress concentrations can be assessed, and significant test data is available to reinforce the analysis.

It would be prudent to verify the assumptions that the developed optimisation methodology is based upon; in particular, verifying the reduction in performance due to a single stringer debond and DSD. The knockdowns in performance witnessed using ESDUpac A0817 seem to match the theory, however, perhaps the global influence needs to be considered, such as the stiffness afforded by the wing box structure. Furthermore, using material allowables that are based on coupon tests can lead to inaccuracies due to scaling effects; however, at this phase, it is difficult to verify the allowables with respect to a global structure.

The strength constraints are based on strains derived for the wing skin, as this is typically the area prone to damage during service. However, as mentioned in Chapter 6, the constraints on the damage tolerance strains can also be due to internal damage caused during manufacturing or inspection. A critical area, for a stringer-stiffened panel with a simple blade stringer (U- and T-profile), is the blade's top edge, which can severely limit the allowable strains to say –3600με, as used by Herencia et al. (2007)[606]. Limiting the strain due to stringer top edge impact could be easily incorporated into the Input/Output spreadsheet. However, having a low allowable strain will limit the weight saving opportunity that is possible with CFRP, and

when out-of-plane effects are considered this will severely exacerbate this situation. It is therefore considered prudent to ensure that the design of the stringer and the manufacturing methods employed eliminate the requirement to consider stringer blade top edge impact.

The manufacturing cost calculator is based on a number of assumptions as well as ground rules, for the production process equations, and material, tool and labour costs, in order to remove the need for company proprietary costs. When using such constant rates for the different processes this will lead to limitations, as some processes, facilities and operator skills will command a larger proportion of the total cost. To understand the trade-offs between different manufacturing processes the variable costs are very important, hence there should be suitable fidelity in the costing calculative data to ensure this is possible, which currently is somewhat lacking. It is for this very reason that companies will not want to give away their cost information, thus creating a major barrier to competition, as less well resourced companies cannot develop such models[572].

The manufacturing processes modelled in the manufacturing cost calculator, in particular for the stringer fabrication, may not be ideal for high-rate manufacture. However, as stringer performing techniques such as roll forming or continuous compression moulding are lacking in maturity it is very hard to comprehend the costs involved, in particular for the capital equipment. It is for this reason that more manual, thus familiar, manufacturing methods have been modelled.

In general, to create the structural optimisation methodology and cost calculator, it has been necessary to parameterise the input data, which has resulted in a simplified problem prognosis that can lead to reduced accuracy. However, generic calculations are typically simplified in order to make them applicable for use. An example of which is the EVWS calculation, which is based on the assumptions of straight and level flight.

11.3 The Novelty Factor

The factors that determine the efficiency of a CFRP stringer-stiffened panel have been investigated, in order to identify the dependencies and constraints of the variables. This ensures that the resultant design from the optimisation methodology is bound within a realistic framework, so that the design is plausible.

The influence of the integration methods of co-curing, co-bonding, or secondary bonding has been considered both from a structural and financial perspective. Typically, the global damage tolerance aspects, such as single stringer debond and DSD, have been previously ignored or not considered.

A great deal of effort was expended in creating a set of realistic material allowables, in order to improve the pragmatism of the optimisation results. This has been done for different fibre types, as well as different CFRP formats, i.e. UD prepreg, NCF, and braid. Typically, previous research has used material properties direct from the material manufacturers, which do not consider any knockdown effects.

A series of strain limits have been calculated, which are dependent on the fibre type, % of ±45° plies, laminate thickness and stringer pitch, in order to constrain the design. Previous work conducted in this field, had, if strain was considered as a constrain, only considered a

blanket strain value such as -3600με. Therefore, the method applied in this optimisation methodology to calculate the strain constraints, has a good rational.

Various additional strength constraints have been included, in particular out-of-plane effects, as well as bearing/bypass. Out-of-plane effects must be considered, as the wing box is an integral fuel tank, and the contour of the wing covers means that the assumption of a flat panel is wrong. These effects are considered under both tensile and compressive loads, which have not previously been considered. Bearing/bypass is a necessary consideration as the influence of a bolted joint will remain a constraint until bonding/integral structures can be relied upon, and bonded repairs can replace the airliner's preferred bolted repair solution. To the author's knowledge, bearing/bypass has not been considered as part of the analysis routine in previous work.

The manufacturing cost calculation process is based on the tried and tested PBCM; this work has identified costs for various capital equipment and materials, which to date has not been widely published. This has been made necessary through direct contact with equipment suppliers, information extracted from Journal papers, and cost data from Cranfield University. In terms of the work rates, many assumptions have been made, due to lack of available data. However, this should provide a good baseline, which can be further developed in the future.

12 Further Work

12.1 Structural Optimisation

Due to the length of time required to manually apply the optimisation methodology it is necessary to automate the procedure. A module from the optimisation process has been automated by Wang Wei (exchange student at Cranfield University from the College of Aeronautical, Shaan Xi'an, China), who optimised the stringer-stiffened panel based on the geometry constraints due to bolted repair. An example of the graphical user interface is shown in Figure 12-1 for an I-profile stringer-stiffened panel. This work demonstrated that it is possible to automate the optimisation methodology.

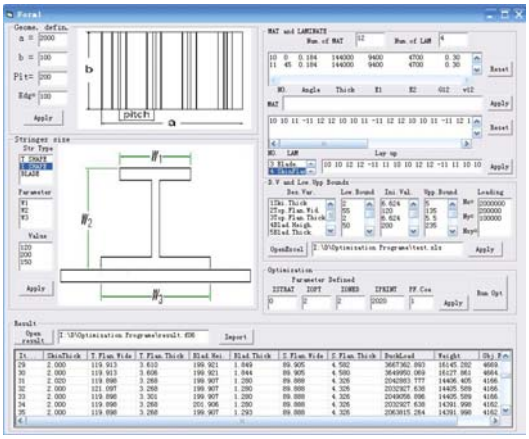

Figure 12-1: Initial attempt to automating optimisation methodology

The optimisation methodology is fairly complex due to the various constraints. This could be simplified, without a major reduction in accuracy for this level of optimisation, at the preliminary design phase, by eliminating the need to take into consideration the particular laminate stacking sequences for a given thickness. This can be achieved by choosing a stacking sequence that has an average modulus for a given laminate, i.e. 50/40/10, therefore the laminate will have a number of plies so that the desired percentages of 0°, ±45°, and 90° plies is achieved. The chosen stacking sequence should also conform to the AsBoDf requirements. Therefore, the particular laminate's moduli will be constant, thus the element stiffness calculations will be slightly easier, as only thickness will change. The thickness of the laminate can be changed, by simply varying the thickness of the individual plies in the laminate, although the overall thickness must remain an integer multiple of the ply thickness. In terms of the manufacturing calculator, the original stacking sequences can be used based on the laminate thickness.

For conventional wing cover design, i.e. when the individual panel's aspect ratio are >3, then the single-term FSM used by ESDUpac A0817, is accurate and comparable to FEM. However, if it is deemed necessary to increase the accuracy, or unconventional designs are investigated with smaller panel aspect ratios, then a multi-term FSM solution could be used. Similarly, the material allowables developed so far, are based on a number of assumptions. It would be beneficial to derive the allowables from a proper test campaign, in order to improve the accuracy.

Approaches to the optimisation routine can be altered, depending on the need. For instance, it could be possible to constrain the thickness of the skin within a rib bay to be the same,

however, how this is accomplished needs further consideration. For example, would each panel be individually optimised, and then the least, greatest or average skin thickness be used to re-optimise all the panels within the rib bay so that they have the same skin thickness? Would this be practicable, both at this level of optimisation, as well as in the end product. Perhaps a better approach would be, to start off the optimisation on the panel with the lowest load, then find the next lowest loaded panel, and use the previously optimised panel as a starting point for optimisation, in terms of the panel's geometry. However, although this principle would be efficient when only axial compression load is considered, the panel will have a shear load applied to it, which can vary considerably relative to the axial load. This can mean that under axial compressive a substantial stringer may be more beneficial, but due to the shear component, a thicker skin could be more efficient.

Currently each panel is optimised individually, and as such there are no constraints imposed between the panels. An example of such a constraint could be to minimise step changes in stringer height, to limit out-of-plane bending stresses[61]. Alternatively, constraints could be set on the maximum change in skin thickness in both spanwise and chordwise directions, based on a strain limitation to avoid delamination.

A major consideration of the lower wing cover is the manhole doubler, which often dominates the design of the wing cover. In principle, this can be factored in to the optimisation by considering the stress concentration caused by the manhole itself, and then increasing the local laminate's thickness so that an RF≥1 is obtained. The stress concentration factor will be dependent on both the percentage of ±45° plies in the laminate, as well as the loading on the panel. Such work has been previously conducted by Wang[607], who compared the thickness required to maintain an RF≥1 for a plain panel, and a panel with a representative manhole in the middle. Although this work showed that multiplication factors can be used for certain laminates under particular loads to take into consideration the influence of the manhole, the work was not, currently, conclusive enough to be incorporated into the optimiser. Another issue is that designing non far-field features, such as doublers, are not best accomplished with a generic optimiser, as highlighted by Hart-Smith (1995)[363]. Finally, the optimisation of the doubler area is only an approximation, and such areas are best designed based on FEM, where 3D effects can be considered.

The incorporation of NCF into the optimisation permutations provides an extra facet to the available manufacturing processes. However, due to the different permutations of NCF textiles, i.e. UD, biaxial, etc, and the different thicknesses of the individual layers, it is not easy to integrate the flexibility of NCF textiles into the optimisation process. For example, a different choice of textile for the 50/40/10, as the one currently used, could ensure that NCF could be used to fabricate a U-profile stringer panel. Therefore, other types of NCF textiles can be integrated into the optimisation methodology.

The T-profile stringer can be enhanced significantly with a bulb to support the free-edge of the web, as has been previously validated. The relationship between the size of the bulb and the blade dimensions is known; therefore, this could be easily integrated into the optimisation methodology.

Simple aero tailoring could also be integrated into the optimisation methodology, as it has been verified that by simply rotating the laminate, the structural performance can be enhanced.

12.1.1 Incorporating other Modules

12.1.1.1 Impact Damage Resistance

The effect of impact on a laminate can be evaluated with FEM; however, such procedures are not pertinent at the preliminary design phase. An easier approach is to employ a damage resistance parameter, using either a relationship between peak contact force and impact damage, or the bending stiffness and strain difference between adjacent plies[608].

Davies and Zhang[414] have shown that the first damage threshold is most likely due to initialisation of delamination failure, and they have developed an equation to calculate the critical peak force at which damage is initiated. The impact requirements are based on energy levels and not force, therefore suitable equations based on energy would need to be developed. This can then be integrated into the optimisation procedure, in order to ensure the panel is resistant against the impact requirements.

Work conducted by Fuoss et al.[608] used an optimisation routine that worked out the best stacking sequence for damage resistance after impact, which should reduce development costs at the preliminary design phase. This could be integrated parallel to the principal optimisation procedure, although the benefit of this at the preliminary design phase, is questionable.

12.2 Life Cycle Cost Calculation

The manufacturing and disposal costs are based on a number of assumptions, thus there will be an acknowledged inaccuracy; whereas the EVWS is very accurate, as it is based on a formula with all components known. There are two principal improvements required to improve the accuracy of the manufacturing cost. The first is to increase the fidelity of the modelling, i.e. to improve the calculation as well as to add more sub-processes. Secondly, the input data must be improved, thus access to manufacturing data is essential, in order to understand the manpower resources required. However, this is proprietary data which cannot be freely accessed, and carrying out time and motion studies in a simulated environment would probably be too inaccurate. In terms of the cost of recycling it is hoped that with increasing market maturity, more research will be conducted into the LCC of CFRP, and financial data will become available.

13 Conclusion

In many ways, MDO is similar to starting any venture, such as a Doctoral thesis, in that good information and therefore reliable knowledge only comes at the latter stages of the design process; however, by then it is often too late, and one must make do with the decisions taken beforehand. At the beginning, it is easy to make changes, however, at this stage the complete picture is incomplete and perhaps even wrong!

The very essence of MDO is to consider all aspects that influence the product, and not just those factors that can be codified and written into an optimisation code. For this reason, it is felt justified to have carried out an extensive literature review and put a large emphasis on a discussion of all factors that contribute to the determination of an optimal CFRP wing cover. In practice design rules, which are essential to ensure an efficient design, are often misconstrued or the basis for the rule is not known. One of the principal reasons for the increase in weight between that estimated by the stress department and that of the design department is due to the conservative nature of the design rules applied. An example of which, as previously highlighted is the tapering of plies due to change in thickness. Often blanket tapering rules are used, which does not consider the implication of the intensity of strain in the taper region, i.e. lower loaded areas can have a steeper taper. Therefore, in order to further optimise the weight of the product, blanket rules should not be relied upon, instead each area should be individually considered and an appropriate design used, as highlighted in this thesis. In practice, this can only be achieved with greater knowledge, in combination with tools developed for particular applications.

One of the major advantages of applying laminated composites is the ability to tailor the stacking sequence to suit the local load conditions, as some areas, for example, may have a greater intensity of axial load relative to shear load. Furthermore, thinner laminates may be constrained by CAI, whereas thicker laminates are typically constrained by notched effects. For each case, the laminate composition should ideally be varied, with a different proportion of ±45° and a distinct stacking sequence. However, the ability to tailor the laminate is constrained due to the fluctuation in thickness across the total part and strength knockdowns due to the termination of plies. For this reason, at the preliminary design phase, defined stacking sequences for laminates with different proportions of ±45° plies has been applied, in this thesis, as this is considered the best approach. A further benefit of this simplistic approach, is that a varying strain limit, based on thickness, to constrain the strength calculations has been used, as opposed to using a blanket strain level, independent of the thickness, as has been applied in most other research. If the stacking sequence itself was allowed to vary, as some research has previously carried out, it is then hard, at this level of optimisation, to estimate the effect this would have on the allowable strain. Thus the approach used here is based on firm assumptions, as strength can be realistically constrained by the allowable strain and with a continuous laminate, i.e. the only termination of plies is due to the change in thickness, then there will be no major reduction in strength through the laminate due to sudden changes in laminate composition.

The broad literature review should portray every major topic that affects a CFRP wing cover, and thus provides a good baseline for all future CFRP wing cover research. Throughout the literature review, which is incorporated within chapter 2 to 9, examples have been assessed in order to verify the findings and to recognise the limitations of both the tools used as part of the optimisation methodology as well as the limitations of the design. These limitations were then used to constrain the boundaries on the design possibilities. In particular the ability to

achieve a 60/30/10 stringer laminate, the stringer pitch, and the difference in Poisson's ratio between the skin and stringer laminates led to some principal constraints on the choice of stringer-stiffened panel configurations. This ensures that practical constraints were considered from the beginning, to minimise the difference in weight between preliminary optimisation and detailed design, which is not only critical but has also often been overlooked in other research. Furthermore, although the MDO methodology does not dynamically factor in the influences from all disciplines that affect the design, it does intrinsically include a number of issues that constrain the design, such as the manufacturing procedure and the necessity to consider bolted repair.

The premise of this thesis is not to recommend the optimum technical solution, from a cover configuration and manufacturing process perspective, as such decisions are influenced by many other non-technical factors. In general it is widely accepted that a CFRP wing cover applied to the right aircraft, at least from a weight perspective, should be advantageous. A large undisturbed wing cover, carrying primarily in-plane loads, should benefit from the application of CFRP, whereas a smaller wing with multiple out-of-plane loads may not, particular when a smaller wing will typically result in a thinner skin, resulting in a wing cover being more prone to impact and not being significantly thick to withstand the out-of-plane loads. However, in terms of manufacturing cost, as seen from the work conducted within the NASA ACT program, the manufacturing cost in comparison to a standard aluminium design is significantly more, when using standard CFRP UD prepreg. Although, as illustrated in this thesis, the market situation needs to be understood in order to determine if that extra outlay in manufacturing cost is negated over the life cycle of the aircraft. However, as demonstrated from the NASA ACT program, LCM manufacturing techniques in combination with dry fibre can reduce the manufacturing cost significantly. This was though based on using untoughened CFRP systems in combination with the through the thickness reinforcement, which today is not being actively pursued, and NCF with toughened resins systems have a similar price to the contemporary UD prepreg systems. Therefore the current benefits of using dry fibre systems is somewhat limited, with only non-autoclave production, decreased deposition time, no shop life issues, and easier recyclability, being the advantages. The future for dry fibre systems can be secured by creating a product that cannot be achieved using UD prepreg, such as a complete perform. Serendipitously, a perform, with local through the thickness support, can also improve the damage tolerance of the wing cover, while minimising the impact on the in-plane properties. Only then, and with increased market competition between suppliers, can the cost of composite manufacture be drastically reduced.

The credentials for a successful design of a CFRP wing cover is very much dependent on the aircraft type and the market conditions. The lightest design will typically be the most expensive, as it will utilise the highest performance fibre, in combination with the thinnest plies, and the smallest stringer pitch. However, dependent on the market conditions the saving in weight, which directly influences the fuel consumption, can then offset the extra cost in production. This hypothesis was proven in the results section of this thesis, albeit the costing is very much dependent on the assumptions made.

The choice between co-curing or bonding parts can influence both the weight and the cost of the wing cover, and is critical to the design, hence why the choice of integration is included as a fundamental part of the optimisation methodology. Due to the necessity to consider single stringer debond for all types of bonded stringer, this will typically increase the weight in comparison to a co-cured design. Furthermore, bonding inherently requires a secondary operation to apply the adhesive and will require another cycle in the autoclave. As the autoclave is defined as capital equipment, it is often the bottleneck in production. The

charging rate for an autoclave is fairly high, although less than an ATL, thus it is costly to run. However, bonding techniques, in particular co-bonding, offers greater flexibility. This is due to a reduction in the risk of having to scrap or carry out major rework at the wing cover level, as well as increasing the flexibility within the constrained time envelope due to the shop life of the prepreg. Alternatively, using a dry fibre can increase the flexibility of the co-curing process as there is no shop life issues, however an infusion process cannot be used in unison with a bonding process. Therefore, a huge advantage can be obtained with co-curing if the deposition and integration times could be vastly reduced for large wing covers, as well as achieving near 100% reliability with the cure cycle. Alternatively if the bonding process had improved dependability, then the need for chicken fasteners to create a quasi hybrid joint could be reduced.

This thesis has established guidelines and an optimisation methodology, with a simple LCC calculator, to compare different solutions from a technical perspective, to identify and validate the relative merits of different configurations. The structural methodology is extensive and explicit, based on proven tools and a well researched realistic process. The cost calculator is based on a number of assumptions, due to the unavailability of such sensitive data and in order to reduce the complexity. In order to improve the accuracy of the manufacturing cost calculator, this would require a lot of knowledge, which is beyond the expertise of a single engineer[609], and hence this thesis. However, a key influence on the overall cost is the factoring in of the recycling costs. Due to the assumptions made in this thesis, the recycling of certain CFRP materials can incur a positive cost, whereas other CFRP material incur a negative cost, which can skew the results to make it favourable for some specific material solutions. However, for the preliminary design phase, it is not the exact end result that is important, instead it is the relative comparison between different cover configurations.

The ability to mathematically calculate the EVWS, based on a number of influential factors, is very beneficial in justifying the merit of saving weight, instead of assuming a blanket-value, such as $1000/kg, as used in other research. If used in the correct framework, an analytical procedure to justify the economic benefit of saving weight can bring a rational to decisions made, which can ensure that the profitability of the program is sustained, as evidenced in this thesis.

It can be concluded that an MDO methodology, which can be integrated into a computer program is very beneficial to the engineer, as a way of automating an optimisation procedure, which has already been defined and verified. Thus, such computer programs can generate much information on generic designs; however, if solely used, new aircraft design knowledge might become an increasingly sparse commodity, resulting in Dwoyer's 1987 prediction that: "If you ask me to envision what I see in the year 2020, there will be no wind tunnels. I would say we would be at the point where airplanes could be designed by rather low-paid technicians"[610]. However, this will not necessarily be the case. Such computer programs can release valuable resources to investigate more novel concepts where the human being's innovative and creative qualities can be most efficiently used.

14 References

1. McMasters, J.H. and Cummings, R.M. (2002), 'Airplane Design - Past, Present, and Future', *Journal of Aircraft,* Vol. 39, No. 1, pp. 10-17.
2. Tan, X., Xu, Y., Early, J., Wang, J., Curran, R., and Raghunathan, S.'A Framework for Systematically Estimating Life Cycle Costs for an Integrated Wing', *7th AIAA Aviation Technology, Integration and Operations Conference,* Sep 18, 2007-Sep 20, 2007, Belfast, Northern Ireland, pp. 1164-1174.
3. Ilcewicz, L.B., Hoffman, D.J. and Fawcett, A.J. (2000), 'Composite Applications in Commercial Airframe Structures', in Kelly, A. and Zweben, C. *Comprehensive Composite Materials*, Vol. 6.07, Pergamon, Oxford, UK., pp. 87-119.
4. Kundu, A.K., Crosby, S., Curran, R., and Raghunathan, S.'Aircraft Component Manufacture Case Studies and Operating Cost Reduction Benefit', *AIAA 3rd Aviation Technology, Integration and Operations Conference,* Vol. AIAA 2003-6829, Nov 17, 2003-Nov 19, 2003, Denver, Colorado, USA,
5. Curran, R., Raghunathan, S. and Price, M. (2004), 'Review of Aerospace Engineering Cost Modelling: The Genetic Casual Approach', *Progress in Aerospace Sciences,* Vol. 40, No. 8, pp. 487-534.
6. Energy Information Administration *Petroleum Navigator - Spot Prices,* available at: http://tonto.eia.doe.gov/dnav/pet/PET_PRI_SPT_S1_D.htm (accessed 2009).
7. Curran, R., Early, J., Price, M., Castagne, S., Mawhinney, P., Butterfield, J., and Raghunathan, S.'Economics Modelling for Systems Engineering in Aircraft', *AIAA 5th Aviation, Technology, Integration, and Operations Conference,* Vol. AIAA 2005-7371, Sep 26, 2005-Sep 28, 2005, Arlington, Virginia, USA,
8. Humphrey, R.J., Venters, K.R., and Witnoskey, L. (1995), 'NASA Baseline Aluminum Aircraft Cost Model', *5th NASA/DoD Advanced Composites Technology Conference,* Vol. 1, May, 1995, Seattle, WA, USA, pp. 182-203.
9. Emirates *Our Fleet,* available at: http://www.emirates.com/english/flying/our_fleet/our_fleet.aspx (accessed 2009).
10. Roberts, W. (2008), 'The New Order', *Airfinance Journal,* No. 311, pp. 40-42.
11. Airbus Industries *Market Demand for 1,200 Aircraft per Year,* available at: http://www.airbus.com/en/corporate/gmf/demand-for-passenger-aircraft/demand-summary/ (accessed 2008).
12. CNN (2006), *Airbus Announces Launch Of A350 XWB,* available at: http://money.cnn.com/services/tickerheadlines/for5/200607170714DOWJONESDJONLINE000182_FORTUNE5.htm (accessed 2006).
13. Perrons, R.K. (1997), *Make-Buy Decisions in the U.S. Aircraft Industry* Massachusetts Institute of Technology, Massachusetts, USA.
14. Phillips, M. (1999), 'Agile Manufacturing in the Aerospace Industry: An Industrial Viewpoint', *International Journal of Agile Management Systems,* Vol. 1, No. 1, pp. 17-22.
15. Jiang, H. and Hansman, J.'An Analysis of Profit Cycles in the Airline Industry', *6th AIAA Aviation Technology, Integration and Operations Conference,* Vol. AIAA 2006-7732, Sep 25, 2006-Sep 27, 2006, Wichita, Kansas, USA, pp. 280-296.
16. Niosi, J. and Zhegu, M. (2005), 'Aerospace Clusters: Local or Global Knowledge Spillovers?', *Industry and Innovation,* Vol. 12, No. 1, pp. 5-29.
17. Hackman, J.R. and Wageman, R. (1995), 'Total Quality Management; Empirical, Conceptual and Practical Issues', *Administration Science Quarterly,* Vol. 40, No. 2, pp. 309-342.
18. Hicks, C., McGovern, T. and Earl, C.F. (2000), 'Supply Chain Management: A

Strategic Issue in Engineer to Order Manufacturing', *International Journal of Production Economics,* Vol. 65, No. 2, pp. 179-190.
19. Fine, C.H. and Whitney, D.E. (1996), *Is the Make-Buy Decision Process a Core Competence,* available at: http://imvp.mit.edu/papers/96/Make_Buy.pdf (accessed 2008).
20. Westre, W.N., Allen-Lilly, H.C., Ayers, D.J., Cregger, S.E., Evans, D.W., Grande, D.L., Hoffmann, D.J., Rogalski, M.E. and Rothschilds, R.J. (inventors) (Sep 5, 2000), *Titanium-Polymer Hybrid Laminates*. US Patent 6,114,050.
21. Madan, R.C. (1988), *Composite Transport Wing Technology Development*, Report no. CR 178409, NASA , Hampton, VA, USA.
22. EADS Deutschland GmbH, C.R.C. *The Research Requirements of the Transport Sectors to Facilitate an Increased Usage of Composite Materials. Part 1:The Composite Material Research Requirements of the Aerospace Industry,* available at: http://www.netcomposites.com/images/CompositeN_Aerospace.pdf (accessed 2006).
23. Marsh, G. (2006), 'Duelling with Composites', *REINFORCEDplastics,* Vol. 50, No. 6, pp. 18-23.
24. Zelinski, P. (2008), *How to Machine Composites: Part 1 - Understanding Composites,* available at: http://www.mmsonline.com/articles/how-to-machine-composites-part-1----understanding-composites.aspx (accessed 2008).
25. Dow, M.B. and Dexter, B. (1997), *Development of Stitched, Braided and Woven Composite Structures in the ACT Program and at Langley Research Center (1985 to 1997) - Summary and Bibliography*, Report no. TP-97-206234, NASA, Hampton, VA, USA.
26. Aoki, Y., Ishikawa, T., Takeda, S., Hayakawa, Y., Harada, A. and Kikukawa, H. (2006), 'Fatigue Test of Lightweight Composite Wing Structure', *International Journal of Fatigue,* Vol. 28, No. 10, pp. 1109-1115.
27. European Commission *Advanced Low-Cost Aircraft Structures,* available at: http://ec.europa.eu/research/transport/projects/article_3675_en.html (accessed 2009).
28. Hedlund-Aström, A. (2005), *Model for End of Life Treatment of Polymer Composite Materials* Royal Institute of Technology, Stockholm, Sweden.
29. Mascarin, A.E., Dieffenbach, R., Brylawski, M.M., Cramer, D.R., and Lovons, A.B.'Costing the Ultralite in Volume Production: Can Advanced Composite Bodies-in-White Be Affordable?', *International Body Engineering Conference & Exposition,* Oct 31, 1995-Nov 2, 1995, Detroit, Michigan, USA,
30. Raghunathan, S., Curran, R., Kundu, A.K., Price, M., and Benard, E.'Research into Integrated Aircraft Technologies', *AIAA 3rd Aviation Technology, Integration and Operations Forum,* Vol. AIAA 2003-6736, Nov 17, 2003-Nov 19, 2003, Denver, Colorado, USA.
31. Xu, Y., Wang, J., Tan, X., Early, J., Curran, R., Raghunathan, S., Doherty, J., and Gore, D.'Life Cycle Cost Modeling for Aircraft Wing Using Object-Oriented Systems Engineering Approach', *46th AIAA Aerospace Sciences Meeting and Exhibit,* Vol. AIAA 2008-1118, Jan 7, 2008-Jan 10, 2008, Reno, Nevada, USA.
32. Marx, W.J., Mavris, D.N., and Schrage, D.P. (1995), 'A Hierarchical Aircraft Life Cycle Cost Analysis Model', *1st AIAA Aircraft Engineering, Technology, and Operations Congress ,* Sep 19, 1995-Sep 21, 1995, Anaheim, CA, USA, pp. 3.
33. Ilcewicz, L.B., Mabson, G.E., Metschan, S.L., Swanson, G.D., Proctor, M.R., Tervo, D.K., Fredrikson, H.G., Gutowski, T.G., Neoh, E.T., and Polgar, K.C. (1996), *Cost Optimization Software for Transport Aircraft Design Evaluation (COSTADE)*, Report no. CR 4737, NASA, Hampton, VA, USA.
34. Porter, M.E. (1985), *Competitive Advantage*, The Free Press, New York, USA.
35. Corbett, J., Dooner, M., Meleka, J. and Pym, C. (1991), 'Design for Manufacture', in

Boothroyd, G. and Dewhurst, P. *Product Design for Manufacture and Assembly*, Addison-Wesley Publishing Co., Wokingham, England, pp. 258-269.
36. Corning, G. (1960), *Airplane Design*, Self Published, College Park, MD, USA.
37. Mileham, A.R., Currie, G.C., Miles, A.W. and Bradford, D.T. (1993), 'A Parametric Approach to Cost Estimating at the Conceptual Stage of Design', *Journal of Engineering Design,* Vol. 4, No. 2, pp. 117-125.
38. Curran, R., Raghunathan, S., Kundu, A.K., Crosby, S., Shields, P., and Eakin, D.'Competitive Aircraft Design and Manufacture', *AIAA Aviation Technology, Integration and Operations Conference,* Vol. AIAA 2002-5852, Oct 1, 2002-Oct 3, 2002, Los Angeles, CA, USA.
39. Grose, D.L.'Reengineering the Aircraft Design Process', *5th AIAA/USAF/NASA/ISSMO Symposium on Multidisciplinary Analysis and Optimization,* Sep 7, 1994-Sep 9, 1994, Panama City Beach, FL, USA, pp. 679-689.
40. Komarov, V.A. and Weisshaar, T.A. (2002), 'New Approach to Improving the Aircraft Structural Design Process', *Journal of Aircraft,* Vol. 39, No. 2, pp. 227-233.
41. Martinez, M.P., Messac, A. and Rais-Rohani, M. (2001), 'Manufacturability-Based Optimization of Aircraft Structures Using Physical Programming', *AIAA Journal,* Vol. 39, No. 3, pp. 517-525.
42. Gillie, J. (2008), *Boeing's 737 Successor May Not Debut Until 2017,* available at: http://blogs.thenewstribune.com/business/2008/03/19/boeing_s_737_successor_may_not_debut_unt_2017 (accessed 2008).
43. Pritchard, D. and MacPherson, A. (2007), 'Strategic Destruction of the Western Commercial Aircraft Sector: Implications of Systems Integration and International Risk-Sharing Business Models', *The Aeronautical Journal,* Vol. 111, No. 1119, pp. 327-334.
44. Hadcock, R.N. and Vosteen, L.F. (1994), *Composites Chronicles: A Study of the Lessons Learned in the Development, Production, and Service of Composite Structures*, Report no. CR 4620, NASA, Springfield, VA, USA.
45. Wessner, C.W. and Wolff, A.W. (1997), *Policy Issues in Aerospace Offsets - Report of a Workshop (1997)*, National Academy Press, Washington, D.C., USA.
46. Bales, R.R., Maull, R.S. and Radnor, Z. (2004), 'The Development of Supply Chain Management within the Aerospace Manufacturing Sector', *Supply Chain Management: An International Journal,* Vol. 9, No. 3, pp. 250-255.
47. Smith, D.J. and Tranfield, D. (2005), 'Talented Suppliers? Strategic Change and Innovation in the UK Aerospace Industry', *R&D Management,* Vol. 35, No. 1, pp. 37-49.
48. Wayne, L. and Shister, N. (2007), 'Boeing Reinvents its Supply Chain', *World Trade,* Vol. 20, No. 4, pp. 36-40.
49. Matlack, C. (2006), *Can Airbus afford the A350?,* available at: http://www.businessweek.com/globalbiz/content/dec2006/gb20061204_704055.htm?chan=rss_topStories_ssi_5 (accessed 2007).
50. Masters, C. (2007), 'How Boeing Got Going', *Time,* No. 17 September 2007, pp. 49-52.
51. Peoples, R. and Willcox, K.'A Value-Based MDO Approach to Assess Business Risk for Commercial Aircraft Design', *10th AIAA/ISSMO Multidisciplinary Analysis and Optimization Conference,* Vol. AIAA 2004-4438, Aug 30, 2004-Sep 1, 2004, Albany, NY, USA, pp. 1568-1579.
52. Castagne, S. , Curran, R., Rothwell, A., Price, M., Benard, E., and Raghunathan, S.'A Generic Tool for Cost Estimating in Aircraft Design', *AIAA 4th Aviation Technology, Integration and Operations Forum,* Vol. AIAA 2004-6235, Sep 20, 2004-Sep 22, 2004, Chicago, Illinois, USA.

53. Wu, H., Liu, Y., Ding, Y. and Liu, J. (2004), 'Methods to Reduce Direct Maintenance Costs for Commercial Aircraft', *Aircraft Engineering and Aerospace Technology,* Vol. 76, No. 1, pp. 15-18.
54. Gantois, K. (1998), *An MDO Concept for Large Civil Airliner Wings* Cranfield University - Cranfield College of Aeronautics, Cranfield.
55. Sobieszczanski-Sobieski, J. (1999), 'Multidisciplinary Design Optimisation (MDO) Methods: Their Synergy With Computer Technology in the Design Process', *The Aeronautical Journal,* Vol. 103, No. 1026, pp. 373-382.
56. Moore, R., Murphy, A., Price, M., and Curran, R.'Analysis Driven Design and Optimization Methods for Aircraft Structures', *47th AIAA/ASME/ASCE/AHS/ASC Structures, Structural Dynamics, and Materials Conference,* May 1, 2006-May 4, 2006, Newport, Rhode Island, USA., pp. 5876-5893.
57. Kim, J.S., Kim, C.G., Hong, C.S. and Hahn, H.T. (2000), 'Development of Concurrent Engineering System for Design of Composite Structures', *Composite Structures,* Vol. 50, No. 3, pp. 297-309.
58. Curran, R., Raghunathan, S., Price, M., Kundu, A.K., Benard, E., Castagne, S., Mawhinney, P., Crosby, S., and Early, J.'A Methodology for Integrated Cost Engineered Systems within Aerospace', *AIAA 4th Aviation Technology, Integration and Operations Conference,* Sep 20, 2004-Sep 22, 2004, Chicago, IL, USA, pp. 58-71.
59. Bettis, R.A. , Bradley, S.P. and Hamel, G. (1992), 'Outsourcing and Industrial Decline', *Academy of Management Executive,* Vol. 6, No. 1, pp. 7-22.
60. McMasters, J.H. and Cummings, R.M. (2004), 'From Farther, Faster, Higher to Leaner, Meaner, Greener: Further Directions in Aeronautics', *Journal of Aircraft,* Vol. 41, No. 1, pp. 51-61.
61. Schuhmacher, G., Murra, I., Wang, L., Laxander, A., O'Leary, O.J., and Herold, M.'Multidisciplinary Design Optimization of a Regional Aircraft Wing Box', *9th AIAA/ISSMO Symposium on Multidisciplinary Analysis and Optimization,* Vol. AIAA 2002-5406, Sep 4, 2002-Sep 6, 2002, Atlanta, Georgia, USA.
62. Markish, J. and Willcox, K. (2002), 'Multidisciplinary Techniques for Commercial Aircraft System Design', *9th AIAA/ISSMO Symposium on Multidisciplinary Analysis and Optimization,* Vol. AIAA 2002-5612, Sep 4, 2002-Sep 6, 2002, Atlanta, GA, USA.
63. Murman, E.M., Walton, W. and Rebentisch, E. (2000), 'Challenges in the Better, Faster, Cheaper era of Aeronautical Design, Engineering and Manufacturing', *The Aeronautical Journal,* Vol. 104, No. 1040, pp. 481-489.
64. Slack, R. (1999), *The Application of Lean Principles to the Military Aerospace Product Development Process* MIT , MA, USA.
65. Williamson, O. *The Economic Institution of Capitalism*, The Free Press, New York, USA.
66. Bakkila, M.V. (1996), *A System Dynamics Analysis of the Interaction Between the U.S. Government and the Defense Aerospace Industry* Massachusetts Institute of Technology, Massachusetts, USA.
67. Coase, R.H. (1972), 'Industrial Organization: A Proposal for Research', in Fuchs, V.R. *Policy Issues and Research Opportunities in Industrial Organization*, Natioanl Bureau of Economic Research, New York, USA, pp. 59-73.
68. Swink, M. and Mabert, V. (2000), 'Product Development Partnerships: Balancing Manufacturers' and Suppliers' Needs', *Business Horizon,* Vol. 43, No. 3, pp. 59-68.
69. Probert, D.R. (1996), 'The Practical Development of a Make or Buy Strategy: The Issues of Process Positioning', *Integrated Manufacturing Systems,* Vol. 7, No. 2, pp. 44-51.

70. Vining, A. and Globerman, S. (1999), 'A Conceptual Framework for Understanding the Outsourcing Decision', *European Management Journal,* Vol. 17, No. 6, pp. 645-654.
71. Akerlof, G. (1970), 'The Market for Lemons: Quality, Uncertainty and the Market Mechanism', *Quarterly Journal of Economics,* Vol. 84, No. 3, pp. 488-500.
72. Krause, D.R., Handfield, R.B. and Scannell, T.V. (1998), 'An Empirical Investigation of Supplier Development: Reactive and Strategic Processes', *Journal of Operations Management,* Vol. 17, No. 1, pp. 39-58.
73. Bradach, J.L. and Eccles, R.G. (1998), 'Price, Authority, and Trust: From Ideal Types to Plural Forms', in Scott, W.R. and Blake, J. *Annual Review of Sociology*, Vol. 15, Annual Reviews, Palo Alto, CA, USA, pp. 97-118.
74. Poppo, L. and Zenger, T. (2002), 'Do Formal Contracts and Relational Governance Function as Substitutes or Complements?', *Strategic Management Journal,* Vol. 23, No. 8, pp. 707-725.
75. Hill, C.W.L. (1990), 'Cooperation, Opportunism, and the Invisible Hand: Implications for Transaction Cost Theory', *Academic Management Review,* Vol. 15, No. 3, pp. 500-513.
76. Williamson, O.E. (1985), *The Economic Institutions of Capitalism*, Free Press, NY, USA.
77. Geyskens, I. , Steenkamp, J.-B.E.M. and Kumar, N. (2006), 'Make, Buy, or Ally: A Transaction Cost Theory Meta-Analysis', *Academy of Management Journal,* Vol. 49, No. 3, pp. 519-543.
78. Hart, O. and Holmstrom, B. (1987), 'Theory of Contracts', Cambridge University Press, Cambridge, UK.
79. Walker, G. and Weber, D. (1984), 'A Transaction Cost Approach to Make or Buy Decisions', *Administrative Science Quarterly,* Vol. 29, No. 3, pp. 373-391.
80. Martin, S. (1996), 'Countertrade and Offsets: An Overview of the Theory and Evidence', in Martin, S. *The Economics of Offsets: Defence Procurement and Countertrade*, Harwood Academic, Amsterdam, The Netherlands, pp. 15-48.
81. Reed, F.M. and Walsh, K. (2002), 'Enhancing Technological Capability through Supplier Development: A Study of the U.K. Aerospace Industry', *IEEE Transactions of Engineering Management,* Vol. 49, No. 3, pp. 231-242.
82. Eppinger, S.D. and Chitkara, A.R. (2006), 'The New Practice of Global Product Development', *MITSloan Management Review,* Vol. 47, No. 4, pp. 22-30.
83. Hickie, D. (2006), 'Knowledge and Competitiveness in the Aerospace Industry: The Cases of Toulouse, Seattle and North-West England', *European Planning Studies,* Vol. 14, No. 5, pp. 697-716.
84. Farrell, J., Monroe, H.K. and Saloner, G. (1994), 'The Vertical Organization of Industry: Systems Competition vs. Component Competition', *Journal of Economics & Management Strategy,* Vol. 7, No. 2, pp. 143-182.
85. Nolan, P. and Zhang, J. (2003), 'Globalization Challenge for Large Firms from Developing Countries: China's Oil and Aerospace Industries', *European Management Journal,* Vol. 21, No. 3, pp. 285-299.
86. Walter, A. (2003), 'Relationship-Specific Factors Influencing Supplier Involvement in Customer New Product Development', *Journal of Business Review,* Vol. 56, No. 9, pp. 721-733.
87. Fan, I.-S., Russell, S. and Lunn, R. (2000), 'Supplier Knowledge Exchange in Aerospace Product Engineering', *Aircraft Engineering and Aerospace Technology: An International Journal,* Vol. 72, No. 1, pp. 14-17.
88. Lewis, E. (2007), 'Suppliers Get Smart', *Product Design and Development,* pp. 32-33.
89. Clark, K., Chew, B. and Fukimoto, T. (1987), 'Product Development in the World

Auto Industry', *Brookings Papers on Economic Activity,* Vol. 3, pp. 729-771.
90. Dankbaar, B. (2007), 'Global Sourcing and Innovation: The Consequences of Losing both Organizational and Geographical Proximity', *European Planning Studies,* Vol. 15, No. 2, pp. 271-288.
91. Vernon, R. (1966), 'International Investment and International Trade in the Product Cycle', *Quarterly Journal of Economics,* Vol. 80, No. 2, pp. 190-207.
92. Wraige, H. (2004), 'The Go-Betweens', *Professional Engineering,* Vol. 16, No. 16, pp. 26.
93. Airbus *Airbus Aircraft Families - Introduction to the A320 Family,* available at: http://www.airbus.com/en/aircraftfamilies/a320/ (accessed 2007).
94. Yoon, K. and Naadimuthu, G. (1994), 'A Make or Buy Decision Analysis Involving Imprecise Data', *International Journal of Production Economics,* Vol. 14, No. 2, pp. 62-69.
95. Rossetti, C. and Choi, T.Y. (2005), 'On the Dark Side of Strategic Sourcing: Experiences from the Aerospace Industry', *Academy of Management Executive,* Vol. 19, No. 1, pp. 46-60.
96. Imrie, R. and Morris, J. (1992), 'A Review of Recent Changes in Buyer-Supplier Relations', *OMEGA International Journal of Management Sciences,* Vol. 20, No. 5-6, pp. 641-652.
97. Rainnie, A. (1991), 'Just in Time, Subcontracting and the Small Firm', *Work, Employment and Society,* Vol. 5, No. 3, pp. 353-375.
98. Probert, D.R., Jones, S.W. and Gregory, M.J. (1993), 'The Make or Buy Decision in the Context of Manufacturing Strategy Development', *Journal of Engineering Manufacture,* Vol. 207, No. B4, pp. 241-250.
99. Burt, D.N. and Doyle, M.F. (1993), *The American Keiretsu, Business One*, Irwin, Homewood, IL.
100. Haftl, L. (2007), 'Aerospace Outsourcing Can Turn Shops into High Flyers', *American Machinist,* Vol. 151, No. 4, pp. 30-32.
101. Teece, D.J. (1982), 'Towards an Economic Theory of the Multiproduct Firm', *Journal of Economic Behavior and Organization,* Vol. 3, No. 1, pp. 39-63.
102. Venkatesan, R. (1992), 'Strategic Sourcing: To Make or not to Make', *Harvard Business Review,* Vol. 70, No. 6, pp. 98-107.
103. McCutcheon, D. and Stuart, F.I. (2000), 'Issues in the Choice of Supplier Alliance Partners', *Journal of Operational Management,* Vol. 18, No. 3, pp. 279-301.
104. Horwitch, M. and Thietart, R.A. (1987), 'The Effect of Business Interdependencies on Product R&D-Intensive Business Performance', *Management Science,* No. 33, pp. 178-197.
105. Swink, M. and Zsidisin, G. (2006), 'On the Benefits and Risks of Focused Commitment to Suppliers', *International Journal of Production Research,* Vol. 44, No. 20, pp. 4223-4240.
106. Burton, B. (2007), *Knowledge: To Share or Protect?,* available at: http://www.ikmagazine.com/xq/asp/txtSearch.culture+cultural/exactphrase.0/sid.0/articleid.36B6D32D-5F37-4874-9139-5AB1B2B1E9B0/qx/display.htm (accessed 2008).
107. Greising, D. and Johnsson, J. (2007), *Behind Boeing's 787 Delays: Problems at One of the Smallest Suppliers in Dreamliner Program Causing Ripple Effect,* available at: www.chicagotribune.com/business/chi-sat_boeing_1208dec08,1,571535.story (accessed 2007).
108. Mecham, M. (2008), *Boeing Buys Vought Share of Fuselage,* available at: http://www.aviationweek.com/aw/generic/story_channel.jsp?channel=comm&id=news/GLOBAL03288.xml&headline=Boeing%20Buys%20Vought%20Share%20Of%20Fuselage%20Builder (accessed 2009).

109. The Economist (2009), 'Time to Change the Act', *The Economist,* Vol. 390, No. 8619, pp. 67-69.
110. Trimble, S. (2007), 'Boeing may Dump Sub-Par Suppliers', *Flight International,* Vol. 172, No. 6-12 Nov 2007, pp. 7.
111. Nellore, R., Söderquist, K. and Eriksson, K.-A. (1999), 'A Specification Model for Product Development', *European Management Journal,* Vol. 17, No. 1, pp. 50-63.
112. Clark, K. and Fujimoto, T. (1991), *Product Development Performance, Strategy, Organization and Management in the World Auto Industry*, Harvard Business School Press, Boston, MA, USA.
113. Clark, K. (1989), 'Project Scope and Project Performance: The Effects of Parts Strategy and Supplier Involvement on Product Development', *Management Science,* Vol. 35, No. 10, pp. 1247-1263.
114. Koufteros, X., Vonderembse, M. and Jayaram, J. (2005), 'Internal and External Integration for Product Development: The Contingency Effects of Uncertainty, Equivocality, and Platform Strategy', *Decision Sciences,* Vol. 36, No. 1, pp. 97-133.
115. Ettlie, J.E. and Pavlou, P.A. (2006), 'Technology-Based New Product Development Partnerships', *Decision Sciences,* Vol. 37, No. 2, pp. 117-147.
116. D'Aveni, R.A. and Ravenscratft, D.J. (1994), 'Economies of Integration versus Bureaucracy Costs: Does Vertical Integration Improve Performance?', *Academy of Managerial Journal,* Vol. 37, No. 5, pp. 1167-1206.
117. O'Sullivan, A. (2006), 'Why Tense, Unstable, and Diverse Relations are Inherent in Co-Designing with Suppliers: An Aerospace Case Study', *Industrial and Corporate Change,* Vol. 15, No. 2, pp. 221-250.
118. Terwiesch, C., Loch, C.H. and De Meyer, A. (2002), 'Exchanging Preliminary Information in Concurrent Engineering: Alternative Coordination Strategies', *Organization Science,* Vol. 13, No. 4, pp. 402-419.
119. Watson, P., Curran, R., Murphy, A., Cowan, S., Hawthorne, P., and Watson, N.'A Cost Estimating Model for Aerospace Procurement Pro-COST EST', *AIAA 4th Aviation Technology, Integration and Operations Conference,* Vol. AIAA 2004-6327, Sep 20, 2004-Sep 22, 2004, Chicago, Illnois, USA, pp. 103-117.
120. Dyer, J.H. and Ouchi, W.G. (1993), 'Japanese-Style Partnerships - Giving Companies a Competitive Edge', *Sloan Management Review,* Vol. 35, No. 1, pp. 51-63.
121. Watts, C.A. and Hahn, C.K. (1993), 'Supplier Development Programs: An Empirical Analysis', *International Journal of Purchasing and Material Management,* Vol. 29, No. 2, pp. 11-17.
122. Kraljic, P. (1983), 'Purchasing must become Supply Management', *Harvard Business Review,* Vol. 61, No. 5, pp. 107-117.
123. Parry, G., Graves, A. and James-Moore, M. (2006), 'The Threat to Core Competence Posed by Developing Closer Supply Chain Relationships', *International Journal of Logistics: Research and Applications,* Vol. 9, No. 3, pp. 295-305.
124. Eisenhardt, K.M. (1989), 'Agency Theory: An Assessment and Review', *Academy of Management Executive,* Vol. 14, No. 1, pp. 57-74.
125. Handfield, R.B. and Ragatz, G.L. (1999), 'Involving Supplier in New Product Development', *California Management Review,* Vol. 42, No. 1, pp. 59-82.
126. Hendry, J. (1995), 'Culture, Community and Networks: The Hidden Cost of Outsourcing', *European Management Journal,* Vol. 13, No. 2, pp. 193-200.
127. Bruce, M. and Moger, S. (1999), 'Dangerous Liaisons: An Application of Supply Chain Modelling for Studying Innovations within the UK Clothing Industry', *Technology Analysis and Strategic Management,* Vol. 11, No. 1, pp. 113-125.
128. Lewicki, R.J., McAllister, D.J. and Bies, R.J. (1998), 'Trust and Distrust: New Relationships and Realities', *Academy of Management Review,* Vol. 23, No. 3, pp.

438-459.
129. Maqsood, T., Walker, D. and Finegan, A. (2007), 'Extending the "Knowledge Advantage": Creating Learning Chains', *The Learning Organization,* Vol. 14, No. 2, pp. 123-141.
130. Williamson, O.E.'Strategy Research: Governance and Competence Perspectives', *Strategic Management Journal,* Vol. 20, No. 12, pp. 1087-1108.
131. Alchian, A.A. and Demsetz, H. (1972), 'Production, Information Costs, and Economic Organization', *American Economic Review,* Vol. 62, pp. 777-795.
132. Langley, M. (1971), 'The History of Metal Aircraft Construction', *Aeronautical Journal of the Royal Aeronautical Society,* Vol. 75, No. 721, pp. 19-30.
133. Harris, C.E., Starnes, J.H., and Shuart, M.J. (2001), *An Assessment of the State-of-the-Art in the Design and Manufacturing of Large Composite Structures for Aerospace Vehicles*, Report no. TM 210844, NASA, Hampton, VA, USA.
134. EADS *Composites in the Aerospace Industry,* available at: http://www.eads.net/xml/content/OF00000000400004/0/16/42251160.jpg (accessed 2008).
135. Paul, D., Kelly, L., Venkayya, V. and Hess, T. (2002), 'Evolution of U.S. Military Aircraft Structures Technology', *Journal of Aircraft,* Vol. 39, No. 1, pp. 18-29.
136. Marsh, G. (2004), 'Composites Lift Off in Primary Aerostructures', *REINFORCEDplastics,* Vol. 48, No. 4, pp. 22-27.
137. Roberts, T. (2007), 'Rapid Growth Forecast for Carbon Fibre Market', *REINFORCEDplastics,* Vol. 51, No. 2, pp. 10-13.
138. CompositesWorld *CompositesWorld Conferences - 2007 Carbon Fibers,* available at: http://compositesworld.com/cf/ (accessed 2008).
139. Marsh, G. (2001), 'Affordability is the Focus for Aerospace Composites', *REINFORCEDplastics,* Vol. 45, No. 1, pp. 34-38.
140. Kedward, K.T. (2000), 'Generic Approaches and Issues for Structural Composite Design',(Kelly, A. Zweben, C.), *Comprehensive Composite Materials*, Vol. 6, Elsevier, Oxford, UK., pp. 15-28.
141. Hexcel *Hexply® M21 - Epoxy Matrix (180°C Curing matrix) - Product Data,* available at: http://www.hexcel.com/NR/rdonlyres/A4AE89BC-0EA6-473A-A3CA-F2F98C13D033/0/HexPly_M21_eu.pdf (accessed 2008).
142. Boshers, C. (2001), 'Design Allowables', in Miracle, D.B. and Donaldson, S.L. *ASM Handbook: Composites v. 21*, ASM International, pp. 360-365.
143. Soutis, C. (2005), 'Carbon Fiber Reinforced Plastics in Aircraft Construction', *Materials Science & Engineering A,* Vol. 412, No. 1-2, pp. 171-176.
144. Grande, D.H., Ilcewicz, L.B., Avery, W.B., and Bascom, W.D. (1993), *Effects of Intra- and Inter-Laminar Resin Content on the Mechanical Properties of Toughened Composite Materials*, Report no. N93-30845, NASA, Hampton, VA, USA.
145. Lee, J. and Soutis, C. (2005), 'Thickness Effect on the Compressive Strength of T800/924C Carbon Fibre-Epoxy Laminates', *Composites: Part A,* Vol. 36, No. 2, pp. 213-227.
146. Mazumdar, S.J. (2002), *Composites Manufacturing - Materials, Product, and Process Engineering*, CRC Press, Fl, USA.
147. Morton, S.K., Webber, J.P.H., and Thomas, D.M.'Design and Assessment of Composite Tapered Laminated Plates', *35th AIAA/ASME/ASCE/AHS/ASC Structures, Structural Dynamics, and Materials Conference,* Apr 18, 1994-Apr 20, 1994, Washington DC, USA, pp. 2763-2773.
148. Baker, A., Dutton, S., and Kelly, D. (2004), *Composite Materials for Aircraft Structures* (2nd edition), AIAA Education Series, Reston, VA, USA.
149. Soutis, C. (2005), 'Fibre Reinforced Composites in Aircraft Construction', *Progress in*

Aerospace Sciences, Vol. 41, No. 2, pp. 143-151.
150. Bader, M.G. 'Designing Composite Materials for Cost-Performance-Effectiveness', *24th International SAMPE Europe Conference of the Society for the Advancement of Materials and Process Engineering,* Apr 1, 2003-Apr 3, 2003, Paris Expo, Porte de Versailles, Paris, France, pp. 59-66.
151. Soutis, C., Smith, F.C. and Matthews, F.L. (2000), 'Predicting the Compressive Engineering Performance of Carbon Fibre-Reinforced Plastics', *Composites: Part A,* Vol. 31, No. 6, pp. 531-536.
152. Richardson, M.O.W. and Wisheart, M.J. (1996), 'Review of Low-Velocity Impact Properties of Composite Materials', *Composites Part A,* Vol. 27, No. 12, pp. 1123-1131.
153. Sookay, N.K., von Klemperer, C.J. and Verijenko, V.E. (2003), 'Environmental Testing of Advanced Epoxy Laminates', *Composite Structures,* Vol. 62, No. 3-4, pp. 429-433.
154. Verrey, J., Wakeman, M.D., Michaud, V. and Manson, J.A.E. (2006), 'Manufacturing Cost Comparison of Thermoplastic and Thermoset RTM for an Automotive Floor Pan', *Composite Part A,* Vol. 37, No. 1, pp. 9-22.
155. Griffin, C.F. and Harvill, W.E. (1988), *Composite Transport Wing Technology Development - Design Development Tests and Advanced Structural Concepts*, Report no. CR 4177, NASA, Hampton, VA, USA.
156. Sela, N. and Ishai, O. (1989), 'Interlaminar Fracture Toughness and Toughening of Laminated Composite Materials: A Review', *Composites,* Vol. 20, No. 5, pp. 423-435.
157. Horton, R.E. and McCarty, J.E. (1987), 'Damage Tolerance of Composites', *Engineered Materials Handbook* , Vol. 1, American Society for Metals, pp. 261-267.
158. SP Systems *Guide to Composites,* available at: http://www.gurit.com/downloads.asp?section=000100010037&sectionTitle=Data+Sheet+and+Brochure+Downloads (accessed 2007).
159. Oxeon (2006), *Increasing Flexibility in the Carbon Fiber Value Chain by Using New Fiber-to-Fabric Converting Technologies,* available at: http://www.oxeon.se/uploads///Media/20061106%20Olofsson_Presentation.pdf (accessed 2008).
160. Bader, M.G. (2002), 'Selection of Composite Materials and Manufacturing Routes for Cost Effective Performance', *Composites Part A,* Vol. 33, No. 7, pp. 913-934.
161. Reeve, S., Robinson, W., Cordell, T., and Rondeau, R.'Carbon Fiber Evaluation for Directed Fiber Preforms', *Fourth International SAMPE Symposium,* May 6, 2001-May 10, 2001, Long Beach, CA, USA, pp. 790-803.
162. Dexter, H.B. (1993), 'An Overview of the NASA Textile Composites Program', *FIBER-TEX 1992: The Sixth Conference on Advanced Engineering Fibers and Textile Structures for Composites,* Oct 27, 1992-Oct 29, 1992, Drexel University, Philadelphia, PA, USA, pp. 1-31.
163. Bibo, G.A., Hogg, P.J. and Kemp, M. (1997), 'Mechanical Characteristics of Glass and Carbon Fibre Reinforced Composites Made with Non-Crimp Fabrics', *Composite Science and Technology,* Vol. 57, No. 9-10, pp. 1221-1241.
164. Tong, L., Mouritz, A.P., and Bannister, M.K. (2002), *3D Fibre Reinforced Polymer Composites*, Elsevier, Netherlands.
165. Kelkar, A.D., Tate, J.S. and Bolick, R. (2006), 'Structural Integrity of Aerospace Textile Composites under Fatigue Loading', *Materials Science and Engineering B,* Vol. 132, No. 1-2, pp. 79-84.
166. Cox, B.N. and Flanagan, G. (1997), *Handbook of Analytical Methods for Textile Composites*, Report no. CR 4750, NASA, Hampton, VA, USA.
167. Thagard, J.R. (2003), *Investigation and Development of the Resin Infusion between Double Flexible Tooling Process for Composite Fabrication,* The Florida State

University, FAMU-FSU College of Engineering, FL, USA.
168. Leong, K.H. , Ramakrishna, S., Huang, Z.M. and Bibo, G.A. (2000), 'The Potential of Knitting for Engineering Composites - A Review', *Composites: Part A,* Vol. 31, No. 3, pp. 197-220.
169. Poe, C.C., Dexter, H.B. and Raju, I.S. (1999), 'Review of the NASA Textile Composites Research', *Journal of Aircraft,* Vol. 36, No. 5, pp. 876-884.
170. Kamiya, R., Cheeseman, B.A., Popper, P. and Chou, T.-W. (2000), 'Some Recent Advances in the Fabrication and Design of Three-Dimensional Textile Preforms: A Review', *Composites Science and Technology,* Vol. 60, No. 1, pp. 33-47.
171. Bannister, M. (2001), 'Challenges for Composites in the New Millenium - A Reinforcement Perspective', *Composite Part A,* Vol. 32, No. 7, pp. 901-910.
172. Edgson, R. and Temple, S. (inventors) (Jul 21, 1998), *Fibre Preforms for Structural Composite Components*. US Patent 5783279.
173. IHS *EN 13473-1 (Reinforcement - Specifications for Multiaxial Multi-Ply Fabrics),* available at: http://necis.ihs.com/document/abstract/CQCOHBAAAAAAAAAA (accessed 2008).
174. REINFORCEDplastics (2003), 'Fabrics Move Forward', *REINFORCEDplastics,* Vol. 47, No. 11, pp. 26-29.
175. Backhouse, R. (1998), *Multiaxial Non-Crimp Fabrics: Characterisation of Manufacturing Capability for Composite Aircraft Primary Structure Applications* Cranfield University, Cranfield, Bedfordshire, UK.
176. Karal, M. (2001), *AST Composite Wing Program - Executive Summary*, Report no. CR 210650, NASA, Hampton, VA, USA.
177. Miller, A.J. (1998), *The Effect of Microstructural Parameters on the Mechanical Properties of Non-Crimp Fabric Composites* School of Industrial and Manufacturing Science, Cranfield University, Bedford, UK.
178. Wouters, M. (2002), *Effects of Fibre Bundle Size and Stitch Pattern on the Static Properties of Unidirectional Carbon-Fibre Non-Crimp Fabric Composites* Lulea University of Technology, Sweden, Lulea, Sweden.
179. Lomov, S.V., Belov, E.B., Bischoff, T., Ghosh, S.B., Truong Chi, T. and Verpoest, I. (2002), 'Carbon Composites Based on Multiaxial Stitched Preforms. Part 1. Geometry of the Preform', *Composites Part A,* Vol. 33, No. 9, pp. 1171-1183.
180. Sigmatex UK Ltd (2005), *High Technology Fabrics - Multi-axial (NCF) Fabrics - Presented to SAMPE - Seattle Chapter ,* available at: http://www.seattlesampe.org/presentations/2005-05.pdf (accessed 2008).
181. Mills, A. (2006), 'Development of an Automated Preforming Technology for Resin Infusion Processing of Aircraft Components', *Journal of Aerospace Industry,* Vol. 220, No. 5, pp. 499-505.
182. Hexcel *Advanced Fibre-Reinforced Matrix Products for Direct Processes,* available at: http://www.hexcel.com/NR/rdonlyres/13080D7F-2058-48B8-A981-256DEC18F086/0/DirectProcessesBrochure.pdf (accessed 2007).
183. TCR Composite *TCR™ Composites - Enhanced Prepreg Braided Sleeves,* available at: http://www.tcrcomposites.com/pdfs/braided.pdf (accessed 2008).
184. A&P Technology *A&P Technology - Braids FAQs,* available at: http://www.braider.com/braidfaqs.html (accessed 2008).
185. Falzon, P.J. and Herszberg, I. (1998), 'Mechanical Performance of 2-D Braided Carbon/Epoxy Composites', *Composites Science and Technology,* Vol. 58, No. 2, pp. 253-265.
186. Braley, M. and Dingeldein, M.'Advancements in Braided Materials Technology', *SAMPE 2001,* May 6, 2001-May 10, 2001, Long Beach, CA, USA, pp. 2445-2454.
187. Davis, J. and Dexter, H.B.'The NASA-ACT program: Examining Innovative Textiles

for Composites', *IFAI Workshop on Advanced Textile Composites,* Mar, 1996, Anaheim, CA, USA,
188. Greenhalgh, E. and Hiley, M. (2003), 'The Assessment of Novel Materials and Processes for the Impact Tolerant Design of Stiffened Composite Aerospace Structures', *Composites: Part A,* Vol. 34, No. 2, pp. 151-161.
189. National Composites Network - DTI (2006), *HYBRIDMAT 3: Advances in the Manufacture of Advanced Structural Composites in Aerospace - a Mission to the USA,* available at: http://www.netcomposites.com/downloads/36642MR.pdf (accessed 2008).
190. Campbell, F.J. (2003), *Manufacturing Processes for Advanced Composites*, Elsevier Science, Oxford, UK.
191. Assyst Bullmer Ltd *Premicut Ultrasonic,* available at: http://www.assystbullmer.co.uk/premiumcut_ultrasonic.shtml (accessed 2009).
192. Jacob, A. (2008), 'Automating Cutting of Composites', *Reinforced Plastics,* Vol. 52, No. 6, pp. 20-23.
193. Grimshaw, M.N., Grant, C.G., and Diaz, J.M.L. *Advanced Technology Tape Laying For Affordable Manufacturing of Large Composite Structures,* available at: http://www.cincinnatilamb.com/downloads/TapeLayingLargeCompositeStructures.pdf (accessed 2008).
194. Izco, L., Isturiz, J., and Motilva, M.'High Speed Tow Placement System for Complex Surfaces with Cut / Clamp / & Restart Capabilities at 85 m/min (3350 IPM) ', *Aerospace Manufacturing and Automated Fastening Conference & Exhibition,* Vol. 2006-01-3138, Sep 12, 2006-Sep 14, 2006, Toulouse, France, SAE International, London, UK.
195. Stockton, D.J., Forster, R. and Messner, B. (1998), 'Developing Time Estimating Models for Advanced Composite Manufacturing Processes', *Aircraft Engineering and Aerospace Technology,* Vol. 70, No. 6, pp. 445-450.
196. Haffner, S.M. (2002), *Cost Modelling and Design for Manufacturing Guidelines for Advanced Composite Fabrication* Massachusetts Institute of Technology, USA.
197. Grimshaw, M.N. *Automated Tape Laying,* available at: http://www.cincinnatilamb .com/downloads/automatedtapelaying.pdf (accessed 2008).
198. Sloan, J. (2008), *ATL and AFP: Signs of Evolution in Machine Process Control,* available at: http://www.compositesworld.com/articles/atl-and-afp-signs-of-evolution-in-machine-process-control.aspx (accessed 2008).
199. Grant, C. (2006), 'Automated Processes for Composite Aircraft Structure', *Industrial Robot: An International Journal,* Vol. 33, No. 2, pp. 117-121.
200. Kosugi, K., Maekawa, S., Hirose, Y., Sana, T., Hatakeyama, T. and Tamura, H. (2001), 'Low Cost Manufacturing Approach for Composite Outer Wing of SST', *Advanced Composite Materials,* Vol. 10, No. 23, pp. 229-236.
201. Sloan, J. (2008), *ATL and AFP: Defining the Megatrends in Composite Aerostructures,* available at: http://www.compositesworld.com/articles/atl-and-afp-defining-the-megatrends-in-composite-aerostructures.aspx (accessed 2008).
202. Groppe, D. (2003), 'Robotic "Layup" of Composite Materials', *Assembly Automation,* Vol. 23, No. 2, pp. 153-158.
203. Groppe, D. (2003), 'Robots Speed Lay-Up of Composite Materials', *Reinforced Plastics,* Vol. 47, No. 4, pp. 44-47.
204. Composite Systems, I. *Aerospace,* available at: http://www.compositemfg.com/ aerpspace.htm (accessed 2009).
205. Buckingham, R.O. and Newell, G.C. (1996), 'Automating the Manufacture of Composite Broadgoods', *Composite Part A,* Vol. 27, No. 3, pp. 191-200.
206. Groppe, D. (2000), 'Robots Improve the Quality and Cost-Effectiveness of Composite

Structures', *Industrial Robot: An International Journal,* Vol. 27, No. 2, pp. 96-102.
207. Cytec *Cycom 790 RTM Modified Epoxy Preform Binder,* available at: http://www.cytec.com/engineered-materials/products/Datasheets/CYCOM%20RTM%20790.pdf (accessed 2009).
208. Glauser, T., Johansson, M. and Hult, A. (2000), 'Electron-Beam Curing of Thick Thermoset Composites: Effect of Temperature and Fiber', *Macromolecular Materials and Engineering,* Vol. 274, pp. 20-24.
209. Clements, L.L. (2000), 'Vacuum Bagging Technology Improved', *High-Performance Composites,* Vol. 8, No. 1, pp. 33-37.
210. Bondline Products, *Industrial Vacuum Bagging Apparatus for Composite Lamina Manufacturers Reduces Energy Use and Waste,* available at: http://www.bondlineproducts.com/vacbagstory.html (accessed 2008).
211. Strong, A.B. (2007), *Fundamentals of Composites Manufacturing: Materials, Methods, and Applications*, Society of Manufacturing Engineers, Dearborn, MI, US.
212. Janardhan, P. (2005), *Tool Wear of Diamond Interlocked Tools in Routing of CFRP Composites* Wichita State University, USA, Wichita, USA.
213. National Center for Defense Manufacturing & Machining (2005), *F-35 Composite Edge of Part Machining,* available at: http://www.dodtechmatch.com/Dod/TechAd/Document.aspx?ID=30190 (accessed 2009).
214. Al-Sulaiman, F.A., Abdul Baseer, M. and Sheikh, A.K. (2005), 'Use of Electrical Power for Online Monitoring of Tool Condition', *Journal of Materials Processing Technology,* Vol. 166, No. 3, pp. 364-371.
215. Subramanian, K. (1977), *Sensing of Drill Wear and Prediction of Drill Life* MIT, Massachusetts, MA, USA.
216. Kurada, S. and Bradley, C. (1997), 'A Review of Machine Vision Sensors for Tool Condition Monitoring', *Computers in Industry,* Vol. 34, No. 1, pp. 55-72.
217. Hashish, M. (2008), 'Abrasive-Waterjet Machining of Composites', *Water Jet Technology Association,* No. Dec, pp. 2-16.
218. Paulo Davim, J. and Reis, P. (2003), 'Drilling Carbon Fiber Reinforced Plastics Manufactured by Autoclave - Experimental and Statistical Study', *Materials and Design,* Vol. 24, No. 5, pp. 315-324.
219. Diamond Tool Coating *How DTC Produces DIA TIGER Diamond,* available at: http://www.diamondtc.com/diatiger/production.html (accessed 2009).
220. M.Torres *Torresmill & Torrestool,* available at: www.afm.es/catalogo_afm-en/catalogo_aeronautica-en/mtorres-en/mtorres_1.pdf (accessed 2009).
221. Kuberski, L.F. (2001), 'Machining, Trimming, and Routing of Polymer-Matrix Composites', in Miracle, D.B. and Donaldson, S.L. *ASM Handbook: Composites v. 21*, ASM International, pp. 616-619.
222. Shanmugam, D.K., Nguyen, T. and Wang, J. (2008), 'A Study of Delamination on Graphite/Epoxy Composites in Abrasive Waterjet Machining', *Composite Part A,* Vol. 39, No. 6, pp. 923-929.
223. Herzog, D., Jaeschke, P., Meier, O. and Haferkamp, H. (2008), 'Investigations on the Thermal Effect Caused by Laser Cutting with Respect to Static Strength of CFRP', *International Journal of Machines Tools & Manufacture,* Vol. 48, No. 12-13, pp. 1464-1473.
224. Alkire, T.D.'Development Trends of Three-Dimensional Waterjet Cutting Systems ', *Industrial Robot,* Vol. 24, No. 1, pp. 24-29.
225. Spadafora, S.J., Eng, A.T., Kovalseki, K.J., Rice, C.E., Pulley, D.F., and Dumsha, D.A.'Aerospace Finishing Systems for Naval Aviation', *42nd International SAMPE Symposium,* May 4, 1997-May 8, 1997, Anaheim, CA, USA, pp. 662-676.
226. Jackson, A. (1993), *Advanced Composite Structural Concepts and Materials* -

Technologies for Primary Aircraft Structures, Report no. N93-30430, Lockheed Aeronautical Systems Company, Burbank, CA, USA.
227. Kim, P., Schuh, T. and Winig, W. (2004), 'CFRP from Motor Sports into Automotive Series: Challenges and Opportunities Facing the Technology Transfer', *Plastic Automotive Engineering (VDI-Gesellschaft Kunststofftechnik),* pp. 457-459.
228. Abel, I. (1997), *Research and Applications in Structures at the NASA Langley Research Center*, Report no. TM 110311, NASA, Hampton, VA, USA.
229. Palmer, R.'Techno-Economic Requirements For Composite Aircraft Components', *New Fabric Technologies, New Manufacturing Processes for Advanced Composite Structures Course,* Vol. NASA NAS1-18862, Mar 29, 1995, Fishermens Bend, Vic., Australia.
230. Jegley, D.C., Bush, H.G. and Lovejoy, A.E. (2003), 'Structural Response and Failure of a Full-Scale Stitched Graphite-Epoxy Wing', *Journal of Aircraft,* Vol. 40, No. 6, pp. 1192-1199.
231. McKague, L. , Gardner, S. and Campbell, J.H. (2005), 'Design and Process Integration for Low Cost Manufacturing', *Journal of Advanced Materials,* Vol. 37, No. 1, pp. 3-10.
232. Cytec *Cycom 5215 Modified Epoxy Resin,* available at: http://www.cytec.com/engineered-materials/products/Cycom%205215.htm (accessed 2008).
233. Hart-Smith, L.J. (1986), *Design and Analysis of Bolted and Riveted Joints in Fibrous Composite Structures*, Report no. 7739, McDonnell Douglas, CA, USA.
234. Kleineberg, M., Wenner, U., and Hanke, M. (2002), *Cost Effective CFRP-Fuselage Manufacturing with Liquid Resin Infusion (LRI) - Technologies,* available at: http://www.dlr.de/fa/PortalData/17/Resources/dokumente/publikationen/2002/14_kleineberg.pdf (accessed 2005).
235. Hitchen, S.A. and Kemp, R.M.J. (1996), 'Development of Novel Cost Effective Hybrid Ply Carbon-Fibre Composites', *Composite Science and Technology,* Vol. 56, No. 9, pp. 1047-1054.
236. Jegley, D.C. and Bush, H.G. (1997), *Structural Test Documentation and Results for the McDonnell Douglas All-Composite Wing Stub Box*, Report no. TM 110204, NASA, Hampton, VA, USA.
237. Kolesnikov, B., Herbeck, L. and Fink, A. (2008), 'CFRP/Titanium Hybrid Material for Improving Composite Bolted Joints', *Composite Structures,* Vol. 83, No. 4, pp. 368-380.
238. Fink, A., Kolesnikov, B. and Wilmes, H. (2004), 'CFRP/Titanium Hybrid Material Improving Composite Structure Coupling', *JEC Composites,* Vol. 7, pp. 64-67.
239. Pantelakis, S., Baxevani, E. and Spelz, U. (1993), 'An Automated Technique for Manufacturing Thermoplastic Stringers in Continuous Length', *Composite Structures,* Vol. 26, No. 3-4, pp. 115-121.
240. Schneider, M. and Wohlmann, B.'Carbon Fibre Sewing Yarn and Binder Yarn For Preform Applications', *26th SAMPE Europe International Conference,* Apr 5, 2005-Apr 7, 2005, Paris, France, pp. 34-39.
241. Rudd, C.D., Turner, M.R., Long, A.C. and Middleton, V. (1999), 'Tow Placement Studies of Liquid Composite Moulding', *Composites Part A,* Vol. 30, No. 9, pp. 1105-1121.
242. Potluri, P. and Atkinson, J. (2003), 'Automated Manufacture of Composites: Handling, Measurement of Properties and Lay-up Simulations', *Composites Part A,* Vol. 34, No. 6, pp. 493-501.
243. Hogg, P.J. (2005), 'Toughening of Thermosetting Composites with Thermoplastic Fibres', *Materials Science and Engineering,* Vol. 412, No. 1-2, pp. 97-103.
244. Hillermeier, R.W. and Seferis, J.C. (2001), 'Interlayer Toughening of Resin Transfer

Molding Composites', *Composites: Part A,* Vol. 32, No. 5, pp. 721-729.
245. McGrail, T. *Polymer Matrix Composites - Opportunities and Challenges,* available at: http://www.soci.org/SCI/groups/mat/2006/reports/pdf/terry_mcgrail.pdf (accessed 2007).
246. Raeckers, B. (2003), *Light Weighting at Airbus,* available at: http://www.compositesintransport.com/pdfs/composit/cluster%2005/presentations/Presentation%20-%20Lightweighting%20-%20Airbus%20-%201pp.pdf (accessed 2008).
247. Morey, B. (2007), 'Processes Reduce Composite Costs', *Manufacturing Engineering,* Vol. 138, No. 4, pp. AT6-12.
248. Coenen, V., Hatrick, M., Law, H., Brosius, D., Nesbitt, A., and Bond, D. *A Feasibility Study of Quickstep Processing of an Aerospace Composite Material,* available at: http://www.quickstep.com.au/files/document/21_Feasibility_Study_Quickstep_SAMPE2005.pdf (accessed 2008).
249. Kaiser, M., Garschke, C., Fox, B., Weimer, C., and Drechsler, K.'Out of Autoclave Manufacture of Structural Aerospace Composite Materials', *SAMPE Europe 28th International Conference and Forums,* Apr 2, 2007-Apr 4, 2007, Paris, France, pp. 468-473.
250. Berejka, A.J. and Eberle, C. (2002), 'Electron Beam Curing of Composites in North America', *Radiation Physics and Chemistry,* Vol. 63, No. 3, pp. 551-556.
251. Materials Science and Technology Division *What is Electron Beam Curing?,* available at: http://www.ms.ornl.gov/researchgroups/composites/new%20orccmt%20pages/pages/ebwhat.html (accessed 2008).
252. Karlsson, K.F. and Aström, B.T. (1997), 'Manufacturing and Applications of Structural Sandwich Components', *Composites Part A,* Vol. 28, No. 2, pp. 97-111.
253. Hexcel *HexWeb Honeycomb Sandwich Design Technology,* available at: http://www.hexcel.com/NR/rdonlyres/80127A98-7DF2-4D06-A7B3-7EFF685966D2/0/7586_HexWeb_Sand_Design.pdf (accessed 2007).
254. Meo, M., Morris, A.J., Vignjevic, R. and Marengo, G. (2003), 'Numerical Simulations of Low-Velocity Impact on an Aircraft Sandwich Panel', *Composite Structures,* Vol. 62, No. 3-4, pp. 353-360.
255. Kuczma, S.K. and Vizzini, A.J. (1999), 'Failure of Sandwich to Laminate Tapered Composite Structures', *AIAA Journal,* Vol. 37, No. 2, pp. 227-231.
256. Potluri, P., Kusak, E. and Reddy, T.Y. (2003), 'Novel Stitch-Bonded Sandwich Composite Structures', *Composite Structures,* Vol. 59, No. 2, pp. 251-259.
257. Scott, M.L., Raju, J.A.S. and Cheung, A.K.H. (1998), 'Design and Manufacture of a Post-Buckling Co-Cured Composite Aileron', *Composites Science and Technology,* Vol. 58, No. 2, pp. 199-210.
258. Mouritz, A.P., Leong, K.H. and Herszberg, I. (1997), 'A Review of the Effect of Stitching on the In-Plane Mechanical Properties of Fiber-Reinforced Polymer Composites', *Composites: Part A,* Vol. 28, No. 12, pp. 979-991.
259. Bibo, G.A., Backhouse, R., Mills, A. and Hogg, P.J. (1998), 'Carbon-Fibre Non-Crimp Fabric Laminates for Cost-Effective Damage-Tolerant Structures', *Composites Science and Technology,* Vol. 58, No. 1, pp. 129-143.
260. Dell'anno, G., Cartie, D.D.R., Allegri, G., Partridge, I.K. and Rezai, A. (2007), 'Exploring Mechanical Property Balance in Tufted Carbon Fabric/Epoxy Composites', *Composites Part A,* Vol. 38, No. 11, pp. 2366-2373.
261. Farley, G.L. and Dickinson, L.C. (1993), *Mechanical Response of Composite Materials with Through-The-Thickness Reinforcement*, Report no. CR14573, NASA, Hampton, VA, USA.
262. Takeda, S., Aoki, Y., Ishikawa, T., Takeda, N. and Kikukawa, H. (2007), 'Structural Health Monitoring of Composite Wing Structure during Durability Test', *Composite*

Structures, Vol. 79, No. 1, pp. 133-139.
263. Partridge, I.K. and Cartie, D.D.R. (2005), 'Delamination Resistant Laminates by Z-Fiber Pinning: Part 1 Manufacture and Fracture Performance', *Composites: Part A,* Vol. 36, No. 1, pp. 55-64.
264. Grassi, M., Zhang, X. and Meo, M. (2002), 'Prediction of Stiffness and Stresses in Z-Fiber Reinforced Composite Laminates', *Composites: Part A,* Vol. 33, No. 12, pp. 1653-1664.
265. Jamco *Advanced Pultrusion (ADP),* available at: http://www.jamco.co.jp/e/e-components/adp2.html (accessed 2008).
266. Pultrusion Dynamics *Pultrusion Dynamics,* available at: http://www.pultrusiondynamics.com/ (accessed 2008).
267. Lee, J.A., Barnes, F.J., and McCarthy, R.J.'Roll-Formed Composite Blade Stiffeners', *International SAMPE Europe Conference No. 23,* Apr 9, 2002-Apr 11, 2002, Paris, France, pp. 737-743.
268. Burley, G.J., Williams, S. and Kaye, A.J. (inventors) (Sep 20, 2005), *A Roll Forming Machine and Method*. Canada. 2346429.
269. Hirose, Y., Taki, T., Mizusaki, Y. and Fujita, T. (2004), 'Low Cost Structural Concept for Composite Trailing Edge Flap', *Advanced Composite Materials,* Vol. 12, No. 4, pp. 281-300.
270. Boeing Commercial Airplane Group (1991), *Advanced Technology Composite Aircraft Structures - Monthly Technical Progress Report No. 25*, Report no. CR 190420 , NASA, Hampton, VA, USA.
271. Willden, K., Gessel, M., Grant, C., and Brown, T. (1995), *Manufacturing Scale-Up of Composite Fuselage Crown Fittings*, Report no. N95-28835, NASA, Hampton, VA, USA.
272. Seibert, H. (2006), 'Applications for PMI Foams in Aerospace Sandwich Structures ', *Reinforced Plastics,* Vol. 50, No. 1, pp. 44-48.
273. Boeing - Environmental Technotes (2003), *Composite Recycling and Disposal An Environmental R&D Issue,* available at: http://www.boeing.com/companyoffices/doingbiz/environmental/TechNotes/TechNotes2003-11.pdf (accessed 2008).
274. Airbus (2005), *Airbus to Protect the Environment in the Recycling of Old Airliners,* available at: http://www.airbus.com/en/corporate/ethics/environment/articles/Environment_PAMELA.html (accessed 2009).
275. Unser, J.F., Staley, T. and Larsen, D. (1996), 'Advanced Composites Recycling', *SAMPE Journal,* Vol. 32, No. 5, pp. 52.
276. Pickering, S.J. (2006), 'Recycling Technologies for Thermoset Composite Materials - Current Status', *Composites: Part A,* Vol. 37, No. 8, pp. 1206-1215.
277. Pinero-Hernanz, R., Dodds, C., Hyde, J., Garcia-Serna, J., Poliakoff, M., Lester, E., Cocero, M.J., Kingman, S., Pickering, S. and Wong, K.H. (2008), 'Chemical Recycling of Carbon Fibre Reinforced Composites in Nearcritical and Supercritical Water', *Composites Part A,* Vol. 39, No. 3, pp. 454-461.
278. CompositesIQ *About Composites - Recycling,* available at: http://www.compositesiq.com/Default.aspx?query=klU73WZFahm4QEktHPAGOA%3D%3D (accessed 2008).
279. Davidson, J. (2006), *Carbon Fiber Composite Recycling: An Industry Perspective,* available at: hhtp://www.compositesworld.com/hpc/issues/2006/September/1410 (accessed 2008).
280. Harris, C.E., Starnes, J.H.J. and Shuart, M.J. (2002), 'Design and Manufacturing of Aerospace Composite Structures, State-of-the-Art Assessment', *Journal of Aircraft,* Vol. 39, No. 4, pp. 545-560.
281. Lee, J. and Soutis, C. (2007), 'Measuring the Notched Compressive Strength of Composite Laminates: Specimen Size Effects', *Composites Science and Technology,*

Vol. 68, No. 12, pp. 2359-2366.
282. Habib, F.A. (2001), 'A New Method for Evaluating the Residual Compression Strength of Composites after Impact', *Composite Structures,* Vol. 53, No. 3, pp. 309-316.
283. Webber, J.P.H. (1996), *Design of Laminated Plates Subjected to In-Plane Loads and Bending Moments*, Report no. ESDU 96036, Engineering Sciences Data Unit, UK.
284. Herencia, J.E., Weaver, P.M., and Friswell, M.I.'Local Optimisation of Anisotropic Composite Panels with T Shape Stiffeners', *48th AIAA/ASME/ASCE/AHS/ASC Structures, Structural Dynamics, and Materials Conference,* Apr 23, 2007-Apr 26, 2007, Honolulu, Hawaii, USA, pp. 6241-6267.
285. Lekhnitskii, S.G. (1968), *Anisotropic Plates*, Gordon and Breach Sci. Publ. Inc., New York, USA.
286. Seydel, E. (1933), 'Über das Ausbeulen von rechteckigen, isotropen oder orthogonalanisotropen Platten bei Schubbeanspruchung', *Archive of Applied Mechanics (Ingenieur Archiv),* Vol. 4, No. 2, pp. 169-191.
287. Grayley, M.E. (1995), *Buckling of Rectangular Specially Orthotropic Plates*, Report no. ESDU 80023, Engineering Science Data Unit , UK.
288. Kim, C.W. and Lee, J.S. (2005), 'Optimal Design of Laminated Composite Plates for Maximum Buckling Load using Genetic Algorithm', *Proc. IMechE: Journal of Mechanical Engineering Science,* Vol. 219, No. 9, pp. 869-878.
289. van der Sloot, J.H. (2009), *Elastic Buckling of Long, Flat, Symmetrically-Laminated (AsBoDf) Composite Stiffened Panels and Struts in Biaxial Compression/Tension and Shear Loading*, Report no. IHS ESDU 08107, Engineering Sciences Data Unit, UK.
290. Adali, S., Richter, A., Verijenko, V.E. and Summers, E.B. (1995), 'Optimal Design of Hybrid Laminates with Discrete Ply Angles for Maximum Buckling Load and Minimum Cost', *Composite Structures,* Vol. 32, No. 1-4, pp. 409-415.
291. Jones, R.M. (1998), *Mechanics of Composite Materials* (2nd edition), Taylor & Francis, Philadelphia, PA, USA.
292. Weaver, P.M. 'Physical Insight into the Buckling Phenomena of Composite Structures', *47th AIAA/ASME/ASCE/AHS/ASC Structures, Structural Dynamics, and Materials Conference,* May 1, 2006-May 4, 2006, Newport, Rhode Island, USA, pp. 5292-5300.
293. Weaver, P.M. 'On Superior Buckling Performance of Flat Plates Through Anisotropy', *44th AIAA/ASME/ASCE/AHS Structures, Structural Dynamics and Materials Conference,* Apr 7, 2003-Apr 10, 2003, Norfolk, Virginia, USA, pp. 219-229.
294. Loughlan, J. (1994), 'A Finite Strip Analysis of the Buckling Characteristics of some Composite Stiffened Shear Panels', *Composite Structures,* Vol. 27, No. 3, pp. 283-294.
295. Choi, H.Y., Downs, R.J. and Chang, F.K. (1991), 'A New Approach Towards Understanding Damage Mechanisms and Mechanics of Laminates Composites due to Low-Velocity Impact: 1, Experiments', *Journal of Composite Materials,* Vol. 25, No. 8, pp. 992-1011.
296. Niu, M.C.Y. (1992), *Composite Airframe Structures*, Conmilit Press Ltd, Hong Kong, PRC.
297. Weaver, P.M. 'On Beneficial Anisotropic Effects in Composite Structures', *43rd AIAA/ASME/ASCE/AHS/ASC Structures, Structural Dynamics, and Materials Conference,* Vol. AIAA-2002-1582, Apr 22, 2002-Apr 25, 2002, Denver, Colorado, USA.
298. Todoroki, A. and Sasai, M. (2004), 'Optimizations of Stacking Sequence and Number of Plies for Laminated Cylinder using GA with Intron Genes', *Advanced Composite Materials,* Vol. 12, No. 4, pp. 331-343.
299. Challenger, K.D. (1986), 'The Damage Tolerance of Carbon Fiber Reinforced

Composites - A Workshop Summary', *Composite Structures,* Vol. 6, No. 4, pp. 295-318.
300. Cantwell, W. and Morton, J. (1991), 'The Impact Resistance of Composite Materials - A Review', *Composites,* Vol. 22, No. 5, pp. 347-362.
301. Lee, J. and Soutis, C. (2007), 'A Study on the Compressive Strength of Thick Carbon Fibre-Epoxy Laminates', *Composites Science and Technology,* Vol. 67, No. 10, pp. 2015-2026.
302. Suarez, J.A. and Buttitta, C. (1996), *Novel Composites for Wing and Fuselage Applications (Task 1 - Novel Wing Design Concepts)*, Report no. CR 198347, NASA, Hampton, VA, USA.
303. Avery, W.B. and Grande, D.H.'Influence of Materials and Layup Parameters on Impact Damage Mechanisms', *22nd International SAMPE Technical Conference,* Nov 6, 1990-Nov 8, 1990, Boston, Massachusetts, pp. 470-483.
304. Powell, P.C. (1993), *Engineering with Fibre-Polymer Laminates*, Chapman & Hall, London, UK.
305. Goerguelue, U.'Investigation of Free Edge Delamination', *International Congress of Multidisciplinary Projecting and Modelling of Building Materials and Elements,* Jun 15, 2007-Jun 16, 2007, Subotica, Serbia.
306. Nagendra, S., Haftka, R.T. and Gürdal, Z. (1991), 'Design of a Blade-Stiffened Composite Panel with a Hole', *Composite Structures,* Vol. 18, No. 3, pp. 195-219.
307. Nagendra, S., Haftka, R.T., and Gürdal, Z.'Design of a Blade Stiffened Composite Panel by a Genetic Algorithm', *34th AIAA/ASME/ASCE/AHS/ASC Structures, Structural Dynamics, and Materials Conference,* Vol. AIAA-93-1584-CP, Apr 19, 1993-Apr 22, 1993, La Jolla, CA, USA, pp. 2418-2436.
308. Wisnom, M.R. (1999), 'Size Effects in the Testing of Fibre-Composite Materials', *Composites Science and Technology,* Vol. 59, No. 13, pp. 1937-1957.
309. Eastep, F.E., Tischler, V.A., Venkayya, V.B. and Khot, N.S. (1999), 'Aeroelastic Tailoring of Composite Structures', *Journal of Aircraft,* Vol. 36, No. 6, pp. 1041-1047.
310. Penning, R.L. (1984), *Failure Analysis of Fibre Reinforced Composite Laminates*, Report no. ESDU 84018, Engineering Sciences Data Unit, UK.
311. Dorey, G. (1975), *Failure Mode of Composite Materials with Organic Matrices and their Consequences in Design*, Report no. CP 163 Paper 8, AGARD, Paris, France.
312. Cantwell, W. and Morton, J. (1985), 'Detection of Impact Damage in CFRP Laminates', *Composite Structures,* Vol. 3, No. 3-4, pp. 241-257.
313. Stevanovic, M., Kostic, M., Stecenko, T. and Briski, D.'Impact Behaviour of CFRP Composites of Different Stacking Geometry', *Composite Evaluation Proceedings TEQC 87,* pp. 78-83.
314. Hitchen, S.A. and Kemp, R.M.J. (1995), 'The Effect of Stacking Sequence on Impact Damage in a Carbon Fibre/Epoxy Composite', *Composites,* Vol. 26, No. 3, pp. 207-214.
315. Hong, S. and Liu, D. (1989), 'On the Relationship between Impact Energy and Delamination Area', *Experimental Mechanics,* Vol. 29, No. 2, pp. 115-120.
316. Liu, D. (1988), 'Impact-Induced Delamination - A View of Bending Stiffness Mismatching', *Journal of Composite Materials,* Vol. 22, No. 7, pp. 674-692.
317. Chang, F.K., Choi, H.Y. and Jeng, S.T. (1990), 'Study on Impact Damage in Laminated Composites', *Mechanics of Materials,* Vol. 10, No. 1-2, pp. 83-95.
318. Cantwell, W., Curtis, P. and Morton, J. (1986), 'An Assessment of the Impact Performance of CFRP Reinforced with High-Strain Carbon Fibres', *Composite Science and Technology,* Vol. 25, No. 2, pp. 133-148.
319. Choi, H.Y., Wang, H.S. and Chang, F.K. (1992), 'Effect of Laminate Configuration and Impactor's Mass on the Initial Impact Damage of Graphite/Epoxy Composite

Plates due to Line Loading Impact', *Journal of Composite Materials,* Vol. 26, No. 6, pp. 804-827.
320. Sihn, S., Kim, R.Y., Kawabe, K. and Tsai, S.W. (2007), 'Experimental Studies of Thin-Ply Laminated Composites', *Composite Science and Technology,* Vol. 67, No. 6, pp. 996-1008.
321. Kim, R.Y. and Soni, S.R. (1984), 'Experimental and Analytical Studies On the Onset of Delamination in Laminated Composites', *Journal of Composite Materials,* Vol. 18, No. 1, pp. 70-80.
322. Wiggenraad, J.F.M., Zhang, X. and Davies, G.A.O. (1999), 'Impact Damage Prediction and Failure Analysis of Heavily Loaded, Blade-Stiffened Composite Wing Panels', *Composite Structures,* Vol. 45, No. 2, pp. 81-103.
323. Wiggenraad, J.F.M. and Ubels, L.C. (1997), *Impact Damage and Failure Mechanisms in Structure Relevant Composite Specimens*, Report no. TP 97006, NLR, Amsterdam, Netherlands.
324. Wiggenraad, J.F.M., Aoki, R., Gaedke, M., Greenhalgh, E., Hachenberg, D., Wolf, K., and Buebl, R. (1996), *Damage Propagation in Composite Structural Elements - Analysis and Experiments on Structures*, Report no. TP 96341, NLR, Amsterdam, Netherlands.
325. Kassapoglou, C. and Lagace, P.A. (1986), 'An Efficient Method for the Calculation of Interlaminar Stresses in Composite Materials', *Journal of Applied Mechanics,* Vol. 53, No. 4, pp. 744-750.
326. Mangalgiri, P.D. (1994), 'An Analytical Study on 0/90 Ply-Drops in Composite Laminates', *Composite Structures,* Vol. 28, No. 2, pp. 181-187.
327. Mukherjee, A. and Varughese, B. (2001), 'Design Guidelines for Ply Drop-Off in Laminated Composite Structures', *Composites: Part B,* Vol. 32, No. 2, pp. 153-164.
328. Brewer, J.C. and Lagace, P.A. (1988), 'Quadratic Stress Criterion for Initiation of Delamination', *Journal of Composite Materials,* Vol. 22, No. 12, pp. 1141-1155.
329. Vidyashankar, B.R. and Krischna Murty, A.V. (2001), 'Analysis of Laminates with Ply Drops', *Composites Science and Technology,* Vol. 61, No. 5, pp. 749-758.
330. Wisnom, M.R., Dixon, R. and Hill, G. (1996), 'Delamination in Asymmetrically Tapered Composites Loaded in Tension', *Composite Structures,* Vol. 35, No. 3, pp. 309-322.
331. Khan, B., Potter, K. and Wisnom, M.R. (2006), 'Suppression of Delamination at Ply Drops in Tapered Composites by Ply Chamfering', *Journal of Composite Materials,* Vol. 40, No. 2, pp. 157-174.
332. He, K., Hoa, S.V. and Ganesan, R. (2000), 'The Study of Tapered Laminated Composite Structures: A Review', *Composites Science and Technology,* Vol. 60, No. 14, pp. 2643-2657.
333. Kemp, B.L. and Johnson, E.R. 'Response and Failure Analysis of a Graphite-Epoxy Laminate Containing Terminating Internal Plies', *AIAA/ASME/ASCE/AHS 26th Structures, Structural Dynamics and Materials Conference (Part 1),* Apr 15, 1985-Apr 17, 1985, Orlando, FL, USA, pp. 13-24.
334. Curry, J.M., Johnson, E.R., and Starnes, J.H.'Effect of Dropped Plies on the Strength of Graphite-Epoxy Laminates ', *AIAA/ASME/ASCE/AHS 28th Structures, Structural Dynamics and Materials Conference (Part 1),* Apr 6, 1987-Apr 8, 1987, Monterey, Canada, pp. 449-456.
335. Webber, J.P.H. (1991), *Delamination of Tapered Composites*, Report no. ESDU 91003, Engineering Science Data Unit, UK.
336. British Aerospace (Warton) (1988), *E.F.A. Joint Structures Team Working Document: CFC Design Rules*, Report no. JST-D-01, BAE, Warton, UK.
337. Varughese, B. and Mukherjee, A. (1997), 'A Ply Drop-Off Element for Analysis of

Tapered Laminated Composites', *Composite Structures,* Vol. 39, No. 1-2, pp. 123-144.
338. Kim, J.S., Kim, C.G. and Hong, C.S. (2001), 'Practical Design of Tapered Composite Structures using the Manufacturing Cost Concept', *Composite Structures,* Vol. 51, No. 3, pp. 285-299.
339. Hart-Smith, L.J. and Heslehurst, R.B. (2001), 'Designing for Repairability', (Miracle, D.B. and Donaldson, S. L.), *ASM Handbook: Composites v. 21*, ASM International, pp. 872-884.
340. Middleton, D.H. (1990), *Composite Materials in Aircraft Structures*, Longman Scientific and Technical, Harlow, Essex, UK.
341. Botting, A.D., Vizzini, A.J. and Lee, S.W. (1996), 'Effect of Ply-Drop Configuration on Delamination Strength of Tapered Composite Structures', *AIAA Journal,* Vol. 34, No. 8, pp. 1650-1656.
342. Fokker *Recommendations for the Design of Composite Laminates Built up from UD-Tape*, Report no. TH 45.108-101, Fokker, Amsterdam, Netherlands.
343. Todoroki, A. and Ishikawa, T. (2004), 'Design of Experiments for Stacking Sequence Optimizations with Genetic Algorithm using Response Surface Approximation', *Composite Structures,* Vol. 64, No. 3-4, pp. 349-357.
344. Seresta, O., Gürdal, Z., Adams, D.B., and Watson, L.T. (2004), 'Optimal Design of Composite Wing Structures with Blended Laminates', *10th AIAA/ISSMO Multidisciplinary Analysis and Optimization Conference,* Vol. AIAA 2004-4349, Aug 30, 2004-Sep 1, 2004, Albany, NY, USA, pp. 603-615.
345. Liu, B. and Haftka, R.T. 'Composite Wing Structural Design Optimization with Continuity Constraints', *42nd AIAA/ASME/ASCE/AHS/ASC Structures, Structural Dynamics and Materials Conference,* Apr 16, 2001-Apr 19, 2001, Seattle, Washington, USA, pp. 205-216.
346. Adams, D.B. (2002), *Blending Methods for Composite Laminate Optimization* Virginia Polytechnic Institute and State University, Blacksburg, Virginia, USA.
347. Liu, B. (2001), *Two-Level Optimization of Composite Wing Structures Based on Panel Genetic Optimization* University of Florida, Florida, USA.
348. Soremekun, G., Gürdal, Z., Kassapoglou, C. and Toni, D. (2002), 'Stacking Sequence Blending of Multiple Composite Laminates using Genetic Algorithms', *Composite Structures,* Vol. 56, No. 1, pp. 53-62.
349. Adams, D.B. (2005), *Optimization Frameworks for Discrete Composite Laminate Stacking Sequences* Virginia Polytechnic Institute and State University, Blacksburg, Virginia, USA.
350. Kristinsdottir, B.P., Zabinsky, Z.B., Tuttle, M.E. and Neogi, S. (2001), 'Optimal Design of Large Composite Panels with Varying Loads', *Composite Structures,* Vol. 51, No. 1, pp. 93-102.
351. Godwin, E.W. and Matthews, F.L. (1980), 'A Review of the Strength of Joints in Fibre-Reinforced Plastics', *Composites,* Vol. 11, No. 3, pp. 155-160.
352. Hart-Smith, L.J. 'Consequences of Interrupted Load Paths in Bonded Laminates Structures caused by Damage and by Poorly Designed Stiffener Runouts', *SAMPE Europe - International Conference 2006 Paris,* Mar 2, 2006-Mar 3, 2006, Paris, France, pp. 1-19.
353. Collings, T.A. (1982), 'On the Bearing Strengths of CFRP Laminates', *Composites,* Vol. 13, No. 3, pp. 241-252.
354. Yan, Y., Wen, W.-D., Chang, F.-K. and Shyprykevich, P. (1999), 'Experimental Study on Clamping Effects on the Tensile Strength of Composite Plates with a Bolt-Filled Hole', *Composites Part A,* Vol. 30, No. 10, pp. 1215-1229.
355. Park, H.-J. (2001), 'Effects of Stacking Sequence and Clamping Force on the Bearing Strengths of Mechanically Fastened Joints in Composite Laminates', *Composite*

Structures, Vol. 53, No. 2, pp. 213-221.
356. Aktas, A. and Dirikolu, M.H. (2003), 'The Effect of Stacking Sequence of Carbon Epoxy Composite on Laminates on Pinned-Joint Strength', *Composite Structures,* Vol. 62, No. 1, pp. 107-111.
357. US DOD, M.S.C. (1999), *The Composite Materials Handbook - Mil 17,* Vol. 3 - Materials Usage, Design and Analysis, CRC Press, Lancaster, PA, USA.
358. Hart-Smith, L.J. (2006), 'An Engineer Asks: Is it really more important that paint stays stuck on the outside of an aircraft than that glue stays stuck on the inside?', *The Journal of Adhesion,* Vol. 82, No. 1-3, pp. 181-214.
359. Gunnion, A.J. and Herszberg, I. (2006), 'Parametric Study of Scarf Joints in Composite Structures', *Composite Structures,* Vol. 75, No. 1-4, pp. 364-376.
360. Oh, J.H., Kim, Y.G. and Lee, D.G. (1997), 'Optimum Bolted Joints for Hybrid Composite Materials', *Composite Structures,* Vol. 38, No. 1-4, pp. 329-341.
361. van Rijn, L.P.V.M. (1996), 'Towards the Fastenerless Composite Design', *Composites Part A,* Vol. 27, No. 10, pp. 915-920.
362. Tomblin, J., Davies, C., Ilcewicz, L., Strole, K., and Dodosh, G.'Assessment of Industry Practices for Aircraft Bonded Joints and Structures (DOT/FAA/AR-05-13)', *FAA Workshop on Adhesive Bonding,* Jun 16, 2004-Jun 18, 2004, Seattle, WA, USA.
363. Hart-Smith, L.J. (1995), 'An Engineer's Viewpoint on Design and Analysis of Aircraft Structural Joints', *Proceedings of the Institution of Mechanical Engineers, Journal of Aerospace Engineering,* Vol. 209, No. G2, pp. 105-129.
364. Akay, M. (1992), 'Bearing Strength of As-Cured and Hygrothermally Conditioned Carbon Fibre/Epoxy Composites under Static and Dynamic Loading', *Composites,* Vol. 23, No. 2, pp. 101-108.
365. Lim, T.S., Kim, B.C. and Lee, D.G. (2006), 'Fatigue Characteristics of the Bolted Joints for Unidirectional Composite Laminates', *Composite Structures,* Vol. 72, No. 1, pp. 58-68.
366. 'ASM Handbook: Volume 21 Composites', in Parker, R.T. (Boeing Commercial Airplane Company), *Mechanical Fastener Selection*, Vol. 21, ASM, pp. 651-658.
367. Ireman, T., Ranvik, T. and Eriksson, I. (2000), 'On Damage Development in Mechanically Fastened Composite Laminates', *Composite Structures,* Vol. 49, No. 2, pp. 151-171.
368. Thoppul, S.D., Finegan, J. and Gibson, R.F. (2009), 'Mechanics of Mechanically Fastened Joint in Polymer-Matrix Composite Structures - A Review', *Composites Science and Technology,* Vol. 69, No. 3-4, pp. 301-329.
369. Mortensen, F. and Thomsen, O.T. (1999), 'A Simple Approach for the Analysis of Embedded Ply Drops in Composite and Sandwich Layers', *Composite Science and Technology,* Vol. 59, No. 8, pp. 1213-1226.
370. Saunders, D.S., Galea, S.C. and Deirmendjian, G.K. (1993), 'The Development of Fatigue Damage around Fastener Holes in Thick Graphite/Epoxy Composite Laminates', *Composites,* Vol. 24, No. 4, pp. 309-321.
371. Chen, W.H., Less, S.S. and Yah, J.T. (1995), 'Three-Dimensional Contact Stresses Analysis of Composite Laminate with Bolted Joint', *Composite Structures,* Vol. 30, No. 3, pp. 287-297.
372. Khashaba, U.A., Sallam, H.E.M. and Al-Shorba (2006), 'Effect of Washer Size and Tightening Torque on the Performance of Bolted Joints in Composite Structures', *Composite Structures,* Vol. 73, No. 3, pp. 310-317.
373. Herbeck, L. and Wilmes, H.'Design Rules for a CFRP Outer Wing', *ICAS 2002 Congress,* Vol. DLR Mitteilung, Sep, 2002, Toronto, Canada, pp. 189-202.
374. Hart-Smith, L.J. (2001), 'Bolted and Bonded Joints', in Miracle, D.B. and Donaldson, S.L. *ASM Handbook: Composites v. 21*, ASM International, pp. 271-289.

375. Liu, D., Gau, W.D., Zhang, K.D. and Ying, B.Z. (1993), 'Empirical Damage Evaluation of Graphite/Epoxy Laminated Bolted Joint in Fatigue', *Theoretical and Applied Fracture Mechanics,* Vol. 19, No. 2, pp. 145-150.
376. Cao, Z. and Cardew-Hall, M. (2006), 'Interference-Fit Riveting Technique in Fiber Composite Laminates', *Aerospace Science and Technology,* Vol. 10, No. 4, pp. 327-330.
377. Cole, R.T., Batch, E.J. and Potter, J. (1982), 'Fasteners for Composite Structure', *Composites,* Vol. 13, No. 3, pp. 233-240.
378. Kelly, G. and Hallstroem, S. (2004), 'Bearing Strength of Carbon Fibre/Epoxy Laminates: Effects of Bolt-Hole Clearance', *Composites: Part B,* Vol. 35, No. 4, pp. 331-343.
379. Grant, P., Nguyen, N., and Sawicki, A.'Bearing Fatigue and Hole Elongation in Composite Bolted Joints', *49th Annual Forum of the American Helicopter Society,* May 19, 1993-May 21, 1993, St. Louis, Missouri, USA, pp. 163-170.
380. Lessard, L.B., Poon, C.J. and Scott, R.F. (1995), 'Design of Joints in Composite Structures', in Hoa, S.V. *Computer-Aided Design of Polymer-Matrix Composite Structures*, CRC Press, pp. 243-284.
381. Crews, J.H.Jr. and Naik, R.A. (1987), *Bearing-Bypass Loading on Bolted Composite Joints*, Report no. M 89153, NASA, Hampton, VA, USA.
382. Clarke, A., Greenhalgh, E., Meeks, C., and Jones, C.'Enhanced Structural Damage Tolerance of CFRP Primary Structures by Z-Pin Reinforcement', *44th AIAA/ASME/ASCE/AHS Structures, Structural Dynamics, and Materials Conference,* Apr, 2003, Norfolk, Virginia, USA, pp. 2525-2535.
383. Xiao, Y. and Ishikawa, T. (2005), 'Bearing Strength and Failure Behavior of Bolted Composite Joints (part I: Experimental Investigation)', *Composites Science and Technology,* Vol. 65, No. 7-8, pp. 1022-1031.
384. Li, R., Kelly, D. and Crosky, A. (2002), 'Strength Improvement by Fiber Steering around a Pin Loaded Hole', *Composite Structures,* Vol. 57, No. 1-4, pp. 377-383.
385. Collings, T.A. (1977), 'The Strength of Bolted Joints in Multi-Directional CFRP Laminates', *Composites,* Vol. 8, No. 1, pp. 43-54.
386. Hart-Smith, L.J. (1980), 'Mechanically-Fastened Joints for Advanced Composites - Phenomenological Consideration and Simple Analyses', in Lenoe, E.M., Oplinger, D.W., and Burke, J.J. *Fourth Conference on Fibrous Composites in Structural Design,* Nov, 1978, San Diego, CA, USA, Plenum Press, New York, USA, pp. 543-574.
387. Banbury, A. and Kelly, D.W. (1999), 'A Study of Fastener Pull-Through Failure of Composite Laminates. Part 1: Experimental', *Composite Structures,* Vol. 45, No. 4, pp. 241-254.
388. Russell, J.D. (2007), 'Composites Affordability Initiative', *Advanced Materials & Processes,* Vol. 165, No. 6, pp. 29.
389. Fernlund, G. and Spelt, J.K. (1994), 'Mixed-Mode Fracture Characterization of Adhesive Joints', *Composite Science and Technology,* Vol. 50, No. 4, pp. 441-449.
390. Potter, K.D., Davies, R., Barrett, M., Godbehere, A., Bateup, L., Wisnom, M. and Mills, A. (2001), 'Heavily Loaded Bonded Composite Structure: Design, Manufacture and Test of 'I' Beam Specimens', *Composite Structures,* Vol. 51, No. 4, pp. 389-399.
391. Forte, M.S., Whitney, J.M. and Schoeppner, G.A. (2000), 'The Influence of Adhesive Reinforcement on the Mode-I Fracture Toughness of a Bonded Joint', *Composites Science and Technology,* Vol. 60, No. 12-13, pp. 2389-2405.
392. Russell, J.Dr. (2007), *The Composites Affordability Initiative, Part 1,* available at: http://www.compositeworld.com/hps/issues/2007/111307 (accessed 2007).
393. Wright-Patterson Air Force Base (2006), *Bonded Composite Wing Surpasses All*

Expectations, available at: http://www.wpafb.af.mil/news/story.asp?id=123035046 (accessed 2007).
394. Huang, C.K. (2003), 'Study on Co-Cured Composite Panels with Blade-Shaped Stiffeners', *Composites Part A,* Vol. 34, No. 5, pp. 403-410.
395. Hill, A.T. 'Hydraulic Ram Ballistic Testing of Low Cost Composite Wing Structure', *37th AIAA/ASME/ASCE/AHS/ASC Structures, Structural Dynamics, and Materials Conference and Exhibit,* Vol. AIAA-96-1327-CP, Apr 15, 1996-Apr 17, 1996, Salt Lake City, UT, USA, pp. 47-52.
396. Composites CRC-ACS *Technologies >> Thermoset Composite Welding (TCW),* available at: http://www.crc-acs.com.au/05tech3.asp (accessed 2008).
397. ESA (1995), *Structural Materials Handbook*, Report no. ESA-PSS-03-203, European Space Agency, Noordwijk, Netherlands.
398. Sahadevan, V., Bonnefon, V. and Edwards, T. (2006), 'A Meta-Heuristic Based Weight Optimisation for Composite Wing Structural Analysis', *Applied Mechanics and Materials,* Vol. 5-6, pp. 305-314.
399. Kedward, K.T. (1981), *Joining of Composite Materials,* Vol. STP 749, ASTM, Baltimore, MD, USA.
400. Laible, R.C. and McGarry, F.J. (1976), 'Toughening of High Temperature Resistant Epoxy Resins ', *Polymer Plastics Technology Engineering,* Vol. 7, No. 1, pp. 27-44.
401. Klapprott, D., Li, H., Wong, R., and Geisendorfer, G. (2004), *Key Factors of the Peel Ply Surface Preparation Process,* available at: http://www.henkelna.com/us/content_data/LT4537_Peel_Ply_Prep_Technical_Paper.pdf (accessed 2009).
402. Hart-Smith, L.J., Redmond, G., and Davis, M.J.'The Curse of the Nylon Peel Ply', *41st International SAMPE Symposium,* Mar 24, 1996-Mar 26, 1996, Anaheim, CA, USA, pp. 303-317.
403. Henkel (2004), *Hysol EA 9895 Peel Ply,* available at: http://www.hysolpeelply.com/assets/downloads/HysolPeelPlyTDS.pdf (accessed 2009).
404. Hart-Smith, L.J. and Strindberg, G. 'Developments in Adhesively Bonding the Wings of the SAAB 340 and 2000 Aircraft', *Proceedings of the Institution of Mechanical Engineers, Part G: Journal of Aerospace Engineering ,* Vol. 211, No. 3, pp. 133-156.
405. Komorowski, J.P., Gould, R.W. and Simpson, D.L. (1998), 'Synergy between Advanced Composites and New NDI Methods', *Advanced Performance Materials,* Vol. 5, No. 1-2, pp. 137-151.
406. Sanchez-Saez, S., Barbero, E., Zaera, R. and Navarro, C. (2005), 'Compression after Impact of Thin Composites Laminates', *Composites Science and Technology,* Vol. 65, No. 13, pp. 1911-1919.
407. Koundouros, M., Falzon, B.G., Soutis, C. and Lord, S.J. (2004), 'Predicting the Ultimate Load of a CFRP Wingbox', *Composites: Part A,* Vol. 35, No. 7-8, pp. 895-903.
408. Baker A, Jones R and Callinan R J (1985), 'Damage Tolerance of Graphite/Epoxy Composites', *Composite Structures,* Vol. 4, No. 1, pp. 15-44.
409. Clarke, A., Creemers, R.J.C., Riccio, A., and Williamson, C. (2005), *Structural Analysis and Optimisation of an All-Composite Damage Tolerant Wingbox*, Report no. TP-2005-478, NLR, Amsterdam, Netherlands.
410. Pagano, N.J. and Schöppner, G.A. (2001), 'Delamination of Polymer Matrix Composites: Problems and Assessment', in Talreja, R., Manson, J.A.E., Kelly, A., and Zweben, C. *Polymer Matrix Composites*, Pergamon, Oxford, UK, pp. 433-528.
411. Naik, N.K., Shrirao, P. and Reddy, B.C.K. (2006), 'Ballistic Impact Behaviour of Woven Fabric Composites: Formulation', *International Journal of Impact Engineering,* Vol. 32, No. 9, pp. 1521-1552.
412. Greenhalgh, E., Bishop, S.M., Bray, D., Hughes, D., Lahiff, S. and Millson, B. (1996),

'Characterisation of Impact Damage in Skin-Stringer Composite Structures', *Composite Structures,* Vol. 36, No. 3-4, pp. 187-207.
413. Wiggenraad, J.F.M., Vercammen, R.W.A., Arendsen, P., and Ubels, L.C. (2000), *Design Optimization of Stiffened Composite Panels for Damage Resistance*, Report no. TP-2000-023, NLR, Amsterdam, Netherlands.
414. Davies, G.A.O. and Zhang, X. (1994), 'Impact Damage Prediction in Carbon Composite Structures', *International Journal of Impact Engineering,* Vol. 16, No. 1, pp. 149-170.
415. Aymerich, F., Pani, C. and Priolo, P. (2007), 'Effect of Stitching on the Low-Velocity Impact Response of [0^3/90^3]s Graphite/Epoxy Laminates', *Composites: Part A,* Vol. 38, No. 4, pp. 1174-1182.
416. Ambur, D.R., Jaunky, N., Hilburger, M. and Davila, C.G. (2004), 'Progressive Failure Analyses of Compression-Loaded Composite Curved Panels with and without Cutouts', *Composite Structures,* Vol. 65, No. 2, pp. 143-155.
417. Park, R. and Jang, J. (2000), 'Effect of Stacking Sequence on the Compressive Performance of Impacted Aramid Fiber/Glass Fiber Hybrid Composite', *Polymer Composites,* Vol. 21, No. 2, pp. 231-237.
418. Davies, G.A.O. and Olsson, R. (2004), 'Impact on Composite Structures', *The Aeronautical Journal,* Vol. 108, No. 1089, pp. 541-563.
419. Stavropoulos, C.D. and Papanicolaou, G.C. (1997), 'Effect of Thickness on the Compressive Performance of Ballistically Impacted Carbon Fibre Reinforced Plastic (CFRP) Laminates', *Journal of Materials Science,* Vol. 32, No. 4, pp. 931-936.
420. Symons, D.D. and Davis, G. (2000), 'Fatigue Testing of Impact-Damaged T300/914 Carbon-Fibre-Reinforced Plastic', *Composites Science and Technology,* Vol. 60, No. 3, pp. 379-389.
421. Wiggenraad, J.F.M., Greenhalgh, E.S., and Olsson, R. (2002), *Design and Analysis of Stiffened Composite Panels for Damage Resistance and Tolerance*, Report no. TP-2002-193, NLR, Amsterdam, Netherlands.
422. Komorowski, J.P., Gould, R.W., and Marincak, A.'Study of the Effect of Time and Load on Impact Damage Visibility', in Wallace, W., Gauvin, R., and Hoa, S.V. *Proceedings of the Second Canadian International Composites Conference and Exhibition (CANCOM),* 1993, Ottawa, Ontario, Canada, pp. 441-446.
423. Thomas, M. 'Study of the Evolution of the Dent Depth due to an Impact on Carbon/Epoxy Laminates - Consequences of Impact Damage Visibility and on In Service Inspection Requirements for Civil Aircraft Composite Structures', *Presented at MIL-HDBK 17 ,* Mar, 1994, Monterey, CA, USA.
424. European Aviation Safety Agency (2003), *Certification Specifications for Large Aeroplanes*, Report no. CS-25, EASA, Europe.
425. Raju, I.S. and Glaessgen, E.H. 'Effect of Stitching on Debonding in Composite Structural Elements', *International Conference on Computational Engineering and Science,* Aug, 2001, Puerto Vallata, Mexico.
426. Choi, H.T. and Chang, F.K. (1992), 'A Model for Predicting Damage in Graphite/Epoxy Laminated Composites Resulting from Low-Velocity Point Impact', *Journal of Composite Materials,* Vol. 26, No. 14, pp. 2134-2169.
427. Tai, N.H., Ma, C.C.M., Lin, J.M. and Wu, G.Y. (1999), 'Effects of Thickness on the Fatigue-Behavior of Quasi-Isotropic Carbon/Epoxy Composites before and after Low Energy Impacts', *Composites Science and Technology,* Vol. 59, No. 11, pp. 1753-1762.
428. Shiau, L.-C. and Chue, Y.-H. (1991), 'Free-Edge Stress Reduction through Fiber Volume Fraction Variation', *Composite Structures,* Vol. 19, No. 2, pp. 145-165.
429. Schellekens, J.C.J. and De Borst, R. (1994), 'Free Edge Delamination in Carbon-

Epoxy Laminates: A Novel Numerical/Experimental Approach', *Composite Structures,* Vol. 28, No. 4, pp. 357-373.
430. Byrd, L.W. and Birman, V. (2006), 'Effectiveness of Z-Pins in Preventing Delamination of Co-Cured Composite Joints on the Example of a Double Cantilever Test', *Composites: Part B,* Vol. 37, No. 4-5, pp. 365-378.
431. Yap, J.W.H., Scott, M.L., Thomson, R.S. and Hachenberg, D. (2002), 'The Analysis of Skin-to-Stiffener Debonding in Composite Aerospace Structures', *Composite Structures,* Vol. 57, No. 1-4, pp. 425-435.
432. van Rijn, J.C.F.N. (2000), *Design Guidelines for the Prevention of Skin-Stiffener Debonding in Composite Aircraft Panels*, Report no. TP-2000-355, NLR, Amsterdam, Netherlands.
433. van Rijn, J.C.F.N. and Wiggenraad, J.F.M. (2000), *A Seven-Point Bending Test to Determine the Strength of the Skin-Stiffener Interface in Composite Aircraft Panels*, Report no. TP-2000-044, NLR, Amsterdam, Netherlands.
434. Meeks, C., Greenhalgh, E. and Falzon, B.G. (2005), 'Stiffener Debonding Mechanisms in Post-Buckled CFRP Aerospace Panels', *Composites: Part A,* Vol. 36, No. 7, pp. 934-946.
435. Greenhalgh, E., Singh, S., Hughes, D. and Roberts, D. (1999), 'Impact Damage Resistance and Tolerance of Stringer-Stiffened Composite Structures', *Plastics, Rubber and Composites,* Vol. 28, No. 5, pp. 228-251.
436. Sawicki, A.J. (2001), 'Testing and Analysis Correlation', in Miracle, D.B. and Donaldson, S.L. *ASM Handbook: Composites v. 21*, ASM International, pp. 344-352.
437. Yokozeki, T., Aoki, Y. and Ogasawara, T. (2008), 'Experimental Characterization of Strength and Damage Resistance Properties of Thin-Ply Carbon Fiber/Toughened Epoxy Laminates', *Composite Structures,* Vol. 82, No. 3, pp. 382-389.
438. Rodini, B.T.Jr. and Eisenmann, J.R.'An Analytical and Experimental Investigation of Edge Delamination in Composite Laminates', *4th Conference Fibrous Composites USA,* Nov, 1978, San Diego, CA, pp. 441-457.
439. Tsai, S.W. and Patterson, J.M., 'Design Rules and Techniques for Composite Materials', in Middleton, D.H. (1990), *Composite Materials in Aircraft Structures*, Longman Scientific and Technical, London, UK, pp. 118-155.
440. Hawyes, V.J., Curtis, P.T. and Soutis, C. (2001), 'Effect of Impact Damage on the Compressive Response of Composite Laminates', *Composites Part A,* Vol. 32, No. 9, pp. 1263-1270.
441. Ruiz, C. and Xia, Y.R. (1991), 'The Significance of Interfaces in Impact Response of Laminated Composites', *14th Annual Energy-Sources Technology Conference and Exhibition,* Vol. Composite Material Technology - 1991, Jan 20, 1991-Jan 23, 1991, Houston, TX, USA., pp. 161-166.
442. Suh, S.S., Han, N.L., Yang, J.M. and Hahn, H.T. (2003), 'Compression Behavior of Stitched Stiffened Panel with a Clearly Visible Stiffener Impact Damage', *Composite Structures,* Vol. 62, No. 2, pp. 213-221.
443. Zhang, X., Hounslow, L. and Grassi, M. (2006), 'Improvement of Low-Velocity Impact and Compression-After-Impact Performance by Z-Fibre Pinning', *Composites Science and Technology,* Vol. 66, No. 15, pp. 2785-2794.
444. Rugg, K.L., Cox, B.N. and Massabo, R. (2002), 'Mixed Mode Delamination of Polymer Composite Laminates Reinforced through the Thickness by Z-Fibers', *Composites: Part A,* Vol. 33, No. 2, pp. 177-190.
445. Greenhalgh, E., Lewis, A., Bowen, R. and Grassi, M. (2006), 'Evaluation of Toughening Concepts at Structural Features in CFRP - Part I: Stringer Pull-Off', *Composites Part A,* Vol. 37, No. 10, pp. 1521-1535.
446. Yang, Q.D., Rugg, K.L., Cox, B.N. and Shaw, M.C. (2003), 'Failure in the Junction

Region of T-Stiffeners 3D-Braided vs. 2D Tape Laminate Stiffeners', *International Journal of Solids and Structures,* Vol. 40, No. 7, pp. 1653-1668.
447. Cartie, D.D.R., Dell'Anno, G., Poulin, E. and Partridge, I.K. (2006), '3D Reinforcement of Stiffener-to-Skin T-Joints by Z-Pinning and Tufting', *Engineering Fracture Mechanics,* Vol. 73, No. 16, pp. 2532-2540.
448. Vijayaraju, K., Mangalgiri, P.D. and Dattaguru, B. (2004), 'Experimental Study of Failure and Failure Progression in T-Stiffened Skins', *Composite Structures,* Vol. 64, No. 2, pp. 227-234.
449. Hayes, B.S. and Seferis, J.C. (2002), 'Preformed Particle Toughening of Epoxy-Based Adhesive Systems: The Effect of Particle Size and Chemistry', *Polymer Composites,* Vol. 23, No. 3, pp. 418-424.
450. Madan, R.C. , Walker, K.A., Hanson, B.A., and Murphy, M.F. 'Impact Damage Analysis for Composite Multistringer Bonded Panels', *Advanced Composites III: Expanding the Technology,* Sep 15, 1987-Sep 17, 1987, Detroit, Michigan, USA.
451. Greenhalgh, E., Meeks, C., Clarke, A. and Thatcher, J. (2003), 'The Effect of Defects on the Performance of Post-Buckled CFRP Stringer-Stiffened Panels', *Composites: Part A,* Vol. 34, No. 7, pp. 623-633.
452. Kradinov, V., Hanauska, J., Barut, A., Madenci, E. and Ambur, D.R. (2002), 'Bolted Patch Repair of Composite Panels with a Cutout', *Composite Structures,* Vol. 56, No. 4, pp. 423-444.
453. Sandow, F. 'A Computer Aided Aircraft Structural Composite Repair System', *32nd International SAMPE Symposium and Exhibitions,* Apr 6, 1987-Apr 9, 1987, Anaheim, CA, USA, pp. 551-557.
454. Tan, S.C. (1991), 'Mechanical Response and the Design of Notched Composite Laminates Filled with a Reinforcement', *Journal of Reinforced Plastics and Composites,* Vol. 10, No. 6, pp. 557-584.
455. Mckenzie, I., Jones, R., Marshall, I.H. and Galea, S. (2000), 'Optical Fibre Sensors for Health Monitoring of Bonded Repair Systems', *Composite Structures,* Vol. 50, No. 4, pp. 405-416.
456. Petersen, D., Rolfes, R. and Zimmermann, R. (2001), 'Thermo-Mechanical Design Aspects for Primary Composite Structures of Large Transport Aircraft', *Aerospace Science Technology,* Vol. 5, No. 2, pp. 135-146.
457. Gardiner, G. *Lightning Strike Protection for Composite Structures,* available at: http://compositesworld.com/hpc/issues/2006/july/1366 (accessed 2008).
458. Crain, B.R. *Lightning Protection of Aircraft Antennas and Radomes,* available at: www.ieeemelbourne.org/Nov8Slides.ppt (accessed 2008).
459. Pridham, B., Jäger, D. and Schreiner, M. (2001), 'BAE Systems and EADS Explore Lightning Strike Protection', *Aerospace Engineering,* available at: http http://www.sae.org/aeromag/features/ace/2001/highlights/page4.htm (accessed 2008).
460. Feraboli, P. and Miller, M. (2009), 'Damage Resistance and Tolerance of Carbon/Epoxy Composite Coupons subjected to Simulated Lightning Strike', *Composite Part A,* Vol. To be Published.
461. World Intellectual Property Organization *(WO/2008/056123) Improved Composite Materials,* available at: http://www.wipo.int/pctdb/en/wo.jsp?WO=2008056123&IA=WO2008056123&DISPLAY=DESC (accessed 2008).
462. Stork Fokker (2007), *Trends in Aerospace Engineering,* available at: http://www.tudelft.nl/live/ServeBinary?id=7801ecbe-cdb8-46bf-ae2a-2a14955855c9&binary=/doc/Trends%20in%20Aerospace%20Engineering.ppt (accessed 2009).
463. Airbus (2008), *A400M Countdown,* available at: http://www.a400m-countdown.com/index.php?page=galerie&v=9&galerie=02_Wing# (accessed 2009).
464. Liu, W., Butler, R. and Kim, H.A. (2008), 'Optimization of Composite Stiffened

Panels Subject to Compression and Lateral Pressure using a Bi-Level Approach', *Structural and Multidisciplinary Optimization,* Vol. 36, No. 3, pp. 235-245.
465. Romeo, G. and Frulla, G. (1996), 'Post-Buckling Behavior of Graphite/Epoxy Wing Boxes Panels under Pure Tension', *20th Congress of the International Council of the Aeronautical Sciences,* Vol. 1, Sep, 1996, Sorrento, Italy., pp. 1156-1166.
466. Negaard, G. (1980), *The History of the Aircraft Structural Integrity Program*, Report no. 680.1B, ASIAC, Wright Patterson AFB, UH, USA.
467. Kropp, Y. 'Development of a Stitched/RFI Composite Transport Wing', *NASA Langley Research Center Mechanics of Textile Composites Conference,* 1995, Hampton, VA, USA, pp. 457-479.
468. Niu, M.C.Y. (1988), *Airframe Structural Design* (2nd edition), Conmilit Press Ltd., North Point, Hong Kong.
469. Liu, W. and Butler, R. 'Optimum Buckling Design of Composite Wing Cover Panels with Manufacturing Constraints', *48th AIAA/ASME/ASCE/AHS/ASC Structures, Structural Dynamics, and Materials Conference,* Apr 23, 2007-Apr 26, 2007, Honolulu, Hawaii, USA, pp. 6072-6082.
470. van Tooren, M.J.L., Schut, E.J., and Berends, J.P.T.J. 'Design "Feasilisation" using Knowledge Based Engineering and Optimization Techniques', *44th AIAA Aerospace Sciences Meeting and Exhibit,* 2006, Reno, NA, USA., pp. 8851-8868.
471. Schafer, B. *CUFSM Advanced Ideas and Examples,* available at: http://www.ce.jhu .edu/bschafer/cufsm/finite_strip_old/cufsm_v2p5_distribute/manual_and_tutorials/cuf sm%20advanced%20ideas.ppt (accessed 2007).
472. Chen, V.L. and Wu, H.-Y.T. (1993), 'A Parametric Study of Residual Strength and Stiffness for Impact Damaged Composites', *Composite Structures,* Vol. 25, No. 1-4, pp. 267-275.
473. Wiggenraad, J.F.M., Arendsen, P., and da Silva Pereira, J.M. (1998), *Design Optimization of Stiffened Composite Panels with Buckling and Damage Tolerance Constraints*, Report no. TP-98024, NLR, Amsterdam, Netherlands.
474. van der Sloot, J.H. (2003), *Elastic Buckling of Long, Flat, Symmetrically-Laminated Composite Stiffened Panels and Struts in Compression*, Report no. IHS ESDU 03001, Engineering Sciences Data Unit, UK.
475. Davies, G.A.O. and Zhang, X. (2000), 'Predicting Impact Damage of Composite Stiffened Panels', *The Aeronautical Journal,* Vol. 104, No. 1032, pp. 97-103.
476. Ubels, L.C. and Wiggenraad, J.F.M. (1997), 'A Method to Apply Structure Relevant Impact Damage to Small Structure Relevant Specimens for Damage Tolerance Studies', *Applied Composite Materials,* Vol. 4, No. 2, pp. 83-94.
477. Miller, A.G., Lovell, D.T. and Seferis, J.C. (1994), 'The Evolution of an Aerospace Material: Influence of Design, Manufacturing and In-Service Performance', *Composite Structures,* Vol. 27, No. 1-2, pp. 193-206.
478. Madan R. C. and Sutton, J.S. 'Design, Testing, and Damage Tolerance Study of Bonded Stiffened Composite Wing Cover Panels', *29th AIAA/ASME/ASCE/AHS/ASC Structures, Structural Dynamic and Materials Conference,* Vol. 88-2291, 1988, Williamsburg, VA, USA, pp. 623-630.
479. Thuis, H.G.S.J. and Wiggenraad, J.F.M. (1992), *Investigation of the Bond Strength of a Discrete Skin-Stiffener Interface*, Report no. TP 92183 L, NLR, Amsterdam, Netherlands.
480. Zhou, G. and Hood, J. (2006), 'Design, Manufacture and Evaluation of Laminated Carbon/Epoxy I-Beams in Bending', *Composites: Part A,* Vol. 37, No. 3, pp. 506-517.
481. Stein, M. and Williams, J.G. (1978), *Buckling and Structural Efficiency of Sandwich-Blade Stiffened Composite Compression Panels*, Report no. TP 1269, NASA, Hampton, VA, USA.

482. Williams, J.G. and Mikulas, M.M.Jr. (1976), *Analytical and Experimental Study of Structurally Efficient Composite Hat-Stiffened Panels Loaded in Axial Compression*, Report no. TM X-72813, NASA, Hampton, VA, USA.
483. Agarwal, B. and Davis, R.C. (1974), *Minimum-Weight Designs for Hat-Stiffened Composite Panels under Uniaxial Compression*, Report no. TN D-7779, NASA, Hampton, VA, USA.
484. Kassapoglou, C. (1997), 'Simultaneous Cost and Weight Minimization of Composite-Stiffened Panels under Compression and Shear', *Composites Part A,* Vol. 28, No. 5, pp. 419-435.
485. Stroud, W.J. and Agranoff, N. (1976), *Minimum-Mass Design of Filamentary Composite Panels under Combined Loads: Design Procedure based on Simplified Buckling Equations*, Report no. TN D-8257, NASA, Hampton, VA, USA.
486. Mittelstedt, C. and Beerhorst, M. (2008), 'Closed-Form Buckling Analysis of Compressively Loaded Composite Plates Braced by Omega-Stringers', *Composite Structures,* Vol. 88, No. 3, pp. 424-435.
487. Baker, D.J. and Rousseau, C.Q. (1996), *Design and Evaluation of a Bolted Joint for a Discrete Carbon-Epoxy Rod-Reinforced Hat Section*, Report no. TM 110277, NASA, Hampton, VA, USA.
488. Bruhn, E.F. (1973), *Analysis and Design of Flight Vehicle Structures*, Jacobs Publishing, Inc., Carmel, IN, USA.
489. Grayley, M.E. (1981), *Buckling of Flat Rectangular Plates*, Report no. ESDU 81047, Engineering Science Data Unit, UK.
490. Weaver, P.M. 'On Optimisation of Long Anisotropic Flat Plates subject to Shear Buckling Loads', *45th AIAA/ASME/ASCE/AHS/ASC Structures, Structural Dynamics, and Materials Conference,* Apr 19, 2004-Apr 22, 2004, Palm Springs, CA, USA, AIAA, pp. 5638-5648.
491. Qi, B., Ness, R. and Tong, L. (2002), 'A Stitched Blade-Stiffened RFI Composite Panel Under Shear Loading', *Journal of Reinforced Plastics and Composites,* Vol. 21, No. 3, pp. 255-276.
492. Kassapoglou, C. and DiNicola, A.J. (1992), 'Efficient Stress Solutions at Skin Stiffener Interfaces of Composite Stiffened Panels', *AIAA Journal,* Vol. 30, No. 7, pp. 1833-1839.
493. Falzon, B.G. and Davies, G.A.O. (2003), 'The Behavior of Compressively Loaded Stiffener Runout Specimens - Part I: Experiments', *Journal of Composite Materials,* Vol. 37, No. 5, pp. 381-400.
494. Stevens, K.A., Ricci, R. and Davies, G.A.O. (1995), 'Buckling and Postbuckling of Composite Structures', *Composites,* Vol. 26, No. 3, pp. 189-199.
495. Jegley, D.C.'Behavior of Compression-Loaded Composite Panels with Stringer Termination and Impact Damage', *AIAA/ASME/ASCE/AHS 39th Structures, Structural Dynamics, and Materials Conference,* Apr 20, 1998-Apr 23, 1998, Long Beach, CA, USA, pp. 733-743.
496. Jegley, D.C. (1999), 'Parametric Study of the Behavior of Graphite/Epoxy Panels with Stiffener Terminations', *Journal of Aircraft,* Vol. 36, No. 6, pp. 1048-1055.
497. Gillespie, L.-R.K. (1988), *Troubleshooting Manufacturing Processes*, Society of Manufacturing Engineers, Dearborn, MI, USA.
498. Paleen, M.J. and Kilwin, J.J. (2001), 'Hole Drilling in Polymer-Matrix Composites', in Miracle, D.B. and Donaldson, S.L. *ASM Handbook: Composites v. 21*, ASM International, pp. 646-650.
499. Paterson, J.H., MacWilkenson, D., and Blackerby, W. (1973), *A Survey of Drag Prediction Techniques Applicable to Subsonic and Transonic Aircraft Design*, Report no. CP-124 Paper 1, AGARD, Paris, France.

500. Anderson, D. (2006), *Fuel Conservation - Airframe Maintenance for Environmental Performance,* available at: http://www.icao.int/env/WorkshopFuelEmissions/Presentations/Anderson.pdf (accessed 2009).
501. Kundu, A.K., Watterson, J., Raghunathan, S. and MacFadden, R. (2002), 'Parametric Optimization of Manufacturing Tolerances at the Aircraft Surface', *Journal of Aircraft,* Vol. 39, No. 2, pp. 271-279.
502. Bootle, J., Burzesi, F. and Fiorini, L. (2001), 'Design Guidelines', in Miracle, D.B. and Donaldson, S.L. *ASM Handbook: Composites v. 21*, ASM International, pp. 388-395.
503. Lanzi, L. (2004), 'A Numerical and Experimental Investigation on Composite Stiffened Panels into Post-Buckling', *Thin-Walled Structures,* Vol. 42, No. 12, pp. 1645-1664.
504. Kong, C.W., Hong, C.S. and Kim, C.G. (2000), 'Postbuckling Strength of Stiffened Composite Plates with Impact Damage', *AIAA Journal,* Vol. 38, No. 10, pp. 1956-1964.
505. Yeh, H.-Y., Lee, J.J., Yang, D.Y.T. and Yeh, H.-L. (2004), 'Study of Stitched and Unstitched Composite Panels Under Shear Loadings', *Journal of Aircraft,* Vol. 41, No. 2, pp. 386-392.
506. Bisagni, C. and Lunzi, L. (2002), 'Post-Buckling Optimization of Composite Stiffened Panels Using Neural Networks', *Composite Structures,* Vol. 58, No. 2, pp. 237-247.
507. Shirk, M.H., Herty, T.J. and Weisshaar, T.A. (1986), 'Aeroelastic Tailoring - Theory, Practice, and Promise', *Journal of Aircraft,* Vol. 23, No. 1, pp. 6-18.
508. Wijayratne, D.D. (2004), *Validation of Design and Analysis Techniques of Tailored Composite Structures*, Report no. CR 212650, NASA, Hampton, VA, USA.
509. Lagace, P.A., Jensen, D.W. and Finch, D.C. (1986), 'Buckling of Unsymmetric Composite Laminates', *Composite Structures,* Vol. 5, No. 2, pp. 101-123.
510. Zink, P.S., Mavris, D.N., Love, M.H., and Karpel, M.'Robust Design for Aeroelastically Tailored / Active Aeroelastic Wing', *7th AIAA/NASA/USAF/ISSMO Symposium on Multidisciplinary Analysis ,* Vol. AIAA-98-4781, Sep 2, 1998-Sep 4, 1998, St. Louis, MO, USA.
511. Vanderplaats, G.N. (1999), 'Structural Design Optimization Status and Direction', *Journal of Aircraft,* Vol. 36, No. 1, pp. 11-19.
512. Wood, R.M. and Bauer, S.X.S. (2002), 'Discussion of Knowledge-Based Design', *Journal of Aircraft,* Vol. 39, No. 6, pp. 1053-1060.
513. Krinis, K. (1997), *Structural Optimization of a Civil Transport Wing* Cranfield University, Bedfordshire, UK.
514. Nonaka, I. and Takeuchi, H. (1995), *The Knowledge Creating Company*, Oxford University Press, Oxford.
515. Mawhinney, P., Price, M., Curran, R., Benard, E., Murphy, A., and Raghunathan, S.'Geometry-Based Approach to Analysis Integration for Aircraft Conceptual Design', *AIAA 5th Aviation, Technology, Integration, and Operations Conference,* Sep 26, 2005-Sep 28, 2005, Arlington, VA, USA, pp. 1699-1707.
516. Egbu, C., Botterill, K., and Bates, M.'The Influence of Knowledge Management and Intellectual Capital on Organizational Innovations', *17th Annual ARCOM Conference ,* Vol. 2, 2001, University of Salford, Salford, UK, pp. 555-574.
517. Love, P.D., Edum-Fotwe, F. and Irani, Z. (2003), 'Management of Knowledge in Project Environments', *International Journal of Project Management,* Vol. 21, No. 3, pp. 155-156.
518. Hajela, P. (2002), 'Soft Computing in Multidisciplinary Aerospace Design - New Directions for Research', *Progress in Aerospace Sciences,* Vol. 38, pp. 1-21.
519. Sobieszczanski-Sobieski, J.'Multidisciplinary Design Optimization: An Emerging New Engineering Discipline', *World Congress on Optimal Design of Structural*

Systems, Aug 2, 1993-Aug 6, 1993, Rio de Janeiro, Brazil.
520. Abbott, E.A. and Scott, M.L. (2002), 'The Case for Multidisciplinary Design Approaches for Smart Fibre Composite Structures', *Composite Structures,* Vol. 58, No. 3, pp. 349-362.
521. Bao, H.P.'In-Depth Survey of Cost/Time Estimating Models', *Multidisciplinary Optimization Branch,* Jul, 2000, NASA Langley Research Center, Hampton, VA, USA.
522. Westphal, R. and Scholz, D. (1997), 'A Method for Predicting Direct Operating Costs During Aircraft System Design', *Cost Engineering,* Vol. 39, No. 6, pp. 35-39.
523. Apostolopoulos, P. and Kassapoglou, C. (2002), 'Recurring Cost Minimization of Composite Laminated Structures - Optimum Part Size as a Function of Learning Curve Effects and Assembly', *Journal of Composite Materials,* Vol. 36, No. 4, pp. 501-518.
524. Korte, J.J., Weston, R.P., and Zang, T.A.'Multidisciplinary Optimization Methods For Preliminary Design', *AGARD CP600 "Future Aerospace Technology in the Service of the Alliance",* Vol. 3, Dec, 1997, Paris, France, pp. C40:1-10.
525. Gunawan, S. and Azarm, S.'On a Combined Multi-Objective and Feasibility Robustness Method for Design Optimization', *AIAA 2004-4357,* pp. 683-692.
526. Gonzalez, L.F., Whitney, E.J., Srinivas, K., and Periaux, J.'Multidisciplinary Aircraft Design and Optimisation Using a Robust Evolutionary Technique with Variable Fidelity Models', *10th AIAA/ISSMO Multidisciplinary Analysis and Optimization Conference,* Aug 30, 2004-Sep 1, 2004, Albany, NY, USA, pp. 3610-3624.
527. Hajela, P. (1999), 'Nongradient Methods in Multidisciplinary Design Optimization - Status and Potential', *Journal of Aircraft,* Vol. 36, No. 1, pp. 255-265.
528. Le Riche, R. and Haftka, R.T. (1993), 'Optimization of Laminate Stacking Sequence for Buckling Load Maximization by Genetic Algorithm', *AIAA Journal,* Vol. 31, No. 5, pp. 951-956.
529. Todoroki, A. and Haftka, R.T.'Lamination Parameters for Efficient Genetic Optimization of the Stacking Sequences of Composite Panel', *Proceedings of the 7th AIAA/USAF/NASA/ISSMO Multidisciplinary Analysis and Optimization Symposium,* Aug 31, 1998-Sep 2, 1998, St. Louis, MO, USA, AIAA, Reston, VA, USA, pp. 870-879.
530. Niu, M.C.Y. (1998), *Airframe Stress Analysis & Sizing*, Conmilit Press Limited, North Point, Hong Kong.
531. Emero, D.H. and Spunt, L.'Optimization of Multirib and Multiweb Wing Box Structures under Shear and Moment Loads', *AIAA 6th Structures and Materials Conference,* 1965, New York, USA, pp. 330-353.
532. Emero, D.H. and Spunt, L. (1966), 'Wing Box Optimization under Combined Shear and Bending', *Journal of Aircraft,* Vol. 3, No. 2, pp. 130-141.
533. van der Sloot, J.H. (2003), *Elastic Buckling of Flat Isotropic Stiffened Panels and Struts in Compression*, Report no. ESDU 98106, Engineering Sciences Data Unit, UK.
534. Grayley, M.E. (1983), *Stiffness of Loaded Flat Strips under Sinusoidally Distributed Bending Couples at Their Edges*, Report no. ESDU 73007, Engineering Sciences Data Unit, UK.
535. Nemeth, M.P. (1986), 'Importance of Anisotropy on Buckling of Compression-Loaded Symmetric Composite Plates ', *AIAA Journal,* Vol. 24, No. 11, pp. 1831-1835.
536. Weaver, P.M. (2006), 'Approximate Analysis for Buckling of Compression Loaded Long Rectangular Plates with Flexural/Twist Anisotropy', *Proceedings of the Royal Society A,* Vol. 462, No. 2065, pp. 59-73.
537. Venkataraman, S., Lamberti, L., Haftka, R.T. and Johnson, T.F. (2003), 'Challenges in Comparing Numerical Solutions for Optimum Weights of Stiffened Shells', *Journal of*

Spacecraft and Rockets, Vol. 40, No. 2, pp. 183-192.
538. Stroud, W.J. and Anderson, M.S. (1981), *PASCO-Structural Panel Analysis and Sizing Code, Capability and Analytical Foundations*, Report no. TM 80181, NASA, Hampton, VA, USA.
539. Anderson, M.S. and Stroud, W.J. (1979), 'General Panel Sizing Computer Code and its Application to Composite Structural Panels', *AIAA Journal,* Vol. 17, No. 8, pp. 892-897.
540. Vanderplaats, G.N. (1973), *CONMIN - a FORTRAN Program for Constrained Function Minimization*, Report no. TM X-62282, NASA, Ames, CA, USA.
541. Stroud, W.J., Greene, W.H., and Anderson, M.S. (1984), *Buckling Loads of Stiffened Panels Subjected to Combined Longitudinal Compression and Shear: Results Obtained With PASCO, EALS, and STAGS Computer*, Report no. TP 2215, NASA, Hampton, VA, USA.
542. Anderson, M.S. and Williams, F.W. (1983), 'Buckling and Vibration of any Prismatic Assembly of Shear and Compression Loaded Anisotropic Plates with an Arbitrary Supporting Structure', *International Journal of Mechanical Science,* Vol. 25, No. 8, pp. 585-596.
543. Williams, F.W., Kennedy, D., Butler, R. and Anderson, M.S. (1991), 'Viconopt: Program for Exact Vibration and Buckling Analysis of Design of Prismatic Plate Assemblies', *AIAA Journal,* Vol. 29, No. 11, pp. 1927-1928.
544. Dawe, D.J. and Peshkam, V. (1989), 'Buckling and Vibration of Finite-Length Composite Prismatic Plate Structures with Diaphragm Ends, Part I: Finite Strip Formulation', *Computer Methods in Applied Mechanics and Engineering,* Vol. 77, No. 1-2, pp. 1-30.
545. Liu, W., Mileham, A.R. and Green, A.J. (2006), 'Bilevel Optimization and Postbuckling of Highly Strained Composite Stiffened Panels', *AIAA Journal,* Vol. 44, No. 11, pp. 2562-2570.
546. Bushnell, D. (1987), 'PANDA2-Program for Minimum Weight Design of Stiffened, Composite, Locally Buckled Panels ', *Computers and Structures,* Vol. 25, No. 4, pp. 469-605.
547. Bushnell, D. and Bushnell, W.D. (1995), 'Optimum Design of Composite Stiffened Panels under Combined Loading', *Computers & Structures,* Vol. 55, No. 5, pp. 819-856.
548. Timoshenko, S.P. and Gere, J.M. (1961), *Theory of Elastic Stability*, McGraw-Hill Book Company Inc., Tokyo, Japan.
549. Williams, J.G. and Stein, M. (1976), 'Buckling Behavior and Structural Efficiency of Open-Section Stiffened Composites Compression Panels', *AIAA Journal,* Vol. 14, No. 11, pp. 1618-1626.
550. Liu, B., Haftka, R.T. and Akguen, M.A. (2000), 'Two-Level Composite Wing Structural Optimization Using Response Surfaces', *Structural and Multidisciplinary Optimization,* Vol. 20, No. 2, pp. 87-96.
551. Herencia, J.E., Weaver, P.M., and Friswell, M.I.'Local Optimisation of Long Anisotropic Laminated Fibre Composite Panels with T Shape Stiffeners', *47th AIAA/ASME/ASCE/AHS/ASC Structures, Structural Dynamics, and Materials Conference,* Vol. AIAA 2006-2171, May 1, 2006-May 4, 2006, Newport, Rhode Island, USA.
552. Kröber, I. *Beulkritischer Schubfluß/Druckspannung randverstärkter Plattenstreifen aus isotropem Werkstoff*, Report no. HSB 45130-01/02, HSB, Germany.
553. Butler, R. (1995), 'Optimum Design of Composite Stiffened Wing Panels - A Parametric Study', *Aeronautical Journal,* Vol. 99, No. 985, pp. 169-177.
554. Nagendra, S., Jestin, D., Gürdal, Z., Haftka, R.T. and Watson, L.T. (1996), 'Improved

Genetic Algorithm for the Design of Stiffened Composite Panels ', *Computers and Science,* Vol. 58, No. 3, pp. 543-555.
555. Liu, B. and Haftka, R.T. (2004), 'Single Level Composite Wing Optimization based on Flexural Lamination Procedures', *Structural and Multidisciplinary Optimization,* Vol. 26, No. 1-2, pp. 111-120.
556. Edwards, D.A., Williams, F.W. and Kennedy, D. (1998), 'Cost Optimization of Stiffened Panels using VICONOPT', *AIAA Journal,* Vol. 36, No. 2, pp. 267-272.
557. Park, C.H., Lee, W.I., Han, W.S. and Vautrin, A. (2004), 'Simultaneous Optimization of Composite Structures considering Mechanical Performance and Manufacturing Cost', *Composite Structures,* Vol. 65, No. 1, pp. 117-127.
558. Henderson, J.L., Gürdal, Z. and Loos, A.C. (1999), 'Combined Structural and Manufacturing Optimization of Stiffened Composite Panels', *Journal of Aircraft,* Vol. 36, No. 1, pp. 246-254.
559. Kaufmann, M. (2008), *Cost/Weight Optimization of Aircraft Structures* KTH School of Engineering Sciences, Stockholm, Sweden.
560. Schmit, L.A. and Mehrinfar, M. (1982), 'Multilevel Optimum Design of Structures with Fiber-Composite Stiffened Panel Components', *AIAA Journal,* Vol. 20, No. 1, pp. 138-147.
561. Schmit, L.A. and Ramannathan, R.K. (1978), 'Multilevel Approach to Minimum Weight Design including Buckling Constraints', *AIAA Journal,* Vol. 16, No. 2, pp. 97-104.
562. Krakers, L.A., Van Tooren, M.J.L., Zaal, K. and Vermeeren, C.A.J.R. (2005), 'Integration of Acoustics and Mechanics in a Stiffened Shell Fuselage. Part III', *Applied Composite Materials,* Vol. 12, No. 1, pp. 21-35.
563. Cheung, Y.K. (1976), *Finite Strip Method in Structural Analysis*, Pergamon, Oxford, UK.
564. Loughlan, J. (1994), 'The Buckling Performance of Composite Stiffened Panel Structures Subjected to Combined In-Plane Compression and Shear Loading', *Composite Structures,* Vol. 29, No. 2, pp. 197-212.
565. Dawe, D.J. (2002), 'Use of the Finite Strip Method in Predicting the Behaviour of Composite Laminated Structures', *Composite Structures,* Vol. 57, No. 1-4, pp. 11-36.
566. Mohd, S. and Dawe, D.J. (1993), 'Finite Strip Method Analysis of Composite Prismatic Shell Structures with Diaphragm Ends', *Computers and Structures,* Vol. 49, No. 5, pp. 753-765.
567. Schafer, B.W. *Elastic Buckling Solution Methods for Cold-Formed Steel Elements and Members,* available at: http://www.ce.jhu.edu/bschafer/cufsm/finite_strip_old/cufsm_v2p5_distribute/manual_and_tutorials/background.pdf (accessed 2008).
568. Peshkam, V. and Dawe, D.J. (1989), 'Buckling and Vibration of Finite-Length Composite Prismatic Plate Structures with Diaphragm Ends, Part II: Computer Programs and Buckling Applications', *Computer Methods in Applied Mechanics and Engineering,* Vol. 77, No. 3, pp. 227-252.
569. Housner, J.M. and Stein, M. (1975), *Numerical Analysis and Parametric Studies of the Buckling of Composite Orthotropic Compression and Shear Panels*, Report no. TN D-7996, NASA, Springfield, VA, USA.
570. Adams, R.D. , Comyn, J., and Wake, W.C. (1997), *Structural Adhesive Joints in Engineering*, Chapman & Hall, London, UK.
571. Humphreys, K. and Wellman, P. (1996), *Basic Cost Engineering* (3rd edition), Marcel Dekker, NZ, USA.
572. Eaglesham, M.A. (1998), *A Decision Support System for Advanced Composite Manufacturing Cost Estimation* Virginia Polytechnic Institute and State University, Blacksburg, VA, USA.

573. Freiman, F. 'The Fast Cost Estimating Models', *Transactions of the 27th Annual Meeting of the American Association of Cost Engineers,* Jun 26, 1983-Jun 29, 1983, Philadelphia, PA, USA.
574. Dean, E.B.'Why Does it Cost How Much?', *Aircraft Design, Systems and Operations Meeting,* Vol. AIAA-93-3966, Aug 11, 1993-Aug 13, 1993, Monterey, CA, USA.
575. Kundu, A.K. , Raghunathan, S., and Curran, R. 'Cost Modelling as a Holistic Tool in the Multi-Disciplinary Systems Architecture of Aircraft Design - The Next Step 'Design for Customer'', *41st Aerospace Sciences Meeting and Exhibit,* Vol. AIAA 2003-1333, Jan 6, 2003-Jan 9, 2003, Reno, Nevada, USA.
576. Aalbrechtse, R.J. *Target Costing in Handbook of Cost Management* (1994 edition), Warren Gorham Lamont, Boston, MA, USA.
577. Hirt, R.J. 'Air Force Design-to-Cost Methodology Development', *21st national SAMPE Symposium and Exhibition,* Apr 6, 1976-Apr 8, 1976, Los Angles, CA, USA.
578. Raffish, N. and Turney, P.B.B. (1991), 'Glossary of Activity-Based Management', *Journal of Cost Management,* Vol. 5, No. 3, pp. 53-63.
579. Curran, R., Raghunathan, S., Rush, C., and Roy, R. 'Cost Estimating Practice in Aerospace: England and Northern Ireland', *CE2000 Conference on Concurrent Engineering: Research and Applications,* 2002, pp. 894-902.
580. Unal, R. and Dean, F.B. (1991), 'Design for Cost and Quality: The Robust Design Approach', *Journal of Parametrics,* Vol. 11, No. 1, pp. 73-93.
581. Wikipedia *Life Cycle Cost Analysis,* available at: http://en.wikipedia.org/wiki/Life_cycle_cost_analysis (accessed 2008).
582. Apgar, H. 'Design-to-life-Cycle-Cost in Aerospace', *AIAA/AHS/ASEE Aerospace Design Conference,* Vol. AIAA-93-1181, Feb, 1993, Irvine, CA, USA.
583. Castagne, S., Curran, R., Rothwell, A., and Murphy, A. 'Development of a Precise Manufacturing Cost Model for the Optimisation of Aircraft Structures', *AIAA 5th Aviation, Technology, Integration, and Operations Conference,* Vol. AIAA 2005-7438, Sep 26, 2005-Sep 28, 2005, Arlington, Virginia, USA.
584. Scanlan, J., Rao, A., Bru, C., Hale, P. and Marsh, R. (2006), 'DATUM Project: Cost Estimating Environment for Support of Aerospace Design Decision Making', *Journal of Aircraft,* Vol. 43, No. 4, pp. 1022-1028.
585. Fabrycky, W.J. and Blanchard, B.S. (1991), *Life-Cycle Cost and Economic Analysis*, Prentice Hall, Engelwoods Cliffs, New Jersey, USA.
586. Collopy, P.D. and Earnes, J.H. (2001), *Aerospace Manufacturing Cost Prediction from a Measure of Part Definition Information*, Report no. 2001-01-3004, Society of Automotive Engineers, Inc., USA.
587. Meyers Aircraft Company *DAPCA IV Model,* available at: http://www.meyersaircraft.com/DAPCA%20IV/DAPCA%20IV%20Intro%20Page.html (accessed 2008).
588. Roskam, J. (1985), *Airplane Design: Part V: Component Weight Estimisation*, Roskam Aviation and Engineering Corp, Ottawa, Kansas, US.
589. Hughes, R.T. (1996), 'Expert Judgement as an Estimating Method', *Information and Software Technology,* Vol. 38, No. 2, pp. 67-75.
590. Thompson, F. (1998), 'Cost Measurement and Analysis', in Meyers, R. *Handbook of Government Budgeting*, Jossey-Bass, San Francisco, CA, USA, pp. 381-411.
591. Yang, S.Y., Girivasan, V., Singh, N.R., Tansel, I.N. and Kropas-Hughes, C.V. (2003), 'Selection of Optimal Material and Operating Conditions in Composite Manufacturing. Part II: Complexity, Representation of Characteristics and Decision Making', *International Journal of Machine Tools & Manufacture,* Vol. 43, No. 2, pp. 175-184.
592. Curran, R., Castagne, S., Rothwell, A., Price, M., and Murphy, A. 'Integrating Manufacturing Cost and Structural Requirements in a Systems Engineering Approach to Aircraft Design', *46th AIAA/ASME/ASCE/AHS/ASC Structures, Structural*

Dynamics, and Materials Conference, Apr 18, 2005-Apr 21, 2005, Austin, Texas, USA, pp. 3283-3300.
593. Mabson, G.E., Ilcewicz, L.B., Graesser, D.L., Metschan, S.L., Proctor, M.R., Tervo, D.K., Tutle, M.E., and Zabinsky, Z.B. (1996), *Cost Optimization Software for Transport Aircraft Design Evaluation (COSTADE) - Overview*, Report no. CR 4736, NASA, Hampton, VA, USA.
594. LeBlanc, D.J. (1976), *Advanced Composite Cost Estimation Manual (ACCEM)*, Report no. AFFDL-TR-76-87, Northrop Corporation, LA, CA, USA.
595. Choi, J.W., Kelly, D. and Raju, J. (2007), 'A Knowledge Based Engineering Tool to Estimate Cost and Weight of Composite Aerospace Structures at the Conceptual Stage of the Design', *Aircraft Engineering and Aerospace Technology: An International Journal,* Vol. 79, No. 5, pp. 459-468.
596. Gutowski, T., Hoult, D., Dillon, G., Neoh, E.T., Muter, S., Kim, E. and Tse, M. (1994), 'Development of a Theoretical Cost Model for Advanced Composite Fabrication', *Composite Manufacturing,* Vol. 5, No. 4, pp. 231-239.
597. Hirsh, J., Hajela, P., Spering, J.C., Coen, G.A. and Mytych, E. (2001), 'MADEsmart: An Environment for Improved Development of Aircraft Components in Preliminary Design', *Engineering with Computers,* Vol. 17, No. 2, pp. 162-185.
598. Neoh, E.T. (1995), *Adaptive Framework for Estimating Fabrication Time* Massachusetts Institute of Technology, MA, USA.
599. Wright, T.P. (1936), 'Factors Affecting the Cost of Airplanes', *Journal of the Aeronautical Sciences,* Vol. 3, No. 2, pp. 122-128.
600. Kendall, K. , Mangin, C. and Ortiz, E. (1998), 'Discrete Event Simulation and Cost Analysis for Manufacturing Optimization of an Automotive LCM Component', *Composites Part A,* Vol. 29, No. 7, pp. 711-720.
601. Ashby, M.F. (2005), *Materials Selection in Mechanical Design*, Elsevier Butterworth-Heinemann, Oxford, UK.
602. Jones, R.I. (1995), *Analysis of the Fuel Penalties of Airframe Systems* Cranfield University, College of Aeronautics Publication.
603. Younossi, O., Kennedy, M., and Graser, J.C. (2001), *Airframe Cost Information*, RAND, Santa Monica, CA, USA.
604. Airport Business (2009), *Mitsubishi Aircraft will Increase Aluminum Demand,* available at: http://www.airportbusiness.com/online/article.jsp?siteSection=1&id=30882 (accessed 2009).
605. Ishikawa, T. (2006), 'Overview of Trends in Advanced Composite Research and Applications in Japan', *Advanced Composite Materials,* Vol. 15, No. 1, pp. 3-37.
606. Herencia, J.E., Weaver, P.M. and Friswell, M.I. (2007), 'Optimization of Long Anisotropic Laminated Fiber Composites Panels with T-Shaped Stiffeners', *AIAA Journal,* Vol. 45, No. 10, pp. 2497-2509.
607. Wang, F. (2008), *Composite Aeroelastic Lifting/Control Surface Structure* School of Engineering, Cranfield University, Bedford, UK.
608. Fuoss, E., Straznicky, P.V. and Poon, C. (1998), 'Effects of Stacking Sequence on the Impact Resistance in Composite Laminates. Part 2: Prediction Method', *Composite Structures,* Vol. 41, No. 2, pp. 177-196.
609. Marx, W.J., Mavris, D.N., and Schrage, D.P.'Knowledge-Based Manufacturing and Structural Design for a High Speed Civil Transport', *1st Industry/Academy Symposium in Research for Future Supersonic and Hypersonic Vehicles,* Dec, 1994, Greensboro, NC, USA.
610. Mayfield, D. (1987), 'Turning Flights of Fancy into Reality', *The Virginia Pilot and Ledger Star, Hampton Roads Business Weekly,* Vol. 2, No. 15, pp. 16-17.
611. Phillips, B.J. and Guo, S. 'Realistic Multidisciplinary Optimization of a Carbon Fibre

Reinforced Plastic Wing Cover', *49th AIAA/ASME/ASCE/AHS/ASC Structures, Structural Dynamics, and Materials Conference,* Vol. AIAA 2008-1980, Apr 7, 2008-Apr 10, 2008, Schaumburg, IL, USA.
612. Kaufmann, M., Zenkert, D. and Mattei, C. (2008), 'Cost Optimization of Composite Aircraft Structures including Variable Laminate Qualities', *Composites Science and Technology,* Vol. 68, No. 13, pp. 2748-2754.
613. Botelho, E.C., Almeida, R.S., Pardini, L.C. and Rezende, M.C. (2007), 'Influence of Hygrothermal Conditioning on the Elastic Properties of Carall Laminates', *Applied Composite Materials,* Vol. 14, No. 3, pp. 209-222.
614. Hexcel *Hexply® 8552 (Epoxy matrix (180°C/356°F curing matrix) - Product Data,* available at: http://www.hexcel.com/NR/rdonlyres/B99A007A-C050-4439-9E59-828F539B03A4/0/HexPly_8552_eu.pdf (accessed 2008).
615. Treasurer, P.J. (2006), *Characterization and Analysis of Damage Progression in Non-Traditional Composite Laminates with Circular Holes* Georgia Institute of Technology, Atlanta, GA, USA.
616. Bau, H., Hoyt, D.M. and Rousseau, C.Q. (2000), 'Open Hole Compression Strength and Failure Characterization in Carbon/Epoxy Tape Laminates', in Grant, P. and Rousseau, C.Q. *Composite Structures Theory and Practice*, American Society for Testing & Materials, pp. 273-292.
617. Kröber, I. (1992), 'Effect of Impacts on CFRP Structures, Results of a Comprehensive Test Program for Practical Use', *74th Meeting of the Structures and Materials Panel of Agard,* Vol. CP-530, May, 1992, Patras, Greece, AGARD, Neuilly sur Seine, France.
618. McCarthy, C.T., McCarthy, M.A. and Gilchrist, M.D. (2005), 'Predicting Failure in Multi-Bolt Composite Joints using Finite Element Analysis and Bearing-bypass Diagrams', *Key Engineering Materials,* Vol. 293-294, pp. 591-598.
619. Hart-Smith, L.J. (1993), 'The Ten-Percent Rule for Preliminary Sizing of Fibrous Composite Structures ', *Aerospace Materials,* Vol. 5, No. 2, pp. 10-16.
620. IHS (2005), *Metallic Materials Data Handbook - Specification prEN3456,* available at: https://extranet.cranfield.ac.uk/cgi-bin/,DanaInfo=www.esdu.com+ps.pl?sess=athens_1090222130758gmv&t=mmdh_spec&p=spec_pren3456_2b (accessed 2008).
621. Grayley, M.E. (1994), *Stiffness of Laminated Plates*, Report no. ESDU 94003, Engineering Sciences Data Unit, UK.
622. Vitali, R., Park, O., Haftka, R.T., Sankar, B.V. and Rose, C.A. (2002), 'Structural Optimization of a Hat-Stiffened Panel using Response Surfaces', *Journal of Aircraft,* Vol. 39, No. 1, pp. 158-166.
623. Giles, G.L. and Anderson, M.S. (1972), *Effects of Eccentricities and Lateral Pressure on the Design of Stiffened Compression Panels*, Report no. TN D-6784, NASA, Hampton, VA. USA.
624. Young, W.C. (1989), *Roark's Formulas for Stress & Strain* (6th edition), McGraw-Hill Inc., New York, USA.
625. Steinke, S. (2008), *Airbus A380 Still under Delivery Pressure,* available at: www.flugrevue.de/index.php?id=3235 (accessed 2008).
626. Aviation Week & Space Technology (2005), 'Gas Turbine Engines - Outlook/Specifications', *Aviation Week & Space Technology,* pp. 122-134.
627. Boeing *Commercial Airplanes - Products,* available at: http://www.boeing.com/commercial/products.html (accessed 2009).
628. Wikipedia *Pareto Principle,* available at: http://en.wikipedia.org/wiki/Pareto_principle (accessed 2009).
629. Alhajri, B. (2008), *Towards a Whole Lifecycle Cost Model for Composite Materials* Cranfield University, Bedford, UK.
630. Boeing (2003), *Composite Recycling and Disposal - An Environmental R&D Issue,*

available at: http://www.boeing.com/companyoffices/doingbiz/environmental/TechNotes/TechNotes2003-11.pdf (accessed 2009).
631. Logsdon, J.R. (2001), 'Electroformed Nickel Tooling', in Miracle, D.B. and Donaldson, S.L. *ASM Handbook: Composites v. 21*, ASM International, pp. 441-444.
632. Wikipedia (2009), *Tool Wear,* available at: http://en.wikipedia.org/wiki/Tool_wear (accessed 2009).
633. Airbus, *Airbus 2007 Results,* available at: http://www.airbus.com/store/mm_repository/pdf/att00011249/media_object_file_Airbus2007resultstable.pdf (accessed 2008).
634. Boeing, *Orders and Deliveries (2007 Deliveries Detail),* available at: http://active.boeing.com/commercial/orders/index.cfm?content=displaystandardreport.cfm&pageid=m25063&RequestTimeout=20000 (accessed 2008).
635. Boeing, *Demand by Airplane Size 2008-2027,* available at: http://www.boeing.com/commercial/cmo/images/2008/lg/lrg_demand_bysize.gif (accessed 2008).
636. Airbus Industries *Flying by Nature - Global Market Forecast 2007 - 2026,* available at: http://www.airbus.com/store/mm_repository/pdf/att00011423/media_object_file_GMF_2007.pdf (accessed 2008).
637. Wikipedia (2009), *Passenger Aircraft,* available at: http://en.wikipedia.org/wiki/Passenger_aircraft (accessed 2009).
638. Bombardier Aerospace (2008), *Commercial Aircraft Market Forecast 2008-2027,* available at: http://www.bombardier.com/files/en/supporting_docs/BCA_Market_Forecast_2008.pdf (accessed 2009).
639. Embrear (2008), *Market Outlook 2008-2027 (5th Edition),* available at: http://www.embraercommercialjets.com/hotsites/market-outlook-2008/english/content/home/default.asp (accessed 2009).
640. Parry, G., James-Moore, M. and Graves, A. (2006), 'Outsourcing Engineering Commodity Procurement', *Supply Chain Management,* Vol. 11, No. 5, pp. 436-445.
641. Grayley, M.E. (1994), *Elastic Buckling of Unbalanced Laminates Fibre Reinforced Composite Plates*, Report no. ESDU 94006, Engineering Sciences Data Unit, UK.

Appendix A – General Laminate Theory

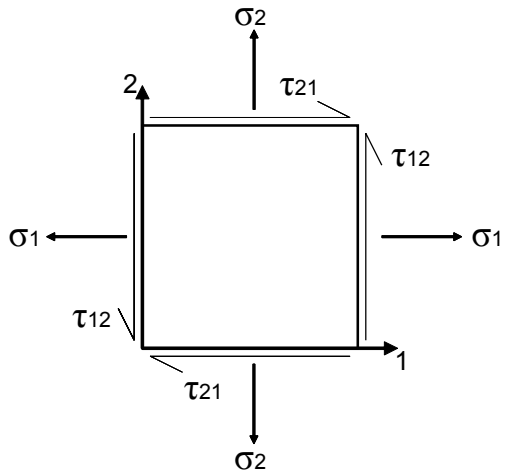

Figure A-1: Constants

The stiffness of a lamina is given by the stress-strain relationship defined by Hooke's law for an isotropic material. As a lamina is orthotropic in nature, there are five elastic constants required, E_{11}, E_{22}, ν_{12}, ν_{21} and G_{12}.

The constitutive equation – equations of strain in terms of stress and stiffness is given by Equation A-1:

$$\begin{bmatrix} \varepsilon_1 \\ \varepsilon_2 \\ \gamma_{12} \end{bmatrix} = \begin{bmatrix} \frac{1}{E_1} & \frac{-\nu_{21}}{E_2} & 0 \\ \frac{-\nu_{12}}{E_1} & \frac{1}{E_2} & 0 \\ 0 & 0 & \frac{1}{G_{12}} \end{bmatrix} \times \begin{bmatrix} \sigma_1 \\ \sigma_2 \\ \tau_{12} \end{bmatrix} \qquad \textbf{A-1}$$

The compliance equations – equations of stress in terms of strain and the inverse stiffness constants are given by Equation A-2.

$$\begin{bmatrix} \sigma_1 \\ \sigma_2 \\ \tau_{12} \end{bmatrix} = \begin{bmatrix} \frac{E_1}{(1-\nu_{12}\nu_{21})} & \frac{\nu_{21}E_1}{(1-\nu_{12}\nu_{21})} & 0 \\ \frac{\nu_{12}E_2}{(1-\nu_{12}\nu_{21})} & \frac{E_2}{(1-\nu_{12}\nu_{21})} & 0 \\ 0 & 0 & G_{12} \end{bmatrix} \times \begin{bmatrix} \varepsilon_1 \\ \varepsilon_2 \\ \gamma_{12} \end{bmatrix} \qquad \textbf{A-2}$$

A.1 Definitions

A.1.1 Isotropic

Material properties are identical in all directions, at all points and every plane is a material plane of symmetry. For a quasi-isotropic laminate, which has the least tailoring of the

laminate's elastic properties, the membrane elastic constants satisfy the conditions of isotropy:

$$E_{11} = E_{22} \quad \textbf{A-3}$$

$$G_{12} = \frac{E_{11}}{2(1+\nu_{12})} \quad \textbf{A-4}$$

$$m_x = m_y = 0 \quad \textbf{A-5}$$

Where m_x and m_y are shear coupling coefficients.

Or in terms of the A Matrix:

$$A_{11} = A_{22} \quad \textbf{A-6}$$

$$A_{66} = \frac{A_{11} - A_{22}}{2} \quad \textbf{A-7}$$

$$A_{16} = A_{26} = 0 \quad \textbf{A-8}$$

A.1.2 Anisotropic

Material properties are different in every direction and at all points, with no planes of material property symmetry existing.

A.1.3 Orthotropic

Three different values of a material property exist in three mutually perpendicular planes of material property symmetry. A specially orthotropic laminate such as 0/0/90/90/0/0 will have D_{16} and D_{26} values of 0, whereas a generally orthotropic 0/30/90/90/30/0 will have flexural/twist anisotropy and hence a fully populated D matrix.

A.2 ABD Matrix

The ABD matrix contains all necessary information to calculate the effective stiffnesses of the laminate and can indicate some issues with the laminate. The ABD matrix is defined as follows, with applied loads and resulting strains and curvatures. Equation A-9 is known as the general constitutive equation for a thin, laminated anisotropic plate:

$$\begin{bmatrix} N_x \\ N_y \\ N_{xy} \\ \hline M_x \\ M_y \\ M_{xy} \end{bmatrix} = \begin{bmatrix} A_{11} & A_{12} & A_{16} \\ A_{12} & A_{22} & A_{26} \\ A_{16} & A_{26} & A_{66} \\ \hline B_{11} & B_{12} & B_{16} \\ B_{12} & B_{22} & B_{26} \\ B_{16} & B_{26} & B_{66} \end{bmatrix} \times \begin{bmatrix} \varepsilon_x \\ \varepsilon_y \\ \gamma_{xy} \end{bmatrix} + \begin{bmatrix} B_{11} & B_{12} & B_{16} \\ B_{12} & B_{22} & B_{26} \\ B_{16} & B_{26} & B_{66} \\ \hline D_{11} & D_{12} & D_{16} \\ D_{12} & D_{22} & D_{26} \\ D_{16} & D_{26} & D_{66} \end{bmatrix} \times \begin{bmatrix} k_x \\ k_y \\ \psi_{xy} \end{bmatrix} \quad \text{A-9}$$

Where ε_x and ε_y are the direct strains in the plate, γ_{xy} is the shear strain in the plate, k_x and k_y are the curvature in the plate, and ψ_{xy} is the twist in the plate.

A.2.1 The A Matrix

The A Matrix is the extensional stiffness, where:

- A_{11} is the stiffness in the laminate in x direction, E_{11}
- A_{22} is the stiffness in the laminate in y direction, E_{22}
- A_{66} is the shear stiffness of the laminate in the x-y plane, G_{12}
- A_{12} is the stiffness that represents Poisson's effects
- A_{16} and A_{26} are the extension-shear coupling effects. These normally have a value of 0 for symmetric and balanced laminates

A.2.2 The B Matrix

The B Matrix is the coupling stiffnesses, which is normally 0 when the laminate is symmetric. Asymmetrical anisotropic laminates will show every type of mechanical coupling[509].

- B_{11}, B_{12} and B_{22} are the Extension-Bending coupling
- B_{16} and B_{26} are the Extension-Twisting or Shear-Bending coupling
- B_{66} is the Shear-Twisting coupling

A.2.3 The D Matrix

The D Matrix is the bending stiffnesses, where:

- D_{11} is the bending stiffness of the laminate about the y-axis, i.e. the bending moment M_x about the y-axis
- D_{22} is the bending stiffness of the laminate about the x-axis
- D_{66} is the torsional stiffness of the laminate
- D_{12} is the stiffness relating to anti-clastic i.e. a moment M_x about the y-axis produces bending about the y-axis and bending of the opposite sign about the x-axis, producing a horse saddle effect
- D_{16} and D_{26} are the bending-twisting coupling effects. These normally have a value of 0 for symmetric and balanced laminates, with only 0° and 90° orientations

A.3 Calculation of Laminate Stiffness Properties

If it is assumed that the laminate is symmetrical then the B matrix can be eliminated, therefore:

$$[N]=[A]\times[\varepsilon] \quad \textbf{A-10}$$

And

$$[M]=-[D]\times[k] \quad \textbf{A-11}$$

Eliminate the shear coupling A_{16} and A_{26} by adopting a balanced lay-up, then the A matrix becomes orthotropic:

$$[A]=\begin{bmatrix} A_{11} & A_{12} & 0 \\ A_{12} & A_{22} & 0 \\ 0 & 0 & A_{66} \end{bmatrix} \quad \textbf{A-12}$$

The D matrix remains anisotropic in nature. Therefore:

$$\begin{bmatrix} N_x \\ N_y \\ N_{xy} \end{bmatrix}=[A]\times\begin{bmatrix} \varepsilon_x \\ \varepsilon_y \\ \gamma_{xy} \end{bmatrix} \quad \textbf{A-13}$$

Dividing by the total laminate thickness, t:

$$\begin{bmatrix} \overline{\sigma}_x \\ \overline{\sigma}_y \\ \overline{\tau}_{xy} \end{bmatrix}=\frac{1}{t}\times[A]\times\begin{bmatrix} \varepsilon_x \\ \varepsilon_y \\ \gamma_{xy} \end{bmatrix} \quad \textbf{A-14}$$

The above equation can calculate the average laminate stresses. The average laminate elastic constants can be obtained from the components of the laminate A matrix, which are given by the following:

$$E_{11}=\frac{A_{11}\times A_{22}-A_{12}^2}{A_{22}\times t} \quad \textbf{A-15}$$

$$E_{22}=\frac{A_{11}\times A_{22}-A_{12}^2}{A_{11}\times t} \quad \textbf{A-16}$$

$$G_{12}=\frac{A_{66}}{t} \quad \textbf{A-17}$$

$$\nu_{12}=\frac{A_{12}}{A_{22}} \quad \textbf{A-18}$$

$$\nu_{21} = \frac{A_{12}}{A_{11}} \qquad \textbf{A-19}$$

Appendix B – Material Allowables & Strain Constraints

B.1 Introduction

The following sub-section is based on the work conducted by Phillips (2008)[611].

It is known that plain strength and modulus should not be used directly to structurally size CFRP structures[148]. Without an established material database, which is readily available to large aircraft manufacturers, it is necessary to use the available data, from open literature collectively to establish design allowables, in order to establish an envelope in which structural sizing can be conducted. Lamina properties alone are insufficient to determine allowables, however using certain analytical assumptions, lamina data can be used to determine laminate allowables[142]. Design allowables are material properties that are statistically determined from test data. Knockdown factors need to be applied to the strength characteristics, and limits applied to the allowable strains, for the reasons shown in Figure B-1. By using such a knockdown factor, this should, in general, take into account of delamination, indentation, localised ply buckling, matrix cracking and fibre breakage[410], under stipulated environmental conditions, and, in particular, defects such as 2% through-the-thickness porosity and flaws with a size of 6mm diameter[612]. These defects should also be taken into account when considering fatigue.

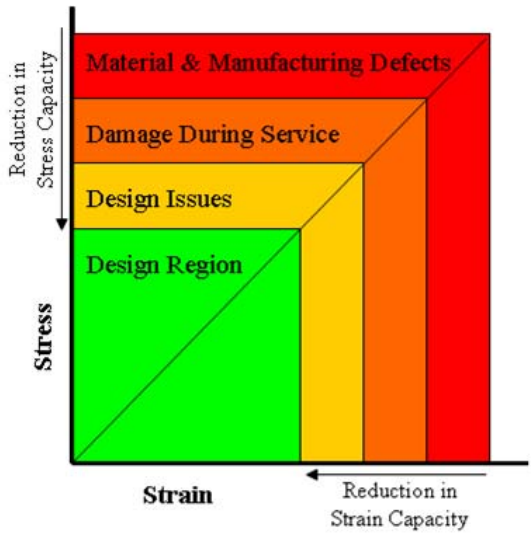

Figure B-1: Allowable design region for stress and strain allowables

Furthermore, environmental conditions can alter the performance of CFRP, in particular the compression and shear strength[148], thus Environmental Knockdown Factors (EKDFs) must also be considered. For example, at an elevated temperature condition of 80°C with 90% relative humidity, a EKDF of 5% under tension and 8% under compression, can occur[613]. The total knockdown applied will include both the knockdown due to the notched effects as well as the EKDF, as shown in Equation B-1.

$$Applied\ KDF = Notched\ KDF \times EKDF \qquad \textbf{B-1}$$

It is known that the allowable strain, for CAI and notched effects is dependent on the percentage of ±45° in the laminate and the stacking sequence. Thus, using a single allowable

strain value, for example -3600με for tension and compression and -7200με for shear, as used by Herencia et al. (2007)[606] and Liu et al. (2006)[545], could lead to inaccurate results.

B.2 UD Laminate

Using the basic properties from Hexcel's M21 datasheet[141], allowables are derived as shown in Table B-1, for both IM and HS material with the EKDF applied. Some data was still missing for a comprehensive overview, so it was necessary to use Hexcel's 8552 datasheets[614] too. HTA/6376 data to obtain ratios in the 90° direction[306] was also used. Obviously, Table B-1 involves a lot of assumptions, and is based on different sources of information; however, it is considered a good baseline with which to size components.

			IM	**HS**
Strength	0°	σc (MPa)	1669 × 0.92 = 1535	1465 × 0.92 = 1348
		σt (MPa)	3039 × 0.95 = 2887	2375 × 0.95 = 2256
	90°[liv]	σc (MPa)	223	196
		σt (MPa)	101	79
		τ12 (MPa)	74	89
Modulus	Average Tension and Compression	E11 (GPa)	((136 × 0.92) + (172 × 0.95))/2 = 144 GPa	((119 × 0.92) + (148 × 0.95))/2 = 125 GPa
		E22[lv] (GPa)	10 × 0.935 = 9.4	8 × 0.935 = 7.4
		G12 (GPa)	5 × 0.935 = 4.7	4.5 × 0.935 = 4.2
	Poisson's Ratio	v12	0.3	0.3
	Ply Thickness	t (mm)	0.125. 0.184 and 0.25	0.125. 0.184 and 0.25

Table B-1: Baseline allowables for HS and IM fibre

B.2.1 Strength

Based on an investigation into the knockdown factors due to OHC, OHT and FHT, on laminates using Toray CFRP IM fibre[615], for both a quasi-isotropic (25/50/25) and a "hard" (60/30/10) laminate, it is possible to establish Table B-2. Although, Table B-2 only provides two points for reference, a graph, as shown in Figure B-2 can be constructed, assuming a linear relationship, to analyse the knockdown based on the percentage of ±45° plies. Bau et al.[616] published similar data for OHC values for various IM laminates.

		Knockdown
Condition	**Laminate**	**Stress**
OHT	25/50/25	0.526
	60/30/10	0.480
FHT	25/50/25	0.468
	60/30/10	0.365
OHC	25/50/25	0.548
	60/30/10	0.505

Table B-2: Knockdown factors

[liv] Tension 2000/70 = 28.57, compression 1650/240 = 6.875. These factors can then be applied to the 0° values to obtain 90° values.
[lv] Based on Hexply 8552 AS4 & IM7 Mechanical Properties.

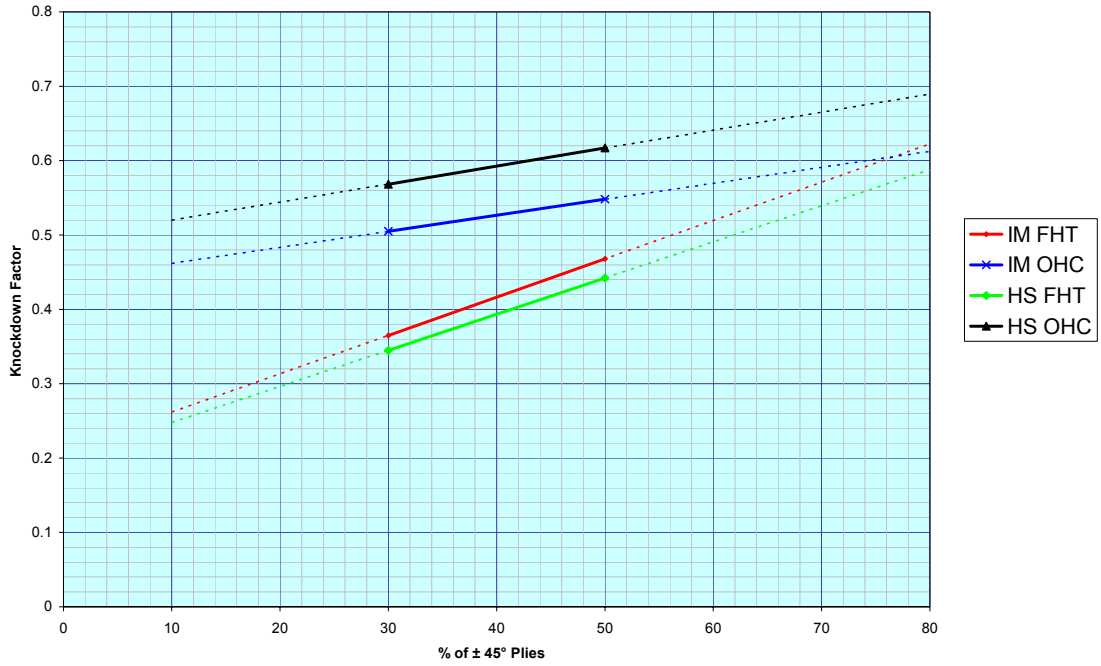

Figure B-2: Knockdown due to OHC and FHT based on percentage of ±45° plies

From Figure B-2 the equations for each line are given by Equations B-2 to B-5.

$$FHT\ HS = 0.0049x + 0.1989 \quad \textbf{B-2}$$

$$FHT\ IM = 0.0052x + 0.2105 \quad \textbf{B-3}$$

$$OHC\ HS = 0.0024x + 0.4959 \quad \textbf{B-4}$$

$$OHC\ IM = 0.0022x + 0.4405 \quad \textbf{B-5}$$

As an example, for an IM 60/30/10 laminate, the following can be obtained:

For 0°:

- $\sigma_c = \left[\left(0.0022 \times 30\right) + 0.4405\right] \times 1535 = 777.5\ MPa$
- $\sigma_t = \left[\left(0.0052 \times 30\right) + 0.2105\right] \times 2887 = 1058\ MPa$

For 90°:

- $\sigma_c = \left[\left(0.0022 \times 30\right) + 0.4405\right] \times 223 = 113\ MPa$
- $\sigma_t = \left[\left(0.0052 \times 30\right) + 0.2105\right] \times 101 = 37\ MPa$

For shear:

- $\tau_{12} = 79\ MPa$

B.2.2 Strain

Strain limitations for compression and tension in the longitudinal direction and for shear are required for ESDUpac A0817, as a means to ensure that the results are realistic. From Hexcel's M21 datasheet[141], CAI strength properties are given for a 4mm quasi-isotropic laminate, which can be converted into a strain, as shown in Table B-3.

		IM (25/50/25)	HS (25/50/25)
Modulus (MPa)		54495	47420
CAI @ 0.3mm BVID	MPa	168	224
	Strain	3080με	4720με
CAI @ 30J	MPa	216	239
	Strain	3960με	5040με

Table B-3: Basic modulus and CAI data for Hexcel's M21/T800 & M21/T700

It has been shown that with an increasing percentage of 0° plies in the laminate, the greater the knockdown in CAI performance[617]. The Hexply datasheet uses a quasi-isotropic laminate; however, compression strain limits are required for laminates with varying amounts of 0° plies. Therefore Figure B-3[617] can be used to factor in the increasing percentage of 0° plies in the laminate.

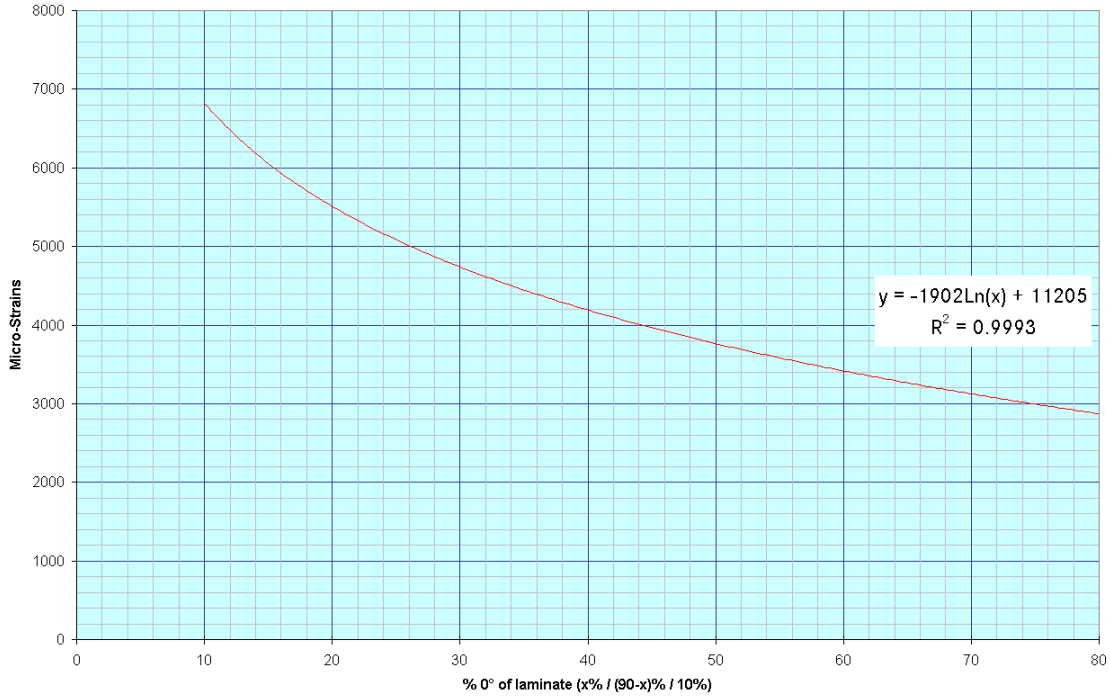

Figure B-3: Residual compressive strain after impact

From Kröber[617] it is known that for a quasi-isotropic laminate, the residual compressive strain is 5100με, and from Table B-3 the quasi-isotropic laminate for CAI @ 0.3mm BVID of 3080με and 4720με for IM and HS respectively. Therefore, for a HS 10/80/10 laminate, the allowable strain for CAI @ 0.3mm BVID is given by:

$$Allowable\ Strain = \left(\frac{\left(-0.1902 \times \ln 10\right) + 1.1205}{0.51} \right) \times 4720 = 6317 \mu\varepsilon$$

Whereas, for a IM 70/20/10 laminate, the allowable strain for CAI @ 0.3 mm BVID is given by:

$$Allowable\ Strain = \left(\frac{\left(-0.1902 \times \ln 70\right) + 1.1205}{0.51} \right) \times 3080 = 1887 \mu\varepsilon$$

It is known that thicker laminates are less sensitive to impact, thus thicker skins will have a higher CAI strength than thinner skins. On that basis, it is known that there will be a crossover

point, where the laminate's compression performance will no longer be limited by CAI but instead OHC, which for a 50/40/10 laminate occurs at 8mm thickness[617]. For a 8mm quasi-isotropic laminate using T800/924, an OHC failure strength of 454MPa is obtained[149]. This was for a laminate with a +/0/-/90 stacking sequence, i.e. a nice stairwell effect. However, typically, the laminate will be ±45°/0/90 or similar, thus a knockdown of 602/718=0.84[440] should be applied, resulting in 454×0.84=381MPa. For the IM fibre in Table B-3 this will give: 381/54495=6991με; and for the HS fibre: 381/47420=8035με. The assumption is that for all laminates, the crossover points between CAI and OHC will be at 8mm, and that the strain limitation due to OHC remains constant after 8mm. An example to work out this strain limitation for a 30/60/10 HS laminate is:

$$Allowable\ Strain = \left(\frac{\left(-0.1902 \times \ln 30\right) + 1.1205}{0.51} \right) \times 8035 = 7461 \mu\varepsilon$$

Shown in Figure B-4, Figure B-5, and Figure B-6 are the strain limitations for IM, HS, and hybrid laminates, with % representing percentage of 0° plies (always 10% 90° plies). As the original quasi-isotropic laminates in Table B-3 are 4mm thick, the linear relationship from 8mm to 4mm was extrapolated to 3mm.

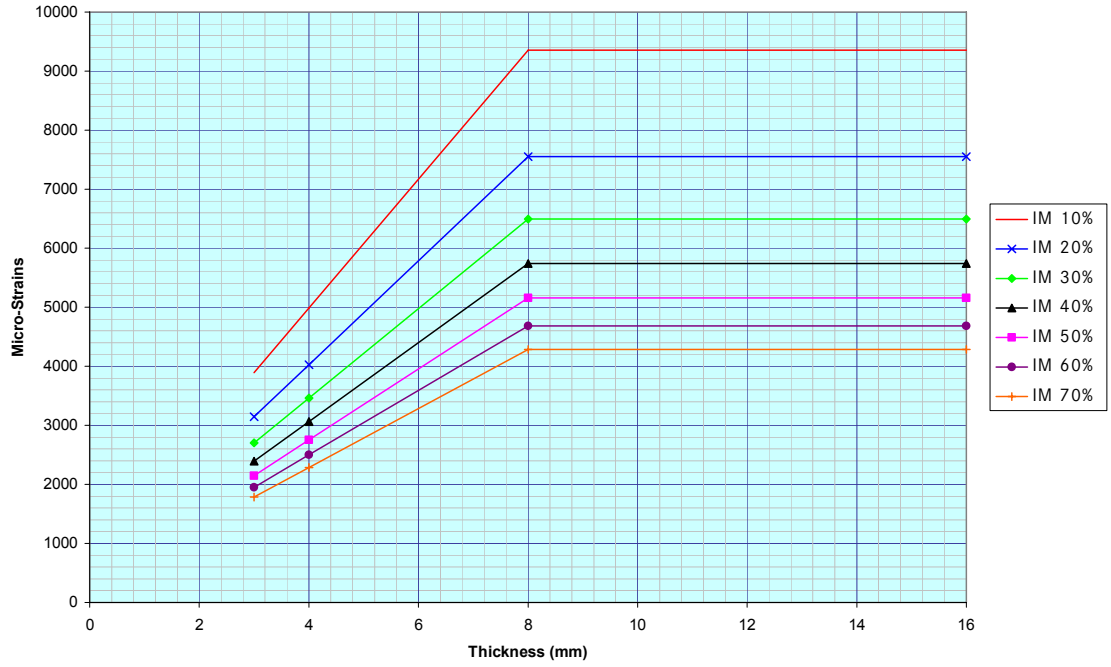

Figure B-4: Strain limit versus panel thickness for IM laminate

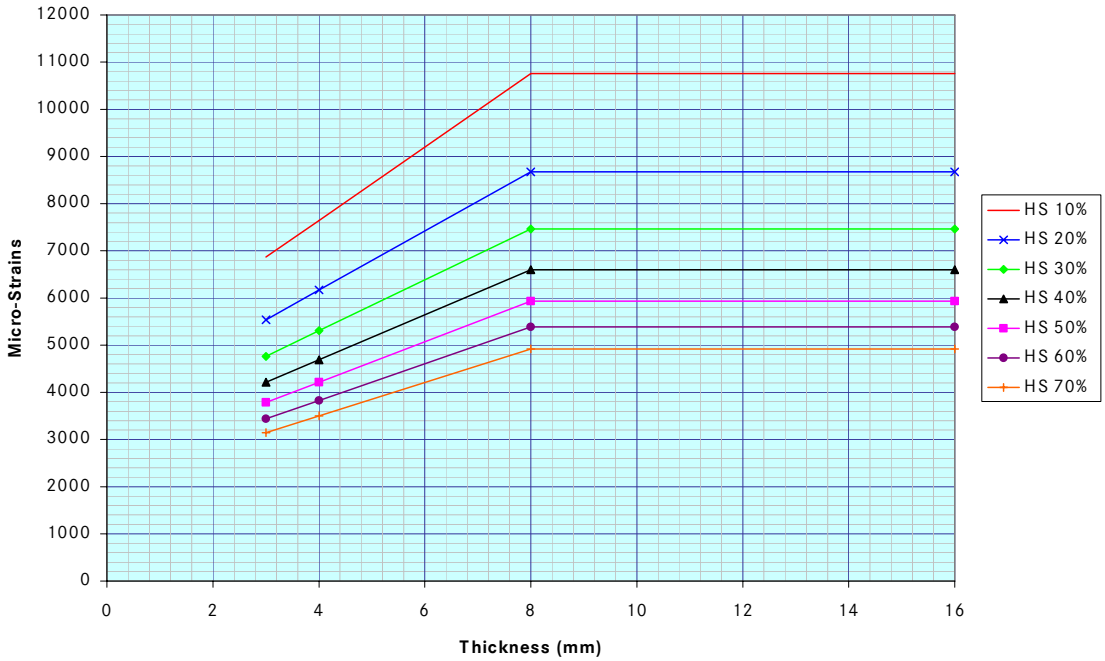

Figure B-5: Strain limit versus panel thickness for HS laminate

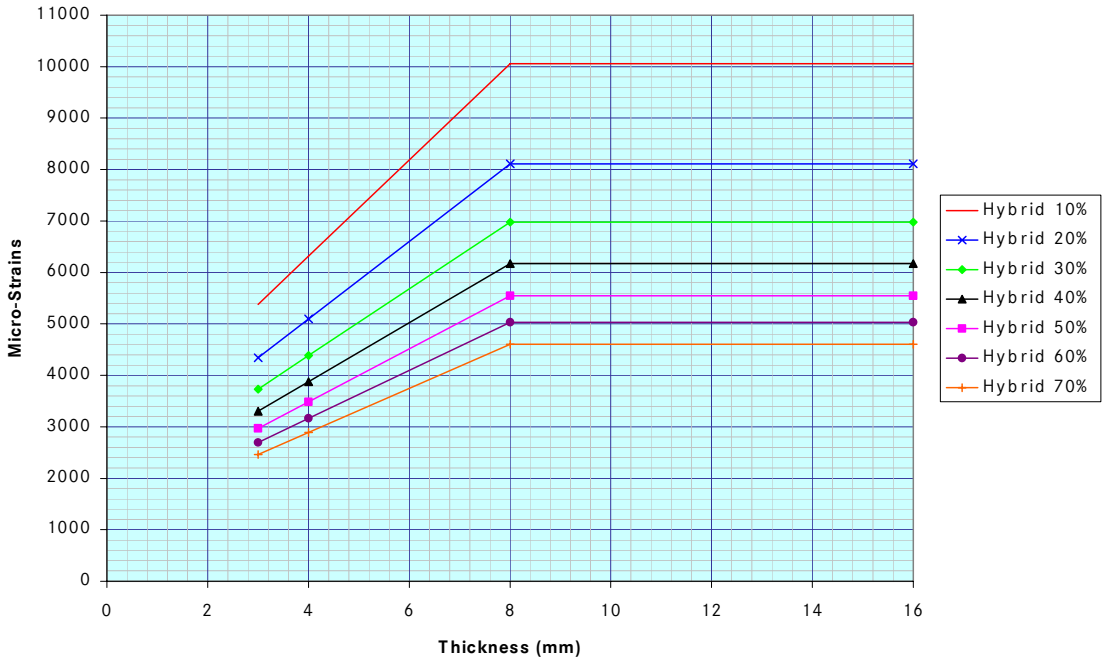

Figure B-6: Strain limit versus panel thickness for hybrid laminate

B.2.2.1 Influence of Stringer Pitch

It is known that the stringer pitch can influence the damage tolerance of the structure, as a wider stringer pitch results in a more compliant structure, thus upon impact the structure should flex more and hence the delamination at a local level should be reduced. Due to a lack of empirical data, the following conditions have been assumed:

- Stringer pitch from 125-165mm is as previously worked out

- Stringer pitch from 165-208mm has at 3mm thickness a CAI strain 1.1 greater than with a stringer pitch from 125-165mm, but the strain at 8mm is the same as for 125-165mm stringer pitch
- Stringer pitch from greater than 208mm has at 3mm thickness a CAI strain 1.21 greater than with a stringer pitch from 125-165mm, but the strain at 8mm is the same as for 125-165mm stringer pitch

The resultant equations for the increase in CAI strain versus thickness are shown in Table B-4, as well as the max strains.

	HS > 208		HS 165 - 208		HS 125 - 165	
0° Percentage	**Equation for Line**	**Max Strain**	**Equation for Line**	**Max Strain**	**Equation for Line**	**Max Strain**
10	y = 777.36x + 4534	10753	y = 951.08x + 3144.3	10753	y = 1109x + 1880.9	10753
20	y = 627.21x + 3658.3	8676	y = 767.37x + 2537	8676	y = 894.79x + 1517.6	8676
30	y = 539.38x + 3146	7461	y = 659.91x + 2181.7	7461	y = 769.49x + 1305.1	7461
40	y = 477.06x + 2782.5	6599	y = 583.67x + 1929.6	6599	y = 680.59x + 1154.3	6599
50	y = 428.73x + 2500.6	5930	y = 524.53x + 1734.1	5930	y = 611.63x + 1037.3	5930
60	y = 389.23x + 2270.2	5384	y = 476.21x + 1574.4	5384	y = 555.28x + 941.78	5384
70	y = 355.84x + 2075.4	4922	y = 435.36x + 1439.3	4922	y = 507.65x + 860.99	4922
Tailored	y = 251.68 + 5448.2	7461	y = 408.54 + 4192.7	7461	y = 551.21 + 3051.3	7461

	IM > 208		IM 165 - 208		IM 125 - 165	
0° Percentage	**Equation for Line**	**Max Strain**	**Equation for Line**	**Max Strain**	**Equation for Line**	**Max Strain**
10	y = 1092.3x + 618.49	9357	y = 1205.7x - 288.37	9357	y = 1308.7x - 1112.8	9357
20	y = 881.32x + 499.02	7550	y = 972.78x - 232.67	7550	y = 1055.9x - 897.84	7550
30	y = 757.9x + 429.14	6492	y = 836.56x - 200.09	6492	y = 908.06x - 772.11	6492
40	y = 670.34x + 379.56	5742	y = 739.9x - 176.97	5742	y = 803.15x - 682.9	5742
50	y = 602.42x + 341.1	5160	y = 664.93x - 159.04	5160	y = 721.77x - 613.71	5160
60	y = 546.92x + 309.68	4685	y = 603.68x - 144.39	4685	y = 655.28x - 557.17	4685
70	y = 500x + 283.11	4283	y = 551.89x - 132	4283	y = 599.06x - 509.37	4283
Tailored	y = 594.64 + 1735.3	6492	y = 697.04 + 916.01	6492	y = 790.14 + 171.21	6492

	Hybrid > 208		Hybrid 165 - 208		Hybrid 125 - 165	
0° Percentage	Equation for Line	Max Strain	Equation for Line	Max Strain	Equation for Line	Max Strain
10	y = 934.83x + 2576.3	10055	y = 1078.4x + 1428	10055	y = 1208.9x + 384.07	10055
20	y = 754.27x + 2078.6	8113	y = 870.08x + 1152.1	8113	y = 975.36x + 309.88	8113
30	y = 648.64x + 1787.6	6977	y = 748.24x + 990.81	6977	y = 838.78x + 266.49	6977
40	y = 573.7x + 1581	6171	y = 661.79x + 876.33	6171	y = 741.87x + 235.7	6171
50	y = 515.57x + 1420.8	5545	y = 594.73x + 787.54	5545	y = 666.7x + 211.82	5545
60	y = 468.08x + 1289.9	5035	y = 539.94x + 714.99	5035	y = 605.28x + 192.3	5035
70	y = 427.92x + 1179.3	4603	y = 493.62x + 653.65	4603	y = 533.35x + 175.81	4603
Tailored	y = 423.12 + 3591.7	6977	y = 552.79 + 2554.3	6977	y = 670.68 + 1611.3	6977

Table B-4: Equations for HS, IM and Hybrid laminates as well as maximum associated strain

B.2.3 Tensile Strain

Any effects of thickness will be ignored for working out the allowable tensile strains. In order to calculate the allowable strains, the following procedure has taken place:

From Hexcel's M21 datasheet[141] the tensile strength of the ply for HS and IM is 2375MPa and 3039MPa respectively. In order to calculate the tensile strength of the laminate, Hart-Smith's 10% rule was used, i.e. every off-axis ply has only 10% of the strength, thus for a 10/80/10 20-ply laminate:

$$10/80/10\ Lam\ Str = \left((2\times 1)+(16\times 0.1)+(2\times 0.1)\right)/20 = 0.19 \quad \textbf{B-6}$$

Using Equation B-6, in combination with Equations B-2 & B-3 to obtain the notched KDF for either a HS or IM laminate, as well as the EKDF, then the resultant stress can be obtained:

$$IM\ 10/80/10\ Lam\ Str = 3039\times 0.19\times\left((0.0052\times 80)+0.2105\right)\times 0.95 = 344\ MPa \quad \textbf{B-7}$$

Using the moduli from Table B-1, except that the pure tensile values of E_{11} were used, i.e. 172GPa and 148GPa respectively, with the 0.95 EKDF applied, to obtain the E_{11} of the overall laminate. Therefore, the stress of the laminate can be divided by the modulus, to obtain the allowable strains as shown in Table B-5.

	Allowable Strains		
	HS	IM	Hybrid
10/80/10	7644	8980	8312
20/70/10	7529	8819	8174
30/60/10	7128	8335	7731
40/50/10	6592	7700	7146
50/40/10	5981	6981	6481
60/30/10	5324	6211	5767
70/20/10	4911	5406	5159

Table B-5: Allowable tensile strains

B.2.4 Shear Strain

$$\gamma_{allow} = 2 \times \varepsilon_{allow\ compr} \qquad \text{B-8}$$

B.2.5 Overall Strain Comparison

Shown in Table B-6 is a comparison of a panel designed with a 10/80/10 skin, with the correct strain allowables, but also those for 50/40/10 applied. As can be seen, when the 50/40/10 strain allowables are applied, there is a significant knockdown in reserve factor, which validates the above calculated strains, as this is the trend expected.

Load		Dimensions (mm)					Strength (RF)			
N/mm	% in	Skin	Stringer				Tension		Compression	
	Str	Thk	BH	BT	LFW	LFT	10/80/10	50/40/10	10/80/10	50/40/10
-1000	30	21.5	28.4	6.0	180	3	5.80	4.51	6.52	3.60
	40	12.8	40.0	6.7	128	3	4.01	3.11	4.50	2.48
	50	6.7	47.0	6.1	76	3	2.51	1.95	2.82	1.56
	60	4.3	48.0	6.1	64	3	1.98	1.54	2.23	1.23
	70	3.6	63.0	7.0	64	3	2.22	1.72	2.49	1.37
-2000	30	21.5	28.4	6.0	180	3	2.90	2.26	3.26	1.63
	40	16.7	50.0	7.1	166	3	2.62	2.04	2.95	0.99
	50	8.6	58.0	6.5	88	3	1.59	1.24	1.79	0.91
	60	6.3	59.0	6.8	103	3	1.46	1.14	1.64	0.88
	70	4.7	64.0	8.9	80	3	1.43	1.11	1.60	1.32
-3000	30	24.0	37.0	6.0	180	3	2.14	1.66	2.40	1.21
	40	18.8	55.0	7.3	180	3	1.95	1.52	2.20	0.82
	50	10.6	69.0	6.7	116	3	1.33	1.03	1.49	0.71
	60	7.4	64.0	8.2	103	3	1.14	0.89	1.28	0.66
	70	5.3	64.0	10.5	80	3	1.07	0.83	1.20	1.06
-4000	30	25.5	49.0	6.0	180	3	1.72	1.34	1.93	0.96
	40	19.7	64.0	7.3	180	3	1.55	1.20	1.74	0.71
	50	12.3	71.0	7.5	128	3	1.14	0.89	1.28	0.59
	60	8.1	73.0	8.3	105	3	0.94	0.73	1.06	0.57
	70	5.9	67.0	12.0	82	3	0.91	0.71	1.03	0.57

Table B-6: Comparison on a T-profile stringer-stiffened panel with a 10/80/10 skin

B.2.6 Bearing/Bypass

To detect failure under bearing-bypass conditions, the conventional method is to identify the highest loaded hole, and evaluate it using semi-empirical criteria[618]. Although this method is appropriate for preliminary design, it does not, however, consider such issues as load distribution, which could be obtained using FEM.

As the load distribution is greater at the outer fasteners[373], then the load distribution for a 4 bolt-row can be assumed to be 35%, 15%, 15%, 35%, which when applied to a stringer blade with a double shear joint, and an applied load of 50kN, with a blade thickness of 6mm and a height of 50mm, has a bearing/bypass load distribution as given in Table B-7

	Bolt 1	Bolt 2	Bolt 3	Bolt 4
Bolt Load (kN)	50 × 0.35 = 17.5	50 × 0.15 = 7.5	50 × 0.15 = 7.5	50 × 0.35 = 17.5
Bypass Load (kN)	50 × 0.65 = 32.5	32.5 – 7.5 = 25	25 – 7.5 = 17.5	0
Bolt Stress (MPa)	17.5 / (6.35 × 6) = 459	7.5 / (6.35 × 6) = 197	7.5 / (6.35 × 6) = 197	17.5 / (6.35 × 6) = 459
Bypass Stress (MPa)	32.5 / ((50 – 6.35) × 6) = 124	25 / ((50 – 6.35) × 6) = 95	17.5 / ((50 – 6.35) × 6) = 67	0

Table B-7: Bearing/bypass load distribution in 4-bolt row

It is difficult to find bearing-bypass information from open-sources, such as journal papers, as to develop such a failure envelope requires a large amount of experimentation with a test machine that has two different actuators to independently vary the bearing and bypass load simultaneously[618]. However Equation B-9 has been developed by Collings[353], to predict the bearing strength of laminates with 3 ply orientations.

$$\sigma_b = \frac{1}{t}\left[\frac{100 \times t_0 \times \sigma_C \times \sigma_{b0}}{\sigma_C(100-\phi)+\phi\sigma_{b0}} + \frac{100^2 \times t_{90} \times \sigma_{TC}}{100^2 + 2.38\phi_{90}^2} + t_{45}\sigma_{b45}\right] \quad \textbf{B-9}$$

Where:

σ_b = Bearing Strength (MPa)
σ_C = Longitudinal Compression Strength (MPa)
σ_{TC} = Constrained Transverse Compression Strength (MPa)
σ_{b0} = Average Constrained Bearing Strength of a 0° laminate (MPa)
σ_{b45} = Average Constrained Bearing Strength of a ±45° laminate (MPa)
φ = combined percentage of ±45° and 90° plies
φ_{90} = percentage of 90° plies
t = total laminate thickness (mm)
t_0 = total thickness of 0° plies (mm)
t_{45} = total thickness of ±45° plies (mm)
t_{90} = total thickness of 90° plies (mm)

The 'constrained' term in some of the above factors means that the coupon was restrained to mitigate Poisson's expansion normal to the load[353]. Using the values of σ_C = 1200MPa, σ_{TC} = 1440MPa, σ_{b0} = 830MPa, and σ_{b45} = 910MPa[353], for a 60/30/10 laminate a σ_b = 982 MPa was obtained, which is independent of thickness. As shown in Table B-8, using the equation, there does not seem to be a large variance in the allowable bearing stress with change in laminate, which has been verified with experimental evidence considering various 0° dominated laminates, but with an increasing percentage of ±45° plies, with only a 14% performance increase being achieved[353]. Therefore, the bearing-bypass diagrams can be based on a single bearing figure, when there is always 10% 90° plies in the laminate.

Laminate	Bearing Stress (MPa)
60/30/10	982
50/40/10	995
30/60/10	1004
10/80/10	984

Table B-8: Bearing stresses

The bearing strength on the y-axis in Figure 5-4 is taken for a HTA/6376 (HS fibre), which has an ultimate bearing stress of 750MPa[618]. The assumption is that for IM fibre, the ultimate bearing stress is 720Mpa. In terms of the two points from Figure 5-4 on the x-axis, these are assumed to be the FHT and FHC values for the laminate. Therefore, the derived FHT and

OHC values can be used, as FHC allowables have not been derived, thus using OHC is considered acceptable, and in fact conservative, as OHC values are typically lower than for FHC. Thus for:

FHT = (0.0052 × % of 45°plies) + 0.2105 **B-10**

OHC = (0.0022 × % of 45° plies) + 0.4405 **B-11**

Using Equations B-10 and B-11, plus Hart-Smith's 10% rule[619], FHT and OHC values can be obtained. For example for 60/30/10:

Tensile Bypass Failure = (((0.0052 × 30) + 0.2105) × 0.64) × 2887.1 = 677MPa

Two simple bearing/bypass diagrams are shown in Figure B-7, for an IM 60/30/10 and HS 10/80/10 respectively. In comparison to the bearing-bypass example in Figure 5-4, it can be seen that the compressive side is fairly simple in Figure B-7. However, as tension is typically more critical, and the curve is usually quite steep, representing the compressive bearing-bypass limit with two lines at right angles is thus acceptable, particularly at this level of analysis. The 50/40/10 bearing/bypass diagram will be assumed to be applicable for use with the tailored laminate.

Figure B-7: Bearing-bypass diagram for IM 60/30/10 (RHS) and HS 10/80/10 (LHS)

B.2.6.1 Fibre Metal Laminate (CFRP/Titanium)

The principal titanium material properties are shown in Table B-9[620], whereas Table B-10 illustrates the change in elastic properties, of a CFRP laminate with an increasing percentage of titanium.

From Kolesnikov et al.[237] a 100/0/0 and a 50/40/10 laminate had bearing strengths of 366MPa and 927MPa, respectively. Whereas, for a hybrid laminate with 50% 0° plies and 50% titanium, the bearing strength was 1570MPa. From previous work conducted, a 60/30/10 laminate with HS fibre had a bearing strength of 750MPa. The difference between the two values of 927MPa and 750MPa, apart from the variation in the laminate percentages, is the definition of bearing and possibly environmental factors. Therefore, the factor used will be 927/750 = 1.236.

Property	Value
E_{11} & E_{22}	110000 MPa
G_{12}	42000 MPa
ν_{12}	0.31

Table B-9: Elastic properties of Titanium 6AL-4V

	E_{11} (MPa)	E_{22} (MPa)	G_{12} (MPa)	ν_{12}	ν_{21}	ρ (kg/m^3)	E_{11}/ρ
60/30/10 [0]	96554	32005	14437	0.37	0.12	1600	60.3
60/30/00 [10]	104232	28958	18167	0.51	0.14	1882	55.4
60/20/00 [20]	113362	36740	18652	0.42	0.14	2164	52.4
60/10/00 [30]	122017	44510	19136	0.35	0.13	2446	49.9
60/00/00 [40]	130400	52272	19620	0.31	0.12	2728	47.8
50/30/00 [50]	126999	62489	23350	0.31	0.15	3010	42.2

Table B-10: Elastic properties of hybrid laminates

Referring back to the difference between the baseline 100/0/0 laminate, the 50/40/10 laminate, and the 50/50 hybrid laminate, it can be seen that a 1% increase of bias plies or titanium provides a bearing strength increase of ((927-366)/50) 11.22MPa and ((1570-366)/50) 24.08MPa, respectively. Thus, the benefit of using titanium over bias plies is (24.08-11.22) 12.86MPa, per 1%. Therefore, the following can be obtained:

- 60/30/10 [0] = 750 + ((12.86 × 0)/1.236) = 750MPa
- 60/30/0 [10] = 750 + ((12.86 × 20)/1.236) = 855MPa
- 60/20/0 [20] = 750 + ((12.86 × 30)/1.236) = 960MPa
- 60/20/0 [30] = 750 + ((12.86 × 40)/1.236) = 1066MPa
- 60/0/0 [40] = 750 + ((12.86 × 50)/1.236) = 1171MPa

For FHT and FHC values, the work from Fink et al.[238] gives FHT values of 685MPa for a 70/20/10 laminate and 697MPa for a 45% 0° and 55% titanium hybrid laminate. In terms of FHC, the values are 629MPa and 750MPa, for the CFRP and hybrid laminate respectively. The numbers previously obtained for a 70/20/10 laminate for FHT and FHC are 518MPa and 476MPa. A factor of 1.32 difference was calculated (685/518 or 629/476) as the disparity between Fink et al. and the previously derived numbers. If the start and end points are known then an improvement based on an increase in titanium can be calculated.

For a 60/30/10 laminate, the FHT and FHC are 529MPa and 436MPa, respectively, whereas a 50/50 hybrid laminate is 528MPa (697/1.32) and 568MPa (750/1.32), respectively. There is very little influence of the titanium on the FHT values, but it varies from 436MPa to 568MPa for FHC, thus a 10% increase of titanium in the laminate gives (568-436)/5=26.4MPa increase. Therefore this can be used to work out Table B-11.

Laminate	FHT (MPa)	FHC (MPa)	Bearing (MPa)
60/30/10	529	436	750
60/30/00 [10]	529	462	855
60/20/00 [20]	529	489	960
60/10/00 [30]	529	515	1066
60/00/00 [40]	529	542	1171

Table B-11: Hybrid laminate data required for bearing/bypass diagram

This data can be plotted to give bearing-bypass diagrams, as shown for two examples in Figure B-8.

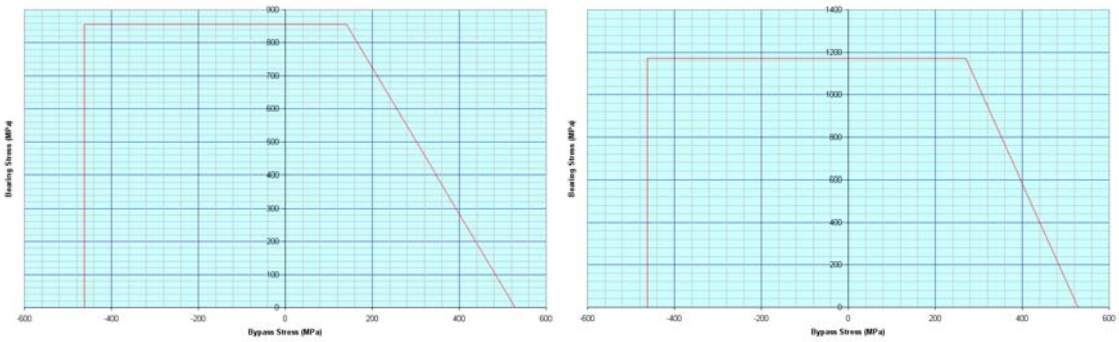

Figure B-8: Bearing-bypass diagram for Hybrid 60/30/00 [10] (RHS) and 60/00/00 [40] (LHS)

B.3 NCF

As previously stated, today's NCFs, using some form of toughening, will have very similar properties to the latest prepreg systems[182]. For this reason, the same developed prepreg allowables will be used for NCF.

B.4 Braids

It is known that 2-D braids suffer from a 10% knockdown in tensile stiffness in comparison to UD tape, as well as a 20-30% knockdown in tensile strength; whereas for compressive properties, the braid has less than a 10% knockdown in stiffness, but more than 40% loss in strength[185]. This is reflected in the mechanical properties for a braid[lvi], as shown in Table B-12.

			IM	HS
Strength	0°	σc (MPa)	1669 × 0.92 × 0.6 = 921	1465 × 0.92 × 0.6 = 809
		σt (MPa)	3039 × 0.95 × 0.75 = 2165	2375 × 0.95 × 0.75 = 1692
	90°[lvii]	σc (MPa)	223 × 0.6 = 134	196 × 0.6 = 118
		σt (MPa)	101 × 0.75 = 76	79 × 0.75 = 59
		τ12 (MPa)	74 × 0.675 = 50	89 × 0.675 = 60
Modulus	Average Tension and Compression	E11 (GPa)	(((136 × 0.92) + (172 × 0.95))/2) × 0.9 = 130 GPa	(((119 × 0.92) + (148 × 0.95))/2) × 0.9 = 113 GPa
		E22[lviii] (GPa)	10 × 0.935 × 0.9 = 8.5	8 × 0.935 × 0.9 = 6.7
		G12 (GPa)	5 × 0.935 × 0.9 = 4.2	4.5 × 0.935 × 0.9 = 3.8
		v12	0.3	0.3

Table B-12: Baseline allowables for HS and IM fibre

[lvi] Adapted from prepreg values, in order to establish baseline properties.
[lvii] Tension 2000/70 = 28.57, compression 1650/240 = 6.875. These factors can then be applied to the 0° values to obtain 90° values.
[lviii] Based on Hexply 8552 AS4 & IM7 Mechanical Properties.

Based on these values, and using data from Cox and Flanagan[166], two braids were designed as follows:

- $[0_{36k}, \pm45_{15k}]$ 46% Axial
  - Equivalent laminate: $[(+/0/-/0)_2/+/0/-]_s$ with 0.184mm plies
- $[0_{36k}, \pm60_{6k}]$ 56% Axial
  - Equivalent laminate: $[(60/0/-60/0)_2/60/0/0]_s$ with 0.184mm plies

To obtain the tensile and compressive strain allowables, the following procedure was used. The overall E_{11} of the 22-ply 4.048mm laminate, using the knocked down compressive and tensile E_{11} values for IM result in:

- $[0_{36k}, \pm45_{15k}]$ 46% Axial
  - Tensile E_{11}: 76022MPa
  - Compressive E_{11}: 59985MPa
- $[0_{36k}, \pm60_{6k}]$ 56% Axial
  - Tensile E_{11}: 84474MPa
  - Compressive E_{11}: 65681MPa

Using Hart-Smith's 10% rule, each braid's resultant stress KDF was worked out:

- $[0_{36k}, \pm45_{15k}]$ 46% Axial
  - 0.51
- $[0_{36k}, \pm60_{6k}]$ 56% Axial
  - 0.59

Taking the compressive and tensile strengths for IM material, which are 921MPa and 2165MPa respectively; this was multiplied by the resultant stress KDF due to Hart-Smith's 10% rule and further multiplied by either Equations B-3 or B-5. Due to the better damage tolerance of braids, for a 6.35mm hole to represent damage, there was no knockdown in tensile strength[166]. It is assumed that this is also the same for compressive strength, thus the knockdown in Equations B-3 and B-5 uses 100% 45° plies, i.e. in order to minimise the KDF, thus the values for Equations B-3 and B-5 are 0.7305 and 0.6605 respectively. Therefore, the tensile strain for the $[0_{36k}, \pm45_{15k}]$ 46% axial braid is:

$$\varepsilon_{IM\ Tension} = \left[\left(2165 \times 0.51 \times 0.7305\right)/76022\right] \times 1 \times 10^6 = 10591\ \mu\varepsilon$$

Based on the work conducted on standard HS and IM laminates, it is known that for a laminate with 50% ±45° plies there is a 1108με difference, thus:

$$\varepsilon_{HS\ Tension} = 10591 - 1108 = 9483\mu\varepsilon$$

Similarly for the $[0_{36k}, \pm60_{6k}]$ 56% axial braid:

$$\varepsilon_{IM\ Tension} = 11063\mu\varepsilon$$
$$\varepsilon_{HS\ Tension} = 9955\mu\varepsilon$$

And for compression, for 4mm:

$$\varepsilon_{IM\ Compression} = \left[\left(921 \times 0.51 \times 0.6605\right)/59985\right] \times 1 \times 10^{6} = 5163\mu\varepsilon$$

From Figure B-4, for IM 40% i.e. there are 50% ±45° plies, the equation of the line between 3 mm and 8 mm is given by:

$$Y = 803.15x - 682.9$$

The assumption is made that the increase in the strain allowable will follow the linear relationship of Y = 803.15x, thus the points at 3mm and 8mm can be obtained, resulting in Figure B-9.

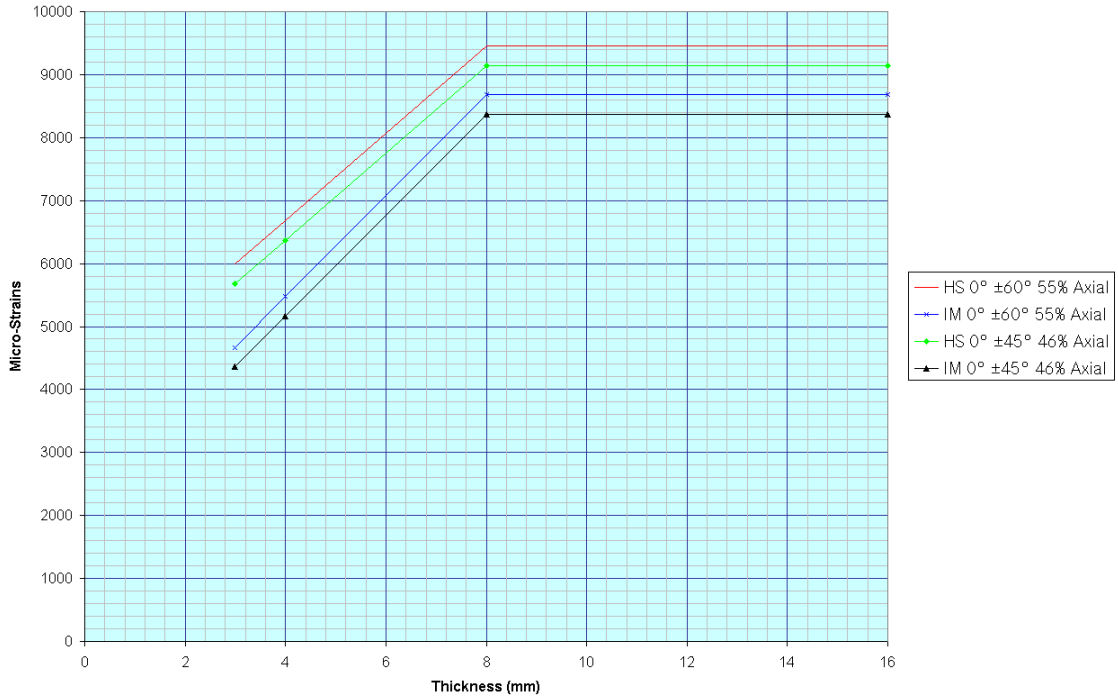

Figure B-9: Strain curves for 2 different 2D braid configurations using either HS or IM fibre

Appendix C – Laminate Configurations

C.1 UD Prepreg Laminates

C.1.1 Skin

4 laminates have been developed, using the interleaved tapering method, as follows:

- 50/40/10
- 30/60/10
- 10/80/10
- Tailored

These laminates are shown in Figure C-1 to Figure C-4. All laminates obey the various stacking rules. The ply thickness used for all laminates is 0.25mm. The 50/40/10, 30/60/10 and 10/80/10 laminates all have defined targets for the percentage of 0°, ±45°, and 90° plies. The tailored laminate however has a higher proportion of ±45°, when the laminate is thinner and hence buckling prone, whereas when the laminate is thicker, there is a higher percentage of 0° plies, as thicker laminates are typically strength critical.

Figure C-1: 50/40/10 UD skin laminate

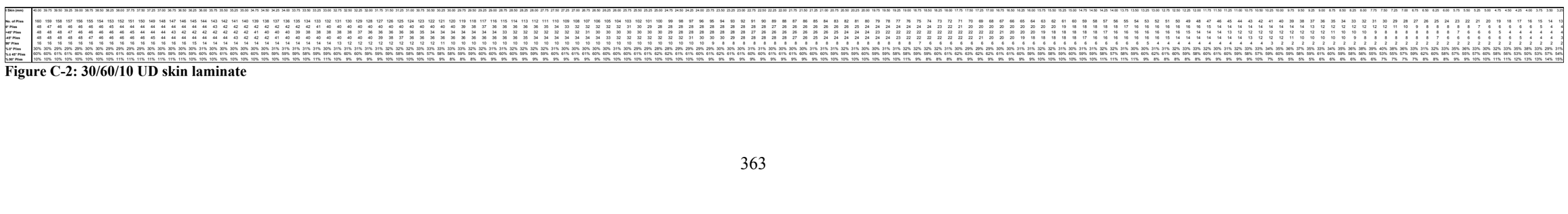

Figure C-2: 30/60/10 UD skin laminate

t Skin (mm)	40.00	39.75	39.50	39.25	39.00	38.75	38.50	38.25	38.00	37.75	37.50	37.25	37.00	36.75	36.50	36.25	36.00	35.75	35.50	35.25	35.00	34.75	34.50	34.25	34.00	33.75	33.50	33.25	33.00	32.75	32.50	32.25	32.00	31.75	31.50	31.25	31.00	30.75	30.50
No. of Plies	160	159	158	157	156	155	154	153	152	151	150	149	148	147	146	145	144	143	142	141	140	139	138	137	136	135	134	133	132	131	130	129	128	127	126	125	124	123	122
0° Plies	18	18	18	18	18	18	18	18	18	18	18	18	18	18	18	17	16	16	16	16	16	15	14	14	14	14	14	14	14	14	14	14	14	14	14	14	14	14	14
+45° Plies	64	64	64	63	62	61	60	60	60	59	58	58	58	57	56	56	56	56	56	55	54	54	54	54	54	53	52	52	52	51	50	50	50	50	50	49	48	48	48
-45° Plies	62	62	62	62	62	62	62	61	60	60	60	59	58	58	58	58	58	57	56	56	56	56	56	55	54	54	54	53	52	52	52	52	52	51	50	50	50	49	48
90° Plies	16	15	14	14	14	14	14	14	14	14	14	14	14	14	14	14	14	14	14	14	14	14	14	14	14	14	14	14	14	14	14	13	12	12	12	12	12	12	12
% 0° Plies	11%	11%	11%	11%	12%	12%	12%	12%	12%	12%	12%	12%	12%	12%	12%	12%	11%	11%	11%	11%	11%	11%	10%	10%	10%	10%	10%	11%	11%	11%	11%	11%	11%	11%	11%	11%	11%	11%	11%
% ± 45° Plies	79%	79%	80%	80%	79%	79%	79%	79%	79%	79%	79%	79%	78%	78%	78%	79%	79%	79%	79%	79%	79%	79%	80%	80%	79%	79%	79%	79%	79%	79%	78%	79%	80%	80%	79%	79%	79%	79%	79%
% 90° Plies	10%	9%	9%	9%	9%	9%	9%	9%	9%	9%	9%	9%	9%	10%	10%	10%	10%	10%	10%	10%	10%	10%	10%	10%	10%	10%	10%	11%	11%	11%	11%	10%	9%	9%	10%	10%	10%	10%	10%

t Skin (mm)	30.25	30.00	29.75	29.50	29.25	29.00	28.75	28.50	28.25	28.00	27.75	27.50	27.25	27.00	26.75	26.50	26.25	26.00	25.75	25.50	25.25	25.00	24.75	24.50	24.25	24.00	23.75	23.50	23.25	23.00	22.75	22.50	22.25	22.00	21.75	21.50	21.25
No. of Plies	121	120	119	118	117	116	115	114	113	112	111	110	109	108	107	106	105	104	103	102	101	100	99	98	97	96	95	94	93	92	91	90	89	88	87	86	85
0° Plies	14	14	14	14	14	14	14	14	13	12	12	12	12	12	12	12	12	12	12	12	12	12	12	12	12	12	11	10	10	10	10	10	10	10	9	8	8
+45° Plies	47	46	46	46	45	44	44	44	44	44	43	42	42	42	42	41	41	40	40	40	39	38	38	38	38	38	38	38	37	36	36	36	35	34	34	34	34
-45° Plies	48	48	47	46	46	46	45	44	44	44	44	44	43	42	41	41	40	40	40	40	40	40	39	38	38	38	38	38	38	38	37	36	36	36	36	36	35
90° Plies	12	12	12	12	12	12	12	12	12	12	12	12	12	12	12	12	12	12	11	10	10	10	10	10	9	8	8	8	8	8	8	8	8	8	8	8	8
% 0° Plies	12%	12%	12%	12%	12%	12%	12%	12%	12%	11%	11%	11%	11%	11%	11%	11%	11%	12%	12%	12%	12%	12%	12%	12%	12%	13%	12%	11%	11%	11%	11%	11%	11%	11%	10%	9%	9%
% ± 45° Plies	79%	78%	78%	78%	78%	78%	77%	77%	78%	79%	78%	78%	78%	78%	78%	77%	77%	77%	78%	78%	78%	78%	78%	78%	78%	79%	80%	81%	81%	80%	80%	80%	80%	80%	80%	81%	81%
% 90° Plies	10%	10%	10%	10%	10%	10%	10%	11%	11%	11%	11%	11%	11%	11%	11%	11%	11%	12%	11%	10%	10%	10%	10%	10%	9%	8%	8%	9%	9%	9%	9%	9%	9%	9%	9%	9%	9%

t Skin (mm)	21.00	20.75	20.50	20.25	20.00	19.75	19.50	19.25	19.00	18.75	18.50	18.25	18.00	17.75	17.50	17.25	17.00	16.75	16.50	16.25	16.00	15.75	15.50	15.25	15.00	14.75	14.50	14.25	14.00	13.75	13.50	13.25	13.00	12.75	12.50	12.25	12.00	11.75
No. of Plies	84	83	82	81	80	79	78	77	76	75	74	73	72	71	70	69	68	67	66	65	64	63	62	61	60	59	58	57	56	55	54	53	52	51	50	49	48	47
0° Plies	8	8	8	8	8	8	8	8	8	8	8	8	8	8	8	7	6	6	6	6	6	6	6	6	6	6	6	6	6	6	6	6	6	6	6	6	6	6
+45° Plies	34	33	32	32	32	32	32	31	30	30	30	29	28	28	28	28	28	27	26	26	26	25	24	24	24	24	24	23	22	22	22	22	22	21	20	20	20	19
-45° Plies	34	34	34	33	32	31	30	30	30	30	30	30	30	29	28	28	28	28	28	27	26	26	26	25	24	23	22	22	22	21	20	20	20	20	20	19	18	18
90° Plies	8	8	8	8	8	8	8	8	8	7	6	6	6	6	6	6	6	6	6	6	6	6	6	6	6	6	6	6	6	6	6	5	4	4	4	4	4	4
% 0° Plies	10%	10%	10%	10%	10%	10%	10%	10%	11%	11%	11%	11%	11%	11%	11%	10%	9%	9%	9%	9%	9%	10%	10%	10%	10%	10%	10%	11%	11%	11%	11%	11%	12%	12%	12%	12%	13%	13%
% ± 45° Plies	81%	81%	80%	80%	80%	80%	79%	79%	79%	80%	81%	81%	81%	80%	80%	81%	82%	82%	82%	82%	81%	81%	81%	80%	80%	80%	79%	79%	79%	78%	78%	79%	81%	80%	80%	80%	79%	79%
% 90° Plies	10%	10%	10%	10%	10%	10%	10%	10%	11%	9%	8%	8%	8%	8%	9%	9%	9%	9%	9%	9%	9%	10%	10%	10%	10%	10%	10%	11%	11%	11%	11%	9%	8%	8%	8%	8%	8%	9%

t Skin (mm)	11.50	11.25	11.00	10.75	10.50	10.25	10.00	9.75	9.50	9.25	9.00	8.75	8.50	8.25	8.00	7.75	7.50	7.25	7.00	6.75	6.50	6.25	6.00	5.75	5.50	5.25	5.00	4.75	4.50	4.25	4.00	3.75	3.50	3.25
No. of Plies	46	45	44	43	42	41	40	39	38	37	36	35	34	33	32	31	30	29	28	27	26	25	24	23	22	21	20	19	18	17	16	15	14	13
0° Plies	6	6	6	6	6	6	6	6	6	5	4	3	2	2	2	2	2	2	2	2	2	2	2	2	2	2	2	2	2	2	2	2	2	2
+45° Plies	18	18	18	17	16	15	14	14	14	14	14	14	14	14	14	13	12	11	10	10	10	9	8	8	8	8	8	7	6	6	6	5	4	4
-45° Plies	18	17	16	16	16	16	16	15	14	14	14	14	14	13	12	12	12	12	12	11	10	10	10	9	8	7	6	6	6	5	4	4	4	3
90° Plies	4	4	4	4	4	4	4	4	4	4	4	4	4	4	4	4	4	4	4	4	4	4	4	4	4	4	4	4	4	4	4	4	4	4
% 0° Plies	13%	13%	14%	14%	14%	15%	15%	15%	16%	14%	11%	9%	6%	6%	6%	6%	7%	7%	7%	7%	8%	8%	8%	9%	9%	10%	10%	11%	11%	12%	13%	13%	14%	15%
% ± 45° Plies	78%	78%	77%	77%	76%	76%	75%	74%	74%	76%	78%	80%	82%	82%	81%	81%	80%	79%	79%	78%	77%	76%	75%	74%	73%	71%	70%	68%	67%	65%	63%	60%	57%	54%
% 90° Plies	9%	9%	9%	9%	10%	10%	10%	10%	11%	11%	11%	11%	12%	12%	13%	13%	13%	14%	14%	15%	15%	16%	17%	17%	18%	19%	20%	21%	22%	24%	25%	27%	29%	31%

Figure C-3: 10/80/10 UD skin laminate

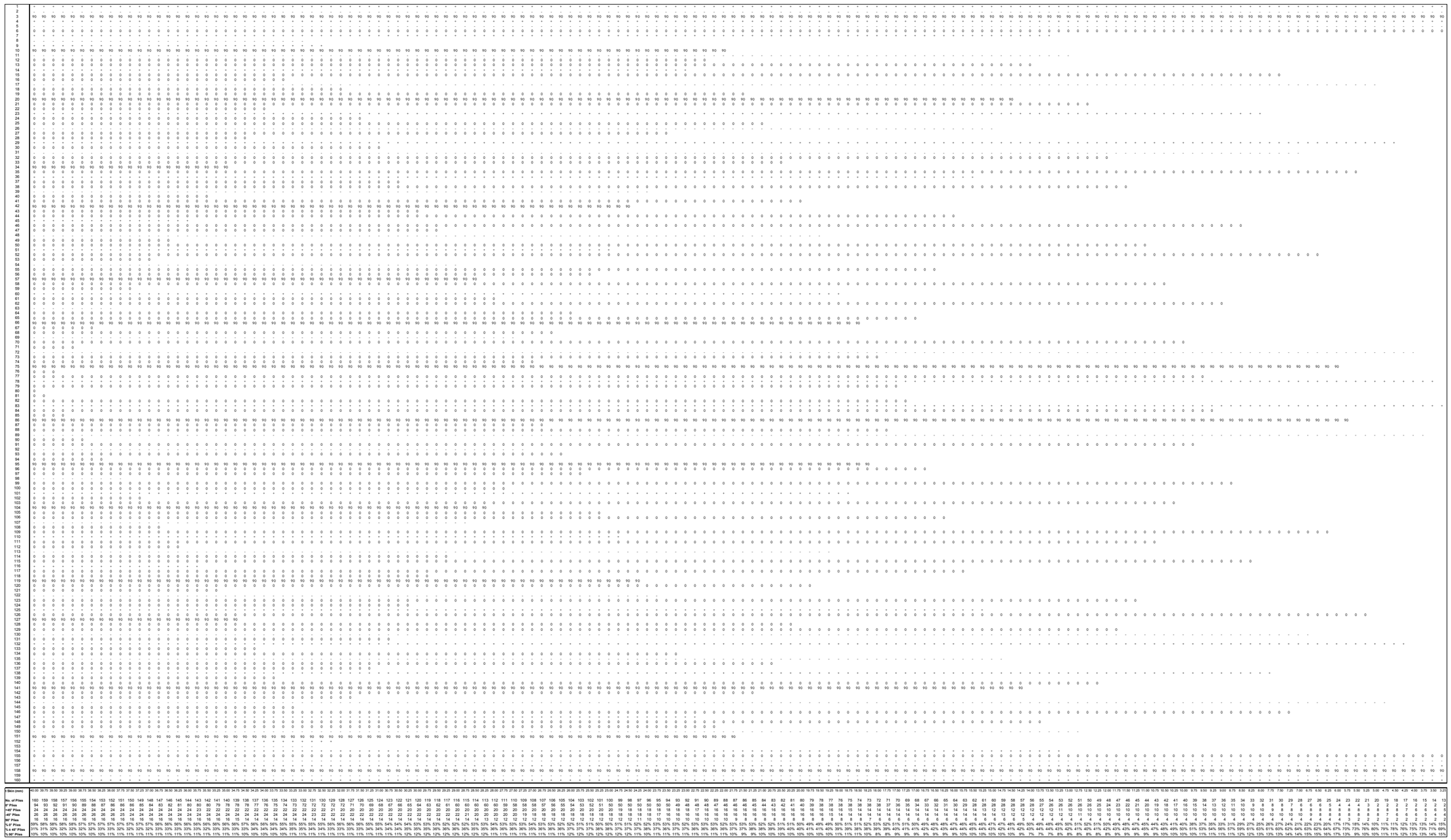

Figure C-4: Tailored UD skin laminate

C.1.2 Stringers

The stringers use 0.184mm thick plies. The stringer foot thickness is related to the skin thickness, and, furthermore, the spine thickness is related to the angle thickness, as follows:

- Stringer foot thickness to skin thickness > than 0.5[176]
- The spine thickness can be 2.4 × the thickness of the angle thickness

Therefore the different stringer configuration required for a skin thickness from 3.25-40.00mm is shown in Table C-1.

	Min Skin Thk (mm)	Max Skin Thk (mm)	Angle Thk (mm)	No. of Plies in Angle	Max Spine Thk (mm)	Max no. of Plies in Spine
Config. 1	3.25	6.50	1.656	9	7.728	42
Config. 2	6.51	9.50	2.392	13	11.224	61
Config. 3	9.51	13.75	3.496	19	16.376	89
Config. 4	13.76	19.50	4.968	27	23.184	126
Config. 5	19.51	27.75	6.992	38	32.568	177
Config. 6	27.76	40.00	9.936	54	46.000	250

Table C-1: UD prepreg stringer details

The stringers are configured as shown in Figure C-5, where the capping plate is the same thickness as the angle, thus they have plies 1-n.

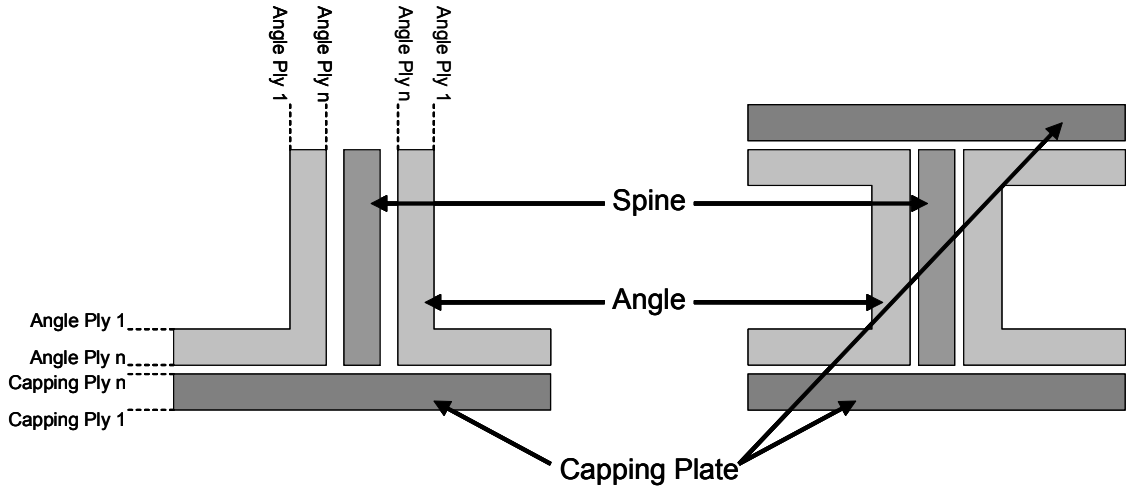

Figure C-5: Configuration for UD prepreg T- and I-profile stringers

The stacking sequences for the angles and capping plates (ply 1 - ply n) are:

- Config 1 (9 plies)
  - (+/-/0/0/90/0/0/+/-)
- Config 2 (13 plies)
  - (+/-/0/0/+/0/90/0/-/0/0/+/-)
- Config 3 (19 plies)
  - (+/-/90/0/0/+/0/0/0/90/0/0/0/-/0/0/90/+/-)
- Config 4 (27 plies)
  - (+/-/90/0/0/0/+/90/0/0/0/0/-/90/+/0/0/0/0/90/-/0/0/0/90/+/-)
- Config 5 (38)
  - (+/-/90/0/0/0/0/+/0/-/0/+/90/0/0/0/0/-/90/90/+/0/0/0/0/90/-/0/+/0/-/0/0/0/0/90/+/-)
- Config 6 (54)
  - (+/-/90/0/0/0/0/+/0/0/-/+/-/0/0/0/0/+/90/0/0/0/0/-/0/0/90/90/0/0/+/0/0/0/0/90/-/0/0/0/0/+/-/+/0/0/-/0/0/0/0/90/+/-)

The spine laminate is shown in Figure C-6 to Figure C-8.

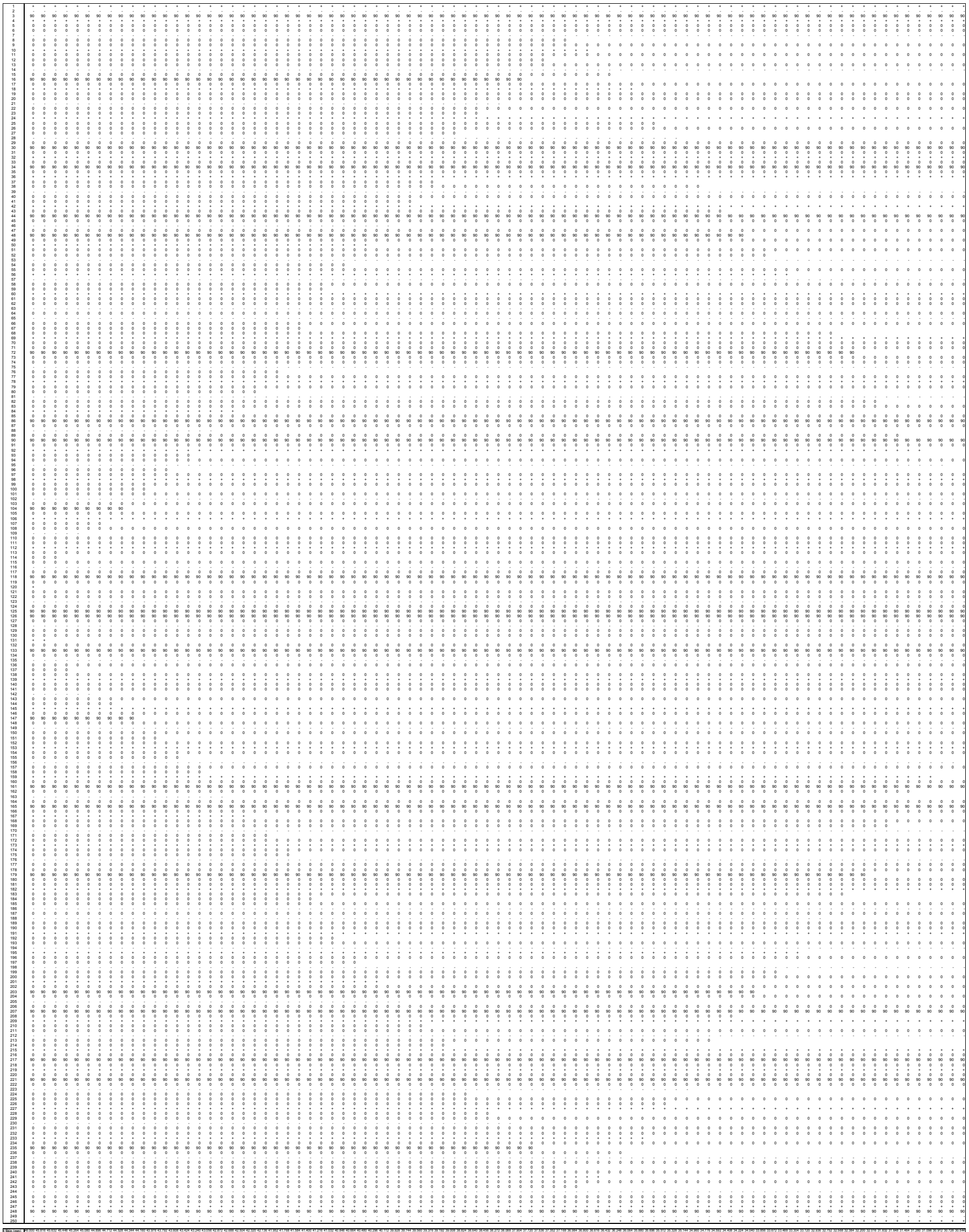

Figure C-6: 60/30/10 conventional UD stringer spine laminate (thickness from 46.000mm to 30.544mm)

1	+	+	+	+	+	+	+	+	+	+	+	+	+	+	+	+	+	+	+	+	+	+	+	+	+	+	+	+	+	+	+	+	+	+	+	+	+	+	+	+	+	+	+	+	+	+	+	+	+	+	+	+	+	+	+	+	+	+	+	+	+	+	+	+	+	+	+	+	+	+	+	+	+	+	+	+	+	+	+	+	+	+	+	+	+
2	-	-	-	-	-	-	-	-	-	-	-	-	-	-	-	-	-	-	-	-	-	-	-	-	-	-	-	-	-	-	-	-	-	-	-	-	-	-	-	-	-	-	-	-	-	-	-	-	-	-	-	-	-	-	-	-	-	-	-	-	-	-	-	-	-	-	-	-	-	-	-	-	-	-	-	-	-	-	-	-	-	-	-	-	-
3	90	90	90	90	90	90	90	90	90	90	90	90	90	90	90	90	90	90	90	90	90	90	90	90	90	90	90	90	90	90	90	90	90	90	90	90	90	90	90	90	90	90	90	90	90	90	90	90	90	90	90	90	90	90	90	90	90	90	90	90	90	90	90	90	90	90	90	90	90	90	90	90	90	90	90	90	90	90	90	90	90	90	90	90	90
4	+	+	+	+	+	+	+	+	+	+	+	+	+	+	+	+	+	+	+	+	+	+	+	+	+	+	+	+	+	+	+	+	+	+	+	+	+	+	+	+	+	+	+	+	+	+	+	+	+	+	+	+	+	+	+	+	+	+	+	+	+	+	+	+	+	+	+	+	+	+	+	+	+	+	+	+	+	+	+	+	+	+	+	+	+
5	0	0	0	0	0	0	0	0	0	0	0	0	0	0	0	0	0	0	0	0	0	0	0	0	0	0	0	0	0	0	0	0	0	0	0	0	0	0	0	0	0	0	0	0	0	0	0	0	0	0	0	0	0	0	0	0	0	0	0	0	0	0	0	0	0	0	0	0	0	0	0	0	0	0	0	0	0	0	0	0	0	0	0	0	0
6	0	0	0	0	0	0	0	0	0	0	0	0	0	0	0	0	0	0	0	0	0	0	0	0	0	0	0	0	0	0	0	0	0	0	0	0	0	0	0	0	0	0	0	0	0	0	0	0	0	0	0	0	0	0	0	0	0	0	0	0	0	0	0	0	0	0	0	0	0	0	0	0	0	0	0	0	0	0	0	0	0	0	0	0	0
7	-	-	-	-	-	-	-	-	-	-	-	-	-	-	-	-	-	-	-	-	-	-	-	-	-	-	-	-	-	-	-	-	-	-	-	-	-	-	-	-	-	-	-	-	-	-	-	-	-	-	-	-	-	-	-	-	-	-	-	-	-	-	-	-	-	-	-	-	-	-	-	-	-	-	-	-	-	-	-	-	-	-	-	-	-
8																																																																																					
9	0	0	0	0	0	0	0	0	0	0	0	0	0	0	0	0	0	0	0	0	0	0	0	0	0	0	0	0	0	0	0	0	0	0	0	0	0	0	0	0	0	0	0	0	0	0	0	0	0	0	0	0	0	0	0	0	0	0	0	0	0	0	0	0	0	0	0	0	0	0	0	0	0	0	0	0	0	0	0	0	0	0	0	0	0
10																																																																																					
11	0	0	0	0	0	0	0	0	0	0	0	0	0	0	0	0	0	0	0	0	0	0	0	0	0	0	0	0	0	0	0	0	0	0	0	0	0	0	0	0	0	0	0	0	0	0	0	0	0	0	0	0	0	0	0	0	0	0	0	0	0	0	0	0	0	0	0	0	0	0	0	0	0	0	0	0	0	0	0	0	0	0	0	0	0
12																																																																																					
13	0	0	0	0	0	0	0	0	0	0	0	0	0	0	0	0	0	0	0	0	0	0	0	0	0	0	0	0	0	0	0	0	0	0	0	0	0	0	0	0																																												
14	-	-	-	-	-	-	-	-	-	-	-	-	-	-	-	-	-	-	-	-	-	-	-	-	-	-	-	-	-	-	-	-	-	-	-	-	-	-	-	-	-	-	-	-	-	-	-	-	-	-	-	-	-	-	-	-	-	-	-	-	-	-	-	-	-	-	-	-	-	-	-	-	-	-	-	-	-	-	-	-	-	-	-	-	-
15																																																																																					
16																																																																																					
17	0	0	0	0	0	0	0	0	0	0	0	0	0	0	0	0	0	0	0	0	0	0	0	0	0	0	0	0	0	0	0	0	0	0	0	0	0	0	0	0	0	0																																										
18																																																																																					
19	0	0	0	0	0	0	0	0	0	0	0	0	0	0	0	0	0	0	0	0	0	0	0	0	0	0	0	0	0	0	0	0	0	0	0	0	0	0	0	0	0	0	0	0	0	0	0	0	0	0	0	0	0	0	0	0	0	0	0	0	0	0	0	0	0	0	0	0	0	0	0	0	0	0	0	0	0	0	0	0	0	0	0	0	0
20	0	0	0	0	0	0	0	0	0	0	0	0	0	0	0	0	0	0	0	0	0	0	0	0	0	0	0	0	0	0	0	0	0	0	0	0	0	0
21																																																																																					
22	0	0	0	0	0	0	0	0	0	0	0	0	0	0	0	0	0	0	0	0	0	0	0	0	0	0	0	0	0	0	0	0	0	0	0	0	0	0	0	0	0	0	0	0																																								
23																																																																																					
24	+	+	+	+	+	+	+	+	+	+	+	+	+	+	+	+	+	+	+	+	+	+	+	+	+	+	+	+	+	+	+	+	+	+	+	+	+	+	+	+	+	+	+	+	+	+																																						
25																																																																																					
26	0	0	0	0	0	0	0	0	0	0	0	0	0	0	0	0	0	0	0	0	0	0	0	0	0	0	0	0	0	0	0	0	0	0	0	0	0	0	0	0	0	0	0	0	0	0	0	0	0	0	0	0	0	0	0	0	0	0	0	0	0	0	0	0	0	0	0	0	0	0	0	0	0	0	0	0	0	0	0	0	0	0	0	0	0
27																																																																																					
28																																																																																					
29	0	0	0	0	0	0	0	0	0	0	0	0	0	0	0	0	0	0	0	0	0	0	0	0	0	0	0	0	0	0	0	0	0	0	0	0	0	0	0	0	0	0	0	0	0	0	0	0	0	0	0	0	0	0	0	0	0	0	0	0	0	0	0	0	0	0	0	0	0	0	0	0	0	0	0	0	0	0	0	0	0	0	0	0	0
30	90	90	90	90	90	90	90	90	90	90	90	90	90	90	90	90	90	90	90	90	90	90	90	90	90	90	90	90	90	90	90	90	90	90	90	90	90	90	90	90	90	90	90	90	90	90	90	90	90	90	90	90	90	90	90	90	90	90	90	90	90	90	90	90	90	90	90	90	90	90	90	90	90	90	90	90	90	90	90	90	90	90	90	90	90
31	0	0	0	0	0	0	0	0	0	0	0	0	0	0	0	0	0	0	0	0	0	0	0	0	0	0	0	0	0	0	0	0	0	0	0	0	0	0	0	0	0	0	0	0	0	0	0	0	0	0	0	0	0	0	0	0	0	0	0	0	0	0	0	0	0	0	0	0	0	0	0	0	0	0	0	0	0	0	0	0	0	0	0	0	0
32	+	+	+	+	+	+	+	+	+	+	+	+	+	+	+	+	+	+	+	+	+	+	+	+	+	+	+	+	+	+	+	+	+	+	+	+	+	+	+	+	+	+	+	+	+	+	+	+	+	+	+	+	+	+	+	+	+	+	+	+	+	+	+	+	+	+	+	+	+	+	+	+	+	+	+	+	+	+	+	+	+	+	+	+	+
33	0	0	0	0	0	0	0	0	0	0	0	0	0	0	0	0	0	0	0	0	0	0	0	0	0	0	0	0	0	0	0	0	0	0	0	0																																																
34	90	90	90	90	90	90	90	90	90	90	90	90	90	90	90	90	90	90	90	90	90	90	90	90	90	90	90	90	90	90	90	90	90	90	90	90	90	90	90	90	90	90	90	90	90	90	90	90	90	90	90	90	90	90	90	90	90	90	90	90	90	90	90	90	90	90	90	90	90	90	90	90	90	90	90	90	90	90	90	90	90	90	90	90	90
35	0	0	0	0	0	0	0	0	0	0	0	0	0	0	0	0	0	0	0	0	0	0	0	0	0	0	0	0	0	0	0	0	0	0	0	0	0	0	0	0	0	0	0	0	0	0	0	0	0	0	0	0	0	0	0	0	0	0	0	0	0	0	0	0	0	0	0	0	0	0	0	0	0	0	0	0	0	0	0	0	0	0	0	0	0
36	+	+	+	+	+	+	+	+	+	+	+	+	+	+	+	+	+	+	+	+	+	+	+	+	+	+	+	+	+	+	+	+	+	+	+	+	+	+	+	+	+	+	+	+	+	+	+	+	+	+	+	+	+	+	+	+	+	+	+	+	+	+	+	+	+	+	+	+	+	+	+	+	+	+	+	+	+	+	+	+	+	+	+	+	+
37																																																																																					
38																																																																																					
39	-	-	-	-	-	-	-	-	-	-	-	-	-	-	-	-	-	-	-	-	-	-	-	-	-	-	-	-	-	-	-	-	-	-	-	-	-	-	-	-	-	-	-	-	-	-	-	-																																				
40	0	0	0	0	0	0	0	0	0	0	0	0	0	0	0	0	0	0	0	0	0	0	0	0	0	0	0	0	0	0	0	0	0	0																																																		
41																																																																																					
42	+	+	+	+	+	+	+	+	+	+	+	+	+	+	+	+	+	+	+	+	+	+	+	+	+	+	+	+	+	+	+	+	+	+	+	+	+	+	+	+	+	+	+	+	+	+	+	+	+	+	+	+	+	+	+	+	+	+	+	+	+	+	+	+	+	+	+	+	+	+	+	+	+	+	+	+	+	+	+	+	+	+	+	+	+
43																																																																																					
44	90	90	90	90	90	90	90	90	90	90	90	90	90	90	90	90	90	90	90	90	90	90	90	90	90	90	90	90	90	90	90	90	90	90	90	90	90	90	90	90	90	90	90	90	90	90	90	90	90	90	90	90	90	90	90	90	90	90	90	90	90	90	90	90	90	90	90	90	90	90	90	90	90	90	90	90	90	90	90	90	90	90	90	90	90
45	0	0	0	0	0	0	0	0	0	0	0	0	0	0	0	0	0	0	0	0	0	0	0	0	0	0	0	0	0	0	0	0	0	0	0	0	0	0	0	0	0	0	0	0	0	0	0	0	0	0	0	0	0	0	0	0	0	0	0	0	0	0	0	0	0	0	0	0	0	0	0	0	0	0	0	0	0	0	0	0	0	0	0	0	0
46																																																																																					
47	0	0	0	0	0	0	0	0	0	0	0	0	0	0	0	0	0	0	0	0	0	0	0	0	0	0	0	0	0	0	0	0	0	0	0	0	0	0	0	0	0	0	0	0	0	0	0	0	0	0																																		
48																																																																																					
49	0	0	0	0	0	0	0	0	0	0	0	0	0	0	0	0	0	0	0	0	0	0	0	0	0	0	0	0	0	0	0	0	0	0	0	0	0	0	0	0	0	0	0	0	0	0	0	0	0	0	0	0	0	0	0	0	0	0	0	0	0	0	0	0	0	0	0	0	0	0	0	0	0	0	0	0	0	0	0	0	0	0	0	0	0
50																																																																																					
51	0	0	0	0	0	0	0	0	0	0	0	0	0	0	0	0	0	0	0	0	0	0	0	0	0	0	0	0	0	0	0	0																																																				
52																																																																																					
53	-	-	-	-	-	-	-	-	-	-	-	-	-	-	-	-	-	-	-	-	-	-	-	-	-	-	-	-	-	-	-	-	-	-	-	-	-	-	-	-	-	-	-	-	-	-	-	-	-	-	-	-	-	-	-	-	-	-	-	-	-	-	-	-	-	-	-	-	-	-	-	-	-	-	-	-	-	-	-	-	-	-	-	-	-
54																																																																																					
55	0	0	0	0	0	0	0	0	0	0	0	0	0	0	0	0	0	0	0	0	0	0	0	0	0	0	0	0	0	0	0	0	0	0	0	0	0	0	0	0	0	0	0	0	0	0	0	0	0	0	0	0																																			
56																																																																																					
57	-	-	-	-	-	-	-	-	-	-	-	-	-	-	-	-	-	-	-	-	-	-	-	-	-	-	-	-	-	-																																																						
58	0	0	0	0	0	0	0	0	0	0	0	0	0	0	0	0	0	0	0	0	0	0	0	0	0	0	0	0	0	0	0	0	0	0	0	0	0	0	0	0	0	0	0	0	0	0	0	0	0	0	0	0	0	0	0	0	0	0	0	0	0	0	0	0	0	0	0	0	0	0	0	0	0	0	0	0	0	0	0	0	0	0	0	0	0
59																																																																																					
60	+	+	+	+	+	+	+	+	+	+	+	+	+	+	+	+	+	+	+	+	+	+	+	+	+	+	+	+	+	+	+	+	+	+	+	+	+	+	+	+	+	+	+	+	+	+	+	+	+	+	+	+	+	+																														
61	0	0	0	0	0	0	0	0	0	0	0	0	0	0	0	0	0	0	0	0	0	0	0	0	0	0	0	0	0	0	0	0	0	0	0	0	0	0	0	0	0	0	0	0	0	0	0	0	0	0	0	0	0	0	0	0	0	0	0	0	0	0	0	0	0	0	0	0	0	0	0	0	0	0	0	0	0	0	0	0	0	0	0	0	0
62	0	0	0	0	0	0	0	0	0	0	0	0	0	0	0	0	0	0	0	0	0	0	0	0	0	0	0	0	0	0	0	0	0	0	0	0	0	0	0	0	0	0	0	0	0	0	0	0	0	0	0	0	0	0	0	0																												
63																																																																																					
64	0	0	0	0	0	0	0	0	0	0	0	0	0	0	0	0	0	0	0	0	0	0	0	0	0	0	0	0																																																								
65	-	-	-	-	-	-	-	-	-	-	-	-	-	-	-	-	-	-	-	-	-	-	-	-	-	-	-	-	-	-	-	-	-	-	-	-	-	-	-	-	-	-	-	-	-	-	-	-	-	-	-	-	-	-	-	-	-	-	-	-	-	-	-	-	-	-	-	-	-	-	-	-	-	-	-	-	-	-	-	-	-	-	-	-	-
66	0	0	0	0	0	0	0	0	0	0	0	0	0	0	0	0	0	0	0	0	0	0	0	0	0	0	0	0	0	0	0	0	0	0	0	0	0	0	0	0	0	0	0	0	0	0	0	0	0	0	0	0	0	0	0	0	0	0																										
67																																																																																					
68																																																																																					
69	+	+	+	+	+	+	+	+	+	+	+	+	+	+	+	+	+	+	+	+	+	+	+	+	+	+																																																										
70	0	0	0	0	0	0	0	0	0	0	0	0	0	0	0	0	0	0	0	0	0	0	0	0	0	0	0	0	0	0	0	0	0	0	0	0	0	0	0	0	0	0	0	0	0	0	0	0	0	0	0	0	0	0	0	0	0	0	0	0	0	0	0	0	0	0	0	0	0	0	0	0	0	0	0	0	0	0	0	0	0	0	0	0	0
71	0	0	0	0	0	0	0	0	0	0	0	0	0	0	0	0	0	0	0	0	0	0	0	0	0	0	0	0	0	0	0	0	0	0	0	0	0	0	0	0	0	0	0	0	0	0	0	0	0	0	0	0	0	0	0	0	0	0	0	0	0	0	0	0	0	0	0	0	0	0	0	0	0	0	0	0	0	0	0	0	0	0	0	0	0
72																																																																																					
73	0	0	0	0	0	0	0	0	0	0	0	0	0	0	0	0	0	0	0	0	0	0	0	0																																																												
74	0	0	0	0	0	0	0	0	0	0	0	0	0	0	0	0	0	0	0	0	0	0	0	0	0	0	0	0	0	0	0	0	0	0	0	0	0	0	0	0	0	0	0	0	0	0	0	0	0	0	0	0	0	0	0	0	0	0	0	0	0	0	0	0	0	0	0	0	0	0	0	0	0	0	0	0	0	0	0	0	0	0	0	0	0
75	-	-	-	-	-	-	-	-	-	-	-	-	-	-	-	-	-	-	-	-	-	-	-	-	-	-	-	-	-	-	-	-	-	-	-	-	-	-	-	-	-	-	-	-	-	-	-	-	-	-	-	-	-	-	-	-	-	-	-	-																								
76																																																																																					
77	0	0	0	0	0	0	0	0	0	0	0	0	0	0	0	0	0	0	0	0	0	0																																																														
78	+	+	+	+	+	+	+	+	+	+	+	+	+	+	+	+	+	+	+	+	+	+	+	+	+	+	+	+	+	+	+	+	+	+	+	+	+	+	+	+	+	+	+	+	+	+	+	+	+	+	+	+	+	+	+	+	+	+	+	+	+	+	+	+	+	+	+	+	+	+	+	+	+	+	+	+	+	+	+	+	+	+	+	+	+
79	0	0	0	0	0	0	0	0	0	0	0	0	0	0	0	0	0	0	0	0	0	0	0	0	0	0	0	0	0	0	0	0	0	0	0	0	0	0	0	0	0	0	0	0	0	0	0	0	0	0	0	0	0	0	0	0	0	0	0	0	0	0	0	0	0	0	0	0	0	0	0	0	0	0	0	0	0	0	0	0	0	0	0	0	0
80																																																																																					
81	-	-	-	-	-	-	-	-	-	-	-	-	-	-	-	-	-	-	-	-	-	-	-	-	-	-	-	-	-	-	-	-	-	-	-	-	-	-	-	-	-	-	-	-	-	-	-	-	-	-	-	-	-	-	-	-	-	-	-	-	-	-	-	-	-	-	-	-	-	-	-	-	-	-	-	-	-	-	-	-	-	-	-	-	-
82																																																																																					
83	0	0	0	0	0	0	0	0	0	0	0	0	0	0	0	0	0	0	0	0																																																																
84																																																																																					
85	0	0	0	0	0	0	0	0	0	0	0	0	0	0	0	0	0	0	0	0	0	0	0	0	0	0	0	0	0	0	0	0	0	0	0	0	0	0	0	0	0	0	0	0	0	0	0	0	0	0	0	0	0	0	0	0	0	0	0	0	0	0																						
86	90	90	90	90	90	90	90	90	90	90	90	90	90	90	90	90	90	90																																																																		
87	0	0	0	0	0	0	0	0	0	0	0	0	0	0	0	0	0	0	0	0	0	0	0	0	0	0	0	0	0	0	0	0	0	0	0	0	0	0	0	0	0	0	0	0	0	0	0	0	0	0	0	0	0	0	0	0	0	0	0	0	0	0	0	0	0	0	0	0	0	0	0	0	0	0	0	0	0	0	0	0	0	0	0	0	0
88																																																																																					
89																																																																																					
90	90	90	90	90	90	90	90	90	90	90	90	90	90	90	90	90	90	90	90	90	90	90	90	90	90	90	90	90	90	90	90	90	90	90	90	90	90	90	90	90	90	90	90	90	90	90	90	90	90	90	90	90	90	90	90	90	90	90	90	90	90	90	90	90																				
91	0	0	0	0	0	0	0	0	0	0	0	0	0	0	0	0	0	0	0	0	0	0	0	0	0	0	0	0	0	0	0	0	0	0	0	0	0	0	0	0	0	0	0	0	0	0	0	0	0	0	0	0	0	0	0	0	0	0	0	0	0	0	0	0	0	0	0	0	0	0	0	0	0	0	0	0	0	0	0	0	0	0	0	0	0
92																																																																																					
93																																																																																					
94	0	0	0	0	0	0	0	0	0	0	0	0	0	0	0	0																																																																				
95																																																																																					
96																																																																																					
97	0	0	0	0	0	0	0	0	0	0	0	0	0	0	0	0	0	0	0	0	0	0	0	0	0	0	0	0	0	0	0	0	0	0	0	0	0	0	0	0	0	0	0	0	0	0	0	0	0	0	0	0	0	0	0	0	0	0	0	0	0	0	0	0	0	0	0	0	0	0	0	0	0	0	0	0	0	0	0	0	0	0	0	0	0
98	+	+	+	+	+	+	+	+	+	+	+	+	+	+	+	+	+	+	+	+	+	+	+	+	+	+	+	+	+	+	+	+	+	+	+	+	+	+	+	+	+	+	+	+	+	+	+	+	+	+	+	+	+	+	+	+	+	+	+	+	+	+	+	+	+	+	+	+	+	+	+	+	+	+	+	+	+	+	+	+	+	+	+		
99	0	0	0	0	0	0	0	0	0	0	0	0	0	0	0	0	0	0	0	0	0	0	0	0	0	0	0	0	0	0	0	0	0	0	0	0	0	0	0	0	0	0	0	0	0	0	0	0	0	0	0	0	0	0	0	0	0	0	0	0	0	0	0	0	0	0																		
100																																																																																					
101																																																																																					
102	-	-	-	-	-	-	-	-	-	-	-	-	-	-																																																																						
103	0	0	0	0	0	0	0	0	0	0	0	0	0	0	0	0	0	0	0	0	0	0	0	0	0	0	0	0	0	0	0	0	0	0	0	0	0	0	0	0	0	0	0	0	0	0	0	0	0	0	0	0	0	0	0	0	0	0	0	0	0	0	0	0	0	0	0	0	0	0	0	0	0	0	0	0	0	0	0	0	0				
104																																																																																					
105	0	0	0	0	0	0	0	0	0	0	0	0	0	0	0	0	0	0	0	0	0	0	0	0	0	0	0	0	0	0	0	0	0	0	0	0	0	0	0	0	0	0	0	0	0	0	0	0	0	0	0	0	0	0	0	0	0	0	0	0	0	0	0	0	0	0	0	0	0	0	0	0	0	0	0	0	0	0	0	0	0	0	0	0	0
106	+	+	+	+	+	+	+	+	+	+	+	+	+	+	+	+	+	+	+	+	+	+	+	+	+	+	+	+	+	+	+	+	+	+	+	+	+	+	+	+	+	+	+	+	+	+	+	+	+	+	+	+	+	+	+	+	+	+	+	+	+	+	+	+	+	+	+	+	+	+	+	+	+	+	+	+	+	+	+	+	+	+	+	+	+
107																																																																																					
108	0	0																																																																																			
109																																																																																					
110	0	0	0	0	0	0	0	0	0	0	0	0	0	0	0	0	0	0	0	0	0	0	0	0	0	0	0	0	0	0	0	0	0	0	0	0	0	0	0	0	0	0	0	0	0	0	0	0	0	0	0	0	0	0	0	0	0	0	0	0	0	0	0	0	0	0	0	0																
111	0	0	0	0	0	0	0	0	0	0	0	0	0	0	0	0	0	0	0	0	0	0	0	0	0	0	0	0	0	0	0	0	0	0	0	0	0	0	0	0	0	0	0	0	0	0	0	0	0	0	0	0	0	0	0	0	0	0	0	0	0	0	0	0	0	0	0	0	0	0	0	0	0	0	0	0	0	0	0	0	0	0	0	0	0
112	+	+	+	+	+	+	+	+	+	+	+	+																																																																									
113	0	0	0	0	0	0	0	0	0	0	0	0	0	0	0	0	0	0	0	0	0	0	0	0	0	0	0	0	0	0	0	0	0	0	0	0	0	0	0	0	0	0	0	0	0	0	0	0	0	0	0	0	0	0	0	0	0	0	0	0	0	0	0	0	0	0	0	0	0	0	0	0	0	0	0	0	0	0	0	0	0	0	0	0	0
114																																																																																					
115	0	0	0	0																																																																																	
116	-	-	-	-	-	-	-	-	-	-	-	-	-	-	-	-	-	-	-	-	-	-	-	-	-	-	-	-	-	-	-	-	-	-	-	-	-	-	-	-	-	-	-	-	-	-	-	-	-	-	-	-	-	-	-	-	-	-	-	-	-	-	-	-	-	-	-	-	-	-														
117	0	0	0	0	0	0	0	0	0	0	0	0	0	0	0	0	0	0	0	0	0	0	0	0	0	0	0	0	0	0	0	0	0	0	0	0	0	0	0	0	0	0	0	0	0	0	0	0	0	0	0	0	0	0	0	0	0	0	0	0	0	0	0	0	0	0	0	0	0	0	0	0	0	0	0	0	0	0	0						
118	90	90	90	90	90	90	90	90	90	90																																																																										
119	0	0	0	0	0	0	0	0	0	0	0	0	0	0	0	0	0	0	0	0	0	0	0	0	0	0	0	0	0	0	0	0	0	0	0	0	0	0	0	0	0	0	0	0	0	0	0	0	0	0	0	0	0	0	0	0	0	0	0	0	0	0	0	0	0	0	0	0	0	0	0	0	0	0	0	0	0	0	0	0	0	0	0	0	0
120																																																																																					
121	0	0	0	0	0	0																																																																															
122	0	0	0	0	0	0	0	0	0	0	0	0	0	0	0	0	0	0	0	0	0	0	0	0	0	0	0	0	0	0	0	0	0	0	0	0	0	0	0	0	0	0	0	0	0	0	0	0	0	0	0	0	0	0	0	0	0	0	0	0	0	0	0	0	0	0	0	0	0	0	0	0	0												
123	-	-	-	-	-	-	-	-	-	-	-	-	-	-	-	-	-	-	-	-	-	-	-	-	-	-	-	-	-	-	-	-	-	-	-	-	-	-	-	-	-	-	-	-	-	-	-	-	-	-	-	-	-	-	-	-	-	-	-	-	-	-	-	-	-	-	-	-	-	-	-	-	-	-	-	-	-	-	-	-	-	-	-	-	-
124	0	0	0	0	0	0	0	0																																																																													
125	90	90	90	90	90	90	90	90	90	90	90	90	90	90	90	90	90	90	90	90	90	90	90	90	90	90	90	90	90	90	90	90	90	90	90	90	90	90	90	90	90	90	90	90	90	90	90	90	90	90	90	90	90	90	90	90	90	90	90	90	90	90	90	90	90	90	90	90	90	90	90	90	90	90	90	90									
126	90	90	90	90	90	90	90	90	90	90	90	90	90	90	90	90	90	90	90	90	90	90	90	90	90	90	90	90	90	90	90	90	90	90	90	90	90	90	90	90	90	90	90	90	90	90	90	90	90	90	90	90	90	90	90	90	90	90	90	90	90	90	90	90	90	90	90	90	90	90	90	90	90	90	90	90	90	90							
127	0	0	0	0	0	0	0	0	0																																																																												
128	-	-	-	-	-	-	-	-	-	-	-	-	-	-	-	-	-	-	-	-	-	-	-	-	-	-	-	-	-	-	-	-	-	-	-	-	-	-	-	-	-	-	-	-	-	-	-	-	-	-	-	-	-	-	-	-	-	-	-	-	-	-	-	-	-	-	-	-	-	-	-	-	-	-	-	-	-	-	-	-	-	-	-	-	-
129	0	0	0	0	0	0	0	0	0	0	0	0	0	0	0	0	0	0	0	0	0	0	0	0	0	0	0	0	0	0	0	0	0	0	0	0	0	0	0	0	0	0	0	0	0	0	0	0	0	0	0	0	0	0	0	0	0	0	0	0	0	0	0	0	0	0	0	0	0	0	0	0	0	0											
130	0	0	0	0	0	0	0																																																																														
131																																																																																					
132	0	0	0	0	0	0	0	0	0	0	0	0	0	0	0	0	0	0	0	0	0	0	0	0	0	0	0	0	0	0	0	0	0	0	0	0	0	0	0	0	0	0	0	0	0	0	0	0	0	0	0	0	0	0	0	0	0	0	0	0	0	0	0	0	0	0	0	0	0	0	0	0	0	0	0	0	0	0	0	0	0	0	0	0	0
133	90	90	90	90	90	90	90	90	90	90	90																																																																									
134	0	0	0	0	0	0	0	0	0	0	0	0	0	0	0	0	0	0	0	0	0	0	0	0	0	0	0	0	0	0	0	0	0	0	0	0	0	0	0	0	0	0	0	0	0	0	0	0	0	0	0	0	0	0	0	0	0	0	0	0	0	0	0	0	0	0	0	0	0	0	0	0	0	0	0	0	0	0	0	0					
135	-	-	-	-	-	-	-	-	-	-	-	-	-	-	-	-	-	-	-	-	-	-	-	-	-	-	-	-	-	-	-	-	-	-	-	-	-	-	-	-	-	-	-	-	-	-	-	-	-	-	-	-	-	-	-	-	-	-	-	-	-	-	-	-	-	-	-	-	-	-	-														
136	0	0	0	0	0																																																																																
137																																																																																					
138	0	0	0	0	0	0	0	0	0	0	0	0	0	0	0	0	0	0	0	0	0	0	0	0	0	0	0	0	0	0	0	0	0	0	0	0	0	0	0	0	0	0	0	0	0	0	0	0	0	0	0	0	0	0	0	0	0	0	0	0	0	0	0	0	0	0	0	0	0	0	0	0	0	0	0	0	0	0	0	0	0	0	0	0	0
139	+	+	+	+	+	+	+	+	+	+	+	+	+																																																																								
140	0	0	0	0	0	0	0	0	0	0	0	0	0	0	0	0	0	0	0	0	0	0	0	0	0	0	0	0	0	0	0	0	0	0	0	0	0	0	0	0	0	0	0	0	0	0	0	0	0	0	0	0	0	0	0	0	0	0	0	0	0	0	0	0	0	0	0	0	0	0	0	0	0	0	0	0	0	0	0	0	0	0	0	0	0
141	0	0	0	0	0	0	0	0	0	0	0	0	0	0	0	0	0	0	0	0	0	0	0	0	0	0	0	0	0	0	0	0	0	0	0	0	0	0	0	0	0	0	0	0	0	0	0	0	0	0	0	0	0	0	0	0	0	0	0	0	0	0	0	0	0	0	0	0	0															
142																																																																																					
143	0	0	0																																																																																		
144																																																																																					
145	+	+	+	+	+	+	+	+	+	+	+	+	+	+	+	+	+	+	+	+	+	+	+	+	+	+	+	+	+	+	+	+	+	+	+	+	+	+	+	+	+	+	+	+	+	+	+	+	+	+	+	+	+	+	+	+	+	+	+	+	+	+	+	+	+	+	+	+	+	+	+	+	+	+	+	+	+	+	+	+	+	+	+	+	+
146	0	0	0	0	0	0	0	0	0	0	0	0	0	0	0	0	0	0	0	0	0	0	0	0	0	0	0	0	0	0	0	0	0	0	0	0	0	0	0	0	0	0	0	0	0	0	0	0	0	0	0	0	0	0	0	0	0	0	0	0	0	0	0	0	0	0	0	0	0	0	0	0	0	0	0	0	0	0	0	0	0	0	0	0	0
147																																																																																					
148	0	0	0	0	0	0	0	0	0	0	0	0	0	0	0	0	0	0	0	0	0	0	0	0	0	0	0	0	0	0	0	0	0	0	0	0	0	0	0	0	0	0	0	0	0	0	0	0	0	0	0	0	0	0	0	0	0	0	0	0	0	0	0	0	0	0	0	0	0	0	0	0	0	0	0	0	0	0	0	0	0	0			
149	-	-	-	-	-	-	-	-	-	-	-	-	-	-	-																																																																					
150	0																																																																																				
151																																																																																					
152	0	0	0	0	0	0	0	0	0	0	0	0	0	0	0	0	0	0	0	0	0	0	0	0	0	0	0	0	0	0	0	0	0	0	0	0	0	0	0	0	0	0	0	0	0	0	0	0	0	0	0	0	0	0	0	0	0	0	0	0	0	0	0	0	0	0	0																	
153	+	+	+	+	+	+	+	+	+	+	+	+	+	+	+	+	+	+	+	+	+	+	+	+	+	+	+	+	+	+	+	+	+	+	+	+	+	+	+	+	+	+	+	+	+	+	+	+	+	+	+	+	+	+	+	+	+	+	+	+	+	+	+	+	+	+	+	+	+	+	+	+	+	+	+	+	+	+	+	+	+	+	+	+	
154	0	0	0	0	0	0	0	0	0	0	0	0	0	0	0	0	0	0	0	0	0	0	0	0	0	0	0	0	0	0	0	0	0	0	0	0	0	0	0	0	0	0	0	0	0	0	0	0	0	0	0	0	0	0	0	0	0	0	0	0	0	0	0	0	0	0	0	0	0	0	0	0	0	0	0	0	0	0	0	0	0	0	0	0	0
155																																																																																					
156																																																																																					
157	0	0	0	0	0	0	0	0	0	0	0	0	0	0	0	0	0																																																																				
158																																																																																					
159																																																																																					
160	0	0	0	0	0	0	0	0	0	0	0	0	0	0	0	0	0	0	0	0	0	0	0	0	0	0	0	0	0	0	0	0	0	0	0	0	0	0	0	0	0	0	0	0	0	0	0	0	0	0	0	0	0	0	0	0	0	0	0	0	0	0	0	0	0	0	0	0	0	0	0	0	0	0	0	0	0	0	0	0	0	0	0	0	0
161	90	90	90	90	90	90	90	90	90	90	90	90	90	90	90	90	90	90	90	90	90	90	90	90	90	90	90	90	90	90	90	90	90	90	90	90	90	90	90	90	90	90	90	90	90	90	90	90	90	90	90	90	90	90	90	90	90	90	90	90	90	90	90	90	90																			
162																																																																																					
163																																																																																					
164	0	0	0	0	0	0	0	0	0	0	0	0	0	0	0	0	0	0	0	0	0	0	0	0	0	0	0	0	0	0	0	0	0	0	0	0	0	0	0	0	0	0	0	0	0	0	0	0	0	0	0	0	0	0	0	0	0	0	0	0	0	0	0	0	0	0	0	0	0	0	0	0	0	0	0	0	0	0	0	0	0	0	0	0	0
165	90	90	90	90	90	90	90	90	90	90	90	90	90	90	90	90	90	90	90																																																																		
166	0	0	0	0	0	0	0	0	0	0	0	0	0	0	0	0	0	0	0	0	0	0	0	0	0	0	0	0	0	0	0	0	0	0	0	0	0	0	0	0	0	0	0	0	0	0	0	0	0	0	0	0	0	0	0	0	0	0	0	0	0	0	0																					
167																																																																																					
168	0	0	0	0	0	0	0	0	0	0	0	0	0	0	0	0	0	0	0	0	0																																																																
169																																																																																					
170	-	-	-	-	-	-	-	-	-	-	-	-	-	-	-	-	-	-	-	-	-	-	-	-	-	-	-	-	-	-	-	-	-	-	-	-	-	-	-	-	-	-	-	-	-	-	-	-	-	-	-	-	-	-	-	-	-	-	-	-	-	-	-	-	-	-	-	-	-	-	-	-	-	-	-	-	-	-	-	-	-	-	-	-	-
171																																																																																					
172	0	0	0	0	0	0	0	0	0	0	0	0	0	0	0	0	0	0	0	0	0	0	0	0	0	0	0	0	0	0	0	0	0	0	0	0	0	0	0	0	0	0	0	0	0	0	0	0	0	0	0	0	0	0	0	0	0	0	0	0	0	0	0	0	0	0	0	0	0	0	0	0	0	0	0	0	0	0	0	0	0	0	0	0	0
173	+	+	+	+	+	+	+	+	+	+	+	+	+	+	+	+	+	+	+	+	+	+	+	+	+	+	+	+	+	+	+	+	+	+	+	+	+	+	+	+	+	+	+	+	+	+	+	+	+	+	+	+	+	+	+	+	+	+	+	+	+	+	+	+	+	+	+	+	+	+	+	+	+	+	+	+	+	+	+	+	+	+	+	+	+
174	0	0	0	0	0	0	0	0	0	0	0	0	0	0	0	0	0	0	0	0	0	0	0																																																															
175																																																																																					
176	-	-	-	-	-	-	-	-	-	-	-	-	-	-	-	-	-	-	-	-	-	-	-	-	-	-	-	-	-	-	-	-	-	-	-	-	-	-	-	-	-	-	-	-	-	-	-	-	-	-	-	-	-	-	-	-	-	-	-	-	-																							
177	0	0	0	0	0	0	0	0	0	0	0	0	0	0	0	0	0	0	0	0	0	0	0	0	0	0	0	0	0	0	0	0	0	0	0	0	0	0	0	0	0	0	0	0	0	0	0	0	0	0	0	0	0	0	0	0	0	0	0	0	0	0	0	0	0	0	0	0	0	0	0	0	0	0	0	0	0	0	0	0	0	0	0	0	0
178	0	0	0	0	0	0	0	0	0	0	0	0	0	0	0	0	0	0	0	0	0	0	0	0	0																																																												
179																																																																																					
180	0	0	0	0	0	0	0	0	0	0	0	0	0	0	0	0	0	0	0	0	0	0	0	0	0	0	0	0	0	0	0	0	0	0	0	0	0	0	0	0	0	0	0	0	0	0	0	0	0	0	0	0	0	0	0	0	0	0	0	0	0	0	0	0	0	0	0	0	0	0	0	0	0	0	0	0	0	0	0	0	0	0	0	0	0
181	0	0	0	0	0	0	0	0	0	0	0	0	0	0	0	0	0	0	0	0	0	0	0	0	0	0	0	0	0	0	0	0	0	0	0	0	0	0	0	0	0	0	0	0	0	0	0	0	0	0	0	0	0	0	0	0	0	0	0	0	0	0	0	0	0	0	0	0	0	0	0	0	0	0	0	0	0	0	0	0	0	0	0	0	0
182	+	+	+	+	+	+	+	+	+	+	+	+	+	+	+	+	+	+	+	+	+	+	+	+	+	+	+																																																									
183																																																																																					
184																																																																																					
185	0	0	0	0	0	0	0	0	0	0	0	0	0	0	0	0	0	0	0	0	0	0	0	0	0	0	0	0	0	0	0	0	0	0	0	0	0	0	0	0	0	0	0	0	0	0	0	0	0	0	0	0	0	0	0	0	0	0	0																									
186	-	-	-	-	-	-	-	-	-	-	-	-	-	-	-	-	-	-	-	-	-	-	-	-	-	-	-	-	-	-	-	-	-	-	-	-	-	-	-	-	-	-	-	-	-	-	-	-	-	-	-	-	-	-	-	-	-	-	-	-	-	-	-	-	-	-	-	-	-	-	-	-	-	-	-	-	-	-	-	-	-	-	-	-	-
187	0	0	0	0	0	0	0	0	0	0	0	0	0	0	0	0	0	0	0	0	0	0	0	0	0	0	0	0	0																																																								
188																																																																																					
189	0	0	0	0	0	0	0	0	0	0	0	0	0	0	0	0	0	0	0	0	0	0	0	0	0	0	0	0	0	0	0	0	0	0	0	0	0	0	0	0	0	0	0	0	0	0	0	0	0	0	0	0	0	0	0	0	0																											
190	0	0	0	0	0	0	0	0	0	0	0	0	0	0	0	0	0	0	0	0	0	0	0	0	0	0	0	0	0	0	0	0	0	0	0	0	0	0	0	0	0	0	0	0	0	0	0	0	0	0	0	0	0	0	0	0	0	0	0	0	0	0	0	0	0	0	0	0	0	0	0	0	0	0	0	0	0	0	0	0	0	0	0	0	0
191	+	+	+	+	+	+	+	+	+	+	+	+	+	+	+	+	+	+	+	+	+	+	+	+	+	+	+	+	+	+	+	+	+	+	+	+	+	+	+	+	+	+	+	+	+	+	+	+	+	+	+	+	+	+	+																													
192																																																																																					
193	0	0	0	0	0	0	0	0	0	0	0	0	0	0	0	0	0	0	0	0	0	0	0	0	0	0	0	0	0	0	0	0	0	0	0	0	0	0	0	0	0	0	0	0	0	0	0	0	0	0	0	0	0	0	0	0	0	0	0	0	0	0	0	0	0	0	0	0	0	0	0	0	0	0	0	0	0	0	0	0	0	0	0	0	0
194	-	-	-	-	-	-	-	-	-	-	-	-	-	-	-	-	-	-	-	-	-	-	-	-	-	-	-	-	-	-	-																																																					
195																																																																																					
196	0	0	0	0	0	0	0	0	0	0	0	0	0	0	0	0	0	0	0	0	0	0	0	0	0	0	0	0	0	0	0	0	0	0	0	0	0	0	0	0	0	0	0	0	0	0	0	0	0	0	0	0	0																															
197																																																																																					
198	-	-	-	-	-	-	-	-	-	-	-	-	-	-	-	-	-	-	-	-	-	-	-	-	-	-	-	-	-	-	-	-	-	-	-	-	-	-	-	-	-	-	-	-	-	-	-	-	-	-	-	-	-	-	-	-	-	-	-	-	-	-	-	-	-	-	-	-	-	-	-	-	-	-	-	-	-	-	-	-	-	-	-	-	-
199																																																																																					
200	0	0	0	0	0	0	0	0	0	0	0	0	0	0	0	0	0	0	0	0	0	0	0	0	0	0	0	0	0	0	0	0	0																																																			
201																																																																																					
202	0	0	0	0	0	0	0	0	0	0	0	0	0	0	0	0	0	0	0	0	0	0	0	0	0	0	0	0	0	0	0	0	0	0	0	0	0	0	0	0	0	0	0	0	0	0	0	0	0	0	0	0	0	0	0	0	0	0	0	0	0	0	0	0	0	0	0	0	0	0	0	0	0	0	0	0	0	0	0	0	0	0	0	0	0
203																																																																																					
204	0	0	0	0	0	0	0	0	0	0	0	0	0	0	0	0	0	0	0	0	0	0	0	0	0	0	0	0	0	0	0	0	0	0	0	0	0	0	0	0	0	0	0	0	0	0	0	0	0	0	0																																	
205																																																																																					
206	0	0	0	0	0	0	0	0	0	0	0	0	0	0	0	0	0	0	0	0	0	0	0	0	0	0	0	0	0	0	0	0	0	0	0	0	0	0	0	0	0	0	0	0	0	0	0	0	0	0	0	0	0	0	0	0	0	0	0	0	0	0	0	0	0	0	0	0	0	0	0	0	0	0	0	0	0	0	0	0	0	0	0	0	0
207	90	90	90	90	90	90	90	90	90	90	90	90	90	90	90	90	90	90	90	90	90	90	90	90	90	90	90	90	90	90	90	90	90	90	90	90	90	90	90	90	90	90	90	90	90	90	90	90	90	90	90	90	90	90	90	90	90	90	90	90	90	90	90	90	90	90	90	90	90	90	90	90	90	90	90	90	90	90	90	90	90	90	90	90	90
208																																																																																					
209	+	+	+	+	+	+	+	+	+	+	+	+	+	+	+	+	+	+	+	+	+	+	+	+	+	+	+	+	+	+	+	+	+	+	+	+	+	+	+	+	+	+	+	+	+	+	+	+	+	+	+	+	+	+	+	+	+	+	+	+	+	+	+	+	+	+	+	+	+	+	+	+	+	+	+	+	+	+	+	+	+	+	+	+	+
210																																																																																					
211	0	0	0	0	0	0	0	0	0	0	0	0	0	0	0	0	0	0	0	0	0	0	0	0	0	0	0	0	0	0	0	0	0	0	0																																																	
212	-	-	-	-	-	-	-	-	-	-	-	-	-	-	-	-	-	-	-	-	-	-	-	-	-	-	-	-	-	-	-	-	-	-	-	-	-	-	-	-	-	-	-	-	-	-	-	-	-																																			
213																																																																																					
214																																																																																					
215	+	+	+	+	+	+	+	+	+	+	+	+	+	+	+	+	+	+	+	+	+	+	+	+	+	+	+	+	+	+	+	+	+	+	+	+	+	+	+	+	+	+	+	+	+	+	+	+	+	+	+	+	+	+	+	+	+	+	+	+	+	+	+	+	+	+	+	+	+	+	+	+	+	+	+	+	+	+	+	+	+	+	+	+	+
216	0	0	0	0	0	0	0	0	0	0	0	0	0	0	0	0	0	0	0	0	0	0	0	0	0	0	0	0	0	0	0	0	0	0	0	0	0	0	0	0	0	0	0	0	0	0	0	0	0	0	0	0	0	0	0	0	0	0	0	0	0	0	0	0	0	0	0	0	0	0	0	0	0	0	0	0	0	0	0	0	0	0	0	0	0
217	90	90	90	90	90	90	90	90	90	90	90	90	90	90	90	90	90	90	90	90	90	90	90	90	90	90	90	90	90	90	90	90	90	90	90	90	90	90	90	90	90	90	90	90	90	90	90	90	90	90	90	90	90	90	90	90	90	90	90	90	90	90	90	90	90	90	90	90	90	90	90	90	90	90	90	90	90	90	90	90	90	90	90	90	90
218	0	0	0	0	0	0	0	0	0	0	0	0	0	0	0	0	0	0	0	0	0	0	0	0	0	0	0	0	0	0	0	0	0	0	0	0	0																																															
219	+	+	+	+	+	+	+	+	+	+	+	+	+	+	+	+	+	+	+	+	+	+	+	+	+	+	+	+	+	+	+	+	+	+	+	+	+	+	+	+	+	+	+	+	+	+	+	+	+	+	+	+	+	+	+	+	+	+	+	+	+	+	+	+	+	+	+	+	+	+	+	+	+	+	+	+	+	+	+	+	+	+	+	+	+
220	0	0	0	0	0	0	0	0	0	0	0	0	0	0	0	0	0	0	0	0	0	0	0	0	0	0	0	0	0	0	0	0	0	0	0	0	0	0	0	0	0	0	0	0	0	0	0	0	0	0	0	0	0	0	0	0	0	0	0	0	0	0	0	0	0	0	0	0	0	0	0	0	0	0	0	0	0	0	0	0	0	0	0	0	0
221	90	90	90	90	90	90	90	90	90	90	90	90	90	90	90	90	90	90	90	90	90	90	90	90	90	90	90	90	90	90	90	90	90	90	90	90	90	90	90	90	90	90	90	90	90	90	90	90	90	90	90	90	90	90	90	90	90	90	90	90	90	90	90	90	90	90	90	90	90	90	90	90	90	90	90	90	90	90	90	90	90	90	90	90	90
222	0	0	0	0	0	0	0	0	0	0	0	0	0	0	0	0	0	0	0	0	0	0	0	0	0	0	0	0	0	0	0	0	0	0	0	0	0	0	0	0	0	0	0	0	0	0	0	0	0	0	0	0	0	0	0	0	0	0	0	0	0	0	0	0	0	0	0	0	0	0	0	0	0	0	0	0	0	0	0	0	0	0	0	0	0
223																																																																																					
224																																																																																					
225	0	0	0	0	0	0	0	0	0	0	0	0	0	0	0	0	0	0	0	0	0	0	0	0	0	0	0	0	0	0	0	0	0	0	0	0	0	0	0	0	0	0	0	0	0	0	0	0	0	0	0	0	0	0	0	0	0	0	0	0	0	0	0	0	0	0	0	0	0	0	0	0	0	0	0	0	0	0	0	0	0	0	0	0	0
226																																																																																					
227	+	+	+	+	+	+	+	+	+	+	+	+	+	+	+	+	+	+	+	+	+	+	+	+	+	+	+	+	+	+	+	+	+	+	+	+	+	+	+	+	+	+	+	+	+	+	+																																					
228																																																																																					
229	0	0	0	0	0	0	0	0	0	0	0	0	0	0	0	0	0	0	0	0	0	0	0	0	0	0	0	0	0	0	0	0	0	0	0	0	0	0	0	0	0	0	0	0	0																																							
230																																																																																					
231	0	0	0	0	0	0	0	0	0	0	0	0	0	0	0	0	0	0	0	0	0	0	0	0	0	0	0	0	0	0	0	0	0	0	0	0	0	0	0																																													
232	0	0	0	0	0	0	0	0	0	0	0	0	0	0	0	0	0	0	0	0	0	0	0	0	0	0	0	0	0	0	0	0	0	0	0	0	0	0	0	0	0	0	0	0	0	0	0	0	0	0	0	0	0	0	0	0	0	0	0	0	0	0	0	0	0	0	0	0	0	0	0	0	0	0	0	0	0	0	0	0	0	0	0	0	0
233																																																																																					
234	0	0	0	0	0	0	0	0	0	0	0	0	0	0	0	0	0	0	0	0	0	0	0	0	0	0	0	0	0	0	0	0	0	0	0	0	0	0	0	0	0	0	0																																									
235																																																																																					
236																																																																																					
237	-	-	-	-	-	-	-	-	-	-	-	-	-	-	-	-	-	-	-	-	-	-	-	-	-	-	-	-	-	-	-	-	-	-	-	-	-	-	-	-	-	-	-	-	-	-	-	-	-	-	-	-	-	-	-	-	-	-	-	-	-	-	-	-	-	-	-	-	-	-	-	-	-	-	-	-	-	-	-	-	-	-	-	-	-
238	0	0	0	0	0	0	0	0	0	0	0	0	0	0	0	0	0	0	0	0	0	0	0	0	0	0	0	0	0	0	0	0	0	0	0	0	0	0	0	0	0																																											
239																																																																																					
240	0	0	0	0	0	0	0	0	0	0	0	0	0	0	0	0	0	0	0	0	0	0	0	0	0	0	0	0	0	0	0	0	0	0	0	0	0	0	0	0	0	0	0	0	0	0	0	0	0	0	0	0	0	0	0	0	0	0	0	0	0	0	0	0	0	0	0	0	0	0	0	0	0	0	0	0	0	0	0	0	0	0	0	0	0
241																																																																																					
242	0	0	0	0	0	0	0	0	0	0	0	0	0	0	0	0	0	0	0	0	0	0	0	0	0	0	0	0	0	0	0	0	0	0	0	0	0	0	0	0	0	0	0	0	0	0	0	0	0	0	0	0	0	0	0	0	0	0	0	0	0	0	0	0	0	0	0	0	0	0	0	0	0	0	0	0	0	0	0	0	0	0	0	0	0
243																																																																																					
244	-	-	-	-	-	-	-	-	-	-	-	-	-	-	-	-	-	-	-	-	-	-	-	-	-	-	-	-	-	-	-	-	-	-	-	-	-	-	-	-	-	-	-	-	-	-	-	-	-	-	-	-	-	-	-	-	-	-	-	-	-	-	-	-	-	-	-	-	-	-	-	-	-	-	-	-	-	-	-	-	-	-	-	-	-
245	0	0	0	0	0	0	0	0	0	0	0	0	0	0	0	0	0	0	0	0	0	0	0	0	0	0	0	0	0	0	0	0	0	0	0	0	0	0	0	0	0	0	0	0	0	0	0	0	0	0	0	0	0	0	0	0	0	0	0	0	0	0	0	0	0	0	0	0	0	0	0	0	0	0	0	0	0	0	0	0	0	0	0	0	0
246	0	0	0	0	0	0	0	0	0	0	0	0	0	0	0	0	0	0	0	0	0	0	0	0	0	0	0	0	0	0	0	0	0	0	0	0	0	0	0	0	0	0	0	0	0	0	0	0	0	0	0	0	0	0	0	0	0	0	0	0	0	0	0	0	0	0	0	0	0	0	0	0	0	0	0	0	0	0	0	0	0	0	0	0	0
247	+	+	+	+	+	+	+	+	+	+	+	+	+	+	+	+	+	+	+	+	+	+	+	+	+	+	+	+	+	+	+	+	+	+	+	+	+	+	+	+	+	+	+	+	+	+	+	+	+	+	+	+	+	+	+	+	+	+	+	+	+	+	+	+	+	+	+	+	+	+	+	+	+	+	+	+	+	+	+	+	+	+	+	+	+
248	90	90	90	90	90	90	90	90	90	90	90	90	90	90	90	90	90	90	90	90	90	90	90	90	90	90	90	90	90	90	90	90	90	90	90	90	90	90	90	90	90	90	90	90	90	90	90	90	90	90	90	90	90	90	90	90	90	90	90	90	90	90	90	90	90	90	90	90	90	90	90	90	90	90	90	90	90	90	90	90	90	90	90	90	90
249	-	-	-	-	-	-	-	-	-	-	-	-	-	-	-	-	-	-	-	-	-	-	-	-	-	-	-	-	-	-	-	-	-	-	-	-	-	-	-	-	-	-	-	-	-	-	-	-	-	-	-	-	-	-	-	-	-	-	-	-	-	-	-	-	-	-	-	-	-	-	-	-	-	-	-	-	-	-	-	-	-	-	-	-	-
250	+	+	+	+	+	+	+	+	+	+	+	+	+	+	+	+	+	+	+	+	+	+	+	+	+	+	+	+	+	+	+	+	+	+	+	+	+	+	+	+	+	+	+	+	+	+	+	+	+	+	+	+	+	+	+	+	+	+	+	+	+	+	+	+	+	+	+	+	+	+	+	+	+	+	+	+	+	+	+	+	+	+	+	+	+

t Skin (mm)	30.360	30.176	29.992	29.808	29.624	29.440	29.256	29.072	28.888	28.704	28.520	28.336	28.152	27.968	27.784	27.600	27.416	27.232	27.048	26.864	26.680	26.496	26.312	26.128	25.944	25.760	25.576	25.392	25.208	25.024	24.840	24.656	24.472	24.288	24.104	23.920	23.736	23.552	23.368	23.184	23.000	22.816	22.632	22.448	22.264	22.080	21.896	21.712	21.528	21.344	21.160	20.976	20.792	20.608	20.424	20.240	20.056	19.872	19.688	19.504	19.320	19.136	18.952	18.768	18.584	18.400	18.216	18.032	17.848	17.664	17.480	17.296	17.296	17.112	16.928	16.928	16.744	16.744	16.560	16.376	16.192	16.008	15.824	15.640	15.456
No. of Plies	165	164	163	162	161	160	159	158	157	156	155	154	153	152	151	150	149	148	147	146	145	144	143	142	141	140	139	138	137	136	135	134	133	132	131	130	129	128	127	126	125	124	123	122	121	120	119	118	117	116	115	114	113	112	111	110	109	108	107	106	105	104	103	102	101	100	99	98	97	96	95	94	94	93	92	92	91	91	90	89	88	87	86	85	84
0° Plies	101	100	99	98	97	96	95	94	93	92	92	92	92	92	92	92	91	90	90	90	89	88	87	86	85	84	84	84	83	82	82	82	81	80	79	78	77	76	75	74	73	72	71	70	69	68	68	68	68	68	67	66	65	64	64	64	63	62	61	60	60	60	59	58	58	58	57	56	55	54	54	54	54	53	52	52	52	52	52	51	50	49	48	48	48
+45° Plies	24	24	24	24	24	24	24	24	24	24	24	24	23	22	22	22	22	22	22	22	22	22	22	22	22	22	21	20	20	20	20	20	20	20	20	20	20	20	20	20	20	20	20	20	20	20	19	18	18	18	18	18	18	18	17	16	16	16	16	16	16	16	16	16	16	16	16	16	16	16	16	16	16	16	16	16	16	16	16	16	16	16	16	15	14
-45° Plies	24	24	24	24	24	24	24	24	24	24	24	24	24	24	23	22	22	22	22	22	22	22	22	22	22	22	22	22	22	22	21	20	20	20	20	20	20	20	20	20	20	20	20	20	20	20	20	20	19	18	18	18	18	18	18	18	18	18	18	18	17	16	16	16	16	16	16	16	16	16	15	14	14	14	14	14	14	14	14	14	14	14	14	14	14
90° Plies	16	16	16	16	16	16	16	16	16	16	15	14	14	14	14	14	14	14	13	12	12	12	12	12	12	12	12	12	12	12	12	12	12	12	12	12	12	12	12	12	12	12	12	12	12	12	12	12	12	12	12	12	12	12	12	12	12	12	12	12	12	12	12	12	11	10	10	10	10	10	10	10	10	10	10	10	9	9	8	8	8	8	8	8	8
% 0° Plies	61%	61%	61%	60%	60%	60%	60%	59%	59%	59%	59%	60%	60%	61%	61%	61%	61%	61%	61%	62%	61%	61%	61%	61%	60%	60%	60%	61%	61%	60%	61%	61%	61%	61%	60%	60%	60%	59%	59%	59%	58%	58%	58%	57%	57%	57%	57%	58%	58%	59%	58%	58%	58%	57%	58%	58%	58%	57%	57%	57%	57%	58%	57%	57%	57%	58%	58%	57%	57%	56%	57%	57%	57%	57%	57%	57%	57%	57%	58%	57%	57%	56%	56%	56%	57%
% ± 45° Plies	29%	29%	29%	30%	30%	30%	30%	30%	31%	31%	31%	31%	31%	30%	30%	29%	30%	30%	30%	30%	30%	31%	31%	31%	31%	31%	31%	30%	31%	31%	30%	30%	30%	30%	31%	31%	31%	31%	31%	32%	32%	32%	33%	33%	33%	33%	33%	32%	32%	31%	31%	32%	32%	32%	32%	31%	31%	31%	32%	32%	31%	31%	31%	31%	32%	32%	32%	33%	33%	33%	33%	32%	32%	32%	33%	33%	33%	33%	33%	34%	34%	34%	35%	34%	33%
% 90° Plies	10%	10%	10%	10%	10%	10%	10%	10%	10%	10%	10%	9%	9%	9%	9%	9%	9%	9%	9%	8%	8%	8%	8%	8%	9%	9%	9%	9%	9%	9%	9%	9%	9%	9%	9%	9%	9%	9%	9%	10%	10%	10%	10%	10%	10%	10%	10%	10%	10%	10%	10%	11%	11%	11%	11%	11%	11%	11%	11%	11%	11%	12%	12%	12%	11%	10%	10%	10%	10%	10%	11%	11%	11%	11%	11%	11%	10%	10%	9%	9%	9%	9%	9%	9%	10%

Figure C-7: 60/30/10 conventional UD stringer spine laminate (thickness from 30.360mm to 15.456mm)

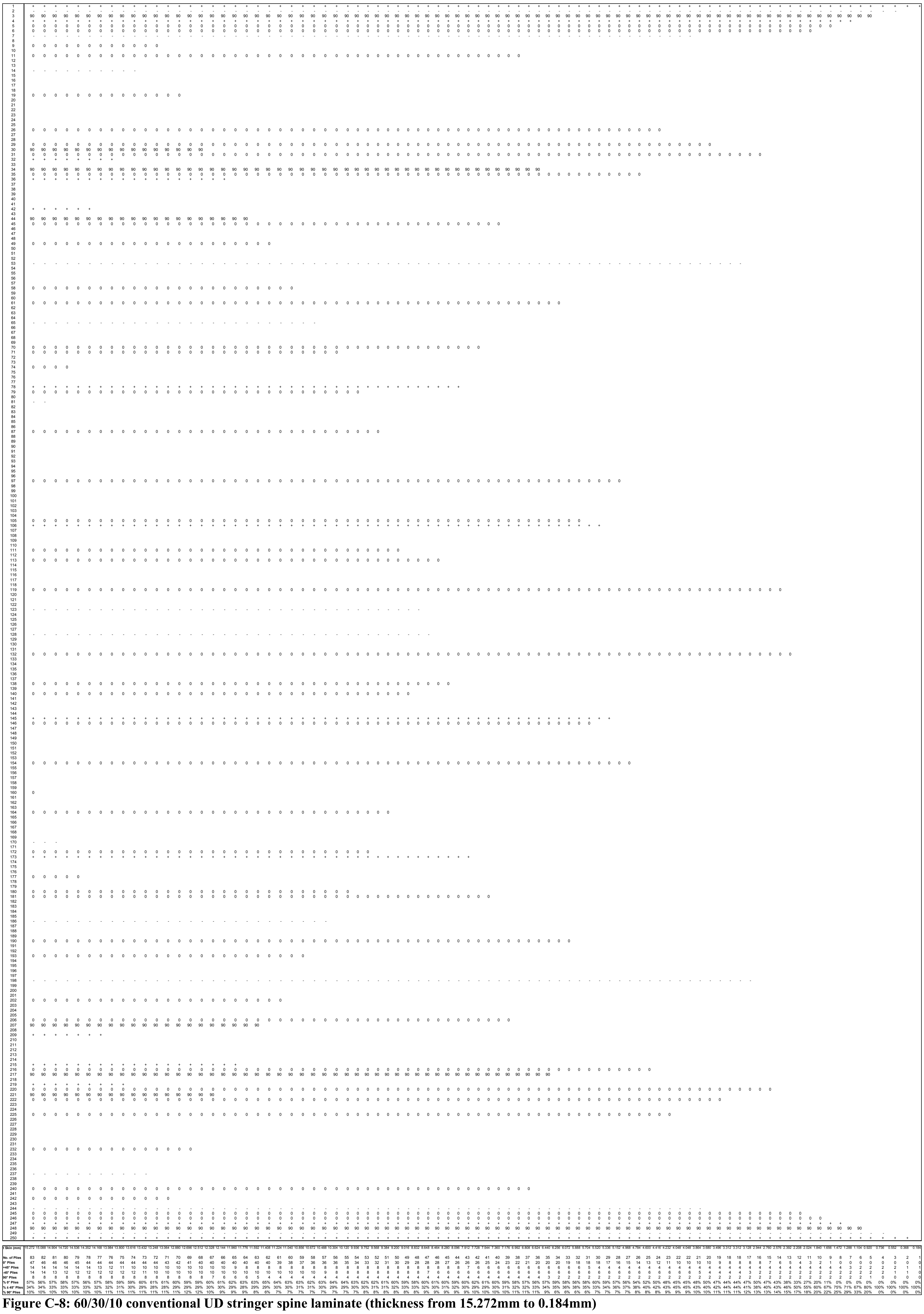

t Skin (mm)	15.272	15.088	14.904	14.720	14.536	14.352	14.168	13.984	13.800	13.616	13.432	13.248	13.064	12.880	12.696	12.512	12.328	12.144	11.960	11.776	11.592	11.408	11.224	11.040	10.856	10.672	10.488	10.304
No. of Plies	83	82	81	80	79	78	77	76	75	74	73	72	71	70	69	68	67	66	65	64	63	62	61	60	59	58	57	56
0° Plies	47	46	46	46	45	44	44	44	44	44	44	44	43	42	41	40	40	40	40	40	40	40	39	38	37	36	36	36
+45° Plies	14	14	14	14	14	14	13	12	11	10	10	10	10	10	10	10	10	10	9	8	8	8	8	8	8	8	8	8
-45° Plies	14	14	13	12	12	12	12	12	12	12	11	10	10	10	10	10	10	10	10	10	10	10	10	10	10	10	9	8
90° Plies	8	8	8	8	8	8	8	8	8	8	8	8	8	8	8	8	7	6	6	6	5	4	4	4	4	4	4	4
% 0° Plies	57%	56%	57%	58%	57%	56%	57%	58%	59%	59%	60%	61%	61%	60%	59%	59%	60%	61%	62%	63%	63%	65%	64%	63%	63%	62%	63%	64%
% ± 45° Plies	34%	34%	33%	33%	33%	33%	32%	32%	31%	30%	29%	28%	28%	29%	29%	29%	30%	30%	29%	28%	29%	29%	30%	30%	31%	31%	30%	29%
% 90° Plies	10%	10%	10%	10%	10%	10%	10%	11%	11%	11%	11%	11%	11%	11%	12%	12%	10%	9%	9%	9%	8%	6%	7%	7%	7%	7%	7%	7%

t Skin (mm)	10.120	9.936	9.752	9.568	9.384	9.200	9.016	8.832	8.648	8.464	8.280	8.096	7.912	7.728	7.544	7.360	7.176	6.992	6.808	6.624	6.440	6.256	6.072	5.888	5.704	5.520	5.336	5.152
No. of Plies	55	54	53	52	51	50	49	48	47	46	45	44	43	42	41	40	39	38	37	36	35	34	33	32	31	30	29	28
0° Plies	35	34	33	32	31	30	29	28	28	28	27	26	26	26	25	24	23	22	21	20	20	20	19	18	18	18	17	16
+45° Plies	8	8	8	8	8	8	8	8	8	8	8	8	7	6	6	6	6	6	6	6	6	6	6	6	5	4	4	4
-45° Plies	8	8	8	8	8	8	8	8	7	6	6	6	6	6	6	6	6	6	6	6	6	6	6	6	6	6	6	6
90° Plies	4	4	4	4	4	4	4	4	4	4	4	4	4	4	4	4	4	4	4	4	3	2	2	2	2	2	2	2
% 0° Plies	64%	63%	62%	62%	61%	60%	59%	58%	60%	61%	60%	59%	60%	62%	61%	60%	59%	58%	57%	56%	57%	59%	58%	56%	58%	60%	59%	57%
% ± 45° Plies	29%	30%	30%	31%	31%	32%	33%	33%	32%	30%	31%	32%	30%	29%	29%	30%	31%	32%	32%	33%	34%	35%	36%	38%	35%	33%	34%	36%
% 90° Plies	7%	7%	8%	8%	8%	8%	8%	8%	9%	9%	9%	9%	9%	10%	10%	10%	10%	11%	11%	11%	9%	6%	6%	6%	6%	7%	7%	7%

t Skin (mm)	4.968	4.784	4.600	4.416	4.232	4.048	4.048	3.864	3.680	3.496	3.312	3.312	3.128	2.944	2.760	2.576	2.392	2.208	2.024	1.840	1.656	1.472	1.288	1.104	0.920	0.736	0.552	0.368	0.184
No. of Plies	27	26	25	24	23	22	22	21	20	19	18	18	17	16	15	14	13	12	11	10	9	8	7	6	5	4	3	2	1
0° Plies	15	14	13	12	11	10	10	10	10	9	8	8	8	8	7	6	5	4	3	2	1	0	0	0	0	0	0	0	0
+45° Plies	4	4	4	4	4	4	4	4	4	4	4	4	4	4	4	4	4	4	4	4	4	4	3	2	2	2	2	1	1
-45° Plies	6	6	6	6	6	6	6	5	4	4	4	4	3	2	2	2	2	2	2	2	2	2	2	2	2	2	1	1	0
90° Plies	2	2	2	2	2	2	2	2	2	2	2	2	2	2	2	2	2	2	2	2	2	2	2	2	1	0	0	0	0
% 0° Plies	56%	54%	52%	50%	48%	45%	45%	48%	50%	47%	44%	44%	47%	50%	47%	43%	38%	33%	27%	20%	11%	0%	0%	0%	0%	0%	0%	0%	0%
% ± 45° Plies	37%	38%	40%	42%	43%	45%	45%	43%	40%	42%	44%	44%	41%	38%	40%	43%	46%	50%	55%	60%	67%	75%	71%	67%	80%	100%	100%	100%	100%
% 90° Plies	7%	8%	8%	8%	9%	9%	9%	10%	10%	11%	11%	11%	12%	13%	13%	14%	15%	17%	18%	20%	22%	25%	29%	33%	20%	0%	0%	0%	0%

Figure C-8: 60/30/10 conventional UD stringer spine laminate (thickness from 15.272mm to 0.184mm)

C.1.3 U-Profile Panel

The U-profile stiffened panel is considered to be made up of 3 laminates. The upper laminate is used to form the channel section for the stringers, whereas the lower laminate is symmetrically similar. As the upper laminate should constitute less than 30% of the total laminate, it is therefore necessary to have a mid-laminate. The U-profile skin laminate is shown in Figure C-9 to Figure C-11.

It is also necessary to have a stringer spine laminate, with a target laminate of 70/20/10, which can be achieved when a basic 60/30/10 laminate is used, but the 0° plies have a thickness of 0.25mm, whereas the ±45° and 90° plies have a thickness of 0.184mm. This stringer spine laminate is shown in Figure C-12 to Figure C-14.

Upper Laminate (U - Part)

| | | |

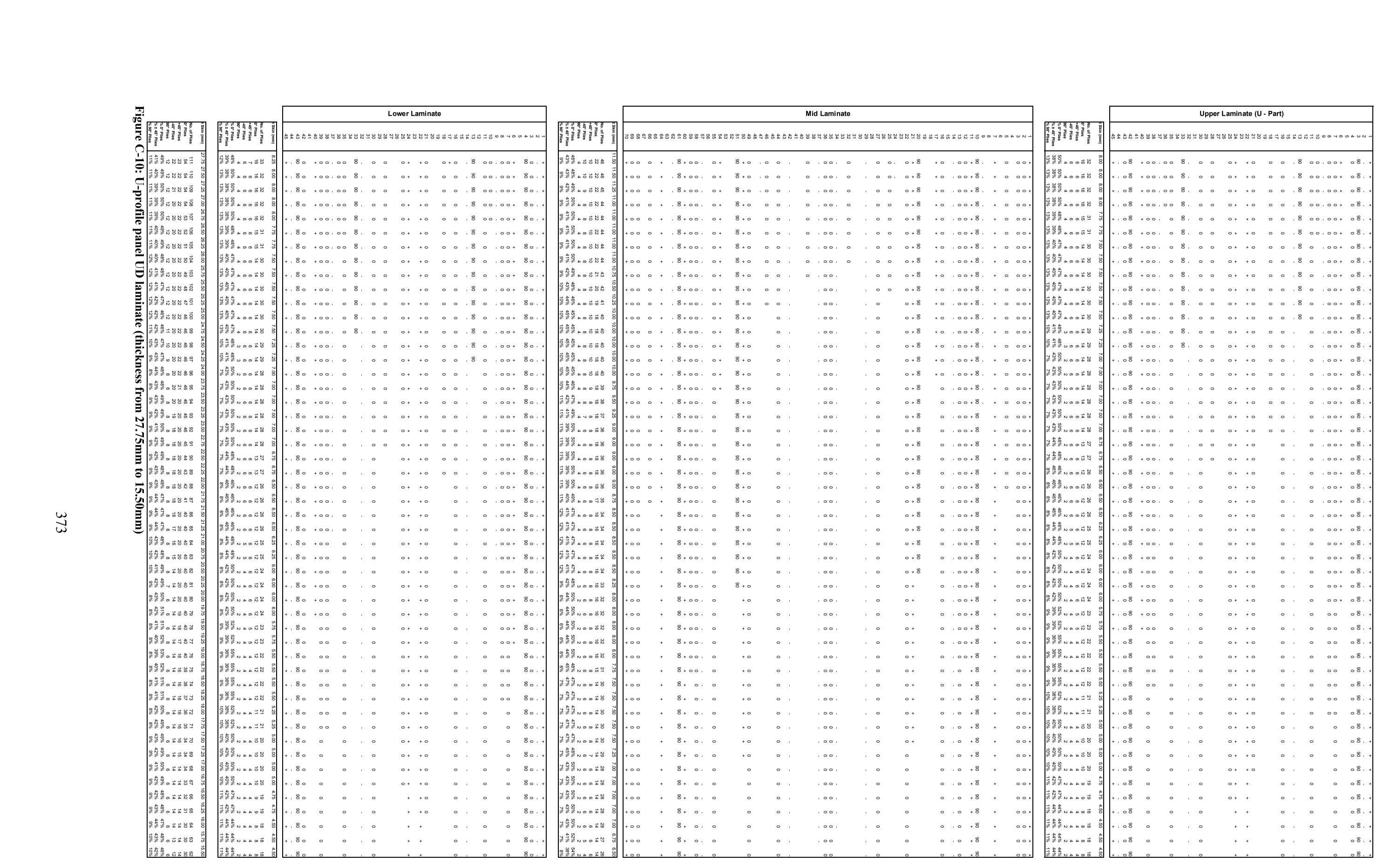

Figure C-10: U-profile panel UD laminate (thickness from 27.75mm to 15.50mm)

Upper Laminate (U - Part)

| | | |

| Skin (mm) | 55.900 | 55.716 | 55.532 | 55.282 | 55.032 | 54.848 | 54.664 | 54.414 | 54.164 | 53.980 | 53.796 | 53.546 | 53.296 | 53.046 | 52.796 | 52.546 | 52.296 | 52.112 | 51.928 | 51.744 | 51.560 | 51.310 | 51.060 | 50.810 | 50.560 | 50.310 | 50.060 | 49.810 | 49.560 | 49.310 | 49.060 | 48.876 | 48.692 | 48.508 | 48.324 | 48.074 | 47.824 | 47.574 | 47.324 | 47.074 | 46.824 | 46.574 | 46.324 | 46.140 | 45.956 | 45.772 | 45.588 | 45.338 | 45.088 | 44.838 | 44.588 | 44.404 | 44.220 | 43.970 | 43.720 | 43.536 | 43.352 | 43.102 | 42.852 | 42.668 | 42.484 | 42.234 | 41.984 | 41.734 | 41.484 | 41.300 | 41.116 | 40.866 | 40.616 | 40.432 | 40.248 | 40.064 | 39.880 | 39.630 | 39.380 | 39.196 | 39.012 | 38.762 | 38.512 | 38.262 | 38.012 | 37.828 | 37.644 | 37.460 | 37.276 |
|---|---|---

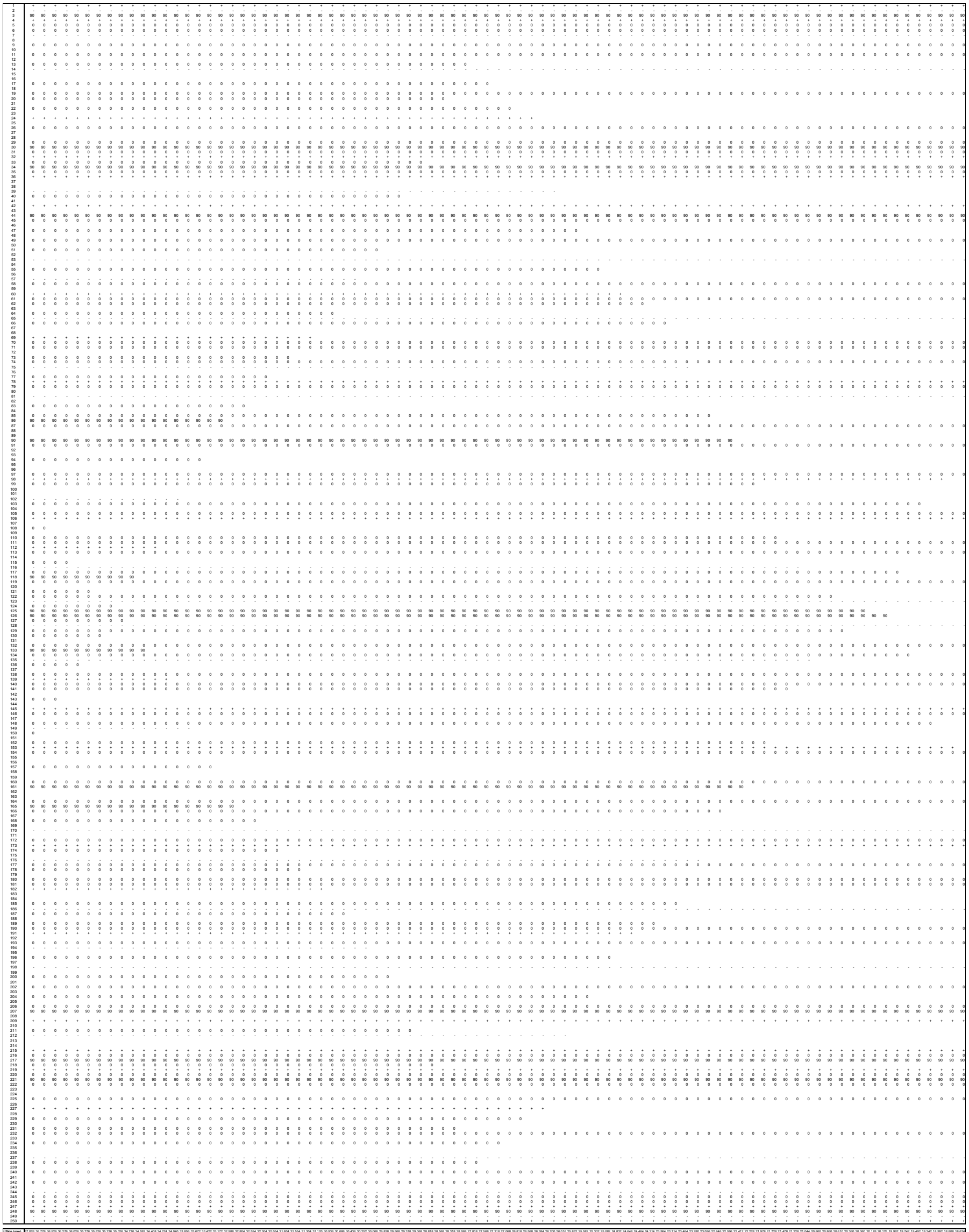

Figure C-13: 70/20/10 U-profile UD stringer spine laminate (thickness from 37.026mm to 18.624mm)

1	+	+	+	+	+	+	+	+	+	+	+	+	+	+	+	+	+	+	+	+	+	+	+	+	+	+	+	+	+	+	+	+	+	+	+	+	+	+	+	+	+	+	+	+	+	+	+	+	+	+	+	+	+	+	+	+	+	+	+	+	+	+	+	+	+	+	+	+	+	+	+	+	+	+	+	+	+	+	+	+	+	+	+	+	+
2	-	-	-	-	-	-	-	-	-	-	-	-	-	-	-	-	-	-	-	-	-	-	-	-	-	-	-	-	-	-	-	-	-	-	-	-	-	-	-	-	-	-	-	-	-	-	-	-	-	-	-	-	-	-	-	-	-	-	-	-	-	-	-	-	-	-	-	-	-	-	-	-	-	-	-	-	-	-	-	-	-	-	-		
3	90	90	90	90	90	90	90	90	90	90	90	90	90	90	90	90	90	90	90	90	90	90	90	90	90	90	90	90	90	90	90	90	90	90	90	90	90	90	90	90	90	90	90	90	90	90	90	90	90	90	90	90	90	90	90	90	90	90	90	90	90	90	90	90	90	90	90	90	90	90	90	90	90	90	90	90	90	90	90	90	90				
4	+	+	+	+	+	+	+	+	+	+	+	+	+	+	+	+	+	+	+	+	+	+	+	+	+	+	+	+	+	+	+	+	+	+	+	+	+	+	+	+	+	+	+	+	+	+	+	+	+	+	+	+	+	+	+	+	+	+	+	+	+	+	+	+	+	+	+	+	+	+	+	+	+	+	+	+	+	+	+						
5	0	0	0	0	0	0	0	0	0	0	0	0	0	0	0	0	0	0	0	0	0	0	0	0	0	0	0	0	0	0	0	0	0	0	0	0	0	0	0	0	0	0	0	0	0	0	0	0	0	0	0	0	0	0	0	0	0	0	0	0	0	0	0	0	0	0	0	0	0	0	0	0	0	0	0	0	0								
6	0	0	0	0	0	0	0	0	0	0	0	0	0	0	0	0	0	0	0	0	0	0	0	0	0	0	0	0	0	0	0	0	0	0	0	0	0	0	0	0	0	0	0	0	0	0	0	0	0	0	0	0	0	0	0	0	0	0	0	0	0	0	0	0	0	0	0	0	0	0	0	0	0	0	0										
7	-	-	-	-	-	-	-	-	-	-	-	-	-	-	-	-	-	-	-	-	-	-	-	-	-	-	-	-	-	-	-	-	-	-	-	-	-	-	-	-	-	-	-	-	-	-	-	-	-	-	-	-	-	-	-	-	-	-	-	-	-	-	-																						
8																																																																																				
9	0	0	0	0	0	0	0	0	0	0	0	0																																																																										
10																																																																																				
11	0	0	0	0	0	0	0	0	0	0	0	0	0	0	0	0	0	0	0	0	0	0	0	0	0	0	0	0	0	0	0	0	0	0	0	0	0	0	0	0	0	0	0	0	0	0																																							
12																																																																																				
13																																																																																				
14	-	-	-	-	-	-	-	-	-	-																																																																											
15																																																																																				
16																																																																																				
17																																																																																				
18																																																																																				
19	0	0	0	0	0	0	0	0	0	0	0	0	0	0																																																																							
20																																																																																				
21																																																																																				
22																																																																																				
23																																																																																				
24																																																																																				
25																																																																																				
26	0	0	0	0	0	0	0	0	0	0	0	0	0	0	0	0	0	0	0	0	0	0	0	0	0	0	0	0	0	0	0	0	0	0	0	0	0	0	0	0	0	0	0	0	0	0	0	0	0	0	0	0	0	0	0	0	0	0	0	0																									
27																																																																																				
28																																																																																				
29	0	0	0	0	0	0	0	0	0	0	0	0	0	0	0	0	0	0	0	0	0	0	0	0	0	0	0	0	0	0	0	0	0	0	0	0	0	0	0	0	0	0	0	0	0	0	0	0	0	0	0	0	0	0	0	0	0	0	0	0	0	0	0	0	0																				
30	90	90	90	90	90	90	90	90	90	90	90	90	90	90	90	90																																																																					
31	0	0	0	0	0	0	0	0	0	0	0	0	0	0	0	0	0	0	0	0	0	0	0	0	0	0	0	0	0	0	0	0	0	0	0	0	0	0	0	0	0	0	0	0	0	0	0	0	0	0	0	0	0	0	0	0	0	0	0	0	0	0	0	0	0	0	0	0	0	0															
32	+	+	+	+	+	+	+	+																																																																													
33																																																																																				
34	90	90	90	90	90	90	90	90	90	90	90	90	90	90	90	90	90	90	90	90	90	90	90	90	90	90	90	90	90	90	90	90	90	90	90	90	90	90	90	90	90	90	90	90	90	90	90	90																																					
35	0	0	0	0	0	0	0	0	0	0	0	0	0	0	0	0	0	0	0	0	0	0	0	0	0	0	0	0	0	0	0	0	0	0	0	0	0	0	0	0	0	0	0	0	0	0	0	0	0	0	0	0	0	0	0	0	0	0																											
36	+	+	+	+	+	+	+	+	+	+	+	+	+	+	+	+	+	+																																																																			
37																																																																																				
38																																																																																				
39																																																																																				
40																																																																																				
41																																																																																				
42	+	+	+	+	+	+																																																																															
43																																																																																				
44	90	90	90	90	90	90	90	90	90	90	90	90	90	90	90	90	90	90	90	90																																																																	
45	0	0	0	0	0	0	0	0	0	0	0	0	0	0	0	0	0	0	0	0	0	0	0	0	0	0	0	0	0	0	0	0	0	0	0	0	0	0	0	0	0	0	0	0																																									
46																																																																																				
47																																																																																				
48																																																																																				
49	0	0	0	0	0	0	0	0	0	0	0	0	0	0	0	0	0	0	0	0	0	0																																																															
50																																																																																				
51																																																																																				
52																																																																																				
53	-	-	-	-	-	-	-	-	-	-	-	-	-	-	-	-	-	-	-	-	-	-	-	-	-	-	-	-	-	-	-	-	-	-	-	-	-	-	-	-	-	-	-	-	-	-	-	-	-	-	-	-	-	-	-	-	-	-	-	-	-	-	-	-	-	-	-	-																	
54																																																																																				
55																																																																																				
56																																																																																				
57																																																																																				
58	0	0	0	0	0	0	0	0	0	0	0	0	0	0	0	0	0	0	0	0	0	0	0	0																																																													
59																																																																																				
60																																																																																				
61	0	0	0	0	0	0	0	0	0	0	0	0	0	0	0	0	0	0	0	0	0	0	0	0	0	0	0	0	0	0	0	0	0	0	0	0	0	0	0	0	0	0	0	0	0	0	0	0	0	0																																			
62																																																																																				
63																																																																																				
64																																																																																				
65	-	-	-	-	-	-	-	-	-	-	-	-	-	-	-	-	-	-	-	-	-	-	-	-	-	-																																																											
66																																																																																				
67																																																																																				
68																																																																																				
69																																																																																				
70	0	0	0	0	0	0	0	0	0	0	0	0	0	0	0	0	0	0	0	0	0	0	0	0	0	0	0	0	0	0	0	0	0	0	0	0	0	0	0	0	0	0																																											
71	0	0	0	0	0	0	0	0	0	0	0	0	0	0	0	0	0	0	0	0	0	0	0	0	0	0	0	0																																																									
72																																																																																				
73																																																																																				
74	0	0	0	0																																																																																	
75																																																																																				
76																																																																																				
77																																																																																				
78	+	+	+	+	+	+	+	+	+	+	+	+	+	+	+	+	+	+	+	+	+	+	+	+	+	+	+	+	+	+	+	+	+	+	+	+	+	+	+	+																																													
79	0	0	0	0	0	0	0	0	0	0	0	0	0	0	0	0	0	0	0	0	0	0	0	0	0	0	0	0	0	0																																																							
80																																																																																				
81	-	-																																																																																			
82																																																																																				
83																																																																																				
84																																																																																				
85																																																																																				
86																																																																																				
87	0	0	0	0	0	0	0	0	0	0	0	0	0	0	0	0	0	0	0	0	0	0	0	0	0	0	0	0	0	0	0	0																																																					
88																																																																																				
89																																																																																				
90																																																																																				
91																																																																																				
92																																																																																				
93																																																																																				
94																																																																																				
95																																																																																				
96																																																																																				
97	0	0	0	0	0	0	0	0	0	0	0	0	0	0	0	0	0	0	0	0	0	0	0	0	0	0	0	0	0	0	0	0	0	0	0	0	0	0	0	0	0	0	0	0	0	0	0	0	0	0	0	0	0	0	0	0																													
98																																																																																				
99																																																																																				
100																																																																																				
101																																																																																				
102																																																																																				
103																																																																																				
104																																																																																				
105	0	0	0	0	0	0	0	0	0	0	0	0	0	0	0	0	0	0	0	0	0	0	0	0	0	0	0	0	0	0	0	0	0	0	0	0	0	0	0	0	0	0	0	0	0	0	0	0	0	0	0	0																																	
106	+	+	+	+	+	+	+	+	+	+	+	+	+	+	+	+	+	+	+	+	+	+	+	+	+	+	+	+	+	+	+	+	+	+	+	+	+	+	+	+	+	+	+	+	+	+	+	+	+	+	+	+	+	+																															
107																																																																																				
108																																																																																				
109																																																																																				
110																																																																																				
111	0	0	0	0	0	0	0	0	0	0	0	0	0	0	0	0	0	0	0	0	0	0	0	0	0	0	0	0	0	0	0	0	0	0																																																			
112																																																																																				
113	0	0	0	0	0	0	0	0	0	0	0	0	0	0	0	0	0	0	0	0	0	0	0	0	0	0	0	0	0	0	0	0	0	0	0	0	0	0																																															
114																																																																																				
115																																																																																				
116																																																																																				
117																																																																																				
118																																																																																				
119	0	0	0	0	0	0	0	0	0	0	0	0	0	0	0	0	0	0	0	0	0	0	0	0	0	0	0	0	0	0	0	0	0	0	0	0	0	0	0	0	0	0	0	0	0	0	0	0	0	0	0	0	0	0	0	0	0	0	0	0	0	0	0	0	0	0	0	0	0	0	0	0													
120																																																																																				
121																																																																																				
122																																																																																				
123	-	-	-	-	-	-	-	-	-	-	-	-	-	-	-	-	-	-	-	-	-	-	-	-	-	-	-	-	-	-	-	-	-	-	-	-																																																	
124																																																																																				
125																																																																																				
126																																																																																				
127																																																																																				
128	-	-	-	-	-	-	-	-	-	-	-	-	-	-	-	-	-	-	-	-	-	-	-	-	-	-	-	-	-	-	-	-	-	-	-	-	-																																																
129																																																																																				
130																																																																																				
131																																																																																				
132	0	0	0	0	0	0	0	0	0	0	0	0	0	0	0	0	0	0	0	0	0	0	0	0	0	0	0	0	0	0	0	0	0	0	0	0	0	0	0	0	0	0	0	0	0	0	0	0	0	0	0	0	0	0	0	0	0	0	0	0	0	0	0	0	0	0	0	0	0	0	0	0	0												
133																																																																																				
134																																																																																				
135																																																																																				
136																																																																																				
137																																																																																				
138	0	0	0	0	0	0	0	0	0	0	0	0	0	0	0	0	0	0	0	0	0	0	0	0	0	0	0	0	0	0	0	0	0	0	0	0	0	0	0																																														
139																																																																																				
140	0	0	0	0	0	0	0	0	0	0	0	0	0	0	0	0	0	0	0	0	0	0	0	0	0	0	0	0	0	0	0	0	0	0	0																																																		
141																																																																																				
142																																																																																				
143																																																																																				
144																																																																																				
145	+	+	+	+	+	+	+	+	+	+	+	+	+	+	+	+	+	+	+	+	+	+	+	+	+	+	+	+	+	+	+	+	+	+	+	+	+	+	+	+	+	+	+	+	+	+	+	+	+	+	+	+	+	+	+																														
146	0	0	0	0	0	0	0	0	0	0	0	0	0	0	0	0	0	0	0	0	0	0	0	0	0	0	0	0	0	0	0	0	0	0	0	0	0	0	0	0	0	0	0	0	0	0	0	0	0	0	0	0	0																																
147																																																																																				
148																																																																																				
149																																																																																				
150																																																																																				
151																																																																																				
152																																																																																				
153																																																																																				
154	0	0	0	0	0	0	0	0	0	0	0	0	0	0	0	0	0	0	0	0	0	0	0	0	0	0	0	0	0	0	0	0	0	0	0	0	0	0	0	0	0	0	0	0	0	0	0	0	0	0	0	0	0	0	0	0	0																												
155																																																																																				
156																																																																																				
157																																																																																				
158																																																																																				
159																																																																																				
160	0																																																																																				
161																																																																																				
162																																																																																				
163																																																																																				
164	0	0	0	0	0	0	0	0	0	0	0	0	0	0	0	0	0	0	0	0	0	0	0	0	0	0	0	0	0	0	0	0	0																																																				
165																																																																																				
166																																																																																				
167																																																																																				
168																																																																																				
169																																																																																				
170	-	-	-																																																																																		
171																																																																																				
172	0	0	0	0	0	0	0	0	0	0	0	0	0	0	0	0	0	0	0	0	0	0	0	0	0	0	0	0	0	0	0																																																						
173	+	+	+	+	+	+	+	+	+	+	+	+	+	+	+	+	+	+	+	+	+	+	+	+	+	+	+	+	+	+	+	+	+	+	+	+	+	+	+	+	+																																												
174																																																																																				
175																																																																																				
176																																																																																				
177	0	0	0	0	0																																																																																
178																																																																																				
179																																																																																				
180	0	0	0	0	0	0	0	0	0	0	0	0	0	0	0	0	0	0	0	0	0	0	0	0	0	0	0	0	0																																																								
181	0	0	0	0	0	0	0	0	0	0	0	0	0	0	0	0	0	0	0	0	0	0	0	0	0	0	0	0	0	0	0	0	0	0	0	0	0	0	0	0	0	0	0																																										
182																																																																																				
183																																																																																				
184																																																																																				
185																																																																																				
186	-	-	-	-	-	-	-	-	-	-	-	-	-	-	-	-	-	-	-	-	-	-	-	-	-	-	-																																																										
187																																																																																				
188																																																																																				
189																																																																																				
190	0	0	0	0	0	0	0	0	0	0	0	0	0	0	0	0	0	0	0	0	0	0	0	0	0	0	0	0	0	0	0	0	0	0	0	0	0	0	0	0	0	0	0	0	0	0	0	0	0	0	0																																		
191																																																																																				
192																																																																																				
193	0	0	0	0	0	0	0	0	0	0	0	0	0	0	0	0	0	0	0	0	0	0	0	0	0																																																												
194																																																																																				
195																																																																																				
196																																																																																				
197																																																																																				
198	-	-	-	-	-	-	-	-	-	-	-	-	-	-	-	-	-	-	-	-	-	-	-	-	-	-	-	-	-	-	-	-	-	-	-	-	-	-	-	-	-	-	-	-	-	-	-	-	-	-	-	-	-	-	-	-	-	-	-	-	-	-	-	-	-	-	-	-	-																
199																																																																																				
200																																																																																				
201																																																																																				
202	0	0	0	0	0	0	0	0	0	0	0	0	0	0	0	0	0	0	0	0	0	0	0																																																														
203																																																																																				
204																																																																																				
205																																																																																				
206	0	0	0	0	0	0	0	0	0	0	0	0	0	0	0	0	0	0	0	0	0	0	0	0	0	0	0	0	0	0	0	0	0	0	0	0	0	0	0	0	0	0	0	0	0																																								
207	90	90	90	90	90	90	90	90	90	90	90	90	90	90	90	90	90	90	90	90	90																																																																
208																																																																																				
209	+	+	+	+	+	+	+																																																																														
210																																																																																				
211																																																																																				
212																																																																																				
213																																																																																				
214																																																																																				
215	+	+	+	+	+	+	+	+	+	+	+	+	+	+	+	+	+	+	+																																																																		
216	0	0	0	0	0	0	0	0	0	0	0	0	0	0	0	0	0	0	0	0	0	0	0	0	0	0	0	0	0	0	0	0	0	0	0	0	0	0	0	0	0	0	0	0	0	0	0	0	0	0	0	0	0	0	0	0	0	0	0																										
217	90	90	90	90	90	90	90	90	90	90	90	90	90	90	90	90	90	90	90	90	90	90	90	90	90	90	90	90	90	90	90	90	90	90	90	90	90	90	90	90	90	90	90	90	90	90	90	90	90	action																																				
218																																																																																				
219	+	+	+	+	+	+	+	+	+																																																																												
220	0	0	0	0	0	0	0	0	0	0	0	0	0	0	0	0	0	0	0	0	0	0	0	0	0	0	0	0	0	0	0	0	0	0	0	0	0	0	0	0	0	0	0	0	0	0	0	0	0	0	0	0	0	0	0	0	0	0	0	0	0	0	0	0	0	0	0	0	0	0	0														
221	90	90	90	90	90	90	90	90	90	90	90	90	90	90	90	90	90																																																																				
222	0	0	0	0	0	0	0	0	0	0	0	0	0	0	0	0	0	0	0	0	0	0	0	0	0	0	0	0	0	0	0	0	0	0	0	0	0	0	0	0	0	0	0	0	0	0	0	0	0	0	0	0	0	0	0	0	0	0	0	0	0	0	0	0	0	0																			
223																																																																																				
224																																																																																				
225	0	0	0	0	0	0	0	0	0	0	0	0	0	0	0	0	0	0	0	0	0	0	0	0	0	0	0	0	0	0	0	0	0	0	0	0	0	0	0	0	0	0	0	0	0	0	0	0	0	0	0	0	0	0	0	0	0	0	0	0	0																								
226																																																																																				
227																																																																																				
228																																																																																				
229																																																																																				
230																																																																																				
231																																																																																				
232	0	0	0	0	0	0	0	0	0	0	0	0	0	0	0																																																																						
233																																																																																				
234																																																																																				
235																																																																																				
236																																																																																				
237	-	-	-	-	-	-	-	-	-	-	-																																																																										
238																																																																																				
239																																																																																				
240	0	0	0	0	0	0	0	0	0	0	0	0	0	0	0	0	0	0	0	0	0	0	0	0	0	0	0	0	0	0	0	0	0	0	0	0	0	0	0	0	0	0	0	0	0	0	0																																					
241																																																																																				
242	0	0	0	0	0	0	0	0	0	0	0	0	0																																																																								
243																																																																																				
244	-	-	-	-	-	-	-	-	-	-	-	-	-	-	-	-	-	-	-	-	-	-	-	-	-	-	-	-	-	-	-	-	-	-	-	-	-	-	-	-	-	-	-	-	-	-	-	-	-	-	-	-	-	-	-	-	-	-	-	-	-	-	-	-																					
245	0	0	0	0	0	0	0	0	0	0	0	0	0	0	0	0	0	0	0	0	0	0	0	0	0	0	0	0	0	0	0	0	0	0	0	0	0	0	0	0	0	0	0	0	0	0	0	0	0	0	0	0	0	0	0	0	0	0	0	0	0	0	0	0	0	0	0	0	0	0	0	0	0	0											
246	0	0	0	0	0	0	0	0	0	0	0	0	0	0	0	0	0	0	0	0	0	0	0	0	0	0	0	0	0	0	0	0	0	0	0	0	0	0	0	0	0	0	0	0	0	0	0	0	0	0	0	0	0	0	0	0	0	0	0	0	0	0	0	0	0	0	0	0	0	0	0	0	0	0	0	0									
247	+	+	+	+	+	+	+	+	+	+	+	+	+	+	+	+	+	+	+	+	+	+	+	+	+	+	+	+	+	+	+	+	+	+	+	+	+	+	+	+	+	+	+	+	+	+	+	+	+	+	+	+	+	+	+	+	+	+	+	+	+	+	+	+	+	+	+	+	+	+	+	+	+	+	+	+	+	+							
248	90	90	90	90	90	90	90	90	90	90	90	90	90	90	90	90	90	90	90	90	90	90	90	90	90	90	90	90	90	90	90	90	90	90	90	90	90	90	90	90	90	90	90	90	90	90	90	90	90	90	90	90	90	90	90	90	90	90	90	90	90	90	90	90	90	90	90	90	90	90	90	90	90	90	90	90	90	90	90	90					
249	-	-	-	-	-	-	-	-	-	-	-	-	-	-	-	-	-	-	-	-	-	-	-	-	-	-	-	-	-	-	-	-	-	-	-	-	-	-	-	-	-	-	-	-	-	-	-	-	-	-	-	-	-	-	-	-	-	-	-	-	-	-	-	-	-	-	-	-	-	-	-	-	-	-	-	-	-	-	-	-	-	-			
250	+	+	+	+	+	+	+	+	+	+	+	+	+	+	+	+	+	+	+	+	+	+	+	+	+	+	+	+	+	+	+	+	+	+	+	+	+	+	+	+	+	+	+	+	+	+	+	+	+	+	+	+	+	+	+	+	+	+	+	+	+	+	+	+	+	+	+	+	+	+	+	+	+	+	+	+	+	+	+	+	+	+	+	+	
t Skin (mm)	18.374	18.124	17.940	17.756	17.506	17.256	17.072	16.888	16.704	16.520	16.336	16.152	15.902	15.652	15.402	15.152	14.968	14.784	14.600	14.416	14.232	14.048	13.798	13.548	13.298	13.048	12.864	12.680	12.430	#####	#####	#####	#####	#####	#####	#####	#####	#####	#####	9.812	9.628	9.444	9.194	8.944	8.694	8.444	8.194	7.944	7.760	7.576	7.326	7.076	6.892	6.708	6.458	6.208	5.958	5.708	5.458	5.208	4.958	4.708	4.708	4.524	4.340	4.090	3.840	3.840	3.656	3.472	3.222	2.972	2.722	2.472	2.222	1.972	1.722	1.472	1.288	1.104	0.920	0.736	0.552	0.368	0.184
No. of Plies	83	82	81	80	79	78	77	76	75	74	73	72	71	70	69	68	67	66	65	64	63	62	61	60	59	58	57	56	55	54	53	52	51	50	49	48	47	46	45	44	43	42	41	40	39	38	37	36	35	34	33	32	31	30	29	28	27	26	25	24	23	22	22	21	20	19	18	18	17	16	15	14	13	12	11	10	9	8	7	6	5	4	3	2	1
0° Plies	47	46	46	46	45	44	44	44	44	44	44	44	43	42	41	40	40	40	40	40	40	40	39	38	37	36	36	36	35	34	33	32	31	30	29	28	28	28	27	26	26	26	25	24	23	22	21	20	20	20	19	18	18	18	17	16	15	14	13	12	11	10	10	10	10	9	8	8	8	8	7	6	5	4	3	2	1	0	0	0	0	0	0	0	0
+45° Plies	14	14	14	14	14	14	13	12	11	10	10	10	10	10	10	10	10	10	9	8	8	8	8	8	8	8	8	8	8	8	8	8	8	8	8	8	8	8	8	8	7	6	6	6	6	6	6	6	6	6	6	6	5	4	4	4	4	4	4	4	4	4	4	4	4	4	4	4	4	4	4	4	4	4	4	4	4	4	3	2	2	2	2	1	1
-45° Plies	14	14	13	12	12	12	12	12	12	12	11	10	10	10	10	10	10	10	10	10	10	10	10	10	10	10	9	8	8	8	8	8	8	8	8	8	7	6	6	6	6	6	6	6	6	6	6	6	6	6	6	6	6	6	6	6	6	6	6	6	6	6	6	5	4	4	4	4	3	2	2	2	2	2	2	2	2	2	2	2	2	2	1	1	0
90° Plies	8	8	8	8	8	8	8	8	8	8	8	8	8	8	8	8	7	6	6	6	5	4	4	4	4	4	4	4	4	4	4	4	4	4	4	4	4	4	4	4	4	4	4	4	4	4	4	4	3	2	2	2	2	2	2	2	2	2	2	2	2	2	2	2	2	2	2	2	2	2	2	2	2	2	2	2	2	2	2	2	1	0	0	0	0
% 0° Plies	64%	63%	64%	65%	64%	64%	64%	65%	66%	67%	67%	68%	68%	67%	67%	66%	67%	68%	68%	69%	70%	71%	71%	70%	70%	69%	70%	71%	70%	70%	69%	68%	68%	67%	66%	66%	67%	68%	67%	66%	68%	69%	68%	67%	66%	65%	64%	63%	64%	66%	65%	64%	65%	67%	66%	64%	63%	61%	60%	58%	55%	53%	53%	55%	58%	55%	52%	52%	55%	58%	54%	50%	46%	40%	34%	25%	15%	0%	0%	0%	0%	0%	0%	0%	0%
% ± 45° Plies	28%	28%	28%	27%	27%	28%	27%	26%	25%	25%	24%	23%	23%	24%	24%	24%	25%	25%	24%	23%	23%	24%	24%	24%	25%	25%	24%	23%	24%	24%	25%	25%	26%	26%	27%	28%	26%	25%	26%	26%	25%	23%	24%	25%	25%	26%	27%	28%	28%	29%	30%	31%	29%	27%	28%	30%	31%	32%	34%	35%	37%	39%	39%	37%	34%	36%	38%	38%	35%	32%	34%	37%	41%	45%	50%	56%	64%	75%	71%	67%	80%	100%	100%	100%	100%
% 90° Plies	8%	8%	8%	8%	8%	9%	9%	9%	9%	9%	9%	9%	9%	9%	9%	10%	10%	9%	7%	8%	8%	6%	5%	5%	5%	6%	6%	6%	6%	6%	6%	6%	6%	7%	7%	7%	7%	7%	7%	8%	8%	8%	8%	8%	8%	9%	9%	9%	7%	5%	5%	5%	5%	5%	6%	6%	6%	6%	7%	7%	7%	8%	8%	8%	8%	9%	10%	10%	10%	11%	11%	12%	14%	15%	17%	19%	21%	25%	29%	33%	20%	0%	0%	0%	0%

Figure C-14: 70/20/10 U-profile UD stringer spine laminate (thickness from 18.374mm to 0.184mm)

C.2 NCF Laminates

C.2.1 Skin

There are 3 NCF laminates developed, using the interleaved tapering method, as follows:

- 50/40/10
- 30/60/10
- 10/80/10

There are a number of permutations for NCF textiles, which can be used to create the skin; however, for simplicity, a basic quad-axial NCF textile was chosen, with each ply in the textile having an orientation of 0°, +45°, -45°, and 90°. The only difference between the textiles for the different laminates is the thickness of each layer, due to the desired target laminate. The thickness of the plies can be worked out using Equation C-1. In order to improve the buckling capability of the laminate, and the bearing strength, a $(+/90/-/0)_s$ was chosen. The only issue with this configuration, is that for a 50/40/10 laminate this would mean that the maximum combined thickness of contiguous 0° plies could be 1.25mm, whereas the stacking sequence rules suggest 1mm should be the maximum thickness. The thinnest laminate is 135gsm or 0.125mm thick. Furthermore, quad-axial laminate will have limited drapeability, but for a wing skin this should be acceptable.

$$Ply\ Thickness = \frac{Areal\ Weight}{Fiber\ Density \times FVF \times 1000} \qquad \textbf{C-1}$$

		50/40/10 Laminate		30/60/10 Laminate		10/80/10 Laminate	
		Areal Weight (gsm)	**Thk (mm)**	**Areal Weight (gsm)**	**Thk (mm)**	**Areal Weight (gsm)**	**Thk (mm)**
TE1	+	270	0.250	405	0.375	540	0.500
	90	135	0.125	135	0.125	135	0.125
	-	270	0.250	405	0.375	540	0.500
	0	675	0.625	405	0.375	135	0.125
	Sub Total	***1350***	***1.250***	***1350***	***1.250***	***1350***	***1.250***
TE2	0	675	0.625	405	0.375	135	0.125
	-	270	0.250	405	0.375	540	0.500
	90	135	0.125	135	0.125	135	0.125
	+	270	0.250	405	0.375	540	0.500
	Sub Total	***1350***	***1.250***	***1350***	***1.250***	***1350***	***1.250***
	Grand Total	**2700**	**2.500**	**2700**	**2.500**	**2700**	**2.500**

Table C-2: NCF skin laminate details

These laminates based on Textile 1 (TE1) and Textile 2 (TE2) are shown in Figure C-15 to Figure C-17.

1	+ 90 - 0	+ 90 - 0	+ 90 - 0	+ 90 - 0	+ 90 - 0	+ 90 - 0	+ 90 - 0	+ 90 - 0	+ 90 - 0	+ 90 - 0	+ 90 - 0	+ 90 - 0	+ 90 - 0	+ 90 - 0	+ 90 - 0	+ 90 - 0	+ 90 - 0	+ 90 - 0	+ 90 - 0	+ 90 - 0	+ 90 - 0	+ 90 - 0	+ 90 - 0	+ 90 - 0	+ 90 - 0	+ 90 - 0	+ 90 - 0	+ 90 - 0	+ 90 - 0	+ 90 - 0
2	+ 90 - 0	+ 90 - 0	+ 90 - 0	+ 90 - 0	+ 90 - 0	+ 90 - 0	+ 90 - 0	+ 90 - 0	+ 90 - 0	+ 90 - 0	+ 90 - 0	+ 90 - 0	+ 90 - 0	+ 90 - 0	+ 90 - 0	+ 90 - 0	+ 90 - 0	+ 90 - 0	+ 90 - 0											
3	+ 90 - 0	+ 90 - 0	+ 90 - 0	+ 90 - 0	+ 90 - 0	+ 90 - 0	+ 90 - 0	+ 90 - 0	+ 90 - 0	+ 90 - 0	+ 90 - 0	+ 90 - 0	+ 90 - 0	+ 90 - 0	+ 90 - 0	+ 90 - 0	+ 90 - 0													
4	+ 90 - 0	+ 90 - 0	+ 90 - 0	+ 90 - 0	+ 90 - 0	+ 90 - 0	+ 90 - 0	+ 90 - 0	+ 90 - 0	+ 90 - 0	+ 90 - 0	+ 90 - 0	+ 90 - 0	+ 90 - 0	+ 90 - 0	+ 90 - 0	+ 90 - 0	+ 90 - 0	+ 90 - 0	+ 90 - 0	+ 90 - 0									
5	+ 90 - 0	+ 90 - 0	+ 90 - 0	+ 90 - 0	+ 90 - 0	+ 90 - 0	+ 90 - 0	+ 90 - 0	+ 90 - 0	+ 90 - 0	+ 90 - 0	+ 90 - 0	+ 90 - 0	+ 90 - 0	+ 90 - 0															
6	+ 90 - 0	+ 90 - 0	+ 90 - 0	+ 90 - 0	+ 90 - 0	+ 90 - 0	+ 90 - 0	+ 90 - 0	+ 90 - 0	+ 90 - 0	+ 90 - 0	+ 90 - 0	+ 90 - 0	+ 90 - 0	+ 90 - 0	+ 90 - 0	+ 90 - 0	+ 90 - 0	+ 90 - 0	+ 90 - 0	+ 90 - 0	+ 90 - 0	+ 90 - 0							
7	+ 90 - 0	+ 90 - 0	+ 90 - 0	+ 90 - 0	+ 90 - 0	+ 90 - 0	+ 90 - 0	+ 90 - 0	+ 90 - 0	+ 90 - 0	+ 90 - 0	+ 90 - 0	+ 90 - 0																	
8	+ 90 - 0																													
9	+ 90 - 0	+ 90 - 0	+ 90 - 0	+ 90 - 0	+ 90 - 0	+ 90 - 0	+ 90 - 0	+ 90 - 0	+ 90 - 0	+ 90 - 0	+ 90 - 0	+ 90 - 0	+ 90 - 0	+ 90 - 0	+ 90 - 0	+ 90 - 0	+ 90 - 0	+ 90 - 0	+ 90 - 0	+ 90 - 0	+ 90 - 0	+ 90 - 0	+ 90 - 0	+ 90 - 0	+ 90 - 0					
10	+ 90 - 0	+ 90 - 0	+ 90 - 0	+ 90 - 0	+ 90 - 0	+ 90 - 0	+ 90 - 0	+ 90 - 0	+ 90 - 0	+ 90 - 0	+ 90 - 0																			
11	+ 90 - 0	+ 90 - 0	+ 90 - 0																											
12	+ 90 - 0	+ 90 - 0	+ 90 - 0	+ 90 - 0	+ 90 - 0	+ 90 - 0	+ 90 - 0	+ 90 - 0	+ 90 - 0	+ 90 - 0	+ 90 - 0	+ 90 - 0	+ 90 - 0	+ 90 - 0	+ 90 - 0	+ 90 - 0	+ 90 - 0	+ 90 - 0	+ 90 - 0	+ 90 - 0	+ 90 - 0	+ 90 - 0	+ 90 - 0	+ 90 - 0	+ 90 - 0	+ 90 - 0	+ 90 - 0			
13	+ 90 - 0	+ 90 - 0	+ 90 - 0	+ 90 - 0	+ 90 - 0	+ 90 - 0	+ 90 - 0	+ 90 - 0	+ 90 - 0																					
14	+ 90 - 0	+ 90 - 0	+ 90 - 0	+ 90 - 0	+ 90 - 0																									
15	+ 90 - 0	+ 90 - 0	+ 90 - 0	+ 90 - 0	+ 90 - 0	+ 90 - 0	+ 90 - 0	+ 90 - 0	+ 90 - 0	+ 90 - 0	+ 90 - 0	+ 90 - 0	+ 90 - 0	+ 90 - 0	+ 90 - 0	+ 90 - 0	+ 90 - 0	+ 90 - 0	+ 90 - 0	+ 90 - 0	+ 90 - 0	+ 90 - 0	+ 90 - 0	+ 90 - 0	+ 90 - 0	+ 90 - 0	+ 90 - 0	+ 90 - 0	+ 90 - 0	
16	+ 90 - 0	+ 90 - 0	+ 90 - 0	+ 90 - 0	+ 90 - 0	+ 90 - 0	+ 90 - 0																							
17	0 - 90 +	0 - 90 +	0 - 90 +	0 - 90 +	0 - 90 +	0 - 90 +	0 - 90 +	0 - 90 +																						
18	0 - 90 +	0 - 90 +	0 - 90 +	0 - 90 +	0 - 90 +	0 - 90 +	0 - 90 +	0 - 90 +	0 - 90 +	0 - 90 +	0 - 90 +	0 - 90 +	0 - 90 +	0 - 90 +	0 - 90 +	0 - 90 +	0 - 90 +	0 - 90 +	0 - 90 +	0 - 90 +	0 - 90 +	0 - 90 +	0 - 90 +	0 - 90 +	0 - 90 +	0 - 90 +	0 - 90 +	0 - 90 +	0 - 90 +	0 - 90 +
19	0 - 90 +	0 - 90 +	0 - 90 +	0 - 90 +	0 - 90 +	0 - 90 +																								
20	0 - 90 +	0 - 90 +	0 - 90 +	0 - 90 +	0 - 90 +	0 - 90 +	0 - 90 +	0 - 90 +	0 - 90 +	0 - 90 +																				
21	0 - 90 +	0 - 90 +	0 - 90 +	0 - 90 +	0 - 90 +	0 - 90 +	0 - 90 +	0 - 90 +	0 - 90 +	0 - 90 +	0 - 90 +	0 - 90 +	0 - 90 +	0 - 90 +	0 - 90 +	0 - 90 +	0 - 90 +	0 - 90 +	0 - 90 +	0 - 90 +	0 - 90 +	0 - 90 +	0 - 90 +	0 - 90 +	0 - 90 +	0 - 90 +	0 - 90 +	0 - 90 +		
22	0 - 90 +	0 - 90 +	0 - 90 +	0 - 90 +																										
23	0 - 90 +	0 - 90 +	0 - 90 +	0 - 90 +	0 - 90 +	0 - 90 +	0 - 90 +	0 - 90 +	0 - 90 +	0 - 90 +	0 - 90 +	0 - 90 +																		
24	0 - 90 +	0 - 90 +	0 - 90 +	0 - 90 +	0 - 90 +	0 - 90 +	0 - 90 +	0 - 90 +	0 - 90 +	0 - 90 +	0 - 90 +	0 - 90 +	0 - 90 +	0 - 90 +	0 - 90 +	0 - 90 +	0 - 90 +	0 - 90 +	0 - 90 +	0 - 90 +	0 - 90 +	0 - 90 +	0 - 90 +	0 - 90 +	0 - 90 +	0 - 90 +				
25	0 - 90 +	0 - 90 +																												
26	0 - 90 +	0 - 90 +	0 - 90 +	0 - 90 +	0 - 90 +	0 - 90 +	0 - 90 +	0 - 90 +	0 - 90 +	0 - 90 +	0 - 90 +	0 - 90 +	0 - 90 +	0 - 90 +																
27	0 - 90 +	0 - 90 +	0 - 90 +	0 - 90 +	0 - 90 +	0 - 90 +	0 - 90 +	0 - 90 +	0 - 90 +	0 - 90 +	0 - 90 +	0 - 90 +	0 - 90 +	0 - 90 +	0 - 90 +	0 - 90 +	0 - 90 +	0 - 90 +	0 - 90 +	0 - 90 +	0 - 90 +	0 - 90 +	0 - 90 +	0 - 90 +						
28	0 - 90 +	0 - 90 +	0 - 90 +	0 - 90 +	0 - 90 +	0 - 90 +	0 - 90 +	0 - 90 +	0 - 90 +	0 - 90 +	0 - 90 +	0 - 90 +	0 - 90 +	0 - 90 +	0 - 90 +	0 - 90 +														
29	0 - 90 +	0 - 90 +	0 - 90 +	0 - 90 +	0 - 90 +	0 - 90 +	0 - 90 +	0 - 90 +	0 - 90 +	0 - 90 +	0 - 90 +	0 - 90 +	0 - 90 +	0 - 90 +	0 - 90 +	0 - 90 +	0 - 90 +	0 - 90 +	0 - 90 +	0 - 90 +	0 - 90 +	0 - 90 +								
30	0 - 90 +	0 - 90 +	0 - 90 +	0 - 90 +	0 - 90 +	0 - 90 +	0 - 90 +	0 - 90 +	0 - 90 +	0 - 90 +	0 - 90 +	0 - 90 +	0 - 90 +	0 - 90 +	0 - 90 +	0 - 90 +	0 - 90 +	0 - 90 +												
31	0 - 90 +	0 - 90 +	0 - 90 +	0 - 90 +	0 - 90 +	0 - 90 +	0 - 90 +	0 - 90 +	0 - 90 +	0 - 90 +	0 - 90 +	0 - 90 +	0 - 90 +	0 - 90 +	0 - 90 +	0 - 90 +	0 - 90 +	0 - 90 +	0 - 90 +	0 - 90 +										
32	0 - 90 +	0 - 90 +	0 - 90 +	0 - 90 +	0 - 90 +	0 - 90 +	0 - 90 +	0 - 90 +	0 - 90 +	0 - 90 +	0 - 90 +	0 - 90 +	0 - 90 +	0 - 90 +	0 - 90 +	0 - 90 +	0 - 90 +	0 - 90 +	0 - 90 +	0 - 90 +	0 - 90 +	0 - 90 +	0 - 90 +	0 - 90 +	0 - 90 +	0 - 90 +	0 - 90 +	0 - 90 +	0 - 90 +	0 - 90 +
t Skin (mm)	40.00	38.75	37.50	36.25	35.00	33.75	32.50	31.25	30.00	28.75	27.50	26.25	25.00	23.75	22.50	21.25	20.00	18.75	17.50	16.25	15.00	13.75	12.50	11.25	10.00	8.75	7.50	6.25	5.00	3.75
No. of Textiles	32	31	30	29	28	27	26	25	24	23	22	21	20	19	18	17	16	15	14	13	12	11	10	9	8	7	6	5	4	3
% 0° Plies	50%	50%	50%	50%	50%	50%	50%	50%	50%	50%	50%	50%	50%	50%	50%	50%	50%	50%	50%	50%	50%	50%	50%	50%	50%	50%	50%	50%	50%	50%
% ± 45° Plies	40%	40%	40%	40%	40%	40%	40%	40%	40%	40%	40%	40%	40%	40%	40%	40%	40%	40%	40%	40%	40%	40%	40%	40%	40%	40%	40%	40%	40%	40%
% 90° Plies	10%	10%	10%	10%	10%	10%	10%	10%	10%	10%	10%	10%	10%	10%	10%	10%	10%	10%	10%	10%	10%	10%	10%	10%	10%	10%	10%	10%	10%	10%

Figure C-15: 50/40/10 NCF skin laminate

1	+ 90 - 0	+ 90 - 0	+ 90 - 0	+ 90 - 0	+ 90 - 0	+ 90 - 0	+ 90 - 0	+ 90 - 0	+ 90 - 0	+ 90 - 0	+ 90 - 0	+ 90 - 0	+ 90 - 0	+ 90 - 0	+ 90 - 0	+ 90 - 0	+ 90 - 0	+ 90 - 0	+ 90 - 0	+ 90 - 0	+ 90 - 0	+ 90 - 0	+ 90 - 0	+ 90 - 0	+ 90 - 0	+ 90 - 0	+ 90 - 0	+ 90 - 0	+ 90 - 0	+ 90 - 0
2	+ 90 - 0	+ 90 - 0	+ 90 - 0	+ 90 - 0	+ 90 - 0	+ 90 - 0	+ 90 - 0	+ 90 - 0	+ 90 - 0	+ 90 - 0	+ 90 - 0	+ 90 - 0	+ 90 - 0	+ 90 - 0	+ 90 - 0	+ 90 - 0	+ 90 - 0	+ 90 - 0	+ 90 - 0											
3	+ 90 - 0	+ 90 - 0	+ 90 - 0	+ 90 - 0	+ 90 - 0	+ 90 - 0	+ 90 - 0	+ 90 - 0	+ 90 - 0	+ 90 - 0	+ 90 - 0	+ 90 - 0	+ 90 - 0	+ 90 - 0	+ 90 - 0	+ 90 - 0	+ 90 - 0													
4	+ 90 - 0	+ 90 - 0	+ 90 - 0	+ 90 - 0	+ 90 - 0	+ 90 - 0	+ 90 - 0	+ 90 - 0	+ 90 - 0	+ 90 - 0	+ 90 - 0	+ 90 - 0	+ 90 - 0	+ 90 - 0	+ 90 - 0	+ 90 - 0	+ 90 - 0	+ 90 - 0	+ 90 - 0	+ 90 - 0	+ 90 - 0									
5	+ 90 - 0	+ 90 - 0	+ 90 - 0	+ 90 - 0	+ 90 - 0	+ 90 - 0	+ 90 - 0	+ 90 - 0	+ 90 - 0	+ 90 - 0	+ 90 - 0	+ 90 - 0	+ 90 - 0	+ 90 - 0	+ 90 - 0															
6	+ 90 - 0	+ 90 - 0	+ 90 - 0	+ 90 - 0	+ 90 - 0	+ 90 - 0	+ 90 - 0	+ 90 - 0	+ 90 - 0	+ 90 - 0	+ 90 - 0	+ 90 - 0	+ 90 - 0	+ 90 - 0	+ 90 - 0	+ 90 - 0	+ 90 - 0	+ 90 - 0	+ 90 - 0	+ 90 - 0	+ 90 - 0	+ 90 - 0	+ 90 - 0							
7	+ 90 - 0	+ 90 - 0	+ 90 - 0	+ 90 - 0	+ 90 - 0	+ 90 - 0	+ 90 - 0	+ 90 - 0	+ 90 - 0	+ 90 - 0	+ 90 - 0	+ 90 - 0	+ 90 - 0																	
8	+ 90 - 0																													
9	+ 90 - 0	+ 90 - 0	+ 90 - 0	+ 90 - 0	+ 90 - 0	+ 90 - 0	+ 90 - 0	+ 90 - 0	+ 90 - 0	+ 90 - 0	+ 90 - 0	+ 90 - 0	+ 90 - 0	+ 90 - 0	+ 90 - 0	+ 90 - 0	+ 90 - 0	+ 90 - 0	+ 90 - 0	+ 90 - 0	+ 90 - 0	+ 90 - 0	+ 90 - 0	+ 90 - 0	+ 90 - 0					
10	+ 90 - 0	+ 90 - 0	+ 90 - 0	+ 90 - 0	+ 90 - 0	+ 90 - 0	+ 90 - 0	+ 90 - 0	+ 90 - 0	+ 90 - 0	+ 90 - 0																			
11	+ 90 - 0	+ 90 - 0	+ 90 - 0																											
12	+ 90 - 0	+ 90 - 0	+ 90 - 0	+ 90 - 0	+ 90 - 0	+ 90 - 0	+ 90 - 0	+ 90 - 0	+ 90 - 0	+ 90 - 0	+ 90 - 0	+ 90 - 0	+ 90 - 0	+ 90 - 0	+ 90 - 0	+ 90 - 0	+ 90 - 0	+ 90 - 0	+ 90 - 0	+ 90 - 0	+ 90 - 0	+ 90 - 0	+ 90 - 0	+ 90 - 0	+ 90 - 0	+ 90 - 0	+ 90 - 0			
13	+ 90 - 0	+ 90 - 0	+ 90 - 0	+ 90 - 0	+ 90 - 0	+ 90 - 0	+ 90 - 0	+ 90 - 0	+ 90 - 0																					
14	+ 90 - 0	+ 90 - 0	+ 90 - 0	+ 90 - 0	+ 90 - 0																									
15	+ 90 - 0	+ 90 - 0	+ 90 - 0	+ 90 - 0	+ 90 - 0	+ 90 - 0	+ 90 - 0	+ 90 - 0	+ 90 - 0	+ 90 - 0	+ 90 - 0	+ 90 - 0	+ 90 - 0	+ 90 - 0	+ 90 - 0	+ 90 - 0	+ 90 - 0	+ 90 - 0	+ 90 - 0	+ 90 - 0	+ 90 - 0	+ 90 - 0	+ 90 - 0	+ 90 - 0	+ 90 - 0	+ 90 - 0	+ 90 - 0	+ 90 - 0	+ 90 - 0	
16	+ 90 - 0	+ 90 - 0	+ 90 - 0	+ 90 - 0	+ 90 - 0	+ 90 - 0	+ 90 - 0																							
17	0 - 90 +	0 - 90 +	0 - 90 +	0 - 90 +	0 - 90 +	0 - 90 +	0 - 90 +	0 - 90 +																						
18	0 - 90 +	0 - 90 +	0 - 90 +	0 - 90 +	0 - 90 +	0 - 90 +	0 - 90 +	0 - 90 +	0 - 90 +	0 - 90 +	0 - 90 +	0 - 90 +	0 - 90 +	0 - 90 +	0 - 90 +	0 - 90 +	0 - 90 +	0 - 90 +	0 - 90 +	0 - 90 +	0 - 90 +	0 - 90 +	0 - 90 +	0 - 90 +	0 - 90 +	0 - 90 +	0 - 90 +	0 - 90 +	0 - 90 +	0 - 90 +
19	0 - 90 +	0 - 90 +	0 - 90 +	0 - 90 +	0 - 90 +	0 - 90 +																								
20	0 - 90 +	0 - 90 +	0 - 90 +	0 - 90 +	0 - 90 +	0 - 90 +	0 - 90 +	0 - 90 +	0 - 90 +	0 - 90 +																				
21	0 - 90 +	0 - 90 +	0 - 90 +	0 - 90 +	0 - 90 +	0 - 90 +	0 - 90 +	0 - 90 +	0 - 90 +	0 - 90 +	0 - 90 +	0 - 90 +	0 - 90 +	0 - 90 +	0 - 90 +	0 - 90 +	0 - 90 +	0 - 90 +	0 - 90 +	0 - 90 +	0 - 90 +	0 - 90 +	0 - 90 +	0 - 90 +	0 - 90 +	0 - 90 +	0 - 90 +	0 - 90 +		
22	0 - 90 +	0 - 90 +	0 - 90 +	0 - 90 +																										
23	0 - 90 +	0 - 90 +	0 - 90 +	0 - 90 +	0 - 90 +	0 - 90 +	0 - 90 +	0 - 90 +	0 - 90 +	0 - 90 +	0 - 90 +	0 - 90 +																		
24	0 - 90 +	0 - 90 +	0 - 90 +	0 - 90 +	0 - 90 +	0 - 90 +	0 - 90 +	0 - 90 +	0 - 90 +	0 - 90 +	0 - 90 +	0 - 90 +	0 - 90 +	0 - 90 +	0 - 90 +	0 - 90 +	0 - 90 +	0 - 90 +	0 - 90 +	0 - 90 +	0 - 90 +	0 - 90 +	0 - 90 +	0 - 90 +	0 - 90 +	0 - 90 +				
25	0 - 90 +	0 - 90 +																												
26	0 - 90 +	0 - 90 +	0 - 90 +	0 - 90 +	0 - 90 +	0 - 90 +	0 - 90 +	0 - 90 +	0 - 90 +	0 - 90 +	0 - 90 +	0 - 90 +	0 - 90 +	0 - 90 +																
27	0 - 90 +	0 - 90 +	0 - 90 +	0 - 90 +	0 - 90 +	0 - 90 +	0 - 90 +	0 - 90 +	0 - 90 +	0 - 90 +	0 - 90 +	0 - 90 +	0 - 90 +	0 - 90 +	0 - 90 +	0 - 90 +	0 - 90 +	0 - 90 +	0 - 90 +	0 - 90 +	0 - 90 +	0 - 90 +	0 - 90 +	0 - 90 +						
28	0 - 90 +	0 - 90 +	0 - 90 +	0 - 90 +	0 - 90 +	0 - 90 +	0 - 90 +	0 - 90 +	0 - 90 +	0 - 90 +	0 - 90 +	0 - 90 +	0 - 90 +	0 - 90 +	0 - 90 +	0 - 90 +														
29	0 - 90 +	0 - 90 +	0 - 90 +	0 - 90 +	0 - 90 +	0 - 90 +	0 - 90 +	0 - 90 +	0 - 90 +	0 - 90 +	0 - 90 +	0 - 90 +	0 - 90 +	0 - 90 +	0 - 90 +	0 - 90 +	0 - 90 +	0 - 90 +	0 - 90 +	0 - 90 +	0 - 90 +	0 - 90 +								
30	0 - 90 +	0 - 90 +	0 - 90 +	0 - 90 +	0 - 90 +	0 - 90 +	0 - 90 +	0 - 90 +	0 - 90 +	0 - 90 +	0 - 90 +	0 - 90 +	0 - 90 +	0 - 90 +	0 - 90 +	0 - 90 +	0 - 90 +	0 - 90 +												
31	0 - 90 +	0 - 90 +	0 - 90 +	0 - 90 +	0 - 90 +	0 - 90 +	0 - 90 +	0 - 90 +	0 - 90 +	0 - 90 +	0 - 90 +	0 - 90 +	0 - 90 +	0 - 90 +	0 - 90 +	0 - 90 +	0 - 90 +	0 - 90 +	0 - 90 +	0 - 90 +										
32	0 - 90 +	0 - 90 +	0 - 90 +	0 - 90 +	0 - 90 +	0 - 90 +	0 - 90 +	0 - 90 +	0 - 90 +	0 - 90 +	0 - 90 +	0 - 90 +	0 - 90 +	0 - 90 +	0 - 90 +	0 - 90 +	0 - 90 +	0 - 90 +	0 - 90 +	0 - 90 +	0 - 90 +	0 - 90 +	0 - 90 +	0 - 90 +	0 - 90 +	0 - 90 +	0 - 90 +	0 - 90 +	0 - 90 +	0 - 90 +

t Skin (mm)	40.00	38.75	37.50	36.25	35.00	33.75	32.50	31.25	30.00	28.75	27.50	26.25	25.00	23.75	22.50	21.25	20.00	18.75	17.50	16.25	15.00	13.75	12.50	11.25	10.00	8.75	7.50	6.25	5.00	3.75
No. of Textiles	32	31	30	29	28	27	26	25	24	23	22	21	20	19	18	17	16	15	14	13	12	11	10	9	8	7	6	5	4	3
% 0° Plies	30%	30%	30%	30%	30%	30%	30%	30%	30%	30%	30%	30%	30%	30%	30%	30%	30%	30%	30%	30%	30%	30%	30%	30%	30%	30%	30%	30%	30%	30%
% ± 45° Plies	60%	60%	60%	60%	60%	60%	60%	60%	60%	60%	60%	60%	60%	60%	60%	60%	60%	60%	60%	60%	60%	60%	60%	60%	60%	60%	60%	60%	60%	60%
% 90° Plies	10%	10%	10%	10%	10%	10%	10%	10%	10%	10%	10%	10%	10%	10%	10%	10%	10%	10%	10%	10%	10%	10%	10%	10%	10%	10%	10%	10%	10%	10%

Figure C-16: 30/60/10 NCF skin laminate

1	+ 90 - 0	+ 90 - 0	+ 90 - 0	+ 90 - 0	+ 90 - 0	+ 90 - 0	+ 90 - 0	+ 90 - 0	+ 90 - 0	+ 90 - 0	+ 90 - 0	+ 90 - 0	+ 90 - 0	+ 90 - 0	+ 90 - 0	+ 90 - 0	+ 90 - 0	+ 90 - 0	+ 90 - 0	+ 90 - 0	+ 90 - 0	+ 90 - 0	+ 90 - 0	+ 90 - 0	+ 90 - 0	+ 90 - 0	+ 90 - 0	+ 90 - 0	+ 90 - 0	+ 90 - 0
2	+ 90 - 0	+ 90 - 0	+ 90 - 0	+ 90 - 0	+ 90 - 0	+ 90 - 0	+ 90 - 0	+ 90 - 0	+ 90 - 0	+ 90 - 0	+ 90 - 0	+ 90 - 0	+ 90 - 0	+ 90 - 0	+ 90 - 0	+ 90 - 0	+ 90 - 0	+ 90 - 0	+ 90 - 0											
3	+ 90 - 0	+ 90 - 0	+ 90 - 0	+ 90 - 0	+ 90 - 0	+ 90 - 0	+ 90 - 0	+ 90 - 0	+ 90 - 0	+ 90 - 0	+ 90 - 0	+ 90 - 0	+ 90 - 0	+ 90 - 0	+ 90 - 0	+ 90 - 0	+ 90 - 0													
4	+ 90 - 0	+ 90 - 0	+ 90 - 0	+ 90 - 0	+ 90 - 0	+ 90 - 0	+ 90 - 0	+ 90 - 0	+ 90 - 0	+ 90 - 0	+ 90 - 0	+ 90 - 0	+ 90 - 0	+ 90 - 0	+ 90 - 0	+ 90 - 0	+ 90 - 0	+ 90 - 0	+ 90 - 0	+ 90 - 0	+ 90 - 0									
5	+ 90 - 0	+ 90 - 0	+ 90 - 0	+ 90 - 0	+ 90 - 0	+ 90 - 0	+ 90 - 0	+ 90 - 0	+ 90 - 0	+ 90 - 0	+ 90 - 0	+ 90 - 0	+ 90 - 0	+ 90 - 0	+ 90 - 0															
6	+ 90 - 0	+ 90 - 0	+ 90 - 0	+ 90 - 0	+ 90 - 0	+ 90 - 0	+ 90 - 0	+ 90 - 0	+ 90 - 0	+ 90 - 0	+ 90 - 0	+ 90 - 0	+ 90 - 0	+ 90 - 0	+ 90 - 0	+ 90 - 0	+ 90 - 0	+ 90 - 0	+ 90 - 0	+ 90 - 0	+ 90 - 0	+ 90 - 0	+ 90 - 0							
7	+ 90 - 0	+ 90 - 0	+ 90 - 0	+ 90 - 0	+ 90 - 0	+ 90 - 0	+ 90 - 0	+ 90 - 0	+ 90 - 0	+ 90 - 0	+ 90 - 0	+ 90 - 0	+ 90 - 0																	
8	+ 90 - 0																													
9	+ 90 - 0	+ 90 - 0	+ 90 - 0	+ 90 - 0	+ 90 - 0	+ 90 - 0	+ 90 - 0	+ 90 - 0	+ 90 - 0	+ 90 - 0	+ 90 - 0	+ 90 - 0	+ 90 - 0	+ 90 - 0	+ 90 - 0	+ 90 - 0	+ 90 - 0	+ 90 - 0	+ 90 - 0	+ 90 - 0	+ 90 - 0	+ 90 - 0	+ 90 - 0	+ 90 - 0	+ 90 - 0					
10	+ 90 - 0	+ 90 - 0	+ 90 - 0	+ 90 - 0	+ 90 - 0	+ 90 - 0	+ 90 - 0	+ 90 - 0	+ 90 - 0	+ 90 - 0	+ 90 - 0																			
11	+ 90 - 0	+ 90 - 0	+ 90 - 0																											
12	+ 90 - 0	+ 90 - 0	+ 90 - 0	+ 90 - 0	+ 90 - 0	+ 90 - 0	+ 90 - 0	+ 90 - 0	+ 90 - 0	+ 90 - 0	+ 90 - 0	+ 90 - 0	+ 90 - 0	+ 90 - 0	+ 90 - 0	+ 90 - 0	+ 90 - 0	+ 90 - 0	+ 90 - 0	+ 90 - 0	+ 90 - 0	+ 90 - 0	+ 90 - 0	+ 90 - 0	+ 90 - 0	+ 90 - 0	+ 90 - 0			
13	+ 90 - 0	+ 90 - 0	+ 90 - 0	+ 90 - 0	+ 90 - 0	+ 90 - 0	+ 90 - 0	+ 90 - 0	+ 90 - 0																					
14	+ 90 - 0	+ 90 - 0	+ 90 - 0	+ 90 - 0	+ 90 - 0																									
15	+ 90 - 0	+ 90 - 0	+ 90 - 0	+ 90 - 0	+ 90 - 0	+ 90 - 0	+ 90 - 0	+ 90 - 0	+ 90 - 0	+ 90 - 0	+ 90 - 0	+ 90 - 0	+ 90 - 0	+ 90 - 0	+ 90 - 0	+ 90 - 0	+ 90 - 0	+ 90 - 0	+ 90 - 0	+ 90 - 0	+ 90 - 0	+ 90 - 0	+ 90 - 0	+ 90 - 0	+ 90 - 0	+ 90 - 0	+ 90 - 0	+ 90 - 0	+ 90 - 0	
16	+ 90 - 0	+ 90 - 0	+ 90 - 0	+ 90 - 0	+ 90 - 0	+ 90 - 0	+ 90 - 0																							
17	0 - 90 +	0 - 90 +	0 - 90 +	0 - 90 +	0 - 90 +	0 - 90 +	0 - 90 +	0 - 90 +																						
18	0 - 90 +	0 - 90 +	0 - 90 +	0 - 90 +	0 - 90 +	0 - 90 +	0 - 90 +	0 - 90 +	0 - 90 +	0 - 90 +	0 - 90 +	0 - 90 +	0 - 90 +	0 - 90 +	0 - 90 +	0 - 90 +	0 - 90 +	0 - 90 +	0 - 90 +	0 - 90 +	0 - 90 +	0 - 90 +	0 - 90 +	0 - 90 +	0 - 90 +	0 - 90 +	0 - 90 +	0 - 90 +	0 - 90 +	0 - 90 +
19	0 - 90 +	0 - 90 +	0 - 90 +	0 - 90 +	0 - 90 +	0 - 90 +																								
20	0 - 90 +	0 - 90 +	0 - 90 +	0 - 90 +	0 - 90 +	0 - 90 +	0 - 90 +	0 - 90 +	0 - 90 +	0 - 90 +																				
21	0 - 90 +	0 - 90 +	0 - 90 +	0 - 90 +	0 - 90 +	0 - 90 +	0 - 90 +	0 - 90 +	0 - 90 +	0 - 90 +	0 - 90 +	0 - 90 +	0 - 90 +	0 - 90 +	0 - 90 +	0 - 90 +	0 - 90 +	0 - 90 +	0 - 90 +	0 - 90 +	0 - 90 +	0 - 90 +	0 - 90 +	0 - 90 +	0 - 90 +	0 - 90 +	0 - 90 +	0 - 90 +		
22	0 - 90 +	0 - 90 +	0 - 90 +	0 - 90 +																										
23	0 - 90 +	0 - 90 +	0 - 90 +	0 - 90 +	0 - 90 +	0 - 90 +	0 - 90 +	0 - 90 +	0 - 90 +	0 - 90 +	0 - 90 +	0 - 90 +																		
24	0 - 90 +	0 - 90 +	0 - 90 +	0 - 90 +	0 - 90 +	0 - 90 +	0 - 90 +	0 - 90 +	0 - 90 +	0 - 90 +	0 - 90 +	0 - 90 +	0 - 90 +	0 - 90 +	0 - 90 +	0 - 90 +	0 - 90 +	0 - 90 +	0 - 90 +	0 - 90 +	0 - 90 +	0 - 90 +	0 - 90 +	0 - 90 +	0 - 90 +	0 - 90 +				
25	0 - 90 +	0 - 90 +																												
26	0 - 90 +	0 - 90 +	0 - 90 +	0 - 90 +	0 - 90 +	0 - 90 +	0 - 90 +	0 - 90 +	0 - 90 +	0 - 90 +	0 - 90 +	0 - 90 +	0 - 90 +	0 - 90 +																
27	0 - 90 +	0 - 90 +	0 - 90 +	0 - 90 +	0 - 90 +	0 - 90 +	0 - 90 +	0 - 90 +	0 - 90 +	0 - 90 +	0 - 90 +	0 - 90 +	0 - 90 +	0 - 90 +	0 - 90 +	0 - 90 +	0 - 90 +	0 - 90 +	0 - 90 +	0 - 90 +	0 - 90 +	0 - 90 +	0 - 90 +	0 - 90 +						
28	0 - 90 +	0 - 90 +	0 - 90 +	0 - 90 +	0 - 90 +	0 - 90 +	0 - 90 +	0 - 90 +	0 - 90 +	0 - 90 +	0 - 90 +	0 - 90 +	0 - 90 +	0 - 90 +	0 - 90 +	0 - 90 +														
29	0 - 90 +	0 - 90 +	0 - 90 +	0 - 90 +	0 - 90 +	0 - 90 +	0 - 90 +	0 - 90 +	0 - 90 +	0 - 90 +	0 - 90 +	0 - 90 +	0 - 90 +	0 - 90 +	0 - 90 +	0 - 90 +	0 - 90 +	0 - 90 +	0 - 90 +	0 - 90 +	0 - 90 +	0 - 90 +								
30	0 - 90 +	0 - 90 +	0 - 90 +	0 - 90 +	0 - 90 +	0 - 90 +	0 - 90 +	0 - 90 +	0 - 90 +	0 - 90 +	0 - 90 +	0 - 90 +	0 - 90 +	0 - 90 +	0 - 90 +	0 - 90 +	0 - 90 +	0 - 90 +												
31	0 - 90 +	0 - 90 +	0 - 90 +	0 - 90 +	0 - 90 +	0 - 90 +	0 - 90 +	0 - 90 +	0 - 90 +	0 - 90 +	0 - 90 +	0 - 90 +	0 - 90 +	0 - 90 +	0 - 90 +	0 - 90 +	0 - 90 +	0 - 90 +	0 - 90 +	0 - 90 +										
32	0 - 90 +	0 - 90 +	0 - 90 +	0 - 90 +	0 - 90 +	0 - 90 +	0 - 90 +	0 - 90 +	0 - 90 +	0 - 90 +	0 - 90 +	0 - 90 +	0 - 90 +	0 - 90 +	0 - 90 +	0 - 90 +	0 - 90 +	0 - 90 +	0 - 90 +	0 - 90 +	0 - 90 +	0 - 90 +	0 - 90 +	0 - 90 +	0 - 90 +	0 - 90 +	0 - 90 +	0 - 90 +	0 - 90 +	0 - 90 +
t Skin (mm)	40.00	38.75	37.50	36.25	35.00	33.75	32.50	31.25	30.00	28.75	27.50	26.25	25.00	23.75	22.50	21.25	20.00	18.75	17.50	16.25	15.00	13.75	12.50	11.25	10.00	8.75	7.50	6.25	5.00	3.75
No. of Textiles	32	31	30	29	28	27	26	25	24	23	22	21	20	19	18	17	16	15	14	13	12	11	10	9	8	7	6	5	4	3
% 0° Plies	10%	10%	10%	10%	10%	10%	10%	10%	10%	10%	10%	10%	10%	10%	10%	10%	10%	10%	10%	10%	10%	10%	10%	10%	10%	10%	10%	10%	10%	10%
% ± 45° Plies	80%	80%	80%	80%	80%	80%	80%	80%	80%	80%	80%	80%	80%	80%	80%	80%	80%	80%	80%	80%	80%	80%	80%	80%	80%	80%	80%	80%	80%	80%
% 90° Plies	10%	10%	10%	10%	10%	10%	10%	10%	10%	10%	10%	10%	10%	10%	10%	10%	10%	10%	10%	10%	10%	10%	10%	10%	10%	10%	10%	10%	10%	10%

Figure C-17: 10/80/10 NCF skin laminate

C.2.2 Stringers

The stringer foot thickness is related to the skin thickness, and furthermore the spine thickness is related to the angle thickness, as for the UD stringers. Therefore, the different stringer configuration required for a skin thickness from 3.25-40.00mm, is shown in Table C-3.

	Min Skin Thk (mm)	Max Skin Thk (mm)	Angle Thk (mm)	No. of Textiles in Angle	Max Spine Thk (mm)	Max no. of Textiles in Spine
Config. 1	3.25	7.25	1.85	3	9.05	15
Config. 2	7.26	11.75	2.95	5	11.45	19
Config. 3	11.76	14.75	3.7	6	15.15	25
Config. 4	14.76	19.00	4.8	8	21.45	35
Config. 5	19.01	26.50	6.65	11	30.15	49
Config. 6	26.51	37.00	9.25	15	38.80	64
Config. 7	37.01	40.00	12.95	19	38.80	64

Table C-3: NCF stringer details

The basic laminate will involve the following 3 textiles:

- TE3/TE4/TE5
  - (+/0/-)/(0/90/0)/(-/0/+)

Where the 90° ply represents the mid-plane of the laminate. This laminate has an overall 62/28/10 proportioning, with the ply thicknesses shown in Table C-4. The reason for the necessity to have 3 tri-axial textiles, as opposed to a simpler twin quad-axial textiles, is to reach the target of a high proportion of 0° plies, whilst not having an overly thick single 0° ply. Furthermore, the ability to finely tailor the thickness is also wished for. Finally, the only difference between TE3 and TE5 is that the position of the +45° and -45° are swapped.

TE3			TE4			TE5		
Ply	Areal Weight (gsm)	Thk. (mm)	Ply	Areal Weight (gsm)	Thk. (mm)	Ply	Areal Weight (gsm)	Thk. (mm)
+	140	0.13	0	310	0.29	-	140	0.13
0	310	0.29	90	190	0.17	0	310	0.29
-	140	0.13	0	310	0.29	+	140	0.13
Total	***590***	***0.55***		***810***	***0.75***		***590***	***0.55***

Table C-4: NCF textile for stringer fabrication

The stringers are configured as shown in Figure C-18, where the capping plate is the same thickness as the angle. For the T-profile and I-profile stringers, the LHS angle and the capping plate will only use TE3 & TE4 textiles, i.e. for TE_Seq; whereas for the T- and I-profile stringers the RHS angle and the I-profile stringer's upper capping plate will only use TE5 & TE4 textiles, i.e. for TE_SeqA.

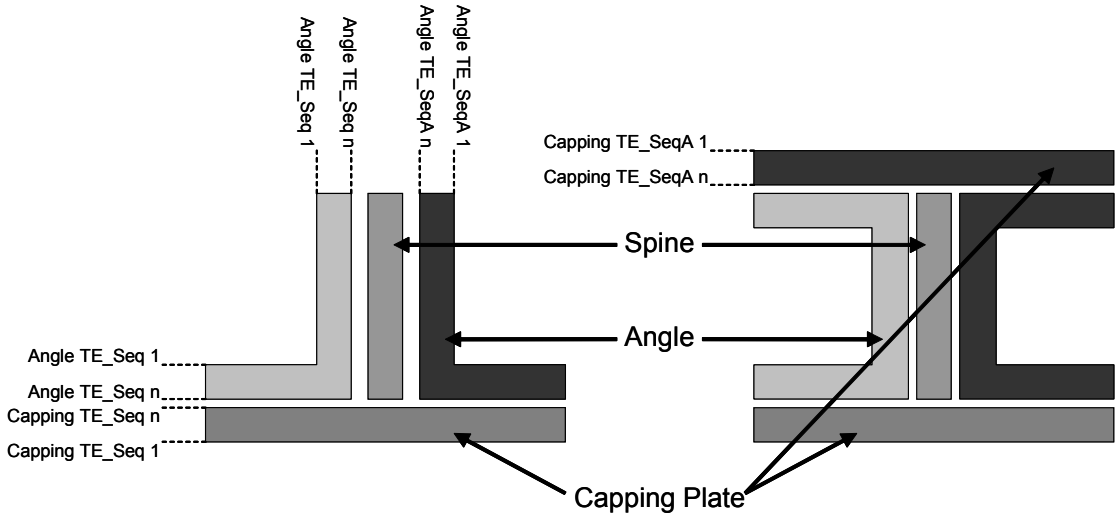

Figure C-18: Configuration for NCF T- and I-profile stringers

The stacking sequences for the angles and capping plates are:

- Config 1 (3 Textiles)
  - LHS Angle and lower capping plate
    - TE3/TE4/TE3
  - RHS Angle and upper capping plate
    - TE5/TE4/TE5
- Config 2 (5 Textiles)
  - LHS Angle and lower capping plate
    - TE3/TE3/TE4/TE3/TE3
  - RHS Angle and upper capping plate
    - TE5/TE5/TE4/TE5/TE5
- Config 3 (6 Textiles)
  - LHS Angle and lower capping plate
    - TE3/TE3/TE4/TE4/TE3/TE3
  - RHS Angle and upper capping plate
    - TE5/TE5/TE4/TE4/TE5/TE5
- Config 4 (8 Textiles)
  - LHS Angle and lower capping plate
    - TE3/TE3/TE3/TE4/TE4/TE3/TE3/TE3
  - RHS Angle and upper capping plate
    - TE5/TE5/TE5/TE4/TE4/TE5/TE5/TE5
- Config 5 (11 Textiles)
  - LHS Angle and lower capping plate
    - TE3/TE3/TE3/TE3/TE4/TE4/TE4/TE3/TE3/TE3/TE3
  - RHS Angle and upper capping plate
    - TE5/TE5/TE5/TE5/TE4/TE4/TE4/TE5/TE5/TE5/TE5
- Config 6 (15 Textiles)
  - LHS Angle and lower capping plate
    - TE3/TE3/TE3/TE3/TE3/TE4/TE4/TE4/TE4/TE4/TE3/TE3/TE3/ TE3/TE3

    - RHS Angle and upper capping plate
        - TE5/TE5/TE5/TE5/TE5/TE4/TE4/TE4/TE4/TE4/TE5/TE5/TE5/TE5/TE5
- Config 6 (19 Textiles)
    - LHS Angle and lower capping plate
        - TE3/TE3/TE3/TE3/TE3/TE3/TE3/TE4/TE4/TE4/TE4/TE4/TE3/TE3/TE3/TE3/TE3/TE3/TE3
    - RHS Angle and upper capping plate
        - TE5/TE5/TE5/TE5/TE5/TE5/TE5/TE4/TE4/TE4/TE4/TE4/TE5/TE5/TE5/TE5/TE5/TE5/TE5

The spine laminate is shown in Figure C-19.

t Skin (mm)	38.80	38.25	37.70	37.15	36.60	36.05	35.50	34.75	34.00	33.45	32.90	32.35	31.80	31.25	30.70	30.15	29.60	28.85	28.10	27.55	27.00	26.25	25.50	24.95	24.40	23.85	23.30	22.75	22.20	21.45	20.70	19.95	19.20	18.65	18.10	17.55	17.00	16.45	15.90	15.15	14.40	13.85	13.30	12.75	12.20	11.45	10.70	10.15	9.60	9.05	8.50	7.95	7.40	6.65	5.90	5.35	4.80	4.25	3.70	3.15	2.60	1.85	1.10
No. of Textiles	64	63	62	61	60	59	58	57	56	55	54	53	52	51	50	49	48	47	46	45	44	43	42	41	40	39	38	37	36	35	34	33	32	31	30	29	28	27	26	25	24	23	22	21	20	19	18	17	16	15	14	13	12	11	10	9	8	7	6	5	4	3	2
% 0° Plies	61%	61%	61%	61%	61%	62%	62%	61%	61%	61%	61%	61%	62%	62%	62%	62%	62%	62%	62%	62%	62%	61%	61%	61%	61%	62%	62%	62%	62%	62%	61%	61%	60%	60%	61%	61%	61%	61%	62%	61%	60%	60%	61%	61%	61%	60%	59%	60%	60%	61%	61%	62%	62%	61%	59%	59%	60%	61%	62%	64%	66%	62%	53%
% ± 45° Plies	31%	31%	30%	30%	30%	30%	29%	30%	31%	30%	30%	30%	29%	29%	29%	28%	28%	29%	30%	29%	29%	30%	31%	30%	30%	29%	29%	29%	28%	29%	30%	31%	33%	32%	32%	31%	31%	30%	29%	31%	33%	32%	31%	31%	30%	32%	34%	33%	33%	32%	31%	29%	28%	31%	35%	34%	33%	31%	28%	25%	20%	28%	47%
% 90° Plies	8%	8%	8%	9%	9%	9%	9%	9%	8%	8%	9%	9%	9%	9%	9%	9%	10%	9%	9%	9%	9%	9%	8%	8%	9%	9%	9%	9%	10%	9%	9%	8%	7%	8%	8%	8%	8%	9%	9%	8%	7%	8%	8%	8%	9%	8%	7%	7%	7%	8%	8%	9%	10%	8%	6%	7%	7%	8%	10%	11%	14%	10%	0%

Figure C-19: 60/30/10 NCF stringer spine laminate

C.3 Braid

C.3.1 Stringers

As a braid can be considered as a single ply, then there are no issues with symmetry. Furthermore, there are no issues with stacking sequence. The braid itself will be considered to be [0_{36k}, $\pm60_{6k}$] 56% Axial, with a cured folded thickness of 0.8mm. In terms of modelling the braid in ESDUpac A0817, it can be as (+60/-60/0/-60/+60), which ensures there is no issue of asymmetry. The associated thicknesses of the plies would be 0.088mm for the ±60° and 0.448mm for the 0° ply.

The stringer foot thickness is related to the skin thickness, and furthermore the spine thickness is related to the angle thickness, as for the UD and NCF stringers. Therefore the different stringer configuration required for a skin thickness from 3.25-40.00mm is shown in Table C-5.

The spine laminate is shown in Figure C-20.

	Min Skin Thk (mm)	Max Skin Thk (mm)	Angle Thk (mm)	No. of Braids in Angle	Max Spine Thk (mm)	Max no. of Textiles in Spine
Config. 1	3.25	6.25	1.6	2	8.0	10
Config. 2	6.26	8.00	2.4	3	11.2	14
Config. 3	8.01	11.25	3.2	4	15.2	19
Config. 4	11.26	16.00	4.0	5	19.2	24
Config. 5	16.01	22.25	5.6	7	26.4	33
Config. 6	22.26	32.00	8.0	10	37.6	47
Config. 7	32.01	40.00	10.4	13	48.8	61

Table C-5: Braid stringer details

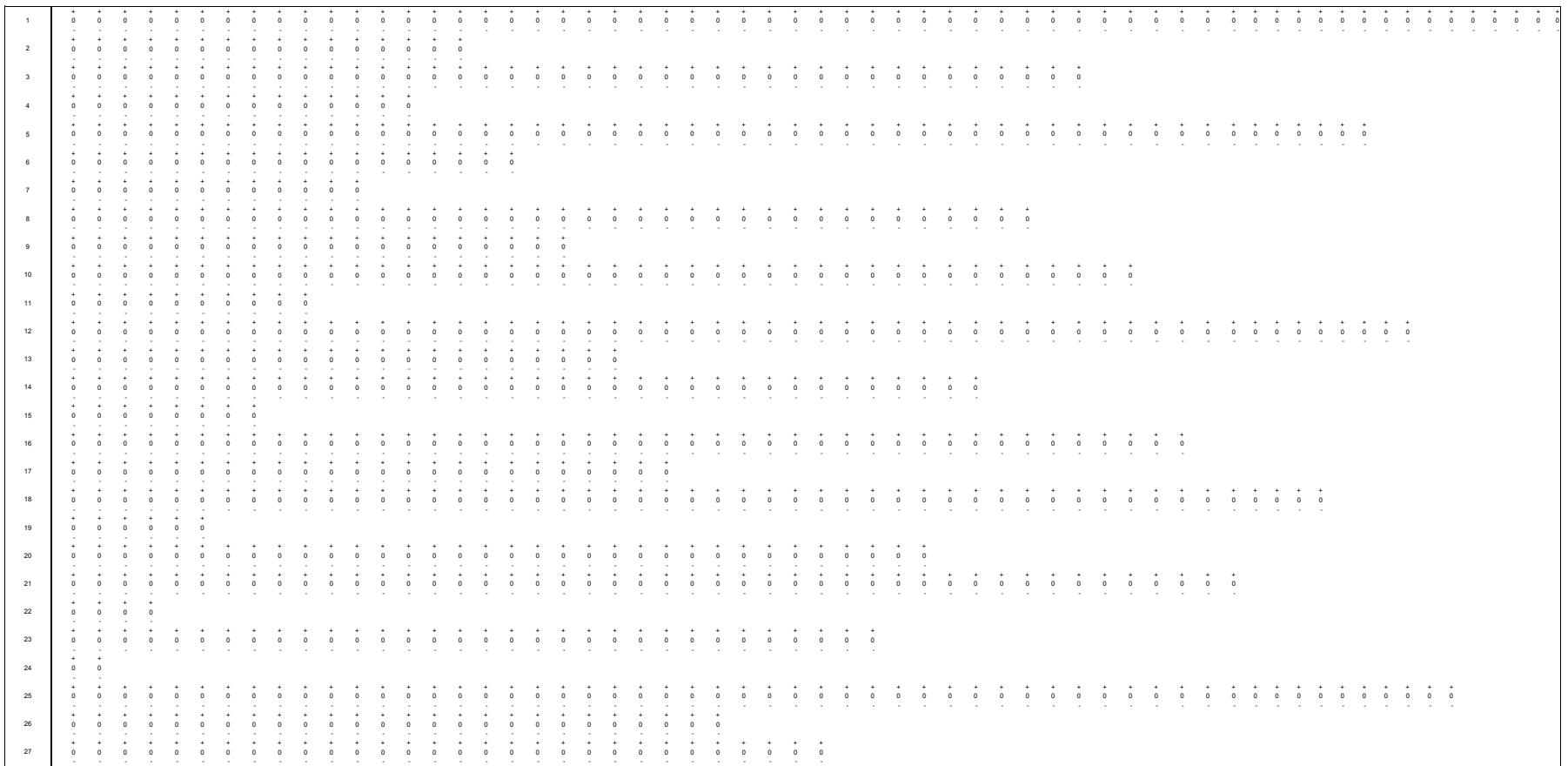

Figure C-20: Braid stringer spine laminate

C.4 Amending Real Laminates for use with ESDUpac A0817 program

A constraint in the ESDUpac A0817 program is that the laminates should be symmetric about the mid-plane, balanced and generally orthotropic, which is defined in ESDU 94003[621] as an "AsBoDf" laminate, i.e. the A-matrix is symmetric, the B-matrix is 0, and the D-matrix is fully populated. This constraint will mean that the laminate data inputted into the program must be amended, when the particular stacking sequence is not AsBoDf. This occurs when plies are terminated, such as when there is an unequal number of 0° or 90° plies above and below the mid-symmetry, or likewise for the ±45° plies, where there should be the same number + and – plies above and below the mid-symmetry.

C.4.1 UD Prepreg

Due to the termination of single plies in the UD prepreg laminate, in order to allow a fine tailoring of thickness, it is likely that slight asymmetry will occur. To ensure that this does not cause an error when using the ESDUpac A0817, the typical laminate shown in Table C-6, has to be modified as shown in Table C-7.

	7.00mm		6.75mm		6.50mm		6.25mm		6.00mm		5.75mm		5.50mm		5.25mm		5.00mm	
	°	mm	°	mm	°	mm	°	mm	°	mm	°	mm	°	mm	°	mm	°	mm
1	0	0.25	0	0.25	0	0.25	0	0.25	0	0.25	0	0.25	0	0.25	0	0.25	0	0.25
2	0	0.25	0	0.25	0	0.25	0	0.25	0	0.25	0	0.25	0	0.25	0	0.25	0	0.25
3	-	0.25	-	0.25	-	0.25	-	0.25	-	0.25	-	0.25	-	0.25	-	0.25	-	0.25
4	0	0.25	0	0.25	0	0.25	0	0.25	0	0.25	0	0.25	0	0.25	0	0.25	0	0.25
5	+	0.25	+	0.25	+	0.25	+	0.25	+	0.25	+	0.25	+	0.25	+	0.25	+	0.25
6	0	0.25	0	0.25	0	0.25	0	0.25	0	0.25	0	0.25	0	0.25	0	0.25	0	0.25
7	0	0.25	0	0.25	0	0.25	0	0.25	0	0.25	0	0.25	0	0.25	0	0.25	0	0.25
8	-	0.25	-	0.25	-	0.25												
9	90	0.25	90	0.25	90	0.25	90	0.25	90	0.25	90	0.25	90	0.25				
10	+	0.25	+	0.25	+	0.25	+	0.25	+	0.25								
11	0	0.25	0	0.25	0	0.25	0	0.25	0	0.25	0	0.25	0	0.25	0	0.25	0	0.25
12	0	0.25																
13	-	0.25	-	0.25	-	0.25	-	0.25	-	0.25	-	0.25	-	0.25	-	0.25	-	0.25
14	0	0.25	0	0.25	0	0.25	0	0.25	0	0.25	0	0.25	0	0.25	0	0.25	0	0.25
14	0	0.25	0	0.25	0	0.25	0	0.25	0	0.25	0	0.25	0	0.25	0	0.25	0	0.25
13	-	0.25	-	0.25	-	0.25	-	0.25	-	0.25	-	0.25	-	0.25	-	0.25	-	0.25
12	0	0.25	0	0.25														
11	0	0.25	0	0.25	0	0.25	0	0.25	0	0.25	0	0.25	0	0.25	0	0.25	0	0.25
10	+	0.25	+	0.25	+	0.25	+	0.25	+	0.25	+	0.25						
9	90	0.25	90	0.25	90	0.25	90	0.25	90	0.25	90	0.25	90	0.25	90	0.25		
8	-	0.25	-	0.25	-	0.25	-	0.25										
7	0	0.25	0	0.25	0	0.25	0	0.25	0	0.25	0	0.25	0	0.25	0	0.25	0	0.25
6	0	0.25	0	0.25	0	0.25	0	0.25	0	0.25	0	0.25	0	0.25	0	0.25	0	0.25
5	+	0.25	+	0.25	+	0.25	+	0.25	+	0.25	+	0.25	+	0.25	+	0.25	+	0.25
4	0	0.25	0	0.25	0	0.25	0	0.25	0	0.25	0	0.25	0	0.25	0	0.25	0	0.25
3	-	0.25	-	0.25	-	0.25	-	0.25	-	0.25	-	0.25	-	0.25	-	0.25	-	0.25
2	0	0.25	0	0.25	0	0.25	0	0.25	0	0.25	0	0.25	0	0.25	0	0.25	0	0.25
1	0	0.25	0	0.25	0	0.25	0	0.25	0	0.25	0	0.25	0	0.25	0	0.25	0	0.25

Table C-6: Conventional ply terminations

	7.00mm		6.75mm		6.50mm		6.25mm		6.00mm		5.75mm		5.50mm		5.25mm		5.00mm	
	°	mm	°	mm	°	mm	°	mm	°	mm	°	mm	°	mm	°	mm	°	mm
1	0	0.25	0	0.25	0	0.25	0	0.25	0	0.25	0	0.25	0	0.25	0	0.25	0	0.25
2	0	0.25	0	0.25	0	0.25	0	0.25	0	0.25	0	0.25	0	0.25	0	0.25	0	0.25
3	-	0.25	-	0.25	-	0.25	-	0.25	-	0.25	-	0.25	-	0.25	-	0.25	-	0.25
4	0	0.25	0	0.25	0	0.25	0	0.25	0	0.25	0	0.25	0	0.25	0	0.25	0	0.25
5	+	0.25	+	0.25	+	0.25	+	0.25	+	0.25	+	0.25	+	0.25	+	0.25	+	0.25
6	0	0.25	0	0.25	0	0.25	0	0.25	0	0.25	0	0.25	0	0.25	0	0.25	0	0.25
7	0	0.25	0	0.25	0	0.25	0	0.25	0	0.25	0	0.25	0	0.25	0	0.25	0	0.25
8	-	0.25	-	0.25	-	0.25	-	0.1875	-	0.125	-	0.0625						
9	90	0.25	90	0.25	90	0.25	90	0.25	90	0.25	90	0.25	90	0.25	90	0.125		
10	+	0.25	+	0.25	+	0.25	+	0.1875	+	0.125	+	0.0625						
11	0	0.25	0	0.25	0	0.25	0	0.25	0	0.25	0	0.25	0	0.25	0	0.25	0	0.25
12	0	0.25	0	0.125														
13	-	0.25	-	0.25	-	0.25	-	0.25	-	0.25	-	0.25	-	0.25	-	0.25	-	0.25
14	0	0.25	0	0.25	0	0.25	0	0.25	0	0.25	0	0.25	0	0.25	0	0.25	0	0.25
14	0	0.25	0	0.25	0	0.25	0	0.25	0	0.25	0	0.25	0	0.25	0	0.25	0	0.25
13	-	0.25	-	0.25	-	0.25	-	0.25	-	0.25	-	0.25	-	0.25	-	0.25	-	0.25
12	0	0.25	0	0.125														
11	0	0.25	0	0.25	0	0.25	0	0.25	0	0.25	0	0.25	0	0.25	0	0.25	0	0.25
10	+	0.25	+	0.25	+	0.25	+	0.1875	+	0.125	+	0.0625						
9	90	0.25	90	0.25	90	0.25	90	0.25	90	0.25	90	0.25	90	0.25	90	0.125		
8	-	0.25	-	0.25	-	0.25	-	0.1875	-	0.125	-	0.0625						
7	0	0.25	0	0.25	0	0.25	0	0.25	0	0.25	0	0.25	0	0.25	0	0.25	0	0.25
6	0	0.25	0	0.25	0	0.25	0	0.25	0	0.25	0	0.25	0	0.25	0	0.25	0	0.25
5	+	0.25	+	0.25	+	0.25	+	0.25	+	0.25	+	0.25	+	0.25	+	0.25	+	0.25
4	0	0.25	0	0.25	0	0.25	0	0.25	0	0.25	0	0.25	0	0.25	0	0.25	0	0.25
3	-	0.25	-	0.25	-	0.25	-	0.25	-	0.25	-	0.25	-	0.25	-	0.25	-	0.25
2	0	0.25	0	0.25	0	0.25	0	0.25	0	0.25	0	0.25	0	0.25	0	0.25	0	0.25
1	0	0.25	0	0.25	0	0.25	0	0.25	0	0.25	0	0.25	0	0.25	0	0.25	0	0.25

Table C-7: Method to terminate plies for ESDU program

It can be seen in Table C-7 that for the termination of a single 0° or 90° ply, the corresponding symmetric ply thickness is halved as well as the thickness of the ply to be terminated. This way, the thickness of the laminate has been reduced by the termination of a single ply but the laminate remains symmetric. For a ±45° ply, in order to keep the laminate balanced and symmetric when terminating an angle ply, it is first necessary to reduce the thickness of the corresponding + and – plies that will be terminated, 4 in total, to 0.75/4 = 0.1875mm. This will represent a reduction of thickness of 0.25mm, i.e. the termination of 1 ply. Following this, all 4 plies will have a thickness of 0.5/4 = 0.125mm, and then the thickness of 0.25/4=0.0625mm, followed by the termination of all plies, as shown in Table C-7.

The effect of this method to terminate plies has been verified using ESDUpac 8147[489]. In Table C-8, the "asymmetric" column represents the real method shown in Table C-6, whereas the "symmetric" column represents the method required for the ESDUpac A0817, or as shown in Table C-7. As can be seen from Table C-8, there is principally no difference in the axial buckling load using ESDUpac A8147 for the two different laminates.

	Running Load (N/mm)	
Thickness (mm)	Asymmetric	Symmetric
6.75	1080	1080
6.25	847	849
5.25	485	485

Table C-8: Comparison between the asymmetric and ESDU amended symmetric laminates

C.4.2 NCF

Due to the nature of NCF there can be situations, such as the middle "3.75mm" column of Table C-9, where asymmetry occurs. In order to ensure that this thickness is compatible with ESDUpac A0817, then it is necessary to ensure symmetry of the laminate. This can be achieved by halving the ply thickness of the textile that is causing the asymmetry of the laminate, and making it symmetric, as shown in Table C-10.

2.50mm			3.75mm			5.00mm		
TE1	+	0.25	TE1	+	0.25	TE1	+	0.25
	90	0.125		90	0.125		90	0.125
	-	0.25		-	0.25		-	0.25
	0	0.625		0	0.625		0	0.625
TE2	0	0.625	TE1	+	0.25	TE1	+	0.25
	-	0.25		90	0.125		90	0.125
	90	0.125		-	0.25		-	0.25
	+	0.25		0	0.625		0	0.625
			TE2	0	0.625	TE2	0	0.625
				-	0.25		-	0.25
				90	0.125		90	0.125
				+	0.25		+	0.25
						TE2	0	0.625
							-	0.25
							90	0.125
							+	0.25

Table C-9: NCF construction in reality

2.50mm			3.75mm			5.00mm		
TE1	+	0.25	TE1	+	0.25	TE1	+	0.25
	90	0.125		90	0.125		90	0.125
	-	0.25		-	0.25		-	0.25
	0	0.625		0	0.625		0	0.625
TE2	0	0.625		+	0.125	TE1	+	0.25
	-	0.25		90	0.0625		90	0.125
	90	0.125		-	0.125		-	0.25
	+	0.25		0	0.3125		0	0.625
				0	0.3125	TE2	0	0.625
				-	0.125		-	0.25
				90	0.0625		90	0.125
				+	0.125		+	0.25
			TE2	0	0.625	TE2	0	0.625
				-	0.25		-	0.25
				90	0.125		90	0.125
				+	0.25		+	0.25

Table C-10: NCF construction due to ESDU FSM constraints

Appendix D – Stability and Strength Calculation

D.1 Load Proportioning

D.1.1 Axial Load

When subjected to a load, the force (F) reacted by the stringer-stiffened panel is distributed between the skin and stringer, as follows[558]:

$$F_{skin} = \frac{(E_{11}A)_{skin}}{(E_{11}A)_{skin} + (E_{11}A)_{str}} \times F_{overall} \quad \textbf{D-1}$$

$$F_{str} = \frac{(E_{11}A)_{str}}{(E_{11}A)_{skin} + (E_{11}A)_{str}} \times F_{overall} \quad \textbf{D-2}$$

Where A is the cross-sectional area of the part. The load reacted by the stringer's web and flanges can also be calculated using a similar method.

D.1.2 Shear Load

The distribution of shear load is different to that of axial load. Axial load runs along the prismatic shape of a stringer-stiffened panel, whereas shear load goes laterally through it. For an integral panel, i.e. a U-profile stringer panel, the shear flows only through the skin. For discrete stringers, such as a T- or I-profile stringer, the shear load is assumed to be distributed between the stringer foot and skin local to where the stringer foot is.

$$q_{local\ skin} = \frac{G_{skin}}{G_{skin} + G_{str\ flange}} \times q \quad \textbf{D-3}$$

$$q_{lower\ flange} = \frac{G_{str\ flange}}{G_{skin} + G_{str\ flange}} \times q \quad \textbf{D-4}$$

D.2 Second Moment of Inertia for Inhomogeneous Beam

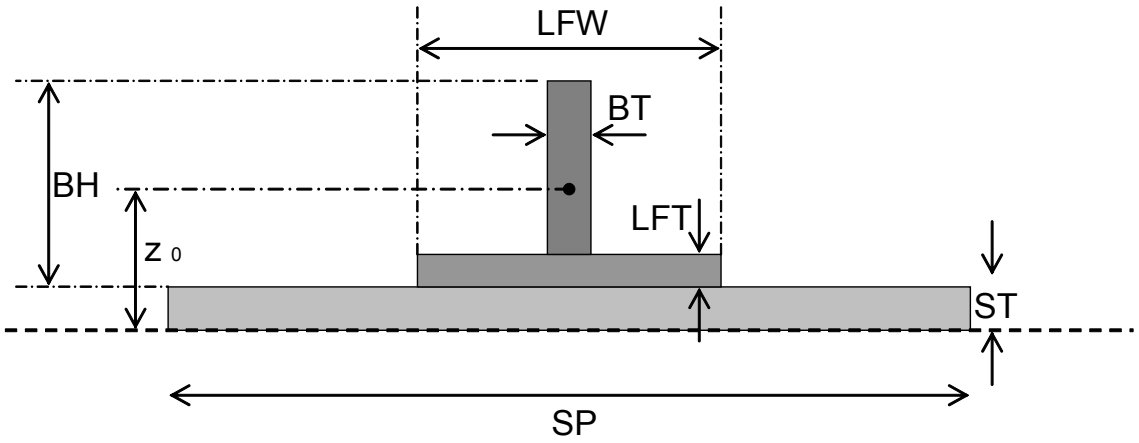

Figure D-1: Second moment of inertia for inhomogeneous stringer panels

	Width (mm)	Thickness (mm)	E (MPa)	A (mm²)	EA (N)	z- (mm)	EAz- (Nmm)	∑EI (Nmm²)
Skin	208.00	3.25	84500	676.00	5.712E+07	1.63	9.282E+07	-4.170E+09
Stringer Foot	60.00	3.00	96500	180.00	1.737E+07	4.75	8.251E+07	-9.242E+08
Stringer Web	5.00	47.00	96500	235.00	2.268E+07	29.75	6.747E+07	-2.251E+10

Table D-1: Basic properties and second moment of inertia of stringer individual section

$$z_0 = \frac{\sum EAz -}{\sum EA} \qquad \textbf{D-5}$$

$$E_{AV} = \frac{\sum EA}{\sum A} \qquad \textbf{D-6}$$

$$I = \frac{\sum EI}{\sum E_{AV}} \qquad \textbf{D-7}$$

D.3 Strain Calculation for Stringer-Stiffened Panel

D.3.1 For Skin

$$\varepsilon_{11\,skin} = \left(\frac{N_x \times (\%E_{11}A)_{skin}}{s_1 \times E_{11\,skin}} \right) \qquad \textbf{D-8}$$

D.3.2 For Stringers

$$\varepsilon_{lower\ flange} = \left(\frac{N_x \times (\%E_{11}A)_{foot}}{LFW \times LFT \times E_{11\ foot}} \right) \quad \textbf{D-9}$$

$$\varepsilon_{blade} = \left(\frac{N_x \times (\%E_{11}A)_{blade}}{(BH - LFT) \times BT \times E_{11\ blade}} \right) \quad \textbf{D-10}$$

$$\overline{G_{xy}} = \frac{(G_{xy}A)_{skin} + (G_{xy}A)_{lower\ flange}}{\left((G_{xy}A)_{skin} / (G_{xy})_{skin}\right) + \left((G_{xy}A)_{lower\ flange} / (G_{xy})_{lower\ flange}\right)} \quad \textbf{D-11}$$

$$\gamma_{12} = \frac{q}{\overline{G_{xy}}} \quad \textbf{D-12}$$

D.3.3 Combined Strain RF

$$\frac{1}{RF} = \sqrt{\left(\frac{\varepsilon_{11}}{\varepsilon_{allow}}\right)^2 + \left(\frac{\gamma_{12}}{\gamma_{allow}}\right)^2} \quad \textbf{D-13}$$

D.4 Strength

In terms of strength; tension, compression and shear must all be considered. There are several methods to calculate the strength of a laminate under combined loading, and hence there are various failure criteria. Typically, each developed failure criterion has been proven through experimental results, although due to the complex stress interactions between the fibres and the matrix, each method cannot be relied on with complete confidence. The chosen criterion will be based on the available information.

ESDUpac 84018[310] is an iterative method, which is based on a Puck modified criterion. The program can differentiate between matrix failure and fibre failure. When matrix failure occurs, the matrix material properties are removed i.e. its in-plane transverse direct and shear stiffnesses are zero. Thereafter, the assumption is that the fibre can still take the load in its longitudinal direction, which can result in further layers of matrix failing. Once either all the matrix layers have failed or the first fibre failure along the lamina's longitudinal direction has occurred, then the laminate is considered to have failed.

However, ESDUpac 84018 requires an extensive set of strength allowables to be developed, which might not be available at the preliminary design phase. A far simpler method, which is applicable at the preliminary design phase, is the maximum strain criteria failure analysis, as shown in Equation D-14.

$$RF = \frac{\varepsilon_{allowable}}{\varepsilon_{applied}}$$ **D-14**

D.4.1 Out-Of-Plane Loading

The effect of out-of-plane loading contributes mainly to the strength of the panel and occurs due to geometric imperfections in the design, eccentricities in the applied in-plane loading, and from fuel pressure[284]. Using Timoshenko's beam-column theory[548], the non-linear bending moments can be calculated. The stringer-stiffened panel will behave like a wide column with either simply supported or clamped boundary conditions at the ends of the stringer, with evaluation points, as shown in Figure D-2[284], where the maximum non-linear bending moments will occur. Vitali et al.[622] assumed clamped boundary conditions to synthesise the ribs, which can cater better for the induced sagging and hogging in the beam due to pressure than simply supported conditions, although it can overestimate the overall buckling load, as the panel's effective length is reduced, which diminishes the interaction with local buckling[464].

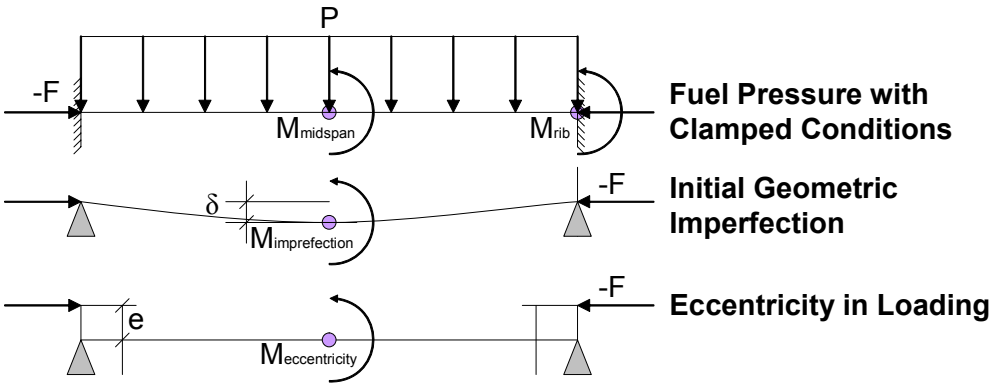

Figure D-2:Out-of-plane loading

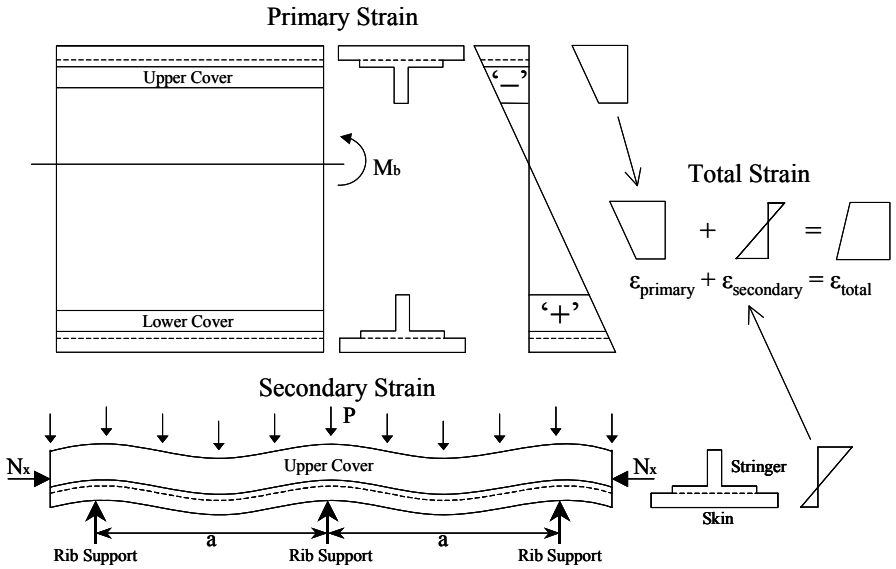

Figure D-3: Out-of-plane effects

The effect of lateral pressure on the assumed beam-column is illustrated in Figure D-3. At the rib stations, there is increased compression in the skin due to the hogging, and at the mid-span there is more compression in the stringer blade due to the sagging. Both the sagging and hogging can reduce the local buckling load of the panel[464], albeit this will not be considered in the stability analysis.

D.4.1.1 Lateral (Fuel) Pressure

Under lateral pressure, for clamped conditions, the non-linear bending moment at the mid-span, and at the extremities, is given by Equations D-15 and D-16, respectively[548].

$$M_{mispan} = \frac{P \times a^2}{4 \times b \times u^2} \times \left(\frac{u}{\sin(u)} - 1 \right) \quad \textbf{D-15}$$

$$M_{rib} = \frac{P \times a^2}{4 \times b \times u^2} \times \left(1 - \frac{u}{\tan(u)} \right) \quad \textbf{D-16}$$

$$\text{Where: } u = \frac{a}{2} \times \sqrt{\frac{-F}{E \times I}} \quad \textbf{D-17}$$

Where 'P' is the fuel pressure, 'a' and 'b' are the rib pitch and stringer pitch respectively. The 'u' factor is the axial load factor for beam-columns[548]. 15 psi was used as fuel overpressure case on the NASA ACT semi-span wing test[176], which at UL is 22.5 psi (0.1551N/mm²).

D.4.1.2 Initial Geometric Imperfections

This is a bow type imperfection, to cater for the difference in the idealised straight line and the actual curve underneath the stringer, due to the wing cover's contour. The non-linear bending moment for a simply supported beam at the mid-span is given by Equation D-18[548]:

$$M_{imperfection} = \frac{-F \times \delta}{1 - \frac{4 \times u^2}{\pi^2}} \quad \textbf{D-18}$$

Where 'F' is the compressive force and δ is the geometric imperfection, which can be considered as ±a/1000[553]. Thus for a 800mm rib pitch, there will be a 0.8mm deviation. This would seem appropriate for a highly contoured wing, or nearer the root, where the gulling effect is more pronounced as shown in Figure D-4. However, for a less contoured wing, or nearer the tip, a value of ±a/2000 is more appropriate.

Figure D-4: Gulling of the A380 wing

D.4.1.3 Load Eccentricities

It is virtually impossible to create a panel that is not eccentric due to imperfections in the panel[623]. An eccentricity factor 'e' of a/1000 has been assumed to correlate between the analytical and experimental data[623]. The non-linear bending moment for a simply supported beam at the mid-span is given by Equation D-19[548]:

$$M_{eccentricities} = \frac{-F \times e}{\cos(u)} \quad \textbf{D-19}$$

D.4.1.4 Combined Compressive Out-of-Plane Load

With clamped boundary conditions the out-of-plane strains are calculated at the mid-span ($M_{total\ mid\ span}$) and the extremities ($M_{extremities}$), which are given by Equations D-20 and D-21, respectively[538]:

$$M_{total\ midpsan} = M_{midspan} + M_{imperfection} + M_{eccentricities} \quad \textbf{D-20}$$

$$M_{total\ ribs} = M_{rib} + M_{imperfection} + M_{eccentricities} \quad \textbf{D-21}$$

D.4.1.5 Out-of Plane Loading Effects on Tension

The simple bending moment formula for a uniformly distributed load (UDL) with clamped ends, at the mid-span and the extremities, is given by Equations D-22 and D-23, respectively[624]:

$$M_{midspan} = \frac{1}{24} \times (P \times b) \times l^2 \quad \textbf{D-22}$$

$$M_{extremities} = -\frac{1}{12} \times (P \times b) \times l^2 \quad \textbf{D-23}$$

D.4.1.6 Converting Bending Moments into in-plane Strains

These non-linear bending moments are assumed to act over the entire length of the stringer, and are used to calculate the out-of-plane strains, using Equation D-24:

$$\varepsilon = \frac{M}{E \times I} \times (h - z_o) \qquad \textbf{D-24}$$

Where 'h' is the extremity of the element (i.e. skin, or stringer element), and 'z_o' is the centroid of the complete panel section.

This out-of-plane strain increment can then be added to the principal strain reacted by the element. The out-of-plane effects are considered to be local, hence they are included at this level of analysis, but they are not added to the overall panel strain for stability analysis.

D.4.2 Anisotropic Compressive Buckling

The skin is considered to be a long flat plate simply supported under normal and shear load. The non-dimensional parameters are given by[535]:

$$\alpha = \sqrt[4]{\frac{D_{22}}{D_{11}}} \qquad \textbf{D-25}$$

$$\beta = \frac{D_{12} + 2D_{66}}{\sqrt{D_{11} \times D_{22}}} \qquad \textbf{D-26}$$

$$\gamma = \frac{D_{16}}{\sqrt[4]{{D_{11}}^3 \times D_{22}}} \qquad \textbf{D-27}$$

$$\delta = \frac{D_{26}}{\sqrt[4]{D_{11} \times {D_{22}}^3}} \qquad \textbf{D-28}$$

For a long anisotropic plate with simply supported boundary conditions under compressive load, the critical buckling load is given by Equation D-29[536]:

$$N_x^{cr} = K_x \frac{\pi^2}{b^2} \sqrt{D_{11} \times D_{22}} \qquad \textbf{D-29}$$

Where K_x is a non-dimensional buckling coefficient given by Equation D-30:

$$K_x = 2(1+\beta) - 2\left(\beta + 3 + 2\gamma^2\right)\frac{(\gamma + 3\delta)^2}{(\beta+3)^2} - 4\left(\delta + 2\gamma^3 - \beta\gamma\right)\frac{(\gamma+3\delta)^3}{(\beta+3)^3} \qquad \textbf{D-30}$$

When $|\gamma|$ and $|\delta|$ < 0.4, K_x should have sufficient accuracy. When laminates with $|\gamma|$ and $|\delta|$ > 0.4 then an interaction scheme to calculate K_x is applied[536].

D.4.3 Anisotropic Shear Buckling

Shear buckling coefficient in terms of the non-dimensional parameters is given by Equation D-31[490].

$$K_{xy} = 3.42 + 2.05\beta - 0.13\beta^2 - 1.79\gamma - 6.89\delta + 0.36\beta(2\gamma + \delta) - 0.25(2\gamma + \delta)^2 \quad \textbf{D-31}$$

The critical shear-buckling load is given by Equation D-32.

$$N_{xy}^{cr} = \frac{\pi^2}{b^2} K_{xy} \sqrt[4]{D_{11} \times D_{22}^{\,3}} \quad \textbf{D-32}$$

D.4.4 Bearing/Bypass Calculation

$$Bearing = \frac{E_{11} A \times F \times b \times Load\ in\ 1st\ Bolt}{Bolt\ Dia \times Thickness} \quad \textbf{D-33}$$

$$Bypass = \frac{E_{11} A \times F \times b \times Load\ in\ 1st\ Bolt}{(Width\ of\ Element - Bolt\ Dia) \times Thickness\ of\ Element} \quad \textbf{D-34}$$

D.5 Input/Output Spreadsheet

Shown in Figure D-5 is an example of the Input/Output spreadsheet. Figure D-5 shows specifically the format for an I-profile stringer-stiffened panel. There is a choice of 3 formats, namely for U-, T-, and I-profile stringers, which can be selected using a decision process, which is integrated into the spreadsheet, to determine the stringer-stiffened panel's configuration. Within the Input/Output spreadsheet, the fields in yellow are for input data, whereas all other fields are automatically updated based on the input data. The "ABD Matrix for Stringer and Skin Elements Input Data", "Stringer and Skin Element Stiffnesses" and "Load Data for .STO File" are linked to the .STO generating spreadsheet, as the loads can only be apportioned to the elements through calculating the size and stiffness of the individual elements.

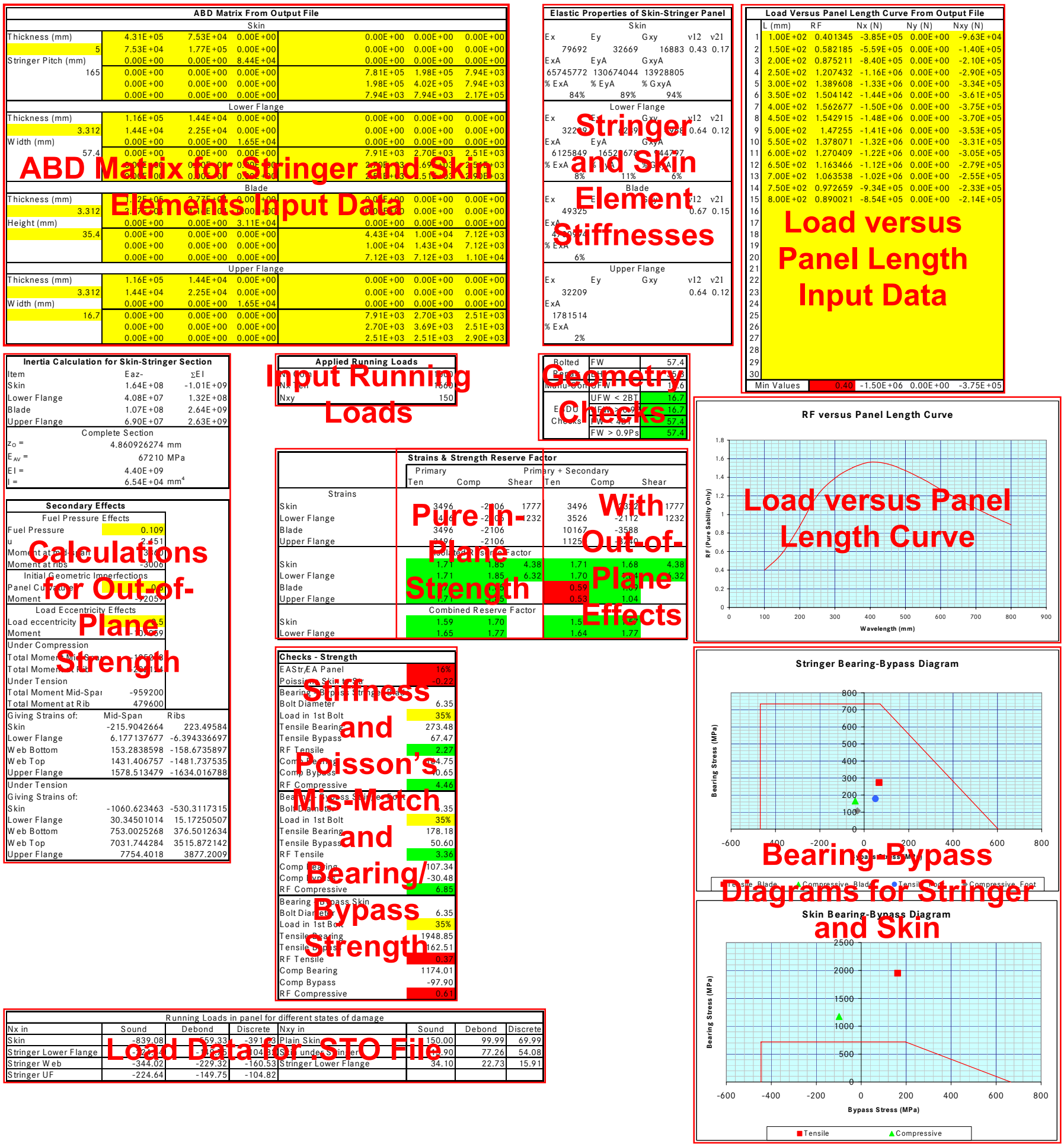

Figure D-5: Spreadsheet for stability and strength RF determination (example for I-profile stringer)

D.6 .STO File

Section 1

Sound_Panel	Debonded_Panel	Discrete_Damaged_Panel
5 T_stringers	5 T_stringers	4 (5) T_stringers
Example_Sound.pgd	Example_Debonded.pgd	Example_Discrete.pgd
Example_Sound.STO	Example_Debonded.STO	Example_Discrete.STO
Example_Sound.lam	Example_Debonded.lam	Example_Discrete.lam
N	N	N
mm	mm	mm

Section 2

2	1				2	1				2	1			
800	53.333	53.333			800	53.333	53.333			800	53.333	53.333		
86	80	20	0		86	80	16	0		77	72	16	0	
2					2					2				

Section 3

1	-78.125	-3.411			1	-78.125	-3.411			1	-78.125	-3.411		
2	-53.563	-3.411			2	-53.563	-3.411			2	-53.563	-3.411		
3	0.000	54.344			3	0.000	54.344			3	0.000	54.344		
4	0.000	40.758			4	0.000	40.758			4	0.000	40.758		
5	-29.000	-3.411			5	-29.000	-3.411			5	-29.000	-3.411		
6	-29.000	0.000			6	-29.000	0.000			6	-29.000	0.000		
7	-14.500	-3.411			7	-14.500	-3.411			7	-14.500	-3.411		
8	0.000	27.172			8	0.000	27.172			8	0.000	27.172		
9	-14.500	0.000			9	-14.500	0.000			9	-14.500	0.000		
10	0.000	-3.411			10	0.000	-3.411			10	0.000	-3.411		
11	0.000	0.000			11	0.000	0.000			11	0.000	0.000		
12	0.000	13.586			12	0.000	13.586			12	0.000	13.586		
13	14.500	-3.411			13	14.500	-3.411			13	14.500	-3.411		
14	14.500	0.000			14	14.500	0.000			14	14.500	0.000		
15	29.000	-3.411			15	29.000	-3.411			15	29.000	-3.411		
16	29.000	0.000			16	29.000	0.000			16	29.000	0.000		
17	53.563	-3.411			17	53.563	-3.411			17	53.563	-3.411		
18	78.125	-3.411			18	78.125	-3.411			18	78.125	-3.411		
19	102.688	-3.411			19	102.688	-3.411			19	102.688	-3.411		
20	156.250	54.344			20	156.250	54.344			20	156.250	54.344		
21	156.250	40.758			21	156.250	40.758			21	156.250	40.758		
22	127.250	-3.411			22	127.250	-3.411			22	127.250	-3.411		
23	127.250	0.000			23	127.250	0.000			23	127.250	0.000		
24	141.750	-3.411			24	141.750	-3.411			24	141.750	-3.411		
25	156.250	27.172			25	156.250	27.172			25	156.250	27.172		
26	141.750	0.000			26	141.750	0.000			26	141.750	0.000		
27	156.250	-3.411			27	156.250	-3.411			27	156.250	-3.411		
28	156.250	0.000			28	156.250	0.000			28	156.250	0.000		
29	156.250	13.586			29	156.250	13.586			29	156.250	13.586		
30	170.750	-3.411			30	170.750	-3.411			30	170.750	-3.411		
31	170.750	0.000			31	170.750	0.000			31	170.750	0.000		
32	185.250	-3.411			32	185.250	-3.411			32	185.250	-3.411		
33	185.250	0.000			33	185.250	0.000			33	185.250	0.000		
34	209.813	-3.411			34	209.813	-3.411			34	209.813	-3.411		
35	234.375	-3.411			35	234.375	-3.411			35	234.375	-3.411		
36	258.938	-3.411			36	258.938	-3.411			36	258.938	-3.411		
37	312.500	54.344			37	312.500	54.344			37	283.500	-3.411		
38	312.500	40.758			38	312.500	40.758			38	298.000	-3.411		
39	283.500	-3.411			39	283.500	-3.411			39	312.500	-3.411		
40	283.500	0.000			40	283.500	0.000			40	327.000	-3.411		
41	298.000	-3.411			41	298.000	-3.411			41	341.500	-3.411		
42	312.500	27.172			42	312.500	27.172			42	366.063	-3.411		
43	298.000	0.000			43	298.000	0.000			43	390.625	-3.411		
44	312.500	-3.411			44	312.500	-3.411							
45	312.500	0.000			45	312.500	0.000							
46	312.500	13.586			46	312.500	13.586			44	415.188	-3.411		
47	327.000	-3.411			47	327.000	-3.411			45	468.750	54.344		
48	327.000	0.000			48	327.000	0.000			46	468.750	40.758		
49	341.500	-3.411			49	341.500	-3.411			47	439.750	-3.411		
50	341.500	0.000			50	341.500	0.000			48	439.750	0.000		
51	366.063	-3.411			51	366.063	-3.411			49	454.250	-3.411		
52	390.625	-3.411			52	390.625	-3.411			50	468.750	27.172		
53	415.188	-3.411			53	415.188	-3.411			53	468.750	0.000		
54	468.750	54.344			54	468.750	54.344			54	468.750	13.586		
55	468.750	40.758			55	468.750	40.758			55	483.250	-3.411		
56	439.750	-3.411			56	439.750	-3.411			56	483.250	0.000		
57	439.750	0.000			57	439.750	0.000			57	497.750	-3.411		
58	454.250	-3.411			58	454.250	-3.411			58	497.750	0.000		
59	468.750	27.172			59	468.750	27.172			59	522.313	-3.411		
60	454.250	0.000			60	454.250	0.000			60	546.875	-3.411		
61	468.750	-3.411			61	468.750	-3.411							
62	468.750	0.000			62	468.750	0.000							
63	468.750	13.586			63	468.750	13.586			61	571.438	-3.411		
64	483.250	-3.411			64	483.250	-3.411			62	625.000	54.344		
65	483.250	0.000			65	483.250	0.000			63	625.000	40.758		
66	497.750	-3.411			66	497.750	-3.411			64	596.000	-3.411		
67	497.750	0.000			67	497.750	0.000			65	596.000	0.000		
68	522.313	-3.411			68	522.313	-3.411			66	610.500	-3.411		
69	546.875	-3.411			69	546.875	-3.411			67	625.000	27.172		
										68	610.500	0.000		
										69	625.000	-3.411		
70	571.438	-3.411			70	571.438	-3.411			70	625.000	0.000		
71	625.000	54.344			71	625.000	54.344			71	625.000	13.586		
72	625.000	40.758			72	625.000	40.758			72	639.500	-3.411		
73	596.000	-3.411			73	596.000	-3.411			73	639.500	0.000		
74	596.000	0.000			74	596.000	0.000			74	654.000	-3.411		
75	610.500	-3.411			75	610.500	-3.411			75	654.000	0.000		
76	625.000	27.172			76	625.000	27.172			76	678.563	-3.411		
77	610.500	0.000			77	610.500	0.000			77	703.125	-3.411		
78	625.000	-3.411			78	625.000	-3.411							
79	625.000	0.000			79	625.000	0.000							
80	625.000	13.586			80	625.000	13.586							
81	639.500	-3.411			81	639.500	-3.411							
82	639.500	0.000			82	639.500	0.000							
83	654.000	-3.411			83	654.000	-3.411							
84	654.000	0.000			84	654.000	0.000							
85	678.563	-3.411			85	678.563	-3.411							
86	703.125	-3.411			86	703.125	-3.411							

Section 4

1	1	2	4.5	1	1	1	2	4.5	1	1	1	2	4.5	1
2	2	5	4.5	1	2	2	5	4.5	1	2	2	5	4.5	1
3	5	7	4.5	1	3	5	7	4.5	1	3	5	7	4.5	1
4	7	10	4.5	1	4	7	10	4.5	1	4	7	10	4.5	1
5	10	13	4.5	1	5	10	13	4.5	1	5	10	13	4.5	1
6	13	15	4.5	1	6	13	15	4.5	1	6	13	15	4.5	1
7	15	17	4.5	1	7	15	17	4.5	1	7	15	17	4.5	1
8	17	18	4.5	1	8	17	18	4.5	1	8	17	18	4.5	1
9	6	9	3.312	3	9	6	9	3.312	3	9	6	9	3.312	3
10	9	11	3.312	3	10	9	11	3.312	3	10	9	11	3.312	3
11	11	14	3.312	3	11	11	14	3.312	3	11	11	14	3.312	3
12	14	16	3.312	3	12	14	16	3.312	3	12	14	16	3.312	3
13	11	12	3.312	2	13	11	12	3.312	2	13	11	12	3.312	2
14	12	8	3.312	2	14	12	8	3.312	2	14	12	8	3.312	2
15	8	4	3.312	2	15	8	4	3.312	2	15	8	4	3.312	2
16	4	3	3.312	2	16	4	3	3.312	2	16	4	3	3.312	2
17	18	19	4.5	1	17	18	19	4.5	1	17	18	19	4.5	1
18	19	22	4.5	1	18	19	22	4.5	1	18	19	22	4.5	1
19	22	24	4.5	1	19	22	24	4.5	1	19	22	24	4.5	1
20	24	27	4.5	1	20	24	27	4.5	1	20	24	27	4.5	1
21	27	30	4.5	1	21	27	30	4.5	1	21	27	30	4.5	1
22	30	32	4.5	1	22	30	32	4.5	1	22	30	32	4.5	1
23	32	34	4.5	1	23	32	34	4.5	1	23	32	34	4.5	1
24	34	35	4.5	1	24	34	35	4.5	1	24	34	35	4.5	1
25	23	26	3.312	3	25	23	26	3.312	3	25	23	26	3.312	3
26	26	28	3.312	3	26	26	28	3.312	3	26	26	28	3.312	3
27	28	31	3.312	3	27	28	31	3.312	3	27	28	31	3.312	3
28	31	33	3.312	3	28	31	33	3.312	3	28	31	33	3.312	3
29	28	29	3.312	2	29	28	29	3.312	2	29	28	29	3.312	2
30	29	25	3.312	2	30	29	25	3.312	2	30	29	25	3.312	2
31	25	21	3.312	2	31	25	21	3.312	2	31	25	21	3.312	2
32	21	20	3.312	2	32	21	20	3.312	2	32	21	20	3.312	2

33	35	36	4.5	1	33	35	36	4.5	1	33	35	36	4.5	1		
34	36	39	4.5	1	34	36	39	4.5	1	34	36	37	4.5	1		
35	39	41	4.5	1	35	39	41	4.5	1	35	37	38	4.5	1		
36	41	44	4.5	1	36	41	44	4.5	1	36	38	39	4.5	1		
37	44	47	4.5	1	37	44	47	4.5	1	37	39	40	4.5	1		
38	47	49	4.5	1	38	47	49	4.5	1	38	40	41	4.5	1		
39	49	51	4.5	1	39	49	51	4.5	1	39	41	42	4.5	1		
40	51	52	4.5	1	40	51	52	4.5	1	40	42	43	4.5	1		
41	40	43	3.312	3	41	40	43	3.312	3							
42	43	45	3.312	3	42	43	45	3.312	3							
43	45	48	3.312	3	43	45	48	3.312	3	41	43	44	4.5	1		
44	48	50	3.312	3	44	48	50	3.312	3	42	44	47	4.5	1		
45	45	46	3.312	2	45	45	46	3.312	2	43	47	49	4.5	1		
46	46	42	3.312	2	46	46	42	3.312	2	44	49	52	4.5	1		
47	42	38	3.312	2	47	42	38	3.312	2	45	52	55	4.5	1		
48	38	37	3.312	2	48	38	37	3.312	2	46	55	57	4.5	1		
										47	57	59	4.5	1		
										48	59	60	4.5	1		
49	52	53	4.5	1	49	52	53	4.5	1	49	48	51	3.312	3		
50	53	56	4.5	1	50	53	56	4.5	1	50	51	53	3.312	3		
51	56	58	4.5	1	51	56	58	4.5	1	51	53	56	3.312	3		
52	58	61	4.5	1	52	58	61	4.5	1	52	56	58	3.312	3		
53	61	64	4.5	1	53	61	64	4.5	1	53	53	54	3.312	2		
54	64	66	4.5	1	54	64	66	4.5	1	54	54	50	3.312	2		
55	66	68	4.5	1	55	66	68	4.5	1	55	50	46	3.312	2		
56	68	69	4.5	1	56	68	69	4.5	1	56	46	45	3.312	2		
57	57	60	3.312	3	57	57	60	3.312	3							
58	60	62	3.312	3	58	60	62	3.312	3							
59	62	65	3.312	3	59	62	65	3.312	3	57	60	61	4.5	1		
60	65	67	3.312	3	60	65	67	3.312	3	58	61	64	4.5	1		
61	62	63	3.312	2	61	62	63	3.312	2	59	64	66	4.5	1		
62	63	59	3.312	2	62	63	59	3.312	2	60	66	69	4.5	1		
63	59	55	3.312	2	63	59	55	3.312	2	61	69	72	4.5	1		
64	55	54	3.312	2	64	55	54	3.312	2	62	72	74	4.5	1		
										63	74	76	4.5	1		
										64	76	77	4.5	1		
65	69	70	4.5	1	65	69	70	4.5	1	65	65	68	3.312	3		
66	70	73	4.5	1	66	70	73	4.5	1	66	68	70	3.312	3		
67	73	75	4.5	1	67	73	75	4.5	1	67	70	73	3.312	3		
68	75	78	4.5	1	68	75	78	4.5	1	68	73	75	3.312	3		
69	78	81	4.5	1	69	78	81	4.5	1	69	70	71	3.312	2		
70	81	83	4.5	1	70	81	83	4.5	1	70	71	67	3.312	2		
71	83	85	4.5	1	71	83	85	4.5	1	71	67	63	3.312	2		
72	85	86	4.5	1	72	85	86	4.5	1	72	63	62	3.312	2		
73	74	77	3.312	3	73	74	77	3.312	3							
74	77	79	3.312	3	74	77	79	3.312	3							
75	79	82	3.312	3	75	79	82	3.312	3							
76	82	84	3.312	3	76	82	84	3.312	3							
77	79	80	3.312	2	77	79	80	3.312	2							
78	80	76	3.312	2	78	80	76	3.312	2							
79	76	72	3.312	2	79	76	72	3.312	2							
80	72	71	3.312	2	80	72	71	3.312	2							

1	3	9	390	1020	0.13	1	3	9	390	1020	0.13	1	3	9	390	1020	0.13
2	4	10	390	1020	0.13	2	4	10	390	1020	0.13	2	4	10	390	1020	0.13
3	5	11	390	1020	0.13	3	5	11	390	1020	0.13	3	5	11	390	1020	0.13
4	6	12	390	1020	0.13	4	6	12	390	1020	0.13	4	6	12	390	1020	0.13
5	19	25	390	1020	0.13	5	19	25	390	1020	0.13	5	19	25	390	1020	0.13
6	20	26	390	1020	0.13	6	20	26	390	1020	0.13	6	20	26	390	1020	0.13
7	21	27	390	1020	0.13	7	21	27	390	1020	0.13	7	21	27	390	1020	0.13
8	22	28	390	1020	0.13	8	22	28	390	1020	0.13	8	22	28	390	1020	0.13
9	35	41	390	1020	0.13	9	51	57	390	1020	0.13	9	43	49	390	1020	0.13
10	36	42	390	1020	0.13	10	52	58	390	1020	0.13	10	44	50	390	1020	0.13
11	37	43	390	1020	0.13	11	53	59	390	1020	0.13	11	45	51	390	1020	0.13
12	38	44	390	1020	0.13	12	54	60	390	1020	0.13	12	46	52	390	1020	0.13
13	51	57	390	1020	0.13	13	67	73	390	1020	0.13	13	59	65	390	1020	0.13
14	52	58	390	1020	0.13	14	68	74	390	1020	0.13	14	60	66	390	1020	0.13
15	53	59	390	1020	0.13	15	69	75	390	1020	0.13	15	61	67	390	1020	0.13
16	54	60	390	1020	0.13	16	70	76	390	1020	0.13	16	62	68	390	1020	0.13
17	67	73	390	1020	0.13												
18	68	74	390	1020	0.13	1	1	3				1	1	3			
19	69	75	390	1020	0.13												
20	70	76	390	1020	0.13	2	86	3				2	77	3			

Section 5

1	1	3				1						1					
2	86	3															
1																	

1	4	-625000	0	78125		1	4	-416625	0	52078.125		1	4	-291637.5	0	36454.6875	
1	-525.839	0	100.000	0		1	-350.524	0	66.660	0		1	-263.422	0	46.662	0	
2	-525.839	0	100.000	0		2	-350.524	0	66.660	0		2	-263.422	0	46.662	0	
3	-525.839	0	50.000	0		3	-350.524	0	33.330	0		3	-263.422	0	23.331	0	
4	-525.839	0	50.000	0		4	-350.524	0	33.330	0		4	-263.422	0	23.331	0	
5	-525.839	0	50.000	0		5	-350.524	0	33.330	0		5	-263.422	0	23.331	0	
6	-525.839	0	50.000	0		6	-350.524	0	33.330	0		6	-263.422	0	23.331	0	
7	-525.839	0	100.000	0		7	-350.524	0	66.660	0		7	-263.422	0	46.662	0	
8	-525.839	0	100.000	0		8	-350.524	0	66.660	0		8	-263.422	0	46.662	0	
9	-387.013	0	50.000	0		9	-257.983	0	33.330	0		9	-193.876	0	23.331	0	
10	-387.013	0	50.000	0		10	-257.983	0	33.330	0		10	-193.876	0	23.331	0	
11	-387.013	0	50.000	0		11	-257.983	0	33.330	0		11	-193.876	0	23.331	0	
12	-387.013	0	50.000	0		12	-257.983	0	33.330	0		12	-193.876	0	23.331	0	
13	-387.013	0	0.000	0		13	-257.983	0	0.000	0		13	-193.876	0	0.000	0	
14	-387.013	0	0.000	0		14	-257.983	0	0.000	0		14	-193.876	0	0.000	0	
15	-387.013	0	0.000	0		15	-257.983	0	0.000	0		15	-193.876	0	0.000	0	
16	-387.013	0	0.000	0		16	-257.983	0	0.000	0		16	-193.876	0	0.000	0	
17	-525.839	0	100.000	0		17	-350.524	0	66.660	0		17	-263.422	0	46.662	0	
18	-525.839	0	100.000	0		18	-350.524	0	66.660	0		18	-263.422	0	46.662	0	
19	-525.839	0	50.000	0		19	-350.524	0	33.330	0		19	-263.422	0	23.331	0	
20	-525.839	0	50.000	0		20	-350.524	0	33.330	0		20	-263.422	0	23.331	0	
21	-525.839	0	50.000	0		21	-350.524	0	33.330	0		21	-263.422	0	23.331	0	
22	-525.839	0	50.000	0		22	-350.524	0	33.330	0		22	-263.422	0	23.331	0	
23	-525.839	0	100.000	0		23	-350.524	0	66.660	0		23	-263.422	0	46.662	0	
24	-525.839	0	100.000	0		24	-350.524	0	66.660	0		24	-263.422	0	46.662	0	
25	-387.013	0	50.000	0		25	-257.983	0	33.330	0		25	-193.876	0	23.331	0	
26	-387.013	0	50.000	0		26	-257.983	0	33.330	0		26	-193.876	0	23.331	0	
27	-387.013	0	50.000	0		27	-257.983	0	33.330	0		27	-193.876	0	23.331	0	
28	-387.013	0	50.000	0		28	-257.983	0	33.330	0		28	-193.876	0	23.331	0	
29	-387.013	0	0.000	0		29	-257.983	0	0.000	0		29	-193.876	0	0.000	0	
30	-387.013	0	0.000	0		30	-257.983	0	0.000	0		30	-193.876	0	0.000	0	
31	-387.013	0	0.000	0		31	-257.983	0	0.000	0		31	-193.876	0	0.000	0	
32	-387.013	0	0.000	0		32	-257.983	0	0.000	0		32	-193.876	0	0.000	0	
33	-525.839	0	100.000	0		33	-350.524	0	66.660	0		33	-263.422	0	46.662	0	
34	-525.839	0	100.000	0		34	-350.524	0	66.660	0		34	-263.422	0	46.662	0	
35	-525.839	0	50.000	0		35	-350.524	0	33.330	0		35	-263.422	0	46.662	0	
36	-525.839	0	50.000	0		36	-350.524	0	33.330	0		36	-263.422	0	46.662	0	
37	-525.839	0	50.000	0		37	-350.524	0	33.330	0		37	-263.422	0	46.662	0	
38	-525.839	0	50.000	0		38	-350.524	0	33.330	0		38	-263.422	0	46.662	0	
39	-525.839	0	100.000	0		39	-350.524	0	66.660	0		39	-263.422	0	46.662	0	
40	-525.839	0	100.000	0		40	-350.524	0	66.660	0		40	-263.422	0	46.662	0	
41	-387.013	0	50.000	0		41	-257.983	0	33.330	0							
42	-387.013	0	50.000	0		42	-257.983	0	33.330	0							
43	-387.013	0	50.000	0		43	-257.983	0	33.330	0		41	-263.422	0	46.662	0	
44	-387.013	0	50.000	0		44	-257.983	0	33.330	0		42	-263.422	0	46.662	0	
45	-387.013	0	0.000	0		45	-257.983	0	0.000	0		43	-263.422	0	23.331	0	
46	-387.013	0	0.000	0		46	-257.983	0	0.000	0		44	-263.422	0	23.331	0	
47	-387.013	0	0.000	0		47	-257.983	0	0.000	0		45	-263.422	0	23.331	0	
48	-387.013	0	0.000	0		48	-257.983	0	0.000	0		46	-263.422	0	23.331	0	

Section 6

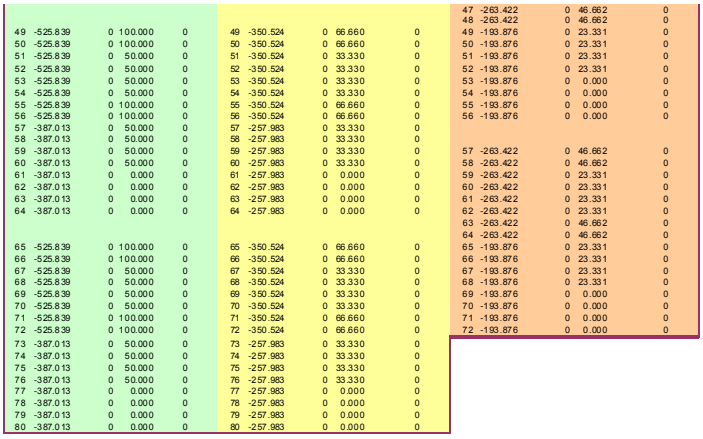

										47	-263.422	0	46.662	0	
										48	-263.422	0	46.662	0	
49	-525.839	0	100.000	0	49	-350.524	0	66.660	0	49	-193.876	0	23.331	0	
50	-525.839	0	100.000	0	50	-350.524	0	66.660	0	50	-193.876	0	23.331	0	
51	-525.839	0	50.000	0	51	-350.524	0	33.330	0	51	-193.876	0	23.331	0	
52	-525.839	0	50.000	0	52	-350.524	0	33.330	0	52	-193.876	0	23.331	0	
53	-525.839	0	50.000	0	53	-350.524	0	33.330	0	53	-193.876	0	0.000	0	
54	-525.839	0	50.000	0	54	-350.524	0	33.330	0	54	-193.876	0	0.000	0	
55	-525.839	0	100.000	0	55	-350.524	0	66.660	0	55	-193.876	0	0.000	0	
56	-525.839	0	100.000	0	56	-350.524	0	66.660	0	56	-193.876	0	0.000	0	
57	-387.013	0	50.000	0	57	-257.983	0	33.330	0						
58	-387.013	0	50.000	0	58	-257.983	0	33.330	0						
59	-387.013	0	50.000	0	59	-257.983	0	33.330	0	57	-263.422	0	46.662	0	
60	-387.013	0	50.000	0	60	-257.983	0	33.330	0	58	-263.422	0	46.662	0	
61	-387.013	0	0.000	0	61	-257.983	0	0.000	0	59	-263.422	0	23.331	0	
62	-387.013	0	0.000	0	62	-257.983	0	0.000	0	60	-263.422	0	23.331	0	
63	-387.013	0	0.000	0	63	-257.983	0	0.000	0	61	-263.422	0	23.331	0	
64	-387.013	0	0.000	0	64	-257.983	0	0.000	0	62	-263.422	0	23.331	0	
										63	-263.422	0	46.662	0	
										64	-263.422	0	46.662	0	
65	-525.839	0	100.000	0	65	-350.524	0	66.660	0	65	-193.876	0	23.331	0	
66	-525.839	0	100.000	0	66	-350.524	0	66.660	0	66	-193.876	0	23.331	0	
67	-525.839	0	50.000	0	67	-350.524	0	33.330	0	67	-193.876	0	23.331	0	
68	-525.839	0	50.000	0	68	-350.524	0	33.330	0	68	-193.876	0	23.331	0	
69	-525.839	0	50.000	0	69	-350.524	0	33.330	0	69	-193.876	0	0.000	0	
70	-525.839	0	50.000	0	70	-350.524	0	33.330	0	70	-193.876	0	0.000	0	
71	-525.839	0	100.000	0	71	-350.524	0	66.660	0	71	-193.876	0	0.000	0	
72	-525.839	0	100.000	0	72	-350.524	0	66.660	0	72	-193.876	0	0.000	0	
73	-387.013	0	50.000	0	73	-257.983	0	33.330	0						
74	-387.013	0	50.000	0	74	-257.983	0	33.330	0						
75	-387.013	0	50.000	0	75	-257.983	0	33.330	0						
76	-387.013	0	50.000	0	76	-257.983	0	33.330	0						
77	-387.013	0	0.000	0	77	-257.983	0	0.000	0						
78	-387.013	0	0.000	0	78	-257.983	0	0.000	0						
79	-387.013	0	0.000	0	79	-257.983	0	0.000	0						
80	-387.013	0	0.000	0	80	-257.983	0	0.000	0						

Figure D-6: Comparison of generated .STO files

A template has been generated in Microsoft Excel to generate the .STO files for the U-, T- and I-profile stringer-stiffened panels. The variables that can change, namely the panel's dimensions and loads are generated using the Input/Output spreadsheet as shown in Figure D-5. The geometry of the panel is taken from the field "ABD Matrix for Stringer and Skin Elements Input Data", whereas load data for is taken from the field "Load Data for .STO file", which is calculated using the field "Stringer and Skin Elements Stiffnesses" and the panel's dimensions.

Figure D-6 illustrates and compares the .STO files for a T-profile stringer-stiffened panel, for a sound panel (green column), debonded (yellow column), and discrete source damage (orange column). Section 1 of the .STO file is the description, naming, and units used by the program. For each case, i.e. sound, debonded, or damaged, this section is similar. Section 2 identifies the program's run type, in this case it generates the full P-λ curve in order to find the lowest load, based upon the panel's length, i.e. 800mm and along the length in 15 equal increments of 53.33mm, which is required to generate the P-λ curve. This section also identifies the number of nodes, strip elements, adhesive layer elements, and the number of boundary conditions. The sound and debonded panel's have 86 nodes and 80 strips, whereas the damaged panel has 77 nodes and 72 strips, as the middle stringer (the panel has nominally 5 stringers) has been removed. There are normally 4 adhesive elements connecting the stringer's lower flange to the skin, thus the sound panel has in total 20 elements, whereas the others have only 16 elements, as for the debonded panel the adhesive elements are removed, and for the damaged panel, as the middle stringer does not exist, there is no need for the adhesive elements for that particular stringer.

Section 3 lists the node numbers and their respective y- and z-coordinates. Section 4 details the strip elements and their related parameters, such as the node numbers at the extremities of the strip, the related thicknesses and the laminate associated to the strip element, which is given in the .LAM file. Section 5 lists the adhesive strip element data as well as the boundary conditions for the panel edges i.e. the first and last node, in this case the number 3 identifies that simply supported boundary conditions are used. Section 6, details the loading data, in this case for a single load case, and only for N_x and N_{xy} loading. The total axial and shear load is given in the first line of Section 6, whereas the elements strips have their respective apportioned load.

D.7 Repair Bolt Diameter to Laminate Thickness

Repair Bolt Dia. (mm)	Double Shear	
	Min. Laminate Thk. (mm)	Max. Laminate Thk. (mm)
6.35	3.250	7.542
7.94	7.543	9.053
9.53	9.054	10.554
11.11	10.555	12.064
12.7	12.065	13.575
14.29	13.576	15.085
15.88	15.086	16.586
17.46	16.587	18.097
19.05	18.098	19.607
20.64	19.608	21.108
22.22	21.109	22.619
23.81	22.620	24.129
25.4	24.130	25.640
26.99	25.641	27.150
28.58	27.151	28.651
30.16	28.652	30.162
31.75	30.163	31.672
33.34	31.673	33.183
34.93	33.184	34.684
36.51	34.685	36.194
38.1	36.195	39.500

Table D-2: Repair bolt diameters and associated laminate thicknesses

Table D-2 highlights the relationship between the different repair bolt diameters and the associated minimum and maximum laminate thicknesses. It has previously been stated that to achieve the highest bearing load, the d/t ratio should be equal to 1. These repair bolt diameters are used with Equations 7-7, 7-8, and 7-9.

D.8 Letter of appreciation from ESDU

Dear Ben,

As your thesis nears completion, I just wanted to write formally to thank you for all the help and feedback that you've given us during the development of the ESDU FSM program. Your uncanny and occasionally (but only momentarily!) irritating talent for rooting out bugs, flaws and inconsistencies in the software and supporting documentation has been invaluable to us. That talent and the obviously deep understanding of the subject that accompanies it have not only saved us large amounts of time but have certainly also helped us to create and deliver a product that is far superior to what it would have been without your input.

I would also like to thank you for the good-humoured spirit in which your comments, criticisms and findings have been delivered and for your long-suffering patience whilst waiting for us to address and resolve the many issues that you identified.

I wish you every success not only with your thesis, but also in all future endeavours.

Yours sincerely,

Adam

Technical Director, Aerospace

ESDU

Appendix E Financial Considerations

E.1 Calculation of Economic Value of Weight Saving

The derivation of EVWS below has been adopted from "Analysis of the Fuel Penalties of Airframe Systems" (A Cranfield University Lecture Note)[602]. A simple representation of aircraft drag is given in Equation E-1.

$$D = \frac{W}{r} \quad \textbf{E-1}$$

Where D = drag, W = weight, and r = lift/drag ratio. Equation E-1 is only true when $(L/D)_{ratio}$ is constant. The range of an aircraft can be expressed in terms of time:

$$dR = \bar{b} \times M \times dt \quad \textbf{E-2}$$

Where dR = range covered, $\bar{b}$ = speed of sound, M = mach number, and dt = time. During the time period dt, the aircraft's fuel mass can be expressed by:

$$\left(f + \Delta f_W\right)dt = -d\left(M_F + \Delta M_F\right) \quad \textbf{E-3}$$

Where f = rate of fuel used by the baseline aircraft, Δf_W = rate of fuel used due to extra weight, M_F = mass of fuel used by the baseline aircraft, and ΔM_f = rate of fuel used due to extra weight. Furthermore, the negative sign on the RHS of the equation represents decrease in fuel weight with increase in time. Rearranging Equation E-2, and substituting it into Equation E-3, gives:

$$dR = \frac{-aM\left[d\left(M_F + \Delta M_F\right)\right]}{f + \Delta f_W} \quad \textbf{E-4}$$

For this case, the thrust specific consumption (c) ($kg.N^{-1}.s^{-1}$) is assumed to be constant and can be expressed as:

$$c = \frac{f + \Delta f_W}{Total\ Drag} \quad \textbf{E-5}$$

Thrust specific fuel consumption is defined as fuel flow rate per unit thrust, and drag, in this case, is equal to the thrust. Therefore, by assuming Equation E-1 is correct, the drag on the aircraft, but excluding the effect of the increased aircraft weight, can be written as:

$$D = \frac{W_A + W_F}{r} \quad \textbf{E-6}$$

Where W_A = empty weight of aircraft excluding system, W_F = weight of fuel used excluding system effect. Thus, incorporating the effect of the incremental drag due to extra weight on the aircraft, the overall drag is given by:

$$Weight\ Drag = \frac{W_A + \Delta W_A + W_F + \Delta W_F}{r} \quad \textbf{E-7}$$

Where ΔW_A = extra weight and ΔW_F = extra weight of fuel used due to extra weight. By substituting Equation E-7 into Equation E-5, the following equation is obtained:

$$c = \frac{f + \Delta f_W}{\left(\left(W_A + \Delta W_A + W_F + \Delta W_F\right) \times \frac{1}{r}\right)} \quad \textbf{E-8}$$

Re-arranging Equation E-8 gives:

$$f + \Delta f_W = \frac{c}{r}\left(\Delta W_A + W_F + \Delta W_F\right) \quad \textbf{E-9}$$

By substituting Equation E-9 into Equation E-4, the following is obtained:

$$dR = \frac{r}{c} \times \frac{-aM\left[d\left(W_F + \Delta W_F\right)\right]}{\left(W_A + \Delta W_A + W_F + \Delta W_F\right)} \quad \textbf{E-10}$$

The range of the aircraft is obtained by substituting $M_F = W_F/g$ and $\Delta M_F = \Delta W_F/g$ and integrating Equation E-10:

$$R = a \times M \times \frac{r}{cg} \times \ln\left[\frac{W_A + \Delta W_A + W_{FO} + \Delta W_{FO}}{W_A + \Delta W_A}\right] \quad \textbf{E-11}$$

Where W_{FO} = weight of fuel used to fly range, R, excluding extra weight, and ΔW_{FO} = extra weight of fuel used to fly range, R, due to extra weight, and g = gravity. By defining t as the time taken to fly the range R ($R=a \times M \times t$), Equation E-11 can be simplified to:

$$t \times \frac{cg}{r} = \ln\left[\frac{W_{FO} + \Delta W_{FO}}{W_A + \Delta W_A} + 1\right] \quad \textbf{E-12}$$

Equation E-12 can be re-arranged to give the total weight of fuel consumed with the extra weight, i.e. $W_{FO} + \Delta W_{FO}$:

$$W_{FO} + \Delta W_{FO} = \left(W_A + \Delta W_A\right) \times \left(e^{\frac{ctg}{r}} - 1\right) \quad \textbf{E-13}$$

From Equation E-13, when $W_{FO} = W_A = 0$, then the weight of the fuel consumed, purely due to the increment in weight, can be obtained:

$$\Delta W_{FO} = \Delta W_A \times \left(e^{\frac{ctg}{r}} - 1 \right) \qquad \textbf{E-14}$$

In order to verify that Equation E-14 is fit for purpose, an example calculation will be performed. For the A320 aircraft[625]:

- Original Life
  - 48,000 pressure cabin cycles
  - 60,000 flying hours
- Enhanced Life
  - 60,000 pressure cabin cycles
  - 120,000 flying hours

Based on these figures, the average original flying time per mission was 1.25 hours, whereas the new average figure is 2.00 hours.

It is known that 1 US gallon is equal to 3.78 litres. It is also known that the density of Kerosene is 817.15kg/m³. Thus 1kg of Kerosene is 1.22 litres (i.e. 1/0.82). Therefore, there are 3.09 kg of fuel in 1 gallon (i.e. 3.79/1.22), which can be used to calculate a cost for the fuel.

- @ $2.60 a gallon it is $0.84/kg (i.e. 2.60/3.09)
- @ $0.75 a gallon it is $0.24/kg (i.e. 0.75/3.09)

For the SFC there are both imperial units of measurement, i.e. lb/(lbf.hr) and SI units of measurement, i.e. g/(kN.s). The conversion from imperial to IS is given by:

1lb = 454g and 1lbf = 0.00448kN, therefore $454/(0.00448 \times 60 \times 60) = 28.14$ conversion factor.

From Aviation Week & Space Technology[626], a list of SFC in Imperial units, for various engines, are given. The SFC is typically given for maximum power, except the figures available for the Rolls Royce engines that are quoted at cruise power. The average value for a commercial modern turbofan is 0.56 lb/(lbf.hr), which equals 15.82 g/(kN.s). However, for the equation we need kg/(N.s), which is 15.82×10^{-6}. Therefore, using the Equation E-14 for an A320, for a 1.25 hour mission:

$$\Delta W_{FO} = 1 \times \left(e^{\frac{\left(15.82 \times 10^{-6}\right) \times 9.8 \times (1.25 \times 60 \times 60)}{16}} - 1 \right) = 0.044568$$

Or for an A320 for a 2.00 hour mission:

$$\Delta W_{FO} = 1 \times \left(e^{\frac{\left(15.82\times10^{-6}\right)\times9.8\times\left(2.00\times60\times60\right)}{16}} - 1 \right) = 0.072257$$

Alternatively for an A330 for a 6 hour mission:

$$\Delta W_{FO} = 1 \times \left(e^{\frac{\left(15.82\times10^{-6}\right)\times9.8\times\left(6.00\times60\times60\right)}{17}} - 1 \right) = 0.217728$$

Or for an A340 for a 8 hour mission:

$$\Delta W_{FO} = 1 \times \left(e^{\frac{\left(15.26\times10^{-6}\right)\times9.8\times\left(8.00\times60\times60\right)}{17}} - 1 \right) = 0.288337$$

For the A320, with a mission time of 1.25 hours and allowable 60,000 flying hours there will be 48,000 missions in total, whereas at 2 hours and an allowable 120,000 there will be 60,000 missions in total. For an A330 and A340, the allowable flying hours is assumed to be 120,000.

Thus:

- For an A320:
  - 0.044568×48,000 = 2139.26
    - 0.24×2139.26= $513/kg of structural weight saved (fuel price low)
    - 0.84×2139.26=$1797/kg of structural weight saved (fuel price high)
  - 0.072257×60,000=4335.42
    - 0.24×4335.42=$1041/kg of structural weight saved (fuel price low)
    - 0.84×4335.42=$3641/kg of structural weight saved (fuel price high)
- For an A330
  - 0.217728×20,000=4354.56
    - 0.24×4354.56=$1045/kg of structural weight saved (fuel price low)
    - 0.84×4354.56=$3658/kg of structural weight saved (fuel price high)
- For an A340
  - 0.288337×15,000=4325.06
    - 0.24×4325.06=$1038/kg of structural weight saved (fuel price low)
    - 0.84×4325.06=$3633/kg of structural weight saved (fuel price high)

These EVWS values would seem fairly representative for the different aircraft types.

Alternatively the following example can also be used to verify the EVWS calculation. Anderson (2006)[500] investigated the approximate percentage in block[lix] fuel savings gained due to a reduction of 453kg in the aircraft's Zero Fuel Weight (ZFW). This investigation was based on a Boeing 747, thus using data for the particular Boeing aircraft[627], this can give a ballpark value for the EVWS. This can be worked out, as follows:

$$EVWS = \frac{FC \times \%Savings\ per\ kg\ ZFW \times Fuel\ Cost \times TAFH \times Speed}{Range} \quad \textbf{E-15}$$

Where FC = fuel capacity and TAFH = total allowable flying hours, thus:

$$EVWS = \frac{(216840/3.09) \times (0.002/453) \times 0.75 \times 120000 \times 890}{13450} = 1845$$

Shown in Table E-1[627], are the different EVWS for 4 different aircraft categories in the Boeing commercial aircraft range, as well as the resultant EVWS at a low and high price of kerosene. These values also compare fairly well with the values obtained by using Equation E-14 to obtain a value for EVWS.

	Range (km)	Fuel Capacity (l)	ZFW (kg)	Approx. % Block Fuel Savings per 453kg ZFW Reduction	EVWS @ $0.75/gallon	EVWS @ $2.60/gallon
737-800	5665	26020	62732	.6	1577	5467
767-300ER	11065	90770	130600	.3	1408	4882
777-300	11135	171160	224528	.2	1759	6099
747-400	13450	216840	246074	.2	1845	3695

Table E-1: Economic value of weight saving

E.2 Process Steps

For each global approach to manufacturing and integration of a wing cover, there are a number of process steps which are the same, regardless of the approach taken. Therefore, it is possible to break down the global manufacturing overall process into common sub-processes, which simplifies and ensures the manufacturing cost calculation is a more tractable problem.

The global process flows are shown in Figure E-2 to Figure E-7, whereas Figure E-8 provides a key to explain the nomenclature for the illustrated global process flows.

[lix] Block fuel saving is the fuel saved from when the engines are started at the beginning of the mission until when they are turned off at the end of the mission

E.2.1 Individual Steps

For each individual process step there can be a number of activities. Each activity has at least a primary characteristic, which identifies a parameter that can be used to calculate the cost of that activity. These factors are identified in the template as shown below:

Process Description	Primary Characteristic	Rate
Apply Vacuum Foil	Area	10 m²/hr

The Pareto 80/20 rule[628] will be assumed (where 80% of the cost is attributable to 20% of the activities), where only the principal process steps are considered, and not ancillary steps which would complicate the calculation without adding to its fidelity. Of interest is the major cost drivers, as well as the approximate duration of the process, thus a process step such as kitting the textiles required to fabricate a stringer is not considered important at this level of analysis.

For all process steps that are dependent on area, it is necessary to increase the number of workers based on the area, as a larger tool for example would have more people working on it, in order to reduce the time needed for that step so that the tool can be expedited in readiness for the next step, and to reduce the number of tools required. In order to harmonise the process the following rates shall be considered:

Area (m²)	0-49	50-99	100-149	150-199	200+
No. of Employees	1	2	3	4	5

The different process steps are coded and listed in alphabetical order, as follows:

ACBD – Autoclave Bond

This manufacturing step is for the secondary bonding process to apply both pressure and heat to cure the adhesive between the skin and stringers. It is assumed that the warm up and cool down from RT (20°C) to 180°C takes 1 hour, whereas the actual cure of the bond requires 2 hours, thus a total of 4 hours is required. This process, if required, is carried out once per cover.

Install in Autoclave	Time	NA	0.33 hrs
Apply Vacuum and Cure	Time	NA	4 hrs

The time required to complete this process is simply the two activity times added together, i.e. 4.33 hours.

ACCU – Autoclave Cure

This manufacturing step is used for the autoclave curing of prepreg skins, stringers and covers. The assumption is that the autoclave will always be fully utilised with multiple stringers or a single skin/cover, thus a long time will be needed to ensure the part and tools are up to temperature, thus a cure cycle will take 8 hours in total, regardless of autoclave size. This process, if required, is carried out once per stringer set/skin/cover.

Install in Autoclave	Time	NA	0.33 hrs
Apply Vacuum and Cure	Time	NA	8 hrs

The time required to complete this process is simply the two activity times added together, i.e. 8.33 hours.

APPP – Apply Peel Ply

This manufacturing step is used to apply peel ply on the skin IML between the stringers, for co-curing and co-bonding (soft skin) integration techniques. This process, if required, is carried out once per cover.

Apply Peel Ply	Area	NA	20 m²/hr

The time required to complete this process can be calculated by subtracting the area of the stringer feet from the total skin area, and dividing this by the application rate of 20m²/hr. The area is given by Equation E-16.

$$Area \approx \sum_{Rib\ Nx}^{Rib\ Na} \left(\left(\left(SP \times No.\ of\ Str\right) - \sum LFW\right) \times a\right) \quad \textbf{E-16}$$

ATPL – Attach Top Plates

This manufacturing step is used to attach the arrestor plate for hot forming of the stringer angles. This process, if required, is carried out twice per stringer (i.e. left and right hand angles), and for every stringer.

Mechanically attach top plates	Length	NA	0.1 hrs (1 person/5 m)

The man-hours required to complete this process for a single angle is the total length of the stringer divided by 5m, which is then multiplied by 0.1hrs to obtain the total time required. The tool time is simply 0.1hrs. The length is given by Equation E-17.

$$Length \approx \sum_{Rib\ Nx}^{Rib\ Na} a \quad \textbf{E-17}$$

ATPP – Apply Total Peel Ply

This manufacturing step is used to apply peel ply on the whole skin IML, for co-bonding (hard skin) and secondary bonding integration techniques. This process, if required, is carried out once per skin.

Apply Peel Ply	Area	NA	20 m²/hr

The time required to complete this process can be calculated by dividing the total area of the skin by the application rate of 20m²/hr. The area is given by Equation E-18.

$$Area \approx \sum_{Rib\ Nx}^{Rib\ Na} \left(\left(SP \times No.\ of\ Str \right) \times a \right) \qquad \textbf{E-18}$$

BRCU – Braid Cut

This manufacturing step is used to cut the braid hose to a desired length for stringer fabrication. This process, if required, is carried out a number of times to obtain the amount of braids for the individual stringer. Furthermore, this process has to be repeated for each stringer.

Roll out Braid	Length	NA	300 m/hr
Cut Braid	Time	NA	0.01 hrs

The time required to complete this process can be calculated based on a breakdown of the braided stringer fabrication. Based on the thickness distribution along the stringer's length a number of braids will commence and terminate. Thus the length can be calculated from this data. This length can be divided by the rate of 300m/hr, to obtain the time it took to roll out the necessary length of braid, and an extra 0.01hrs is added to cater for the cutting of the braid. The lengths of braids can be worked out using the manufacturing cost calculator spreadsheet.

CLHB – Crane Lift onto Hot Form Bed

This manufacturing step is used to lift the stringer forming tools onto the hot forming bed. Assumption is that 2 people are required to carry out this operation. This process is carried out twice per stringer (i.e. left and right hand angles), and for every stringer.

Crane Lift	Time	NA	0.2 hrs (2 people)

The time required to complete this process for a single angle is simply 0.2hrs, with associated man-hours of 0.4hrs.

CLNS – Crane Lift to Next Stage

This manufacturing step is used to lift and remove the stringer forming tool from the hot forming bed. Assumption is that 2 people are required to carry out this operation. This process is carried out twice per stringer (i.e. left and right hand angles), and for every stringer, for a prepreg stringer, and furthermore for an NCF or braided stringer the other constituent parts must be consolidated, thus they also need to be moved.

Crane Lift	Time	NA	0.2 hrs (2 people)

The time required to complete this process for a single angle is simply 0.2hrs, with associated man-hours of 0.4hrs

DFFP – Dry Fibre Flat Preform

This manufacturing step is used to lay the textile on the forming tool. This process, if required, is carried out for the spine and lower and upper flanges, but only once for the complete thickness.

Insert Textile onto Hot Form Tool	Length	NA	0.1 hrs (1 person/5 m)

The man hours required to complete this process for a single angle is the total length of the stringer divided by 5m, which is then multiplied by 0.1hrs to obtain the total time required. The tool time is simply 0.1hrs. The length is given by Equation E-17.

DFPF – Dry Fibre Preform

This manufacturing step is used to attach the textile to the forming block and arrest the stringer preform for a single handed stringer. This process, if required, is carried out for both the left and right hand angles, after every 3 dry textiles are deposited.

Insert Textile onto Hot Form Tool	Length	NA	0.1 hrs (1 person/5 m)
Mechanically Attach Preform Arrestors	Length	NA	0.1 hrs (1 person/5 m)

The man hours required to complete this process for a single angle is the total length of the stringer divided by 5m, which is then multiplied by 0.1hrs to obtain the total time required. The tool time is simply 0.1hrs. This is then doubled to get the total time. The length is given by Equation E-17.

DFRA – Dry Fibre Remove Arrestors

This manufacturing step is used to remove the arrestors applied to the dry fibre textile after hot forming. This process, if required, is carried out for both the left and right hand angles, after every 3 dry textiles are deposited.

Mechanically Detach Preform Arrestors	Length	NA	0.1 hrs (1 person/5 m)

The man hours required to complete this process for a single angle is the total length of the stringer divided by 5m, which is then multiplied by 0.1hrs to obtain the total time required. The tool time is simply 0.1hrs. Due to the change in thickness of the stringer along its length, this can only be worked out using the manufacturing cost calculator spreadsheet.

DTPL – Detach Top Plates

This manufacturing step is used to remove the plate used for forming the stringer after hot forming. This process is carried out twice per stringer (i.e. left and right hand angles), and for every stringer.

Mechanically Detach Top Plates	Length	NA	0.1 hrs (1 person/5 m)

The man hours required to complete this process for a single angle is the total length of the stringer divided by 5m, which is then multiplied by 0.1hrs to obtain the total time required. The tool time is simply 0.1hrs. The length is given by Equation E-17.

LSMD – Lightning Strike Mesh Deposition

This manufacturing step is used to deposit the lightning strike mesh. In order to simplify this whole process, a single layer with a constant density is considered. This process is carried out once per cover.

Roll out required Length	Length	NA	120 m/hr
Cut Mesh	Time	NA	0.03 hrs
Mesh Deposition	Area	NA	15 m²/hr

The rolling out of mesh to the correct length will be worked out using the manufacturing cost calculator cost spreadsheet, using the four points at the corner of the first and last rib datums, and taking into consideration that the roll width is 1m. The cutting of the mesh is the number of lengths required, divided by the mesh cutting time. The mesh deposition can be calculated from Equation E-18.

MACO – Mandrel Collation

This manufacturing step is used for consolidating the mandrels for the U-profile co-cured stringer-stiffened panel. This process, if required, is repeated for all mandrels expect the last one, when step MASU is conducted.

Slide Mandrel into Jig	Time	NA	0.03 hrs
Insert Spine Laminate	Length	NA	0.05 hrs (1 person/5 m)

The time required to complete this process for a single mandrel is the total length of the stringer divided by 5m, and then multiplied by 0.05hrs. A further 0.03hrs is added on to obtain the total time required. The length is given by Equation E-17.

MASU – Mandrel Setup

This manufacturing step is used for collating the final mandrel and then preparing the mandrel set in readiness for the integration of the U-stringers to the skin, i.e. the noodle must be inserted. This process, if required, is carried out once per cover.

Slide Final Mandrel into Jig	Time	NA	0.03 hrs
Fix Mandrels into Jig	Time	NA	0.15 hrs
Insert Noodles	Length	NA	20m/hr
Rotate Jig	Time	NA	0.1 hrs

The man hours required to complete this process for a set of stringers is the total length of all the stringer blades divided by the rate for inserting the noodle, i.e. 20m/hr. A further 0.28hrs is added on to obtain the total time required. The total length is given by Equation E-19.

$$Total\ Length \approx \sum_{Str\ Nx}^{Str\ Na} \sum_{Rib\ Nx}^{Rib\ Na} a \qquad \textbf{E-19}$$

MATS – Mandrel to Skin

This manufacturing step is used to lower the mandrel set onto the skin/cover tool and secure. 3 people are required to carry out this operation. This process, if required, is carried out once per cover.

Lower Mandrel Jig onto Skin	Time	NA	0.15 hrs
Lock into Position	Time	NA	0.5 hrs

The time required to complete this process is simply 0.65hrs.

MCDS – Machining Discrete Stringer

This manufacturing step is used for trimming the T-profile stringer's blade and lower flange, and the I-profile's stringer upper and lower flanges, after being cured in readiness for bonding to the skin. This process, if required, is carried out for every stringer per cover.

Fix Stringer into Trim Tool	Time	NA	0.2 hrs (2 people)
Trim using Router	Length	NA	30 m/hr

The time required to complete the machining of a discrete stringer is calculated from the total length of the stringer multiplied by 3 for a T-profile stringer (both sides of the feet and the blade) or multiplied by 4 for an I-profile stringer (both sides of the feet and the upper flange) divided by 30m/hr. A further 0.2hrs is added on to obtain the total time required. The length is given by Equation E-17.

MCSB – Machine Stringer Blade

This manufacturing step is used to trim the stringer blade for either a co-curing (including co-infusion and U-profile panel) or co-bonding integration process, with hard skin. This process, if required, is carried out once per cover but for every stringer.

Machine Stringer Blade	Length	NA	30 m/hr

The time required to complete the machining of a cured stringer blade is calculated from the total length of the stringer for a T-profile stringer or multiplied by 2 for an I-profile stringer (both sides of the upper flange) divided by 30m/hr. The length is given by Equation E-17.

MCSK – Machining Skin

This manufacturing step is used to trim the outer profile of the skin, after cure. This process is carried out once per cover.

Place Cover/Skin onto Jig	Time	NA	2 hrs
Machine Edge of Skin to Profile	Perimeter	NA	30 m/hr

The setup of the cover/skin into the jig is assumed to require 3 people. The time required to complete the machining of a cured skin perimeter is calculated by dividing the skin's perimeter by the rate of 30m/hr. The perimeter of the skin/cover is given, thus it must not be calculated.

NCCU – NCF Clean Up

This manufacturing step is used to remove unwanted material, i.e. off-cut NCF and vacuum foil, for recycling, after the individual textiles have been cut. This process, if required, is carried out once per textile.

Remove Off-Cut NCF	Length	NA	200 m/hr
Remove all other Material	Length	NA	300 m/hr

The time required to complete this process is calculated from the total length of the material used divided by the rates. This should be done once for removing off-cut NCF and again to remove the other materials. The total lengths are derived from the process NCPC.

NCDP – NCF Deposition

This manufacturing step is used to deposit the NCF band onto the tool, with the maximum permissible width being 1.5m. The assumption for the NCF is that there will be no scrap incurred with this process, as this will be incurred instead by the material supplier, who supplies the rolls. With NCF deposition there will be a need to apply heat locally to activate the binder, hence despite the simple unidirectional rolling, the deposition rate is fairly slow. This process, if required, is carried out a number of times, until the skin is deposited. After every strip is deposited, 0.03hrs is required to reposition the machine's head.

NCF Deposition	Length	NA	150 m/hr
NCF Deposition	Piece	NA	0.03 hr

The lengths can be worked out using the manufacturing cost calculator spreadsheet.

NCPC – NCF Pre-Cutting

For the NCF stringers it is considered that the individual blanks will be cut out of 1.5m wide rolls of NCF. However, for the skin it will be assumed that the NCF is delivered to the manufacturer on rolls compatible to the NCF deposition machine, with the correct width and length as required to fabricate the skin preform. Therefore, this manufacturing step is used to pre-cut the NCF to the desired shape for the stringers. This process, if required, is carried out a number of times.

Roll out NCF from Roll	Length	NA	200 m/hr
Roll out Plastic Film	Length	NA	300 m/hr
Cut out NCF to Profile	Perimeter	NA	100 m/hr

The time required to complete this process can be calculated based on a breakdown of the NCF stringer fabrication. Based on the thickness distribution along the stringer's length a number of NCF textiles will commence and terminate. Thus the length can be calculated from this data. The width of the desired NCF textile can also be obtained from the stringer dimensions. The length and the width can be multiplied together to obtain the total area for the particular NCF textile, i.e. TE3, TE4 or TE5. This can be repeated for all stringers associated with the cover. Once the total area required for each particular NCF textile is calculated, this can be multiplied by the monthly production rate, while ensuring a distance of 10mm exists between each blank for nesting purposes, in order to obtain the total area required. This can then be divided by the standard width of NCF, i.e. 1.5m. Therefore, for each particular textile, the total length required can be divided by the length rates shown in the table above to obtain the time for rolling out the NCF and the plastic foil. The actual cutting out time required can be calculated from the perimeter of each individual textile blank divided by the rate of 100m/hr. The manufacturing cost calculator spreadsheet is required to work out this cost.

NDBC – Non Destructive Inspection Bond Check

This manufacturing step is used to inspect the bonds connecting the stringers to the skin. This process, if required, is carried out once for every stringer bonded to the cover.

Run NDT Machine	Area	NA	15 m²/hr

The time required to complete this process can be calculated from the total bond area, which is the combined area of all the stringers' feet. Therefore, per stringer, the cumulative area per local rib length multiplied by the foot width is calculated to obtain the total foot area for the particular stringer. This is repeated for every stringer to obtain the total area, which is then divided by the rate, i.e. 15m²/hr, to obtain the time required. The area is given by Equation E-20.

$$Area \approx \sum_{Str\ Nx}^{Str\ Na} \sum_{Rib\ Nx}^{Rib\ Na} \left(LFW \times a\right) \qquad \textbf{E-20}$$

NDDS – Non Destructive Inspection Discrete Stringer

This manufacturing step is used to inspect discrete stringers that are pre-cured. This process, if required, is carried out once per stringer, and for all the stringers needed for the cover.

Setup NDT Machine	Time	NA	0.2 hrs (2 people)
Run NDT Machine	Area	NA	25 m²/hr

The time required to complete this process can be calculated from the combined surface area of the stringer's lower flange, the blade, and for an I-profile stringer the upper

flange also. It should be noted that the NDT machine needs access from only one side. The total area is divided by the rate of 25m²/hr with an additional 0.2hrs for setup time to obtain the total time required. The area for a T- and I-profile stringers is given by Equation E-21and E-22 respectively.

$$Area \approx \sum_{Rib\ Nx}^{Rib\ Na} \left((LFW + BH) \times a \right) \quad \textbf{E-21}$$

$$Area \approx \sum_{Rib\ Nx}^{Rib\ Na} \left((LFW + BH + UFW) \times a \right) \quad \textbf{E-22}$$

NDSK – Non Destructive Inspection Skin

This manufacturing step is used to inspect the skin. This process is carried out once per skin/cover.

Run NDT Machine	Area	NA	25 m²/hr

The time required to complete this process can be calculated from the total surface area of the skin, which is calculated by the cumulative area per rib bay, divided by the rate of 25m²/hr to obtain the total time required. The area is given by Equation E-18.

NDST – Non Destructive Inspection Stringer

This manufacturing step is used to inspect the stringer that is already cured/bonded to the skin. This process, if required, is carried out once for every stringer bonded to the cover.

Run NDT Machine	Area	NA	25 m²/hr

The time required to complete this process can be calculated from the total surface area of all the stringer blades and the upper flange for an I-profile stringer, divided by the rate of 25m²/hr to obtain the total time required. The area for a T- and I-profile stringers is given by Equation E-23 and E-24 respectively.

$$Area \approx \sum_{Str\ Nx}^{Str\ Na} \sum_{Rib\ Nx}^{Rib\ Na} \left(BH \times a \right) \quad \textbf{E-23}$$

$$Area \approx \sum_{Str\ Nx}^{Str\ Na} \sum_{Rib\ Nx}^{Rib\ Na} \left((BH + UFW) \times a \right) \quad \textbf{E-24}$$

NDSU – Non Destructive Inspection Setup

This manufacturing step is used to setup the skin or cover into the jig in readiness for inspection. For secondary bonding and co-bonding (hard skin) the process is carried out once to check the cured skin and again to check the cover. For all other processes it is only carried out once for the complete cover. It is assumed 3 people are required for this operation.

Setup Vertically in NDT Jig	Time	NA	2 hrs

The time required to complete this process is simply 2hrs.

OVCU – Oven Cure

This manufacturing step is used for the dry fibre processes. It is assumed that an oven will have capacity for the skin/cover, or a whole set of stringers. The cure cycle requires 3 hours to elevate the temperature of the preform and tooling to 135°C, the resin is injected at an assumed rate of 150kg per hour, the oven temperature is then increased to 180°C, which takes an hour, this temperature is held for 1.5 hours and then the oven is cooled down for 3 hours. This process, if required, is carried out once per set of stringers or once per skin/cover.

Install in Oven	Time	NA	0.33 hrs
Oven Cycle	Time	Amount of Resin	Variable

The time required to complete this process is the standard time of 8.83hrs plus a variable time based on the amount of resin needed. Based on a resin and fibre density of 1.28kg/m³ and 1.8kg/m³ [141] respectively, and an assumed FVF of 60%, then the resin will constitute 32% of the laminate's weight, i.e. (1.28×0.4)/((1.8×0.6)+(1.28×0.4)). Thus the components weight multiplied by 0.32 will result in the weight of the resin required to be infused. This can be divided by the rate of 150kg/hr to obtain the injection time.

OVPF – Oven Cure

This manufacturing step is used for both dry fibre and prepreg stringers. This process, if required, is carried out once per stringer, and for every stringer in the set.

Install in Oven	Time	NA	0.33 hrs
Oven Cycle	Time	NA	4 hrs

The time required to complete this process is simply 4.33hrs.

PFMT – Preform into Mould Tool

This manufacturing step is used to insert an uncured stringers into an encompassing mould tool. This process, if required, is carried out once per stringer, and for every stringer in the set.

Install stringer preform	Length	NA	0.1 hrs (1 person/5 m)
Install tool into holding fixture	Length	NA	0.1 hrs (1 person/5 m)

The man hours required to complete this process for a single stringer is the total length of the stringer divided by 5m, which is then multiplied by 0.1hrs to obtain the total time required. The tool time is simply 0.2hrs. These times are doubled to get the time for the complete sub-process. The length is given by Equation E-17.

PFPT – Preform into Partial Mould Tool

This manufacturing step is used to insert cured stringers into a partial mould tool, i.e. there is only a fixture at each end of the stringer. This process, if required, is carried out once per stringer, and for every stringer in the set.

Install stringer preform	Length	NA	0.1 hrs (1 person/5 m)
Install tool into holding fixture	Length	NA	0.1 hrs (1 person/5 m)

The man hours required to complete this process for a single angle is the total length of the stringer divided by 5m, which is then multiplied by 0.1hrs to obtain the total time required. The tool time is simply 0.2hrs. These times are doubled to get the time for the complete sub-process. The length is given by Equation E-17.

RMPP – Remove Peel Ply

This manufacturing step is used for skins that have been pre-cured, prior to the stringers being bonded to the cover. This process, if required, removes the peel ply directly underneath the stringer's foot. After removal of peel ply, the surface will require no further treatment in readiness for bonding. This process, if required, is carried out once per stringer, and for every stringer in the set.

Remove Peel Ply Local to Stringer Foot	Area	NA	5 m²/hr

The time required to complete this process can be calculated based on the combined area of all the stringers' feet. Therefore, per stringer, the cumulative area per local rib length multiplied by the foot width is calculated to obtain the total foot area for the particular stringer. This is repeated for every stringer to obtain the total area, which is then divided by the rate, i.e. 5m²/hr, to obtain the time required. The area is given by Equation E-20.

SFAA – Stringer Foot Adhesive Application

This manufacturing step is used to apply the adhesive film to the bottom of the stringer feet, by first fixing the stringer in a jig and then applying heat first and thereafter the adhesive film to the stringer foot. This process, if required, is carried out once per stringer, and for every stringer in the set.

Install Stringer into Holding Fixture	Time	NA	0.1 hrs (2 people required)
Heat Stringer Foot and Apply Adhesive	Area	NA	6 m²/hr

The time required to complete this process can be calculated based on the combined area of all the stringers' feet. Therefore, per stringer, the cumulative area per local rib length multiplied by the foot width is calculated to obtain the total foot area for the particular stringer. This is then divided by the rate, i.e. 6m²/hr, to obtain the time required. A further 0.1hrs is added on. This is done for each stringer and the combined times are added together. The area is given by Equation E-25.

$$Area \approx \sum_{Rib\ Nx}^{Rib\ Na} \left(LFW \times a\right) \qquad \textbf{E-25}$$

SPHF – Stringer Preform Hot Form

This manufacturing step is used to preform the stringer angle. This process is carried out once per angle. For dry fibre application i.e. with NCF and braids, this process needs to be repeated after every 3 dry textiles are deposited for each angle.

Apply Heat and Lower Diaphragm	Time	NA	0.8 hrs

The time required to complete this process is simply 0.8hrs.

STLP – Stringer L Preform

This manufacturing step is used for preforming the complete T-profile stringer, after the angles have been formed. This process, if required, is carried once per stringer, and for every stringer in the set.

Bring L's with Spine Together	Length	NA	0.1 hrs (1 person/5 m)
Insert Noodle	Length	NA	20m/hr
Place Capping Plate	Length	NA	0.1 hrs (1 person/5 m)
Insert Pressure Plate	Length	NA	0.1 hrs (1 person/5 m)

The man hours required to complete this process for a complete stringer is the total length of the stringer divided by 5m, which is then multiplied by 0.1hrs to obtain the total time required. These times are trebled to get the time for the complete sub-process except the noodle insertion. The length of the stringer blade divided by the rate for inserting the noodle, i.e. 20m/hr, gives the time for inserting the noodle, and this is added to the other times for this sub-process. The length is given by Equation E-17.

STPF – Stringer Preform

This manufacturing step is used to preform the complete stringer under vacuum in readiness for the oven. This process, if required, is carried out once per stringer, and for every stringer in the set.

Lay Vacuum Foil on Flat Surface	Area	NA	10 m²/hr (for flat area)
Lay Bleeder Ply on Vacuum Foil	Area	NA	20 m²/hr (for flat area)
Place Tool into Vacuum Bag Using Crane	Time	NA	0.2 hrs (2 people)
Apply Sealant Tape	Length	NA	20 m/hr
Check Seals	Length	NA	100 m/hr

The areas of vacuum foil and bleeder ply will be assumed to be 1.5 times the area of the stringer's lower flange and 2.5 times the area of the blade for a T-profile stringer, or 2 times the combined area of the stringer upper and lower flange and blade for an I-profile stringer. These areas can be simply divided by the rates shown in the table above, to get the times. The crane time is simply 0.2 hours. For applying the sealant and checking the seals, it will be assumed that as the stringer is a long and slender object, that the seal length will be twice the overall stringer length, as normally sealant tape is applied back

to back, thus these lengths can be simply divided by the rates to obtain the time. The area for a T- and I-profile stringers is given by Equation E-26 and E-27 respectively. The length is given by Equation E-17.

$$Area \approx \sum_{Rib\ Nx}^{Rib\ Na} \left(\left(\left(LFW \times 1.5\right) + \left(BH \times 2.5\right)\right) \times a\right) \quad \textbf{E-26}$$

$$Area \approx \sum_{Rib\ Nx}^{Rib\ Na} \left(\left(LFW + BH + UFW\right) \times 2 \times a\right) \quad \textbf{E-27}$$

STSI – Stringer to Skin Integration

This manufacturing step is used to position the stringers to the skin, using holding fixtures on the skin/cover tool. This process, if required, is carried out once per stringer, and for every stringer in the set.

Install Holding Fixtures around Skin Tool	Time	NA	0.1 hrs (1 each end)
Move Over Skin Tool and Position	Time	NA	0.1 hrs
Lower Individual Stringer onto Fixtures	Time	NA	0.1 hrs

The first part of this sub-process is per stringer, so 0.2hrs is required per stringer. The other two times are added together and are considered only once for the stringer to skin integration phase. Thus, the total time is simply 0.4hrs.

STUP – Stringer U Preform

This manufacturing step is used for preforming the complete I-profile stringer, after the angles have been formed. This process, if required, is carried out once per stringer, and for every stringer in the set.

Bring U's with Spine Together	Length	NA	0.1 hrs (1 person per 5 m)
Insert Noodles	Length	NA	20m/hr
Place Capping Plates	Length	NA	0.1 hrs (1 person per 5 m)
Insert Pressure Plates	Length	NA	0.1 hrs (1 person per 5 m)

The man hours required to complete this process for a complete stringer is the total length of the stringer divided by 5m, which is then multiplied by 0.1hrs to obtain the total time required. These times are trebled to get the time for the complete sub-process except the noodle insertion. The length of the stringer blade, multiplied by 2, divided by the rate for inserting the noodle, i.e. 20m/hr, gives the time for inserting the noodle, and this is added to the other times for this sub-process. The length is given by Equation E-17.

TLCL – Tool Cleaning

This manufacturing step is used to clean tooling. This process is carried out a number of times, each time a tool is used.

Tool Cleaning	Area	NA	4 m²/hr for skin/cover and 1 m²/hr for stringer tooling

It is necessary to first of all calculate the areas to be cleaned.

For UD operations:

- UD Skin and Stringer (Angle, spine, lower and optional upper plate) Deposition
    - Area of the two-dimensional laminate required

The skin area is given by Equation E-18. For the stringer constituent parts, the laminate area can be worked out based on the manufacturing cost calculator spreadsheet.

- Angle Forming
    - T-profile stringers – Surface area of the blade and half of the lower flange
    - I-profile stringers – Surface area of the blade and half of the upper and lower flanges

The area for a T- and I-profile stringer is given by Equation E-28 and E-29 respectively, for each forming block, i.e. per stringer there will be two.

$$Area \approx \sum_{Rib\ Nx}^{Rib\ Na} \left(\left(\left(LFW \div 2\right) + \left(BH\right)\right) \times a\right) \quad \textbf{E-28}$$

$$Area \approx \sum_{Rib\ Nx}^{Rib\ Na} \left(\left(\left(\left(LFW + UFW\right) \div 2\right) + BH\right) \times a\right) \quad \textbf{E-29}$$

- Stringer Preforming (for capping plates only)
    - T-profile stringers – Surface area of the lower flange
    - I-profile stringers – Surface area of the upper and lower flanges

The area for a T- and I-profile stringers is given by Equation E-25 and E-30 respectively.

$$Area \approx \sum_{Rib\ Nx}^{Rib\ Na} \left(\left(LFW + UFW\right) \times a\right) \quad \textbf{E-30}$$

- Stringer Holding Tools
    - T-profile stringers – Twice the surface area of the blade and the lower flange (for partial tooling divide the complete area by the length of the stringer to obtain the surface area for 1m of tooling)
    - I-profile stringers – Twice the surface area of the blade and the upper and lower flanges (for partial tooling divide the complete area by the length of the stringer to obtain the surface area for 1m of tooling)

The area for a T- and I-profile stringer is given by Equation E-31 and E-32 respectively. The length is given by Equation E-17.

$$Area \approx \sum_{Rib\ Nx}^{Rib\ Na} \left(\left(\left(LFW\right) + \left(BH \times 2\right)\right) \times a\right) \quad \textbf{E-31}$$

$$Area \approx \sum_{Rib\ Nx}^{Rib\ Na} \left(\left(\left(LFW + UFW\right) + \left(BH \times 2\right)\right) \times a\right) \quad \textbf{E-32}$$

- Mandrels
  - Height of adjacent stringers and pitch between stringers multiplied by the stringer length, remembering that the number of mandrels required is the number of stringers plus 1

The area is given by Equation E-33.

$$Area \approx \sum_{Rib\ Nx}^{Rib\ Na} \left(BH_{Str\ Na} + BH_{Str\ Na+1} + SP\right) \times a \quad \textbf{E-33}$$

For Dry Fibre operations:

- Skin
  - Area of the two-dimensional laminate required

The skin area is given by Equation E-18.

- Angle consolidation and forming
  - T-profile stringers – Surface area of the blade and half of the lower flange
  - I-profile stringers – Surface area of the blade and half of the upper and lower flanges

The area for a T- and I-profile stringer is given by Equation E-28 and E-29 respectively.

- Spine, lower and optional upper plate consolidation
  - Area of the two-dimensional laminate required

The area for the lower and upper plate and is given by Equation E-25 and Equation E-34, respectively. The area for the spine is given by Equation E-35.

$$Area \approx \sum_{Rib\ Nx}^{Rib\ Na} \left(UFW \times a\right) \quad \textbf{E-34}$$

$$Area \approx \sum_{Rib\ Nx}^{Rib\ Na} \left(BH \times a\right) \quad \textbf{E-35}$$

- Stringer Preforming (for capping plates only)
  - T-profile stringers – Surface area of the lower flange
  - I-profile stringers – Surface area of the upper and lower flanges

The area for a T- and I-profile stringer is given by Equation E-25 and E-30 respectively.

- Stringer Holding Tools

- T-profile stringers – Twice the surface area of the blade and the lower flange (for partial tooling divide the complete area by the length of the stringer to obtain the surface area for 1m of tooling)
- I-profile stringers – Twice the surface area of the blade and the upper and lower flanges (for partial tooling divide the complete area by the length of the stringer to obtain the surface area for 1m of tooling)

The area for a T- and I-profile stringers is given by Equation E-31 and E-32 respectively. The length is given by Equation E-17.

These areas are simply divided by the cleaning rates.

TLPP –Tool Preparation

This manufacturing step is used to prepare the tooling in readiness for a curing operation. This process is carried out a number of times, each time a tool is used for curing a part.

Tool Sealing	Area	NA	30 m²/hr for skin/cover and 5 m²/hr for stringer tooling
Tool Release Agent	Area	NA	30 m²/hr for skin/cover and 5 m²/hr for stringer tooling

It is necessary to first of all calculate the areas to be cleaned.

For UD operations:

- UD Skin Deposition
  - Area of the two-dimensional laminate required

The skin area is given by Equation E-18.

- Angle Forming (when stringer is pre-cured)
  - T-profile stringers – Surface area of the blade and half of the lower flange
  - I-profile stringers – Surface area of the blade and half of the upper and lower flanges

The area for a T- and I-profile stringer is given by Equation E-28 and E-29 respectively.

- Stringer Preforming (for capping plates only)
  - T-profile stringers – Surface area of the lower flange
  - I-profile stringers – Surface area of the upper and lower flanges

The area for a T- and I-profile stringer is given by Equation E-25 and E-30 respectively.

- Stringer Holding Tools
  - T-profile stringers – Twice the surface area of the blade and the lower flange (for partial tooling divide the complete area by the length of the stringer to obtain the surface area for 1m of tooling)

    - I-profile stringers – Twice the surface area of the blade and the upper and lower flanges (for partial tooling divide the complete area by the length of the stringer to obtain the surface area for 1m of tooling)

The area for a T- and I-profile stringer is given by Equation E-31 and E-32 respectively. The length is given by Equation E-17.

- Mandrels
    - Average height of adjacent stringers and pitch between stringers multiplied by the stringer length

The area is given by Equation E-33.

For Dry Fibre operations:

- Skin
    - Area of the two-dimensional laminate required

The skin area is given by Equation E-18.

- Angle consolidation and forming (when stringer is pre-cured)
    - T-profile stringers – Surface area of the blade and half of the lower flange
    - I-profile stringers – Surface area of the blade and half of the upper and lower flanges

The area for a T- and I-profile stringer is given by Equation E-28 and E-29 respectively.

- Stringer Preforming (for capping plates only when stringer is pre-cured)
    - T-profile stringers – Surface area of the lower flange
    - I-profile stringers – Surface area of the upper and lower flanges

The area for a T- and I-profile stringers is given by Equation E-25 and E-30 respectively.

- Stringer Holding Tools
    - T-profile stringers – Twice the surface area of the blade and the lower flange (for partial tooling divide the complete area by the length of the stringer to obtain the surface area for 1m of tooling)
    - I-profile stringers – Twice the surface area of the blade and the upper and lower flanges (for partial tooling divide the complete area by the length of the stringer to obtain the surface area for 1m of tooling)

The area for a T- and I-profile stringer is given by Equation E-31 and E-32 respectively. The length is given by Equation E-17.

These areas are simply divided by the cleaning rates.

UDDP – UD Deposition

This manufacturing step is used to deposit the UD prepreg, either for the skin or stringers. This process, if required, is carried out once for the skin, and once for each constituent laminate of the stringer, so that enough blanks can be produced for one month's production. After every strip is deposited 0.006hrs is required to reposition the head of the machine.

Carbon Fibre Deposition	Volume	NA	250m/hr
Head Reposition	Piece	NA	0.006 hr
Edge of Part Ultrasonic Cutting	Perimeter	NA	50 m/hr

The carbon fibre deposition time can be worked out using the manufacturing cost calculator spreadsheet. The perimeter of the skin/cover is given, thus it must not be calculated.

Shown in Figure E-1 is a plot for the deposition rate on a contoured surface for a 4 ply quasi-isotropic laminate using a 300mm wide, 0.25 mm thick ply (E-mail from Coyle, E. from MAG Advanced Technologies 09/03/09). As the typical laminate width is constrained, then an assumed average deposition rate of 30kg/hr is chosen. In order to make this applicable to the manufacturing cost calculator, a rate based on length is required, thus 30kg/hr results in a deposition rate of 250m/hr. This deposition rate, based on length is applicable to all UD prepreg ply thicknesses.

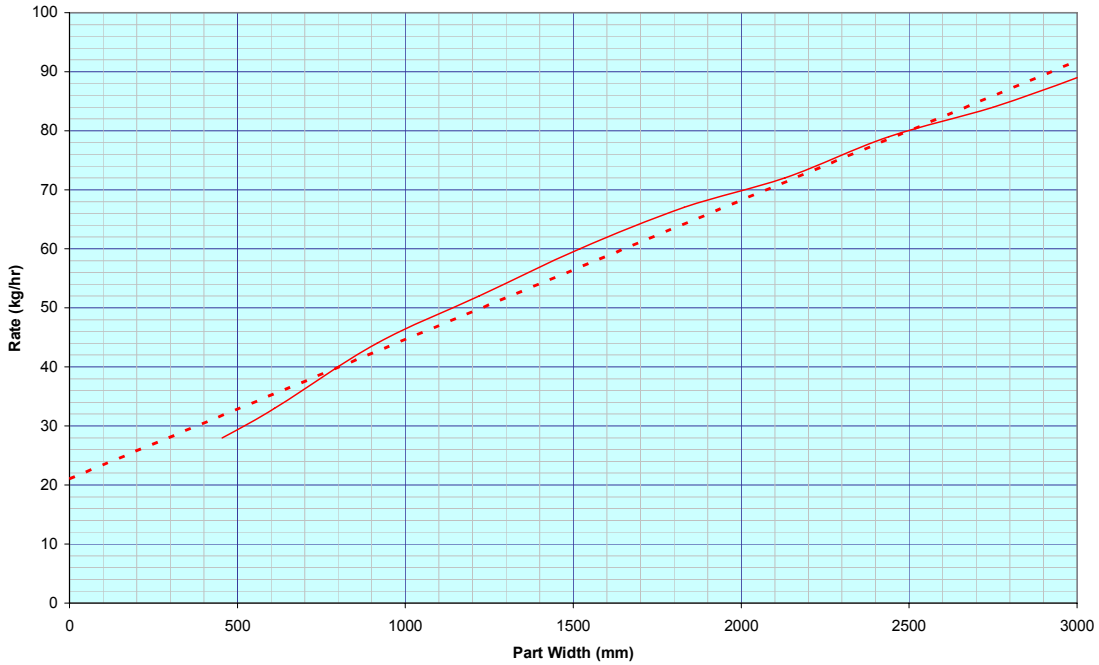

Figure E-1: ATL rate for a 4 ply quasi-isotropic laminate using 0.25mm thick plies

UDIB – UD Insert Blank

This manufacturing step is used to insert the blank for a single handed stringer onto the form tool. This process, if required, is carried out twice per stringer (i.e. left and right hand angles), and for every stringer.

Insert Blank onto Hot Form Tool	Length	NA	0.1 hrs (1 person/5 m)

The man-hours required to complete this process for a single angle is the total length of the stringer divided by 5m, which is then multiplied by 0.1hrs to obtain the total time required. The tool time is simply 0.1hrs. The length is given by Equation E-17.

VBAP – Vacuum Bag Application

This manufacturing step is used for applying a vacuum bag. This process is carried out for consolidating the lightning strike mesh, debulking the NCF after every 6 textiles have been deposited, for curing the skin and curing/bonding the cover.

Apply Vacuum Foil	Area	NA	10 (for skin or LS mesh) or 8 to 4 m²/hr (i.e. SP from 312.5 to 125 mm)
Apply Sealant Tape	Perimeter	NA	20 m/hr
Check Seals	Perimeter	NA	100 m/hr

The area of vacuum foil will be assumed to be 1.1 times the area of the skin/cover surface area. This area is divided by the rate shown in the table above, to get the times. For applying the sealant tape and checking the seals, the perimeter of the skin/cover can be used, thus these lengths can be simply divided by the rates to obtain the time. The skin area is given by Equation E-18. The perimeter of the skin/cover is given, thus it must not be calculated.

VBDB – Vacuum Bag Debagging

This manufacturing step is used to remove the vacuum bag. This process is carried each time a vacuum bag is used.

Debagging	Perimeter	NA	40 m/hr

For debagging, the perimeter of the skin/cover can be used, thus this length can be simply divided by the rate of 40 m/hr to obtain the time. The perimeter of the skin/cover is given, thus it must not be calculated. For debagging a stringer, it will be assumed that as the stringer is a long and slender object, that the perimeter is the length of the stringer. The length is given by Equation E-17.

VBDM – Vacuum Bag Demoulding

This manufacturing step is used to demould the part after cure. The process is carried out after curing of the skin or cover.

Demoulding	Perimeter	NA	20 m/hr

For demoulding, the perimeter of the skin/cover can be used, thus this length can be simply divided by the rate of 20 m/hr to obtain the time. The perimeter of the skin/cover is given, thus it must not be calculated. For demoulding a stringer, it will be assumed that as the stringer is a long and slender object, that the perimeter is twice the length of the stringer. The length is given by Equation E-17.

VBFC – Vacuum Bag For Cure

This manufacturing step is used only when the function of the vacuum bag is to cure the part. In this case both release film and bleeder plies are required. This process is therefore carried out each time a part is cured.

Apply Release Film	Area	NA	18 (for skin) or 10 to 6 m²/hr (i.e. SP from 312.5 to 125 mm)
Apply Bleeder Ply	Area	NA	22 (for skin) or 12 to 8 m²/hr (i.e. SP from 312.5 to 125 mm)

The areas of release film and bleeder ply will be assumed to be 1.1 times the area of the skin/cover surface area. This area is divided by the rates shown in the table above, to obtain the man-hours. The skin area is given by Equation E-18.

VBRF – Vacuum Bag Release Film

This manufacturing step is used only for secondary bonding stringers to the skin. This process, if required, is carried out once per stringer, and for every stringer.

Apply Release Film	Stringer Perimeter	NA	20 m/hr

For applying 30mm wide strips of release film, it can be assumed that the perimeter of the stringer's foot is twice its length, as given by Equation E-36. This length is divided by the rate of 20 m/hr to obtain the time.

$$Area \approx \sum_{Str\ Nx}^{Str\ Na} \sum_{Rib\ Nx}^{Rib\ Na} (2 \times a) \qquad \textbf{E-36}$$

VBUT – Vacuum Bag Utilized

This manufacturing step is used when applying vacuum bag pressure, i.e. there is no external heat or pressure from an oven or autoclave. This process is carried out for the consolidation of the lightning strike mesh, and the debulking of the NCF for the skin.

Apply Vacuum	Time	NA	6 hrs
Debagging	Perimeter	NA	40 m/hr

The vacuum time is simply 6hrs. For debagging, the perimeter of the skin/cover can be used, thus this length is simply divided by the rate of 40 m/hr to obtain the time.

VBWE – Vacuum Bag Wedges

This manufacturing step is used to insert wedges both sides of the stringer or stringer tooling to aid the vacuum bagging of the cover. This process, if required, is carried out twice per stringer, i.e. a wedge each side, and for every stringer.

Install Wedges for Stringers	Length	NA	0.05 hrs (1 person / 5 m)

The man-hours required to complete this process per stringer is the total length of the stringer divided by 5m, which is then multiplied by 0.05hrs and then by 2 (2 wedges per stringer) to obtain the total time required. The tool time is simply 0.1hrs. The length is given by Equation E-17.

E.2.2 Global Process Flow

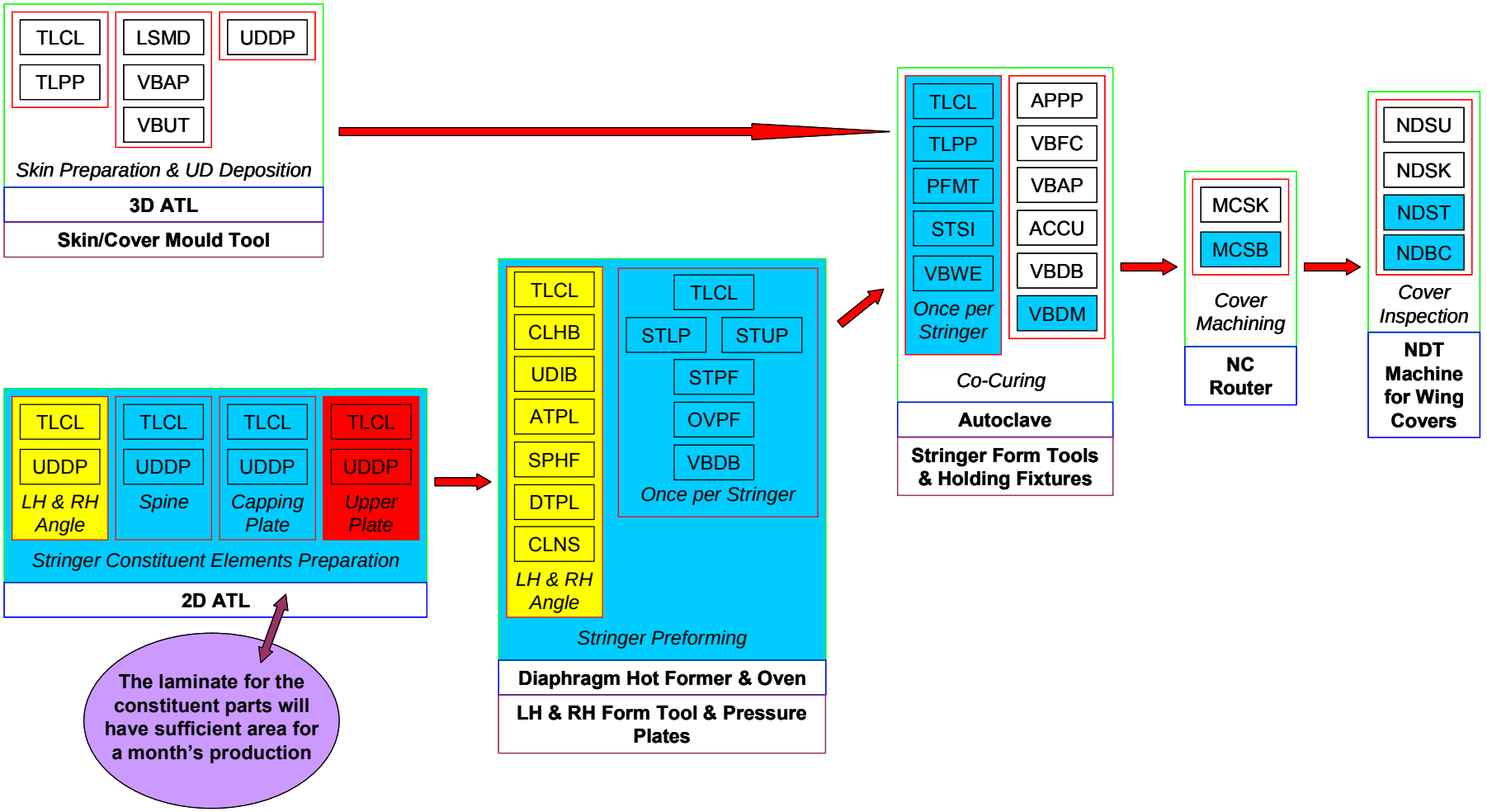

Figure E-2: Co-Cure

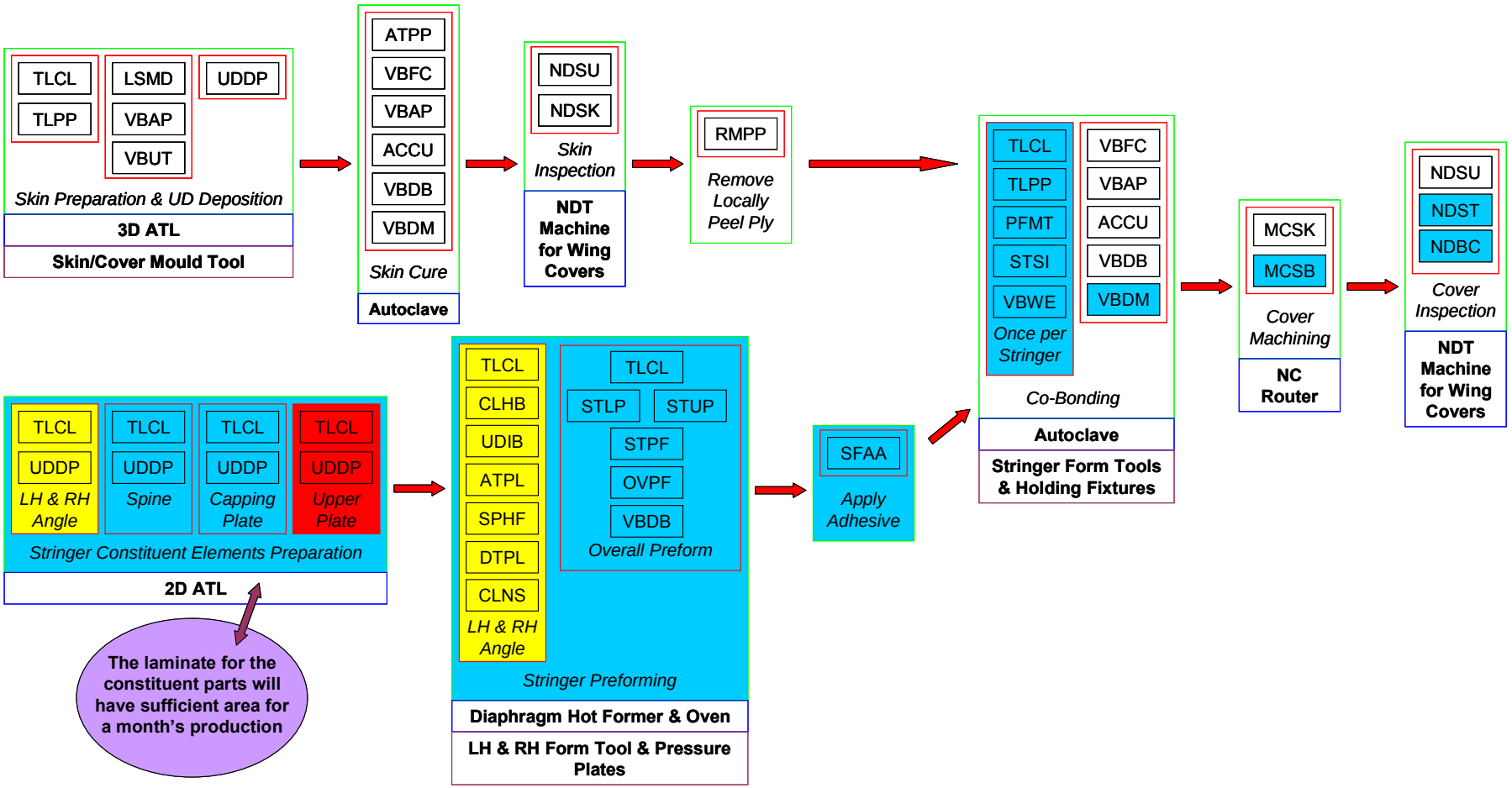

Figure E-3: Co-Bond (Hard Skin)

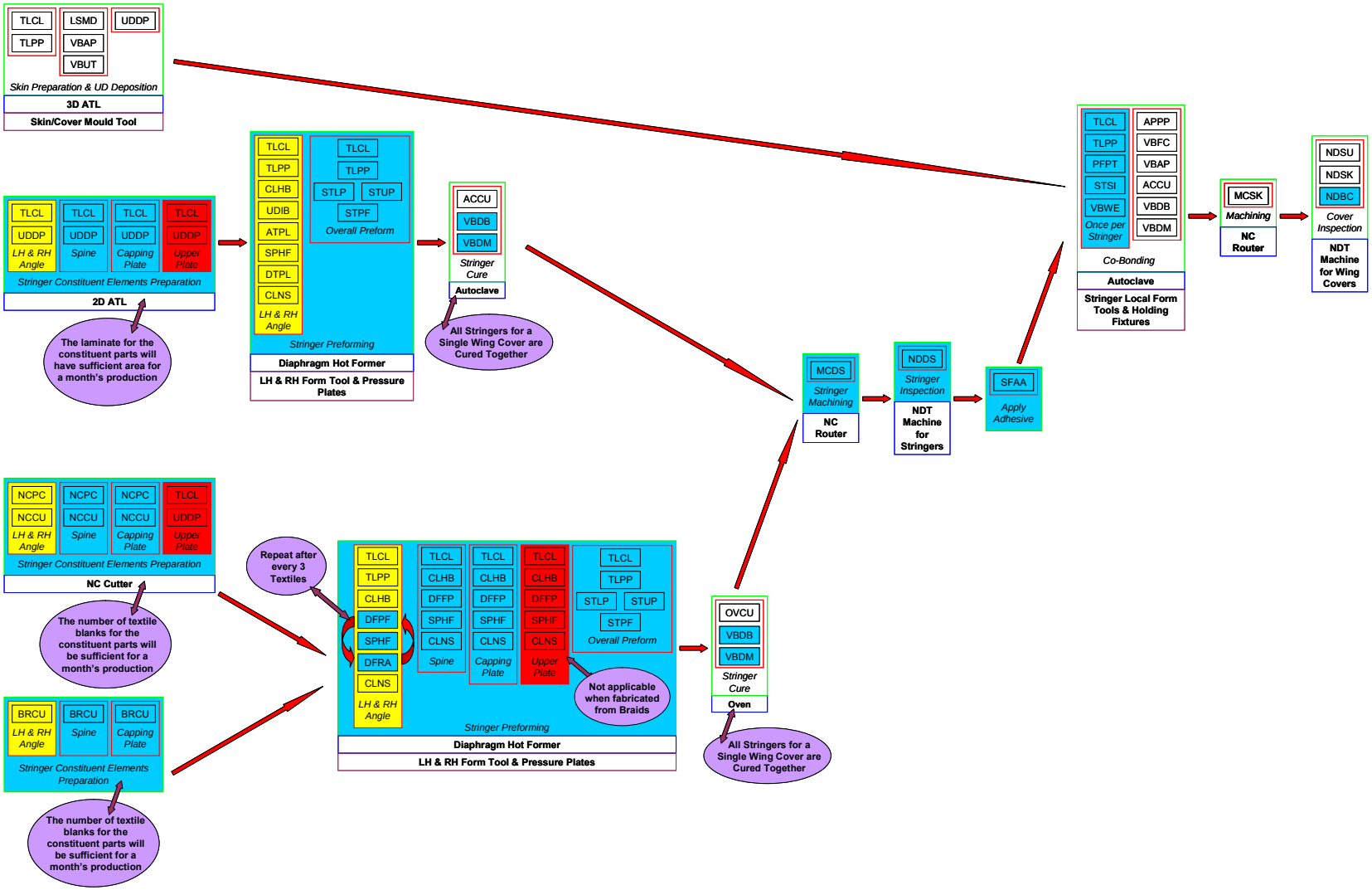

Figure E-4: Co-Bond (Hard Stringer)

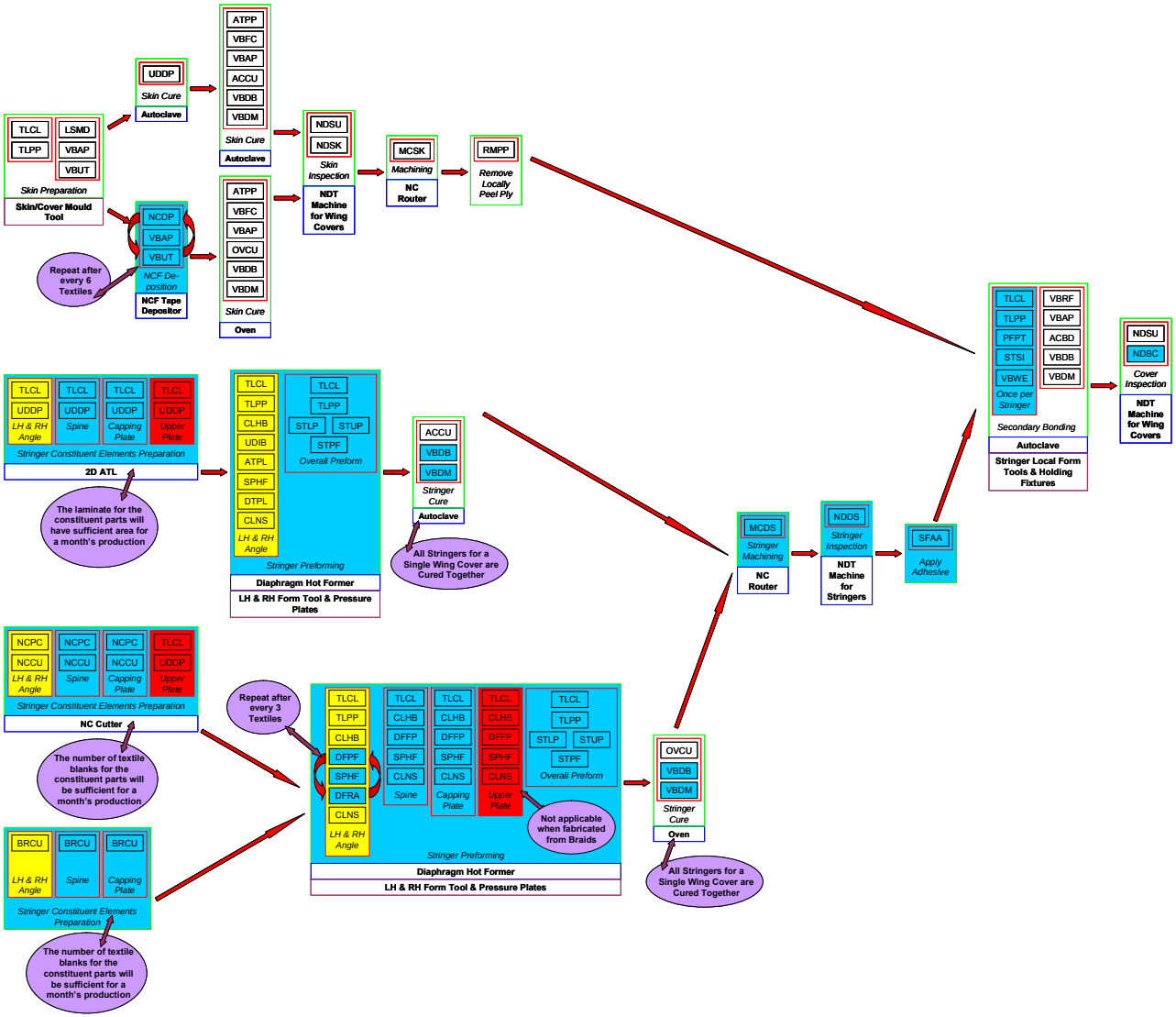

Figure E-5: Secondary Bond

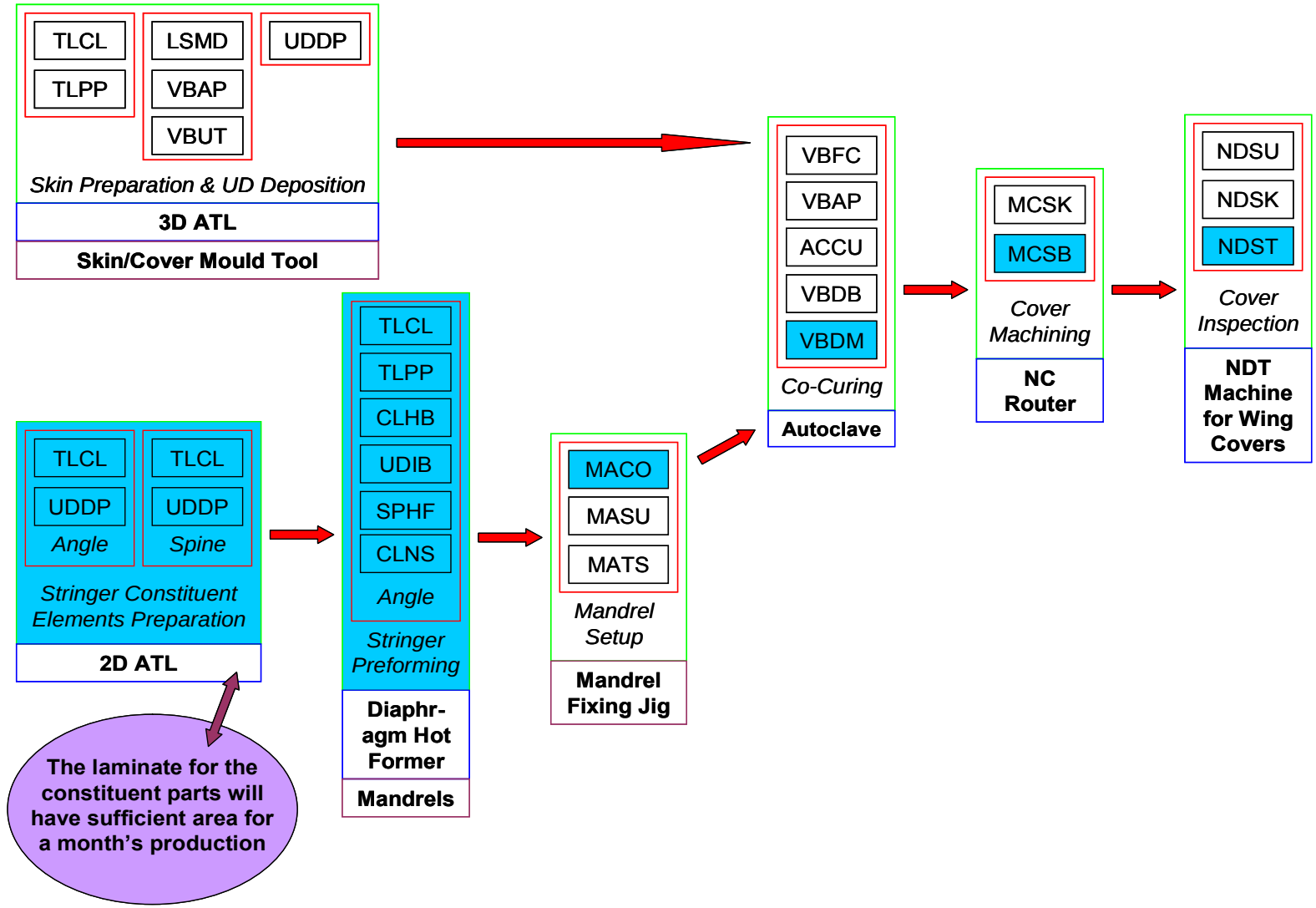

Figure E-6: U-profile

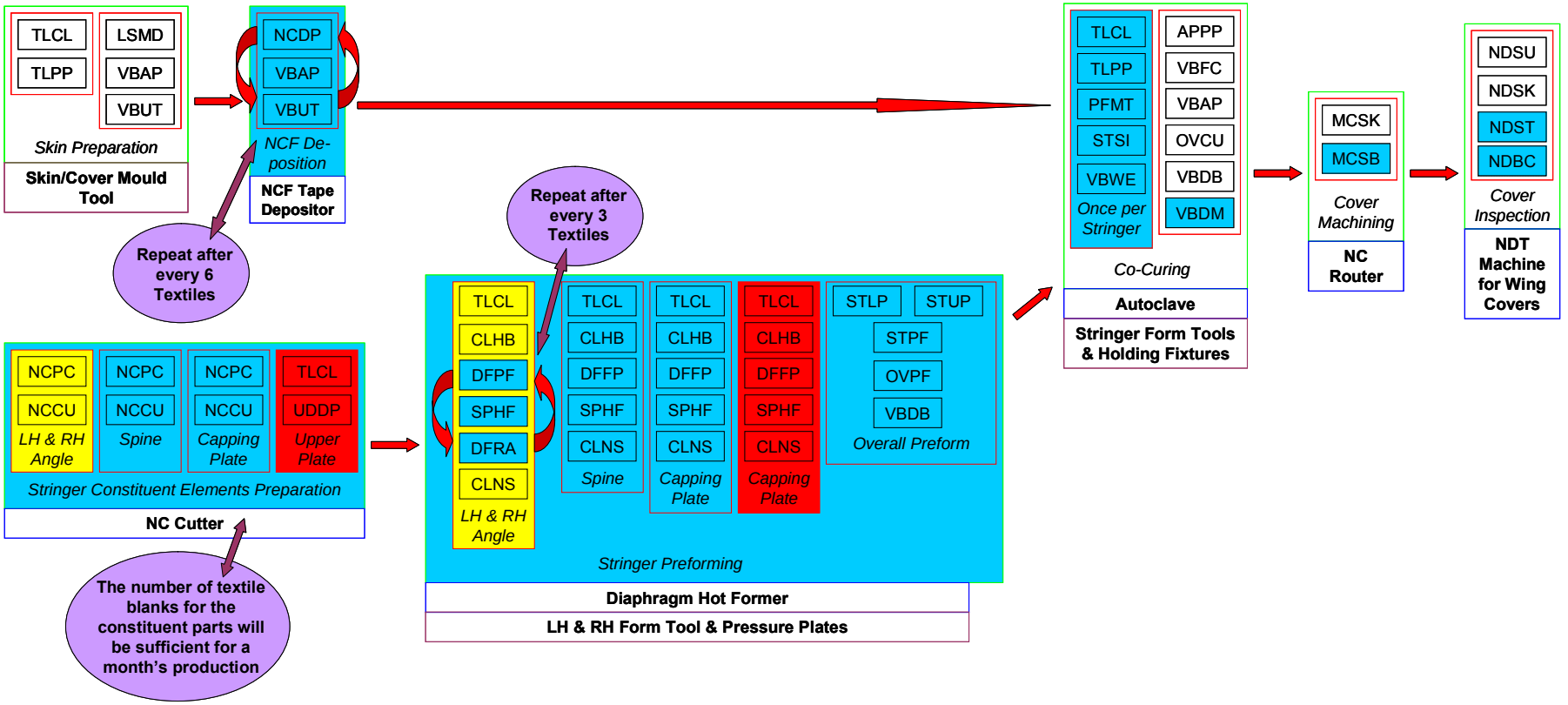

Figure E-7: Co-Infuse

Figure E-8: Key

E.2.3 Particular Process Steps

The manufacturing cost calculator spreadsheet has a specific template for each manufacturing process and stringer-stiffened panel configuration. Thus once the input data for a stringer-stiffened panel is given, i.e. its dimensions, the manufacturing cost can be calculated. In general all process steps are based on simple length or area relationships, therefore the manufacturing cost calculator spreadsheet can simply work out the cost by integrating Equations E-16 to E-36 into the spreadsheet. There are however 3 process steps that require a more complicated calculation procedure than the other steps, which are simply based on area or length. These process steps are:

- LSMD
- NCDP
- UDDP

All these process steps require rolls of material, with a finite width, to be deposited over a particular area. The simplest of the above process steps is LSMD as the area is simply the area of the complete skin/cover, thus it is only the number of strips and length of each strip that needs to be calculated.

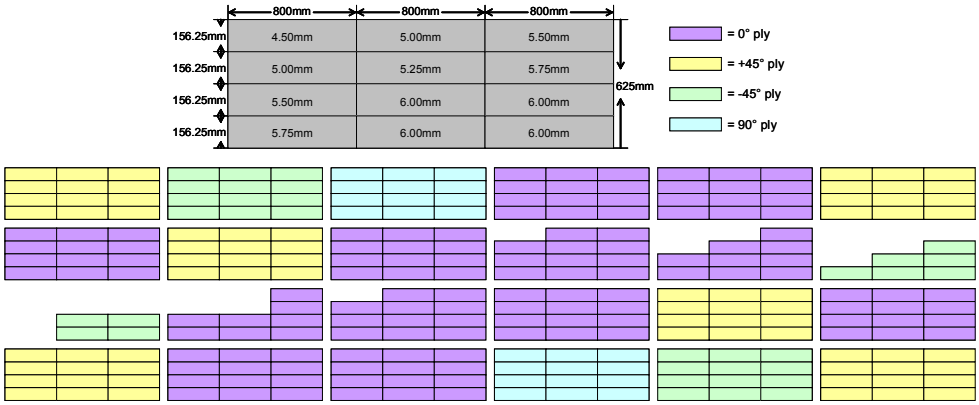

Figure E-9: Ply definition breakdown for skin

The remaining two steps are more complicated, as the area is based on the extent of each ply/textile, which is dependent on the thickness distribution of the skin and for UD

prepreg stringers the laminate to fabricate the constituent parts. An example of the complicated layer structure based on one of the examples shown in Chapter 10 is shown in Figure E-9. It can be seen that due to the thickness varying from 4.50 to 6.00mm, a number of the plies near to the laminate's mid-plane do not extend across the complete area of the skin/cover.

An additional complication for the UDDP process step is that the plies have 4 different orientations, namely 0°, ±45°, and 90°. Therefore, it is necessary that the manufacturing cost calculator can take into consideration the implications of the different orientations, which influences both the deposition time, and the resultant amount of off-cut material, as illustrated in Figure E-10. This example uses a standard tape width of 300mm, on a panel with a rib and stringer pitch of 800mm and 165mm, respectively. It can be seen that in this case the 90° ply has the best material utilisation, whereas the 0° and 45° plies have a lot of off-cut material, although this is dependent on the shape of the ply to be deposited.

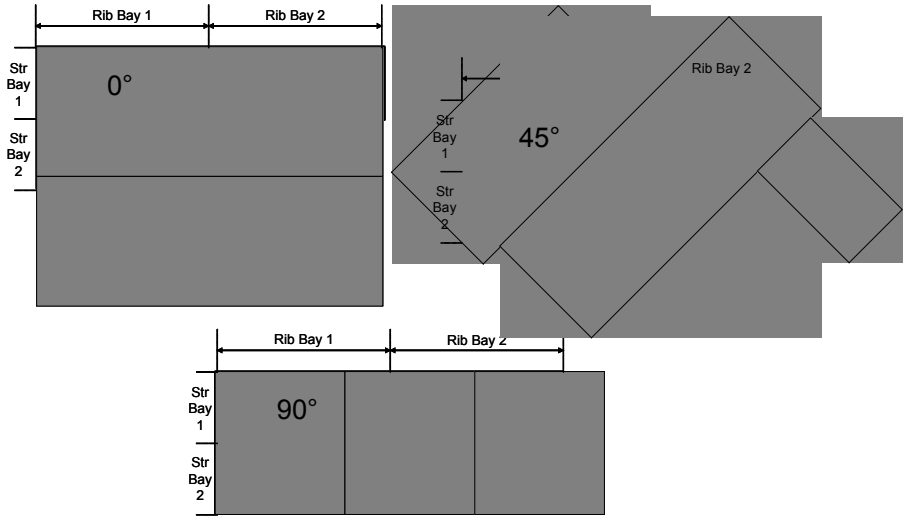

Figure E-10: Material utilisation rates for 0°, 45°, and 90° on a simple ply contour

Previous endeavours into this field for calculating the cost of depositing UD prepreg has been carried out by Stockton et al.[195] and Kim et al. (2001)[338]. Stockton et al. broke down the deposition of a laminate using an ATL into constant and variable activities. The approach uses trigonometry to work out the length and number of strips required to layup a rectangular shape.

An alternative method from Kim et al. (2001) is to calculate an index of the complete laminate based on the cost parameters such as the number of prepreg layers, the cutting length and the stacking area[338]. Thus a laminate made from a greater number of separate plies will be more expensive relative to a laminate with a smaller number of plies. This method could be applicable to NCF deposition as the orientation of the layer is not considered, however for the deposition of UD prepreg this method is not applicable.

E.2.3.1 Developed Solution

The method developed by Iyiyazici, A. (MSc Thesis [not yet published] "Linking Design Data to Manufacturing Recurring Costs" at Chalmers University of Technology, Gothenburg, Sweden) can calculate the deposition of UD tape for shapes as shown in Figure E-11. As can be seen in Figure E-11 the green shapes can be analysed, however the purple shapes with an indented profile or with a blank area within the shape cannot be analysed. However, as identified in Figure E-11 with the yellow shapes, it is possible to decompose the purple shapes so that they can be analysed, although due to the decomposition of the shape the accuracy of the analysis will be reduced by a certain factor.

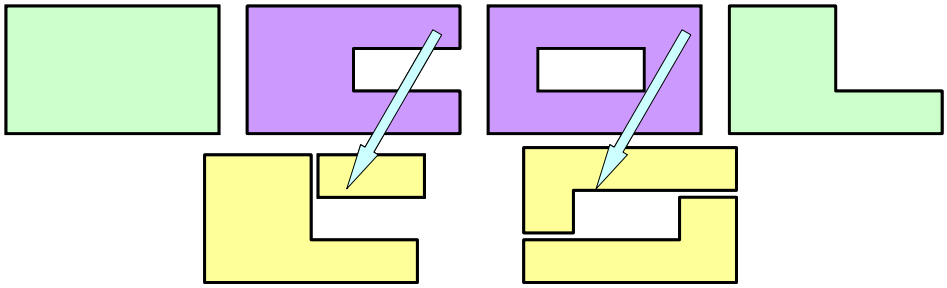

Figure E-11: Different ply shapes

The method has been programmed within Microsoft Excel Visual Basic, as shown in Figure E-12. This program needs the basic 2D coordinates of the ply/layer, which is inputted directly into Microsoft Excel. As input data for the macro, the basic 2D coordinates are required, as well as the ply width and its orientation. The ply width will typically be 300mm, however for sub-processes LSMD and NCDP the width must vary, to either 1m or 1.5m, respectively, although for these two processes the orientation is always 0°. Once this data is known, the number of strips, the length of the strips in total, as well as the amount of off-cut material is given as output.

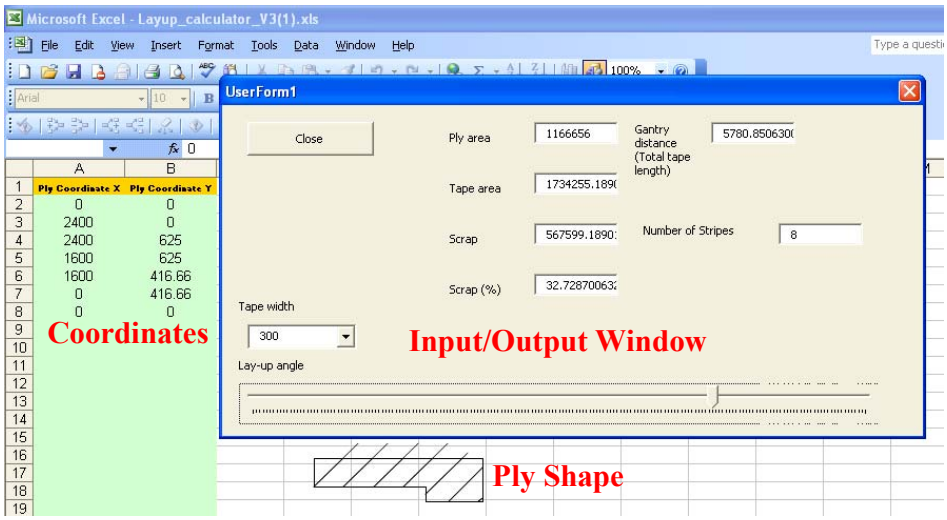

Figure E-12: Deposition calculator

The macro is based on an trigonometric and algebraic algorithm. The basic principle of the algorithm is to scan the desired laminate profile with a horizontal line for 0° plies.

For ±45° and 90° plies the horizontal line is rotated by the required angle. The first line originates from coordinate 0,0 and then the next line is generated parallel to the first line, at a distance that is equivalent to the ply/layer width, as shown in Figure E-13. This is repeated until the final line no longer intersects with the desired laminate profile. The next phase is to calculate the intersection points between the lines and the desired laminate profile, as illustrated in Figure E-13 by the red points. Finally, a comparison is conducted between adjacent lines to see which line has the intersection points the furthest distance away, once those points are identified then the ply/layer strip area can be identified, as illustrated in Figure E-13 by the green lines. These strips are added together to obtain the total ply area required; and the lengths are added together to calculate the total length required for the laminate profile.

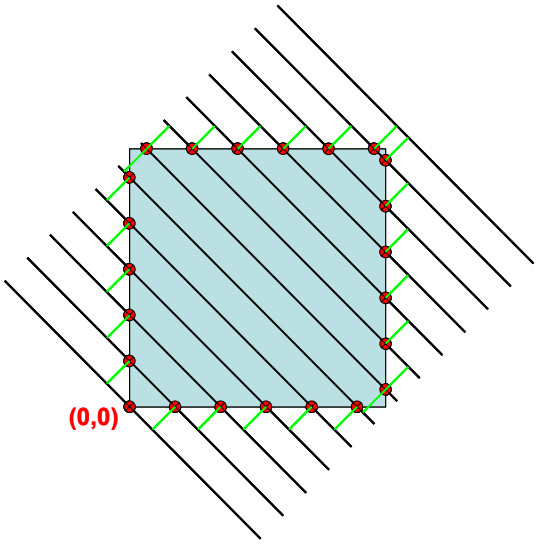

Figure E-13: Deposition breakdown using algorithm

The individual ply/layer data itself can be obtained from the manufacturing cost calculator spreadsheet, an excerpt of which is shown in Figure E-14. The manufacturing cost calculator spreadsheet is setup to determine the number of plies required and their extent, by simply dividing the skin laminate thickness per cell (a cell represents the panel) by the thickness of the ply. Furthermore, the ply orientation is known from the stacking sequence, i.e. for a certain thickness there is a given stacking sequence. This procedure is similar for the stringers, although the stringer needs to be broken down into their constituent elements, i.e. angles, spines, capping plates, as well as the associated elements height or width.

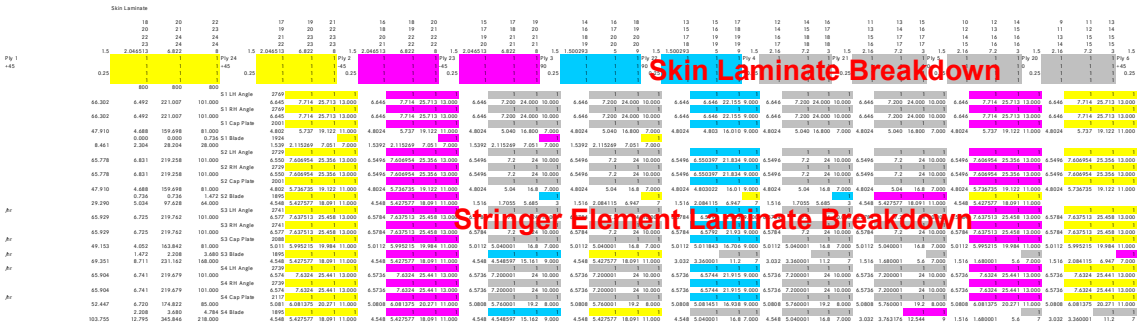

Figure E-14: Manufacturing cost calculator laminate breakdown

E.3 Material Costs

From Bader (2002)[160], the price of HS and IM prepreg is \$120/kg and \$240/kg, respectively. Typically the unit cost per kg for material will be higher for thinner UD prepreg, i.e. 0.184 mm thickness, than for thicker UD prepreg, i.e. 0.25mm thickness, however this will not be considered here. Furthermore HS NCF is \$70/kg[160], thus based on the prepreg costs, an IM NCF should cost \$140/kg. However, in reality, once the cost of the resin is included, as well as the toughening agent, to ensure that the NCF's performance is similar to the prepreg, then the cost per kg can be assumed to be the same as for the prepreg. The cost for a HS triaxial braid is assumed to cost \$50/kg (E-Mail from Andrew Mills, Cranfield University 03/03/09), thus including resin and toughening agent, the cost would be \$85/kg, whereas for IM the cost would be \$170/kg.

The following prices were obtained from Andrew Mills (E-Mail 12/06/09 & 07/09/09 & 14/09/09), based on \$1.6=£1, for secondary and tertiary materials:

- Bleeder Ply: \$2/m²
- Lightning strike mesh: \$58/m² (On a 1m roll)
- Noodle: \$72/m
- Peel Ply: \$1.75/m²
- Release Film: \$3/m²
- Resin film (e.g. FM300): \$50/m²
- Vacuum Film: \$1.5/m²

The following prices and application data for tool preparation fluids were obtained from Mike Rigby from Marbocote Ltd (E-mail 03/07/09), based on \$1.6=£1:

- Tool cleaning agent: \$9.30/ltr & 0.04l/m²
- Mould Sealer: \$120/ltr & 0.04l/m²
- Release Agent: \$23/ltr & 0.04l/m²

Initial work has been conducted into the modelling of the life cycle cost of composite materials, however due to the unavailability of published cost data from composite recyclers, it has not been possible to estimate the cost of recycling[629]. It could be assumed that the cost of disposal to recycle is simply \$0, as today without a market in place, composite manufacturers simply give their scrap material to recyclers for free [meeting with J. Davidson (Milled Carbon Ltd) 27/02/08].

However, the author has calculated some primitive disposal costs based on a number of assumptions. The principal assumption is that the fibres will always be recovered to create short-fibre for use with a BMC process. This is because a grinding process would be wasteful with the premium aerospace long fibres. It has been estimated that virgin carbon fibre is roughly \$50/kg, whereas the reclaimed fibres cost \$11.50/kg[630], i.e. the cost factor difference is approximately 4.3. However, the raw material costs for UD prepreg, NCF and braids, have previously been set. Therefore, applying the 4.3 factor to the HS prepreg price of \$120/kg, gives a value of resale value of \$27.5/kg as chopped fibre, similarly for IM the resale value is \$55/kg. However, this is the resale value, the

disposal cost is of interest for this study. Due to processing costs, and overhead charges the costs of disposal is shown in Table E-2.

For pre-cured material, i.e. all off-cut material, the NCF and braid will cost less to recycle of as it is already in a dry state, so it can be simply chopped, whereas the prepreg will cost more. The post-cured CFRP, entails both cured scrap during the manufacture, such as trimming of the part, as well as the recycling of the wing cover at the end of its service life. This will need to be machined into suitable pieces in order to process it, hence why it is more expensive to recycle it.

	Pre-Cured ($/kg)		Post-Cured ($/kg)
	Prepreg	NCF/Braid	
HS Fibre	-27	0	-37
IM Fibre	0	27	-10

Table E-2: Disposal costs for CFRP

E.4 Capital Equipment Hourly Rates

2D ATL

Acquisition cost:	$4,350,000	
Expected life:	15 years	
Depreciation charge:	$290,000	
Adjustment to value:	$130,500	(@ 3% per year increase)
Finance cost:	$217,500	(@ 5% on average book value)
Maintenance cost:	$304,500	(@ 7% on average book value)

The cost of operating the machine per year is:
290,000+130,500+217,500+304,500=$942,500.

If the machine operates 16 hours a day for 235 days a year, then the hourly rate for the 2D ATL is: 942,500/(16×235)=$251/hr.

3D ATL

Acquisition cost:	$5,075,000	
Expected life:	15 years	
Depreciation charge:	$338,333	
Adjustment to value:	$152,250	(@ 3% per year increase)
Finance cost:	$253,750	(@ 5% on average book value)
Maintenance cost:	$355,250	(@ 7% on average book value)

If the machine operates 16 hours a day for 235 days a year, then the hourly rate for the 3D ATL is: $292/hr.

NC ROUTER

Acquisition cost:	$1,900,000	
Expected life:	15 years	
Depreciation charge:	$126,667	
Adjustment to value:	$57,000	(@ 3% per year increase)
Finance cost:	$95,000	(@ 5% on average book value)
Maintenance cost:	$76,000	(@ 4% on average book value)

If the machine operates 16 hours a day for 235 days a year, then the hourly rate for the NC Cutter is: $94/hr.

NCF TAPE DEPOSITOR

Acquisition cost:	$1,500,000 (assumed – no information available)	
Expected life:	15 years	
Depreciation charge:	$100,000	
Adjustment to value:	$45,000	(@ 3% per year increase)
Finance cost:	$75,000	(@ 5% on average book value)
Maintenance cost:	$75,000	(@ 5% on average book value)

If the machine operates 16 hours a day for 235 days a year, then the hourly rate for the NCF Tape Depositor is: $78/hr.

AUTOCLAVE

Acquisition cost:	$2,000,000	
Expected life:	20 years	
Depreciation charge:	$100,000	
Adjustment to value:	$60,000	(@ 3% per year increase)
Finance cost:	$100,000	(@ 5% on average book value)
Maintenance cost:	$60,000	(@ 3% on average book value)

If the machine operates 8 hours a day for 235 days a year, then the hourly rate for the Autoclave is: $170/hr.

OVEN

Acquisition cost:	$500,000	
Expected life:	20 years	
Depreciation charge:	$25,000	
Adjustment to value:	$15,000	(@ 3% per year increase)
Finance cost:	$25,000	(@ 5% on average book value)
Maintenance cost:	$10,000	(@ 2% on average book value)

If the machine operates 8 hours a day for 235 days a year, then the hourly rate for the Oven is: $40/hr.

NDT MACHINE FOR WING COVERS

Acquisition cost:	$2,000,000	
Expected life:	15 years	
Depreciation charge:	$133,333	
Adjustment to value:	$60,000	(@ 3% per year increase)
Finance cost:	$100,000	(@ 5% on average book value)
Maintenance cost:	$60,000	(@ 3% on average book value)

If the machine operates 16 hours a day for 235 days a year, then the hourly rate for the NDT machine is: $94/hr.

NDT MACHINE FOR STRINGERS

Acquisition cost:	$400,000	(assumed – no information available)
Expected life:	15 years	
Depreciation charge:	$26,667	
Adjustment to value:	$12,000	(@ 3% per year increase)
Finance cost:	$20,000	(@ 5% on average book value)
Maintenance cost:	$12,000	(@ 3% on average book value)

If the machine operates 16 hours a day for 235 days a year, then the hourly rate for the Stringer NDT machine is: $19/hr.

DIAPHRAGM HOT FORMING

Acquisition cost:	$125,000	(assumed – no information available)
Expected life:	3 years	
Depreciation charge:	$41,667	
Adjustment to value:	$3,750	(@ 3% per year increase)
Finance cost:	$6,250	(@ 5% on average book value)
Maintenance cost:	$1,250	(@ 1% on average book value)

If the machine operates 16 hours a day for 235 days a year, then the hourly rate for the Diaphragm Hot Former is: $14/hr.

E.5 Tooling Costs and Rates

The costs for the skin/cover and stringer tooling can be calculated with the following methods. Once the costs are known, then the tooling costs can be amortized over the complete production run, in order to calculate the tooling rate per part.

SKIN/COVER TOOLING

From Haffner[196], for an Invar® steel open mould tool, suitable for a HTP skin, the cost per area is given as $19/in², which is $29,450/m². Similarly, Logsdon[631], estimated open mould tooling at $2000-3000/ft², which is $22,222-33,333/m². Large tool surfaces, such

as for a HTP skin or wing skin, will require an electroformed nickel surface, which ensures a uniform thickness to minimise any thermally induced deformations during cure[196]. Therefore, the upper cost from Logsdon would seem more appropriate, thus a cost of $30,000/m² shall be used for skin/cover tooling.

Once the surface area of the tool is known then the cost can be worked out, for example a 40m² tool would cost (40×30,000) $1.2m.

STRINGER TOOLING

From Haffner[196], the cost of raw Invar® steel is $22/kg. Haffner also stipulated that the material cost normally accounts for over 30% of the total cost. The tooling, for T- and I-profile stringers, can be listed as:

- Preforming tools
  - Co-Cure & Co-Bond (Soft Stringers)
    - Preforming tool
    - Full length stringer mould/positioning tooling
  - Secondary Bond & Co-Bond (Hard Stringers)
    - Preforming/curing tool
    - Partial length stringer positional tooling

In order to reduce calculation complexity, the preforming tool for co-cure and co-bond (soft stringers) will be considered to be the same as for the preforming/curing tool for secondary bond and co-bond (hard stringers). The cost for these tools is based on the stringer size, and calculated by using Equation E-37:

$$Cost = BH_{AVG} \times \left(\frac{LFW_{AVG}}{2} \right) \times Str.\,Length \times \rho \times COM \times CF \qquad \textbf{E-37}$$

Where ρ is the density of the material (kg/m³) (Steel ≈ 7800 kg/m³); COM is the Cost of the Material per kg; and CF is the Cost Factor based on the proportion of raw material cost to overall cost. The CF for the preforming/curing tool will be considered to be 2, i.e. 50% of the total cost is the raw material cost.

Similarly for the full and partial length stringer mould/positioning tools, the cost for T-profile and I-profile stringers are given in Equations E-38 and E-39, respectively. Where CF has a value of 3.5 as the raw material cost is minimal to the overall cost of the tool. Furthermore, the Length Factor (LF) is 1 for the full length tools and 1/Str. Length for the partial length tools. The factor 0.005 is the material thickness, i.e. 5mm.

$$T - \mathrm{Pr}ofile\,Cost = \left(BH_{AVG} \times \frac{LFW_{AVG}}{2} \right) \times Str.\,Length \times \rho \times 0.005 \times COM \times CF \times LF \qquad \textbf{E-38}$$

$$I - \mathrm{Pr}ofile\,Cost = \left(BH_{AVG} \times \left(\frac{LFW_{AVG}}{2} + \frac{UFW_{AVG}}{2} \right) \div 2 \right) \times Str.\,Length \times \rho \times 0.005 \times COM \times CF \times LF \qquad \textbf{E-39}$$

For U-profile stringers, the stringer tooling is a series of matched mandrels, which are then fixed in a jig so that they can be brought together with the skin tool. As cost data is difficult to obtain, a simple factor will be added for each mandrel to cater for the overall holding jig. For this case the CF is 2.5 as the tooling is slightly more complicated than the normal preforming/curing tools used for the discrete tooling, and JF, i.e. the Jig Factor, is 1.15 to include the cost of the holding jig.

$$Cost = \frac{BH_{StrA\ AVG} + BH_{StrA+1\ AVG}}{2} \times SP \times Str.\ Length \times \rho \times COM \times CF \times JF \quad \textbf{E-40}$$

All other tooling such as pressure plates or jigs for applying adhesive to the stringer foot will be considered as shop aids, and thus their costs will be ignored.

The only other cost to be considered will be the router cost for machining the profile of the skin/cover and stringers. If the data would be available, it could be possible to use Taylor's equation for tool life expectancy[632], so aspects such as cut depth and feed rate could be considered, in order to improve the accuracy of the calculation. However without this data it is known that a PCD router costs $300 per piece, and is disposed of after use. For IM fibre the PCD router can machine a length of 17m, whereas for HS a length of 34m is possible, thus for a hybrid, a length of 25.5m can be considered.

E.6 Production Rates

Airbus in 2007 sold the following aircraft[633]:

- A320 Family: 367 aircraft
- A330/A340: 79 aircraft

Boeing in 2007 sold the following aircraft[634]:

- B737 Family: 330 aircraft
- B767/B777: 95 aircraft
- B747: 16 aircraft

Future total market predictions are as follows:
Boeing[635]:

- Very Large Aircraft: 49 per year
- Wide Body: 338 per year
- Single Aisle: 958 per year

Airbus[636]:

- Very Large Aircraft: 64 per year
- Wide Body: 274 per year
- Single Aisle: 831 per year

So on average the market requires per year:

- Very Large Aircraft: 57
- Wide Body: 306

- Single Aisle: 895

In terms of regional aircraft, i.e. aircraft with a seating capacity less than 120 seats, Bombardier from Canada, and Embrear from Brazil dominate the market currently. However, there are a number of other manufacturers who are or will be entering this market [637]:

- ACAC (AVIC I Commercial Aircraft Company) ARJ21 (China)
- Antonov 148 (Russia)
- Mitsubishi Regional Jet (Japan)
- Sukhoi Superjet 100 (Russia)

Future total market predictions are as follows:

Bombardier[638]:
- 20-59 seats: 25 per year
- 60-99 seats: 305 per year
- 100-149 seats: 315 per year

Enbrear[639]:
- 30-60 seats: 55 per year
- 61-90 seats: 130 per year
- 91-120 seats: 188 per year

So on average the market requires per year:
- 20-60 seats: 40
- 61-90 seats: 180
- 91-120 seats: 195

For example 61-90 was worked out by:

For Bombardier between 60-99 seater requires 305 per year, so 305/40=7.625.
7.625×30=229, therefore 229 + Embrear's prediction of 130, gives an average of 180.